György Inzelt
Andrzej Lewenstam
Fritz Scholz *Editors*

Handbook of Reference Electrodes

Springer

Handbook of Reference Electrodes

György Inzelt • Andrzej Lewenstam • Fritz Scholz
Editors

Handbook of Reference Electrodes

With contributions by

F.G.K. Baucke, A.I. Bhatt, Z. Galus, G. Gritzner, G. Inzelt, K. Izutsu, H. Kahlert, T. Kakiuchi, V.V. Kharton, A. Kisiel, A. Lewenstam, K. Maksymiuk, A. Michalska, J. Migdalski, M. Rohwerder, F. Scholz, G.A. Snook, P. Spitzer, G. Tauber, E.V. Tsipis, G. Tsirlina, S. Wunderli

Springer

Editors
György Inzelt
Department of Physical Chemistry
Eötvös Loránd University
Budapest
Hungary

Andrzej Lewenstam
Center for Process Analytical Chemistry
and Sensor Technology 'ProSens'
Process Chemistry Center
Åbo Akademi University
Åbo, Finland

Faculty of Materials Science and Ceramics
AGH University of Science and Technology
Krakow, Poland

Fritz Scholz
Institute of Biochemistry
University of Greifswald
Greifswald
Germany

ISBN 978-3-642-36187-6 ISBN 978-3-642-36188-3 (eBook)
DOI 10.1007/978-3-642-36188-3
Springer Heidelberg New York Dordrecht London

Library of Congress Control Number: 2013936741

Printed on acid-free paper

Springer is part of Springer Science+Business Media (www.springer.com)

In Memoriam,

The editors dedicate this book to the memory of Dr. Friedrich G. K. Baucke (October 30th, 1930–March 4th, 2013), famed expert in the study of solid glasses and glass melts, and elucidator of the mechanism of the glass electrode. He was a fine scholar, thoughtful scientist, and sincere friend. Chapter 8 of this handbook, written by Dr. F. G. K. Baucke at the age of 82, testifies to his indefatigable search for truth.

Preface

One of the fundamental problems of the electrochemistry is that the Galvani potential difference across an interface, i.e., the difference of inner potentials of two adjacent phases, is not experimentally accessible. Consequently, the potential of a single electrode, i.e., a so-called half-cell consisting of one electron conductor and at least one ionic conductor cannot be determined. By combining two electrodes to a complete galvanic cell or electrolytic cell, potential difference between the two metallic terminals can be measured. The two metallic terminals should be identical for any meaningful potential measurement, and under certain conditions the measured potential is characteristic to the electrode potential intended to determine. For this purpose we use reference electrodes. Reference electrodes are galvanic half-cells which are designed to provide a stable and reproducible Galvani potential difference, either as a primary standard (the standard hydrogen electrode) or as secondary standards. In order to produce reliable experimental data, reference electrodes have to fulfill many, partly contradictory conditions, which practically never can be met to full satisfaction. For the choice and application of a particular reference electrode it is of utmost importance to know its properties as detailed as possible.

It is of great theoretical interest to relate a Galvani potential difference to the absolute potential of a clearly defined species, e.g., the potential of a free electron in vacuum. This defines an absolute potential scale (see Chap. 15), for which the *precise* relation to the conventional standard hydrogen electrode scale for aqueous solutions is still debated. Hence, a consistent system based on the standard hydrogen electrode (SHE) definition still serves the fundamental needs of measuring and calculating redox equilibria, and coupled chemical equilibria in aqueous systems. The relation of the electrode potentials in nonaqueous systems, be they liquid or solid, to the (aqueous) SHE, is of fundamental importance in chemistry because nonaqueous systems play an important role in modern technologies and research, and in many cases aqueous and nonaqueous systems are even directly coupled, as, e.g., in ion partition systems.

Therefore, the authors of this *Handbook of Reference Electrodes* were guided by the idea to provide all necessary and reliable data. The last and only handbook on

reference electrodes was published in 1961 [Ives DJG, Janz GJ (1961) Reference electrodes. Theory and practice. Academic, New York]. Although the progress in this field of research and technology was rather steady and not revolutionary in the last half century, a lot of information vital for modern electrochemistry has been added during that time. Naturally, the Ives/Janz book could not contain information on reference electrodes for solid-state electrolyte systems and nothing about room temperature ionic liquids, glass melts, reference electrodes based on conducting polymers, etc., since these topics strongly developed in the last decades.

In the first section this handbook provides the fundamentals of thermodynamics and kinetics of reference electrodes, and then liquid junction potentials and salt bridges are discussed, as they are involved in almost all reference systems. The following chapters present the various reference electrodes and systems as they are presently used. A final chapter is devoted to the Kelvin probe and discusses this instrument as a reference electrode for contact potential measurements.

Budapest, Hungary — György Inzelt
Åbo, Finland and Krakow, Poland — Andrzej Lewenstam
Greifswald, Germany — Fritz Scholz
Aug 2012

Contents

1 Electrode Potentials 1
György Inzelt

2 Reference Redox Systems in Nonaqueous Systems and the Relation of Electrode Potentials in Nonaqueous and Mixed Solvents to Standard Potentials in Water 25
Gerhard Gritzner

3 Liquid Junction Potentials 33
Galina Tsirlina

4 Salt Bridges and Diaphragms 49
Fritz Scholz and Takashi Kakiuchi

5 Reference Electrodes for Aqueous Solutions 77
Petra Spitzer, Samuel Wunderli, Krzysztof Maksymiuk, Agata Michalska, Anna Kisiel, Zbigniew Galus, and Günter Tauber

6 Reference Electrodes for Use in Nonaqueous Solutions 145
Kosuke Izutsu

7 Reference Electrodes for Ionic Liquids and Molten Salts 189
Anand I. Bhatt and Graeme A. Snook

8 Reference Electrodes in Oxidic Glass Melts 229
Friedrich G.K. Baucke

9 Reference Electrodes for Solid-Electrolyte Devices 243
Vladislav V. Kharton and Ekaterina V. Tsipis

10 Direct Solid Contact in Reference Electrodes 279
Andrzej Lewenstam

11 Micro-reference Electrodes 289
Heike Kahlert

12 Conducting Polymer-Based Reference Electrodes 305
Jan Migdalski and Andrzej Lewenstam

13 Screen-Printed Disposable Reference Electrodes 325
Agata Michalska, Anna Kisiel, and Krzysztof Maksymiuk

14 Pseudo-reference Electrodes 331
György Inzelt

15 The Kelvin Probe Technique as Reference Electrode for Application on Thin and Ultrathin Electrolyte Films 333
Michael Rohwerder

Index 341

List of Contributors

Friedrich G.K. Baucke (†) Formerly affiliated with SCHOTT AG, Mainz, Germany

Anand I. Bhatt CSIRO, Clayton South, VIC, Australia

Zbigniew Galus Department of Chemistry, University of Warsaw, Warszawa, Poland

Gerhard Gritzner Institut für Chemische Technologie Anorganischer Stoffe, Johannes Kepler Universität, Linz, Austria

György Inzelt Department of Physical Chemistry, Eötvös Loránd University, Budapest, Hungary

Kosuke Izutsu Faculty of Science, Shinshu University, Musashino, Japan

Heike Kahlert Institute of Biochemistry, University of Greifswald, Greifswald, Germany

Takashi Kakiuchi Department of Energy and Hydrocarbon Chemistry, Graduate School of Engineering, Kyoto University, Kyoto, Japan

Vladislav V. Kharton Department of Materials and Ceramic Engineering, CICECO, University of Aveiro, Aveiro, Portugal

Anna Kisiel Department of Chemistry, Warsaw University, Warsaw, Poland

Andrzej Lewenstam Center for Process Analytical Chemistry and Sensor Technology 'ProSens', Process Chemistry Center, Åbo Akademi University, Åbo, Finland

Faculty of Materials Science and Ceramics, AGH University of Science and Technology, Krakow, Poland

Krzysztof Maksymiuk Department of Chemistry, University of Warsaw, Warszawa, Poland

Agata Michalska Department of Chemistry, University of Warsaw, Warszawa, Poland

Jan Migdalski AGH University of Science and Technology, Faculty of Materials Science and Ceramics, Krakow, Poland

Michael Rohwerder Max-Planck-Institut für Eisenforschung, Düsseldorf, Germany

Fritz Scholz Institute of Biochemistry, University of Greifswald, Greifswald, Germany

Graeme A. Snook CSIRO, Clayton South, VIC, Australia

Petra Spitzer Physikalisch-Technische Bundesanstalt (PTB), Braunschweig, Germany

Günter Tauber Leiter Forschung, SI Analytics GmbH, Mainz, Germany

Ekaterina V. Tsipis UCQR, IST/ITN, Instituto Superior Técnico, Universidade Técnica de Lisboa, CFMC-UL, Sacavém, Portugal

Galina Tsirlina Chemical Faculty, Department of Electrochemistry, Moscow State University, Moscow, Russia

Samuel Wunderli METAS, Chemistry, Bern-Wabern, Switzerland

Chapter 1
Electrode Potentials

György Inzelt

1.1 Introduction

As it has been pointed out in the Preface the reference electrode allows the control of the potential of a working electrode or the measurement of the potential of an indicator electrode relative to that reference electrode. The rate, the product, and the product distribution of electrode reactions depend on the electrode potential. A knowledge of the electrode potential is of utmost importance in order to design any electrochemical device or to carry out any meaningful measurement. When current flows through an electrochemical cell the potential of one of the electrodes should remain practically constant—it is the reference electrode—in order to have a well-defined value for the electrode potential of the electrode under investigation or to control its potential. An ideally non-polarizable electrode or an electrode the behavior of which is close to it may serve as a reference electrode. The choice and the construction of the reference electrode depend on the experimental or technical conditions, among others on the current applied, the nature and composition of the electrolyte (e.g., aqueous solution, nonaqueous solution, melts), and temperature.

We have already mentioned several notions, which have to be defined. In the following subsections we will give a more detailed picture; however, it seems to be useful to summarize the most important features herein.

It is worth to start with the definition of the electrode, which is certainly not an easy task.

G. Inzelt (✉)
Department of Physical Chemistry, Eötvös Loránd University, Pázmány Péter sétány 1A, 1117 Budapest, Hungary
e-mail: inzeltgy@chem.elte.hu

G. Inzelt et al. (eds.), *Handbook of Reference Electrodes*,
DOI 10.1007/978-3-642-36188-3_1,

1.1.1 Electrodes

There are currently two usages for the term electrode, namely, either (1) the electron conductor connected to the external leads or (2) the half-cell between one electron conductor and at least one ionic conductor. The latter version has usually been favored in electrochemistry [1, 2]. The half-cell, i.e., the electrode, may have a rather complicated structure. In the simplest case a pure solid metal is in contact with an electrolyte solution containing its own ions. However, the electronic conductor may be also an alloy (e.g., an amalgam), carbon (e.g., graphite, glassy carbon), boron-doped diamond, a semiconductor (e.g., a metal oxide, metal salt, doped silicon, germanium alloys), and metal oxides (e.g., iridium dioxide, titanium covered with ruthenium dioxide). It should also be mentioned that even when a pure metal is immersed into an electrolyte solution, its surface may be covered, e.g., with an oxide layer. Typical examples are magnesium or aluminum; however, even the surface of platinum is covered with oxides when it is stored in air or at higher positive potentials. Besides the spontaneously formed surface layers, the surface of metals or other substances is often modified on purpose to obtain electrodes for special functions. When a metal surface is covered by an electrochemically active polymer layer, we speak of polymer modified or (polymer film) electrodes which become an important class of electrodes. A satisfactory definition, which includes the factors and problems mentioned above, may be as follows. *The electrode consists of two or more electrically conducting phases switched in series between which charge carriers (ions or electrons) can be exchanged, one of the terminal phases being an electron conductor and the other an electrolyte*. The electrode can be schematically denoted by these two terminal phases, e.g., Cu(s)$\vert$ $CuSO_4$ (aq), disregarding all other phases that may be interposed. However, in certain cases more phases are displayed, e.g., Ag(s)$\vert$ AgCl(s)$\vert$ KCl(aq) or Pt(s)$\vert$ Polyaniline(s)$\vert$ H_2SO_4(aq), since the consideration of those phases is essential regarding the equilibria and the thermodynamic description.

The electrodes can be classified in several ways. The electrode on which reduction (transfer or electrons from the metal to the dissolved species) occurs is called cathode and on which oxidation takes place is called anode. The positive electrode is the cathode in a galvanic cell and the anode in an electrolytic cell. In a galvanic cell the negative electrode is the anode, while in an electrolytic cell it is the cathode. According to the nature of species participating in electrochemical equilibria and the realization of the equilibria, we may speak of electrodes of the first kind, electrodes of the second kind, electrodes of the third kind, redox electrodes, and membrane electrodes. When more than one electrode reaction takes place simultaneously at the interface, the electrode is a mixed electrode. Another important distinction is based on whether charged species cross the interface or not. In the former case, when the charge transfer is infinitely fast, the electrode is called ideally non-polarizable electrode. When no charge transfer occurs through the interface and the current (charge) that can be measured merely contributes to the establishment of the electrical double layer, the term is ideally polarizable electrode.

There are also names which express the function of the electrode and refer to the whole construction including mechanical parts of the electrode, e.g., dropping mercury or hanging mercury drop electrodes, rotating disk electrodes, combination glass electrodes, optically transparent electrodes, and photoelectrodes. Electrodes with different properties can be constructed by using the same element or compound for the solid phase, however, in various crystal forms, morphologies, and surface structures, with or without additives. For instance, carbon electrodes are made of various materials, such as graphite of spectral purity, graphite powder with liquid or solid binders, glassy carbon, carbon fibers, highly oriented pyrolytic graphite, paraffin-impregnated graphite (PIGE), or diamond. Platinum might be polycrystalline or in forms of different single crystals (well-defined electrodes). The electrode geometry plays also an important role. We may classify electrodes according to their forms such as inlaid disk, sphere, cylinder, sheet, net, spiral wire, sponge, inlaid ring, inlaid plate, ring-disk, etc. The electrode size is also an important factor, and consequently macroelectrodes, microelectrodes, and ultramicroelectrodes are distinguished.

The functional grouping is as follows. The electrode which is under study is called working electrode in voltammetry or indicator electrode in potentiometry. The electrode the potential of which is practically constant and used to make comparison of electrode potentials, i.e., to define the value of the potential of the electrode on the scale based on standard hydrogen electrode, is called a reference electrode. The electrode that serves to maintain the current in the circuit formed with the working electrode in voltammetric experiments in three-compartment cells is the auxiliary (or counter) electrode.

1.1.2 Electrochemical Cells, Cell Diagram, Cell Voltage

For all mobile species, i.e., for species present in the contacting phases the equilibrium condition is

$$\tilde{\mu}_i^{\alpha} = \tilde{\mu}_i^{\beta}, \quad \mu_i^{\alpha} + z_i F \varphi^{\alpha} = \mu_i^{\beta} + z_i F \varphi^{\beta}, \tag{1.1}$$

where $\tilde{\mu}_i^{\alpha}$ and $\tilde{\mu}_i^{\beta}$ are the electrochemical potentials of the ith species in phase α (e.g., in the metal phase) and phase β (solution), respectively, z_i is the charge number of the species, φ^{α} and φ^{β} are the inner electric potentials of the respective phases, and F is the Faraday constant. For a neutral entity (solvent or salt molecules) $\tilde{\mu}_i = \mu_i$, where μ_i is the chemical potential.

Galvani potential difference, i.e., the difference of inner electric potentials of the contacting phases, $\Delta_{\alpha}^{\beta}\varphi$, determines the electrostatic component of the work term corresponding to the transfer of charge across the interface between the phases α and β whose inner electric potentials are φ^{α} and φ^{β}, respectively. The electrical

potential drop can be measured only between the points of contacting phases, whose chemical composition is the same. In this case $\mu_i^{\beta} = \mu_i^{\alpha}$. When the points belong to two different phases, the experimental determination of the potential drop is impossible.

Because the absolute or single electrode potential, i.e., the difference of inner potentials (Galvani potential difference) between contacting phases, cannot be measured or calculated, therefore we measure the electric potential difference of a galvanic cell (cell voltage), E_{meas}, which is the difference of electric potential between a metallic terminal attached to the right-hand electrode in the cell diagram and identical metallic terminal attached to the left-hand electrode. E_{meas} includes the condition when current flows through the cell. The value of E_{meas} measured when the left-hand electrode is at virtual equilibrium, and hence acting as a reference electrode, may be called the potential of the (right-hand) electrode with respect to the (left-hand) reference electrode, E.

Electrochemical cells consist of at least two electron conductors (usually metals) in contact with ionic conductors (electrolytes). The current flow through electrochemical cells may be zero or nonzero. Electrochemical cells with current flow can operate either as galvanic cells, in which chemical reactions occur spontaneously and chemical energy is converted into electrical energy, or as electrolytic cells (also called electrolysis cells), in which electrical energy is converted into chemical energy. The electrodes may be separated by a salt bridge or a glass frit, or an ion-permeable (exchange) membrane or a porous inert diaphragm, or in the case of concentration cells without transference even with a metal in contact with its poorly soluble salts. The galvanic cell is represented by a cell diagram.

Thus, the chemical cell, consisting of an aqueous solution of hydrogen chloride (activity: a, concentration: c), a platinum-hydrogen electrode (partial pressure of hydrogen: p), and a silver–silver chloride electrode, both with copper terminals, is represented by the diagram

$$\mathrm{Cu(s)|Pt(s)|}\underset{p}{\mathrm{H_2(g)}}\Big|\underset{a\text{ or }c}{\mathrm{HCl(aq)}}\Big|\mathrm{AgCl(s)|Ag(s)|Cu(s)}$$

Although this diagram has been recommended by the IUPAC Commission of Electrochemistry [1, 3] it is not entirely correct. It would be better to write as follows:

$$\ldots \Big|\, \mathrm{H_2(g)} \,\Big|\, \underset{c_1}{\mathrm{HCl(aq)}} \,\Big|\Big|\, \underset{c_1}{\mathrm{HCl(aq)}} \,\Big|\, \mathrm{AgCl(s)}$$

since liquid junction potential may arise even in this case because at the hydrogen electrode HCl solution is saturated by H_2, while at the silver–silver chloride electrode HCl solution is saturated by AgCl.

The cell diagram of the Daniell cell is

$$\mathrm{Cu(s)} \,\vert\, \mathrm{Zn(s)} \,\vert\, \mathrm{ZnSO_4(aq)} \,\vdots\, \mathrm{CuSO_4(aq)} \,\vert\, \mathrm{Cu(s)}$$

The diagram of the cell for pH measurements when glass electrode is used [4]:

$$\mathrm{Cu(s)} \,\vert\, \mathrm{Hg(l)} \,\vert\, \mathrm{H_2Cl_2(s)} \,\vert\, \mathrm{KCl(aq)} \,\vdots\!\vdots\, \text{solution} \,\vert\, \text{glass} \,\vert\, \mathrm{HCl(aq)\ or\ buffer} \,\vert\, \mathrm{AgCl(s)} \,\vert\, \mathrm{Ag(s)} \,\vert\, \mathrm{Cu(s)}$$

$$m > 3.5\,\mathrm{mol\,kg^{-1}} \quad a_{\pm} = ?\,\mathrm{pH} = ?$$

A single vertical bar ($\vert$) should be used to represent a phase boundary, a dashed vertical ($\vdots$) bar to represent a junction between miscible liquids, and double, dashed vertical bars ($\vdots\!\vdots$) to represent a liquid junction, in which the liquid junction potential has been assumed to be eliminated.

1.2 Electrode Potential, Equilibrium Electrode Potential, Standard Electrode Potential, Electromotive Force

The electrode potential, E (SI unit is V), is the electric potential difference of an electrochemical cell (including the condition when current flows through the cell), and the left-hand electrode in the diagram of the galvanic cell (cell diagram) is at virtual equilibrium, and hence acting as a reference electrode. In electrolysis cells the potential of the working electrode is compared to a reference electrode which is practically at equilibrium. The liquid junction potential is assumed to be eliminated. When the right-hand electrode is also at equilibrium the measured potential is the equilibrium electrode potential. In this case we measure the electromotive force (emf) of the cell.

The electromotive force is the limiting value of the electric potential difference of a galvanic cell when the current through the external circuit of the cell becomes zero, all local charge transfer equilibria across phase boundaries—except at electrolyte | electrolyte junctions—and local chemical equilibria within phases being established. (The cell as a whole is not at equilibrium since if the cell reaction reaches its equilibrium then $E_{\mathrm{cell}} = \Delta G_{\mathrm{cell}} = 0$.)

When the electrode investigated in aqueous medium is at equilibrium and in its standard state as well as the reference electrode is the standard hydrogen electrode, the standard electrode potential can be determined. In nonaqueous solvents it is necessary to use another standard reaction than the ionization of hydrogen (see below and Chaps. 2, 6–9).

There is an inherent link between emf and the potential of the electrochemical cell reaction (E_{cell}); however, the definition of E_{cell} is purely thermodynamic (see below), while that of the emf is operational. In order to avoid confusion regarding the

sign (+ or −) of emf (and E_{cell}) it is necessary to introduce an unambiguous convention. The cell diagram has to be drawn in such a way that the oxidation always occurs at the left-hand side electrode while the reduction takes place at the right-hand side electrode, i.e., the positive electricity flows through the cell from left to right. Therefore, the positive electricity flows from right to left through the outer part of the circuit. In this way, for a spontaneous reaction when the Gibbs energy change of reaction, $\Delta G < 0$, the value of emf and E_{cell} will be positive.

1.2.1 Thermodynamical Basis of the Electrode Potential

A chemical reaction occurring spontaneously in a galvanic cell is called the cell reaction. The Gibbs energy change of the reaction (ΔG) is converted into electrical energy (current) and heat. The cell reaction in a galvanic cell is spontaneous, i.e., ΔG is negative. The reaction equation should be written in such a way that $\Delta G < 0$ when it proceeds from left to right. The peculiarity of the cell reaction is that the chemical processes (oxidation and reduction) take place spatially separated at the electrodes in such a way that they are interconnected by the ion transport through the solution separating the two electrodes. They are called half-reactions or electrode reactions. Oxidation takes place at the anode, and reduction at the cathode.

We define a term called the potential of the cell reaction (E_{cell}), which is a thermodynamic quantity. The relationship between the molar Gibbs (free) energy change (ΔG) of the cell reaction and the potential of the cell reaction (E_{cell}) is as follows [1, 3, 5–9]:

$$E_{cell} = -\frac{\Delta G}{nF}, \tag{1.2}$$

where n is the charge number of the cell reaction and F is the Faraday constant.

The reaction to which ΔG and the potential of the cell reaction (E_{cell}) refer should be clearly indicated, for example

$$CuSO_4(aq) + Zn(s) \rightarrow Cu(s) + ZnSO_4(aq) \tag{1.3}$$

$$2H_2(g) + O_2(g) \rightarrow 2H_2O(l) \tag{1.4}$$

$$H_2(g) + {}^1\!/_2 O_2(g) \rightarrow H_2O(l) \tag{1.5}$$

$$2CH_3OH(aq) + 3O_2(g) \rightarrow 2CO_2(g) + 4H_2O(l) \tag{1.6}$$

The respective half-reactions are as follows:

$$Cu^{2+}(aq) + 2e^- \rightarrow Cu(s) \tag{1.3a}$$

$$\mathrm{Zn(s)} \rightarrow \mathrm{Zn^{2+}(aq)} + 2\mathrm{e^-} \tag{1.3b}$$

$$\mathrm{O_2(g)} + 4\mathrm{e^-} + 4\mathrm{H^+} \rightarrow 2\mathrm{H_2O(l)} \tag{1.4a}$$

$$2\mathrm{H_2(g)} \rightarrow 4\mathrm{H^+(aq)} + 4\mathrm{e^-} \tag{1.4b}$$

$$^1\!/_2\mathrm{O_2(g)} + 2\mathrm{e^-} + 2\mathrm{H^+(aq)} \rightarrow \mathrm{H_2O(l)} \tag{1.5a}$$

$$\mathrm{H_2(g)} \rightarrow 2\mathrm{H^+(aq)} + 2\mathrm{e^-} \tag{1.5b}$$

$$3\mathrm{O_2(g)} + 12\mathrm{e^-} + 12\mathrm{H^+(aq)} \rightarrow 6\mathrm{H_2O(l)} \tag{1.6a}$$

$$2\mathrm{CH_3OH(aq)} + 2\mathrm{H_2O(l)} \rightarrow 2\mathrm{CO_2(g)} + 12\mathrm{H^+(aq)} + 12\mathrm{e^-} \tag{1.6b}$$

The expression, "cell reaction," is used almost exclusively for the spontaneous reactions occurring in galvanic cells. However, also in electrolysis cells (electrochemical cells) chemical transformations take place, when current is passed through the cell from an external source. Evidently, we may also speak of cell reactions even in this case, albeit additional energy is needed for the reaction to proceed since $\Delta G > 0$.

1.2.2 From the Cell Potential to the Electrode Potential. The Dependence of the Potential of Cell Reaction on the Composition

If the stoichiometric equation of the cell reaction is

$$\sum_{\alpha}\sum_{i} \nu_i^{\alpha} A_i^{\alpha} = 0, \tag{1.7}$$

where A_i is for the components, α is for the phases, and ν_i is for the stoichiometric coefficients,

$$\Delta G = \sum_{\alpha}\sum_{i} \nu_i^{\alpha} \mu_i^{\alpha}, \tag{1.8}$$

where μ_i^{α} is the chemical potential of species i in phase α.

At equilibrium between each contacting phase for the common constituents

$$\sum_{\alpha}\sum_{i} \nu_i^{\alpha} \mu_i^{\alpha} = 0. \tag{1.9}$$

If we consider a cell without liquid junction—which in fact is nonexistent but the effect of the liquid junction potential can be made negligible

$$\Delta G = \sum_{\alpha} \sum_{i} \nu_i^{\alpha} \mu_i^{\alpha} = -nFE_{\text{cell}}. \tag{1.10}$$

Taking into account the relationship between μ_i and the relative activity of species i, a_i, i.e.,

$$\mu_i = \mu_i^{\circ} + RT \ln a_i, \tag{1.11}$$

where R is the gas constant and T is the thermodynamic temperature, it follows that (for the sake of simplicity neglecting the indication of phases further on)

$$E_{\text{cell}} = -\frac{1}{nF} \sum \nu_i \mu^{\circ} - \frac{RT}{nF} \sum \nu_i \ln a_i = E_{\text{cell}}^{\circ} - \frac{RT}{nF} \sum \nu_i \ln a_i. \tag{1.12}$$

If the reference electrode is the standard hydrogen electrode (SHE)

$$E_{\text{cell}}^{\circ} = -\frac{1}{F}(\mu_{\text{H}^+}^{\circ} - 0.5\mu_{\text{H}_2}^{\circ}) - \frac{1}{nF} \sum \nu_i \mu_i^{\circ}. \tag{1.13}$$

It has been mentioned that $E_{\text{cell}}^{\circ} = E^{\circ}$ when the reference system is the oxidation of molecular hydrogen to solvated (hydrated) protons. The standard electrode potential of the hydrogen electrode is chosen as 0 V. Thermodynamically it means that not only the standard free energy of formation of hydrogen ($\mu_{\text{H}_2}^{\circ}$) is zero—which is a rule in thermodynamics—but that of the solvated hydrogen ion ($\mu_{\text{H}^+}^{\circ} = 0$!) at all temperatures. In contrast to the common thermodynamic definition of the standard state, the temperature is ignored. The zero temperature coefficient of the SHE corresponds to the conventional assumption of the zero standard entropy of H^+ ions. This extra-thermodynamic assumption induces the impossibility of comparing the values referred to the hydrogen electrodes, in different solvents.

The old standard values of E° were calculated by using $p^{\circ} = 1$ atm = 101,325 Pa. The new ones are related to 10^5 Pa (1 bar). It causes a difference in potential of the standard hydrogen electrode of +0.169 mV, that is, this value has to be subtracted from the E° values given previously in different tables. Since the large majority of the E° values have an uncertainty of at least 1 mV, this correction can be neglected.

When all components are in their standard states ($a_i = 1$ and $p^{\circ} = 1$ bar) $E_{\text{cell}} = E_{\text{cell}}^{\circ} = E^{\circ}$. However, a_i is not accessible by any electrochemical measurements, only the mean activity ($a_{\pm}$) can be determined. The cell represented by the cell diagram

$$\text{Cu(s)|Pt(s)|H}_2\text{(g)|HCl(aq)|AgCl(s)|Ag(s)|Cu(s)}$$

$$p = 1 \text{ bar} \quad c = 1 \text{ mol dm}^{-3}$$

is usually considered as a cell without liquid junction. As it has been mentioned earlier it is not entirely true since the electrolyte saturated with hydrogen and AgCl near the Pt and Ag | AgCl electrodes, respectively (see above). In order to avoid the direct reaction between AgCl and H_2 a long path is applied between the electrodes or the HCl solution is divided into two parts separated by a diaphragm.

In this case the cell reaction is as follows:

$$\mathrm{AgCl} + {}^1\!/_2\mathrm{H_2} \rightleftarrows \mathrm{Ag} + \mathrm{Cl^-} + \mathrm{H^+} \tag{1.14}$$

From Eq. (1.14)

$$E_{\mathrm{cell}} = E^{\ominus}_{\mathrm{Ag/AgCl}} - \frac{RT}{F} \ln a_{\mathrm{H^+}} a_{\mathrm{Cl^-}}, \tag{1.15}$$

where $a_{\mathrm{H^+}} a_{\mathrm{Cl^-}} = a_{\pm}^2 = (\gamma_{\pm} c_{\mathrm{HCl}}/c^{\ominus})^2 = (\gamma_{\pm} m_{\mathrm{HCl}}/m^{\ominus})^2$.

1.2.3 Determination of the Standard Potential

The standard potential of a cell reaction ($E^{\ominus}_{\mathrm{cell}}$) values can be calculated from the standard molar free (Gibbs) energy change ($\Delta G^{\ominus}$) for the same reaction with a simple relationship:

$$E^{\ominus}_{\mathrm{cell}} = \Delta G^{\ominus}/nF = (RT/nF) \ln K, \tag{1.16}$$

where n is the charge number of the cell reaction which is the stoichiometric number equal to the number of electrons transferred in the cell reaction as formulated, F is the Faraday constant, K is the equilibrium constant of the reaction, R is the gas constant, and T is the thermodynamic temperature. However, $E^{\ominus}_{\mathrm{cell}}$ is not the standard potential of the electrode reaction (or sometimes called half-cell reaction) which is tabulated in the tables. It is the standard potential of the reaction in a chemical cell which is equal to the standard potential of an electrode reaction (abbreviated as standard electrode potential), $E^{\ominus}$, when the reaction involves the oxidation of molecular hydrogen to solvated protons:

$${}^1\!/_2\,\mathrm{H_2(g)} \rightarrow \mathrm{H^+(aq)} + \mathrm{e^-} \tag{1.17}$$

The notation H^+ (aq) represents the hydrated proton in aqueous solution without specifying the hydration sphere. It means that the species being oxidized is always H_2 molecule and $E^{\ominus}$ is always related to a reduction. It is the reason why we speak of reduction potentials. In the opposite case the numerical value of $E^{\ominus}$ would be the same but the sign would differ. It should be mentioned that in old books, e.g., in Latimer's book [10], the other sign convention was used; however, the International

Union of Pure and Applied Chemistry (IUPAC) has introduced the unambiguous and authoritative usage in 1974 [1, 3].

Although the standard potentials at least in aqueous solutions are always related to reaction [Eq. (1.17)], i.e., the standard hydrogen electrode, it does not mean that other reference systems cannot be used or ΔG° of any electrochemically accessible reaction cannot be determined by measuring emf. One may think that ΔG° and E° values in the tables of different books [10–19] are determined by calorimetry and electrochemical measurements, respectively. It is not so, the way of tabulations mentioned serves practical purposes only. Several "thermodynamic" quantities (ΔG°, ΔH°, ΔS°, etc.) have been determined electrochemically, especially when these measurements were easier or more reliable. On the other hand, E° values displayed in the tables mentioned have been determined mostly by calorimetric measurements since in many cases—due to kinetic reasons, too slow or too violent reactions—it has been impossible to collect these data by using the measurement of the electric potential difference of a cell at suitable conditions and in some cases its application is limited by a chemical reaction with the solvent.

The tables compiled usually contain E° values for simple inorganic reactions in aqueous solution mostly involving metals and their ions, oxides and salts, as well as some other important elements (H, N, O, S, and halogens). Many values of ΔG°, ΔH°, ΔS°, and E° that can be found in these sources are based on rather old reports. The thermodynamic data have been continuously renewed by the US National Institute for Standards and Technology (NIST, earlier NBS = National Bureau of Standards and Technology) and its reports supply reliable data which are widely used by the scientific community [20]. The numerical values of the quantities have also been changed due to the variation of the standard states and constants. Therefore, it is not surprising that E° values are somewhat different depending on the year of publication of the books. Despite the—usually slight—difference in the data and their uncertainty, E° values are very useful for predicting the course of any redox reactions including electrode processes.

1.2.4 The Formal Potential ($E_{\mathrm{c}}^{\circ'}$)

Besides $E_{\mathrm{cell}}^{\circ}$ and E° the so-called formal potentials ($E_{\mathrm{cell,c}}^{\circ'}$ and $E_{\mathrm{c}}^{\circ'}$) are frequently used [5, 7]. The purpose of defining formal potentials is to have "conditional constant" that takes into account activity coefficients and side reaction coefficients (chemical equilibria of the redox species), since in many cases it is impossible to calculate the resulting deviations because neither the thermodynamic equilibrium constants are known, nor it is possible to calculate the activity coefficients. Therefore, the potential of the cell reaction and the potential of the electrode reaction are expressed in terms of concentrations:

$$E_{\mathrm{cell}} = E_{\mathrm{cell,c}}^{\circ'} - \frac{RT}{nF} \sum \nu_i \ln \frac{c_i}{c^{\circ}}, \tag{1.18}$$

$$E = E_{\mathrm{c}}^{\ominus'} - \frac{RT}{nF} \sum \nu_i \ln \frac{c_i}{c^{\ominus}}, \tag{1.19}$$

where

$$E_{\mathrm{cell,c}}^{\ominus'} = E_{\mathrm{cell}}^{\ominus} - \frac{RT}{nF} \sum \nu_i \ln \gamma_i \tag{1.20}$$

and

$$E_{\mathrm{c}}^{\ominus'} = E^{\ominus} - \frac{RT}{nF} \sum \nu_i \ln \gamma_i \tag{1.21}$$

when SHE is the reference electrode ($a_{\mathrm{H}^+} = \frac{p_{\mathrm{H_2}}}{p^{\ominus}} = 1$). Equation (1.19) is the well-known Nernst equation:

$$E = E_{\mathrm{c}}^{\ominus'} + \frac{RT}{nF} \ln \frac{\pi\, c_{\mathrm{ox}}^{\nu_{\mathrm{ox}}}}{\pi\, c_{\mathrm{red}}^{\nu_{\mathrm{red}}}}, \tag{1.22}$$

where π is for the multiplication of the concentrations of the oxidized (ox) and reduced (red) forms, respectively. The Nernst equation provides the relationship between the equilibrium electrode potential and the composition of the electrochemically active species. Note that the Nernst equation can be used only at equilibrium conditions! The formal potential is sometimes called as conditional potential, indicating that it relates to specific conditions (e.g., solution composition) which usually deviate from the standard conditions. In this way, the complex or acid–base equilibria are also considered since the total concentrations of oxidized and reduced species considered can be determined, e.g., by potentiometric titration, however, without a knowledge of the actual compositions of the complexes. In the case of potentiometric titration the effect of the change of activity coefficients of the electrochemically active components can be diminished by applying inert electrolyte in high concentration (almost constant ionic strength). If the solution equilibria are known from other sources, it is relatively easy to include their parameters into the respective equations related to $E_{\mathrm{c}}^{\ominus'}$. The most common equilibria are the acid–base and the complex equilibria. In acid media a general equation for the proton transfer accompanying the electron transfer is

$$\mathrm{Ox} + n\,\mathrm{e}^- + m\mathrm{H}^+ \rightleftarrows \mathrm{H}_m\mathrm{Red}^{(m-n)+} \qquad E_{\mathrm{c}}^{\ominus'}, \tag{1.23}$$

$$\mathrm{H}_m\mathrm{Red}^{(m-n)+} \rightleftarrows \mathrm{H}_{m-1}\mathrm{Red}^{(m-n-1)+} + \mathrm{H}^+ \qquad K_{\mathrm{a1}}, \tag{1.24}$$

$$\mathrm{H}_{m-1}\mathrm{Red}^{(m-n-1)+} \rightleftarrows \mathrm{H}_{m-2}\mathrm{Red}^{(m-n-2)+} + \mathrm{H}^+ \qquad K_{\mathrm{a2}}, \tag{1.25}$$

etc. For $m = n = 2$

$$E = E_c^{\Theta'} + \frac{RT}{2F} \ln\left(\frac{c_{ox}}{c_{red}} \frac{K_{a1}\ K_{a2} + K_{a1} a_{H^+} + a_{H^+}^2}{K_{a1} K_{a2}}\right). \tag{1.26}$$

The complex equilibria can be treated in a similar manner; however, one should not forget that each stability constant (K_i) of a metal complex depends on the pH and ionic strength.

The simplest and frequent case is when metal ions (M^{z+}) can be reduced to the metal which means that all the ligands (L^{n-}) will be liberated, i.e.,

$$ML_\nu^{(z-\nu n)+}(aq) + ze^- = M(s) + \nu L^{n-}(aq). \tag{1.27}$$

In this case the equilibrium potential is as follows:

$$E = E_{c,ML/M}^{\Theta'} + \frac{RT}{zF} \ln \frac{c_{ML}}{c_L}, \tag{1.28}$$

where c_{ML} and c_L are the concentrations of the complex and the ligand, respectively, and $E_{c,ML/M}^{\Theta'}$ is the formal potential of reaction [Eq. (1.27)]. At certain conditions ($c_M{}^+ \ll c_L$) the stability constant (K) of the complex and ν can be estimated from the E vs. ln c_L plot by using the following equation:

$$E = E_c^{\Theta'} - \frac{RT}{zF} \ln K \frac{RT}{zF} \ln c_L^{\nu}. \tag{1.29}$$

Amalgam formation shifts the equilibrium potential of a metal (polarographic half-wave potential, $E_{½}$) into the direction of higher potentials due to the free energy of the amalgam formation (ΔG_{amal})

$$E = E_c^{\Theta'} - (\Delta G_{amal}/nF) + (RT/nF) \ln(c_{M^+}/c_M), \tag{1.30}$$

$$E_{1/2} = E_c^{\Theta'} - (\Delta G_{amal}/nF) + (RT/nF) \ln\ c_M(\text{sat}), \tag{1.31}$$

where c_M (sat) is the saturation concentration of the metal in the mercury. It is assumed that a_{Hg} is not altered, and $D_{red} = D_{ox}$, where D_{red} and D_{ox} are the respective diffusion coefficients.

In principle, $E_c^{\Theta'}$ can be determined by the widely used electroanalytical techniques (e.g., polarography, cyclic voltammetry). The combination of the techniques is also useful.

1.2.5 The Problem to Relate to Each Other Electrode Potentials Between Different Media

In several nonaqueous solvents it is necessary to use a standard reaction other than the oxidation of molecular hydrogen. At present there is no general choice of such standard reaction (reference electrode) [3, 5]. Although in some cases the traditional reference electrodes (e.g., saturated calomel, SCE, or silver/silver chloride) can also be used in organic solvents, much effort has been made to find reliable reference reactions. The system has to meet the following criteria:

(i) The reaction should be a one-electron transfer
(ii) The reduced form should be a neutral molecule, and the oxidized form a cation
(iii) The two components should have large sizes and spherical structures, i.e., the $\Delta G_{\text{solvation}}$ should be low and practically independent from the nature of the solvent (the free energy of ion transfer from one solution to the other is small)
(iv) Equilibrium at the electrode must be established rapidly
(v) The standard potential must not be too high so that solvents are not oxidized
(vi) The system must not change structure upon electron transfer

The ferrocene/ferrocenium reference redox system at platinum fulfills these requirements fairly well [5, 21–23]. Another system which has been recommended is bis(biphenyl)chromium (0)/bis(biphenyl)chromium (+1) (BCr^+/BCr) [5, 22, 23]. Several other systems have been suggested and sporadically used such as cobaltocene/cobaltocenium, tris(2,2′-bipyridine) iron (I)/tris(2,2′-bipyridine) iron (0), $Rb^+/Rb(Hg)$, etc. $Ag/AgClO_4$ or $AgNO_3$ dissolved in the nonaqueous solvent is also frequently used.

It yields stable potentials in many solvents (e.g., in CH_3CN); however, in some cases its application is limited by chemical reaction with the solvent.

This problem will be addressed in detail in Chap. 2.

When the electrolysis is carried out in molten salts at high temperatures, special, chemically highly resistant reference electrodes should be used. In most cases pseudo-reference electrodes or quasi-reference electrodes, such as a piece of metal (Mo, Al–Li alloy, etc.), are used (see Chap. 14). However, in many two-electrode systems one of the electrodes consists of a metal and its fused salt, e.g., Ag | AgCl, Mg | $MgCl_2$, Pb | $PbCl_2$, Tl | TlCl, and Zn | $ZnCl_2$ or oxide, e.g., Al | Al_2O_3 which makes the comparison of the electrode potentials possible (see Chap. 8).

1.3 The Role of the Kinetics of the Electrode Reaction

We have mentioned that the reference electrodes should behave as practically ideally non-polarizable electrodes. Ideally non-polarizable electrodes are those for which the exchange of common charged components between phases proceeds unhindered. This is the case when the exchange current density (j_o) and the standard

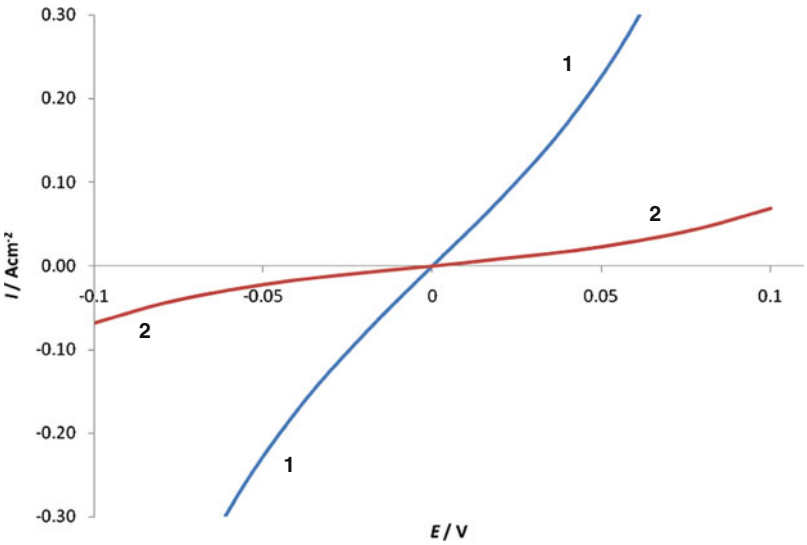

Fig. 1.1 The current density vs. electrode potential function (the polarization curves) for electrodes with exchange current densities (*1*) 0.1 mA cm^{-2} and (*2*) 0.01 mA cm^{-2}, respectively

rate constant ($k^{\circ\prime}$) of the electrode reaction are high, i.e., the activation energy is small. The potential is practically unaffected by small current densities (j) until $j_o \gg j$. The situation is illustrated in Fig. 1.1. It can be seen that 0.01 mA cm^{-2} current density causes only 1–2 mV if $j_o = 0.1$ mA cm^{-2}; however, the potential shift is tenths of mVs when $j_o = 0.01$ mA cm^{-2}. At high current density diffusion (concentration) polarization becomes operative. Such electrodes show electrochemical reversibility and Nernstian behavior. A thermodynamic equilibrium exists, and the Nernst equation can be applied regardless of the current flow. The surface equilibrium is a consequence of the very fast charge transfer kinetics. Polarizability and non-polarizability are not absolute properties of an electrode (interface) but depend on a number of conditions, e.g., on the timescale of the experiment, and it is assumed that the mass transport is fast [6, 24].

The respective equations can easily be derived from the fundamental relationship between the current density (j) and electrode potential (E) under steady-state conditions

$$j = k^{\circ\prime}F\left\{-c_o(x=0)\exp\left[-\frac{\alpha_c F(E-E^{\circ\prime})}{RT}\right] + c_R(x=0)\exp\left[\frac{\alpha_a F(E-E^{\circ\prime})}{RT}\right]\right\}, \tag{1.32}$$

where $c_o(x=0)$ and $c_R(x=0)$ are the concentration of the oxidized and reduced forms of the species at the site of the reaction (at the electrode surface) taking part in the electron exchange process, respectively, α_a an α_c are the anodic and cathodic

transfer coefficients, respectively, R is the gas constant, T is the thermodynamic temperature, and $E^{\Phi'}$ is the formal electrode potential.

The exchange current density can be expressed as follows:

$$j_o = k^{\Phi} F c_o^* \exp\left[\frac{\alpha_c F(E_e - E^{\Phi'})}{RT}\right], \tag{1.33}$$

where c_o^* is the bulk concentration of the oxidized form of the redox couple, and E_e is the equilibrium electrode potential.

If the exchange current density is much higher than the current applied

$$j_o \gg j, \text{ i.e.}, j/j_o \to 0, \tag{1.34}$$

we obtain

$$c_o(0,t)/c_R(0,t) = (c_o^*/c_R^*)\exp[nf(E - E_e)]. \tag{1.35}$$

By substituting (c_o^*/c_R^*) from the Nernst equation

$$\exp\left[nf(E_e - E_c^{\Phi'})\right] = c_o^*/c_R^*, \tag{1.36}$$

the following relationships can be derived:

$$c_o(0,t)/c_R(0,t) = \exp\left[nf(E - E_c^{\Phi'})\right] \tag{1.37}$$

or

$$E = E_c^{\Phi'} + \frac{RT}{nF}\ln\frac{c_o(0,\ t)}{c_R(0,\ t)}, \tag{1.38}$$

i.e., the Nernst equation expresses the relationship between the surface concentrations and the electrode potential regardless of the current flow.

In the case of three-electrode system by using potentiostat/galvanostat the change of the potential (polarization) of the reference electrode usually causes no problem, since the current flows between the working and the reference electrode is always very small. However, in two-electrode system it can effect the potential of the reference electrode substantially. One of the old practices to avoid this problem is the use of working electrode of much smaller real surface area than that of the reference electrode. In this way the current density of the reference electrode is always much smaller than that of the working electrode; consequently while I current flows through the cell and the external circuit, the polarization of the reference electrode will be negligible in comparison with the working electrode. This strategy is still used in the case of polarography (large area mercury pool) or electrochemical impedance spectroscopy.

1.4 Instruments for Potential Measurements

In all electrochemical methods the potential difference between a working or an indicator electrode and a reference electrode, which in two-electrode system is also the counter electrode in electrolytic cells, is measured. In the case of galvanic cells emf is aimed to determine or in potentiometry the measurement is made under equilibrium (or near equilibrium) conditions, which means that the concentrations of all species are uniform throughout the solution, equilibrium prevails within and between the phases, and all other parameters (pressure, temperature) are constant. Of course, a cell voltage can be measured when no current is being applied in an electrolysis cell. However, the rest or open-circuit potential is not necessarily an equilibrium potential, e.g., it is a mixed potential in the case of a corroding system, which is called corrosion potential. Voltage meters with high-input impedance are used, so that the current flowing through the cell is as small as possible; consequently the potential is only slightly affected. Most of the potential drops on the outer resistance (R_{outer}) of the voltage meter. If it were not be the case, i.e., at comparable cell (inner) resistance (R_{inner}) and outer resistance, the voltage measured would depend on the ratio of $R_{\text{outer}}/R_{\text{outer}} + R_{\text{inner}}$; consequently unreliable data can be obtained. The outer resistance, which is the input resistance or impedance of the voltmeters (pH meters), is very high, typically in the region of 10^{14} Ω.

It may need an explanation why we consider a current flow during the measurement of the cell potential even in the case of a galvanic cell or an electrolysis cell at so-called open-circuit conditions. If we close any electric circuit and there is a potential difference between the two terminals, current should flow. If we want to measure the potential we have to make a circuit; otherwise no measurement can be made. In this sense the open-circuit potential only means that no current is applied in an electrolysis cell. While the classical compensation method can still be used, nowadays almost exclusively, high impedance voltmeters are applied. In an electrolysis cell the potential of the working electrode can be controlled by using a potentiostat.

1.4.1 Compensation Method

For the measurement of electromotive force of a galvanic cell a compensation method, based on the principle of counter emf, was elaborated by Poggendorff (1796–1877) in 1841 (Pogg Ann 54:161). Later it was developed further by others. The method is also called du Bois-Reymond–Poggendorff compensation method which is an acknowledgement of the contribution of Emil du Bois-Reymond (1798–1896). The zero current condition is established by using another power supply (**A**), which is connected with an opposite polarity. The currentless circuit is realized by changing in the resistances of the potentiometer until the "null indicator," i.e., the galvanometer (**G**) shows zero (Fig. 1.2).

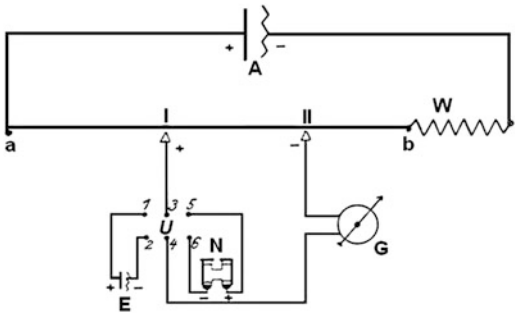

Fig. 1.2 The drawing of the Poggendorff compensation circuit

The measurement is carried out as follows.

The circuit of the secondary battery (**A**) or other power supply is closed by a measuring wire which is uniform in diameter, and is mounted on a board above a meter rule. The galvanic cell (**E**) whose emf to be measured is connected oppositely to the battery in the auxiliary circuit established between points **a** and **b**. By the help of the variation of the position of the sliding contact it can be achieved that the potential difference between points **I** and **II** will correspond to the emf of **E** cell, providing that its emf is smaller than that of the battery (**A**) which is usually 2 V. The contact at any intermediate point is done with a squareended metal probe, which presses the wire on the scale ("tapping"). The switch is closed for an instant, and the galvanometer indicates the direction of the current. This technique permits length measurement to ±1 mm which—choosing an appropriate **a**–**b** length—corresponds to 1 mV accuracy. Then the sub-circuit will be currentless, which is indicated by the sensitive (ca. 10 μA) center-reading galvanometer (**G**). Since the voltage of the battery may change, it is of importance to use standard reference source, which is usually a Weston cell developed by Edward Weston (1850–1936). The potential of the Weston cell is 1.0183 V at 25 °C, and it is very stable and reproducible. In Fig. 1.2 this cell is marked by **N** which is related to the German name: "Normalelement" (normal element). Thus, the measurement is repeated by replacing **E** with **N**. The currentless situation is achieved in a different position of **II** which is denoted by **II**′. The ratio of the two different lengths (l) is equal to the ratio of the electromotive forces of **E** and **N**, respectively, i.e., emf (**E**):emf (**N**) = l(**I–II**):l(**I–II**′). The serial resistance **W** (rheostat) serves for the setting of the value of the current. It should be done when the test with the Weston element is carried out, and the value of the resistance should not be varied afterwards. Instead of the measuring wire other types of resistances, resistance series, which brought into circuit by a dial switch, can also be used (Fig. 1.3).

The emf value of the cell (E) can be calculated from the following relationship:

$$\frac{E}{E_n} = \frac{R_1(x)}{R_1(n)} \frac{R_1(n) + R_2(n)}{R_1(x) + R_2(x)} \frac{U(x)}{U(n)}, \tag{1.39}$$

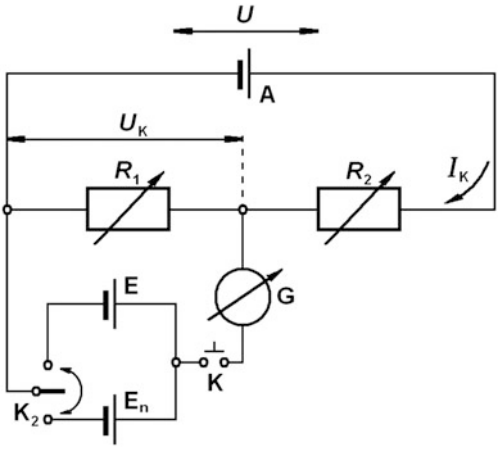

Fig. 1.3 Compensation circuit with variable resistances (R_1 and R_2). U is the voltage of the DC power supply (battery) A, U_k is the compensating voltage, E_n is the standard reference source (normal element), E is the cell whose voltage to be measured, and K is a dial switch

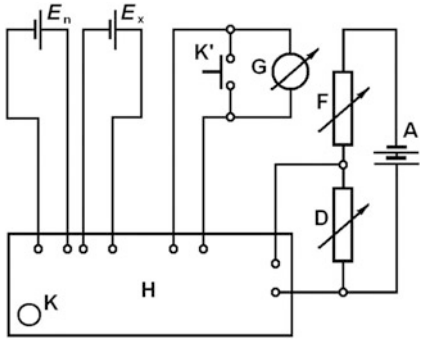

Fig. 1.4 The measurement of emf by a compensator. F and D are the fine and course potentiometers, H is the compensator, K is a momentary switch

where x and n refer to values measured for the cell E and normal element E_n, whose cell voltage is E and E_n, respectively.

The accuracy of the measurement has been enhanced by the application of "compensators." The principle of compensators was elaborated by Feussner in 1890 (Z Instrumentenkunde 10:113). The compensators worked with two or more identical series of resistances, sometimes combined with a Wheatstone bridge and a Thomson bridge. Many variants such as Franke, Wilsmore, Rapsor Siemens-Halske, and Lindeck-Rothe compensators were used (Fig. 1.4).

With the appearance of the valve voltmeter in 1935 the compensation method has been gradually displaced from the everyday laboratory practice [25], and nowadays almost exclusively electronic voltmeters equipped with transistors and integrated circuits are being used.

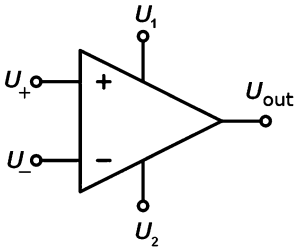

Fig. 1.5 The schematic picture of an operational amplifier. U_+ is the non-inverting input, U_- is the inverting input, U_{out} is the output voltage, and U_1 and U_2 are the positive and negative power supplies, respectively. U_1 is usually between +9 and +15 V and U_2 is respectively between −9 and −15 V

1.4.2 Voltmeters, pH Meters, Potentiostats

Besides the measurement of the cell voltage under (near) equilibrium conditions, the potential between the working and the reference electrodes, i.e., the electrode potential of the electrode under investigation, is measured and controlled. For this purpose a potentiostat is used. (The current can also be controlled in galvanostatic regime.) For transient measurements a function generator, which produces the desired perturbation, is also built in the potentiostat. Earlier the analog signals (potential, current, time) have been recorded by X-Y recorders or oscilloscopes; however, nowadays almost exclusively digital-to-analog converters are used for the control of the device, and analog-to-digital converters for the data acquisition, and as the results, the respective functions appear on the screen of computers [6].

1.4.2.1 Operational Amplifiers

The most important parts of all voltmeters and potentiostats used are the general-purpose amplifiers called operational amplifiers (OPAs) [6, 26–29]. An operational amplifier (Fig. 1.5) is a DC-coupled high-gain electronic voltage amplifier with a differential input and, usually, a single-ended output. An OPA produces an output voltage that is typically millions of times larger than the voltage difference between its input terminals.

The operational amplifiers have five connections. The output voltage is a function of the difference between the two input voltages according to the equation:

$$U_{out} = A(U_+ - U_-), \tag{1.40}$$

where A is the gain of the amplifier. The ideal gain is infinite; practical gains are in the region of 10^5–10^{17}.

One of the inputs or the output maybe grounded (connected to the earth ground).

Usually the output is connected back to one or other inputs (feedback circuit). With this configuration, the output voltage will be almost exactly the same as the

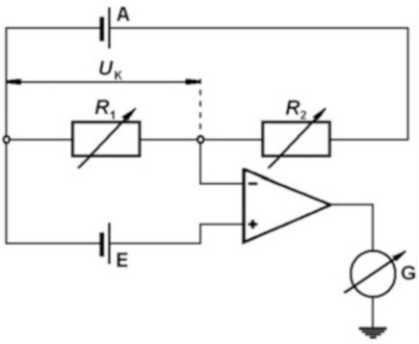

Fig. 1.6 Schematic diagram of the voltmeter (pH meter), which consists of high-input-impedance operational amplifier. The cell (pH probe) of the meter is connected to the non-inverting input. The output voltage, which is directly proportional to pH, is read with a voltmeter (in this and the following figures the two power supply connections to the operational amplifier are omitted for the sake of clarity)

input voltage. There are different types of operational amplifier circuits for different purposes, such as unity-gain non-inverting buffer, non-inverting voltage amplifier, differential voltage amplifier, current amplifier, etc. Active filters are used to compensate the effect of the impedance of passive frequency-determining elements.

1.4.2.2 Voltmeters, pH Meters

For measuring cell potentials highly sensitive electronic voltmeters (pH meters) with very high-input impedance allowing the precise measurements of small potential differences are used (Fig. 1.6). Earlier vacuum tubes (electrometer tubes) were applied, which have been replaced by field effect transistors. (The first commercial pH meter was built by Arnold Orville Beckman (1900–2004) in the United States in 1935, based on vacuum tube amplifiers).

1.4.2.3 Potentiostat

Potentiostats are based on electronic amplifiers, which control the potential drop between an electrode (the working electrode) and the electrolyte. The working electrode is normally connected to ground potential; the potential of the electrolyte is measured by a special probe, by the reference electrode. Effects of the counter and the electrolyte (especially the solution resistance) can be suppressed by this technique. The simplest potentiostat circuit is shown in Fig. 1.7.

The difference between the desired U_1 potential and the reference potential is amplified, resulting in currents via counter and working electrode until this

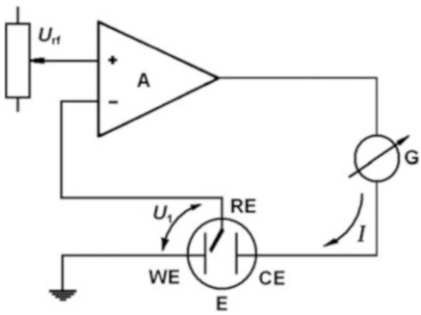

Fig. 1.7 Potentiostat circuit. A is the operational amplifier, U_1 is the regulated potential between WE working and RE reference electrode, CE is the counter electrode, U_{rf} is the internal reference voltage

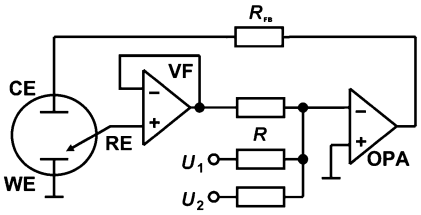

Fig. 1.8 An adder potentiostat circuit

difference becomes (almost) zero. The internal reference voltage can be varied by different impulse or sinusoidal signals.

A different design, an adder potentiostat, is shown in Fig. 1.8. The RE is buffered by a voltage follower (VF) and separate input signals U_1, U_2, . . . such as rectangular pulses, ramps, or sine waves can be mixed.

A potentiostat as a laboratory device is normally equipped with further features such as monitoring of the reference electrode, current detection by current-to-voltage converters or differential amplifiers, pulse form generators, displays of current and potential, as well as computer interfaces. The ohmic potential drop in the electrolyte or at the electrode | electrolyte interface may induce a difference between the bias potential and the desired electrode potential of the working electrode. The modern potentiostats are also equipped by an automatic ohmic drop compensation (see below). A frequency dependence should also be considered due to the different *RC* circuits in the cell and in the potentiostats. For instance, source resistance of the reference electrode is typically in the range from 1 kΩ to 10 MΩ and—together with the input capacity C of the inverting input of the amplifier (typically 20 pF)—results in a time constant $\tau = R \times C$ which limits the high-frequency response. The potentiostats also have a limited range of potential and power. Above these limits the potentiostats cannot control and regulate the potential.

There are techniques, e.g., rotating ring-disk electrodes and scanning electrochemical microscope, which require simultaneous potential control of two working electrodes. For these purposes bipotentiostats are used. Multipotentiostats, which can control the potential of more than two working electrodes, have also been developed.

1.5 Accuracy of the Potential Measurement Related to the Cell Construction

The position of the reference electrode and the separation of the compartments of the reference and working electrodes are crucial to obtain reliable data for the electrode potential of the indicator electrode or to control the potential of the working electrode. In order to decrease the effect of the ohmic potential drop (ohmic overpotential, *IR* drop), which arises between the working and the reference electrode, it is a general rule that the working and the reference electrodes can be positioned as near as possible. For this purpose the Luggin capillary is also recommended. Ohmic overpotential always lowers the actual biased or measured potential. This potential drop is mainly due to the resistance of the electrolyte phase; however, when large currents flow, ohmic overpotentials can also be caused by the resistance of conductors (wires, contacts). In cases when electrodes made of materials of low electronic conductivity are used or formation of poorly conducting surface films occurs, ohmic potential drop arises, which may also change with time. The *IR* drop can be corrected by using the values of the current I and the resistance R of the electrolyte between the working and the reference electrodes. Electronic *IR* drop correction/compensation possibilities are integrated in most modern potentiostats. Positive feedback or interruption compensation techniques are applied. In the case of positive feedback technique the resistance is set in advance or measured and the correction is made by adding the potential loss to the bias potential. However, in this way the ohmic potential drop cannot be fully compensated because it may lead to instability (potential oscillation). The interruption technique is based on the determination of the value of the ohmic drop by interrupting the current flow for some μs, measuring the change of the potential, and the automatical correction of the bias potential with this value. (The ohmic drop immediately decreases to zero when no current flows, while the change of the electrode potential, i.e., discharge of the double layer is a much slower event.) However, this method limits the timescale of the experiment; it cannot be applied at fast voltammetry or chronoamperometry.

In order to prevent the mixing of the electrolytes of the reference electrode and the working electrode a diaphragm and often a double salt bridge are used. The diaphragm is most often some kind of porous material (sintered glass, ceramics, organic polymer membrane, or gel) or a wetted stopper without grease (the thin electrolyte film is enough to maintain an appropriate electrolytic conductivity). One must be careful in respect of the choice of the material since glass diaphragms will easily be dissolved in strongly alkaline solutions, while organic solvent may attack organic membranes. The diaphragm has to be cleaned from time to time. (See in detail in Chap. 4.)

Electrodes of the second kind such as Ag | AgCl and the calomel electrode (Hg | Hg_2Cl_2) are the most frequently used reference electrodes. In solutions containing sulfuric acid Hg | Hg_2SO_4 are applied, while in alkaline media Hg | HgO are also applied. The potential of these electrodes depends on the concentration (activity) of the electrolyte used. In the commercial calomel electrodes usually KCl

solutions are applied. However, if the supporting electrolyte in the cell is $HClO_4$ or any perchlorate salt it is advisable to use NaCl since $KClO_4$ is a sparingly soluble salt and may fill up the diaphragm (frit) and insulate the reference electrode. It should be noted that by changing KCl for NaCl the potential of the saturated calomel electrode (SCE) will be varied which is due to the different solubilities. In the case of electrodes of the second kind the effect of temperature on the solubility has to be considered, too.

References

1. Cohen ER, Cvitas T, Fry J et al (eds) (2007) IUPAC quantities, units and symbols in physical chemistry, 3rd edn. RSC, Cambridge, 73
2. Inzelt G (2012) Electrode. In: Bard AJ, Inzelt G, Scholz F (eds) Electrochemical dictionary, 2nd edn. Springer, Heidelberg, pp 273–277
3. Parsons R (1974) Pure Appl Chem 37:503
4. Buck P, Rondinini S, Covington AK et al (2002) Pure Appl Chem 74:2169–2200
5. Inzelt G (2006) Standard potentials. In: Bard AJ, Stratmann M, Scholz F, Pickett CJ (eds) Inorganic electrochemistry. Encyclopedia of electrochemistry, vol 7a. Wiley, Weinheim, pp 1–15
6. Bard AJ, Faulkner LR (2001) Electrochemical methods, 2nd edn. Wiley, New York, pp 44–54, Chap 2
7. Scholz F (2010) Thermodynamics of electrochemical reactions. In: Scholz F (ed) Electroanalytical methods, 2nd edn. Springer, Berlin, pp 11–31
8. Petrii OA, Tsirlina GA (2002) Electrode potentials. In: Bard AJ, Stratmann M, Gileadi E, Urbakh M (eds) Encyclopedia of electrochemistry, vol 1. Wiley-VCH, Weinheim, pp 1–23
9. Bard AJ, Parsons R, Jordan J (1985) Standard potentials in aqueous solutions. Marcel Dekker, New York
10. Latimer WM (1952) Oxidation potentials. Prentice-Hall, Englewood Cliffs
11. Pourbaix M (1963) Atlas d'equilibres electrochemiques. Gauthier-Villars, Paris
12. Pourbaix M, Zoubov N, van Muylder J (1963) Atlas d' Equilibres Electrochimiques a 25 °C. Gauthier-Villars, Paris
13. Pourbaix M (ed) (1966) Atlas of Electrochemical Equilibria in Aqueous Solutions. Pergamon-CEBELCOR, Brussels
14. Charlot G, Collumeau A, Marchot MJC (1971) Selected constants. Oxidation-reduction potentials of inorganic substances in aqueous solution. IUPAC, Butterworths, London
15. Milazzo G, Caroli S (1977) Tables of standard electrode potentials. Wiley-Interscience, New York
16. Antelman MS, Harris FJ (eds) (1982) The encyclopedia of chemical electrode potentials. Plenum, New York
17. Parsons R (1985) Redox potentials in aqueous solutions: a selective and critical source book. Marcel Dekker, New York
18. Bratsch SG (1989) J Phys Chem Ref Data 18:1
19. Inzelt G (2006) Standard potentials. In: Bard AJ, Stratmann M, Scholz F, Pickett CJ (eds) Inorganic electrochemistry. Encyclopedia of electrochemistry, vol 7a. Wiley, Weinheim, pp 17–75
20. Case MW Jr (1998) NIST-JANAF thermodynamical tables. Am. Chem. Soc., Am. Inst. Phys., NIST, Maryland
21. Lund H (1983) Practical problems in electrolysis. In: Baizer MM, Lund H (eds) Organic electrochemistry. Marcel Dekker, New York, p 187219

22. Gritzner G, Kuta J (1984) Pure Appl Chem 56:461
23. Gritzner G (1990) Pure Appl Chem 62:1839
24. Inzelt G (2010) Kinetics of electrochemical reactions. In: Scholz F (ed) Electroanalytical methods, 2nd edn. Springer, Berlin, pp 33–53
25. Selley NJ (1977) Experimental approach to electrochemistry. Edward Arnold, London, pp 64–66
26. Lohrengel MM (2008) Potentiostat, potentiostatic circuit. In: Bard AJ, Inzelt G, Scholz F (eds) Electrochemical dictionary. Springer, Heidelberg, pp 544–545
27. Clayton G, Winder S (2003) Operational amplifiers. Newnes, Oxford
28. Huijsing JH (2001) Operational amplifiers: theory and design. Kluwer Academic, Boston
29. Kissinger PT (1996) In: Kissinger PT, Heineman WR (eds) Laboratory techniques in electroanalytical chemistry, 2nd edn. Marcel Dekker, New York, Chapter 6

Chapter 2
Reference Redox Systems in Nonaqueous Systems and the Relation of Electrode Potentials in Nonaqueous and Mixed Solvents to Standard Potentials in Water

Gerhard Gritzner

2.1 Introduction

NOTE: Throughout this chapter recommendations by the International Union of Pure and Applied Chemistry (IUPAC) [1, 2] for representing electrochemical cells will be followed stating that a single vertical bar (|) should be used to represent a phase boundary, a dashed vertical bar (¦) to represent a junction between miscible liquids, and a double dashed bar (‖) to represent a liquid junction, in which the liquid junction (potential) is assumed to be eliminated. The subscripts account for the following: (s), solid; (l), liquid; (aq), aqueous; and (Hg), amalgam. A slash (/) is used for cases where both forms of the redox couple are assumed to be in solution.

As electrochemistry moved into mixed and nonaqueous electrolytes it became of interest to compare potentials in different media. Serious problems preventing comparison are the liquid junction potentials between different electrolytes. Such liquid junction potentials also occur in the measurement in aqueous systems, but they are generally suppressed by a salt bridge. Salt bridges for aqueous systems usually consist of (saturated) solutions of KCl or NH_4NO_3. For both KCl and NH_4NO_3 similar mobilities for the cation and the anion of the respective salt were measured in aqueous solutions. Thus the liquid junction potential between two aqueous electrolytes connected via such a bridge should be smaller than the experimental error (see Chap. 1). Data in aqueous systems without liquid junction potentials are obtained from measurements in cells without transference such as:

$$\mathrm{Pt|H_2(g, } p = p^\circ)\mathrm{|HCl(aq, } a_\pm = 1)\mathrm{¦HCl(aq, } a_\pm = 1)\mathrm{|AgCl|Ag.}$$

A liquid junction potential will, however, occur even in water whenever the activity of HCl [$a_\pm$(HCl)] on the right differs from the activity of HCl on the left.

G. Gritzner (✉)
Institut für Chemische Technologie Anorganischer Stoffe, Johannes Kepler Universität, Altenbergerstraße 69, 4040 Linz, Austria
e-mail: Gerhard.Gritzner@jku.at

G. Inzelt et al. (eds.), *Handbook of Reference Electrodes*,
DOI 10.1007/978-3-642-36188-3_2,

An electrochemical cell consisting of an aqueous and a nonaqueous half-cell or two different nonaqueous solvents in the half-cells always includes a liquid junction potential. Quite frequently the liquid junction potential is ignored and aqueous reference electrodes such as the silver–silver chloride electrodes in various concentrations of KCl or calomel electrodes are used. Care was at best taken that water cannot diffuse into the nonaqueous system. It is important to note that the liquid junction potential is a transport—not a thermodynamic—property (see Chap. 3). This is generally ignored or not fully understood. Thus the literature is full of papers for conversion factors to aqueous reference electrodes [3]. Experimental evaluations of liquid junction potentials were carried out, but always refer to a given setup of the junction [4]. Its value depends on the design of the diaphragm and on time. Thus a given reference cell with a special diaphragm may yield reproducible data when used in electrochemical measurements. However, the reported potential includes the unknown liquid junction potential. Thus using the very same reference electrode may—due to a different separator—yield different potential values. Electrochemical measurements in the same electrolyte, on the other hand, always present thermodynamic values and thus reproducible values (within the experimental skills of the researcher).

Two different approaches are used to establish electrochemical series in nonaqueous and mixed aqueous–nonaqueous systems: (1) a reference redox system [5] or (2) a reference electrode in combination with a bridge to suppress the liquid junction potential [6].

2.2 Reference Redox Systems

Pleskov proposed the redox systems $Rb^+|Rb$ and $Rb^+|Rb(Hg)$, respectively, as reference redox systems (pilot ion) to correlate data in aqueous and nonaqueous systems [7]. He proposed this system, because of the large ionic radius of Rb^+, assuming that interactions of solvent molecules with the Rb^+ cation would be small. His assumption was strongly influenced by the Born model [8]. The Born model is based on purely electrostatic considerations and considers the change in Gibbs energy of an ion by the transfer from vacuum into water. The dominating properties in such transfer are the ionic charge and the ionic radius. The larger the radius and the smaller the charge, the weaker is the ion solvent–ion interaction according to the Born model. Such consideration made Pleskov to propose the redox systems $Rb^+|Rb$ and $Rb^+|Rb(Hg)$ as reference (pilot ion).

Studies on Gibbs energies of transfer of Rb^+ [9–11] showed that the interaction of Rb^+ with different solvents is not negligible. The $Rb^+|Rb$ couple turned out to be too much solvent dependent to be used as a reference redox system to relate electrochemical properties in different solvents.

Strehlow and coworkers studied various organometallic complexes. They formulated requirements for suitable reference redox systems [12] (1) The ions or molecules forming the reference redox system should preferably be spherical with as

large a radius as possible, (2) the ions should carry a low charge, (3) the equilibrium at the electrode should be rapid and reversible, (4) both components of the redox couple should be soluble, (5) no change in the geometry of the ligands should occur upon the redox process, (6) the redox potential should be in a potential range that is accessible in as many solvents as possible, and (7) both forms should be stable enough to permit potentiometric measurements. Strehlow suggested the systems ferrocene/ferrocenium ion (ferrocene: *bis*(η-cyclopentadienyl)iron(II)) and cobaltocene/cobaltocenium ion (cobaltocene: *bis*(η-cyclopentadienyl)cobalt(II)). While some of the arguments used in this publication are strongly influenced by the Born concept of ion–solvent interactions, this paper became very influential in establishing reference redox systems. Unfortunately the ferrocenium/ferrocene couple is affected by interactions of water with the ferrocenium ion. Thus the ferrocenium/ferrocene couple should not be used in water, making this couple unsuited for establishing a general electrochemical series versus the standard hydrogen electrode [13]. The ferrocenium ion/ferrocene couple consists of cation and a neutral molecule. It is the typical example of a cation/neutral analogue redox couple. Studies in ionic liquids indicate problems with the ferrocenium ion/ferrocene couple [14]. Cobaltocenium ion/cobaltocene, which was also used in nonaqueous solvents but never properly connected to the ferroceniumion ion/ferrocene scale [15, 16], is currently favored in electrolytes based on ionic liquids, but recent publications indicate that ferrocenium ion/ferrocene and *bis*(biphenyl)chromium(I)/*bis*(biphenyl)chromium(0) may also be used in room temperature ionic liquids [17, 18]. Decamethylferrocene was later suggested to be superior to ferrocene due to its larger ionic radius [19, 20] as claimed by the authors.

Other reference redox systems have been proposed and used, such as *tris*(2,2′-bipyridine)iron(I)/*tris*(2,2′-bipyridine)iron(0) [21], 4,7-dimethyl-1,10 phenanthroline iron(II) [4], and redox systems based on polynuclear aromatic hydrocarbons and the respective radical ions [22–24].

Most data in nonaqueous and mixed solvents have been published versus the *bis*(biphenyl)chromium(I)|*bis*(biphenyl)chromium(0) redox couple [25].

The use of reference redox systems became very popular in connection with polarographic and cyclovoltammetric studies. Generally the respective reference redox system was added to the electrolyte with the studied redox system, thus avoiding any liquid junction potential (internal standard). An additional advantage of using a reference redox system is that only one form of the redox couple may be used. The second partner of the redox couple is generated during the polarographic or cyclovoltammetric study. In the case of the redox couple the oxidized form *bis*(biphenyl) chromium(I) tetraphenylborate [25] (earlier *bis*(biphenyl)chromium(I) iodide [26] is added; in case of the ferrocenium ion/ferrocene couple the reduced form, namely, ferrocene, is added.

2.3 Reference Electrodes in Combination with a Bridge

Pleskov, during his investigations in acetonitrile, introduced the system Ag| 0.1 mol dm^{-3} $AgNO_3$ as a reference electrode in this solvent [27]. This electrode, later coined Pleskov electrode [28], is an electrode of the first kind. Reversibility of the $Ag^+|Ag$ system in many nonaqueous electrolytes led to reference electrodes based on $Ag^+|Ag$ in many solvents. Reversibility of this electrode was proven in some solvents by varying the Ag^+ concentration and observing Nernstian behavior of the electrode in a Ag^+ salt solution, maintaining constant ionic strength by adding a supporting electrolyte. Measurements of such a reference electrode with the same supporting electrolyte in both half-cells should yield potentials free of liquid junction potentials. Thus one could establish an electrochemical series in the solvent chosen. But such series are solvent specific and do not allow comparison of potential data in different solvents. Thus an assumption is necessary to allow establishing a universal scale of redox potentials.

Such an assumption was proposed, namely that a bridge consisting of a 0.1 mol dm^{-3} tetraethylammonium picrate in acetonitrile suppresses the liquid junction potential between two different nonaqueous electrolytes [6]. The argument in favor of such a salt bridge for nonaqueous electrolytes is the similar electrical mobility of the tetraethylammonium cation and the picrate anion in acetonitrile. This assumption was later expanded to allow for other nonaqueous solvents [28]. Agreement for the electrochemical data was found if the nonaqueous solvents did not have acidic hydrogen atom(s) in the solvent molecule (aprotic solvents) [29]. 0.1 mol dm^{-3} solutions of either tetrabutylammonium picrate or pyridinium trifluorosulfonate [30] were also used.

Occasionally also the use of so-called pseudo “reference electrodes” has been reported (see Chap. 14). Such “pseudo reference electrodes” became popular in polarography but especially in cyclic voltammetry, employing three electrode arrangements. They consist of a silver or platinum wire or activated carbon dipping into the electrolyte. They substitute for a reference electrode. Such electrodes were reported to exhibit very stable potentials. The ease of such an arrangement was also used in electrochemical studies in (room temperature) ionic liquids. It must be pointed out that electrode potentials versus such electrodes are meaningless as such arrangements do not constitute thermodynamic values.

2.4 Concentration and Activities

Electrochemical measurements especially in polarography and cyclic voltammetry are frequently carried out in the presence of a supporting electrolyte. Concentrations of the supporting electrolyte in aqueous and nonaqueous solutions are usually 0.1 mol dm^{-3}, but may reach 1 mol dm^{-3} or more. Analysis of activity coefficients for the salt under study is not possible. Conductance studies in nonaqueous solvents

were carried out and equations to analyze 1:1 and later 2:2 and other symmetrical and unsymmetrical electrolytes were developed. From such measurements association constants were derived.

2.5 Summary and Recommendation

Electrode potentials should only be reported in thermodynamic arrangements. The most convenient way in polarography and cyclic voltammetry is the use of a reference redox system in the same electrolyte as the system under study. The $Ag^{+}|Ag$ electrode seems applicable to many solvents and may be used as reference electrode in potentiometric investigations.

There are two aspects to reference redox systems. One point is the possibility of compiling electrode potentials in a variety of solvents and solvent mixtures, which are not affected by unknown liquid junction potentials. Unfortunately very frequently aqueous reference electrodes are employed in electrochemical studies in nonaqueous electrolytes. Such data, however, include an unknown, irreproducible phase boundary potential. Electrode potentials of a redox couple measured in the same electrolyte together with the reference redox system constitute reproducible, thermodynamic data. In order to stop the proliferation of—in the view of the respective authors—better and better reference redox systems, the IUPAC recommended that either ferrocenium ion/ferrocene or *bis*(biphenyl)chromium(I)/*bis*(biphenyl)chromium(0) be used as a reference redox system [5].

The second point is the assumption that the potential of a half-cell containing the reference redox system is—within experimental error—independent of the nature of the solvent. This assumption is outside the realm of exact thermodynamics and thus open to discussion. As for any extra-thermodynamic assumption it is impossible to prove its validity. This point should be kept in mind especially when discussing single-ion transfer properties.

2.6 The Relation of Redox Potentials in Nonaqueous or Mixed Electrolytes to the Aqueous Standard Hydrogen Electrode

The conversion to the aqueous standard hydrogen electrode as reference half-cell requires an extra-thermodynamic assumption, either the assumption of a solvent independent reference redox system or other assumptions employed in calculating single-ion transfer properties. Details about the procedure and data for univalent cation|metal systems were published [13]. The redox couple ferrocenium ion/ferrocene as reference electrode system is not very suited for such a conversion as the ferrocenium cation undergoes interactions with water and thus impairs the extra-thermodynamic assumption for aqueous solutions. This becomes apparent when

Table 2.1 Difference of the half-wave potentials and ½ (E_{pa} + E_{pc}) potentials, respectively, of the ferrocenium ion/ferrocene and *bis*(biphenyl)chromium(I)/*bis*(biphenyl)chromium couples in several solvents

Solvent	Abbr.	$\Delta E_{(Fc-BCr)}$[a]	Solvent	Abbr.	$\Delta E_{(Fc-BCr)}$[a]
1,2-Dichlorethane	DCE	1.131	*N*-Methylformamide	NMF	1.135
Nitromethane	NM	1.112	*N*,*N*-Dimethylformamide	DMF	1.127
Nitrobenzene	NB	1.130	*N*,*N*-Dimethylacetamide	DMA	1.131
Acetonitrile	AN	1.118	*N*,*N*-Diethylacetamide	DEA	1.135
Propylene carbonate	PC	1.114	*N*-Methylpyrrolidone(2)	NMP	1.126
Butyrolactone	BL	1.112	Tetramethylurea	TMU	1.130
Acetone	AC	1.130	Dimethylsulfoxide	DMSO	1.123
Methanol	MeOH	1.134	Tetramethylene sulfone	TMS	1.114
Ethanol	EtOH	1.134	2,2′-Thiodiethanol	TDE	1.121
Formamide	FA	1.129	Trimethyl phosphate	TMP	1.130
Water	W	0.98	Hexamethylphosphoric triamide	HMP	1.124

[a]Difference in the electrode potentials of ferrocenium/ferrocene and *bis*(biphenyl)chromium(I)/*bis*(biphenyl)chromium(0)

comparing the difference in electrode potentials for the ferrocenium ion/ferrocene couple and the *bis*(biphenyl)chromium(I)/*bis*(biphenyl)chromium(0) redox couples (Table 2.1). Most of the organic reference redox couples (at least one form) are practically insoluble in water. This makes measurement of reliable electrode potentials very difficult. In some solvents the electrode potential of the ferrocenium ion/ferrocene couple is more positive than the solvent oxidation (especially in sulfur donor solvents) and thus cannot be measured.

Table 2.1 clearly shows that the water value for the relation between ferrocene and bis(biphenyl)chromium ($\Delta E_{(Fc-BCr)}$) is too small and transfer properties using ferrocene as base from water will be incorrect.

References[1]

1. Quack M, Stohner J, Strauss HL, Takami M, Thor AJ, Cohen ER, Cvitas T, Frey JG, Holström B, Kuchitsu K, Marquard R, Mills I, Pavese F (eds) (2007) Quantities, units and symbols in physical chemistry, 3rd edn. RSC Publishing, Cambridge
2. Mills I, Cvitas T, Homann K, Kallay N, Kuchitsu K (1991) Quantities, units and symbols in physical chemistry, 2nd edn. Blackwell Science, Oxford. ISBN 0-632-03583-8
3. Pavlishuk VV, Addison AW (2000) Inorg Chim Acta 298:97
4. Nelson IV, Iwamoto RT (1961) Anal Chem 33:1795
5. Gritzner G, Kůta J (1983) Pure Appl Chem 56:461
6. Owensby DA, Parker AJ, Diggle JW (1974) J Am Chem Soc 96:2683

[1] The author apologizes for not including all pertinent references, but such references are cited in the respective publication and may be checked there.

7. Pleskov VA (1947) Usp Chim 16:2514
8. Born M (1920) Z Phys 1:45
9. Gritzner G, Auinger M (2009) Acta Chim Slov 56:86
10. Cox BG, Hedwig GR, Parker AJ, Watts DW (1974) Aust J Chem 27:477
11. Johnsson M, Persson I (1987) Inorg Chim Acta 127:15
12. Koepp HM, Wendt H, Strehlow H (1960) Z Elektrochem 64:483
13. Gritzner G (2010) J Mol Liq 156:103
14. Sukardi SK, Zhang J, Burgar I, Horne MD, Hollenkamp AF, MacFarlane DR, Bond AM (2008) Electrochem Commun 8:250
15. Behr B, Gutknecht J, Schneider H, Stroka J (1978) J Electroanal Chem 86:289
16. Topolev VV, Khanova LA, Krishtalik LI (2006) Chem Phys 326:33
17. Waligora L, Lewandowski A, Gritzner G (2009) Electrochim Acta 54:1419
18. De Vreese P, Haerens K, Matthijs E, Binnemans K (2012) Electrochim Acta 76:242
19. Bashkin JK, Kinlen PJ (1990) Inorg Chem 29:4507
20. Noviandri I, Brown KN, Fleming DS, Gulyas PT, Lay PA, Masters AF, Phillips L (1999) J Phys Chem B 103:6713
21. Tanaka N, Ogata T (1974) Inorg Nucl Chem Lett 10:511
22. Madec C, Courtez-Coupez J (1977) J Electroanal Chem 84:177
23. Bauer D, Beck J-P (1973) Bull Soc Chim (France) 1252
24. Kakutani T, Morihori Y, Senda M, Takahashi R, Matsumoto K (1978) Bull Chem Soc Jpn 51:2847
25. Gritzner G (1990) Pure Appl Chem 62:1839
26. Duschek O, Gutmann V (1973) Monatsh Chem 104:990
27. Pleskov VA (1948) J Phys Chem USSR 22:351
28. Diggle JW, Parker AJ (1973) Electrochim Acta 18:975
29. Gritzner G (2010) J Chem Eng Data 55:1014
30. Chaudry M, Dash KC, Kamienska-Piotrowicz E, Kinjo Y, Persson I (1994) J Chem Soc Faraday Trans 90:2235

Chapter 3
Liquid Junction Potentials

Galina Tsirlina

3.1 Introduction

The liquid junction potential (LJP), as considered in relation to practical aspects of reference electrodes, is a rather bothering experimental problem. The additional and always unknown potential drop between the electrolytes of the electrode under study and of the reference electrode is harmful for the accuracy of potential measurements. In addition, the existence of this drop disturbs the equilibrium in the circuit (if any) and complicates stabilization of nonequilibrium systems.

Simultaneously, the LJP is an exciting phenomenon for the theory of electrochemical systems. Its modeling combines various types of theory and provides the results widely accepted in practice. Another remarkable aspect is the existence of LJPs in a wide variety of systems with essentially different viscosity, permittivity, and molecular structure. This is always advantageous for theory verification.

The LJP has a meaning of Galvani potential, i.e., *its exact value cannot be measured by definition* [1]. This results in the need of various approximations from both experimental and modeling sides. Generally, both the solvent and the electrolyte can be different in two contacting liquid phases (1) and (2), and it is assumed [2] that the quantity of the LJP can be presented by two additive contributions induced by heterogeneous distribution of ions and polar molecules, respectively:

$$\Delta\phi_{\mathrm{LJ}} = \Delta\phi_{\mathrm{ion}} + \Delta\phi_{\mathrm{solv}}. \tag{3.1}$$

The ionic contribution is given by the equation:

G. Tsirlina (✉)
Department of Electrochemistry, Chemical Faculty, Moscow State University, Leninskie Gory, 1 - str.3, Moscow 119991, Russia
e-mail: tsir@elch.chem.msu.ru

G. Inzelt et al. (eds.), *Handbook of Reference Electrodes*,
DOI 10.1007/978-3-642-36188-3_3,

$$\Delta\phi_{\text{ion}} = -\frac{RT}{F}\int_{(1)}^{(2)}\sum\frac{t_i}{z_i}\,\mathrm{d}\ln a_i - \frac{RT}{F}\int_{(1)}^{(2)}\sum\frac{t_i}{z_i}\,\mathrm{d}\mu_i^{\ominus}, \tag{3.2}$$

where t_i is the transport number of the i-th ion, that is, the portion of current transferred by this ion through the solution, a_i is the individual activity of the i-th ion (*immeasurable quantity!*), and $\mu_i^{\ominus}$ is the standard chemical potential of the i-th ion. For scientists mostly working in a single solvent (e.g., with aqueous potentiometric techniques), the definition of the LJP is typically limited to the first right-hand term in Eq. (3.2), and they associate the LJP with the so-named diffusion potential: $\Delta\phi_{\text{LJ}} = \Delta\phi_{\text{diff}}$.

The term "diffusion potential" results from the fact that the space separation of charge is initially induced by diffusion. In contrast, for people dealing with solvent effects (e.g., in organic electrochemistry), the solvent contribution attracts more attention, including solvent effect on $\mu_i^{\ominus}$. The principle (mostly psychological) difference results from strongly different experimental and model approaches applied under these two circumstances. Strictly speaking, even in the absence of electrolyte, the diffusion layer exists at the boundary of two miscible liquids [2–4]. However, usually an inhomogeneous distribution of molecules (dipoles) results in a lower potential drop than the drop resulting from the redistribution of ions.

The classification of LJP effect considered below, mainly takes into account the nature of the potential drop at various types of liquid–liquid boundaries. One should realize that the problem of quantitative modeling and/or precise experimental separation of various contributions to the LJP of mixed nature still remain a challenge, when the limiting cases (predominating contribution of one type) already found more or less reasonable solutions.

This chapter is arranged as follows: Sect. 3.2 presents brief comments to the LJP between two different molecular solvents; Sect. 3.3 is devoted to the most advanced area, the LJP between two different electrolyte solutions in a certain solvent (known also as diffusion potential) and includes some comments concerning the temperature-induced LJP in these systems; Sect. 3.4 contains brief notes about LJPs in solvent-free systems, namely melts and room temperature ionic liquids (RTILs); the concluding Sect. 3.5 presents various specific cases of LJPs and outlines the links with electroanalysis, especially ion-selective electrodes, the functional properties of which are strongly affected by diffusion potentials. This specific case should be considered separately because the membrane/solution interfaces (as well as the boundaries of immiscible liquids) keep the exact geometry of boundaries.

This chapter could not be written in the traditional encyclopedic style because the understanding of LJPs is still under development. In the new millennium, the boom of RTIL's introduced new ideas and systems into chemistry and physics of liquids. In parallel, computational modeling of liquid systems became more powerful. New experimental and computational results require joint fermentation under the supervision of theory, and this process will take some time. The goal of this chapter is to collect and to structure currently available facts and hypothesis and to warn the reader of simplified and straightforward considerations of LJPs.

3.2 The LJP Between Two Different Molecular Solvents

The most traditional approach to an experimental estimation of the LJP between two polar solvents consists in the measurement of the emf between two identical redox electrodes in these liquids. Basically this measurable quantity contains the difference of redox potentials in the solvents coexisting in the cell and $\Delta\phi_{LJ}$ as described by Eqs. (3.1) and (3.2). The most usual goal of scientists is not to separate $\Delta\phi_{solv}$ (and/or contributions to $\Delta\phi_{ion}$), but to account for $\Delta\phi_{LJ}$ as a whole when constructing universal potential scales for various solvents. However, a parallel analysis of the contributions to $\Delta\phi_{LJ}$ is unavoidable in these studies; so fundamental information accumulates in the course of "more applied" research as a sort of by-product. One important note is necessary concerning the ionic contribution $\Delta\phi_{ion}$ in experiments considered below: even if one and the same electrolyte is dissolved in two solvents forming a LJP, and concentrations in both solvents are equal, $\Delta\phi_{ion}$ is in general nonzero [both right-hand terms in Eq. (3.2) are solvent dependent]. In general one even cannot consider this contribution as minor (it is only possible for chemically related solvents).

The requirements for a redox probe operating as a reference system in various solvents are listed in Sect. 1.2.5 (see also Chaps. 1, 2, and 6). The most popular is the *ferrocene/ferrocenium* (Fc^+/Fc) system proposed for the first time more than 50 years ago [5] and recommended by authoritative sources [6, 7]. The problem is typically considered for the case when temperature and pressure gradients are zero. The earlier (slightly naive) idea of this sort [8, 9] was to use Rb^+/Rb as an inorganic reference. The size of rubidium ions is certainly insufficient to provide low enough solvation energy, but this suggestion stimulated a number of detailed experimental studies of reference systems for nonaqueous electrochemistry (see e.g., [10, 11]) and by these means created a firm basis for the Fc^+/Fc research. Interesting historical remarks are given by Krishtalik [12–14].

The solvation energies of ferrocene and ferrocenium, being the crucial values, are often considered to be the sum of electrostatic, solvophobic (cavitational), and specific (dispersion/repulsion) components. In the framework of the usual simplified models, the cavitational specific contributions of Fc^+ and Fc species are thought to cancel out due to minor changes in size of the molecule upon reduction/oxidation and effective screening of the metal center by the cyclopentadienyl rings (this assumption agrees with recent quantum chemistry results [15]). The second assumption about small electrostatic contribution to the solvation energy of Fc^+, which can be neglected when transferring the system from one solvent into the other, seems more risky from a first glance. A simple analysis of the solvation of Fc^+ in terms of the Born model predicts the solvation energy difference of Fc^+/Fc in, to say, water and benzonitrile of ~10 kJ/mol, corresponding to a possible difference of standard potentials of ca. 0.1 V. Unfortunately computational results are still helpless: the variation of DFT functional and basis sets induces an uncertainty comparable with 0.1 V for Fc^+/Fc couple [16]. When dealing with solvation energy differences rather than absolute values, the discrepancies are undoubtedly smaller, but the accuracy of these calculations still remains questionable [17, 18].

The comparison becomes more solid when the data for Fc^+/Fc and relative redox pairs in different solvents are considered in parallel [e.g., for *bis*(*biphenyl*)*chromium* (1/0) (BCr^+/BCr) or for *cobaltocenium*/*cobaltocene* (Cc^+/Cc)]. A relative redox probe containing the anion (carborane compound, bis-*o*-dicarbollyl-nickel) was studied for comparison [12]. A consideration of the potential differences in various solvents, rather than relative redox potential values, eliminates the LJP. The tabulated values for differences between the formal potentials of BCr^+/BCr and Fc^+/Fc couples in 22 solvents with significantly different static permittivity values are equal within the accuracy of few mV [7]. Similarly, the differences of the formal potentials of Fc^+/Fc and Cc^+/Cc in five aprotic solvents and three aqueous–organic mixtures remain practically constant within the limits of experimental error [12], when the difference in water is somewhat larger, ca 40 mV. The comparison with aqueous systems is slightly risky, as the reactants under study are not so stable in water.

The cobaltocenium system is of special interest, as in some solvents the second (reductive) process can be observed for Cc, and one can extract the experimental difference of two redox potentials dealing with only one model reactant. The redox potentials of the $Cc^+/Cc/Cc$ couples were reported for usual aprotic solvents [12] and some specific low-dielectric solvents (namely monoglyme, dichloromethane, and diglyme) [19], as well as for water mixtures with these solvents [19, 20]. Corresponding water−solvent LJP values were evaluated on the basis of these data, mostly finding themselves in the range of 0.2–0.3 V. In general LJPs do not correlate with the solvent dielectric constant, but they are possibly affected by the hydrophylic or hydrophobic nature of the solvent. This result indicates indirectly the pronounced contribution of $\Delta\phi_{solv}$.

To separate approximately this contribution to $\Delta\phi_{LJ}$ [Eq. (3.1)], the studies of (mixed solvent)/(pure solvent) junctions [3] are rather informative. Under more or less ideal conditions (no hydrogen bonds, etc.), the dipole–dipole interactions at the boundary are expected to result in a linear dependence of $\Delta\phi_{solv}$ on the molar composition of the mixed solvent. Correspondingly, the same trend is expected for measurable emf's of the model cells with the above-mentioned junction, and it was really observed for usual aprotic solvents with not too low polarity. The qualitative models of smooth and stepped dipoles distribution in the diffusion layer [3, 4] were suggested in relation to these experiments (see also discussion in review [2]). These models can be further improved if the molecular structure of the solvents is involved. The topic is surely "under construction," as well as more bulky mixed solvent research.

Despite the history of LJPs at solvent/solvent interface is rather old, the area is still opened for scientific novelty. This results from the endless diversity of mixed solvents and less predictable trends in applied electrochemistry. Namely, new challenges arise from the development of lithium batteries [21], and it is natural to assume that future trends in electrochemical energy conversion will be also "nonaqueous" because of the crucial role of wide potential windows. It is difficult to predict whether molecular or ionic liquids will dominate in these future applications, but the background for LJP phenomena in both media goes from the basic knowledge of LJP for molecular solvents.

For solvents (1) and (2) with a common binary electrolyte, the LJP can be presented by combination of chemical potentials of ions (or, in other words, by the energies of ions transfer):

$$\Delta\phi_{\mathrm{LJ}} = \left[\mu^{(1)}_{\mathrm{cation}} - \mu^{(2)}_{\mathrm{cation}} - \mu^{(1)}_{\mathrm{anion}} + \mu^{(2)}_{\mathrm{anion}}\right]/2. \tag{3.3}$$

This equation certainly contains the unknown values related to individual ions. However, it is sometimes useful for the estimation of the LJP from the data on the energy transfer of salts (of course with inclusion of some extrathermodynamic assumptions concerning the energies of single ions transfer).

The energy of ions transfer can be estimated from potentiometric data for the interfaces of two immiscible electrolyte solutions (ITIES) [22]. Early data for water/octane are tabulated in ref. [8]. However, "oil-type" solvents forming ITIES are not so common in usual nonaqueous electrochemistry. The specific details of the estimation of LJPs for completely and partly miscible organic liquids can be found in ref. [23].

3.3 The LJP at Solution/Solution Interface

Really inspiring fragments of the history of science are concerned with the quantitative theory of the LJP and its experimental verification just for the case when the nature of solvent is the same for both solutions (1) and (2) having equal temperatures and pressures. Another general assumption is the absence of convection (however, slow time-independent convection is not crucial for model estimates). The goal of this section is to present briefly the links between basic LJP knowledge and modern practice of LJP arrangement.

3.3.1 The LJP at Solution/Solution Interface (One and the Same Solvent)

A LJP resulting exclusively from concentration gradients of ions is most frequently called a diffusion potential drop $\Delta\phi_{\mathrm{diff}}$. If the solvent from both sides of junction is the same, $\mu_i^{\ominus}$ is constant along the boundary, and Eq. (3.2) is reduced to

$$\Delta\phi_{\mathrm{LJ}} = \Delta\phi_{\mathrm{diff}} = -\frac{RT}{F}\int_{(1)}^{(2)}\sum\frac{t_i}{z_i}\mathrm{d}\ln a_i. \tag{3.4}$$

In the first approximation, $\Delta\phi_{\text{diff}}$ can be estimated by substituting corresponding concentrations c_i for the partial activities a_i. The resulting value looses the meaning of Galvani potential, but despite the left-hand quantity still cannot be measured, the right-hand term can be calculated by adopting a model approach to the concentration distribution of ions in the boundary region. The basis for this calculation is the electroneutrality approximation discussed in ref. [24] in a popular form with impressive historic notes.

There are two types of $\Delta\phi_{\text{diff}}$-related model problems, dynamic and steady state, both being of high practical interest. Informative brief reviews of dynamic solutions for various types of electrolyte combinations in the junctions are available in refs. [5, 25] in addition to original simulation results. Principle explanations concerning model assumptions and limitations can be found in ref. [26]. The dynamic problem consists in the simulation of charge separation transients and/or spatial distribution of ions concentrations. At the starting point (zero time) the diffusion gradients between solutions (1) and (2) for all ions are determined by the bulk concentrations, which are the principle parameters being experimentally controllable. Typically the mobilities of ions are also available parameters depending on the electrolyte nature and concentration, solvent nature (mostly viscosity), pressure, and temperature. When the diffusion of ions starts, and the mobilities of the ions of at least two types are different (which is typical), a spatial charge separation appears immediately. This prompts a migration component, which facilitates the transport of the "slower" ions, and hinders the movement of the "faster" ions. After some period (up to a μs for usual molecular solvents at room temperature) the interplay of the opposite diffusion and migration flows results in a steady state. Under these stationary conditions, the total fluxes of anions and cations of one and the same electrolyte are equal and no further charge separation takes place. Correspondingly, electrolytes continue to move as a single whole with time-independent rate.

It should be stressed that this stationary situation is still a nonequilibrium one. The quantitative result depends on parameters mentioned above and on the geometry of the boundary region. The latter, in its turn, depends on the degree of spreading of the initial sharp boundary during the period until the steady state is established. Typically, the steady-state $\Delta\phi_{\text{diff}}$ values are calculated in the framework of the models of Planck [26, 27] and Henderson [26, 28, 29], as the most conventional.

In Planck's model for a sharp boundary, for 1,1-electrolyte,

$$\Delta\phi_{\text{diff}} = \frac{RT}{F} \ln \xi, \tag{3.5}$$

where function ξ can be found from a transcendent equation in which "+" and "−" denote the sets, which consist of all cations and of all anions, respectively, and λ denotes the limiting conductivity of the corresponding ion:

$$\frac{\xi\sum\limits_{+}\lambda_{+}^{(2)}c_{+}^{(2)}-\sum\limits_{+}\lambda_{+}^{(1)}c_{+}^{(1)}}{\sum\limits_{-}\lambda_{-}^{(2)}c_{-}^{(2)}-\xi\sum\limits_{-}\lambda_{-}^{(1)}c_{-}^{(1)}}=\frac{\ln\left(\dfrac{\sum\limits_{i}c_{i}^{(2)}}{\sum\limits_{i}c_{i}^{(1)}}\right)-\ln\xi}{\ln\left(\dfrac{\sum\limits_{i}c_{i}^{(2)}}{\sum\limits_{i}c_{i}^{(1)}}\right)+\ln\xi}\cdot\frac{\xi\sum\limits_{i}c_{i}^{(2)}-\sum\limits_{i}c_{i}^{(1)}}{\sum\limits_{i}c_{i}^{(2)}-\xi\sum\limits_{i}c_{i}^{(1)}}. \tag{3.6}$$

Henderson equation, which has gained wider acceptance, corresponds to the so-called free diffusion boundary, i.e., to a degraded diffusion layer with approximately linear concentration distribution along the normal to the boundary. The traditional form of Henderson equation (for concentrations c having the units of normality) is as follows:

$$\Delta\phi_{\text{diff}}=\frac{RT}{F}\cdot\frac{\sum\limits_{i}\left(\frac{\lambda_i}{z_i}\right)\cdot\left(c_i^{(2)}-c_i^{(1)}\right)}{\sum\limits_{i}\lambda_i\cdot\left(c_i^{(2)}-c_i^{(1)}\right)}\ln\frac{\sum\limits_{i}\lambda_i c_i^{(1)}}{\sum\limits_{i}\lambda_i c_i^{(2)}}. \tag{3.7}$$

The equation was derived for the case of a smeared-out boundary and linear spatial distributions of concentrations.

Two particular types of simplified systems attracted special attention. The first is the liquid junction between solutions of one and the same electrolyte with different concentrations (sometimes called liquid junctions of Lingane's type 1 [30]). For such a junction formed by 1,1-electrolyte solutions, both Eqs. (3.6) and (3.7) are reduced to the formula

$$\Delta\phi_{\text{diff}}=\frac{RT}{F}\cdot\frac{\lambda_{-}-\lambda_{+}}{\lambda_{-}+\lambda_{+}}\ln\frac{c^{(1)}}{c^{(2)}}, \tag{3.8}$$

where c without subscript stands for concentrations of solutions. The actively studied junctions of another type (liquid junctions of Lingane's type 2 [30]) are formed by different electrolytes of equal concentrations. In this case

$$\Delta\phi_{\text{diff}}=\frac{RT}{F}\cdot\ln\frac{\Lambda^{(1)}}{\Lambda^{(2)}}. \tag{3.9}$$

Equation (3.9) is also known as the Lewis–Sargent formula [31]. This formula operates with equivalent conductivities of solutions Λ, not of the ions. The paper [31] published 1 year after Henderson's papers played a historical role. The cells of the same geometry as were used in [31] are still utilized for emf measurements. These cells with free diffusion boundary are sometimes called Lewis–Sargent cells. Another important note in ref. [31] concerns the search of conductivity values.

In contrast to Planck's initial idea, it was suggested to use concentration-dependent conductivities instead of the limiting values.[1]

To judge what boundary is "sharp" (Planck's model) or smoothed (Henderson's model), one should consider the thickness of the real diffusion layer under steady-state conditions. Typically it is of the order of μm, i.e., much larger than the ionic size, if the shape of the boundary is not regulated by some mechanical means. The specific size effect appears if the boundary is formed in microchannel configuration and when the diffusion length is comparable with the total distance between the channel walls. The problem is considered quantitatively in refs. [32, 33], in relation to devices for microanalysis.

Generally, Eqs. (3.5)–(3.7) yield very similar results; however, for junctions with a pronounced difference in ion mobilities (like HCl⋮LiCl), the difference of the two model predictions can reach up to 10 mV. A specific feature of the Planck equation is the existence of two mathematical solutions, the first being close to that of Henderson, and the second one being independent of the solution concentration and of no physical meaning [34].

It is useful to mention a number of early experimental studies aimed at estimation of LJPs and verification of Eqs. (3.5)–(3.7). These studies are still of interest as a source of precise tabulated data with the accuracy achieving at least 0.1 mV, and they contain a lot of experimental details sometimes missed in modern measurements despite the seemingly higher technical level of electronic voltmeters. The earliest stage of this research, when the data on ionic mobilities were rather limited, can be imagined from the papers of Gumming [35, 36]. From the later (most active) period of 1910–1930s, the conclusive or most detailed papers of each series are mentioned here. Very important series in relation to both LJPs and single ion activities (these problems cannot be separated) were published by MacInnes (see, e.g., [37–39]) and Harned (see, e.g., [40, 41]; note that the most popular cell for pH measurements is still the Harned cell [42]). These data were collected for a wide range of concentrations, conductivities, and transfer numbers, and by these means formed the basis to verify theoretical relationships. Experiments with sucrose solutions instead of water [43] should be also mentioned, as important for involvement of even more wider range of conductivities. Critical reviews of earlier works, in combination with original data, were published by Guggenheim [44, 45].

The determination of activity coefficients of individual ions is still a widely discussed application of LJP models. From thermodynamic point of view it is impossible, so the problems of diffusion potential calculation and single ion activities determination form a sort of vicious circle. To calculate the former

[1] The problem looks slightly philosophic, as any calculated $\Delta\phi_{\text{diff}}$ values cannot pretend on exact agreement with experiment because of model approximations. In [31] the values computed on the basis of concentration-dependent conductivity for 0.1–0.2 M solutions demonstrated better agreement with experimental emf data as compared to the values based on the limiting conductivity, but both experimental and theoretical values have no exact meaning of LJP. In practice, when calculations are required for junctions with high solution concentration, there are simply no quantitative data on conductivity.

value, one should know the latter values. These values, in their term, can be only determined if the diffusion potential is completely eliminated (which is impossible in general), or its values for the both sides of salt bridge are known. This finally means that the former values can be calculated by some other ways, which means some model approximations, etc. State of the art can be understood from the brief reviews "Single-Ion Activity: Experiment versus Theory" [46], "The Impossibility of Measuring Individual Ion Activity Coefficients Using Ion-Selective Electrodes," [47] and "The nature of single-ion activity coefficients calculated from potentiometric measurements on cells with liquid junctions" [48], and the follow-up discussion [49]. About recurrent attempts of a mathematical factorizing concentration functions to access individual activity coefficients of ions see refs. [50–52].

Another area in near relation to diffusion potential and individual ions activity is the physical chemistry of ion selective electrodes.

3.3.2 Elimination of Diffusion Potential (Principal Aspects)

In practice, in place of model LJP calculations and corresponding emf corrections, the elimination of the diffusion potential is conventionally applied. This is achieved by introducing the so-called "salt bridges" filled with concentrated solutions of salts, which satisfy the condition $t_+/z_+ = t_-/z_-$ (see Chap. 4). For a symmetric electrolyte, this simply means that anions and cations have very close diffusion coefficients, and transport numbers of both ions are ~0.5. When the salt bridge is located between the solutions of the working and reference electrodes, two LJPs appear instead of the initial single LJP (which is attempted to be eliminated). Both new LJPs are nonzero and can be rather high. However, under the above-mentioned condition these two potential drops are of close absolute value and of the opposite sign, compensating each other to some extent. One can easily obtain this result, e.g., from Eq. (3.7).

A widely known example is a saturated KCl solution (which concentration achieves 4.8 mol/kg at 25 °C, $t_+ = 0.48$, $t_- = 0.52$). In aqueous solutions, potassium and ammonium nitrates are also suitable, as well as some rubidium and cesium salts. Expensive but impressive versions are CsCl (11.3 mol/kg at 25 °C, $t_+ = 0.5025$, $t_- = 0.4975$) and RbCl (7 mol/kg at 25 °C, $t_+ = 0.5009$, $t_- = 0.4991$) [53]. The requirement of equal transport numbers is less important as compared with that of high concentration of electrolyte solution, which fills the bridge [54–56]. There is also an interesting example of an unsymmetrical electrolyte, lithium sulfate, which satisfies the requirement mentioned above because the lithium cation has a transfer number ca. twice lower than the sulfate anion [57]. Lithium sulfate bridges are of interest for organic and water–organic media with low KCl solubility. A suitable version of the salt bridge can be chosen for any type of cells, when taking into account the purposes of research or application [56].

Recently, salt bridges containing water-stable and moderately hydrophobic RTIL's with substituted phosphonium cation and fluorinated sulfonyl amide

anion [58–60] were demonstrated to be advantageous, as well as mixtures with more hydrophobic RTIL [61]. The cell stability provides a satisfactory accuracy for the determination of pH and individual activity coefficients of small ions. The prospects of RTIL salt bridges are considered below in Sect. 4.2. Here, we should mention that this useful invention can stimulate the development of theory for solution|RTIL boundaries and interfaces. To extend the traditional approaches mentioned in Sect. 3.3.1, one should consider the transport of large RTIL ions first in RTIL and later in water, which is not so trivial and requires additional parameters. This theoretical problem is important for practice as well, at least in relation to the stabilization time of the bridge. Currently available data [58, 61] demonstrate that stabilization of potential drops at water|RTIL boundary requires up to 10^3 s, which exceeds the values for solution|solution interfaces by many orders of magnitude and can be hardly explained by the difference in viscosities. The initial idea of the authors [62] was to escape this problem by using quasi-Nernstian boundaries.

Special difficulties arise when suspensions of solid particles (e.g., soil) are studied instead of solutions. For suspensions, the diffusion potential appears to be anomalously high as compared to the parent solutions because the diffuse layers of suspended particles contribute to the apparent quantity. The technique of LJP elimination for suspensions assumes the comparative measurements in the cells of various configurations [63].

3.3.3 LJP Optimization by Means of Cell and Salt Bridge Construction

The early studies of aqueous LJPs were concentrated on experimental verification of Planck and Henderson models. As the difference of these models was related in particular to the geometry of the diffusion layer, some efforts were made to study various cell/salt bridge geometries. To ensure steady state LJPs, the “free diffusion” configuration was compared with a cell possessing a “continuous mixture layer” [44]. Early experiments with flowing junction [45, 64] resulted in a very stable cell operation (see also about stopping of the flow effect in ref. [65]). The general approach was always a comparison of data of cells with and without transference, the control experiments in symmetric cells, and in the cells with various types of salt bridges. Despite classical early studies were never reduced to determination of LJP by simple subtraction of the data for various cells, the simplified procedure of this sort is frequently applied for the rough estimate of LJP contributions.

These estimates are really useful for stability tests when new constructions of salt bridges are considered. A respective review is available now [66] (see also Chap. 4). A special comment is required concerning the mutual location of a Luggin capillary salt bridge and the main compartment of the electrochemical cell when a penetration of KCl (or another LJP eliminating electrolyte) is undesirable. In this

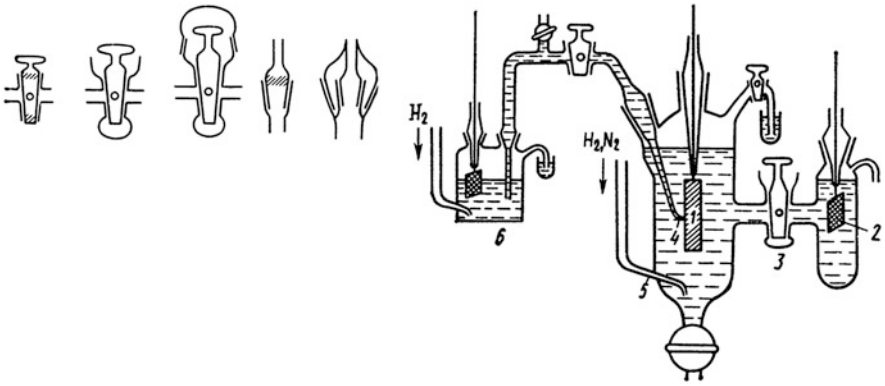

Fig. 3.1 Various types of glass junctions for electrochemical cells (*left*) and an example of the cell with separated compartments (*right 1*: working electrode, *2*: counter electrode, *3*: stopcock junction, *4*: Luggin capillary, *5*: gas inlet, *6*: hydrogen reference electrode) [71]

case it is always advantageous to locate the bridge below the main compartment of the cell, not above, because gravitationally induced convection provides an essential contribution to electrolyte transfer.

Various permeable membranes were applied to decrease the rate of electrolyte diffusion under steady state [67], in particular a collodion membrane first proposed in ref. [68] became rather popular. In contrast to ion-selective membranes, no Donnan potential is established when collodion membrane is used. These membranes are introduced to stabilize the system for long-term operation, not to affect LJP as is. Many inert viscous substances and porous inert ceramics can serve for the same purpose, and this approach is widely used in modern technologies of miniaturized reference electrodes for applications. Various types of diaphragms (including polymer and ceramics) are used in industrial pH measurements as well [69].

For basic interfacial electrochemistry, it is always better to use cells with reliably separated compartments. For glass cells, the best is to use thoroughly finished glass stopcocks. In this case the thickness of liquid layer is of the order of μm, and electrolyte diffusion from the salt bridge is rather slow. For long experiments and/or solutions with highly mobile hydronium ions, the bridges with two consecutive stopcocks can be recommended, like applied for the measurements in deuterated aqueous solutions with the use of protium-based hydrogen [70]. A classical design of these cells for precise electrochemical measurements is presented in ref. [71] (despite this book is published in Russian, the pictures themselves can be informative for any audience, see, e.g., in Figure 3.1).

The most illustrative examples of LJP minimization and optimization can be found in the traditional area of pH measurements [42, 72]. It forms an important part of Bates–Guggenheim convention [21]. However, one should note that this convention also assumes an extrathermodynamic assumption, in which unknown accuracy is partly compensated by numerous calibrations. The example of later attempts to further improve LJP aspects of the glass electrode can be found in ref. [73].

Going to more technical applications, a simplified (and probably sufficient) approach to the estimation of LJPs is typical for channel devices in flow injection electroanalysis (see, e.g., [74]). The injection of solutions of different composition provides a serious risk of local compositional changes and by these means can affect the LJP. The goal of research in this area is mostly to minimize nonstationary LJP contributions. The measurements of pH in large-scale flows related to industrial applications are discussed in refs. [69, 75].

The problem of LJP correction of pH values for highly diluted solutions remains essential, and empiric corrections are still under discussion in practical analytical chemistry [76]. In relation to this problem, the study of "electrochemistry in pure water" [77] is of interest. In this case (no electrolyte added to high purity water) the LJP is unpredictably high and sensitive to occasional solution composition. The sometimes used Nafion membrane to separate the working electrode and a hydrogen reference electrode is certainly to be discouraged because of the introduction of an additional membrane potential.

3.3.4 Thermal LJP Between Solutions Having Different Temperatures

In early studies [78], the effect of temperature on LJP was considered exclusively in terms of Eq. (3.7). It was believed that the increase of T in RT/F multiplier is compensated partly or completely by temperature dependences of ionic mobilities. Much later Thermal LJP (TLJP) phenomenon was treated theoretically for balanced external pressure [79]. For the junction of two solutions of equal concentrations (the solvent and electrolyte has one common ion) with the temperatures T_1 and T_2 ($T_2 > T_1$), the equation for temperature-induced contribution contains new parameters the entropies of the transport of individual i-th ions (S_i):

$$\Delta\phi_{\mathrm{TLJ}} = -\frac{RT}{F}\int_{T_1}^{T_2}\sum\frac{t_i S_i}{z_i}\mathrm{d}T. \tag{3.10}$$

This TLJP is important for pH measurements at elevated temperatures. Key values of high temperature parameters for some usual 1,1-electrolytes are reported in ref. [79], and the equations for solid electrolyte-containing cells with temperature gradient are presented as well. Important note specially marked in later review [80] is related to the changes of the customary transport numbers with temperature (at elevated temperatures, NaCl is more suitable for LJP elimination than KCl). Quantitative information for both chlorides is available in ref. [81]. TLJP at solution/solution boundary is also of interest for applications related to corrosion. In this case the medium is technical water being rather diluted electrolyte, and not so low potential drops can arise (see example of TLJP research, e.g., in ref. [82]).

In melts, problem of TLJP (thermo-emf) always arises, and the emf correction is typically calculated from thermoelectric coefficients of phases in contact [83]. However, no detailed research of TLJP contribution to this correction is known. The problem is probably close to solvent/solvent junctions.

In [75], various advancements related to industrial pH control are considered as related to temperature effects on the uncertainty of the key quantity (automatically retractable probes, contactless connectors, "intelligent electrodes"). However, the author sadly concludes that recent developments have no or only a little improving effect.

3.4 LJP in Condensed Ionic Systems

The traditional treatment of LJP for melts is outlined in a classical monograph "Reference Electrodes Theory and Practice" [84]. For melt/melt junction containing three types of species ($i = 1$, 2, or 3), forming the salts "1–3" and "2–3" with equivalent conductivities Λ

$$\Delta\phi_{\text{diff}} = \frac{RT}{F} \cdot \left(\frac{\Lambda_{1-3} - \Lambda_{2-3}}{z_1\Lambda_{1-3} - z_2\Lambda_{2-3}} \right) \ln \frac{z_1\Lambda_{1-3}}{z_2\Lambda_{2-3}}. \tag{3.11}$$

Very approximate verification of this formula for RTILs can be arranged with the use of Ag-containing RTIL, which supports Ag^+/Ag reference [85]. For a single system with one common ion studied in ref. [85], Eq. (3.11) results in the value of ca. 80 mV, i.e., much higher than the values obtained earlier for high temperature melts. Comparison with experimental results is limited to assumptions related to model redox probes (Fc and Cc), as always.

Many questions still remain opened in fundamental research of RTILs, including LJP at the boundary of two ionic liquids and LJP at RTIL/molecular solvent boundary. The progress is expected from the studies of Fc^+/Fc and Cc^+/Cc reference scales by analogy with approach mentioned above in Sect. 3.2. It is already evident from comparison of formal potentials for Fc^+/Fc and similar decamethylferrocenium redox probe that the difference of solvation energy in various RTILs can result in potential shift up to 0.1 V [86]. Due to experimental difficulties related to high ohmic drops in RTIL, as well as to moisture and air sensitivity, the accuracy of potential measurements for redox couples is lower than compared to conventional interfacial electrochemistry [87–89], but it is enough to approach the same accuracy of LJP estimates. It is already evident that Born-like approaches are helpless for RTILs (even more than for molecular liquids).

To extend the traditional models of LJP to RTILs, one should solve the problem of possible changes of ion mobility after penetration into another medium.

The specific aspect for RTILs is the possibility of specific solvation of model redox reactant with either anion or cation. In the former case one cannot exclude that the traditional requirement for redox probe (point (ii) in Sect. 1.2.5, resulting from specific solvation of anions supported by hydrogen bonds) can be

reconsidered, i.e., the redox couples containing neutral molecule as the oxidized (not reduced) form can be less sensitive to solvent nature.

In relation to LJP in condensed ionic systems, it is of interest to mention LJP in ionized gas formed by injection of salt solutions into high-temperature (1,800 K) flame located between two solution compartments with Pt reference electrodes [90]. Surprisingly, the dependence of potential difference on ions concentration in the flame and mobilities follows the trends for solution/solution LJP.

3.5 Membranes and Immiscible Liquids

These systems only rarely assume true equilibrium between solution and membrane. Typically they work under the mode of steady state nonequilibrium ions distribution, which means that stable diffusion potential is settled at membrane/solution interface.

The examples of unified approach to diffusion potential modeling for solution/solution (immiscible liquids) and solution/membrane boundaries can be found in refs. [25–27] and [91, 92]. There are already no doubts that diffusion potential contributes to the apparent membrane potential and affects strongly the calibration curves of ion-selective electrodes [26, 93, 94]. This can take place for glass electrode as well (see refs. related to pH measurements in Sect. 3.3.3).

The geometry of real polymer membranes still induces some problems with quantitative application of model calculations, and calibration procedure remains more or less empiric. However, the model systems imitating membranes, the interfaces of two immiscible electrolyte solutions (ITIES), are free from this shortcoming. Various types of LJP behavior for ITIES dependent on the ratios of ion partition coefficients are considered in ref. [95]; remarks in ref. [96] are also useful. The effect of initial concentration distribution on the temporal LJP behavior is considered in ref. [97] self-consistently for the limiting cases of thick membranes (assumed to operate as ion-selective electrodes) and thin membranes (assumed to imitate biological membranes).

General consideration of membrane potential and LJP in the context of experimental errors in potential measurements is available in a brief review [98]. The specific details for so-called “biological liquids” (like blood, urine, etc.) can be found in review [99].

References

1. Petrii OA, Tsirlina GA (2003) Electrode potentials. In: Bard AJ, Stratmann M, Gileadi E, Urbakh M (eds) Encyclopedia of electrochemistry, vol 1. Wiley-VCH, New York, pp 1–25
2. Izutsu K (2011) Anal Sci 27:685
3. Izutsu K (2008) Bull Chem Soc Jpn 81:703

4. Izutsu K (2010) Bull Chem Soc Jpn 83:39
5. Koepp HM, Wendt H, Strehlow H (1960) Z Elektrochem 64:483
6. Izutsu K (2002) Electrochemistry in nonaqueous solutions. Wiley-VCH, Darmstadt
7. Gritzner G, Kuta J (1984) Pure Appl Chem 56:461
8. Pleskov VA (1947) Uspekhi Khimii 16:254
9. Pleskov VA (1949) Zh Fiz Khimii 23:104
10. Kolthoff IM, Thomas FG (1965) J Phys Chem 69:3049
11. Parker AJ (1976) Electrochim Acta 21:671
12. Krishtalik LI, Alpatova NM, Ovsyannikova EV (1991) Electrochim Acta 36:435
13. Krishtalik LI (2008) Electrochim Acta 53:3722 [Erratum (2009) Electrochim Acta 54:4741]
14. Krishtalik LI (2008) Russ J Electrochem 44:43
15. Kuznetsov AnM, Maslii AN, Krishtalik LI (2009) Russ J Electrochem 45:87
16. Roy LE, Jakubikova E, Guthrie MG, Batista ER (2009) J Phys Chem A 113:6745
17. Namazian M, Lin CY, Coote ML (2010) J Chem Theory Comput 6:2721
18. Baik M-H, Friesner RA (2002) J Phys Chem A 106:7407
19. Bunakova LV, Khanova LA, Topolev VV, Krishtalik LI (2004) J New Mater Electrochem Syst 7:241
20. Khanova LA, Topolev VV, Krishtalik LI (2006) Chem Phys 326:33
21. Izutsu K (2011) J Solid State Electrochem 15:1719
22. Samec Z (2008) Interface of the immiscible liquids. In: Bard AJ, Inzelt G, Scholz F (eds) Electrochemical dictionary. Springer, Berlin, pp 359–360
23. Izutsu K, Kobayashi N (2005) J Electroanal Chem 574:197
24. Dickson EJF, Limon-Petersen JG, Compton RG (2011) J Solid State Electrochem 15:1335
25. Ward KR, Dickson EJF, Compton RG (2010) J Phys Chem B 114:4521
26. Sokalski T, Lingenfelter P, Lewenstam A (2003) J Phys Chem B 107:2443
27. Planck M (1890) Ann Physik 40:561
28. Henderson P (1907) Z Phys Chem 59:118
29. Henderson P (1908) Z Phys Chem 63:325
30. Lingane JJ (1958) Electroanalytical chemistry, 2nd edn. Prentice Hall, New York
31. Lewis GN, Sargent LW (1909) J Am Chem Soc 31:636
32. Kang KH, Kang IS (2004) J Electroanal Chem 566:331
33. Park J, Hun KY, Li X (2006) J Electroanal Chem 591:141
34. Damaskin BB, Tsirlina GA, Borzenko MI (1998) Russ J Electrochem 34:199
35. Gumming AC (1907) Trans Faraday Soc 2:213
36. Gumming AC (1912) Trans Faraday Soc 8:86
37. MacInnes DA (1915) J Am Chem Soc 37:2301
38. Noyes AA, MacInnes DA (1920) J Am Chem Soc 42:239
39. MacInnes DA, Yeh YL (1921) J Am Chem Soc 43:239
40. Harned HS (1916) J Am Chem Soc 38:1986
41. Harned HS (1926) J Phys Chem 30:433
42. Buck RP, Rondinini S, Covington AK, Baucke FGK, Brett CMA, Camxes MF, Milton MJT, Mussini T, Naumann R, Pratt KW, Spitzer P, Wilson GS (2002) Pure Appl Chem 74:2169
43. Scatchard G (1923) J Am Chem Soc 45:1716
44. Guggenheim EA (1930) J Am Chem Soc 52:1315
45. Guggenheim EA (1930) J Phys Chem 34:1758
46. Fraenkel D (2012) J Phys Chem B 116:3603
47. Zarubin DP (2011) J Chem Thermodyn 43:1135
48. Malatesta F (2000) J Solut Chem 29:771
49. Vera JH, Wilczek-Vera G (2012) J Chem Thermodyn 47:442 (continued in the same issue, pp 445, 449, 451)
50. Ferse A, Müller HO (2011) J Solid State Electrochem 10:2149
51. Malatesta F (2011) J Solid State Electrochem 10:2169
52. Ferse A (2011) J Solid State Electrochem 10:2173

53. Buizza C, Mussini PR, Mussini T, Rondinini S (1996) J Appl Electrochem 26:337
54. Chloupek JB, Danes VZ, Danesova BA (1933) Coll Czech Chem Commun 5:469
55. Chloupek JB, Danes VZ, Danesova BA (1933) Coll Czech Chem Commun 5:527
56. Sokalski T, Maj-Zurawska M, Hulanicki A, Lewenstam A (1999) Electroanalysis 11:632
57. Faverio CL, Mussini PR, Mussini T (1998) Anal Chem 70:2589
58. Sakaida H, Kakiuchi T (2011) J Phys Chem B 115:13222
59. Shimata M, Sakaida H, Kakiuchi T (2011) Anal Chem 83:164
60. Fujino Y, Kakiuchi T (2011) J Electroanal Chem 651:61
61. Zhang L, Miyazawa T, Kitazumi Y, Kakiuchi T (2012) Anal Chem 84:3461
62. Kakiuchi T, Tsujioka N, Kurita S, Iwami Y (2003) Electrochem Commun 5:159
63. Oman RF, Camxes MF, Powell KJ, Rajagopalan R, Spitzer P (2007) Pure Appl Chem 79:67, 81
64. MacInnes DA, Yeh YL (1921) J Am Chem Soc 43:2563
65. Scatchard G (1925) J Am Chem Soc 47:697
66. Kakiuchi T (2011) J Solid State Electrochem 15:1661
67. Lamb AB, Larson AT (1920) J Am Chem Soc 42:229
68. Fales HA, Stammelman MJ (1923) J Am Chem Soc 45:1271
69. Tauber G (2009) Technisches Messen 76:308
70. Rusanova MY, Tsirlina GA, Petrii OA (1993) Russ J Electrochem 29:412
71. Damaskin BB (ed) (1991) Praktikum po elektrokhimii (Lab works on electrochemistry). Vysshaya Shkola, Moscow, pp 5–23
72. Bates R, Popovych O (1981) Crit Rev Anal Chem 10:247
73. Brandariz I, Barriada JL, Taboada-Pan C, de Vicente MES (2001) Electroanalysis 13:1110
74. Adachi T, Suzuki H (2011) Sens Actuators B 156:228
75. Tauber G (2010) Technisches Messen 77:150
76. Kadis R, Leito I (2010) Anal Chim Acta 664:129
77. Huang H, Wang Q, Cha C-S, Lu J, Zhuang L (2011) Electroanalysis 23:577
78. Prideaux EBR (1928) Trans Faraday Soc 24:11
79. Lvov SN, Macdonald DD (1996) J Electroanal Chem 403:25
80. Wildgoose GG, Giovanelli D, Lawrence NS, Compton RG (2004) Electroanalysis 16:421
81. Macdonald DD, Scott AC, Wentrcek P (1979) J Electrochem Soc 126:1618
82. Oh SH, Bahn CB, Hwang IS (2003) J Electrochem Soc 150:E321
83. Minh NQ, Redey L (1987) Reference electrodes for molten electrolytes. In: Lovering DG, Gale RJ (eds) Molten salt techniques, vol 3. Plenum, New York, pp 105–287
84. Laity RW (1961) Electrodes in fused salt systems. In: Ives DJG, Janz GJ (eds) Reference electrodes. Theory and practice. Academic, New York, pp 524–606
85. Snook GA, Best AS, Pandolfo AG, Hollenkamp AF (2006) Electrochem Commun 8:1405
86. Torriero AAJ, Howlett PC (2012) Electrochem Commun 16:84
87. Rogers EI, Silvester DS, Poole DL, Aldous L, Hardacre C, Compton RG (2008) J Phys Chem C 112:2729
88. Lewandowski A, Waligora L, Galinski M (2009) Electroanalysis 21:2221
89. Sukardi SK, Zhang J, Burgar I, Horne MD, Hollenkamp AF, MacFarlane DR, Bond AM (2008) Electrochem Commun 12:250
90. Caruana DJ, McCormack SP (2001) Electrochem Commun 3:675
91. Ward KR, Freitag L, Compton RG (2010) J Phys Chem B 114:10763
92. Dickson EJF, Freitag L, Compton RG (2010) J Phys Chem B 114:187
93. Lewenstam A (2011) J Solid State Electrochem 15: 15.
94. Jasielec JJ, Filipek R, Szyszkiewicz K, Fausek J, Danielewski M, Lewenstam, A (2012) Comput Mater Sci 63: 75.
95. Zhurov K, Dickson EJF, Freitag L, Compton RG (2011) J Phys Chem B 115:6909
96. Perram JW, Stiles PJ (2006) Phys Chem Chem Phys 8:4200N10
97. Koryta J (1984) Electrochim Acta 29:445
98. Angst U, Vennesland O, Myrdal R (2009) Mater Struct 42:365
99. Lewenstam A (2007) In: Alegret S, Merkoci A (eds) Comprehensive analytical chemistry. Elsevier, Amsterdam, pp 5–24

Chapter 4
Salt Bridges and Diaphragms

4.1 Common Types of Salt Bridges and Diaphragms

Fritz Scholz

4.1.1 Introduction

Whenever the reference electrode compartment has to be separated by electrolyte bridges and diaphragms from the other parts of the electrochemical cell, the separation has to meet the following requirements:

(i) The electrolytic contact between the electrodes must be maintained.
(ii) The ohmic resistance R_Ω of the electrolyte bridge(s) and diaphragm(s) must be small enough so that the voltage drop iR_Ω is minimal or, if possible, negligible. (Electronic iR_Ω compensation will not be considered here.)
(iii) The diffusion potentials at all places were different electrolyte solutions border, must be as small as possible, and they must be as stable (time invariant) as possible. *It is the major task of a salt bridge to reduce the diffusion potential which would build up at the junction of the electrolytes A and A′ of the two electrode compartments by interposing the bridge electrolyte B.*
(iv) The electrolyte of the reference electrode should not be contaminated by the electrolyte (or generally the solution) of the working electrode and vice versa.

Strictly taken, these requirements can never be completely met, and at best some good compromise can be achieved. One fact facilitates these problems: to maintain a constant potential of the reference electrode, generally high-input impedance

F. Scholz (✉)
Institute of Biochemistry, University of Greifswald, 17487 Greifswald, Germany
e-mail: fscholz@uni-greifswald.de

G. Inzelt et al. (eds.), *Handbook of Reference Electrodes*,
DOI 10.1007/978-3-642-36188-3_4,

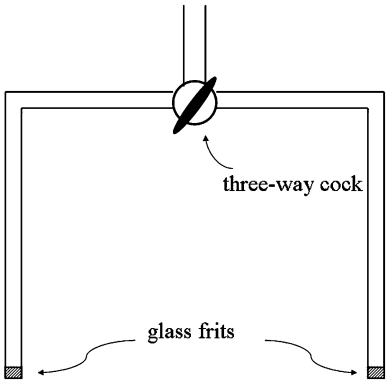

Fig. 4.1.1 Salt bridge constructed from glass tubes, glass frits, and a 3-way cock

measuring instruments are used, so that the current flowing through the salt bridge and diaphragms is practically negligible.

The term *salt bridge* means a device containing an electrolyte solution and placed between two electrodes or electrode compartments in such way that the electrolyte solution serves as the ionic conductor between the two electrodes. Normally, a salt bridge is constructed of tubes containing the electrolyte solution. The ends of the tubes may have diaphragms (e.g., glass frits) to keep the solution as good as possible confined to the inner of the tubes. Another possibility is that one end of the tube is drawn out to a capillary, the orifice of which can be placed very near to the surface of the working electrode. This is called a Luggin capillary.[1] A very simple salt bridge is depicted in Fig. 4.1.1. Such salt bridge is filled by sucking the electrolyte solutions through the frits and glass tubes. It is possible to fill both sides of the bridge with different solutions, provided they are chemically compatible. If the electrolyte bridge is filled with only one solution, a two-way cock can be placed in the top glass tube. The sleeve of the cock should be free of any grease as the electrolyte film in the annular gab between the cone and the sleeve of the glass cock provides the ionic conductivity. When the three-way cock is closed and the bridge is in use, the cock acts as a *ground-joint diaphragm*. The cock should possess high-precision grounds of a large ground surface area. The high-precision grounding is important to minimize leakage by still guaranteeing low resistance of the electrolyte film. It was the important discovery of Olin Freeman Tower (1872–1945), an American student of F. W. Ostwald in Leipzig, that rather concentrated solutions of potassium chloride offer the great advantage that the diffusion potentials are very small because the effects of potassium cations and chloride anions almost cancel (for a detailed discussion, see Chap. 3). Still today, there is no better salt for the aqueous electrolyte bridges than KCl, if possible at saturation concentration. In case that the two solutions which need to be separated by a diaphragm are chemically incompatible (e.g., one solution containing K^+ and

[1] This kind of capillary salt bridge was suggested by Hans Luggin, an Austrian scientist (1863–1899), to Fritz Haber (1868–1934) when both worked in Karlsruhe, Germany.

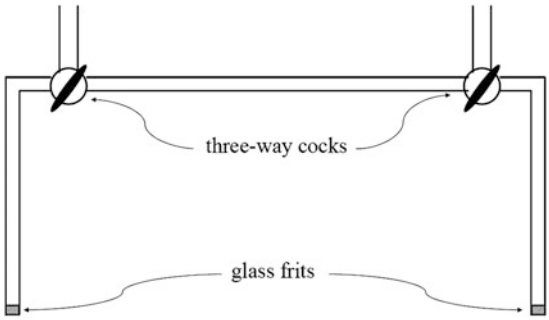

Fig. 4.1.2 Salt bridge constructed from glass tubes, glass frits, and two 3-way cocks for the purpose of separating chemically incompatible electrolyte solutions by a third solution which is compatible with the two terminal solutions

the other ClO_4^- ions) one needs to use a salt bridge as depicted in Fig. 4.1.2: that bridge allows the tube between the two cocks to be filled with an electrolyte solution which is compatible with the two other electrolytes (e.g., NaCl in the above given example). Bates et al. reported in 1950 [1] a special salt bridge for high-accuracy measurements which allowed to form a very stable liquid‖liquid electrolyte junction in two vertical glass tubes. That bridge, and also others, has two cocks, so that the two electrolytes of the electrodes can be separated by a third electrolyte. Bridges like that depicted in Fig. 4.1.1 always possess the property of a siphon, the flow of liquids being only impeded by the frits at the two ends and the cock. Nevertheless, it is important to arrange the hydrostatic pressure on both sides in such way that no pressure gradient will drive the liquids from one to the other side. Very small pore frits are also helpful to limit the contamination of solutions by a directed flow. Especially for reference electrodes, the described problem of pressure gradient can be easily solved by using a single glass tube with one frit at the lower end, and tightly fitting the reference electrode to the tube as shown in Fig. 4.1.3. Here the frit is a small stick of magnesia (MgO) melted in the glass. Several other materials can be also used as diaphragm. The construction shown in Fig. 4.1.3 has the advantage that normally no pressure can force the solution to flow in or out; however, a pressure gradient can build up when the bridge/electrode system is subjected to temperature changes as the thermal contraction or expansion of the inner solutions may lead to pressure gradients. When very tight frits (like a magnesia stick or Vycor® plate) are used, this is no issue in case of normal room temperature variations of some Kelvin. In any case, care must be taken to prevent any air bubbles inside the bridge and electrode, as gas has a much higher temperature coefficient of volume, and thus a gas bubble would create larger pressure gradients in response to temperature changes. Figure 4.1.4 depicts some common diaphragms used for salt bridges. Diaphragms for reference electrodes may be made of (1) sintered glass frits, (2) sintered ceramics (e.g., sintered magnesia (MgO), (3) asbestos fiber (not anymore used), (4) Vycor®, (5) organic polymer membranes, (6) stopper-in-sleeve constructions (glass), (7) stopper with thread (any material), (8) sintered platinum, and (9) they may also be simply a plug of a gel, like Agar. Vycor® (registered trademark of Corning, Inc.) is a porous glass possessing a sufficient conductivity and being very well suited to be used as diaphragm between

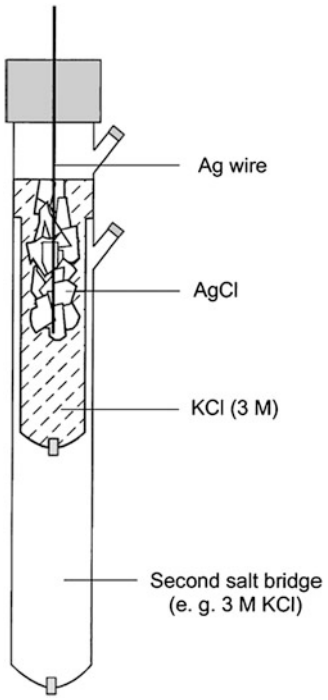

Fig. 4.1.3 Construction of a silver/silver chloride reference electrode with a second salt bridge. Reproduced with permission from [20]

aqueous and nonaqueous solutions. Thin plates of about 2 mm thickness are cut from a rod and fitted to the end of a glass tube with the help of a shrink tube or in another suitable way. Vycor® diaphragms cannot be used in strongly alkaline solutions as they will crack and deteriorate rapidly. All diaphragms have specific properties, of which the following are of special importance: (a) ohmic resistance, (b) chemical stability towards the used electrolyte solutions, and (c) leaking rate (permeability for solutions). Of course, thermal stability, pressure stability, etc. may be also important in some cases. Table 4.1.1 gives a compilation of properties of common diaphragms. Pore diaphragms (e.g., the Twin Pore Diaphragm of Metrohm AG, Switzerland) consist of open pores which connect the analyte solution and the reference electrode solution with a gel electrolyte. The gel practically does not interact with the analyte solution, so that interference by blocking (e.g., protein precipitation) is negligible. A platinum thread consisting of fine twinned Pt wires has similar advantages. Platinum threads, however, may suffer from wrong potentials in strongly redox buffered solutions.

Diaphragms tend to fail because of (1) leakage of electrolyte leading to higher resistance, because the diaphragm may contain gas (air) instead of electrolyte solution and (2) precipitations of sparingly soluble salts, proteins, etc., leading also to higher resistance or even complete blocking. The leakage can be diminished by adding glycerol or similar liquids to the aqueous electrolyte solution, and or

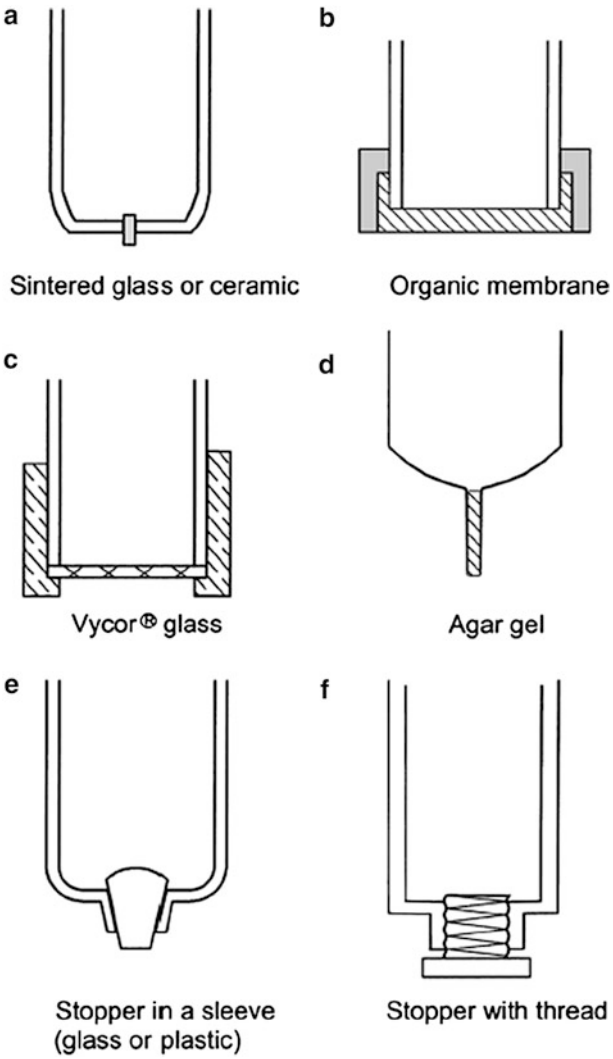

Fig. 4.1.4 Common diaphragms for salt bridges. The stopper/sleeve shown in (**e**) is usually made in an inverted way, so that the stopper can be removed from the outside of the tube. Reproduced with permission from [21]

gelling agents. Adding viscous water-miscible solvents also diminishes the mobility of the ions [9] according to the Stokes–Einstein law and thus considerably contributes to a decrease of the junction potentials.

Table 4.1.1 Properties of common diaphragms

Diaphragm	Impedance (sat. KCl)	Pore size	Leak rate (μl h^{-1})	Application
Vycor® 7930 porous glass	500 Ω for sat. KCl [3]	4 nm [4] 10–20 nm [5]	Modest [2]	Cannot be used in strongly alkaline solutions
Glass frit		*American standard:* Fine: 4–5.5 μm Very fine: 2–2.5 μm Ultra fine: 0.9–1.4 μm *European standard:* P3: 16–40 μm P4: 10–16 μm P5: 1–1.6 μm		
Pt thread	30 k Ω with *Idrolyt*[1] electrolyte [6]		3–30 [5]	Especially suitable for applications in protein solutions
Ceramic/ conductive Polymer composite	500 Ω–2.7 k Ω for sat. KCl [2]		7.4×10^{-4}–5.7×10^{-5} [2]	
Twin pore	<20 k Ω for gel electrolyte [7]		0 [6]	
Ground-joint diaphragm	5–100 k Ω for 3 M KCl [8]		5–100 for 3 M KCl [7]	

[1] *Idrolyt* is the name of a glycerin-based electrolyte of Metrohm AG, Switzerland, having the same Cl^- activity as a 3 M KCl solution. It is a 9 %-ic solution of KCl in a 3:2 mixture of glycerol to water [2]

4.1.2 Gels for Stabilizing Salt Bridges

To decrease the leakage of salt solutions from bridges, especially in case of reference electrodes, glass electrodes, etc., the viscosity of the salt solutions is increased with gelling agents. Gelling also contributes to decreased diffusion coefficients [10, 11] of the salt ions and thus to diminished liquid junction potentials. The decreased ion mobility in gels results from geometric obstructions, and in case of polyelectrolyte gels also from electrostatic obstruction [12]. A very convenient way to prepare gelled salt bridges for connecting a reference electrode compartment with an electrochemical cell housing the other electrode(s) is as follows: A thin polyethylene tube (e.g., 0.5–1 mm inner diameter) is filled with

the liquid gel electrolyte solutions, and after gelling the tube can be cut in appropriate pieces to make the solution connections. Such tubes can be easily exchanged, or the end pieces can be cut and disposed off if contamination has occurred. The tubes may also be thrown out before filling, so that the cut can be performed at places of diminished radius, allowing to decrease the contact area at the orifice, i.e., at the gel solution junction. To fill a tube, e.g., with warm agar gel, a syringe has to be used. The tube can be kept very long times. Before use one end has to be cut and disposed, and then a part of appropriate length can be cut for use. Such tubes are especially useful to contact small electrochemical cells, as e.g., for in situ AFM/STM [13], or also flow-through cells [14]. Such tubes can be also used like Luggin capillaries to approach the surface of a working electrode.

4.1.2.1 Agar and Pure Agarose Gels

Agar (also called agar-agar) is a mixture of agarose and agaropectin. Agarose is a polymer build up of the repeating units of agarobiose. Agarobiose is a disaccharide from D-galactose and 3,6-anhydro-L-galactopyranose. Agaropectin is a heterogeneous mixture of smaller acidic molecules that gel poorly. Instead of using agar, one can purchase purified agarose and use it for the gelation of electrolyte solutions: typically the salt solution contains 2–5 % (w/v) agar (or agarose). Agarose gels have a concentration-dependent pore structure: the pore size varies from 100 to several hundred nanometers [15, 16]. The gel is prepared by gently heating the agar (or agarose) with the salt solution and the liquid is allowed to cool down in the appropriate tubes. Solidification occurs between 40 and 32 °C. Agar and agarose gels are probably most popular for self-made laboratory diaphragms, but they suffer from an easy drying out at air, and microbes like to settle and grow on the gel. Therefore commercial reference electrode systems use synthetic polymers for gel formation.

4.1.2.2 Cellulose Gel

Hydroxyethyl cellulose is the gelling ingredient of a gel commercially used in the reference gel electrolyte of Ionode Pty Ltd, Australia. It consists of KCl 26 %, triethylene glycol 21 %, hydroxyethyl cellulose 2 %, and water to 100 % [17]. This gel is a highly viscous liquid minimizing leakage.

In another commercial product, methyl cellulose is used as gelling agent, with 40 % KCl (KCl saturated) and a not specified amount of water [18].

4.1.2.3 Acrylate Hydrogels

Among the methacrylate hydrogels, the most common gelating polymer is poly-2-hydroxyethyl-methacrylate (p-HEMA) [19]. The monomer and the aqueous

electrolyte solutions are mixed, degassed, and kept on ice when 100 µl of a 6 % solution of sodium bisulfite and 100 µl of a 12 % solution of ammonium persulfate are added per 1 ml of monomer. The mixture is left for solidification in an appropriate vessel (or tube) at 37 °C for 2 h. The polymerized material has to be dialyzed against the used electrolyte solution to remove non-polymerized monomers and catalyst. Generally, health hazard issues have to be severely observed in case of acrylates.

References

1. Bates RG, Pinching GD, Smith ER (1950) J Res Natl Bur Stand 45:418–429
2. Material safety data sheet (21 April 2009) 6.2308.040 Idrolyte. Metrohm Ltd., CH-9101 Herisau, Switzerland
3. Smith TJ, Stevenson KJ (2007) Reference electrodes. In: Zoski CG (ed) Handbook of electrochemistry. Elsevier, Amsterdam, p 96
4. Data sheet: VYCOR® Brand Porous Glass 7930, Corning Incorporated, 2001
5. Gille W, Enke D, Janowski F (2002) J Porous Mater 9:221–230
6. Technical speciation of pH glass electrode 6.0224.100 of Metrohm AG, Switzerland
7. Technical speciation of pH glass electrode 6.0221.100 of Metrohm AG, Switzerland
8. Technical speciations of various glass electrodes 6.01 – 6.02 of Metrohm AG, Switzerland
9. Steel BJ, Stokes JM, Stokes RH (1958) J Phys Chem 62:1514–1516
10. Fuji T, Thomas HC (1958) J Phys Chem 62:1566–1568
11. Gokarn NA, Rajurkar NS (2006) J Solut Chem 35:1673–1685
12. Darwish MIM, van der Maarel JRC, Zitha PLJ (2004) Macromolecules 37:2307–2312
13. Hasse U, Scholz F (2005) Electrochem Commun 7:173–176
14. Vahl K, Kahlert H, Scholz F (2010) Electroanalysis 22:2172–2178
15. Narayanan J, Xiong J-Y, Liu X-Y (2006) J Phys Conf Ser 28:83–86
16. Hasse U, Scholz F (2006) J Solid State Electrochem 10:380–382
17. Material safety data sheet (April 2011, Version 3) Reference Gel Electrolyte RE45. Ionode Pty Ltd, 8/148 Tennyson Memorial Avenue, Tennyson Qld 4105, Australia
18. Material safety data sheet (21 April 2009) 6.2308.030 Electrolyte KCl sat. gel. Metrohm Ltd., CH-9101 Herisau, Switzerland
19. Kindler DD, Bergethon PR (1990) J Appl Physiol 69:371–375
20. Kahlert H (2010) In: Scholz F (ed) Electroanalytical methods. Guide to experiments and applications, 2nd edn. Springer, Berlin, p 305
21. Kahlert H (2010) In: Scholz F (ed) Electroanalytical methods. Guide to experiments and applications, 2nd edn. Springer, Berlin, p 304

4.2 Ionic Liquid Salt Bridge

Takashi Kakiuchi

4.2.1 Introduction

Ionic liquid salt bridge (ILSB) [22, 23] is a promising alternative to KCl-based salt bridge (KClSB) and is capable of solving many of the problems intrinsic to KClSB: unstable liquid junction potential in low-ionic-strength sample solutions, clogging of the junction plug in pH composite electrodes, frequent necessity of renewing internal solution, contamination of sample solutions with KCl, and the dependence of liquid junction potential on the type of the junction [23].

ILSB is not omnipotent, because the liquid junction potential is interfered by ions whose hydrophobicity is nearly comparable to or higher than that of ions constituting the ILSB, when the concentration of the ion is comparable to or higher than the solubility of ILSB-constituent ions in a sample solution [23]. Nevertheless, ILSB outperforms KClSB in certain important applications of electroanalytical chemistry, notably, precise pH measurements [24, 25]. The stable liquid junction potential that formed when an ILSB is in contact with a low-ionic-strength aqueous solution is a strong advantage of ILSB over KClSB in that the former enables the determination of single ion activities in aqueous solutions with the precision on the order of 1 mV or better [24, 26]. Unlike KClSB, ILSB is currently in the development phase in view of optimization of ionic liquids depending on the purposes. Nonetheless, ILSB has been shown to be a workable and superior alternative to KClSB in a few important applications and it seems worthwhile at the current stage to describe the principles and applications of ILSB.

4.2.2 Principles of ILSB

A hydrophobic ionic liquid (IL) forms in contact with water (W) a liquid–liquid two-phase system. A notable feature of this two-phase system is that the phase-boundary potential, that is, the potential drop across the interface that develops in the IL-W two-phase system, is mainly determined by the partitioning of the IL-constituent ions between ILSB and W. First, this principle is briefly introduced.

T. Kakiuchi (✉)
pH Science and Technology Laboratory, Kinomoto 1058, Wakayama 640-8453, Japan
e-mail: kakiuchi.takashi.55e@st.kyoto-u.ac.jp

Following sections summarize other factors that can influence the phase-boundary potential at the contact of an IL with W.

4.2.2.1 Distribution Potential

When an ionic liquid that consists of moderately hydrophobic cationic and anionic species is in contact with an aqueous solution, the phase-boundary potential, $\Delta_{IL}^{W}\phi$, which is the inner potential of the W phase with respect to that of IL phase, is established across the interface at a distribution equilibrium, where the superscript W and subscript IL stand for the aqueous phase and the IL phase, respectively.

We consider the simplest case when the ions in W phase are all hydrophilic and do not significantly partition into the IL phase and an ILSB, which is made of a 1–1 electrolyte. In such an expedient case, $\Delta_{IL}^{W}\phi$ is determined by the partitioning of the IL-constituent ions, C^+ and A^-, and is given by [23]

$$\Delta_{IL}^{W}\phi = \frac{1}{2}\left(\Delta_{IL}^{W}\phi_{C^+}^{\ominus} + \Delta_{IL}^{W}\phi_{A^-}^{\ominus}\right) + \frac{RT}{2F}\ln\frac{\gamma_{A^-}^{W}\gamma_{C^+}^{IL}}{\gamma_{C^+}^{W}\gamma_{A^-}^{IL}}, \tag{4.2.1}$$

where $\Delta_{IL}^{W}\phi_{C^+}^{\ominus}$ and $\Delta_{IL}^{W}\phi_{A^-}^{\ominus}$ are the standard ion transfer potentials of C^+ and A^-, which is defined in terms of the standard Gibbs energy of the transfer of ion, j, from IL to W, $\Delta G_j^{IL\to W,\ominus}$, as $\Delta_{IL}^{W}\phi_j^{\ominus} = -\Delta G_j^{IL\to W,\ominus}/(z_j F)$. $\gamma_{C^+}^{\alpha}$ and $\gamma_{A^-}^{\alpha}$ in Eq. (4.2.1) are the activity coefficients of C^+ and A^- in phase α (α = W or IL) and z_j is the ionic charge on ion j in signed units of electronic charge.

Usually, $\Delta_{IL}^{W}\phi_{C^+}^{\ominus} \neq -\Delta_{IL}^{W}\phi_{A^-}^{\ominus}$ and, hence, $\Delta_{IL}^{W}\phi$ is not null. However, in an IL sandwiched by two aqueous solutions, $\Delta_{IL}^{W}\phi$ values on both sides of the IL phase have the same magnitudes but with opposite signs, and the second term on the right-hand side of Eq. (4.2.1) does not strongly depend on the electrolyte composition of the aqueous solution. Hence, the IL phase functions as an ILSB, because the liquid junction potential, which would develop if the ILSB is absent, is effectively canceled out by the IL phase inserted in between.

4.2.2.2 Contributions of Ion Transport to the Phase-Boundary Potential

In many cases of practical applications of ILSB, the distribution equilibrium throughout a two-phase system of an ILSB and a sample solution is seldom achieved. In the course of the dissolution of the IL into the sample solution, a quasi-distribution equilibrium is established within the diffusion layer in the sample solution side of the interface and the Nernst equation [27] for the distribution of an ionic species holds only for surface concentrations of the ions on both sides of the interface [28]. The phase-boundary potential at zero current is then characterized as

a mixed potential [29] determined by the sum of the partial currents caused by the transfer of different ions across the interface [30].

To calculate partial currents, the Nernst–Planck equation may be used to describe the mass transfer of C^+ and A^- in ILSB. In W, the mode of mass transfer of C^+ and A^- depends on the electrolyte composition. In the simplest case when only C^+ and A^- transfer across a planar interface by diffusion and the aqueous phase contains sufficient amount of indifferent electrolytes, so that the diffusion is the mode of mass transfer of C^+ and A^- in W, the value of $\Delta_{IL}^{W}\phi$ is determined by the potential at which the sum of two partial currents due to the transfer of C^+ and A^- across the phase boundary is null. Then, the mixed potential, $\Delta_{IL}^{W}\phi_{mix}$, is described by [31]:

$$\Delta_{IL}^{W}\phi_{mix} = \frac{RT}{2F}\ln\left(\frac{D_{C^+}^{W}}{D_{A^-}^{W}}\right)^{1/2} + \frac{\Delta_{R}^{W}\phi_{C^+}^{o} + \Delta_{R}^{W}\phi_{A^-}^{o}}{2}, \tag{4.2.2}$$

where $D_{C^+}^{W}$ and $D_{A^-}^{W}$ are the diffusion coefficients of C^+ and A^- in W.

When the concentration of indifferent electrolytes in W is low, the mixed potential simply reduces to

$$\Delta_{IL}^{W}\phi = \frac{1}{2}\left(\Delta_{IL}^{W}\phi_{C^+}^{o} + \Delta_{IL}^{W}\phi_{A^-}^{o}\right). \tag{4.2.3}$$

However, in this case the diffusion potential on the aqueous solution side of the interface due to the difference in $D_{C^+}^{W}$ and $D_{A^-}^{W}$ may become significant [32]. When the aqueous phase contains a salt MX, where M^+ and X^- do not partition in the ILSB, the Henderson equation [33] for the diffusion potential takes the form

$$\Delta\phi_{diff}^{W} = \left(\frac{u_{c^+} - u_{A^-}}{u_{c^+} + u_{A^-}}\right) \times \frac{RT}{F}\ln\frac{c_{CA}^{W}\left(u_{c^+} + u_{A^-}\right) + c_{MX}^{W}\left(u_{M^+} + u_{X^-}\right)}{c_{MX}^{W}\left(u_{M^+} + u_{X^-}\right)}, \tag{4.2.4}$$

where $\Delta\phi_{diff}^{W}$ is the diffusion potential in W referred to the electrostatic potential in W at the interface between the IL and W, c_{CA}^{W} is the concentration of $[C^+][A^-]$ in the aqueous solution side of the interface determined by the solubility of $[C^+][A^-]$, c_{MX}^{W} is the concentration of MX in W, and u_i is the mobility of ion i ($i = M^+, X^-, C^+$, or A^-) in W. From Eq. (4.2.4) it is seen that $\Delta\phi_{diff}^{W}$ becomes negligible when a sufficient amount of hydrophilic salt, MX, is in W.

Note the difference in the length scales between the distribution potential and the diffusion potential. In the latter, the region where the potential drop develops is a function of time and spans across the diffusion layer [34], whereas in the former the potential drop is limited within the diffuse part of the electrical double layer and is time-invariant. In the case when $\Delta\phi_{diff}^{W}$ is not negligible, $\Delta_{IL}^{W}\phi$ is thus given by the sum of the two quantities given in Eqs. (4.2.3) and (4.2.4). To minimize the

deviation of the phase-boundary potential from that determined by the distribution potential of C^+ and A^-, the use of an ionic liquid that consists of cation and anion having similar mobility values in W is recommended [32, 35].

4.2.2.3 Experimental Examination of the Constancy of Liquid Junction Potential at ILSB

Although any phase-boundary potential is not thermodynamically accessible, it is possible to examine the constancy of the liquid junction potential at ILSB, for example, by use of the following cell:

I	II	III	IV	V	VI	VII	
Ag	AgX	a mol dm^{-3} Aqueous M_1X solution	ILSB	x mol dm^{-3} Aqueous M_2X' solution	AgX'	Ag	(A)

where M_1X and M_2X' are salts of monovalent cations, such as H^+ and Na^+, with halogen ions, X^- and X'^-. By changing x in phase V while keeping a in phase III constant, the cell voltage, E, should vary with the single ion activity of X'^-, provided that the phase-boundary potential at the interface between IV and V, $\Delta^{\mathrm{W}}_{\mathrm{IL}}\phi_{\mathrm{SB}}$, and the Ag/AgX' electrode on the right-hand side of cell (A) responds to the activity of X'^- in phase V according to the Nernst equation; the constancy of the potential of the Ag/AgX electrode on the left-hand side at a given a value is naturally expected as long as the compositions of phases III and V are independent of each other.

As an example, the results when the ILSB is made of *N*-heptyl-*N*-methylpyrrolidinium bis(pentafluoroethanesulfonyl)amide, $[C_{1,7}pyrr^+][C_2C_2N^-]$, are shown in Figs. 4.2.1 and 4.2.2. The concentration of HBr in phase V (M_2X') was changed from 5 μmol kg^{-1} to 2 mol kg^{-1}, whereas the composition of phase III was kept constant at 10 mmol dm^{-3} chloride salt of $C_{1,7}pyrr^+$ (M_1X). The latter salt was chosen to lower the electrochemical polarizability of the interface between III and V [31] and fix the phase-boundary potential across the interface between III and IV at a value determined by the Nernst equation for the partition of $C_{1,7}pyrr^+$ between III and IV [22].

Figure 4.2.1 displays stable time courses of E for 15 min at 11 different concentrations of HBr. The constancy of E is seen at all concentrations. The stability of $\Delta^{\mathrm{W}}_{\mathrm{IL}}\phi_{\mathrm{SB}}$ over 1 h has been published for a similar ILSB [36].

E values in Fig. 4.2.1 are plotted against the decadic logarithm of the mean activity of HBr, $a^{\pm}_{\mathrm{HBr}}$, in Fig. 4.2.2 (filled circles) [36]. The dashed line has a slope of 59.16 mV per decade expected for the Nernstian response of the Ag|AgBr electrode at 25 °C. Except at the low and high extremes of the HBr concentrations, the variation of E with $\log_{10} a^{\pm}_{\mathrm{HBr}}$ is well explained by the Nernstian slope, which suggests

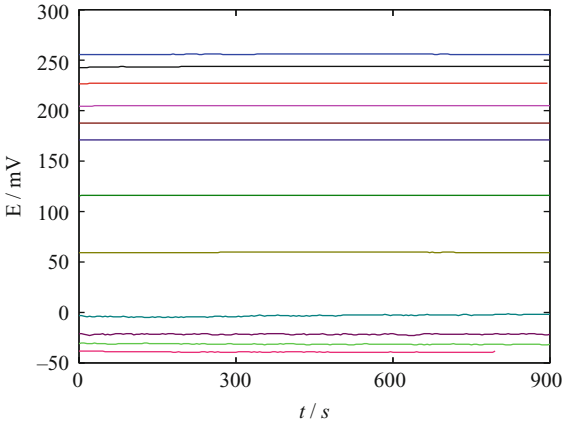

Fig. 4.2.1 Time courses of E at 25 °C for $[C_{1,7}pyrr^+]$ $[C_2C_2N^-]$ ILSB at 11 different concentrations of HBr: 5×10^{-6}, 1×10^{-5}, 2×10^{-5}, 5×10^{-5}, 1×10^{-4}, 2×10^{-4}, 2×10^{-3}, 2×10^{-2}, 2×10^{-1}, 5×10^{-1}, and 2 mol kg^{-1} from *top* to *bottom* [37]

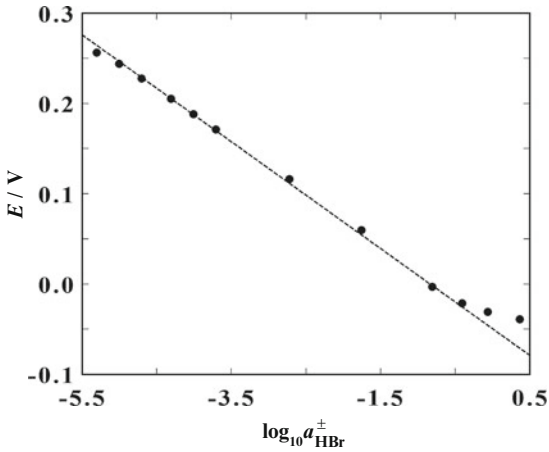

Fig. 4.2.2 Plots of E as a function of the mean activity of HBr, $a^{\pm}_{HBr}$, corresponding to data in Fig. 4.2.1. Replot of the same data in ref. [36]. *Dashed line* has a slope of 59.16 mV per decade change in $a^{\pm}_{HBr}$

the constancy of $\Delta^{W}_{IL}\phi_{SB}$ over four orders of magnitude change in the HBr concentration.

Note that the phase-boundary potential at III and IV includes a contribution of the transfer Gibbs energy of $C_{1,7}pyrr^+$ between III and IV [22], which shifts E up to a positive value of a few tens mV.

The deviations at the low and high extremes probably have different origins. At the low ionic strength, the diffusion potential can be significant as described above. On the other hand, the deviation at the high extreme is likely to be due to the response of the Ag|AgBr electrode to the single ion activity of Br^-, and not to the mean activity of HBr; the single ion activity of Br^- is smaller than the mean activity of HBr [38] and the difference becomes greater with increasing concentration of HBr. The applicability of the ILSB then extends to higher concentrations of HBr to 1 mol dm^{-3} [39].

4.2.2.4 Interference by Other Ions

When ions dissolved in W are not hydrophilic enough, the partition of these ions into ILSB can participate in the distribution equilibrium and can shift $\Delta_{IL}^{W}\phi$ from the value given by Eq. (4.2.1) in a way similar to the interference by foreign ions in ion-exchange-membrane-type ion-selective electrodes [30, 40]. To estimate the degree of interference, we need to know for a particular ionic liquid used for an ILSB the values of $\Delta_{IL}^{W}\phi_i^{\ominus}$, which are thermodynamically not accessible in principle and their estimates for each IL based on an extrathermodynamic assumption are also not usually available. Because most of the ILs are similar to a polar aprotic solvent with regard to the partition of a number of substances [41], a good quantitative measure of the hydrophobicity of ions between an IL and W is the standard ion transfer potential of the ions between nitrobenzene (NB) and W, $\Delta_{NB}^{W}\phi_i^{\ominus}$, whose values are available for ions relevant to ILs [42, 43].

Figure 4.2.3 shows apparent values of $\Delta_{NB}^{W}\phi_i^{\ominus}$ for moderately hydrophobic ions that are relevant to ILSB, together with typical ions employed in electrochemistry of liquid–liquid interfaces.

As an example, the vertical upward arrow indicates the location of $\Delta_{NB}^{W}\phi$ at -0.051 V when the NB phase contains 1-methyl-3-octylimidazolium (C_8mim^+) and bis(trifluoromethanesulfonyl)amide ($C_1C_1N^-$), which suggests that $\Delta_{IL}^{W}\phi$ between the ILSB made of these ions and an aqueous solution, $\Delta_{IL}^{W}\phi_{ILSB}$, would have a small negative value.

The degree of interference by a hydrophobic ion becomes significant when its surface concentration at $\Delta_{IL}^{W}\phi_{ILSB}$ is comparable to the solubility of the ILSB-constituent ions and, hence, depends on the relative magnitude of $\Delta_{IL}^{W}\phi_i^{\ominus}$ with respect to $\Delta_{IL}^{W}\phi_{ILSB}$, that is, $|\Delta_{IL}^{W}\phi_i^{\ominus} - \Delta_{IL}^{W}\phi_{ILSB}|$. This interference is basically the same as those seen in the case of ion-exchange-type liquid-membrane ion-selective electrodes [30].

4.2.2.5 Solubility of IL in W and Electrochemical Polarizability at the ILSB|W Interface

The solubility is another important factor in designing ILSB. It directly determines the degree of contamination of a sample solution by ILSB-constituent salts, and also the duration of life of an ILSB. The solubility product, K_s^W, of an ILSB-constituent salt, $[C^+][A^-]$, in water is quantitatively related to the difference between $\Delta_{IL}^{W}\phi_{C^+}^{\ominus}$ and $\Delta_{IL}^{W}\phi_{A^-}^{\ominus}$ through

$$\ln K_s^W = \frac{F}{RT}\left(\Delta_{IL}^{W}\phi_{C^+}^{\ominus} - \Delta_{IL}^{W}\phi_{A^-}^{\ominus}\right). \tag{4.2.5}$$

The length of the horizontal bar in Fig. 4.2.3 is thus a direct measure of K_s^W.

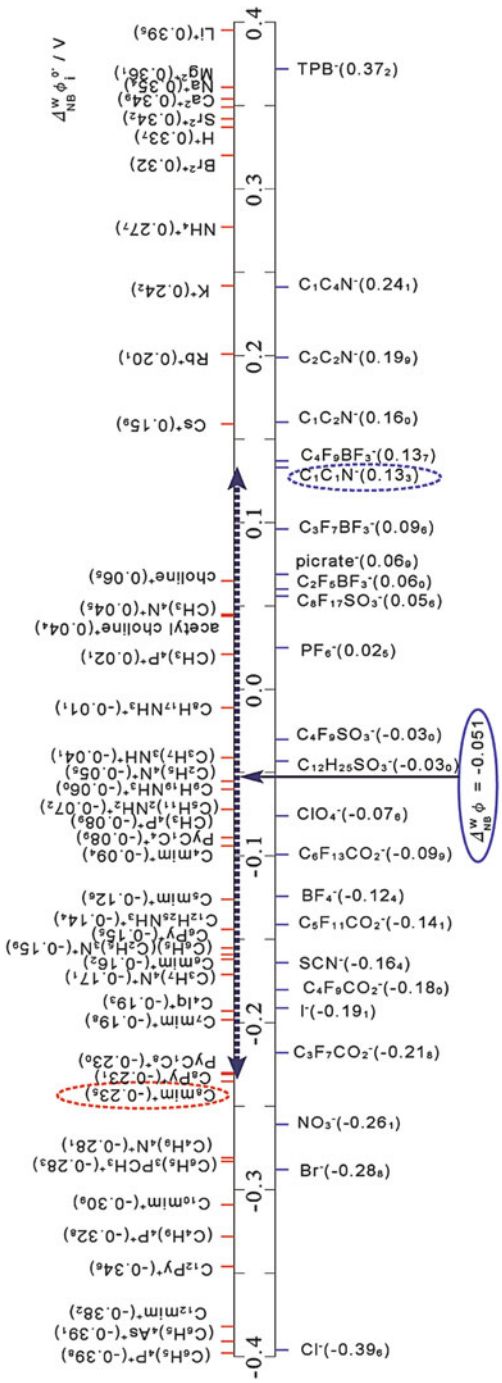

Fig. 4.2.3 Apparent standard ion transfer potentials of some hydrophobic ions across nitrobenzene and water interface for preparing moderately hydrophobic ionic liquids 25 °C [43] $C_n mim^+$: 1-alkyl-3-methylimidazolium (alkyl = butyl ($n = 4$), pentyl($n = 5$), hexyl($n = 6$), heptyl($n = 7$), octyl($n = 8$), decyl ($n = 10$), dodecyl($n = 12$)); $PyC_1C_n^+$: *N*-alkyl-*N*-methylpyrrolidinium (aklyl = butyl($n = 4$), octyl($n = 8$)); C_nPy^+: *N*-alkylpyridinium (alkyl hexyl ($n = 6$), octyl($n = 8$), decyl($n = 10$), dodecyl($n = 12$)); C_nIq^+: *N*-alkyllisoquinolinium (alkyl = butyl($n = 4$), dodecyl($n = 12$), hexadecyl($n = 14$)); $C_mC_nN^-$ (bis (perfluoroalkanesulfonyl)amide: *m* and *n* stand for the number of difluoromethylene moiety). The value after each abbreviated name of ion indicates the value of $\Delta^{W}_{NB}\phi^{o'}_{i}$ in V

Table 4.2.1 Mutual solubility of ionic liquid and water for moderately hydrophobic ionic liquids suitable to ionic liquid salt bridge at 25 °C

Ionic liquid	T_g / K	S_{IL} / mmol dm^{-3}	S_W / wt%
$[C_6mim^+][C_1C_1N^-]$		4.9	1.6
$[C_6mim^+][C_2C_2N^-]$		1.1	1.1
$[C_8mim^+][C_1C_1N^-]$		0.9	0.9
$[C_8mim^+][C_2C_2N^-]$		0.4	0.5
$[TBMOEP^+][C_2C_2N^-]$		0.2	0.8
$[C_{1,6}pyrr^+][C_2C_2N^-]$		~0.2	<0.5
$[C_{1,8}pyrr^+][C_2C_2N^-]$		~0.2	<0.5

Importantly, the electrochemical polarizability of the interface is inversely proportional to the solubility of the ILSB-constituent salt in water [31]. The electrical resistance may not be a serious problem in conventional potentiometry with a high-input impedance electrometer or voltammetry with a potentiostat. Nonetheless, it is preferable to lower the polarizability of the ILSB|W interface as low as possible to minimize the interference by other ions on $\Delta_{IL}^{W}\phi$ determined by Eq. (4.2.3).

$[C_nmim^+][C_1C_1N^-]$: 1-alkyl-3-methylimidazolium bis(trifluoromethanesulfonyl)amide (hexyl ($n = 6$), octyl($n = 8$)); $[C_nmim^+][C_2C_2N^-]$: 1-alkyl-3-methylimidazolium bis(pentafluoroethanesulfonyl)amide (hexyl ($n = 6$), octyl ($n = 8$)); $[TBMOEP^+][C_2C_2N^-]$: tributylmethoxyethylphosphonium bis(pentafluoroethanesulfonyl)amide; $[C_{2,n}pyrr^+][C_2C_2N^-]$: *N*-alkyl-*N*-methylpyrrolidinium bis(pentafluoroethanesulfonyl)amide (hexyl ($n = 6$), octyl($n = 8$)).

Table 4.2.1 lists the solubility of some moderately hydrophobic ILs suitable to ILSBs in water. A practical range of the solubility of ILSB-constituent ILs is between a few tenth and a few mmol dm^{-3}. The lower end, ~0.1 mmol dm^{-3}, is mainly for of ILSBs specialized for low-ionic-strength samples, and the higher end is of ILSBs for samples with high ionic strength or those that may contain a certain level of hydrophobic ions.

4.2.2.6 Dissolution of Water in ILSB

Usually, the more hydrophobic an IL, the higher the solubility of water in the IL is. The solubility of water in moderately hydrophobic ILs suitable to an ILSB is typically 0.5–1 weight percent, which corresponds to the mole fraction of water being ca. 0.2 at room temperature, and increases with temperature [44–46]. A high content of water in an ILSB is unwelcome. When the ambient temperature varies during use or storage of ILSB, tiny water droplets may appear as suspensions in the ILSB or may absorb more water from a sample solution than that at a normal operating temperature. Such variability of water content in ILSB can be deleterious for the reproducible liquid junction potential, and minimization of water dissolution is preferable. However, the use of more hydrophobic ILs than those exemplified in

Table 4.2.1 is bound by the electrochemical polarizability and the vulnerability to interfering ions, as described above.

4.2.2.7 ILSB Based on Mixed ILs

A simple possibility to overcome the above dichotomy regarding the water dissolution in ILSB is the use of a mixture of two ionic liquids, a very hydrophobic and a moderately hydrophobic IL [47]. The former works simply as a hydrophobic medium to suppress water dissolution and the latter does as a potential determining salt [47].

A mixture of pentyltripropylammonium bis(pentafluoroethanesulfonyl)amide as a potential determining salt and heptadecafluorodecyltrioctylphosphonium tetrakis [3,5-bis (trifluoromethyl)phenyl]borate as a very hydrophobic liquid matrix shows a reproducibility of $\pm$ 0.6 mV (95 % confidence interval) for aqueous KCl solutions in the range between 0.5 mmol dm^{-3} and 0.5 mol dm^{-3}; the average excursion of E over 1 h is within $\pm$ 0.3 mV [47]. Moreover, such a strategy of using mixed ILs for ILSB allows us to employ moderately hydrophobic salts having melting points higher than room temperature or target temperature for use as ILSBs because of the lower melting points of the mixtures than their component salts.

4.2.3 Preparation of ILSB

4.2.3.1 Selection of Ionic Liquids for ILSB

Guidelines in selecting ionic liquids for ILSB with regard to the value of $\Delta_{IL}^{W}\phi_{ILSB}$, the mutual solubility, and the diffusion potential are described in the preceding sections. In addition, there are several factors to be considered.

4.2.3.2 Chemical Stability and Purity of ILs

Moderately hydrophobic ILs for ILSB are preferably inert. However, ILs are not necessarily chemically "innocent" [48, 49], nor green [50, 51]. The electrochemical stability of cation and anions used for moderately hydrophobic ILs in its ionic liquid states has been studied extensively in the relevance with their applications to electrochemical devices. Aside from impurities, such as water, both ends of the polarization windows are limited by redox reactions of cations and anions [52, 53]. For our interest in ILSB aimed to be used in aqueous solutions, ILSB-constituent ions dissolved in aqueous sample solutions are electrochemically inactive within potential window available in aqueous solutions.

Anions

PF_6, which has been used for preparing moderately hydrophobic ILs, is hydrolyzed in water, though its rate is slower than that of BF_4^- [54, 55]. A more hydrophobic tri(pentafluoroethyl)trifluorophosphate is more stable against hydrolysis in water, but the hydrolysis is discernible [54]. These anions are therefore not suitable for ILSB. Perfluoroalkyltrifluoroborates are stable in water and tuning of hydrophobicity is feasible by changing the length of perfluoroalkane moiety [56].

Bis(perfluoroalkanesulfonyl)amides are stable in water. The hydrophobicity can be tuned by changing the length of the perfluoroalkyl moieties. The complexation with metal ions in IL is probably weak, but the ion pair formation with transition metal ions, such as Cd^{2+}, can be appreciable when the concentrations of metal ions are high. $\Delta_{IL}^{W}\phi_{ILSB}$ is then affected by such extraction of the ions in ILSB [57].

Cations

Quaternary ammonium and phosphonium, as well as dialkylimidazolium ions, are typical ions used for preparing moderately hydrophobic ILs. It is known that these ions decompose through Hofmann elimination or ylide formation in strongly alkaline environment, e.g., solid alkyltrimethylammonium hydroxide hydrate, even at room temperature and the decomposition rate increases with elevating temperature [58, 59]. However, these cations are stable in an aqueous alkaline solution [58, 60], and, hence, ILSBs made of these ions are stable when they are in contact with an aqueous alkaline solution, e.g., 0.1 mol dm^{-3} NaOH.

Purification

The purity of ILs is an important issue for characterization of the physicochemical properties of ILs. For example, in application of $[TBMOEP^+][C_2C_2N^-]$ (see Table 4.2.1) to an ILSB, the removal of unreacted tributylphosphine and other impurities is essential to obtain a stable liquid junction potential [61].

For moderately hydrophobic ILs, washing of ILs with copious water repeatedly, typically 30 times, is highly recommended to remove extraneous ions and other hydrophilic impurities. Decolorization based on a silica-charcoal column [62] or a treatment with charcoal [63] is simple yet powerful, though the loss of the IL is considerable.

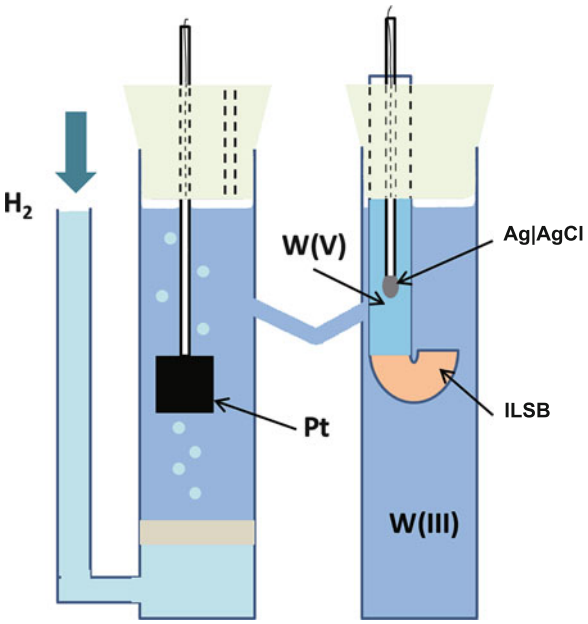

Fig. 4.2.4 Illustration of cell configuration for a fluid ILSB inserted between a hydrogen electrode and a Ag|AgCl electrode, corresponding to cell (B)

4.2.3.3 Type of Liquid Junction

The thermodynamic nature of the working mechanism of ILSB liberates us from concern about the shape of the liquid junction in designing ILSBs. This is a distinctive advantage of ILSB over KClSB.

It has been shown by using cell (A) that the ILSB made of [$TBMOEP^+$] [$C_2C_2N^-$] gives a stable $\Delta_{IL}^{W}\phi_{ILSB}$ down to 1 μmol dm^{-3} LiI, NaI, KI, and HI [10, 14]. This stability of $\Delta_{IL}^{W}\phi_{ILSB}$ of the ILSB at low-ionic-strength solutions allows us to more reliably estimate single ion activities. For example, by inserting [$TBMOEP^+$][$C_2C_2N^-$] in a Harned cell,

I	II	III	IV	V	VI	
Pt	H_2 (*g*), aqueous HCl soln.	ILSB	Aqueous HCl soln.	AgCl	Ag	(B)

it is possible to determine the activity coefficients of hydrogen ions and chloride ions, independently, by changing the concentration of HCl in phase IV, while keeping the solution composition in phase II, or vice versa [26]. The shape of the cell is shown in Fig. 4.2.4, in which the liquid ILSB is in the bottom of a J-shaped glass tube in the right-hand side compartment of the cell.

Another simple water-jacketed cell is illustrated in Fig. 4.2.5, in which a liquid ILSB is supported on a glass frit of ca. 4 mm thickness. The upper aqueous phase is conveniently changed, while the lower aqueous phase remains unchanged. It is important to avoid electrical leakage between upper and lower solutions through

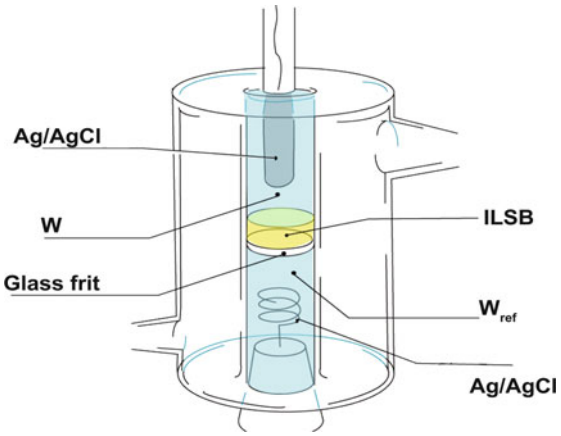

Fig. 4.2.5 Illustration of a cell configuration for a fluid ILSB supported by a glass frit

inner glass wall. A way to minimize this effect is the silanization of the inner glass wall where the IL is in contact.

4.2.3.4 Gelation of ILSB

In most of practical applications of ILSB-equipped reference electrodes, it is preferable to have a solidified ILSB. For example, 1-methyl-3-octylimidazolium bis(trifluoromethanesulfonyl)amide, $[C_8mim^+][C_1C_1N^-]$, is gelled at room temperature with poly (vinylidenefluoride-*co*-hexafluoropropylene) [64, 65] (PVDF-HFP), when the weight percent of $[C_8mim^+][C_1C_1N^-]$ is below 80.

A 1:1 mixture of an IL and PVDF-HFP has been used for ILSB. There is no difference in performance of gelled and non-gelled ionic liquids for ILSB [23]. A gelled ILSB membrane can be mounted in a membrane holder, as the one used for liquid-membrane-type ion-selective electrodes [66].

Gelation of ionic liquid with PVDF-HFP apparently suppresses the intake of water into ILSB and improves the reproducibility of $\Delta_{IL}^{W}\phi$. The IL gradually leaches out from the gelled ILSB into a bathing aqueous solution, which causes a gradual thinning of the membrane and eventual loss of its function in a long time use.

An example of a gelled ILSB assembled in a glass composite electrode for pH measurements is shown in Fig. 4.2.6 [67]. A torus-shaped ring of a gelled IL is held between the upper and lower plastic cylinders through two O-rings. The inner wall of the IL ring is in contact with an internal solution. Accurate determination of the pH of dilute sulfuric acid solutions has been successfully made with this composite

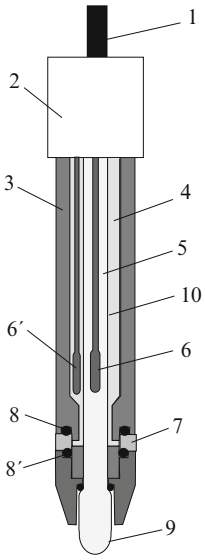

Fig. 4.2.6 Structure of a glass composite electrode equipped with a gelled ILSB torus ring [67]. *1*: electric cable; *2*: a plastic cap; *3*: cylindrical plastic body; *4*: internal solution of reference electrode; *5*: internal solution of glass electrode; *6* and *6′*: Ag/AgCl electrodes; *7*: gelled ILSB; *8* and *8′*: silicon O-ring; *9*: glass membrane; *10*: stem glass tube

electrode [67]. A smaller version of a glass composite pH electrode equipped with an ILSB is commercially available.

4.2.3.5 ILSB-Coated Reference Electrodes

The presence of an internal solution is the bottleneck in miniaturization of reference electrodes. A reference electrode with gelled ILSB coated on a Ag|AgCl electrode has been proposed [68] in which a gelled ILSB layer in contact with AgCl is saturated with AgCl.

As an example of a miniature reference electrode, Fig. 4.2.7 illustrates a glass capillary, with 150 μm inner diameter at the tip, filled with an non-gelled $[C_8mim^+][C_1C_1N^-]$. A AgCl-coated silver wire is inserted in the capillary.

Figure 4.2.8 shows cyclic voltammograms in the presence (solid line) and absence (dotted line) of 1 mmol dm^{-3} ferrocenedimethanol in an aqueous KCl solution. Voltammograms in Fig. 4.2.8a were recorded with the miniature $[C_8mim^+][C_1C_1N^-]$-coated AgCl reference electrode, and those in Fig. 4.2.8b are obtained with a conventional Ag|AgCl electrode.

Although a calibration of potential is required to compare data obtained with a ILSB-coated electrodes with those obtained with traditional reference electrodes, such a small reference electrode will find certain applications, e.g., electrophysiology.

Fig. 4.2.7 Ag|AgCl electrode inserted in $[C_8mim^+][C_1C_1N^-]$ filled with a glass capillary with 150 μm inner diameter at the tip [69]

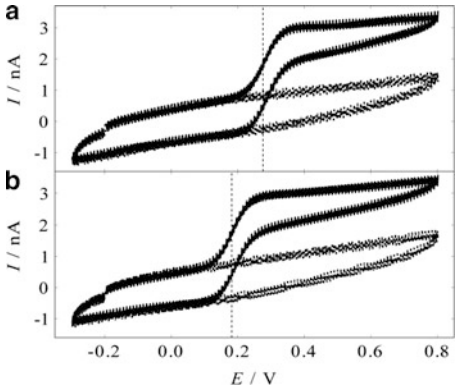

Fig. 4.2.8 Cyclic voltammograms for oxidation–reduction of ferrocenedimethanol in 0.1 mol dm^{-3} KCl at 15 μm diameter Pt disk electrode referred to Ag|AgCl electrode inserted in $[C_8mim^+][C_1C_1N^-]$ filled with a glass capillary with 150 μm inner diameter at the tip (**a**) and referred to a conventional Ag|AgCl electrode in a saturated KCl solution (**b**). Counterelectrode is a 6-mm diameter Pt electrode in both cases. Scan rate: 50 mV s^{-1} [69]

4.2.4 Some Remarks on ILSB

4.2.4.1 Difference and Similarity of KClSB and ILSB

Salt bridge is an electrochemical device interposed between two electrolyte solutions of different compositions to isolate two solutions from each other while keeping the electrical connection, and hence is intrinsically nonthermodynamic in nature. The reason is easily seen in the case of KClSB; a system of an internal solution, KClSB, and a sample solution eventually end up with a homogeneous solution phase, sooner or later. In the case of ILSB, because of finite solubility of any kind of ions into the ILSB, the compositions of the two solution phases eventually become equal at equilibrium. Both solution phases are saturated with ILSB-constituting ions, whereas the ILSB is saturated with the components originally contained in the sample solution. There is therefore no fundamental or thermodynamically distinctive difference between KClSB and ILSB, although the working principle of minimizing the liquid junction potential between two electrolyte solutions is conceptually different [23]. Both KClSB and ILSB are useful only before, well before, the system reaches a thermodynamic equilibrium. In this sense, the ILSB is based on a quasi-thermodynamic basis. However, even technically, the difference between them is substantial, and is of considerable significance inasmuch as only technically both find raison d'etre. Aside from technical advantages of ILSB over KClSB described in Introduction (see also [23]) originated with the quasi-thermodynamic nature of ILSB, there are some more points worth mentioning.

The liquid junction potential at the interface between an ILSB and an aqueous solution of a simple mineral acid or an alkali hydroxide is distinctively more stable and accountable than that in the case of KClSB with regard to a much wider concentration range of an electrolyte, more than five orders of magnitude, and much wider acidity range, about 14 pH units. Such stability of phase-boundary potential over the wide pH range at ILSB stems from the working principle based on the distributing potential, distinguished from the diffusion potential to which the difference in the mobility of H^+ and OH^- and that of other ions contributes significantly, and enables many experiments in chemistry of electrolyte solutions that have been not possible or not reliable enough with KClSB.

The magnitude of the contamination of a sample solution by dissolution of electrolytes from an SB is more than three orders of magnitude lower in ILSB. These constitute the basis of reliable estimates of single ion activities [24, 26], including pH measurements, and other subjects related to liquid junction potential.

4.2.4.2 Comparison of Electrode Potentials Obtained with KClSB and ILSB

A comparison of the cell voltage data obtained with an ILSB or the potential of a working electrode with respect to an ILSB-equipped reference electrode, such as half-wave potential in voltammetry, with those obtained with an KClSB is made

without any difficulty. A cell voltage of the cell (B), E, that is, the electrode potential of the working electrode

I	II	III	IV	V	VI	
Ag	Ag X	a mol dm^{-3} MX	SB	Sample solution	Working electrode	(B)

does not depend on the type of the salt bridge, as long as the salt bridge works ideally, that is, it nullifies the liquid junction potential otherwise formed at the direct contact of phases III and V without disturbing the compositions of II and V. Therefore, there is no conceptual difference in E obtained with ILSB and that obtained with KClSB.

Many of half-wave potentials and formal potentials in electrochemistry have been compiled with respect to a calomel electrode or Ag|AgCl electrode in contact with a concentrated KCl solution (phases III and IV in cell (B)), e.g., saturated or 3 mol dm^{-3} KCl. By replacing the KClSB with and ILSB in cell (B), however, we would not be able to directly compare the electrode potential because of a possible dissolution of K^+ in ILSB at such high concentrations. It is recommended to examine E at a lower KCl concentration in phase III in cell (B) with an ILSB, e.g., $a = 0.01$, and then convert E with a known difference in the electrode potential of Ag|AgCl electrodes at 10 mmol dm^{-3} and saturated KCl.

4.2.4.3 Challenges in Future Studies

The reproducibility of $\Delta_{\mathrm{IL}}^{\mathrm{W}}\phi_{\mathrm{ILSB}}$ of one type of ILSB prepared and tested on different days is 0.6 mV (95 % confidence interval) [47]. This is comparable or slightly less reproducible than that reported in the liquid junction potential of KClSB at the optimized conditions [70, 71]. Further studies seem to be required to experimentally establish the highly reproducible liquid junction potential at ILSB. On the one hand, the wide degree of freedom in selecting ILs for ILSB allows us to optimize the composition of ILSBs depending on particular purposes. It is preferable, on the other hand, to narrow them down to one or few ILs for the ILSB on which more extensive and intensive studies are to be made for standardizing this new salt bridge.

Temperature and pressure dependence of the performance of ILSB have not been elucidated. There is no conceivable obstacle in applying ILSB at wider temperature and pressure conditions.

The use of ILSB in organic solvents has not been challenged. Because ILs are considerably, if not completely, miscible with polar protic and aprotic solvents, the formation of phase-separated systems is not expected. Even in such cases, ILSBs described above presumably work as conventional salt bridges based on diffusion potential, as is the case of KClSB. As ILs are not completely miscible with nonpolar organic solvents, ILSB should work to correlate electrode potentials in such solvents with those in aqueous solutions.

References

22. Kakiuchi T, Tsujioka N, Kurita S, Iwami Y (2003) Electrochem Commun 5 (2):159–164
23. Kakiuchi T, Yoshimatsu T (2006) Bull Chem Soc Jpn 79(7):1017–1024
24. Shibata M, Sakaida H, Kakiuchi T (2011) Anal Chem 83(1):164–168
25. Kakiuchi T (2011) J Solid State Electrochem 15(7–8):1661–1671
26. Sakaida H, Kakiuchi T (2011) J Phys Chem B 115(45):13222–13226
27. Nernst W (1889) Z Phys Chem 8:129–181
28. Kakiuchi T (2001) J Electroanal Chem 496(1–2):137–142
29. Kolthoff IM, Miller CS (1940) J Am Chem Soc 62:2171–2174
30. Kakiuchi T, Senda M (1984) Bull Chem Soc Jpn 57(7):1801–1808
31. Kakiuchi T, Tsujioka N (2007) J Electroanal Chem 599(2):209–212
32. Yoshimatsu T, Kakiuchi T (2007) Anal Sci 23(9):1049–1052
33. Henderson P (1907) Z Phys Chem 59(1):118–127
34. Dickinson EJF, Freitag L, Compton RG (2010) J Phys Chem B 114(1):187–197
35. Sakaida H, Kitazumi Y, Kakiuchi T (2010) Talanta 83(2):663–666
36. Fujino Y, Kakiuchi T (2011) J Electroanal Chem 651(1):61–66
37. Fujino Y, Kakiuchi T (2010) Unpublished work
38. Fraenkel D (2011) J Phys Chem B 115:557–568
39. Sakaida Y, Kakiuchi T, to be published
40. Kakiuchi T, Obi I, Senda M (1985) Bull Chem Soc Jpn 58(6):1636–1641
41. Abraham MH, Acree WE (2006) Green Chem 8(10):906–915
42. Kakiuchi T (2007) Anal Chem 79(17):6442–6449
43. Tanaka S, Matsuoka Y, Belkada F, Kitazumi Y, Suzuki A, Nishi N, Kakiuchi T, in preparation
44. Freire MG, Carvalho PJ, Gardas RL, Marrucho IM, Santos LMNBF, Coutinho JAP (2008) J Phys Chem B 112(6):1604–1610
45. Ferreira AR, Freire MG, Ribeiro JC, Lopes FM, Crespo JG, Coutinho JAP (2011) Ind Eng Chem Res 50(9):5279–5294
46. Rehak K, Moravek P, Strejc M (2012) Fluid Phase Equil 316:17–25
47. Zhang LM, Miyazawa T, Kitazumi Y, Kakiuchi T (2012) Anal Chem 84 (7):3461–3464
48. Dupont J, Spencer J (2004) Angew Chem Int Ed 43(40):5296–5297
49. Chowdhury S, Mohan RS, Scott JL (2007) Tetrahedron 63(11):2363–2389
50. Frade RFM, Afonso CAM (2010) Hum Exp Toxicol 29(12):1038–1054
51. Petkovic M, Seddon KR, Rebelo LPN, Pereira CS (2011) Chem Soc Rev 40 (3):1383–1403
52. Opallo M, Lesniewski A (2011) J Electroanal Chem 656(1–2):2–16
53. Silvester DS (2011) Analyst 136(23):4871–4882
54. Schmidt M, Heider U, Kuehner A, Oesten R, Jungnitz M, Ignat'ev N, Sartori P (2001) J Power Sources 97–98:557–560
55. Freire MG, Neves CMSS, Marrucho IM, Coutinho JAP, Fernandes AM (2010) J Phys Chem A 114(11):3744–3749
56. Nishi N, Suzuki A, Kakiuchi T (2009) Bull Chem Soc Jpn 82(1):86–92

57. Yoshimatsu T (2007) Thesis of the master's degree, Department of Energy and Hydrocarbon Chemistry, Graduate School of Engineering, Kyoto University
58. Macomber CS, Boncella JM, Pivovar BS, Rau JA (2008) J Therm Anal Calorim 93(1):225–229
59. Edson JB, Macomber CS, Pivovar BS, Boncella JM (2012) J Membr Sci 399:49–59
60. Ye YS, Elabd YA (2011) Macromolecules 44(21):8494–8503
61. Sakaida H (2010) Master's Thesis of Graduate School of Engineering, Department of Energy and Hydrocarbon Chemistry, Kyoto University
62. Earle MJ, Gordon CM, Plechkova NV, Seddon KR, Welton T (2007) Anal Chem 79(2):758–764
63. Stark A, Behrend P, Braun O, Muller A, Ranke J, Ondruschka B, Jastorff B (2008) Green Chem 10(11):1152–1161
64. Fuller J, Breda AC, Carlin RT (1997) J Electrochem Soc 144(4):L67–L70
65. Fuller J, Breda AC, Carlin RT (1998) J Electroanal Chem 459(1):29–34
66. Shibata M, Yamanuki M, Iwamoto Y, Nomura S, Kakiuchi T (2010) Anal Sci 26(11):1203–1206
67. Shibata M, Kato M, Iwamoto Y, Nomura S, Kakiuchi T, submitted for publication
68. Kakiuchi T, Yoshimatsu T, Nishi N (2007) Anal Chem 79(18):7187–7191
69. Kitazumi Y, Kakiuchi T (2012) Unpublished
70. Covington AK, Rebelo MJF (1987) Anal Chim Acta 200(1):245–260
71. Davison W, Covington AK, Whalley PD (1989) Anal Chim Acta 223 (2):441–447

References

References to Sect. 4.1

1. Bates RG, Pinching GD, Smith ER (1950) J Res Natl Bur Stand 45:418–429
2. Material safety data sheet (21 April 2009) 6.2308.040 Idrolyte. Metrohm Ltd., CH-9101 Herisau, Switzerland
3. Smith TJ, Stevenson KJ (2007) Reference electrodes. In: Zoski CG (ed) Handbook of electrochemistry. Elsevier, Amsterdam, p 96
4. Data sheet: Vycor® Brand Porous Glass 7930, Corning Incorporated, 2001
5. Gille W, Enke D, Janowski F (2002) J Porous Mater 9:221–230
6. Technical speciation of pH glass electrode 6.0224.100 of Metrohm AG, Switzerland
7. Technical speciation of pH glass electrode 6.0221.100 of Metrohm AG, Switzerland
8. Technical speciations of various glass electrodes 6.01 – 6.02 of Metrohm AG, Switzerland
9. Steel BJ, Stokes JM, Stokes RH (1958) J Phys Chem 62:1514–1516
10. Fuji T, Thomas HC (1958) J Phys Chem 62:1566–1568
11. Gokarn NA, Rajurkar NS (2006) J Solut Chem 35:1673–1685
12. Darwish MIM, van der Maarel JRC, Zitha PLJ (2004) Macromolecules 37:2307–2312
13. Hasse U, Scholz F (2005) Electrochem Commun 7:173–176
14. Vahl K, Kahlert H, Scholz F (2010) Electroanalysis 22:2172–2178

15. Narayanan J, Xiong J-Y, Liu X-Y (2006) J Phys Conf Ser 28:83–86
16. Hasse U, Scholz F (2006) J Solid State Electrochem 10:380–382
17. Material safety data sheet (April 2011, Version 3) Reference Gel Electrolyte RE45. Ionode Pty Ltd, 8/148 Tennyson Memorial Avenue, Tennyson Qld 4105, Australia
18. Material safety data sheet (21 April 2009) 6.2308.030 Electrolyte KCl sat. gel. Metrohm Ltd., CH-9101 Herisau, Switzerland
19. Kindler DD, Bergethon PR (1990) J Appl Physiol 69:371–375
20. Kahlert H (2010) In: Scholz F (ed) Electroanalytical methods. Guide to experiments and applications, 2nd edn. Springer, Berlin, p 305
21. Kahlert H (2010) In: Scholz F (ed) Electroanalytical methods. Guide to experiments and applications, 2nd edn. Springer, Berlin, p 304

References to Sect. 4.2

22. Kakiuchi T, Tsujioka N, Kurita S, Iwami Y (2003) Electrochem Commun 5(2):159–164
23. Kakiuchi T, Yoshimatsu T (2006) Bull Chem Soc Jpn 79(7):1017–1024
24. Shibata M, Sakaida H, Kakiuchi T (2011) Anal Chem 83(1):164–168
25. Kakiuchi T (2011) J Solid State Electrochem 15(7–8):1661–1671
26. Sakaida H, Kakiuchi T (2011) J Phys Chem B 115(45):13222–13226
27. Nernst W (1889) Z Phys Chem 8:129–181
28. Kakiuchi T (2001) J Electroanal Chem 496(1–2):137–142
29. Kolthoff IM, Miller CS (1940) J Am Chem Soc 62:2171–2174
30. Kakiuchi T, Senda M (1984) Bull Chem Soc Jpn 57(7):1801–1808
31. Kakiuchi T, Tsujioka N (2007) J Electroanal Chem 599(2):209–212
32. Yoshimatsu T, Kakiuchi T (2007) Anal Sci 23(9):1049–1052
33. Henderson P (1907) Z Phys Chem 59(1):118–127
34. Dickinson EJF, Freitag L, Compton RG (2010) J Phys Chem B 114(1):187–197
35. Sakaida H, Kitazumi Y, Kakiuchi T (2010) Talanta 83(2):663–666
36. Fujino Y, Kakiuchi T (2011) J Electroanal Chem 651(1):61–66
37. Fujino Y, Kakiuchi T (2010) Unpublished work
38. Fraenkel D (2011) J Phys Chem B 115:557–568
39. Sakaida Y, Kakiuchi T, to be published
40. Kakiuchi T, Obi I, Senda M (1985) Bull Chem Soc Jpn 58(6):1636–1641
41. Abraham MH, Acree WE (2006) Green Chem 8(10):906–915
42. Kakiuchi T (2007) Anal Chem 79(17):6442–6449
43. Tanaka S, Matsuoka Y, Belkada F, Kitazumi Y, Suzuki A, Nishi N, Kakiuchi T, in preparation
44. Freire MG, Carvalho PJ, Gardas RL, Marrucho IM, Santos LMNBF, Coutinho JAP (2008) J Phys Chem B 112(6):1604–1610
45. Ferreira AR, Freire MG, Ribeiro JC, Lopes FM, Crespo JG, Coutinho JAP (2011) Ind Eng Chem Res 50(9):5279–5294
46. Rehak K, Moravek P, Strejc M (2012) Fluid Phase Equil 316:17–25
47. Zhang LM, Miyazawa T, Kitazumi Y, Kakiuchi T (2012) Anal Chem 84(7):3461–3464
48. Dupont J, Spencer J (2004) Angew Chem Int Ed 43(40):5296–5297
49. Chowdhury S, Mohan RS, Scott JL (2007) Tetrahedron 63(11):2363–2389
50. Frade RFM, Afonso CAM (2010) Hum Exp Toxicol 29(12):1038–1054
51. Petkovic M, Seddon KR, Rebelo LPN, Pereira CS (2011) Chem Soc Rev 40(3):1383–1403
52. Opallo M, Lesniewski A (2011) J Electroanal Chem 656(1–2):2–16
53. Silvester DS (2011) Analyst 136(23):4871–4882
54. Schmidt M, Heider U, Kuehner A, Oesten R, Jungnitz M, Ignat'ev N, Sartori P (2001) J Power Sources 97–98:557–560

55. Freire MG, Neves CMSS, Marrucho IM, Coutinho JAP, Fernandes AM (2010) J Phys Chem A 114(11):3744–3749
56. Nishi N, Suzuki A, Kakiuchi T (2009) Bull Chem Soc Jpn 82(1):86–92
57. Yoshimatsu T (2007) Thesis of the master's degree, Department of Energy and Hydrocarbon Chemistry, Graduate School of Engineering, Kyoto University
58. Macomber CS, Boncella JM, Pivovar BS, Rau JA (2008) J Therm Anal Calorim 93 (1):225–229
59. Edson JB, Macomber CS, Pivovar BS, Boncella JM (2012) J Membr Sci 399:49–59
60. Ye YS, Elabd YA (2011) Macromolecules 44(21):8494–8503
61. Sakaida H (2010) Master's Thesis of Graduate School of Engineering, Department of Energy and Hydrocarbon Chemistry, Kyoto University
62. Earle MJ, Gordon CM, Plechkova NV, Seddon KR, Welton T (2007) Anal Chem 79 (2):758–764
63. Stark A, Behrend P, Braun O, Muller A, Ranke J, Ondruschka B, Jastorff B (2008) Green Chem 10(11):1152–1161
64. Fuller J, Breda AC, Carlin RT (1997) J Electrochem Soc 144(4):L67–L70
65. Fuller J, Breda AC, Carlin RT (1998) J Electroanal Chem 459(1):29–34
66. Shibata M, Yamanuki M, Iwamoto Y, Nomura S, Kakiuchi T (2010) Anal Sci 26(11):1203–1206
67. Shibata M, Kato M, Iwamoto Y, Nomura S, Kakiuchi T, in preparation
68. Kakiuchi T, Yoshimatsu T, Nishi N (2007) Anal Chem 79(18):7187–7191
69. Kitazumi Y, Kakiuchi T (2012) Unpublished
70. Covington AK, Rebelo MJF (1987) Anal Chim Acta 200(1):245–260
71. Davison W, Covington AK, Whalley PD (1989) Anal Chim Acta 223(2):441–447

Chapter 5
Reference Electrodes for Aqueous Solutions

5.1 The Hydrogen Electrode

Petra Spitzer and Samuel Wunderli

The standard hydrogen electrode (SHE) acts as a primary reference in electrochemistry. The standard potentials of all other reference electrodes are linked to that of the SHE at the same temperature. The SHE contribution to the cell potential is by convention zero at all temperatures (see Chap. 1).

The IUPAC (International Union of Pure and Applied Chemistry) defines the SHE in 2008 [1]: "The standard hydrogen electrode consists of a platinum electrode in contact with a solution of H^+ at unit activity and saturated with H_2 gas with a fugacity referred to the standard pressure $p^\ominus$ of 10^5 Pa.[1]" It is assumed that the hydrogen ions at an activity of 1 mol kg^{-1} have no interactions with other ions.

In textbooks and scientific publications often the expression normal hydrogen electrode (NHE) is used as synonym for SHE. Occasionally [3] it is stated that the only difference between the two standards is the reference to standard state pressure: one atm for the NHE and one bar for the SHE. This is not correct. The NHE is the historical standard suggested by Nernst in 1889 [4]. Nernst defined the NHE as a metal in contact with a solution saturated with hydrogen gas at 1 atm partial

[1] The value for $p^\ominus = 100$ kPa (standard state pressure) is the IUPAC recommended value since 1982 [2]. Prior to 1982 the standard pressure was usually taken to be $p^\ominus = 101{,}325$ Pa (=1 atm, called the standard atmosphere). In the primary method for pH and general in electrochemistry $p^\ominus = 101{,}325$ Pa is still the preferred standard.

P. Spitzer (✉)
Physikalisch-Technische Bundesanstalt (PTB), Bundesallee 100, 38116 Braunschweig, Germany
e-mail: petra.spitzer@ptb.de

S. Wunderli
METAS, Chemistry, Lindenweg 50, CH-3003 Bern-Wabern, Switzerland
e-mail: samuel.wunderli@metas.ch

G. Inzelt et al. (eds.), *Handbook of Reference Electrodes*,
DOI 10.1007/978-3-642-36188-3_5,

pressure and containing 1 mol L^{-1} sulfuric acid. As the concept of activity was not yet developed at that time the definition is related to concentration. Furthermore the sufuric acid could cause high liquid junction potentials and limit the reproducibility of the electrode/solution interface [5].

In contrast the SHE is an ideal device and cannot be rigorously realized experimentally. For the practical realization the standard potential of the hydrogen electrode is not measured at standard conditions but recalculated to H^+ at unit activity and 10^5 Pa. These electrodes are often called reversible hydrogen electrodes (RHE). The acronym RHE is also used for relative hydrogen electrode. In this special case both electrodes, the hydrogen reference electrode and the electrode to be studied, are immersed in the same electrolyte. In this way the junction potential between the reference and the sensing electrode is reduced [6].

The classical platinum hydrogen electrode consists of a platinum wire connected with a platinum "flag" of ~1 cm^2. In order to increase the effective surface finely divided platinum, so-called platinum black, is electrochemically precipitated on the platinum sheet.

The electrode is directly immersed in the electrolyte solution without liquid junction. In general hydrochloric acid of 0.01 or 0.001 mol kg^{-1} molality is used as electrolyte [7]. The equilibrium potential depends on the hydrogen ion activity and therefore on the pH of the sample electrolyte. The electrode surface and therefore also the solution must be saturated with hydrogen.

Hydrogen electrodes are experimentally realized in various designs [8]. The hydrogen in most cases is continuously generated from a hydrogen generator or delivered from gas cylinders. This makes the handling and maintenance cumbersome and restricts currently the application of the hydrogen electrodes to some special applications. Certainly the most important one is the determination of the standard potential of the silver/silver chloride electrodes in the standardization of pH buffer.

Hydrogen electrodes having an internal cartridge that continuously generates a low volume of hydrogen are working independently from external hydrogen sources. They are also commercially available (Hydroflex™ [9]). This design uses a carbon supported platinum catalyst as a gas diffusion electrode. Through a small channel the in situ produced hydrogen gas is brought to an inert palladium containing sensor element. The sensor electrode is immersed in the acidic electrolyte. The sample solution is separated from the electrode by a polymer membrane. The leak rate is smaller than 250 µL over 24 h. These electrodes can be used in strong acids as well as in strong alkali media [10].

A typical application of the hydrogen electrode as a reference electrode is the determination of the standard potential of other reference systems. The potential of the hydrogen electrode referred to standard conditions is stable over time. Hydrogen electrodes are therefore ideally suited for the characterization of reference electrodes in terms of their electrochemical potential and stability versus time. Reference values from the hydrogen electrode are transferred either directly or via additionally characterized reference electrodes.

The hydrogen electrode is still the basis for all pH measurements to date. The pH of the standard buffers used to calibrate pH electrodes is traced back to primary buffer solutions [11]. The primary method for pH is based on the measurement of the potential of an electrochemical cell without liquid junction, involving a selected buffer solution, a platinum hydrogen electrode, and a silver/silver chloride reference electrode. The standard potential of the silver/silver chloride electrode in hydrochloric acid at a molality of 0.01 mol kg^{-1} is determined simultaneously.

5.1.1 Practical Realization of the Hydrogen Electrode

The hydrogen electrode can be described as red/ox electrode at which molecular hydrogen is oxidized to hydrogen ions (solvated protons).

$$2H^+(aq) + 2e^- \rightarrow H_2(g) \tag{5.1.1}$$

The electrode potential is given by the Nernst equation:

$$E = E^\ominus + \frac{RT}{2F} \cdot \ln\left[\frac{(m_{H^+}\gamma_{H^+}/m^\ominus)^2}{p_{H_2}/p^\ominus}\right]. \tag{5.1.2}$$

In Eq. (5.1.2), γ_{H^+} is the molal activity coefficient of the hydrogen ion H^+ at the molality m_{H^+}, and $m^\ominus$ is a standard state, chosen to be equal to 1 mol kg^{-1}; p_{H_2} is the partial pressure of hydrogen and $p^\ominus$ the standard pressure 101,325 Pa. R is the gas constant, T the thermodynamic temperature, and F is the Faraday constant.

The equilibrium potential between the adsorbed hydrogen gas on the electrode surface and the dissolved hydrogen ions in the electrolyte at all temperatures corresponds to an electrochemical potential $E^\ominus$ of 0 V by definition (5.1.3). The hydrogen activity depends on the activity of the hydrogen ions in the electrolyte solution (5.1.4).

$$E^\ominus(H_2/H^+) = 0\,V, \tag{5.1.3}$$

$$pH = -\log a_{H^+} = -\log(m_{H^+}\gamma_{H^+}/m^\ominus). \tag{5.1.4}$$

For hydrogen electrodes having hydrochloric acid as electrolyte within the range of validity of the Debye–Hückel limiting law the mean activity coefficient of HCl ($m_{HCl} \leq 0.01$ mol kg^{-1}) is set equal to the single-ion activity coefficient of the hydrogen ion [12]. The molar mean activity coefficient of HCl, $\gamma_{\pm HCl}$, at various temperatures is best known at the molality 0.01 mol kg^{-1} [13]. These values are for instance used in the primary method for pH to determine the standard potential of the silver/silver chloride.

Fig. 5.1.1 Platinum hydrogen cell (Harned cell) designed at Physikalisch-Technische Bundesanstalt (PTB) and produced by Fa. Rettberg, Göttingen

In the primary method for pH the hydrogen electrode is combined with a silver/silver chloride reference electrode in a so-called Harned cell [14].

The primary procedure for pH is based on the measurement of the potential difference of a electrochemical cell without liquid junction, involving a selected buffer solution, a platinum hydrogen electrode, and a silver/silver chloride reference electrode, in cell I [15]:

$$\mathrm{Pt|H_2|buffer, Cl^-|AgCl|Ag} \qquad \text{(Cell I)}$$

The cell is shown in Fig. 5.1.1. and schematically depicted in Fig. 5.1.2. This special designed cell consists of a hydrogen electrode compartment containing the platinum hydrogen electrode (1), the hydrogen inlet bubbler (2), and the silver/silver chloride reference electrode (3) compartment. Both half-cells are connected by a capillary (4). No hydrogen bubbles can enter the silver/silver chloride electrode compartment. The hydrogen flows through two humidifier units (5) before entering the hydrogen electrode compartment. The hydrogen leaves the cell by the exhaust (6).

The experimental details of the primary method for pH are described elsewhere [16]. The pH of primary buffer solutions is measured in a temperature range between 5 and 80 °C.

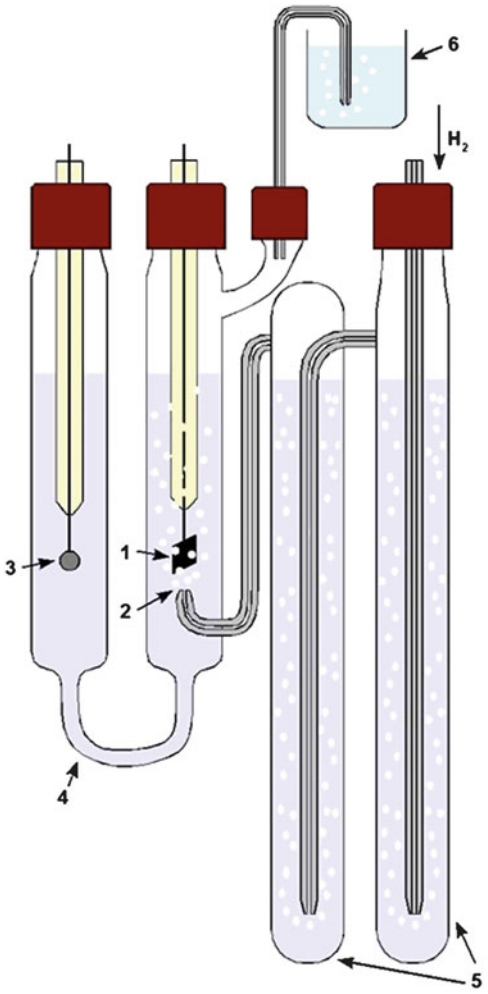

Fig. 5.1.2 Schematic representation of the platinum hydrogen cell (Harned cell). (1) Platinum hydrogen electrode, (2) inlet bubbler, (3) silver/silver chloride reference electrode, (4) capillary, (5) humidifiers, (6) exhaust

It is impossible to build absolute identical silver/silver chloride electrodes. The standard potential difference depends in some unknown way on the method of preparation [11]. For the Ag/AgCl electrodes of the thermo-electrical type [17], the cell potential variations in preparation cause variations in potential in the order of 0.2 mV. The standard potential is therefore determined simultaneously to the electrochemical potentials measured in the primary pH standard buffer solutions. Chloride ions are added to the chloride-free buffer at several chloride molalities in order to stabilize the potential of the silver–silver chloride electrode. The electrochemical cell potential consists merely of the difference in the two electrode potentials [18].

A convention is necessary to obtain the single-ion activity embodied in the definition of the pH according to Eq. (5.1.4). The application of the

Bates–Guggenheim convention is restricted to solutions of low ionic strength, $I \leq 0.1$ mol kg^{-1}. Values of pH that include all sources of uncertainty excepting that of the Bates–Guggenheim convention, as is the common practice, are considered conventional pH values, which is sufficient for most applications [18].

The standard potential $E^{\ominus}$ is determined according to Eq. (5.1.5) using cell II. The Harned cell is filled with hydrochloric acid of known molality ($m_{\mathrm{HCl}} = 0.01$ mol kg^{1}). The mean activity coefficient of HCl, $\gamma_{\pm\mathrm{HCl}}$, at various temperatures is taken from the literature [13].

$$\mathrm{Pt|\ H_2|HCl}(m)\mathrm{|AgCl|Ag} \qquad \text{(Cell II)}$$

$$E^{\ominus} = E + \left[\frac{2RT\ln(10)}{F}\right]\left(\log(m_{\mathrm{HCl}}) + \log(\gamma_{\pm\mathrm{HCl}}) + 0.25\left(\log\left(\frac{p^{\ominus}}{p_{\mathrm{H_2}}}\right)\right)\right). \quad (5.1.5)$$

γ_{HCl} is the mean activity coefficient of the hydrochloric acid at the molality m_{HCl}, $p_{\mathrm{H_2}}$ is the partial pressure of hydrogen, and $p^{\ominus}$ the standard pressure 101,325 Pa. R is the gas constant, T the thermodynamic temperature, and F is the Faraday constant. E is the cell voltage measured in cell II.

5.1.2 *Pressure Dependency of the Practical Realization of the SHE*

The electrochemical potential of hydrogen electrode depends on the partial pressure of hydrogen gas with which electrolyte is brought into equilibrium. To be able to correct the observed cell voltage to 101,325 Pa standard pressures, the partial pressure of the hydrogen must be determined. The partial pressure of hydrogen $p_{\mathrm{H_2}}$ is defined as the difference between the atmospheric pressure p_{at} and the vapor pressure of the solution at the measurement temperature. For dilute aqueous solutions not exceeding a molality of 0.5 mol kg^{-1} at 25 °C [19] the vapor pressure can be identified with that of pure water, $p_{\mathrm{H_2O}}$, at the same temperature. In addition to the atmospheric pressure a hydrostatic pressure p_{hy} appears which depends on the immersion of the hydrogen inlet bubbler in the solution. The partial pressure of hydrogen is taken from Eq. (5.1.6):

$$p_{\mathrm{H_2}} = p_{\mathrm{at}} - p_{\mathrm{H_2O}} + p_{\mathrm{hy}} \qquad (5.1.6)$$

The atmospheric pressure is measured by a pressure sensor near to the electrochemical cell.

The influence of the hydrostatic pressure is empirically investigated for aqueous solutions. According to [19] the correction of the depth of immersion h of the

hydrogen inlet bubbler (the capillary tube the hydrogen enters the electrode) is calculated in Pa by Eq. (5.1.7). Thereby h is given in mm[2].

$$p_{\mathrm{hy}} = 4 \cdot h \tag{5.1.7}$$

This correction to the hydrogen electrode potential is in the order of 10 μV for 20 mm bubbler depth up to 50 μV for 100 mm bubbler depth [19].

The partial pressure of the saturated water vapor can be calculated from the Wagner equation [20] for the highest accuracy according to Eq. (5.1.8):

$$\ln p_{\mathrm{r}} = \ln \frac{p_{\mathrm{H_2O}}}{p_{\mathrm{c}}} = \frac{1}{T_r} \cdot \left[\begin{array}{l} -7.85951783 \cdot \tau + 1.84408259 \cdot \tau^{1.5} - 11.7866497 \cdot \tau^3 \\ +22.6807411 \cdot \tau^{3.5} - 15.9618719 \cdot \tau^4 + 1.80122502 \cdot \tau^{7.5} \end{array} \right], \tag{5.1.8}$$

where p is the pressure and T is the thermodynamic temperature; the subscript c indicates the values at the critical point.

$$T_{\mathrm{c}} = 647.096\,\mathrm{K}; \quad p_{\mathrm{c}} = 22,064\,\mathrm{kPa}$$

$$\tau = 1 - T_{\mathrm{r}} = 1 - \frac{T}{T_{\mathrm{c}}} \tag{5.1.9}$$

$$p_{\mathrm{H_2O}} = p_{\mathrm{r}} \cdot p_{\mathrm{c}} \tag{5.1.10}$$

The vapor pressure of water at temperatures between 0 °C and 360 °C is also tabulated [21]. Also calculation software is available [22].

The correction to be added to the measured cell potential is assumed to be equal to the potential difference between two hydrogen electrodes immersed in the same solution. One electrode is at partial pressure $p_{\mathrm{H_2}}$ and one at 101,325 Pa. The pressure correction is calculated according to Eq. (5.1.11). The correction is in the order of −1 mV at 25 °C as can be seen from the example given below.

$$\Delta E = \frac{RT}{2F} \cdot \ln\left(\frac{p(\mathrm{H_2})}{p^{\ominus}}\right). \tag{5.1.11}$$

Example: By inserting Eq. (5.1.6) into Eq. (5.1.11), the pressure correction of the electrode potential can be calculated by (5.1.12):

$$\Delta E = \frac{RT}{2F} \cdot \ln\left(\frac{p_{\mathrm{at}} - p_{\mathrm{H_2O}} + 4h}{p^{\ominus}}\right). \tag{5.1.12}$$

[2] In [19] the empirical relation for the bubbler depth correction is given in mmHg as $0.4h/13.6$, and the depth of immersion of the bubbler in mm.

Input quantities:

$R = 8.3145$ J mol^{-1} K^{-1}, $T = 298.15$ K, $F = 96{,}485$ As mol^{-1}, $p^{\ominus} = 101,325$ Pa, $p_{at} = 101{,}308$ Pa, $p_{H_2O} = p_r \cdot p_c = 3,170$ Pa, $T_c = 647.096$ K, $1 - T/T_c = 0.5392492$, $p_r = 0.000143667$ Pa, $\ln(p_r) = -8.848009889$, $p_c = 22{,}064{,}000$ Pa

$$\Delta E = -0.9 \text{ mV}.$$

5.1.3 Purity of Hydrogen

In general hydrogen of highest purity from cylinders (purity better than 99.999 %) is used as external source. Also hydrogen generators are possible depending on the flow rate of hydrogen needed. It is important to use tight gas lines made from electroplated stainless steel to avoid contaminations especially from oxygen.

Oxygen, hydrogen sulfide, hydrogen cyanide, and carbon monoxide poison the platinum electrode. In solution volatile substances can be purged from the solution by the hydrogen gas and cations of metals more noble than hydrogen, e.g., silver and mercury can be reduced at the electrode. Some aromatic compounds like 4-hydroxynitrobenzene and benzoic acid may be reduced by hydrogen in the presence of finely divided platinum (platinum black) [7].[3] This sensitivity of the hydrogen electrode compared to other reference systems is the main reason why the SHE lost its practical relevance but still remains its role as primary reference.

5.1.4 Electrode Preparation

The hydrogen electrode is formed by bubbling hydrogen gas over platinum wire, foil, or plate, the surface of which is able to catalyze the reaction (5.1.1). The platinum can be replaced by other metals having similar properties, e.g., palladium.

The surface of the electrodes in most applications is specially treated to increase the surface and to fasten the kinetics of the electrode. In general hydrogen electrodes are platinized. The electrode surface is covered with finely divided platinum, so-called platinum black.

A common design consists of an electrode body made from an 8-mm glass tube with a sealed platinum wire of 0.5 mm diameter. A platinum sheet of 10 × 10 mm and a thickness of 0.2 mm ("flaks") is spot welded close to the center of the free end of the wire. Electrical contact is realized as solid contact between the platinum wire and a copper wire. Further details of the preparation are given in [17] and [8].

[3] The widely used buffer solution potassium hydrogen phthalate (pH = 4.1 at 25 °C) cannot be measured by the platinum hydrogen electrode due to reduction of the phthalate. In this case a palladium electrode is used.

New electrodes are cleaned before use by brief immersion in a cleaning mixture, sometimes called "50 Vol% Aqua Regia", prepared by combining three volumes of 12 mol L^{-1} hydrochloric acid with one volume of 16 mol L^{-1} nitric acid and four volumes of water. After thoroughly rinsing the electrodes in distilled water they are platinized in a simple U-tube device using a platinum wire as counter electrode in such a direction that the electrode to be coated is negative. The stabilization time of the electrode depends on the thickness of the platinum black layer. A typical value is a current density of 45 mA cm^{-2} for 540 s in 3.5 wt% hexachloroplatinic acid (H_2PtCl_6) + 0.005 wt% lead acetate ($Pb(C_2H_3O_2)_2$). The latter is added to the solution to improve the plating characterization of the electrode. The plating should be uniformly black and adhere firmly to the electrode. The potential of the hydrogen electrode is in general reproducible within 5 μV. Coverage values of about 0.5 mol L^{-1} are sufficient. A typical flow rate of the hydrogen is 0.1 mL s^{-1}. Very small flow rates can cause imperfect saturation of the solution. At high flow rates parts of the solution can purged from the solution.

References

1. Cohen ER, Cvitas T, Frey JG, Holmström B, Kuchitsu K, Marquardt R, Mills I, Pavese F, Quack M, Stohner J, StraussHL, Takami M, Thor AJ (2008) Quantities, units and symbols in physical chemistry, IUPAC Green Book, 3rd edn, 2nd printing. IUPAC & RSC Publishing, Cambridge, p 74
2. Cox JD (1982) Pure Appl Chem 54:1239
3. Wanner H, Östhols E (2000) Standards and conventions for TDB publications. OECD Nuclear Energy Agency, TDB-5, 3rd revision, p 3
4. Nernst W(1900) Z Elektrochem 7:253
5. Galster H (1991) pH measurement: fundamentals, methods, applications, instrumentation, VCH, Weinheim, p 68
6. Inzelt G (2008) Electrodes: In: Bard AJ, Inzelt G, Scholz F (eds) Electrochemical dictionary. Springer, Berlin, pp 202–205
7. Kahlert H (2010) Reference elctrodes. In: Scholz F (ed) Electroanalytical methods. Springer, Berlin, pp 263–264
8. Bates RG (1973) Determination of pH—theory and practise. Wiley, New York, pp 280–294
9. RHE. Available from http://www.gaskatel.de/english/hydroflex/theory.html
10. Schwarz J, Hörig A, Oelssner W, Vonau W, Kohnke H-J (2012) GIT and US-Patent 5′407′555 Hydrogen rod electrode with integrated hydrogen source (1995), August Winsel 56:99
11. Buck RP, Rondinini S, Baucke FGK, Camoes MF, Covington AK, Milton MJT, Mussini T, Naumann R, Pratt KW, Spitzer P, Wilson GS (2002) Pure Appl Chem 74:2169
12. Spitzer P,Werner B (2002) Anal Bioanal Chem 374:787
13. Bates RG, Robinson RA (1980) J Solution Chem 9:455
14. Harned HS, Robinson RA (1928) J Am Chem Soc 50:3157
15. Mariassy M, Pratt KW, Spitzer P (2009) Metrologia 46:199

16. Spitzer P, Eberhardt R, Schmidt I, Sudmeier U (1996) Fresenius J Anal Chem 356:178
17. Hills GJ, Ives DJG (1951) J Chem Soc 318:305
18. Spitzer P, Pratt KW (2011) J Solid State Electrochem 15:69
19. Hills GJ, Ives DJG (1961) The hydrogen electrode. In: Ives DJG, Janz GJ (eds) Reference electrodes. Theory and practice. Academic, New York, p 96
20. Wagner W, Pruss A (2002) Phys Chem Ref Data 31:387
21. Tables of physical and chemical constants. Available from http://www.kayelaby.npl.co.uk/chemistry/3_4/3_4_2.html
22. IAPWS-97. Available from http://www.iapws.org/newform.htm

5.2 Silver Electrodes

Krzysztof Maksymiuk, Agata Michalska, Anna Kisiel, and Zbigniew Galus

5.2.1 The Silver–Silver Chloride Electrode

In the group of second-kind electrodes, half-cells based on the charge transfer reactions of silver play a very important role. Silver(I) forms many ill-soluble compounds with a variety of anions. Among these compounds silver(I) halides, mainly silver chloride, were used quite intensely for the formation of electrodes with different applications including potentiometric measurements. There are advantages of these electrodes [23] such as simple preparation, possibility to make them very compact, and also possibility to use them in some cases directly in the solution, which avoids the uncertainties connected with liquid junction.

The silver–silver chloride electrode consists of silver covered by solid silver chloride which stays in contact with the solution containing chloride anions. It is probably the most frequently used reference electrode in modern electrochemical and electroanalytical practice. The most important properties which led this electrode to so wide applications were use of material which does not contaminate the medium, easy miniaturization, and possibility of using the electrode in any orientation.

Half-cell reaction of the silver–silver chloride electrode is as follows:

$$\mathrm{AgCl} + \mathrm{e}^- \rightleftharpoons \mathrm{Ag} + \mathrm{Cl}^- \tag{5.2.1}$$

This reaction is fast which is important for proper functioning of this electrode.

K. Maksymiuk • A. Michalska • A. Kisiel • Z. Galus (✉)
Department of Chemistry, University of Warsaw, Pasteura 1, 02-093 Warsaw, Poland
e-mail: kmaks@chem.uw.edu.pl; agatam@chem.uw.edu.pl; akisiel@chem.uw.edu.pl; zbgalus@chem.uw.edu.pl

The potential of this electrode is dependent on chloride ion activity according to the relation:

$$E = E^{\ominus}_{\mathrm{Ag/Ag^+}} + \frac{RT}{F}\ln a_{\mathrm{Ag^+}} = E^{\ominus}_{\mathrm{Ag/Ag^+}} + \frac{RT}{F}\ln K_{\mathrm{sol(AgCl)}} - \frac{RT}{F}\ln a_{\mathrm{Cl^-}}. \quad (5.2.2)$$

The standard potential of the silver–silver chloride electrode, when $a_{\mathrm{Cl^-}} = 1$, is expressed as a sum of the standard potential of the Ag^+/Ag system and additional term with the solubility product of AgCl, $K_{\mathrm{sol(AgCl)}}$.

As it follows from Eq. (5.2.3) the solubility product of AgCl may be calculated from precisely determined standard potentials of $E^{\ominus}_{\mathrm{Ag/AgCl}}$ and $E^{\ominus}_{\mathrm{Ag/Ag^+}}$:

$$E^{\ominus}_{\mathrm{Ag/AgCl}} = E^{\ominus}_{\mathrm{Ag/Ag^+}} + \frac{RT}{F}\ln K_{\mathrm{sol(AgCl)}}. \quad (5.2.3)$$

Different methods were used for the preparation of silver chloride electrodes. They were listed by Shumilova and Zhutaeva [23] and will be briefly discussed later.

In order to get the standard potentials of the $\mathrm{Ag|AgCl|Cl^-}$ electrode the emf of the following cell:

$$\mathrm{H_2(g)|HCl(aq)|AgCl(s)|Ag(s)} \quad (5.2.4)$$

was determined.

When all reactants in the cell (5.2.4) are in the standard states, the emf should be equal to the standard potential of the silver–silver chloride electrode. The values of the standard potential of this electrode were reported by several workers: Harned and Ehlers [24], Bates and Bower [25], and Harned and Paxton [26]. In the latter case [26] strontium chloride and hydrochloric acid were used as electrolyte. $E^{\ominus}$ values were given in those papers for certain ranges of temperature: 0–60 °C [24], 0–50 °C [26], and 0–95 °C [25].

In the careful work of Bates and Bower [25] with many measurements and many different cells applied, the standard deviations of the individual $E^{\ominus}$ values were quite low at lower temperatures, but at 95 °C they were estimated to be 0.28 mV. At 25 °C the values of $E^{\ominus}$ reported by these three groups of workers are equal: 0.2224_6 V [24], 0.2223_4 V [25], and 0.2223_9 V [26]. Bates and Bower [25] represent the $E^{\ominus}$ values obtained at different temperatures in the range 0–95 °C by the following equation:

$$E^{\ominus}(\mathrm{V}) = 0.2365_9 - 4.8564 \times 10^{-4}T - 3.4205 \times 10^{-6}T^2 + 5.869 \times 10^{-9}T^3. \quad (5.2.5)$$

One should add that Bates and Bower [25] applied, as did also Harned and Ehlers [24], so-called thermal-electrolytic electrodes (see below). Equation 5.2.5 is incorrectly given in [27].

Greeley et al. [28] have reported also the values of standard potentials of the Ag | AgCl electrode at temperatures exceeding 100 °C. These results were obtained

using the cell of type (5.2.4) and the apparatus adapted to the work at higher temperatures with thermal silver–silver chloride electrodes. We give the $E^{\ominus}$ values at selected temperatures [28]: 0.1330 V (125 °C), 0.0708 V (175 °C), and −0.0051 V (225 °C).

In general, $E^{\ominus}$ results at higher temperatures obtained by Greeley et al. [28] were represented satisfactorily by the equation:

$$E^{\ominus}(\mathrm{V}) = 0.2373_5 - 5.3783 \times 10^{-4}T - 2.3728 \times 10^{-6}T^2. \tag{5.2.6}$$

The standard error of fit of the results obtained for the range 25–200 °C to this equation was 0.19 mV. In 1978 Bates and Macaskill [29] have collected 35 values of $E^{\ominus}$ including published and non-published data (personal communications) for the cell of type (5.2.4), starting since 1953. Mostly thermal type electrodes were used in the collected works and the procedure developed over 20 years earlier by Bates and Bower. As a result the mean value was found [29], $E^{\ominus} = 0.22249$ V with a standard deviation of 0.13 mV. This $E^{\ominus}$ value may be suggested for a practical use. The specific cause of the significant variability of the results was not identified.

5.2.1.1 Preparation of the Ag | AgCl Electrodes

Following Shumilova and Zhutaeva [23] we list the methods of the preparation of the silver–silver chloride electrodes:

1. Electrolytic methods where silver and silver halides have been electrolytically deposited usually on a platinum support
2. So-called thermal electrodes formed by the thermolysis of a paste composed of silver oxide from one side and silver chlorate, bromate, or iodate from the other. Such paste was deposited on platinum and decomposed at higher temperature (500–600 °C), resulting in the formation of a mixture of silver and silver halide. Such paste deposition was repeated to get platinum well covered by silver–silver halide mixture
3. Thermoelectrolytic electrodes when the electrolytic formation of a silver halide occurs on the silver oxide paste decomposed thermally
4. Preparation of silver chloride on the silver surface, which leads to combined electrodes resulting from silver halide precipitation on the silver surface

Probably the most popular is the third method where thermal decomposition of silver oxide is combined with the following anodic formation of AgCl.

Below we present the recently described such thermoelectric procedure [30].

After careful washing of Ag and Pt wires in HNO_3 in order to remove impurities the Ag_2O paste was placed on a Pt wire (0.5 mm diameter) and heated for 1 h at 100 °C. Next heating was prolonged for 2 h at 500 °C.

Around 15 % of the deposited silver was anodically oxidized in 0.1 mol dm^{-3} HCl, at potential 50 mV more positive than the open circuit potential for each electrode. All solutions were deoxygenated by nitrogen.

As a result of extensive studies these authors have found that electrodes with AgCl prepared at constant potential exhibit considerably more reproducible values with a standard deviation of the equilibrium potential of 9 μV compared to 31 μV found for electrodes with AgCl formed with the use of a constant current.

These authors [30] have found the 189 μV difference between the average values of the set of electrodes prepared by two different methods of anodization. Also such factors as the equilibration time before measurement and porosity of the silver before anodization may influence the quality of such Ag|AgCl electrodes.

5.2.1.2 Novel Trends in the Construction of the Ag|AgCl Electrodes

Recently the influence of various procedures oriented on the optimization of Ag|AgCl electrodes was studied. Among them five different procedures of chloridizing and conditioning of such electrodes with the aim of minimizing the bias potential and increasing the long-term stability were examined [31]. Several parameters such as size and mass of electrodes, chloridization, conditioning, and storage of obtained electrodes were varied [31]. A thermal-electrolytic-type procedure of the preparation of Ag|AgCl electrodes earlier recommended by Bates was used [32]. Such electrodes were used also by other researchers [30, 31]. It was shown that the microstructure of applied AgCl influences significantly the behavior of such reference electrodes [33, 34]. Porous electrodes with a highly developed surface may have high exchange current at equilibrium which results in better reproducibility and stability of their potential [30]. However, the same authors write also about drawbacks which exhibit highly porous electrodes such as a deep penetration of the electrolyte sometimes even to the Pt support and formation of the mixed potential. Also the adsorption of impurities may increase [35].

Recently attention was paid [30] to the electrooxidation of silver deposited on a support (Pt). Silver was formed in a thermal decomposition at around 500 °C of Ag_2O in a furnace. Usually the electrooxidation was carried out in 0.1 mol dm^{-3} HCl using a constant current (usually around 1 mA), for a fixed time to pass a charge necessary for a silver conversion to AgCl in 10–25 %.

Since the shape of deposited silver may change from electrode to electrode, using constant current, also the current density may change accordingly. Therefore during anodic process the potential of the anode, especially at the end of the process, may be considerably different for different electrodes.

Brewer et al. [30], to overcome these difficulties, used the anodization at a constant potential with its value slightly above the open circuit potential. Under such conditions the current decreased in time, not forcing the process and blocking solution penetration to the deeper part of the silver anode. The electrode is not polarized to higher harmful potentials which could happen during constant current anodization. In this case the role of the AgCl formation is independent of the geometric surface area.

The comparison of such electrodes, prepared at constant potential, with those prepared with the use of a constant current, has revealed that the former electrodes better reproduce their properties than the latter ones [30].

A special care was taken [31] to get the silver deposit with smooth surface and with a low porosity. Silver had a shape of small spheres with diameter not exceeding 3 mm. Such Ag spheres were anodized in different HCl solutions using 10 mA current and different time of electrolysis. The procedures involved also the conditioning of the prepared Ag | AgCl electrodes in HCl solutions of different concentrations for different time, searching for the most favorable conditions for the stabilization of the potential. The electrodes were tested in the measurements of the emf of the Harned cell. Almost all electrodes were used for several months with the bias potential smaller than 0.03 mV.

In recent years also simple methods of the construction of the Ag | AgCl electrode were described [36, 37]. The proposed construction [37] was a gel-filled Ag | AgCl electrode for use in a student laboratory, especially useful in potentiometric titrations. The simple method of the preparation of the Ag | AgCl electrode was described also by other authors [38]. In this case [38] Ag wire, after cleaning, was covered with AgCl by anodization in 0.05 mol dm^{-3} KCl, applying for 10 min 3 V voltage to silver and the second Pt electrode. The silver wire completely covered by AgCl was placed in a solution of agar dissolved in hot 3 mol dm^{-3} KCl [38]. Another simple procedure consists of immersion of a silver wire in $FeCl_3$ solution—silver is oxidized to AgCl coating the surface of silver.

Silver thin films were modified using a novel plasma chloriding modification process for the development of thin silver film/silver chloride reference electrodes [39]. The influence of the formation of the silver chloride complexes ($AgCl_2^-$ and others) on the potential of the silver/silver chloride electrode was analyzed [40] at higher temperatures. At temperatures exceeding 150 °C the solubility products, the concentration of silver complexes and the concentration of free chloride ions are significantly different from those existing at 25 °C.

Pressure-balanced Ag|AgCl reference electrodes have been extensively used for corrosion monitoring in boiling water reactor environment [41]. The potential of the thermoelectrochemical cell Ag|AgCl versus the standard hydrogen electrode at temperature, T, was expressed as a sum of the isothermal potential and thermal liquid-junction potential.

Kim et al. [42] have studied the behavior and physical–chemical properties of thin-film Ag | AgCl reference electrodes using different supports. To make the electrode resistant to heat treatment a metal adhesive layer in used thin-film Ag | AgCl electrodes was replaced by a polyimide layer and a gold backbone structure was employed [43], which made the electrode resistant to heating even at 300 °C. There was also developed [44] a porous polytetrafluoroethylene junction reference electrode with an airtight inner solution chamber containing saturated KCl. Such reference electrode is not influenced by a change in the sample pressure and also it is not necessary to supply the KCl inner solution. The relationship between the diffusion rate through the introduced junction and its characteristics was investigated. It was found that such reference electrode which contains 8 mL of KCl inner solution was able to be used continuously up to 2 years.

Also quartz-sealed Ag | AgCl reference electrode was fabricated and investigated in $CaCl_2$-based molten salts [45]. Such electrode is important for the

study of processes in melts (above 700 °C), where good reference electrodes practically do not exist. There were only used different pseudo-reference electrodes placed in the molten salt, but their potentials were not stable and were dependent on various factors. The Ag | AgCl reference electrode may be useful in such electrolytes, but in view of higher solubility of AgCl at temperatures exceeding 700 °C in molten salts to avoid contamination by silver(I) ions, a completely sealed electrode was proposed. In the study of molten salts with temperatures up to 650 °C the common sodium glass could be used, since it was easy from such glass to prepare a thin wall tube to place the Ag | AgCl electrode there. Such glass walls exhibit sufficiently high ionic conductivity. However, at temperatures exceeding 700 °C the sodium glass cannot be used because of its low melting point; therefore quartz was used to form sealed tubes. A method of the preparation of sodium ion conducting quartz membrane (0.5 mm thick) was elaborated. It was suggested [45] that the same procedure with completely sealed quartz structure may be used for preparation of other reference electrodes, for instance, metal | metal sulfide and metal | metal oxide electrodes which may function at higher temperatures. The silver chloride electrodes gave reproducible results and were stable in experiments performed at high temperatures (700–950 °C) for rather long time ranging from hours to days. The electrical resistance of such electrodes decreased from 10^5 to 10^3 Ω, following the Arrhenius law, when increasing the molten salt temperature from 600 to 950 °C. The potential variation of the electrode upon changing the electrolyte composition ($CaCl_2$, NaCl, KCl) suggested the selective conduction of Na^+ ions and possibly Ca^{2+} ions through the thin wall of the sealed quartz tube. However, the long use of such electrode (2 or 3 days) in molten chlorides in the presence of oxygen led to some erosion of quartz.

Shankenberg et al. [46] in their work on the novel potentiometric sensor for medical devices developed a novel evaporation process for the deposition of an Ag | AgCl | Ag layer combination serving as a thin-film reference electrode.

Further work on the adaptation of the Ag | AgCl electrode to different conditions is expected.

The majority of classical reference electrodes use aqueous solutions of ions participating in the potential-determining reactions. The connection of such electrodes with the electrochemical cell occurred either by a direct contact of the solution filling the electrode or by the use of an electrolytic bridge. Though different junctions were used, in order to minimize the contamination of the studied solution, the problem of a proper contact still exists. The diffusion and change of concentration of electrolytes at the liquid junction lead to some change of measured emf.

Very frequently the Ag | AgCl electrode is connected with the electrolytic cell by a porous plug. However, such connection brings difficulties, because of the contributions to the measured emf from the liquid junction. It is difficult to control it, because of the continuous nature of the diffusion in the plug [47]. These contributions may be calculated using a proper model; however, the assumption on the linear change of concentrations may be not exactly obeyed [48, 49] and under some conditions the emf of the cell deviated from the Nernstian behavior. Because of such influences, sometimes it is not possible to say whether changes of

the measured emf originated from the reference electrode or from other parts of the cell [50].

Also when an Ag | AgCl reference electrode was used for long time in a low conductivity solution or reductive solution, it was often found that the liquid-junction potential becomes unstable [43]. This behavior was characteristic for silver chloride electrode, while it was significantly less expressed when the calomel electrode was used. The authors have found [43] that 340 mg L^{-1} of silver chloride was dissolved in 3 mol dm^{-3} KCl as silver complex ions $AgCl_x^{-(x-1)}$ (for $x = 2$ or 3), while in water only 1.93 mg L^{-1} of AgCl may be dissolved. These complex ions when diffusing through the liquid junction have been transformed into AgCl and blocked the junction (e.g., porous ceramic). In reducing solutions also metallic silver resulting from silver complexes may change the junction. Due to those phenomena the liquid-junction potential became unstable or fluctuating. To eliminate these effects the authors [43] have developed a new electrode with the use of gels and chelating resins.

5.2.1.3 Electrodes with Gel-Solidified Internal Electrolyte, Membranes, or Crystalline Components

The development of above-mentioned solidified reference electrodes is very frequently connected with their miniaturization in order to enable their use in different conditions including those where the application of large electrodes is not possible. The development of such electrodes with gel-solidified electrolyte was initiated long time ago, also because they could be connected with the electrochemical cell in different space orientations. The use of solidified electrolyte makes the electrode more resistant to the influence of pressure, which is one of the most significant advantages of such electrodes [51]. External high pressure does not push the solution into the electrode space. Agar–agar and gelatin earlier used were substituted later by more robust compounds such as poly(vinyl alcohol), poly (vinyl acrylamide), methylcellulose, hydroxyethylcellulose, and aerosil. The use of such gelling compounds widens the range of temperatures in which the reference electrode may be used, quite limited in the presence of aqueous solutions. It is important that the rate of transport of ions in such gels is not much influenced by this medium and in consequence the conductivity and also potential of such electrodes are not significantly changed in comparison to the aqueous solutions.

The properties of such gels and their change under the influence of variable conditions and concentrations of salts were aptly discussed by Guth et al. [52]. Some gels often swell by absorbing solvent molecules; some others with stronger chemical bonds exhibit lower tendency to swelling. It should be stressed that for gel electrodes in contact with sample solution change the concentration of the electrolyte (e.g., KCl) by diffusion may influence the potential of the reference electrode. Such changes of the potential under influence of a solution composition were earlier

Table 5.2.1 Advantages and drawbacks of gel reference electrodes [52]

Advantages	Drawbacks
Electrode potentials comparable with those of conventional electrodes with liquid electrolytes	Increased diffusion potentials when changing solutions
Increased ability to work at high temperature (depending on gel type, up to 121 °C)	Irreversible bleeding
Applicable with hole diaphragm	Biofouling (for several gels)
Pressure resistant	Electrolyte not renewable
Sterilizable in steam	Gel aging
Retarded diffusion of solutions into the electrolyte	Decolorization
Position-independent usage is possible	Cumbersome preparation
	Some gels contain toxic/ carcinogenic substrates

discussed in the literature [53]. The advantages and drawbacks of such gel reference electrodes summarized by Guth et al. [52] are given in Table 5.2.1.

It is not our intention to discuss more extensively and in detail the published changes and improvements, but we will try to show briefly only some recent modifications and trends. Ciobanu and coworkers [54, 55] prepared and studied miniaturized reference electrodes made of silver and its ill-soluble salts (Cl^-, SCN^-, PO_4^{3-}, S^{2-}) located in the photopolymerized acryl hydrogel with the addition of tetramethylammonium chloride. Figure 5.2.1 shows a schematic representation of such an electrode.

The active part of such electrode has been located in the ending part of a micropipette which had a volume from 0.5 to 10 μL. The highest stability of potential (±0.5 mV) during 30 h was observed in 3 mol dm^{-3} KCl for the Ag | AgCl and Ag | Ag_3PO_4 electrodes with a photopolymerized hydrogel. The potentials of prepared electrodes were only slightly dependent on the concentration of anions present in the salt of the electrode, in contrast to electrodes not covered by hydrogel.

There were also constructed Ag | AgCl reference electrodes [56] covered by the hydrophobic ionic liquid bis-(trifluoromethylsulfonyl) imide-1-methyl-3-octylimidazole or covered by a 1.5 mm thick gel modification of this liquid saturated with AgCl. This gel not only partly dissolves AgCl but also plays a role of the electrolyte bridge between this reference electrode and aqueous samples. Using this gel-type salt one may construct the reference electrode with well-defined thermodynamic potential stable during the change of the KCl concentration in the limits $5 \times 10^{-5} - 2$ mol dm^{-3}. This type of reference electrodes without aqueous liquid phase exhibits thermal stability and resistivity against redox reagents such as for instance oxygen. However, hydrophobic ions may influence their potential; therefore their use in organic solvents is not advised because of the easy solubility of the gelling compounds and their derivatives.

Polymers instead of water were used to immobilize chloride ions by many researchers (see, for instance, [57–60]). In these works [60] the preparation of a miniaturized Ag | AgCl reference electrode (0.8 mm in diameter and 5 mm in length) was described, with KCl solution solidified by agar. There was also a

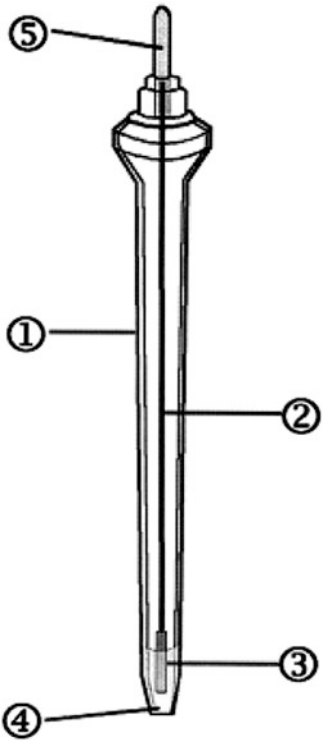

Fig. 5.2.1 Schematic view of the miniaturized reference electrode design contained in the tip of a micropipette (1); silver wire (2); AgX coating layer (3) (X = Cl^-, SCN^-, or PO_4^{3-}); photopolymerized hydrogel (4); gold-plated lid which supports and centers the internal reference element (5) [54]. Reprinted with permission from Wiley

different approach to construct a solid reference electrode based on a composite containing a mixture of Ag, AgCl, graphite, and epoxy resin [60].

In a few recent years Kisiel et al. [61–63] published a series of papers concerning reference electrodes for applications in potentiometric cells. Construction of these electrodes was similar to that of ion-selective electrodes, as potentially advantageous from the point of view of mass production of electrodes and complete cells. In this approach the Ag│AgCl couple with the addition of solid KCl was incorporated into a poly(vinyl chloride)- or poly(*n*-butyl acrylate)-based membrane (i.e., membranes typical for ion-selective electrodes) with lipophilic ionic components ensuring independence of potential on kind and concentration of the sample solution. Additionally, conducting polymers—polypyrrole [61, 63], poly (3,4-ethylenedioxythiophene) [61, 62], or carbon nanotubes [64] were used as a solid contact between the membrane and the substrate electrode, stabilizing the potential. The role of organic components present in the poly(vinyl chloride)-based membrane hosting Ag│AgCl system was discussed by Mattinen et al. [65].

In a recent work [66] inorganic components (Ag, AgCl, KCl) were closed in polyacrylate microspheres and in this form incorporated into the poly(*n*-butyl acrylate) membrane. For this arrangement, improved potential stability of the electrode was obtained, resulting from more uniform distribution of the components and their reduced leakage from the membrane.

O'Neil et al. [67] proposed an Ag | AgCl-based reference electrode incorporating a junction consisting of poly(methyl methacrylate) and graphene-stacked nanofibers.

Also conducting polymers were used as a membrane for the preparation of Ag | AgCl solid-state reference electrodes [61, 68]. Mangold and coworkers [69] have studied the behavior of the electrode Pt | PPy | Ag | AgCl | Cl^-, where silver and AgCl were deposited on platinum support and covered by a layer of polypyrrole doped with chloride ions. The formation of such electrode occurred in the process of electropolymerization of pyrrole from NaCl solutions using Pt electrode covered by Ag accompanied by simultaneous oxidation of Ag to AgCl. However, potential of such electrodes exhibited significant dependence on the change of NaCl concentration in the solution. The electrode system was protected from the influence of a solution by a membrane.

Kounaves and coworkers [70] have studied the Ag | AgCl systems covered by membrane made of Nafion or polyurethane. These polymers were used to protect the studied solution from a NaCl leakage from the electrode solution. The studies on the stability of potentials of such electrodes have shown that the potentials of the electrodes protected by Nafion were significantly less stable than those covered by the polyurethane membrane. The drift of the potential, in the initial stage, could result from a slow equilibration between the Ag | AgCl phase and KCl immobilized in the internal membrane. Further drift could be a consequence of the hydration of the external Nafion membrane. In the case of chloride solutions electrodes of both types exhibited decrease of the potential (about -41 (± 1) mV dec^{-1}) with the increase of chloride ions concentrations (from 10^{-3} mol dm^{-3} to 1 mol dm^{-3}), showing a behavior similar to that of an indicator electrode. This change could result from the diffusion of more concentrated solution of chloride ions to the electrolyte immobilized in the poly(vinyl chloride) membrane situated under the external protective layer made of Nafion or polyurethane.

Maminska et al. [71] worked on all-solid-state micro-reference electrodes dedicated to the flow-through analysis. A flat Ag | AgCl microelectrode was covered by a membrane made from poly(vinyl chloride) which contained ionic liquid 1-dodecylo-3-methyl-imidazol chloride. The presence of this ionic liquid kept the concentration of chloride ions constant which stabilized the potential. The potential of such electrodes was found to be independent of the concentration of such anions as Cl^-, Br^-, and NO_3^-.

Another interesting example is electrode described by Eine et al. [47]. In its construction the cation and anion exchangers were placed in a poly(vinyl chloride)-based membrane containing lipophilic salts different in the case of the cation and anion exchange membrane. In that work [47] poly[*N*-(4-vinylbenzyl)-*N*,*N*′-dimethylamine] was used as the anion exchanging substance and a copolymer of methacrylic acid and methyl methacrylate in a molar ratio 1:1 as the cation exchangers. The measured membrane resistance varied from 0.01 to 0.09 MΩ. The performance of such reference electrode was good, since it avoids problems with liquid junction and has several practical advantages.

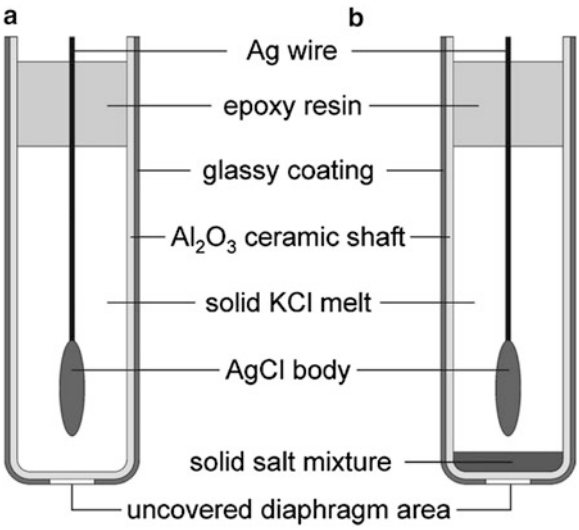

Fig. 5.2.2 Scheme of reference electrodes with solidified KCl reference electrolyte [74]. Reprinted with permission from Elsevier

Also the reference electrode on the front side was covered with a photosensitive poly-2-hydroxyethyl methacrylate layer. This layer served as a protection against variation of the chloride concentration in the analyte. One may add that Yu and Dong [72] in their work compared several different procedures of the preparation of the Ag | AgCl electrodes.

A concept of electrode with reference electrolyte solidified in a crystalline form was also developed [52, 73]. In this case a sintered Ag | AgCl mixture was embedded in a solid melt of KCl forming a solid crystalline body. In Fig. 5.2.2 we show the schemes of such electrodes [74].

At the bottom a porous alumina ceramic acts as a diaphragm which forms electrolytic junction with the studied medium (Fig. 5.2.2a). In a slightly changed modification (Fig. 5.2.2b) the bottom of the cylinder is filled with an additional solid salt mixture which plays a role of a bridge electrolyte.

The potential of such all-solid-state reference electrode was found to be very stable in time of several months. It was not affected by the change of pH of the investigated solutions. However, at present the behavior of such all-solid-state reference electrodes is not as good as that of conventional electrodes [52].

5.2.1.4 Miniaturized Electrodes

Very frequently the solidification of the chloride solution was developed parallel with the miniaturization of electrodes. Therefore, it is not easy to discuss these two trends of improvements separately.

Below we present selected papers which paid more attention to the small size of the Ag | AgCl electrodes.

A micro-planar electrode with long-term stability was developed by Matsumoto et al. [75], who used a perfluorocarbon polymer membrane. The electrode was not influenced by interferences (with exception of K_2S with concentration exceeding 0.001 mol dm^{-3}). Yalcinkaya and Powner [76] have introduced a new type of miniaturized coated silver stripe reference electrode without internal solution for single use.

Also a needle-type ultramicro Ag | AgCl reference electrode having a micro-capillary with outer and inner diameters of 1.0 μm and 0.5 (±0.2) μm, respectively, was constructed by Kitade et al. [77]. This micro-reference electrode can be introduced into a living cell and may be used in very small environments, for instance, in a cell of an electrochemical scanning tunneling microscopy. It was found that such electrode with the micro-capillary filled with agar gel containing 3.33 mol dm^{-3} KCl as a salt bridge exhibited very good stability and reproducibility of the potential.

On the other side, Zhang et al. [78] have prepared and characterized a carbon fiber cone nanometric sized ultramicroelectrodes equipped with an integrated micro Ag | AgCl reference electrode. The introduction of such integrated Ag | AgCl electrode located at the bottom edge of the carbon fiber tip led to the determination of dopamine in extremely small volumes. This leads to the conclusion that such electrode system may be used for in vivo and/or single cell studies.

A disposable Ag | AgCl electrode with potential practically not influenced by concentration changes and pH of the analyte solution was developed by Mroz et al. [79]. The electrode was prepared from inexpensive materials with screen printing and encapsulation by lamination. Miniaturized Ag | AgCl electrodes were developed also by other authors (see, for instance, [80–82]). Liquid-junction Ag | AgCl reference electrodes were developed using microfabrication techniques [80–82].

A novel thin-film Ag | AgCl structure was used. A pinhole or a combination of a pinhole and a cellulose acetate plug was used for the liquid junction [80]. Although the electrode with the pinhole junction showed potential drift to the positive side due to KCl effusion, the electrode with the combinatory junction could give a stable electrode potential within ±1 mV for several hours. No dependence on KCl concentration or pH of the external electrolyte solution was observed in the latter type of electrode. The behavior of such miniature electrode was comparable to that of the commercial liquid-junction electrodes.

In another work [81] a silver thin-film pattern was covered with a polyimide protection layer with a 50 μm wide slit at the center of the pattern and the Ag | AgCl layer was grown from there into the silver layer. A liquid junction was formed with a photocurable hydrophilic polymer. A silicone rubber passivation covered the entire area except for the pad and the end of the junction. The complete miniature liquid-junction reference electrode could maintain a stable level within ±1 mV for time longer than 100 h with the aid of poly(vinyl pyrrolidone) matrix in the electrolyte layer.

A miniature liquid-junction reference electrode was employed to integrate the three-electrode system on a chip [82]. The reference electrode features a durable

thin-film Ag | AgCl element whose entire surface was coated with a hydrophobic membrane.

No substantial difference was observed in the cyclic voltammograms between the integrated system and the macroscopic three-electrode system in terms of their peak current and half-wave potential. The integrated electrode system was also applied to fabricate one-chip biochemical sensors.

A study was also undertaken [72] to develop fast in situ Ag | AgCl reference electrodes well suited for repeatable several hundred times use in human serum. The authors give the technical details of the electrode preparation. The electrode exhibited satisfactory stability of the potential.

Also two Ag | AgCl electrodes, one uncoated and the second coated by a polymer, were implanted subcutaneously in rats [50]. After 1 week of implantation uncoated electrode potential, measured in 0.1 mol dm^{-3} KCl, shifted by about −180 mV and it was shown that all AgCl was removed from the electrode. The electrode could be efficiently protected by coating with polyurethane or Nafion. Electron micrographs showed that after 2 weeks this coating remained intact.

In the literature there are numerous papers on different micro-biosensors used to measure, for instance, glucose or lactate concentration in the body. Some of these sensors use Ag | AgCl electrodes with AgCl formed on a silver surface. Potential of such electrodes may be influenced either by some anions such as S^{2-}, I^-, Br^-, which react with AgCl, or by change of the ionic strength.

Evidently when the micro Ag | AgCl electrodes are used in such media, they should be protected by membranes from the influence of different interferents.

In recent years there are numerous papers published in which the authors use silver–silver chloride reference electrodes. Very frequently the construction of these electrodes is changed in order to adapt them to the need of the potentiometric or electrolytic cells used in the study. One may expect that in the future this trend will be observed.

5.2.2 *The Silver–Silver Bromide Electrode*

The silver–silver bromide electrode was not frequently described and used in the published works. This electrode is formed from silver covered by silver bromide placed in bromide ions solutions. The potential of this electrode may be described similarly to that of the Ag | AgCl electrode. The electrode reaction of silver bromide is

$$AgBr + e^- \rightleftharpoons Ag + Br^- \tag{5.2.7}$$

The potential of this electrode is dependent on the bromide ion activity according to the equation:

$$E = E^{\ominus}_{\mathrm{Ag/Ag^+}} + \frac{RT}{F} \ln a_{\mathrm{Ag^+}} = E^{\ominus}_{\mathrm{Ag/AgBr}} - \frac{RT}{F} \ln a_{\mathrm{Br^-}}, \tag{5.2.8}$$

where

$$E^{\ominus}_{\mathrm{Ag/AgBr}} = E^{\ominus}_{\mathrm{Ag/Ag^+}} + \frac{RT}{F} \ln K_{\mathrm{sol(AgBr)}}. \tag{5.2.9}$$

The standard potential of the Ag | AgBr electrode was determined by a number of workers; however, there is a significant discrepancy between reported values amounting to 0.37 mV. These discrepancies were briefly discussed by Hetzer et al. [83]. Since these earlier studies were conducted with a care for reliability, it was not easy to say which result from those reported is the most reliable.

In order to resolve these differences Hetzer et al. [83] undertook the redetermination of that standard potential using the cell:

$$\mathrm{H_2(g)|HBr(aq)|AgBr(s)|Ag(s)} \tag{5.2.10}$$

with HBr concentration varying from 0.005125 to 0.10085 mol $\mathrm{kg^{-1}}$ in the temperature range 0–50 °C. These authors have used the silver bromide electrodes of the thermal type formed by heating at 550 °C of a paste composed of 10 wt% of silver bromate and 90 wt% of silver oxide. In the measurements, the cell solutions were deaerated using hydrogen.

The carefully measured emfs after averaging from several measurements were analyzed and the values of the standard potentials were obtained by the method of least squares. The numerical values of $E^{\ominus}$ were measured in the range from 0 to 50 °C every 5 K. The $E^{\ominus}$ value at 25 °C is equal to 0.0710_6 V and is very near to that found by Harned et al. [84] (0.0710_5 V).

Also results at other temperatures in the range 0–50 °C are quite similar.

The results of Hetzer et al. [83], obtained at different temperatures, were given by them in a form of the following dependence:

$$E^{\ominus}(\mathrm{V}) = 0.0710_9 - 4.87 \times 10^{-4}(T - 25) - 3.08 \times 10^{-6}(T - 25)^2. \tag{5.2.11}$$

The discrepancies observed between earlier data reported by different authors [83] were explained by Hetzer et al. to be due to the difference in the preparation of electrodes. These discrepancies between potentials of different silver bromide electrodes may also result from the influence of oxygen as found by Harned et al. [84]. This remark relates especially to dilute solutions of hydrobromic acid.

According to Harned oxygen is the main cause of differences in results since differently prepared electrodes in the absence of oxygen give quite similar results [84].

The potential of the Ag | AgBr electrode was determined by Towns et al. [85] also at temperatures higher than 50 °C. They measured the emf of the cell (5.2.10) from 25 to 200 °C using hydrogen pressures of about 1 atm and HBr concentrations from 0.005 to 0.5 mol $\mathrm{kg^{-1}}$ in the special bomb-type experimental apparatus. They

used the thermal-type silver halogenide electrodes. The determined standard potential of the cell (5.2.10) was found to fit the following equation:

$$E^{\ominus}(\mathrm{V}) = 0.0828_9 - 4.0647 \times 10^{-4}T - 2.3986 \times 10^{-6}T^2 \qquad (5.2.12)$$

with a standard error of fit of 1.1 mV.

The values of $E^{\ominus}$ obtained at 25 and 60 °C agree with those of Harned et al. [84] within 0.3 and 0.5 mV, respectively. The decrease of $E^{\ominus}$ with the rise of temperature is for the Ag | AgBr electrode slightly greater than the decrease of $E^{\ominus}$ observed for the Ag | AgCl electrode.

We recommend the value 0.0710_9 V as a standard potential of the Ag | AgBr electrode.

Mainly two methods were used for the preparation of the Ag | AgBr electrodes: thermal method used by Hetzer et al. [83] and electrolytic method where silver deposited on Pt spiral was anodized either in hydrobromic acid or in bromide solutions.

The properties of the silver bromide coated ion-selective electrode were also studied [86].

5.2.3 *The Silver–Silver Iodide Electrode*

The silver–silver iodide electrode similarly as silver chloride and silver bromide electrodes is the second-kind electrode with metallic silver covered by silver iodide and placed in a solution of iodide ions. It has rather no practical importance because of instability of iodide ions in the presence of oxygen. This instability was probably the main cause of the discrepancies between earlier results which were briefly summarized by Hetzer et al. [87]. These significant discrepancies among several values of $E^{\ominus}$ at 25 °C were the main reason of the careful work undertaken by Hetzer et al. [87] on the cell:

$$\mathrm{H_2(g)|HI(aq)|AgI(s)|Ag(s)} \qquad (5.2.13)$$

carried out at different temperatures in the range 0–50 °C. All solutions were prepared and handled by them under nitrogen atmosphere. For 25 °C they found [87] the standard value equal to -0.1524_4 V. The nearest to that value, considering earlier data, is the result found by Owen [88] equal to -0.1523_0 V. The results of other earlier workers were even more lower.

The agreement of the emf of cell (5.2.13) with different pairs of electrodes obtained by Hetzer et al. [87] was very good, about 0.04 mV at 25 °C. Of course, the cells were protected from oxygen to increase the stability of iodide solutions. It was found [87] that the lifetime of cells which contain acid of concentration higher than 0.2 mol $\mathrm{kg^{-1}}$ was much shorter than the lifetime of cells with more diluted acid. The authors explained that [87] by increased solubility of AgI in more concentrated

iodide solutions. This explanation, assuming that the electrode is well equilibrated before use, is not quite clear. The values of $E^{\ominus}_{Ag/AgI}$ obtained by Hetzer et al. [87] at different temperatures were described by the equation:

$$E^{\ominus}(\mathrm{V}) = -0.1524_2 - 3.19 \times 10^{-4}(T-25) - 2.84 \times 10^{-6}(T-25)^2 \quad (5.2.14)$$

with an average deviation of 0.05 mV, and these values are recommended by the present authors.

The silver–silver iodide electrodes were prepared by using the thermal method. A paste of 10 % wt silver iodide and 90 % wt silver oxide was heated at 450 °C (15 min), ground together with small quantities of water and placed on platinum helices.

The electrodes were covered two times by such paste and this was followed each time by heating. As the authors write [87] the potentials of the electrodes in each set agreed to better than 0.08 mV.

More recently a needle-type Ag | AgI micro-reference electrode was developed [89] with a stagnant electrolyte layer and an active liquid junction. The properties of the silver iodide coated ion-selective electrode were also studied [90].

5.2.4 The Silver–Silver Sulfide Electrode

There are known two modifications of Ag_2S α and β. The transition from β to α form, which is stable at lower temperatures, occurs at 178 °C.

The β form exhibits semiconducting properties (n-type). The solubility product of Ag_2S in water $K_{sol(Ag_2S)}$ is very small 6.2×10^{-52}. Therefore the use of the system $Ag \mid Ag_2S \mid S^{2-}$ with the concentration of S^{2-} ions of the order of 0.1 mol dm^{-3} raises the question of the nature of the mechanism of functioning of this electrode at so extremely low concentration of the Ag^+ ion in the solution. Probably some complexes of silver(I) with sulfide ions play some role, since the $Ag \mid Ag_2S \mid S^{2-}$ electrode exhibits relatively good performance and Golding [91] has proposed to apply it as a reference electrode.

Noyes and Freed [92] have studied the behavior and emf of the cell:

$$Ag\,(s) \mid Ag_2S\,(s) \mid HCl\,(aq) \mid H_2S\,(g) \,\|\, HCl\,(aq) \mid Pt\,(s) \mid H_2\,(g) \quad (5.2.15)$$

using $Ag \mid Ag_2S$ electrodes prepared in different fashions and also changing the concentration of HCl. The following values of emf of above cell were found [92]: 0.0380_5, 0.0376_7, 0.0365_8, and 0.0357 V at 5, 10, 25, and 35 °C, respectively. The result at 25 °C was later confirmed in some limits by other researchers who found for 25 °C 0.0362 V [92], 0.0368 V [93], and 0.0362 V [94]. From these measurements a mean value 0.0364 (±0.00025) V was reported by Ives and Janz [95].

Goates et al. [94] have measured also the emf of another cell, where the $Ag \mid Ag_2S \mid S^{2-}$ electrode was combined with the normal calomel electrode (NCE):

$$\mathrm{Ag\ (s)} \,\big|\, \mathrm{Ag_2S\ (s)} \,\big|\, \mathrm{Na_2S} \,\|\, \mathrm{NCE} \tag{5.2.16}$$

Several concentrations of Na_2S were used. From these measurements the standard potential of the silver sulfide electrode was calculated as equal to $E^{\circ}_{Ag/Ag_2S/S^{2-}} = -0.7125(\pm 0.0004)$ V at 25 °C. Several millivolts more negative value −0.7180 V was reported later [96]. However, Zhutaeva and Shumilova [23] reported considerably less negative value equal to −0.691 V.

The temperature coefficient of the emf of cell (5.2.15), determined by several workers, shows significant differences, namely, -0.81×10^{-4} V K^{-1} [97], -0.80×10^{-4} V K^{-1} [92], and -1.04×10^{-4} V K^{-1} [94]. Estimation given by Ives and Janz [95], based on non-electrochemical results, is the lowest of all these data, being equal to -0.53×10^{-4} V K^{-1}. Under such condition it is rather difficult to recommend a specific value. The needed temperature coefficient should be rather determined by the researchers for the electrode used by them.

The silver sulfide electrode was suggested to be used as a reference electrode for the study of sulfide systems. This suggestion was based on the reproducible potential of the electrode, though its electrode behavior was found to be not quite reversible [91]. The problem of reproducibility and its origin calls for more extensive studies in order to understand the mechanism of the potential response on the change of concentrations of the potential-determining ions. At present, this electrode should be rather considered as a quasi-reference system, though Golding [91] has proposed to apply it as a reference electrode.

In recent years Ciobanu et al. [55] paid attention to the Ag | Ag_2S electrode embedded into an acrylic copolymer matrix. Their studies have shown that such electrode exhibits stable potential in different media including aqueous solutions of different species and in mixed (aqueous/nonaqueous) and nonaqueous solvents. As the authors suggest [55] such electrodes may be successfully applied in electrochemical microanalysis when the volume of the analyzed sample is on the μm level. The open circuit potential was stable in the limits ±2 mV in different solvents.

From different ways of the preparation of this electrode [92–94], the method of anodization of a silver plate (wire) or silver deposited on a Pt support in sulfide solution is advised. Also the platinum support covered by porous silver (prepared from thermal decomposition of silver oxide paste) placed into aqueous solution of hydrogen sulfide led to the formation of the Ag | Ag_2S system.

5.2.5 *Other Electrode Systems Based on the Silver Redox Reaction*

In addition to the Ag | AgCl, Ag | AgBr, Ag | AgI, and Ag | Ag_2S electrodes, which were discussed above, there are also other silver electrode systems, which may be used for the formation of the second-kind reference electrodes. Some of these systems with their redox potentials are listed [23] in Table 5.2.2.

Table 5.2.2 Selected silver electrode systems in aqueous solutions at 25 °C

Silver redox reaction	E°/V
$AgSCN + e^- \rightleftharpoons Ag + SCN^-$	0.0894_9
$Ag_4[Fe(CN)_6] + 4e^- \rightleftharpoons 4Ag + [Fe(CN)_6]^{4-}$	0.1478
$AgN_3 + e^- \rightleftharpoons Ag + N_3^-$	0.295
$Ag_3PO_4 + 3e^- \rightleftharpoons 3Ag + PO_4^{3-}$	0.3402
$AgIO_3 + e^- \rightleftharpoons Ag + IO_3^-$	0.354
$AgCNO + e^- \rightleftharpoons Ag + CNO^-$	0.41
$Ag_2C_2O_4 + 2e^- \rightleftharpoons 2Ag + C_2O_4^{2-}$	0.4647
$AgBrO_3 + e^- \rightleftharpoons Ag + BrO_3^-$	0.548
$AgCH_3COO + e^- \rightleftharpoons Ag + CH_3COO^-$	0.643
$Ag_2SO_4 + 2e^- \rightleftharpoons 2Ag + SO_4^{2-}$	0.654

Some of these systems were occasionally considered as potential candidates for the construction of reference electrodes. Their limited use in that role results, among others reasons, from sometimes complicated chemical equilibria and formation of complexes in addition to ill-soluble compound (Ag^+–SCN^- system) or from relatively higher solubility of the silver compound ($AgBrO_3$, $AgCH_3COO$, or Ag_2SO_4). Also the use of too many reference electrodes is not practical.

References

23. Shumilova NA, Zhutaeva GV (1978) In: Bard AJ (ed) Encyclopedia of electrochemistry of the elements. Dekker, New York
24. Harned HS, Ehlers RW (1933) J Am Chem Soc 55:2179
25. Bates RG, Bower VE (1954) J Res Natl Bur Stand 53:282
26. Harned HS, Paxton TR (1953) J Phys Chem 57:531
27. Bard AJ, Parsons R, Jordan J (1985) Standard potentials in aqueous solutions. Marcel Dekker, New York, p 304
28. Greeley RS, Smith WT, Lietzke MH, Stanghton RW (1960) J Phys Chem 64:652
29. Bates RG, Macaskill JB (1978) Pure Appl Chem 50:1701
30. Brewer PJ, Leese RJ, Brown RJC (2012) Electrochim Acta 71:252
31. Guiomar Lito MJ, Filomena Camoes M (2009) J Solution Chem 38:1471
32. Bates RG (1973) Determination of pH. Theory and practice, 2nd edn. Wiley, New York
33. Brewer PJ, Brown RJC (2010) Sensors 10:2202
34. Brown RJC, Milton MJT (2005) Accred Qual Assur 10:352
35. Brewer PJ, Stoica D, Brown RJC (2011) Sensors 11:8072
36. East GA, del Valle MA (2000) J Chem Educ 77:97
37. Thomas JM (1999) J Chem Educ 76:97
38. Inamdar SN, Bhat MA, Haram SK (2009) J Chem Educ 86:355
39. Escoffier C, Maguire PD, Mahony C, Graham WG, MacAdams EM, McLaughlin JA (2002) J Electrochem Soc 149:H98
40. Oijerholm J, Forsberg S, Hermansson HP, Ullberg M (2009) J Electrochem Soc 156:P56

41. Oh SH, Bahn CB, Hwang IS (2003) J Electrochem Soc 150:E321
42. Kim HR, Kim YD, Kim KI, Shim JH, Nam H, Kong BK (2004) Sens Actuators B 97:348
43. Ito S, Hachiya H, Baba K, Asano Y, Wada H (1995) Talanta 42:1685
44. Ito S, Kobayashi F, Baba K, Asano Y, Wada H (1996) Talanta 40:135
45. Gao P, Jin XB, Wang DH, Wu XH, Chen GZ (2005) J Electroanal Chem 579:321
46. Shankenberg U, Lisec T, Hintsche R, Kuna I, Uhlig A, Wagner B (1996) Sens Actuators B 34:476
47. Eine K, Kjelstrup S, Nagy K, Syverud K (1997) Sens Actuators B 44:381
48. Johnsen EE, Kjelstrup Ratkje S, Førland T, Førland KS (1990) Z Physik Chem 168:101
49. Beer J, Kjelstrup Ratkje S, Olsen GF (1991) Z Physik Chem 174:179
50. Moussy F, Harrison DJ (1994) Anal Chem 66:674
51. Galster H (1980) GIT Fachz Lab 24:744
52. Guth U, Gerlach F, Decker M, Oelßner W, Vonau W (2009) J Solid State Electrochem 13:27
53. Gabel J, Vonau W, Lange R, Barthold K (2000) GIT-Laborfachzeitschrift 45:366
54. Ciobanu M, Wilburn JP, Buss NL, Ditavong P, Lowy DA (2002) Electroanalysis 14:989
55. Ciobanu M, Wilburn JP, Lowy DA (2004) Electroanalysis 16:1351
56. Kakiuchi T, Yoshimatsu T, Nishi N (2007) Anal Chem 79:7187
57. Bakker E (1999) Electroanalysis 11:788
58. Lindner E (2000) Anal Chem 68:336A
59. Lee HJ, Hong US, Lee DK, Shin JH, Nam H, Cha GS (1998) Anal Chem 70:3377
60. Valdes-Ramirez G, Alvarez-Romero G, Galan-Vidal CA, Hernandez-Rodriguez PR, Ramirez-Silva MT (2005) Sens Actuators B 110:264
61. Kisiel A, Marcisz H, Michalska A, Maksymiuk K (2005) Analyst 130:1655
62. Kisiel A, Michalska A, Maksymiuk K (2007) Bioelectrochem 71:75
63. Kisiel A, Michalska A, Maksymiuk K, Hall EAH (2008) Electroanalysis 20:318
64. Rius-Ruiz FX, Kisiel A, Michalska A, Maksymiuk K, Riu J, Xavier RF (2011) Anal Bioanal Chem 399:3613
65. Mattinen U, Bobacka J, Lewenstam A (2009) Electroanalysis 21:1955
66. Kisiel A, Donten M, Mieczkowski J, Rius-Ruiz FX, Maksymiuk K, Michalska A (2010) Analyst 135:2420
67. O'Neil GD, Buiculescu R, Kounaves SP, Chaniotakis NA (2011) Anal Chem 83: 5749
68. Blaz T, Migdalski J, Lewenstam A (2005) Analyst 130:637
69. Mangold K-M, Schäfer S, Jüttner K (2000) Fresenius J Anal Chem 367:340
70. Nolan MA, Tan SH, Kounaves SP (1997) Anal Chem 69:1244
71. Maminska R, Dybko A, Wróblewski W (2006) Sens Actuators B 115:552
72. Yu P, Dong S (1996) Anal Chim Acta 330:767

73. Vonau W, Oelßner W, Sikora RJ, Henze J (2003) Referenzelektrode DE 10305005
74. Vonau W, Oelßner W, Guth U, Henze J (2010) Sens Actuators B 144:368
75. Matsumoto T, Oashi A, Ito N (2002) Anal Chim Acta 462:253
76. Yalcinkaya F, Powner ET (1997) Med Eng Phys 19:299
77. Kitade T, Kitamura M, Takegami S, Miyata Y, Nagatomo M, Sakaguchi T, Furukawa M (2005) Anal Sci 21:907
78. Zhang X, Ogorevec B, Tavcar G, Grabec Svegl I (1996) Analyst 121:1817
79. Mroz A, Borchardt M, Diekmann C, Cammann K, Knoll M, Dumschat C (1998) Analyst 123:1373
80. Suzuki H, Hirakawa I, Sasaki S, Karube I (1998) Sens Actuators B 46:146
81. Suzuki H, Shiroishi H, Sasaki S, Karube I (1999) Anal Chem 71:5069
82. Suzuki H, Hirakawa I, Sasaki S, Karube I (1999) Anal Chim Acta 387:103
83. Hetzer HB, Robinson RA, Bates RG (1962) J Phys Chem 66:1423
84. Harned HS, Keston AS, Donelson JG (1936) J Am Chem Soc 58:989
85. Towns MB, Greeley RS, Lietzke MH (1960) J Phys Chem 64:1861
86. Strydom CA, Van Staden JF, Strydom HJ (1991) Electroanalysis 3:815
87. Hetzer HB, Robinson RA, Bates RG (1964) J Phys Chem 68:1929
88. Owen BB (1935) J Am Chem Soc 57:1226
89. Hashimoto M, Upadhyay S, Kojima S, Suzuki H, Hayashi K, Sunagawa K (2006) J Electrochem Soc 153:H155
90. Strydom CA, Van Staden JF, Strydom HJ (1992) Electroanalysis 4:969
91. Golding M (1959) J Chem Soc 1838
92. Noyes AA, Freed ES (1920) J Am Chem Soc 42:476
93. Kimura G (1935) Bull Inst Phys Chem Res (Tokyo) 14:94
94. Goates RJ, Cole AG, Gray EL, Faux ND (1951) J Am Chem Soc 73:707
95. Ives DJG, Janz GJ (eds) (1961) Reference electrodes. Theory and practice. Academic, New York, Chapter 7.V, pp 381–382
96. Freiberger WI, de Bruyn PL (1957) J Phys Chem 61:586
97. Nakolkin IA (1942) Zh Fiz Khim 16:18

5.3 Mercury Electrodes

Krzysztof Maksymiuk, Agata Michalska, Anna Kisiel, and Zbigniew Galus

Reference electrodes based on mercury are second-kind electrodes composed of pure mercury and a sparingly soluble mercury salt [98, 99]. Due to environmental concerns in recent years these electrodes are less frequently used compared to their

K. Maksymiuk (✉) • A. Michalska • A. Kisiel • Z. Galus
Department of Chemistry, University of Warsaw, Pasteura 1, 02-093 Warsaw, Poland
e-mail: kmaks@chem.uw.edu.pl; agatam@chem.uw.edu.pl; akisiel@chem.uw.edu.pl; zbgalus@chem.uw.edu.pl

silver-based counterparts. To the most popular mercury-based reference electrodes belong calomel and mercury sulfate electrodes.

5.3.1 Mercury/Mercury(I) Chloride (Calomel) Electrode

The mercury/mercury(I) chloride (calomel) electrode is a second-kind electrode composed typically of metallic mercury and excess of hardly soluble mercury(I) chloride with addition of a paste of mercury with calomel in contact with KCl solution [98, 100]. It was introduced by Ostwald in 1890 and is now the most popular mercury reference electrode. The scheme of this electrode is shown below:

$$\mathrm{Hg|Hg_2Cl_2(s), KCl(s)|KCl(l)||}$$

A typical construction of calomel electrode (Fig. 5.3.1) consists of an outer glass tube with a frit at the bottom to enable electrical contact with the solution. Inside the

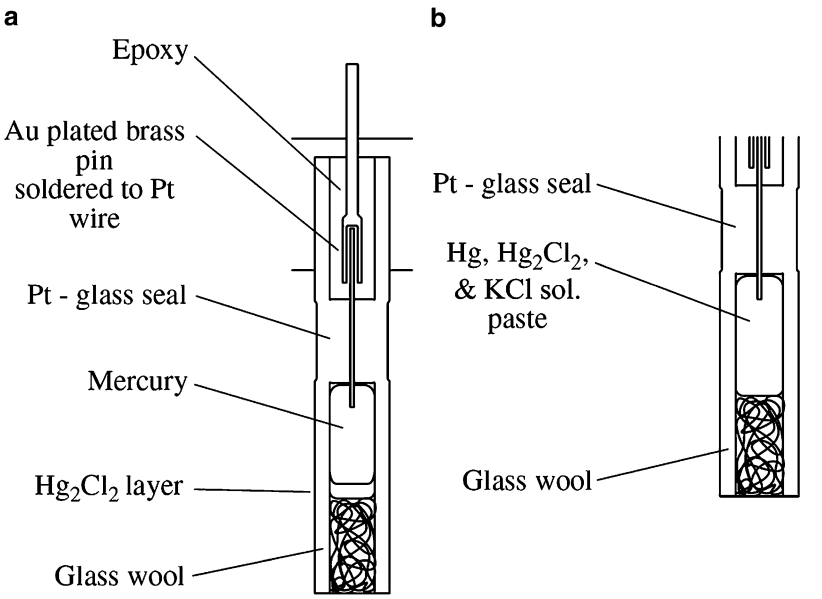

Fig. 5.3.1 Scheme of saturated calomel electrode constructions. (**a**) Dry mercury covered by a layer of Hg_2Cl_2, (**b**) grinded Hg and Hg_2Cl_2 together with a few drops of KCl filling solution [99]. Reprinted with permission from Elsevier

tube another tube is placed, containing a paste of mercury and mercury(I) chloride dispersed in a saturated solution of potassium chloride. The bottom part of the inner tube can be filled with glass wool to enable electrical contact of the contents of the inner tube with that of the outer tube. The outer tube is usually filled with saturated solution of potassium chloride.

Half-cell reaction of calomel electrode is expressed as follows:

$$Hg_2Cl_2 + 2e^- \rightleftharpoons 2Hg + 2Cl^- \tag{5.3.1}$$

and the potential is described by equation:

$$E = E^{\ominus}_{Hg_2^{2+}/Hg} + RT/F \ln K_{sol(Hg_2Cl_2)} - RT/F \ln a_{Cl^-}. \tag{5.3.2}$$

The standard potential $E^{\ominus}_{Hg_2Cl_2/Hg}$ (for $a_{Cl^-} = 1$) is a sum of standard potential of the Hg_2^{2+}/Hg couple and logarithmic term containing solubility product of Hg_2Cl_2, $K_{sol(Hg_2Cl_2)}$. This potential, at temperature 25 °C, is $E^{\ominus}_{Hg_2Cl_2/Hg} = 0.268\,V$ vs. standard hydrogen electrode (SHE) (25 °C), according to early works reviewed by Wrona and Galus [101]. Hills and Ives [102] using a cell without liquid junction, by extrapolation to infinite dilution, obtained $E^{\ominus} = 0.26796\,V$ at 25 °C, which can be recommended. Elaboration of their experimental results by Guggenheim and Prue's method [103] led to identical results; the same results have been obtained also by Schwabe and Ziegenbalg [104]. Some small differences reported in paper of Grzybowski [105] were explained by the role of cell design and effect of smoothing the values over a number of temperatures. Similar studies were also carried out by other authors (references given in [101]).

According to Nernst equation the potential of calomel electrode is dependent on chloride ions' activity (concentration). In practice, three cases are encountered: "normal" calomel electrode (with KCl solution of concentration 1 mol dm^{-3}), "0.1 normal" calomel electrode (with KCl solution concentration 0.1 mol dm^{-3}), and most often used "saturated" calomel electrode (with saturated KCl solution and the presence of KCl crystals), abbreviated as the "saturated calomel electrode", SCE. A version with saturated NaCl solution ("sodium chloride saturated calomel electrode", SSCE) is also widely used in solution, where risk of a potassium salt precipitation occurs, e.g., in perchlorate ions containing solutions.

Because saturated calomel electrode forms its own salt bridge and transference numbers of K^+ and Cl^- ions are similar, the influence of liquid-junction potential is negligibly small.

Potential values corresponding to different calomel electrodes, at temperature 25 °C, were collected in Table 5.3.1 [106]:

As filling solution hydrochloric acid can be also used; however, the potential under these conditions is not sufficiently reproducible and this arrangement is not recommended for reference electrodes. This effect can result from oxidation of mercury occurring in acidic medium:

$$2Hg + 2H^+ + 2Cl^- + {}^1/_2\,O_2 \rightarrow Hg_2Cl_2 + H_2O \tag{5.3.3}$$

Potential of the calomel electrode is dependent on temperature, described by formulae [101]:

$E(V) = 0.2412 - 6.61 \times 10^{-4}(T - 25\ °C) - 1.75 \times 10^{-6}(T - 25\ °C)^2 - 9 \times 10^{-10}(T - 25\ °C)^3$ for saturated electrode, [107].
$E(V) = 0.3337 - 8.75 \times 10^{-5}(T - 25\ °C) - 3 \times 10^{-6}(T - 25\ °C)^2$ for 0.1 normal (0.1 mol dm^{-3} KCl) electrode, [107].

Table 5.3.1 Potentials of calomel electrodes: Hg_2Cl_2 | Hg [106]

Electrolyte solution	Temperature (°C)	Potential vs. SHE (V)
Saturated KCl (~4 mol dm^{-3})	25	0.2412 [98, 107]
	0	0.2568 [107]
	10	0.2507 [107]
	20	0.2444 [107]
	30	0.2378 [107]
	40	0.2307 [107]
	50	0.2233 [107]
	60	0.2154 [107]
	70	0.2071 [107]
0.1 mol dm^{-3} KCl	25	0.3337 [107, 108]
1 mol dm^{-3} KCl	25	0.2801 [98, 107]
0.1 m KCl	25	0.339 [107]
1 m KCl	25	0.2809 [107]

$E(\mathrm{V}) = 0.2801 - 2.75 \times 10^{-4}(T - 25°\mathrm{C}) - 2.5 \times 10^{-6}(T - 25°\mathrm{C})^2 - 4 \times 10^{-9}(T - 25\ °\mathrm{C})^3$ for normal (1 mol dm^{-3} KCl) electrode, where T is temperature in °C. These formulae are correct for the temperatures given in Table 5.3.1.

The potential of calomel electrode is very reproducible if the electrode is produced and operated carefully.

Instead of pure mercury less toxic solid silver amalgam has been also proposed for construction of calomel electrodes [109, 110]. Long-term as well as short-time test confirms the potential of the new electrode equal to that of classical calomel electrode within the limits of 1 mV. This electrode was also found to be non-polarized in the presence of current below 2 mA.

A reference electrode with glassy carbon substrate modified by polypyrrole with mercury and solid Hg_2Cl_2 has been also proposed [111]. More details can be found in Sect. 12.2.1.

5.3.1.1 Electrode Preparation

Electrode preparation consists of mercury and mercury salt preparation [98, 99]:

Mercury preparation. No particular preparative steps are necessary unless mercury of sufficient purity is used.

Hg_2Cl_2 preparation. High purity Hg_2Cl_2 is available commercially or it can be obtained by chemical precipitation and should be finely powdered (0.1–5 μm).

In chemical preparation [98] about 1 g of reagent-grade mercury(I) nitrate dihydrate, $Hg_2(NO_3)_2{\cdot}2H_2O$, is mixed with 0.2 mL of concentrated nitric acid and ~20 mL of water. This solution is added dropwise for 2 min into a covered beaker containing ~100 mL of 0.1 mol dm^{-3} HCl. After addition, the resulting solution is

stirred using a magnetic stir bar for 1 h. After precipitate settling, the supernatant solution is decanted; this procedure is repeated twice to rinse the precipitate. The precipitated mercury(I) chloride is then filtered using a sintered glass crucible, rinsed quickly with four portions of cold distilled water, and then transferred to a vacuum desiccator. The hydrochloric acid used should be free of halogens, to avoid deposition of other mercury(I) halides.

Mercury(I) chloride can be obtained electrochemically [98], but is less stable than the product obtained chemically.

$Hg|Hg_2Cl_2$ electrode preparation. Method 1 [98]. Hg_2Cl_2 is added to dry mercury. After complete coverage of the surface with the salt, addition of Hg_2Cl_2 is stopped; otherwise the electrode response will be slow. The $Hg|Hg_2Cl_2$ interface must be prepared before introduction of filling solution.
Method 2 [99]. Mercury and Hg_2Cl_2 are ground together with a few drops of KCl filling solution using a mortar and pestle to obtain a paste. The paste is placed in a tube, in direct contact with a platinum wire.

5.3.1.2 Electrochemical Properties and Side Reactions

Many works concerning calomel electrode operation appeared in the decade 1950–1960 and these papers were reviewed by Ives and Janz [98] and later by Wrona and Galus [101].

Kinetics of charge transfer reaction for calomel electrode has been studied by Bockris et al. [112]; the reported exchange current density is around 1 A cm^{-2}. The electrochemical behavior of the calomel electrode is determined both by this high charge transfer density and very low concentration of Hg_2^{2+} ions. This suggests existence of other species determining the electrochemical response. Hills and Ives [113] postulated existence of chloro compounds as Hg_2Cl^+ and $HgCl^+$. Some information about the nature of calomel formation could be obtained by studying process of the anodic oxidation of mercury in chloride ions containing solutions (e.g., [114–120]), pointing to the presence of soluble forms of mercury with calomel formation as a secondary reaction and tendency to calomel disproportionation. Formation of chloromercury compounds monolayer with covalently bound Cl atoms was postulated [116]. More detailed and quantitative studies were reported by Bockris et al. [112]. The authors concluded generation of calomel through ionic intermediate Hg_2Cl^+ entering the solution phase and reacting then with Cl^- ions (Hg_2Cl^+ form can also disproportionate to yield mercury(II) species). This process has been also studied by Armstrong et al. [121]. The rate of mercury dissolution was found diffusion controlled and the estimated electrode reaction rate constant was found to be above 1.5 cm s^{-1}. Existence of $HgCl_4^{2-}$ was postulated as the reaction product in 2 or 5 mol dm^{-3} HCl. Behr and Taraszewska [122] determined quantitatively the concentration of mercury compounds in equilibrium with solid Hg_2Cl_2 and metallic Hg in KCl solutions (Fig. 5.3.2); the slow step of the

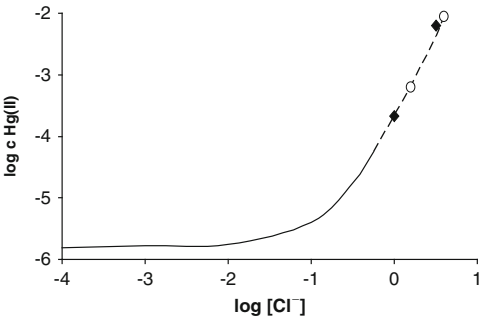

Fig. 5.3.2 Total mercury forms concentration in equilibrium with Hg and Hg_2Cl_2 vs. log[Cl^-] [122], determined in [122] (*diamonds*), obtained according to Sillén [147] (*line*) or calculated by Armstrong et al. [121] (*circles*) (see details in [122])

process was found to be crystallization or disproportionation of Hg_2Cl_2. Bewick et al. [123] explained the process in terms of monolayer deposition with two-dimensional growth of two-dimensional nuclei and determined nucleation rate constants for different steps. The proposed mechanism of the growth process consists of the following reactions:

$$Cl^-_{solution} \rightleftharpoons Cl^-_{ads} \rightleftharpoons Cl^-_{lattice} \tag{5.3.4a}$$

$$Cl^-_{solution} \rightleftharpoons Cl^-_{lattice} \tag{5.3.4b}$$

$$Hg \rightarrow Hg^+_{ads(slow)} \tag{5.3.4c}$$

$$Hg^+_{ads} \rightarrow Hg^+_{lattice} \tag{5.3.4d}$$

More details of calomel formation in anodic oxidation of mercury can be found in [101].

Hills and Ives [98] explained origin of possible problems concerning potential instability, observed mainly in acidic solutions; these effects have been also summarized in [101].

1. Introduction of oxygen into the electrode system shifts the potential to more positive values, also due to occurrence of reaction described by Eq. (5.3.3). However, this process is reversible and the initial potential can be restored after passing an inert gas through the system.
2. A thick layer of calomel upon the mercury surface leads to unsatisfactory results. Thin layers are advantageous to obtain good properties of the electrode.
3. An aqueous solution layer formed between the mercury and glass wall of the tube, with properties different from those of bulk solution, may affect the potential. This effect can be considerably reduced by hydrophobization of the glass surface.
4. Coarsely crystalline calomel may result in positive deviation of the potential; thus finely dispersed calomel is recommended.

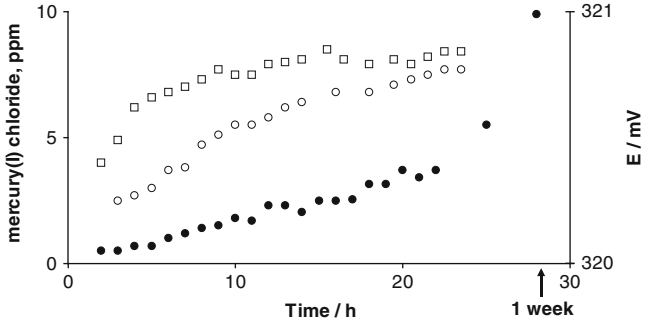

Fig. 5.3.3 Variation of calomel electrode potential with time (*open symbols*) and of mercuric species concentration measured spectrophotometrically (*filled symbols*) [126]. The *upper series* (*open symbols*) and concentration changes refer to a "thick-skin" type electrode, and the *lower series* to Hills and Ives' type electrode (see details in [126])

5. Interaction of calomel with mercury can be of some significance. Therefore, it is advised to store calomel and mercury in dry state. If calomel is introduced into a vessel, where the mercury is already covered by a solution layer, the parameters of the electrode are usually not satisfactory.

A difficulty which was not resolved by the electrode construction is slow establishment of disproportionation equilibrium of calomel. The nature of disproportionation was studied in [124] using a circulation cell. This process is of significance at temperatures above 80 °C; thus in this temperature range the calomel electrode cannot be used. On the other hand, the above-mentioned problems with disproportionation equilibrium can be important, if measurements are carried out at various temperatures. This difficulty can be partly reduced by using a vessel with high ratio of mercury surface area to the volume of solution [124]. Such a new type of cell has been proposed by Ives and Prassad [125], with a small volume of the solution which reduces the time needed for equilibration. Covington et al. have shown [126] that the electrode gives more reproducible results if new cells are prepared and used at each temperature and are not thermally cycled in the usual manner.

Covington et al. [127], taking into account the disproportionation reaction resulting in formation of mercuric-chloride complexes, reevaluated the standard potential of calomel electrode to $E^{\ominus} = 0.2679_6$V.

The same group of researchers [126] have studied also variations in time of the potential of the calomel electrode and pointed to slow rise of potential over several hours (Fig. 5.3.3). This increase was dependent on amount of calomel; the electrode with greater amount of calomel reached a steady state value more quickly. Simultaneous spectrophotometric analysis of the solution confirmed accumulation of ionic mercury species in solution (at concentration around 10^{-8} mol dm^{-3}) resulting from disproportionation of calomel.

Studies carried out by Schwabe and Ferse [128] revealed significant temperature hysteresis effect; particularly erroneous results (potential shifts from the correct value were around 1 mV) were observed by Covington et al. [126] when the temperature was lowered.

Another problem is related to applications of calomel electrodes in samples where traces of sulfide ions can be present. In this case Hg(II) ions as disproportionation product of Hg_2Cl_2 can react with sulfide ions producing black deposit of HgS in the vicinity of reference electrode junction [129].

The conclusion resulting from Covington's studies is that the silver/silver chloride reference electrode is much preferred than the calomel electrode.

5.3.2 Other Mercury/Mercury(I) Halide Electrodes

Electrodes similar to the calomel electrode can be also constructed, utilizing sparingly soluble mercury(I) halides instead of calomel. These mercury(I) compounds are less soluble in water than calomel; however, complexes of Hg(I) with halide ions are stronger than those with chloride anions. On the other hand, these compounds are more photosensitive.

Gerke [130] and Hills and Ives [98] have reviewed papers concerning the electrode: $Hg \mid Hg_2Br_2 \mid Br^-$. Standard potentials of this couple have been determined using mean molal ionic activity coefficients of HBr or by using the standard potential of the silver/silver bromide electrode. The obtained standard potential is 0.139 V, with deviations within the range of 1 mV.

This electrode is characterized by equilibria analogous to those typical for calomel electrode. Due to these processes potential measurements carried out at various temperatures may not be reproducible. Results with reproducibility lower than 40 μV were presented by Gupta et al. [131]. Hg_2Br_2 is less soluble than Hg_2Cl_2; however, it easily forms complexes, disadvantageous from the point of view of reference electrode applications [132].

A similar system with mercury(I) iodide has been reviewed by Gerke [130]. The standard potential was found to be −0.0404 V at 25 °C; however, this electrode is not recommended as reference electrode.

5.3.3 Mercury/Mercury(I) Sulfate Electrode

The mercury/mercury(I) sulfate electrode, abbreviated as mercury sulfate reference electrode (MSRE), is a second-kind electrode which consists of metallic mercury coated with slurry of mercury(I) sulfate (Hg_2SO_4) [100, 133] (Fig. 5.3.4). The properties of this electrode have been reviewed in [101].

This reference electrode is frequently used due to its outstanding reproducibility [134], following only the hydrogen electrode. The redox equilibrium:

$$Hg_2SO_{4(s)} + 2e^- \rightleftharpoons 2Hg + SO_4^{2-} \tag{5.3.5}$$

is represented by the Nernst equation:

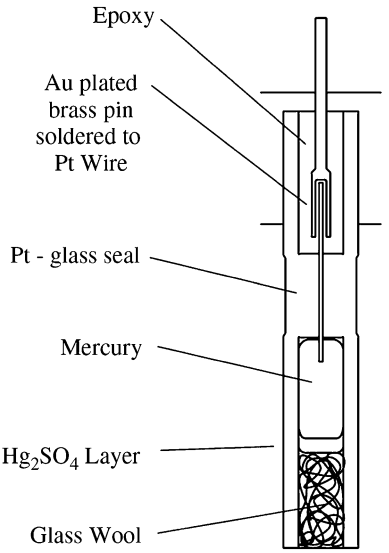

Fig. 5.3.4 Schematic view of mercury sulfate reference electrode [99]. Reprinted with permission from Elsevier

$$E = E^{\ominus}_{Hg_2SO_4/Hg} - RT/F \ln a_{SO_4^{2-}} \tag{5.3.6}$$

pointing to the linear dependence on a sulfate ion activity. It is applied mainly in chloride ion free solutions or in systems sensitive to chloride ions. These electrodes are often used to study processes occurring in lead-acid batteries, e.g. [135].

The standard potential data, $E^{\ominus}_{Hg_2SO_4/Hg}$ (25 °C), vary in the range from 0.6125 to 0.6294 V [136]; for instance, 0.6158_7 V vs. hydrogen electrode was initially reported by Beck et al. [137]. A slightly lower value (0.6151_5 V at 25 °C), but with lower reproducibility, was earlier obtained by Harned and Hamer [138]. A considerably lower value (0.6125 V) was found by Covington et al. [139]. The difference between above given data can result from difference in data extrapolation to infinite dilution. Clegg et al. [140] postulated 0.6123_6 V, based mainly on emf results from [139]; this value can be recommended. Later, Hamer and Wu [141], carrying out measurements for cells with zinc or cadmium amalgams and mercury(I) sulfate electrodes, proposed the standard potential value: 0.6154_4 V.

Gardner et al. [142], basing on the formal potential reported by Covington [139], studied the influence of temperature on the standard potentials; results are collected in Table 5.3.2. The temperature, T, dependence of the standard potential can be described by equation [138]:

$$E(\mathrm{V}) = 0.6349_5 - 781.44 \times 10^{-6}T - 426.89 \times 10^{-9}T^2,$$

valid in the temperature range 0–60 °C.

Schwabe and Ferse [128] have studied also influence of higher concentrations (above 0.5 m) of Li_2SO_4 and Na_2SO_4 on potential at different temperatures.

Table 5.3.2 Standard potentials for mercury/mercury(I) sulfate reference electrode [101, 142]

Temperature (°C)	E°/V
0	0.6305_8
5	0.6277_4
15	0.6203_8
25	0.6125_0
35	0.6039_2
45	0.5947_1
55	0.5848_9
65	0.5745_0
75	0.5635_4
85	0.5519_9
95	0.5398_1
100	0.5334_7

5.3.3.1 Electrode Preparation

Mercury preparation. No particular preparative steps are necessary unless mercury of sufficient purity is used.

Hg_2SO_4 preparation [99]. High purity Hg_2SO_4 is available commercially; it can be also produced chemically or electrochemically.

In chemical preparation mercury(I) sulfate can be obtained similarly as mercury (I) chloride. First, about 1 g of reagent-grade mercury(I) nitrate dihydrate, $Hg_2(NO_3)_2{\cdot}2H_2O$, is moistened with 0.2 mL of concentrated nitric acid and dissolved in 20 mL of water. This solution is then added dropwise for 2 min into a covered beaker containing ~100 mL of 1 mol dm^{-3} H_2SO_4 while using a magnetic stir bar to continuously stir the solution. The resulting suspension should be stirred for an hour. The precipitated mercury(I) sulfate is rinsed in sintered glass crucible with ample cold 1 mol dm^{-3} H_2SO_4 and then stored in $\geq$1 mol dm^{-3} H_2SO_4, protected from light. Chemically precipitated mercury(I) sulfate can be recrystallized by dissolving Hg_2SO_4 in concentrated sulfuric acid in the presence of mercury and the resulting solution should be added dropwise to an excess of absolute methanol causing precipitation of the mercury(I) sulfate. The white precipitate should be washed 20 times employing decantation and the Hg_2SO_4 should be stored in $\geq$1 mol dm^{-3} H_2SO_4 and protected from light.

In electrochemical preparation either galvanostatic or potentiostatic procedure can be applied. In galvanostatic method mercury can be oxidized in 2.5 mol dm^{-3} H_2SO_4 by applying a current density of 40 mA cm^{-2} between an Hg pool electrode and a platinum coil counter electrode. This setup consists of a glass stirrer which should not agitate the mercury pool electrode, but to keep the Hg_2SO_4 in suspension and allow for mixing of the solution. Using this method 1–1.2 g of Hg_2SO_4 from 1 mL Hg is obtained. The Hg_2SO_4 is gray and contains finely divided mercury.

In potentiostatic method mercury can be oxidized using a dropping mercury electrode made of a funnel filled with Hg. The Hg is dropped into 2.5 mol dm^{-3} H_2SO_4 at an applied potential of 2 V. The Hg_2SO_4 produced is gray and contains finely divided mercury as above.

The obtained product, independently of the method used, should be stored in acidic medium ($\geq$1 m H_2SO_4) as hydrolysis occurs in neutral solutions, and protected from light.

The electrode is prepared by coating the mercury with ~2.5 mm thick layer of Hg_2SO_4 before flushing out the assembly five times with the filling solution. To equilibrate, the reference electrode should be conditioned overnight in fresh filling solution.

Filling solution is either saturated K_2SO_4 or H_2SO_4 of concentration higher than 1 mol dm^{-3}. Electrodes with more dilute solutions exhibit poor reversibility.

The potential of this electrode is less sensitive to mercury purity than that of SCE. When using the electrode, the disadvantageous properties of mercury(I) sulfate (hydrolysis and relatively high solubility) should be taken into account. It is also known that mercury can dissolve in aerated dilute sulfuric acid; however, this process is hindered by high overpotential of hydrogen evolution on mercury.

5.3.4 Mercury/Mercury(I) Sulfide Electrode

There are known two sulfides of mercury HgS and Hg_2S. However, the latter of these compounds is not stable because of the disproportionation reaction:

$$Hg_2^{2+} + H_2S \rightarrow HgS + Hg + 2H^+ \tag{5.3.7}$$

This reaction occurs due to the very low solubility of HgS in water (solubility product, $K_{sol(HgS)} = 9 \times 10^{-52}$ at 25 °C). The given value is from the chemical tables.

HgS is known in two forms with different colors, black and red. From these two forms, at room temperature, the red one is thermodynamically more stable; however, usually the black modification is formed when HgS is precipitated in aqueous solutions. Therefore, in the collections of potentials often the values for both forms are reported.

Ives [143] reported the work of Makolkin [144] who studied the hydrogen sulfide cell:

$$\begin{gathered}\mathrm{Pt\,(s)} \,\big|\, \mathrm{H_2\,(g)} \,\big|\, \mathrm{KCl\,(aq)} \,\|\, \mathrm{KCl\,(aq)} \,\big|\, \mathrm{H_2S\,(g)} \,\big|\, \mathrm{HgS\,(s)} \,\big|\, \mathrm{Hg\,(l)} \\ c = 0.01 \ \mathrm{mol\ dm^{-3}}\end{gathered} \tag{5.3.8}$$

using the red modification of HgS.

The emf of such a cell at temperatures 15, 25, and 35 °C was found to be 0.0628, 0.0569, and 0.0525 V, respectively. The temperature coefficient at 25 °C was determined as equal to -5×10^{-4} V K^{-1}.

A similar cell was also studied [145], but in this case black HgS was used. At 25 °C the emf of the cell was equal to 0.0504 ± 0.009 V, lower than that found for the red modification. Also the emf of the following cell:

$$\mathrm{Hg(l)|HgS(s)|Na_2S(aq)|KCl(aq)|Hg_2Cl_2(s)|Hg(l)} \tag{5.3.9}$$

was measured [143]. Careful elaboration of the experimental data led the authors to the determination of a standard free energy of formation of HgS, $\Delta G^{\circ} = -10.5 \pm 0.07$ kcal at 25 °C. From their results Ives [143] found the standard potential of that electrode $E^{\circ}_{\mathrm{Hg/HgS/S^{2-}}} = -0.661 \pm 0.0015$ V at 25 °C.

Using thermodynamic data ($E^{\circ}_{\mathrm{Hg/Hg^{2+}}}$ and $K_{\mathrm{sol(HgS)}}$) one arrives to a few millivolts more negative value (dependent on the $K_{\mathrm{sol(HgS)}}$ which is reported by different authors in the range 10^{-51}–10^{-52}). The mechanism of the formation of the potential in the system with so low concentration of Hg^{2+} ions in the solution is not clear.

However, there are reports in the literature, briefly summarized [146] on the formation of complex species HgS_2^{2-}, $Hg(HS)_2$, and $HgS(HS)_2^{2-}$, which may play some role in the formation of potential. Though in principle the $Hg|HgS|S^{2-}$ system could be used as a reference electrode redox couple, its applicability is in practice very limited. This system may be considered as a quasi-reference electrode one, in view of the extremely small solubility product of HgS. Therefore, the potential of such electrode may be not well reproducible and not sufficiently stable in time. The wider use of such electrode would need more profound and extensive studies on its nature and performance.

Different methods may be applied for the preparation of HgS. Anodization of mercury in the presence of sulfide may be used, but even direct longer action of H_2S on mercury in the presence of air leads to the formation of black HgS.

In the preparation of the red form, Makolkin [144] has used a solution of $HgCl_2$ heated to 60 °C which reacted with an excess of aqueous ammonia and next with an excess of solution of $Na_2S_2O_3$.

Construction of such electrode may be similar to that used in the case of the HgO electrode.

5.3.5 *Other Electrode Systems Based on the Mercury Redox Reaction*

There are also other electrode systems of the type $Hg\,|\,Hg_2X_2$, $Hg_2Y\,|\,X^-$, or $Hg_2Y\,|\,Y^{2-}$ which may be potentially used for the construction of a reference electrode. In theory such electrodes of the second kind should maintain a constant potential at a constant activity of X^- or Y^{2-}. In Table 5.3.3 some of such systems were listed with their standard or formal potentials [101].

Table 5.3.3 Selected mercury electrode systems in aqueous solutions at 25 °C

Mercury redox reaction	E°/V
$Hg_2(C_6H_5COO)_2 + 2e^- \rightleftharpoons 2Hg + 2C_6H_5COO^-$	0.4623_0
$Hg_2Pc_2 + 2e^- \rightleftharpoons 2Hg + 2Pc^-$, Pc = picrate	0.4924_0
$Hg_2HPO_4 + 2e^- \rightleftharpoons 2Hg + HPO_4^{2-}$	0.6359_0
$Hg_2C_2O_4 + 2e^- \rightleftharpoons 2Hg + C_2O_4^{2-}$	0.4166_0
$Hg(IO_3)_2 + 2e^- \rightleftharpoons 2Hg + 2IO_3^-$	0.3939_0
$Hg_2Ac_2 + 2e^- \rightleftharpoons 2Hg + 2Ac^-$, Ac = acetate	0.5115_6
$Hg_2(HCOO)_2 + 2e^- \rightleftharpoons 2Hg + 2HCOO^-$	0.5113_0

Some of these systems were only occasionally used as reference electrodes. Different reasons limited their application. For practical reasons the use of many, different types of reference electrodes is confusing and not practical.

References

98. Hills GJ, Ives DJG (1961) The calomel electrode and other mercury-mercurous salt electrodes. In: Ives DJG, Janz GJ (ed) Reference electrodes. Theory and practice. Academic, New York, pp 127–178
99. Smith TJ, Stevenson KJ (2007) Reference electrodes. In: Zoski CG (ed) Handbook of electrochemistry, Elsevier, pp 73–110
100. Szabó S, Bakos I (2010) Int J Corros, article ID 756950
101. Wrona PK, Galus Z (1982) Mercury. In: Bard AJ (ed) Encyclopedia of electrochemistry of the elements, vol 9, part A. Dekker, New York
102. Hills GJ, Ives DJG (1951) J Chem Soc 319
103. Guggenheim EA, Prue JE (1954) Trans Faraday Soc 50:231
104. Schwabe K, Ziegenbalg S (1958) Z Elektrochem 62:172
105. Grzybowski AK (1958) J Phys Chem 62:550
106. Holze R (2007) Electrochemical thermodynamics and kinetics. In: Lechner MD (ed) Landolt-Börnstein numeric data and functional relationships in science and technology, group IV physical chemistry, vol 9 Electrochemistry. Springer, Berlin, subvolume A
107. Chateau H (1954) J Chim Phys 51:590
108. Bard AJ, Faulkner LR (2001) Electrochemical methods, 2nd edn. Wiley, New York
109. Yosypchuk B, Novotny L (2003) Chem Listy 97:1083
110. Yosypchuk B, Novotny L (2004) Electroanalysis 16:238
111. Pickup NL, Lam M, Milojevic D, Bi RY, Shapiro JS, Wong DKY (1997) Polymer 38:2561
112. Bockris JO'M, Devanathan MAU, Reddy AKN (1964) Proc R Soc London A279:324
113. Hills GJ, Ives DJG (1951) J Chem Soc 313
114. Cousens RH, Ives DJG, Pittman RW (1953) J Chem Soc 3972
115. Cousens RH, Ives DJG, Pittman RW (1953) J Chem Soc 3980
116. Dibbs HP, Ives DJG, Pittman RW (1957) J Chem Soc 3370
117. Boult EH, Thirsk HR (1954) Trans Faraday Soc 50:376

118. Cornish DC, Dibbs HP, Feates FS, Ives DJG, Pittman RW (1962) J Chem Soc 4104
119. Cornish DC, Das SN, Ives DJG, Pittman RW (1966) J Chem Soc A 111
120. Cornish DC, Ives DJG, Pittman RW (1966) J Chem Soc A 116
121. Armstrong RD, Fleischmann M, Thirsk HR (1965) Trans Faraday Soc 61:2238
122. Behr B, Taraszewska J (1968) J Electroanal Chem 19:373
123. Bewick A, Fleischmann M, Thirsk HR (1962) Trans Faraday Soc 58:2200
124. Das SN, Ives DJG (1962) J Chem Soc 1619
125. Ives DJG, Prasad D (1970) J Chem Soc B 1649
126. Covington AK, Dobson JV, Wynne-Jones L (1967) Electrochim Acta 12:525
127. Covington AK, Dobson JV, Wynne-Jones L (1967) Electrochim Acta 12:513
128. Schwabe K, Ferse E (1965) Z Elektrochem 69:383
129. Vitiello JD, Pistone D, Cormier AD (1996) Scand J Clin Lab Invest 56 (Suppl 224):165
130. Gerke RH (1925) Chem Rev 1:377
131. Gupta SR, Hills DJ, Ives DJG (1963) Trans Faraday Soc 59:1886
132. Cornish DC, Ives DJG, Pittman RW (1966) J Chem Soc A 120
133. Ives DJG, Smith FR (1961) Electrodes reversible to sulfate ions. In: Ives DJG, Janz GJ (ed) Reference electrodes. Theory and practice. Academic, New York, pp 393–410
134. Antropov LI (1972) Tankonyvkiado. Budapest in Hungarian; (1969) Theoreticheskaya Elektrokhimiya. Visshaya Skola, Moscow
135. Carpenter MK, Bernardi DM, Wertz JA (1996) J Power Sources 63:15
136. Hamer WJ (1972) J Res Natl Bur Stand 76A:185
137. Beck WH, Dobson JV, Wynne-Jones WFK (1960) Trans Faraday Soc 56:1172
138. Harned HS, Hamer WJ (1935) J Am Chem Soc 57:27
139. Covington AK, Dobson JV, Wynne-Jones WFK (1965) Trans Faraday Soc 61:2050
140. Clegg SL, Rard JA, Pitzer KS (1994) J Chem Soc Faraday Trans 90:1875
141. Hamer WJ, Wu YC (1995) J Solution Chem 24:1013
142. Gardner WL, Mitchell RE, Cobble JW (1969) J Phys Chem 73:2021
143. Ives DJG (1961) Oxide, oxygen and sulfide electrodes. In: Ives DJG, Janz GJ (ed) Reference electrodes. Theory and practice. Academic, New York, pp 322–392
144. Makolkin IA (1942) Zhur Fiz Khim 16:18
145. Goates RJ, Cole AG, Gray EL (1951) J Am Chem Soc 73:3596
146. Balej J (1985) Standard potentials in aqueous solution. In: Bard AJ, Parson R, Jordan J (eds) Mercury, Dekker, New York, Chapter 10.III
147. Sillén LG (1949) Acta Chem Scand 3:539

5.4 Thallium Electrode

Krzysztof Maksymiuk, Agata Michalska, Anna Kisiel, and Zbigniew Galus

Thallium electrode is a second-kind electrode composed of thallium amalgam (40 %) and a thallium salt, most often thallium(I) chloride, but also thallium(I) bromide or sulfate can be used [148, 149]:

$$\mathrm{Hg, Tl(40\,wt\%)|TlCl(s), KCl(s)||}$$

Half-cell reaction of thallium(I) chloride electrode is similar to that of silver/silver chloride electrode:

$$\mathrm{TlCl + e^- \rightleftharpoons Tl(Hg) + Cl^-} \tag{5.4.1}$$

and the potential is described by equation:

$$E_{\mathrm{TlCl/Tl}} = E^{\ominus}_{\mathrm{Tl^+/Tl}} + \frac{RT}{F}\ln K_{\mathrm{sol}}(\mathrm{TlCl}) - \varepsilon(\mathrm{Tl-Hg, Tl}) - \frac{RT}{F}\ln a_{\mathrm{Cl}^-}. \tag{5.4.2}$$

Taking into account the standard potential $E^{\ominus}_{\mathrm{Tl^+/Tl}} = -0.3363$ V, solubility product of TlCl (1.805×10^{-4}), and potential shift resulting from amalgam formation (ε, studied, e.g., by Mussini and Longhi [150]), the standard potential (for $a_{\mathrm{Cl}^-} = 1$) at temperature 25 °C is as follows:

$$E^{\ominus}_{\mathrm{TlCl/Tl}} = -0.5784\ \mathrm{V}.$$

Values of the formal potential corresponding to TlCl/Tl(Hg) electrode for various solutions were collected in Table 5.4.1 [151, 152]:

Thallium(I) chloride and bromide do not form stable complexes with typical anions and do not undergo disproportionation; thus electrodes using these salts are characterized by good performance and low temperature hysteresis [153, 154]. Upon galvanostatic polarization they exhibit slight hysteresis, however, lower than for calomel electrode. Electrode potentials are reversible with respect to temperature changes and the dependence of potential on temperature is described by third-degree polynomial functions [153, 154]:

$E(\mathrm{V}) = -0.5734 - 8.297 \times 10^{-4}(T-25) - 2.007 \times 10^{-6}(T-25)^2 + 1.345 \times 10^{-8}(T-25)^3$, for electrode with thallium chloride.

K. Maksymiuk (✉) • A. Michalska • A. Kisiel • Z. Galus
Department of Chemistry, University of Warsaw, Pasteura 1, 02-093 Warsaw, Poland
e-mail: kmaks@chem.uw.edu.pl; agatam@chem.uw.edu.pl; akisiel@chem.uw.edu.pl; zbgalus@chem.uw.edu.pl

Table 5.4.1 Potentials of thallium electrode: TlCl/Tl(Hg)

Electrolyte solution	Temperature (°C)	Potential vs. SHE (V)
3.5 mol dm^{-3} KCl, HCl[a]	25	−0.5706
3.5 mol dm^{-3} KCl, oxalate	25	−0.5703
3.5 mol dm^{-3} KCl, phosphate	25	−0.5713
3.5 mol dm^{-3} KCl, borax	25	−0.5709
Sat. KCl, HCl	25	−0.5734
Sat. KCl, phosphate	25	−0.5766
Sat. KCl, borax	25	−0.5795

[a]Thalamid™ electrode

$E(\mathrm{V}) = -0.6826 - 7.289 \times 10^{-4}(T-25) - 2.438 \times 10^{-6}(T-25)^2 + 2.622 \times 10^{-8}(T-25)^3$, for electrode with thallium bromide; in both cases the dependences relate to 0.1 mol dm^{-3} HCl solutions.

Thallium(I) sulfate is more soluble than halides and this limits its suitability for reference electrode purposes.

Thallium(I) chloride reference electrode was commercialized by Schott Glaswerke (Mainz, Germany) as Thalamid™ electrode. Thallium amalgam and thallium(I) chloride stay in contact with solution saturated with TlCl, NaCl, or KCl. Oxygen access should be restricted to avoid amalgam decomposition. This electrode is stable at temperatures up to 135 °C, in contrast to calomel electrode working at temperatures up to 80 °C and the electrode resumes very fast its potential after a temperature change. However, a significant drawback of Thalamid electrode is toxicity of thallium and its compounds. Performance of classical silver/silver chloride or calomel electrodes under typical conditions for potentiometric applications was found, however, better than for thallium electrode [155].

Owing to low solubility of thallium halides in organic solvent, the thallium reference electrode was successfully used in dimethylsulfoxide [156–158], dimethylformamide [159], propylene carbonate [160], and acetonitrile [161].

References

148. Bates RG (1961) The glass electrode. In: Ives DJG, Janz GJ (ed) Reference electrodes. Theory and practice. Academic, New York, pp 270–321
149. Szabó S, Bakos I (2010) Int J Corros, article ID 756950
150. Mussini T, Longhi P (1965) Ric Sci Rend A8:1352
151. Baucke FGK (1974) Chem Ing Tech 46:71
152. Holze R (2007) Electrochemical thermodynamics and kinetics. In: Lechner MD (ed) Landolt-Börnstein numeric data and functional relationships in science and technology, group IV physical chemistry, vol 9 Electrochemistry. Springer, Berlin, subvolume A
153. Baucke FGK (1971) J Electroanal Chem 33:135
154. Baucke FGK (1972) J Electroanal Chem 39:263
155. Midgley D, Torrance K (1978) Analyst 101:833
156. Cogley DR, Butler JN (1966) J Electrochem Soc 113:1074

157. Smyrl WH, Tobias CW (1966) J Electrochem Soc 113:754
158. Smyrl WH, Tobias CW (1968) J Electrochem Soc 115:33
159. Delahay P, Tobias CW (eds) (1970) Advances in electrochemistry and electrochemical engineering, vol 7. Interscience, New York
160. Baucke FGK, Tobias CW (1969) J Electrochem Soc 116:34
161. Coetzee JE, Campion JJ (1967) J Am Chem Soc 89:2513

5.5 Iodine–Iodide Electrode

Günter Tauber

5.5.1 Iodine–Iodide Electrode

The iodine–iodide electrode has been investigated and reported by many authors. Brunner [162] and Vetter [163] have given comprehensive and detailed descriptions of the chemical reactions, the equilibrium potential, polarization phenomena, and current density vs. potential curves of the iodine–iodide redox system, obtained with platinum as the noble metal electrode.

This chapter will describe the iodine–iodide electrode with respect to properties that are relevant for practical applications, i.e., as a reference electrode for potentiometry as typically used in measuring chains with pH glass electrodes, which was introduced by Ross [164].

The iodine–iodide electrode is a redox electrode. It consists of two phases: an electrolyte with iodide and triiodide ions and a noble metal. The reaction partners are the ions dissolved in the electrolyte only, which are adsorbed at the noble metal surface, exchange electrons with the noble metal, and define its potential in that way. No ions but only electrons are the charge carrying species passing the liquid/solid interface. Owing to the high exchange current density of the electrode reaction this redox electrode has a very stable potential with a fast response during temperature cycling and it has a very small sensitivity to polarization.

The basic reaction of the iodine–iodide electrode is

$$2I^- \rightleftarrows I_2 + 2e^- \tag{5.5.1}$$

with the standard potential of $E_1{}^{\ominus} = +0.6276\,\mathrm{V}$ according to Vetter [163].

For higher iodide concentrations the reaction

G. Tauber
Leiter Forschung, SI Analytics GmbH, Hattenbergstraße 10, 55122 Mainz, Germany
e-mail: guenter.tauber@si-analytics.com

$$I_2 + I^- \rightleftarrows I_3^- \tag{5.5.2}$$

is reported with an equilibrium constant $K = \frac{c_{I_2} c_{I^-}}{c_{I_3^-}} = 0.0015$ at 25 °C [163, 165].

In this case the electrode reaction is

$$3I^- \rightleftarrows I_3^- + 2e^- \tag{5.5.3}$$

with the standard potential of $E_2^{\ominus} = +0.5446$ V according to Vetter [163].

Equation (5.5.3) describes the reaction of practically used reference electrodes with high iodide concentrations. The potential of the iodine–iodide electrode is given by the Nernst equation

$$E = E^{\ominus} + \frac{RT}{2F} \ln \frac{c_{I_2}}{c_{I^-}^2} \tag{5.5.4}$$

or

$$E = E^{\ominus} + \frac{RT}{2F} \ln \frac{c_{I_3^-}}{c_{I^-}^3} \tag{5.5.5}$$

where R is the gas constant, T is the absolute temperature, and F is the Faraday constant. Equations (5.5.4) and (5.5.5) lead to the same electrode potential at 25 °C.

For other temperatures the temperature dependence of the formation of triiodide must be taken into account when calculating the potential.

The temperature dependence of the equilibrium constant K_1 for the reverse of reaction (5.5.2) was determined spectrophotometrically by Palmer et al. [165].

$$\log K_1 = \log K^{-1} = A/T + B + C \log T. \tag{5.5.6}$$

The values of the parameters were found to be $A = 550.0$, $B = 7.355$, and $C = -2.575$ for solutions with an ionic strength of 0.02 mol L^{-1}.

With Eqs. (5.5.4) and (5.5.6) the electrode potential for all temperatures can be calculated when the concentrations of iodine and iodide are known.

A reference electrode suitable for practical use must have a well-known potential in the specified temperature range, reproducible and stable over a long period of time. The liquid-junction potentials should be small and reproducible in the specified applications and finally its production should be easy and inexpensive. These expectations will be proved next for the iodine–iodide electrode.

5.5.2 *Temperature Coefficient*

The temperature function of the iodine–iodide electrode was investigated by Ross [164], who described the optimum electrolyte composition with 2.84 mol L^{-1} KI and 0.00458 mol L^{-1} I_3^-. This electrolyte results in an electrode potential with a temperature coefficient close to zero.

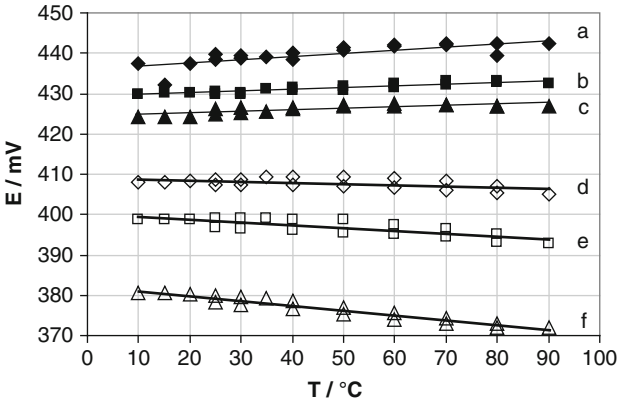

Fig. 5.5.1 Potentials of iodine–iodide electrodes vs. a saturated silver–silver chloride reference electrode with $E = 197$ mV at 25 °C connected via a salt bridge. The concentrations of KI were, (a) $c_{I^-} = 1.8$ mol L^{-1}, (b) $c_{I^-} = 2.8$ mol L^{-1}, (c) $c_{I^-} = 3.8$ mol L^{-1}, (d) $c_{I^-} = 2.8$ mol L^{-1}, (e) $c_{I^-} = 3.8$ mol L^{-1}, (f) $c_{I^-} = 3.8$ mol L^{-1}. The potentials at 25 °C were adjusted by addition of iodine solution

The very small temperature function of the electrode potential was confirmed by measurements of Tauber [166]. Figure 5.5.1 shows the electrode potentials measured vs. a saturated silver/silver chloride electrode at 25 °C using the following cell:

$$\mathrm{Ag/AgCl, KCl_{sat}(25\,^{\circ}C)//3\,mol\,L^{-1}\ KCl//3\,mol\,L^{-1}\ KCl//(}T/^{\circ}\mathrm{C)I_3^-/I^-, Pt} \tag{5.5.7}$$

The potential of the Ag/AgCl, KCl_{sat} electrode was assumed to $E = +197$ mV at 25 °C [167–169].

The temperature coefficient T_c of the iodine–iodide redox electrode can be taken from the data of Fig. 5.5.1. Figure 5.5.2 shows a plot of T_c vs. the electrode potential E at 25 °C.

It is important to mention that all potentials of Figs. 5.5.1 and 5.5.2 are referenced to the standard hydrogen electrode at 25 °C. This is useful for practical applications because the potential of the standard hydrogen electrode has a high "relative" temperature coefficient.

Palmer et al. [165] have determined the temperature dependence of the equilibrium constant of reaction (5.5.2). Using their data to calculate the potentials for different temperatures would lead to a shift of the line in Fig. 5.5.2 to lower potentials, but having the same slope. The reason for the shift may be the much smaller ionic strength of the solutions used in the spectrophotometrical studies by Palmer.

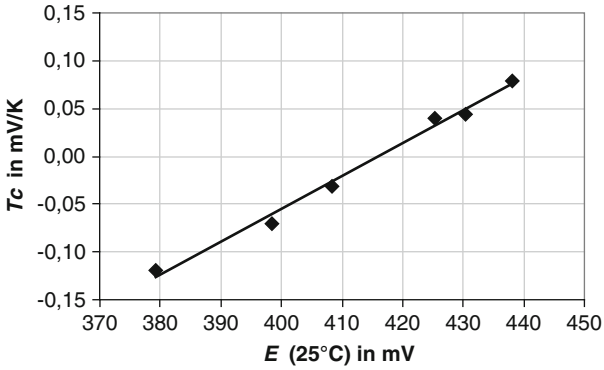

Fig. 5.5.2 Temperature coefficient T_c of the iodine–iodide electrode vs. the potential E at 25 °C. The iodine–iodide electrode with the smallest temperature coefficient close to zero has a potential around $E = 415$ mV at 25 °C and an electrolyte with a high KI concentrations of over 1.5 mol L^{-1}

5.5.3 *Dilution Effect*

Equation (5.5.5) describes the relationship between the electrode potential and the concentrations of dissolved triiodide and iodide ions at a given temperature. The manufacturing of this redox electrode is easy and gives reproducible reference potentials if suitable housing materials like glass, platinum, and ceramic are used.

If the reference electrolyte is diluted by 10 %, the potential changes by only 1.4 mV, half as much as the change of a silver–silver chloride electrode potential. This is explained by the two-electron reaction (5.5.3), which causes only half the slope. Therefore, the potential of the iodine–iodide electrode is less sensitive to the dilution of the electrolyte compared to the silver/silver chloride, for instance.

If the electrode construction allows the refilling or replacement of the reference electrolyte, a reliable potential can be established over a long period of time. If the reference chamber is closed as obtained in commercial electrodes, the loss of ions by diffusion is a problem. Improvements were obtained by a larger electrolyte volume [170] or the introduction of an iodine reservoir or other means to stabilize the electrolyte composition [171].

5.5.4 *Liquid Junction*

In most practical cases reference electrodes are in contact with the sample solution via a diaphragm, which is typically a porous ceramic plug. The diaphragm is filled with the usually used KCl solution as reference electrolyte to form a liquid junction at its outer surface. Details and characteristics of liquid junctions are described elsewhere. Especially for the iodine–iodide electrode it should be mentioned that

iodine or iodide will penetrate the diaphragm and may cause problems by reaction with the sample solution or by coloring organic material.

The diffusion potentials as an important source of uncertainties are of the same order of magnitude for potassium iodide solutions as for the usually used potassium chloride solutions, because the relative ion mobilities of chloride and iodide are similar within 0.6 % [172].

Because of possible interference of the iodide or triiodide ions with sample solutions a KCl bridge electrolyte is introduced for practical applications. In this case a very small and constant liquid-junction potential is obtained at the inner junction of triiodide–iodide solution and the KCl solution and at the outer bridge diaphragm the same junction potentials with KCl solution are obtained as with other reference electrodes too.

5.5.5 Polarization

Another important property of a reference electrode for practical use is its sensitivity to polarization. If the reference electrode is burdened with a small current under bad measuring conditions, not well-suited equipment or by electromagnetic interference, then the reference potential should be affected as little as possible.

Vetter [161] has investigated the polarization of platinum electrodes in the iodine–iodide system. A current density of 1 mA cm^{-2} causes a potential shift of less than 1 mV, corresponding to a current of about 0.3 mA to a platinum wire with 0.3 mm diameter and a length of 3 cm. This is a very small polarization. A current of 0.3 mA would cause a potential drop of 300 mV at a 1 kΩ diaphragm.

Hence, the iodine–iodide electrode is well suited for practical applications in a harsh environment with electromagnetic interferences.

5.5.6 Long Time Stability

Since the electrolyte is in contact via a diaphragm with a KCl bridge electrolyte or the measuring solution the concentration of both components I_3^- and I^-, respectively, may change with time due to dilution or diffusion. In both cases it is expected that the dilution rate of $c_{I_3^-}$ and c_{I^-} is of the same order of magnitude. This would result in an increase of the potential.

Usually in practice a decrease of the potential with time is observed, which can be explained by a faster loss of c_{I_2}. A reason for a faster loss of iodine may be the diffusion through the diaphragm, by reaction with components from the sample solution, or by absorption of iodine in organic materials being in contact with the

electrolyte. Hence, a replenishment of iodine can increase the lifetime of the electrode and establish a longer period of constant potential.

Suggestions for the replenishment of iodine using absorbed iodine to organic materials like polyamid, for instance, as an iodine reservoir are described in [169]. On the other hand, it is possible to reduce the iodide loss by diffusion by the addition of iodide to the bridge electrolyte.

An effect of oxygen from the air on the long time stability could not be obtained. This is in accordance with Vetter [163].

5.5.7 Conclusion

The main advantage is the zero temperature coefficient of the iodine–iodide reference system and the very small hysteresis. On the other hand, this reference electrode is free of silver ions to avoid problems due to interactions with sulfide ions or proteins at the liquid junction. In harsh environments the iodine–iodide electrode is almost insensitive to small currents and to electromagnetic interferences.

The use of the iodine–iodide system is not restricted to aqueous electrolytes. Baucke [173] has investigated the iodine–iodide system in acetonitrile for special applications.

References

162. Brunner E (1907) Z phys Chem 58:1
163. Vetter KJ (1952) Z phys Chem 199:22
164. Ross JW, Potentiometric electrode, UK Patent GB 2 088 565 A
165. Palmer DA, Ramette RW, Mesmer RE (1984) J Solution Chem 13:9
166. Tauber G (2006) Presentation on ELACH7 conference in Waldheim, Germany
167. Bates RG (1954) Electrometric pH determinations, theory and practice. Wiley, New York
168. Galster H (1990) pH-Messung, VCH Verlagsgesellschaft mbH, Weinheim
169. Hamann CH, Vielstich W (1998) Elektrochemie, Wiley-VCH Verlag GmbH, Weinheim
170. Hirshberg M, West SJ, Barbookles J, Ion-selective electrode, US Patent No. US 6,793,787 B1
171. Tauber G, Potentiometrische Messkette, Patent No. D 10 2006 012 799 B4
172. Milazzo G (1952) Elektrochemie, Springer, Wien
173. Baucke FGK, Bertram R, Cruse K (1971) J Electroanal Chem 32:247

5.6 Oxide Systems

Krzysztof Maksymiuk, Agata Michalska, Anna Kisiel, and Zbigniew Galus

Only two metal oxides were in practice used to construct the reference electrodes of the second kind, namely, HgO and Ag_2O. The other metal oxides electrodes were used only occasionally sometimes as pH sensors.

5.6.1 The Mercury–Mercury(II) Oxide Electrode

This electrode has been known for rather long time. Already in 1909 Brönsted [174] has carried out measurements of the emf of the cell:

$$\mathrm{Pt(s)|H_2(g)|NaOH(aq)|HgO(s)|Hg(l)|Pt(s)} \tag{5.6.1}$$

These measurements were extended in 1926 by Fried [175]. Changing the NaOH concentration from 1 to 10 mol dm^{-3} it was found that emf of this cell was independent of NaOH concentration.

The Hg | HgO electrode should give rather reproducible results since the species which form this electrode, HgO and Hg, are stable.

On the other side, highly unstable is Hg_2O. The addition of alkali to salts of mercury(I) leads to the mixture of HgO and Hg due to the disproportionation reaction:

$$\mathrm{Hg_2^{2+} + 2OH^- \rightarrow HgO + Hg + H_2O} \tag{5.6.2}$$

The report of Longhi and others [176], on a good behavior of the Hg | HgO electrode, was confirmed later by several researchers who studied also the performance of this electrode at temperatures lower and higher than room temperature.

It should be mentioned that HgO is known in two forms: yellow and red; however, this difference in color may be due to the size of the particles of these species [177]. The red form which exhibits slightly lower solubility in water than the yellow one should be thermodynamically more stable; therefore the potentials given refer to the red form.

Several authors, including Hamer and Craig [178], have proposed to use the mercury(II) oxide electrode as a reference, especially for higher concentrations of alkali solutions including higher temperatures. The use of such an electrode, for instance, in the study of corrosion, fuel, and storage cells, is especially advised.

K. Maksymiuk • A. Michalska • A. Kisiel • Z. Galus (✉)
Department of Chemistry, University of Warsaw, Pasteura 1, 02-093 Warsaw, Poland
e-mail: kmaks@chem.uw.edu.pl; agatam@chem.uw.edu.pl; akisiel@chem.uw.edu.pl; zbgalus@chem.uw.edu.pl

Longhi et al. [176] carried out the careful redetermination of the standard potential of the Hg | HgO electrode at temperatures which covered the range from 283 to 363 K.

Potentials of this electrode were reported for two reference standard states.

Taking as a reference state $a_{H^+} = 1$ one may write the electrode reaction:

$$HgO + 2H^+ + 2e^- \rightleftharpoons Hg + H_2O \tag{5.6.3}$$

On the other side assuming $a_{OH^-} = 1$ one has

$$HgO + H_2O + 2e^- \rightleftharpoons Hg + 2OH^- \tag{5.6.4}$$

where HgO is in the following equilibrium:

$$HgO + H_2O \rightleftharpoons Hg(OH)_2 \rightleftharpoons Hg^{2+} + 2OH^- \tag{5.6.5}$$

Using the expression for potential of the Hg | Hg^{2+} electrode:

$$E_{Hg/Hg^{2+}} = E^{\ominus}_{Hg/Hg^{2+}} + \frac{RT}{2F} \ln a_{Hg^{2+}} \tag{5.6.6}$$

and the solubility product of $Hg(OH)_2$—$K_{sol(Hg(OH)_2)}$ [equilibrium (5.6.5)] one obtains for the reference state $a_{OH^-} = 1$:

$$E_{Hg/HgO/OH^-} = E^{\ominus}_{Hg/Hg^{2+}} + \frac{RT}{2F} \ln K_{sol(Hg(OH)_2)} - \frac{RT}{F} \ln a_{OH^-}. \tag{5.6.7}$$

Using further the ionic product of water one gets from Eq. (5.6.7) the following relation:

$$E_{Hg/HgO/H^+} = E^{\ominus}_{Hg/Hg^{2+}} + \frac{RT}{2F} \ln \frac{K_{sol(Hg(OH)_2)}}{K_w^2} + \frac{RT}{F} \ln a_{H^+} \tag{5.6.8}$$

valid for reference state $a_{H^+} = 1$.

Both these potentials [Eqs. (5.6.7) and (5.6.8)] are obviously combined by the simple equation:

$$E^{\ominus}_{Hg/HgO/OH^-} = E^{\ominus}_{Hg/HgO/H^+} + \frac{RT}{F} \ln K_w. \tag{5.6.9}$$

The early works on the Hg | HgO electrode were critically discussed and reported by Ives and Janz [177] who followed the critical evaluation of Hamer and Craig [178]. The characteristic feature of these early measurements is the agreement of obtained data up to 1 mV.

The average potential for the $E^{\ominus}_{Hg/HgO/H^+}$ electrode, corrected to zero concentration, was found to be 0.9258_1 (± 0.00036) V at 25 °C. The temperature coefficient of that potential at the same temperature is $-0.0002878\ V\ K^{-1}$. Reported data show that they were determined with a high precision.

Also Balej [179] gives the potential of this electrode practically equal to the above given value, adopted from the critical review of Hepler and Olofson [180]. Balej [179] reported also $E^{\ominus}$ for the Hg | HgO electrode in alkaline solutions [Eq. (5.6.4)] equal to 0.0977 V.

The Hg | HgO system was suggested to be a reference electrode with a constant concentration of hydroxide ion, maintained by $Ba(OH)_2$ and $Ca(OH)_2$ saturated solutions.

For the electrode systems: Hg | HgO | $Ba(OH)_{2(sat)}$ and Hg | HgO | $Ca(OH)_{2(sat)}$, Samuelson and Brown [181] reported the following potentials:

$$E(\mathrm{V}) = 0.1462 - 0.00060(T - 25)(\mathrm{to} \pm 0.00020\,\mathrm{V}) \tag{5.6.10}$$

and

$$E(\mathrm{V}) = 0.1923 - 0.00010(T - 25)(\mathrm{to} \pm 0.00010\,\mathrm{V}), \tag{5.6.11}$$

respectively, where T stands for temperature in °C and potentials are reported in the hydrogen scale.

Longhi et al. [176] redetermined and extended measurements of the standard potential of the mercury(II) oxide electrode for the temperature ranging from 283 to 363 K. These authors [176] have discussed also the reasons leading to discrepancies observed in the reported earlier data.

In the Technical Report on mercury(II) and silver(I) oxide electrodes, prepared by Rondinini et al. in the frame of the Commission on Electroanalytical Chemistry of IUPAC [182], the results obtained by Longhi et al. [176] were taken as the basic data. Table 5.6.1 shows the standard potentials of the Hg | HgO electrode given in this report. Potentials of both electrodes Hg | HgO | H^+ and Hg | HgO | OH^- at different temperatures were reported.

The authors of the IUPAC report [182] give the standard potentials as a function of temperature also in the form of the least-square polynomials.

$$E^{\ominus}_{Hg/HgO/H^+}(\mathrm{mV}) = 992.7_4 - 0.18081T - 0.00012958T^2 \tag{5.6.12}$$

$$E^{\ominus}_{Hg/HgO/OH^-}(\mathrm{mV}) = 109.2_7 - 1.0042T - 0.0034805T^2 \tag{5.6.13}$$

with the estimated standard error not greater than ± 0.20 and ± 0.23 mV, respectively.

There were estimated also the temperature coefficients. At 298.15 K these coefficients are equal to

Table 5.6.1 Values of the standard acid potential $E^{\ominus}_{Hg/HgO/H^+}$ and of the standard basic potential $E^{\ominus}_{Hg/HgO/OH^-}$ of the HgO electrode in aqueous solution at various temperatures T, with ultimate reference to 1 bar (10^5 Pa) standard-state pressure of H_2, columns A, with mean absolute deviations

	$E^{\ominus}_{Hg/HgO/H^+}$(mV)			$E^{\ominus}_{Hg/HgO/OH^-}$(mV)		
T (K)	A	B[a]	C	A	B[a]	C
283.15	931.4 ± 0.2	931.5	$931.2_0 \pm 0.18$	114.7 ± 0.2	114.9	$114.5_7 \pm 0.21$
298.15	$926.9_9 \pm 0.03$	927.1_6	$927.3_0 \pm 0.14$	$99.0_0 \pm 0.03$	99.1_7	$99.3_4 \pm 0.16$
313.15	922.5 ± 0.2	922.7	$923.3_7 \pm 0.16$	81.5 ± 0.2	81.7	$82.4_4 \pm 0.18$
333.15	$918.5_7 \pm 0.04$	918.7_6	$918.0_8 \pm 0.15$	$58.0_9 \pm 0.04$	58.2_8	$57.4_5 \pm 0.17$
348.15	$914.0_6 \pm 0.04$	914.2_6	$914.0_7 \pm 0.13$	$36.7_4 \pm 0.04$	36.9_4	$36.9_5 \pm 0.15$
363.15	909.9 ± 0.1	910.1	$910.0_4 \pm 0.20$	14.9 ± 0.1	15.1	$15.0_2 \pm 0.24$

[Corresponding values referred to 1 atm (101,325 Pa) are quoted (column B) to facilitate comparison with earlier data in the literature]. Parallel values from the multi-linear regression analysis with standard errors are given in columns C [182]

[a]The uncertainty figures are the same as those in columns A

$$\frac{dE^{\ominus}_{Hg/HgO/H^+}}{dT} = -0.2581\,\text{mV}\,\text{K}^{-1} \tag{5.6.14}$$

and

$$\frac{dE^{\ominus}_{Hg/HgO/OH^-}}{dT} = -1.0712\,\text{mV}\,\text{K}^{-1}. \tag{5.6.15}$$

Longhi et al. [176] proposed to use the mercury(II) oxide electrode for estimation of OH^- concentration at high temperatures in strongly alkaline solutions (e.g., 1–10 mol dm^{-3} NaOH), where typical electrodes such as glass or antimony cannot be rather applied. The dependence of the potential of such electrode on NaOH molality, m, was expressed as follows:

$$E_{Hg/HgO/OH^-} = E^{\ominus}_{Hg/HgO/OH^-} - \frac{RT}{F}\ln(m_{OH^-}\gamma_{OH^-}) + \frac{RT}{2F}\ln a_{H_2O}, \tag{5.6.16}$$

where a_{H_2O} and γ_{OH^-} denote water activity and activity coefficient of OH^- ion, respectively. This equation may supply the potential of this reference electrode of aqueous NaOH in higher concentration solutions, and also at higher temperatures.

Every and Banks [183] have shown that the Hg | HgO electrode may be used in 5 mol dm^{-3} NaOH up to 100 °C. Case and Bignold [184] have used this electrode also at higher temperatures. They have shown that mercury(II) oxide did not decompose when electrodes were heated in autoclave (in 0.1 mol dm^{-3} NaOH) up to 280 °C. They measured the temperature dependence of the emf of the cell similar to cell (5.6.1). The results are presented in Fig. 5.6.1.

The results shown in Fig. 5.6.1 represent mean values taken from two identical pairs of electrodes. Deviations from these mean values are small being equal to ±0.1 mV at 20 °C and ±1 mV at 200 °C. At 25 °C and 1 atm, the cell exhibited the

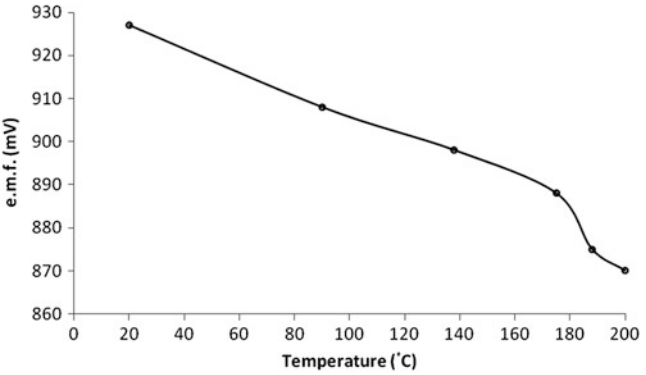

Fig. 5.6.1 Temperature variation of the potential of the cell: Pt(s)| H_2(g)| NaOH(aq)| HgO(s)| Hg(l); $p = 1$ atm [184]. Reprinted with permission from Springer

Table 5.6.2 The Hg| HgO| OH^- electrode potentials vs. SHE

m_{NaOH} (mol kg^{-1})	γ_{NaOH}	a_{H_2O}	E (V)
0.001	0.9655	1.0000	0.2763
0.1	0.7820	0.9981	0.1634
1	0.6774	0.9757	0.1077
1.45	0.6862	0.9605	0.0976
5.00	1.092	0.7892	0.0514
8.78	2.570	0.5597	0.0105
10.71	4.114	0.4497	−0.0095

equilibrium value of 0.926 V in agreement with Ives and Janz [177]. As it follows from Fig. 5.6.1, the emf changes practically linearly with temperature in the range of 20–120 °C and the temperature coefficient in this range dE/dT is equal to −0.25 mV $°C^{-1}$ in both 0.1 and 1.0 mol dm^{-3} NaOH.

Nickell et al. [185] have used the Hg| HgO| OH^- electrode for the determination of hydrogen evolution potentials in aqueous sodium hydroxide. They determined and calculated the potentials of this electrode in the temperature range from 0 to 90 °C for NaOH concentrations changed in the limits 0.10–12.8 m.

In Table 5.6.2 we report, following Nickell et al. [185], several numerical values of the Hg| HgO| OH^- electrode potentials at different NaOH molalities but at constant temperature 25 °C.

The potential of this electrode is dependent on OH^- and water activity in the following way:

$$E_{Hg/HgO/OH^-} = E^{\ominus}_{Hg/HgO/OH^-} - \frac{RT}{F} \ln \frac{a_{OH^-}}{\sqrt{a_{H_2O}}}. \tag{5.6.17}$$

The Hg| HgO electrode may be used also for measurements of potentials in the alkaline battery formation process. The knowledge of such potentials is very

important for the elucidation of the real electrode reactions and in the case of battery for understanding of reactions which occur during their charging and discharging. This electrode is stable during days and due to the fast electrode reaction the potential is reproducible to 0.1 mV. For short discussion see [177].

Also solid-state Hg(Au)│HgO reference electrode was prepared [186] using gold amalgam solid particles. This gold amalgam was prepared by chemical reduction of Au(III) with $NaBH_4$ followed by reduction of Hg(II) in the presence of gold fine particles. The solid content in the suspension of the gold amalgam and fine mercury oxide particles in dimethylformamide containing poly(vinyl chloride) (PVC) was precipitated by the addition of a large amount of water to give solid Hg(Au)│HgO│PVC mixture. After drying, the mixture was pressure molded to a physically stable Hg(Au)│HgO composite reference electrode material. The electrochemical characteristics of the electrode as a reference system were very similar to that of a traditional Hg│HgO reference electrode.

Concluding we may advise to use the standard potentials reported by the IUPAC group [182].

5.6.1.1 Preparation of the Mercury–Mercury(II) Oxide Hg│HgO Electrode

There are no difficulties in preparing the mercury–mercury(II) oxide electrode. It is advised [177] to prepare HgO by gentle heating of $Hg(NO_3)_2$. However, also reagent-grade HgO washed on the steam bath may be accepted [177]. It is obvious that mercury should be also of high purity. Earlier studies on the anodic polarization of mercury in alkaline solutions [187] confirmed the formation of only HgO and absence of other oxides.

In the constructed electrode, mercury should be in contact with a HgO layer and with an hydroxide solution. Different variants in the construction of such electrode may be realized. Figure 5.6.2 shows [188] the electrode prepared in a fashion which may be used in construction of other reference electrodes based on the reaction of mercury.

5.6.2 The Silver–Silver Oxide Electrode

The electrode constructed from silver which is in contact with Ag_2O should be thermodynamically stable. The influence of higher oxides on the potential of such electrode should not be important, since the stability of Ag^{2+} in aqueous solutions is very low. In fact Ag^{2+} ions practically do not exist in aqueous solutions, since for the reaction:

$$Ag^{2+} + Ag \rightleftarrows 2Ag^{+} \tag{5.6.18}$$

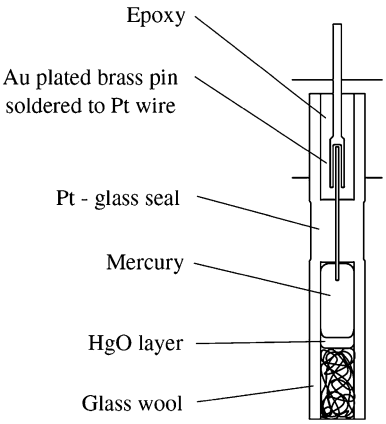

Fig. 5.6.2 Scheme of the Hg | HgO electrode with filling solution saturated $Ca(OH)_2$ [188]. Reprinted with permission from Elsevier

the equilibrium constant $K = \dfrac{[Ag^+]^2}{[Ag^{2+}]} \cong 10^{20}$ at 25 °C

The limited stability of higher silver oxides is well indicated by their redox potentials; however, oxides AgO and Ag_2O_3 may be formed and they are used, e.g., in batteries.

The potential of the reaction:

$$2AgO + 2H^+ + 2e^- \rightleftharpoons Ag_2O + H_2O \tag{5.6.19}$$

is for nonhydrated oxide equal to 1.398 V [189], while the potential of the hydrated form is 1.066 V. The potential of the Ag_2O_3 | AgO couple in acidic media is even more positive being equal to 1.569 V [189].

The Ag | Ag_2O electrode was not frequently used. Earlier works on the Ag | Ag_2O electrode were discussed by Hamer and Craig [178] and briefly summarized by Ives and Janz [177]. Evidently the potential of such electrodes, as found in earlier works, was not quite stable and its drift to more negative values was observed in time. Hamer and Craig [178] explained these changes as due to not proper preparation of the electrode. Namely the Pt with deposited porous silver was dipped in a slurry of silver oxide before use. Instability could result from the oxygen adsorption on silver and the formation of a film of nonstoichiometric oxides on the surface.

Hamer and Craig [178] have modified the preparation of the electrode which now exhibited stable potential. Their method briefly described below led to the presence of only Ag_2O in contact with silver. Using such electrode with a stable potential, Hamer and Craig [178] have measured the emf of the following cell:

$$Hg(l)|HgO(s)|NaOH(aq)|Ag_2O(s)|Ag(s) \tag{5.6.20}$$

It was found to be equal to 0.2440 (±0.0005) V.

Table 5.6.3 Values of the standard acid potential $E^{\ominus}_{Ag/Ag_2O/H^+}$ and of the standard basic potential $E^{\ominus}_{Ag/Ag_2O/OH^-}$ of the Ag_2O electrode (standard errors: ±0.5 mV) in aqueous solution at various temperatures T; standard-state pressure: 1 bar (10^5 Pa)

T (K)	$E^{\ominus}_{Ag/Ag_2O/H^+}$(mV)	$E^{\ominus}_{Ag/Ag_2O/OH^-}$(mV)	$pK^{\ominus}_{sol\ (AgOH)}$
283.15	1,178.3	361.7	8.044
288.15	1,176.0	355.7	7.922
293.15	1,173.6	349.6	7.809
298.15	1,171.3	343.3	7.702
303.15	1,169.0	336.9	7.598
308.15	1,166.7	330.3	7.502
313.15	1,164.4	323.4	7.411
318.15	1,162.0	316.4	7.327

Corresponding values of the standard solubility product $pK^{\ominus}_{sol\ (AgOH)}$ of AgOH (standard errors: 0.008) are also given [182]

The emfs were not dependent on electrolyte concentration except of the range 5–30 wt% of NaOH.

The standard emf $E^{\ominus}_1$ of cell (5.6.20) is

$$E^{\ominus}_1 = E^{\ominus}_{Ag/Ag_2O/OH^-} - E^{\ominus}_{Hg/HgO/OH^-}. \tag{5.6.21}$$

Therefore, using $E^{\ominus}_{Hg/HgO/OH^-}$ given in Sect. 5.6.1 and measured $E^{\ominus}_1$ one gets the standard potential of the $Ag \mid Ag_2O \mid OH^-$ electrode.

Hamer and Craig [178] have measured the emf of cell (5.6.20) at several temperatures, ranging from 273 to 363 K. The standard emf of cell (5.6.20) changes with temperature in the following way:

$$E^{\ominus}_1(\text{mV}) = 305.5_0 - 0.2063T(\text{to} \pm 0.5\,\text{mV}). \tag{5.6.22}$$

The formal potential of the $Ag \mid Ag_2O \mid OH^-$ electrode may be calculated from these data at different temperatures. Such calculations were made by Longhi et al. [176] using $E^{\ominus}_{Hg/HgO/OH^-}$ potential determined by them. Later these potentials were also reexamined by the IUPAC group [182]. The calculated critical results of both $E^{\ominus}_{Ag/Ag_2O/OH^-}$ and $E^{\ominus}_{Ag/Ag_2O/H^+}$ potentials are given in Table 5.6.3.

As in the case of mercury–mercury(II) oxide electrodes also, the dependence of the silver–silver oxide electrode potential on temperature was described by the simple equations:

$$E^{\ominus}_{Ag/Ag_2O/H^+}(\text{mV}) = 1{,}309.8_2 - 0.4645T \tag{5.6.23}$$

and

$$E^{\ominus}_{Ag/Ag_2O/OH^-}(\text{mV}) = 410.6_0 + 0.82506T - 0.003524T^2. \tag{5.6.24}$$

There are also given [182] the corresponding temperature coefficients at 298.15 K:

$$\frac{\mathrm{d}E^{\ominus}_{\mathrm{Ag/Ag_2O/H^+}}}{\mathrm{d}T} = -0.4645\,\mathrm{mV\,K^{-1}} \tag{5.6.25}$$

and

$$\frac{\mathrm{d}E^{\ominus}_{\mathrm{Ag/Ag_2O/OH^-}}}{\mathrm{d}T} = -1.2763\,\mathrm{mV\,K^{-1}}. \tag{5.6.26}$$

In conclusion, we may advise to use the potentials reported by the IUPAC group [182], though in some cases the number of significant digits is probably exaggerated.

5.6.2.1 Preparation of the Silver–Silver Oxide Ag | Ag_2O Electrode

Different methods were applied in preparation of this electrode. However, as we wrote earlier, the method, which uses the Pt wire covered by porous silver and subsequently placed in slurry of silver oxide and later in a cell solution, did not lead to correct results.

The method used by Hamer and Craig [178] may be advised because it led these authors to satisfactory results. They used platinum gauze (with a 1.5 cm^2 of surface area) which was covered by wetted silver oxide, and this layer of oxide was dried. Such procedure was repeated several times until the platinum was well covered by dry Ag_2O. Subsequently, the layer of Ag_2O was partly reduced by hydrogen at 60 °C (the extent of reduction was estimated basing on the gray color of the layer).

Such electrode after cooling in hydrogen was introduced to the cell. Potential of such electrode was stable (after several hours of equilibration) within 1 mV even for 38 days.

5.6.3 Other Oxide Electrodes

In the book edited by Ives and Janz [177] there are described other oxide electrodes, namely, Sb | Sb_2O_3, Bi | Bi_2O_3, As | As_2O_3, and also W, Mo, and Te oxide electrodes. However, all these electrodes were discussed as pH sensors, but not as reference electrodes. The authors list also other systems which were described by Pourbaix and coworkers in their "Atlas of Electrochemical Equilibria in Aqueous Solutions," [190] which deals with different redox systems and their dependence on pH.

These redox systems in principle could be applied as the reference electrodes; however, their use in strongly alkaline solutions is rather problematic because of the amphoteric nature of oxides which form these electrodes. Therefore, an increased solubility of M_2O_3 oxides is observed; also in acidic solutions these oxides are more easily soluble. Hence, these systems could be used as reference electrodes only in the intermediate pH range. However, even small changes of pH of the solution could then influence the potential of such electrodes according to the equation:

$$E^{\ominus} = E + \frac{2.303RT}{F}\text{pH}. \tag{5.6.27}$$

Under such conditions these electrodes cannot play properly the role of reference electrodes. For the sake of completeness, we list the standard potentials of the most frequently used metal–metal oxide electrodes:

$$E^{\ominus}_{\text{Sb/Sb}_2\text{O}_3} = 0.1445\,\text{V},$$

$$E^{\ominus}_{\text{Bi/Bi}_2\text{O}_3} = 0.3890\,\text{V},$$

$$E^{\ominus}_{\text{Pb/PbO}} = 0.5785\,\text{V}.$$

On the other side, there are efforts to use some bronzes as reference electrodes. Gabel et al. [191] who studied the behavior of several polycrystalline bronzes found that tungsten substituted lithium molybdenum oxide bronzes with general formula $A_xMo_{1-y}W_yO_3$ may be applied as materials for solid-state reference electrodes. They found that the potential of such electrodes does not change significantly with the change of pH, sodium ion concentration, and redox potential of a studied solution.

Earlier [192] some bronzes with bivalent cations were examined as candidates for construction of reference electrodes; however, their potential was not stable.

Other oxides, mainly transition metal oxides, were used as reference systems in the potentiometric CO_2 sensors. Such solid systems were introduced in late 1970s.

In 1986 Maier et al. [193] have proposed a cell, which responds thermodynamically on CO_2:

$$\begin{aligned}&\text{Au(s)}|\text{O}_2\text{(g)}\text{CO}_2\text{(g)}|\text{Na}_2\text{CO}_3\text{(aq)}|\text{Na}^+ - \text{conductor}|\text{Na}_2\text{ZrO}_3\text{(aq)}\\ &\times|\text{ZrO}_2\text{(s)}|\text{O}_2\text{(g)}|\text{Au(s)}\end{aligned} \tag{5.6.28}$$

with the reference electrode reaction:

$$\text{ZrO}_2 + 2\text{e}^- + {}^1\!/_2\,\text{O}_2 + 2\text{Na}^+ \rightleftharpoons \text{Na}_2\text{ZrO}_3 \tag{5.6.29}$$

Evidently the reference electrode is the oxygen electrode of the second kind. Other reference systems, based on that electrode, were proposed: $\text{SnO}_2 \,|\, \text{Na}_2\text{SnO}_3$

and $TiO_2 | Na_2TiO_3$ [194], $LiMn_2O_4$ [195], $LiCoO_2 | Co_3O_4$ [196], and others [197]. The sensors constructed with the use of such reference electrodes operate at high temperatures in a solid state and exhibit the Nernstian response on the change of CO_2.

References

174. Brönsted JN (1909) Z Physik Chem 65:84
175. Fried F (1926) Z Physik Chem 123:406
176. Longhi P, Mussini T, Orsenigo R, Rondinini S (1987) J Appl Electrochem 17:505
177. Ives DJG, Janz GJ (eds) (1961) Reference electrodes. Theory and practice. Academic, New York, Chapter 7.II, pp 333–335
178. Hamer WJ, Craig DN (1957) J Electrochem Soc 104:206
179. Balej J (1985) Standard potentials in aqueous solution. In: Bard AJ, Parsons R, Jordan J (eds) Mercury. Dekker, New York, Chapter 10.III
180. Hepler LG, Olofson G (1975) Chem Rev 75:585
181. Samuelson GJ, Brown DJ (1935) J Am Chem Soc 57:2711
182. Rondinini S, Longhi P, Mussini PR, Mussini T (1994) Pure Appl Chem 66:641 @ 1994 IUPAC
183. Every RL, Banks WP (1967) Corrosion 23:151
184. Case B, Bignold GJ (1971) J Appl Electrochem 1:141
185. Nickell RA, Zhu WH, Payne RU, Cahela DR, Tatarchule BJ (2006) J Power Sources 161:1217
186. Kim W, Park J (2007) Bull Korean Chem Soc 28:439
187. El Wakkad SES, Salem TM (1952) J Phys Chem 56:621
188. Smith TJ, Stevenson KJ (2007) Reference electrodes. In: Zoski CG (ed) Handbook of electrochemistry, Elsevier, pp 73–110
189. Zhutaeva GV, Shumilova NA (1985) In: Bard AJ, Parsons R, Jordan J (eds) Standard potentials in aqueous solution. Dekker, New York, Chapter 11.II
190. Pourbaix M (ed) (1966) Atlas of electrochemical equilibria in aqueous solutions. Pergamon Press, Oxford
191. Gabel J, Vonau W, Shuk P, Guth U (2004) Solid State Ionics 169:75
192. Lukowski R, Guth U, Schäf O (1999) DE—Pat 19.823.056:A1
193. Maier J, Warhus U (1986) J Chem Thermodyn 18:309
194. Maier J, Holzinger M, Sitte W (1994) Solid State Ionics 74:5
195. Salem F, Birke P, Weppner W (1999) Electrochem Solid State Lett 2:201
196. Zhang YC, Tagawa H, Asakura S, Mizusaki J, Narita H (1997) J Electrochem Soc 144:4345
197. Ramirez J, Fabry P (2001) Sens Actuators B 77:339

References

References to Sect. 5.1

1. Cohen ER, Cvitas T, Frey JG, Holmström B, Kuchitsu K, Marquardt R, Mills I, Pavese F, Quack M, Stohner J, Strauss HL, Takami M, Thor AJ (2008) Quantities, units and symbols in physical chemistry, IUPAC Green Book, 3rd edn. IUPAC & RSC Publishing, Cambridge, p 74, 2nd printing
2. Cox JD (1982) Pure Appl Chem 54:1239
3. Wanner H, Önsted E (2000) Standards and conventions for TDB Publications. OECD Nuclear Energy Agency, p 3
4. Nernst W (1900) Z Elektrochem7:253
5. Galster H (1991) pH measurement: fundamentals, methods, applications, instrumentation. Weinheim, VCH, p 68
6. Inzelt G (2008) Electrodes. In: Bard AJ, Inzelt G, Scholz F (eds) Electrochemical dictionary. Springer, Berlin, pp 202–205
7. Kahlert H (2010) Reference elctrodes. In: Scholz F (ed) Electroanalytical methods. Springer, Berlin, pp 263–264
8. Bates RG (1973) Determination of pH—theory and practise. Wiley, New York, pp 280–294
9. RHE. Available from http://www.gaskatel.de/english/hydroflex/theory.html
10. Schwarz J, Hörig A, Oelssner W, Vonau W, Kohnke H-J (2012) GIT 56:99
11. Buck RP, Rondinini S, Baucke FGK, Camoes MF, Covington AK, Milton MJT, Mussini T, Naumann R, Pratt KW, Spitzer P, Wilson GS (2002) Pure Appl Chem 74:2169
12. Spitzer P, Werner B (2002) Anal Bioanal Chem 374:787
13. Bates RG, Robinson RA (1980) J Solution Chem 9:455
14. Harned HS, Robinson RA (1928) J Am Chem Soc 50:3157
15. Mariassy M, Pratt KW, Spitzer P (2009) Metrologia 46:199
16. Spitzer P, Eberhardt R, Schmidt I, Sudmeier U (1996) Fresenius J Anal Chem 356:178
17. Hills GJ, Ives DJG (1951) J Chem Soc 318:305
18. Spitzer P, Pratt KW (2011) J Solid State Electrochem 15:69
19. Hills GJ, Ives DJG (1961) The hydrogen electrode. In: Ives DJG, Janz GJ (eds) Reference electrodes. Theory and practice. Academic, New York, p 96
20. Wagner W, Pruss A (2002) Phys Chem Ref Data 31:387
21. Tables of physical and chemical constants. Available from http://www.kayelaby.npl.co.uk/chemistry/3_4/3_4_2.html
22. IAPWS-97. Available from http://www.iapws.org/newform.htm

References to Sect. 5.2

23. Shumilova NA, Zhutaeva GV (1978) In: Bard AJ (ed) Encyclopedia of electrochemistry of the elements. Dekker, New York
24. Harned HS, Ehlers RW (1933) J Am Chem Soc 55:2179
25. Bates RG, Bower VE (1954) J Res Natl Bur Stand 53:282
26. Harned HS, Paxton TR (1953) J Phys Chem 57:531
27. Bard AJ, Parsons R, Jordan J (1985) Standard potentials in aqueous solutions. Marcel Dekker, New York, p 304
28. Greeley RS, Smith WT, Lietzke MH, Stanghton RW (1960) J Phys Chem 64:652
29. Bates RG, Macaskill JB (1978) Pure Appl Chem 50:1701
30. Brewer PJ, Leese RJ, Brown RJC (2012) Electrochim Acta 71:252

31. Guiomar Lito MJ, Filomena Camoes M (2009) J Solution Chem 38:1471
32. Bates RG (1973) Determination of pH. Theory and practice, 2nd edn. Wiley, New York
33. Brewer PJ, Brown RJC (2010) Sensors 10:2202
34. Brown RJC, Milton MJT (2005) Accred Qual Assur 10:352
35. Brewer PJ, Stoica D, Brown RJC (2011) Sensors 11:8072
36. East GA, del Valle MA (2000) J Chem Educ 77:97
37. Thomas JM (1999) J Chem Educ 76:97
38. Inamdar SN, Bhat MA, Haram SK (2009) J Chem Educ 86:355
39. Escoffier C, Maguire PD, Mahony C, Graham WG, MacAdams EM, McLaughlin JA (2002) J Electrochem Soc 149:H98
40. Oijerholm J, Forsberg S, Hermansson HP, Ullberg M (2009) J Electrochem Soc 156:P56
41. Oh SH, Bahn CB, Hwang IS (2003) J Electrochem Soc 150:E321
42. Kim HR, Kim YD, Kim KI, Shim JH, Nam H, Kong BK (2004) Sens Actuators B 97:348
43. Ito S, Hachiya H, Baba K, Asano Y, Wada H (1995) Talanta 42:1685
44. Ito S, Kobayashi F, Baba K, Asano Y, Wada H (1996) Talanta 40:135
45. Gao P, Jin XB, Wang DH, Wu XH, Chen GZ (2005) J Electroanal Chem 579:321
46. Shankenberg U, Lisec T, Hintsche R, Kuna I, Uhlig A, Wagner B (1996) Sens Actuators B 34:476
47. Eine K, Kjelstrup S, Nagy K, Syverud K (1997) Sens Actuators B 44:381
48. Johnsen EE, Kjelstrup Ratkje S, Førland T, Førland KS (1990) Z Physik Chem 168:101
49. Beer J, Kjelstrup Ratkje S, Olsen GF (1991) Z Physik Chem 174:179
50. Moussy F, Harrison DJ (1994) Anal Chem 66:674
51. Galster H (1980) GIT Fachz Lab 24:744
52. Guth U, Gerlach F, Decker M, Oelßner W, Vonau W (2009) J Solid State Electrochem 13:27
53. Gabel J, Vonau W, Lange R, Barthold K (2000) GIT-Laborfachzeitschrift 45:366
54. Ciobanu M, Wilburn JP, Buss NL, Ditavong P, Lowy DA (2002) Electroanalysis 14:989
55. Ciobanu M, Wilburn JP, Lowy DA (2004) Electroanalysis 16:1351
56. Kakiuchi T, Yoshimatsu T, Nishi N (2007) Anal Chem 79:7187
57. Bakker E (1999) Electroanalysis 11:788
58. Lindner E (2000) Anal Chem 68:336A
59. Lee HJ, Hong US, Lee DK, Shin JH, Nam H, Cha GS (1998) Anal Chem 70:3377
60. Valdes-Ramirez G, Alvarez-Romero G, Galan-Vidal CA, Hernandez-Rodriguez PR, Ramirez-Silva MT (2005) Sens Actuators B 110:264
61. Kisiel A, Marcisz H, Michalska A, Maksymiuk K (2005) Analyst 130:1655
62. Kisiel A, Michalska A, Maksymiuk K (2007) Bioelectrochem 71:75
63. Kisiel A, Michalska A, Maksymiuk K, Hall EAH (2008) Electroanalysis 20:318
64. Rius-Ruiz FX, Kisiel A, Michalska A, Maksymiuk K, Riu J, Xavier RF (2011) Anal Bioanal Chem 399:3613
65. Mattinen U, Bobacka J, Lewenstam A (2009) Electroanalysis 21:1955
66. Kisiel A, Donten M, Mieczkowski J, Rius-Ruiz FX, Maksymiuk K, Michalska A (2010) Analyst 135:2420
67. O'Neil GD, Buiculescu R, Kounaves SP, Chaniotakis NA (2011) Anal Chem 83:5749
68. Blaz T, Migdalski J, Lewenstam A (2005) Analyst 130:637
69. Mangold K-M, Schäfer S, Jüttner K (2000) Fresenius J Anal Chem 367:340
70. Nolan MA, Tan SH, Kounaves SP (1997) Anal Chem 69:1244
71. Maminska R, Dybko A, Wróblewski W (2006) Sens Actuators B 115:552
72. Yu P, Dong S (1996) Anal Chim Acta 330:767
73. Vonau W, Oelßner W, Sikora RJ, Henze J (2003) Referenzelektrode DE 10305005
74. Vonau W, Oelßner W, Guth U, Henze J (2010) Sens Actuators B 144:368
75. Matsumoto T, Oashi A, Ito N (2002) Anal Chim Acta 462:253
76. Yalcinkaya F, Powner ET (1997) Med Eng Phys 19:299
77. Kitade T, Kitamura M, Takegami S, Miyata Y, Nagatomo M, Sakaguchi T, Furukawa M (2005) Anal Sci 21:907

78. Zhang X, Ogorevec B, Tavcar G, Grabec Svegl I (1996) Analyst 121:1817
79. Mroz A, Borchardt M, Diekmann C, Cammann K, Knoll M, Dumschat C (1998) Analyst 123:1373
80. Suzuki H, Hirakawa I, Sasaki S, Karube I (1998) Sens Actuators B 46:146
81. Suzuki H, Shiroishi H, Sasaki S, Karube I (1999) Anal Chem 71:5069
82. Suzuki H, Hirakawa I, Sasaki S, Karube I (1999) Anal Chim Acta 387:103
83. Hetzer HB, Robinson RA, Bates RG (1962) J Phys Chem 66:1423
84. Harned HS, Keston AS, Donelson JG (1936) J Am Chem Soc 58:989
85. Towns MB, Greeley RS, Lietzke MH (1960) J Phys Chem 64:1861
86. Strydom CA, Van Staden JF, Strydom HJ (1991) Electroanalysis 3:815
87. Hetzer HB, Robinson RA, Bates RG (1964) J Phys Chem 68:1929
88. Owen BB (1935) J Am Chem Soc 57:1226
89. Hashimoto M, Upadhyay S, Kojima S, Suzuki H, Hayashi K, Sunagawa K (2006) J Electrochem Soc 153:H155
90. Strydom CA, Van Staden JF, Strydom HJ (1992) Electroanalysis 4:969
91. Golding M (1959) J Chem Soc 1838
92. Noyes AA, Freed ES (1920) J Am Chem Soc 42:476
93. Kimura G (1935) Bull Inst Phys Chem Res (Tokyo) 14:94
94. Goates RJ, Cole AG, Gray EL, Faux ND (1951) J Am Chem Soc 73:707
95. Ives DJG, Janz GJ (eds) (1961) Reference electrodes. Theory and practice. Academic, New York, Chapter 7.V, pp 381–382
96. Freiberger WI, de Bruyn PL (1957) J Phys Chem 61:586
97. Nakolkin IA (1942) Zh Fiz Khim 16:18

References to Sect. 5.3

98. Hills GJ, Ives DJG (1961) The calomel electrode and other mercury-mercurous salt electrodes. In: Ives DJG, Janz GJ (eds) Reference electrodes. Theory and practice. Academic, New York, pp 127–178
99. Smith TJ, Stevenson KJ (2007) Reference electrodes. In: Zoski CG (ed) Handbook of electrochemistry. Elsevier, pp 73–110
100. Szabó S, Bakos I (2010) Int J Corros, article ID 756950
101. Wrona PK, Galus Z (1982) Mercury. In: Bard AJ (ed) Encyclopedia of electrochemistry of the elements, part A, vol 9. Dekker, New York
102. Hills GJ, Ives DJG (1951) J Chem Soc 319
103. Guggenheim EA, Prue JE (1954) Trans Faraday Soc 50:231
104. Schwabe K, Ziegenbalg S (1958) Z Elektrochem 62:172
105. Grzybowski AK (1958) J Phys Chem 62:550
106. Holze R (2007) Electrochemical thermodynamics and kinetics. In: Lechner MD (ed) Landolt-Börnstein numeric data and functional relationships in science and technology, group IV physical chemistry, vol 9 Electrochemistry. Springer, Berlin, subvolume A
107. Chateau H (1954) J Chim Phys 51:590
108. Bard AJ, Faulkner LR (2001) Electrochemical methods, 2nd edn. Wiley, New York
109. Yosypchuk B, Novotny L (2003) Chem Listy 97:1083
110. Yosypchuk B, Novotny L (2004) Electroanalysis 16:238
111. Pickup NL, Lam M, Milojevic D, Bi RY, Shapiro JS, Wong DKY (1997) Polymer 38:2561
112. Bockris JO'M, Devanathan MAU, Reddy AKN (1964) Proc R Soc London A279:324
113. Hills GJ, Ives DJG (1951) J Chem Soc 313
114. Cousens RH, Ives DJG, Pittman RW (1953) J Chem Soc 3972
115. Cousens RH, Ives DJG, Pittman RW (1953) J Chem Soc 3980

116. Dibbs HP, Ives DJG, Pittman RW (1957) J Chem Soc 3370
117. Boult EH, Thirsk HR (1954) Trans Faraday Soc 50:376
118. Cornish DC, Dibbs HP, Feates FS, Ives DJG, Pittman RW (1962) J Chem Soc 4104
119. Cornish DC, Das SN, Ives DJG, Pittman RW (1966) J Chem Soc A 111
120. Cornish DC, Ives DJG, Pittman RW (1966) J Chem Soc A 116
121. Armstrong RD, Fleischmann M, Thirsk HR (1965) Trans Faraday Soc 61:2238
122. Behr B, Taraszewska J (1968) J Electroanal Chem 19:373
123. Bewick A, Fleischmann M, Thirsk HR (1962) Trans Faraday Soc 58:2200
124. Das SN, Ives DJG (1962) J Chem Soc 1619
125. Ives DJG, Prasad D (1970) J Chem Soc B 1649
126. Covington AK, Dobson JV, Wynne-Jones L (1967) Electrochim Acta 12:525
127. Covington AK, Dobson JV, Wynne-Jones L (1967) Electrochim Acta 12:513
128. Schwabe K, Ferse E (1965) Z Elektrochem 69:383
129. Vitiello JD, Pistone D, Cormier AD (1996) Scand J Clin Lab Invest 56(Suppl 224):165
130. Gerke RH (1925) Chem Rev 1:377
131. Gupta SR, Hills DJ, Ives DJG (1963) Trans Faraday Soc 59:1886
132. Cornish DC, Ives DJG, Pittman RW (1966) J Chem Soc A 120
133. Ives DJG, Smith FR (1961) Electrodes reversible to sulfate ions. In: Ives DJG, Janz GJ (eds) Reference electrodes. Theory and practice. Academic, New York, pp 393–410
134. Antropov LI (1972) Tankonyvkiado. Budapest in Hungarian; (1969) Theoreticheskaya Elektrokhimiya. Visshaya Skola, Moscow
135. Carpenter MK, Bernardi DM, Wertz JA (1996) J Power Sources 63:15
136. Hamer WJ (1972) J Res Natl Bur Stand 76A:185
137. Beck WH, Dobson JV, Wynne-Jones WFK (1960) Trans Faraday Soc 56:1172
138. Harned HS, Hamer WJ (1935) J Am Chem Soc 57:27
139. Covington AK, Dobson JV, Wynne-Jones WFK (1965) Trans Faraday Soc 61:2050
140. Clegg SL, Rard JA, Pitzer KS (1994) J Chem Soc Faraday Trans 90:1875
141. Hamer WJ, Wu YC (1995) J Solution Chem 24:1013
142. Gardner WL, Mitchell RE, Cobble JW (1969) J Phys Chem 73:2021
143. Ives DJG (1961) Oxide, oxygen and sulfide electrodes. In: Ives DJG, Janz GJ (eds) Reference electrodes. Theory and practice. Academic, New York, pp 322–392
144. Makolkin IA (1942) Zhur Fiz Khim 16:18
145. Goates RJ, Cole AG, Gray EL (1951) J Am Chem Soc 73:3596
146. Balej J (1985) Standard potentials in aqueous solution. In: Bard AJ, Parson R, Jordan J (eds) Mercury. Dekker, New York, Chapter 10.III
147. Sillén LG (1949) Acta Chem Scand 3:539

References to Sect. 5.4

148. Bates RG (1961) The glass electrode. In: Ives DJG, Janz GJ (eds) Reference electrodes. Theory and practice. Academic, New York, pp 270–321
149. SzabóS, Bakos I (2010) Int J Corros, article ID 756950
150. Mussini T, Longhi P (1965) Ric Sci Rend A8:1352
151. Baucke FGK (1974) Chem Ing Tech 46:71
152. Holze R (2007) Electrochemical thermodynamics and kinetics. In: Lechner MD (ed) Landolt-Börnstein numeric data and functional relationships in science and technology, group IV physical chemistry, vol 9 Electrochemistry. Springer, Berlin, subvolume A
153. Baucke FGK (1971) J Electroanal Chem 33:135
154. Baucke FGK (1972) J Electroanal Chem 39:263
155. Midgley D, Torrance K (1978) Analyst 101:833

156. Cogley DR, Butler JN (1966) J Electrochem Soc 113:1074
157. Smyrl WH, Tobias CW (1966) J Electrochem Soc 113:754
158. Smyrl WH, Tobias CW (1968) J Electrochem Soc 115:33
159. Delahay P, Tobias CW (eds) (1970) Advances in electrochemistry and electrochemical engineering, vol 7. Interscience, New York
160. Baucke FGK, Tobias CW (1969) J Electrochem Soc 116:34
161. Coetzee JE, Campion JJ (1967) J Am Chem Soc 89:2513

References to Sect. 5.5

162. Brunner E (1907) Z Phys Chem 58:1
163. Vetter KJ (1952) Z Phys Chem 199:22
164. Ross JW, Potentiometric electrode, UK patent GB 2 088 565 A
165. Palmer DA, Ramette RW, Mesmer RE (1984) J Solution Chem 13:9
166. Tauber G (2006) Presentation on ELACH7 conference in Waldheim, Germany
167. Bates RG (1954) Electrometric pH determinations, theory and practice. Wiley, New York
168. Galster H (1990) pH-Messung. VCH Verlagsgesellschaft mbH, Weinheim
169. Hamann CH, Vielstich W (1998) Elektrochemie. Wiley-VCH Verlag GmbH, Weinheim
170. Hirshberg M, West SJ, Barbookles J, Ion-selective electrode, US Patent No. US 6,793,787 B1
171. Tauber G, Potentiometrische Messkette, Patent Nr. D 10 2006 012 799 B4
172. Milazzo G (1952) Elektrochemie. Springer, Wien
173. Baucke FGK, Bertram R, Cruse K (1971) J Electroanal Chem 32:247

References to Sect. 5.6

174. Brönsted JN (1909) Z Physik Chem 65:84
175. Fried F (1926) Z Physik Chem 123:406
176. Longhi P, Mussini T, Orsenigo R, Rondinini S (1987) J Appl Electrochem 17:505
177. Ives DJG, Janz GJ (eds) (1961) Reference electrodes. Theory and practice. Academic, New York, Chapter 7.II, pp 333–335
178. Hamer WJ, Craig DN (1957) J Electrochem Soc 104:206
179. Balej J (1985) Standard potentials in aqueous solution. In: Bard AJ, Parsons R, Jordan J (eds) Mercury. Dekker, New York, Chapter 10.III
180. Hepler LG, Olofson G (1975) Chem Rev 75:585
181. Samuelson GJ, Brown DJ (1935) J Am Chem Soc 57:2711
182. Rondinini S, Longhi P, Mussini PR, Mussini T (1994) Pure Appl Chem 66:641 @ 1994 IUPAC
183. Every RL, Banks WP (1967) Corrosion 23:151
184. Case B, Bignold GJ (1971) J Appl Electrochem 1:141
185. Nickell RA, Zhu WH, Payne RU, Cahela DR, Tatarchule BJ (2006) J Power Sources 161:1217
186. Kim W, Park J (2007) Bull Korean Chem Soc 28:439
187. El Wakkad SES, Salem TM (1952) J Phys Chem 56:621
188. Smith TJ, Stevenson KJ (2007) Reference electrodes. In: Zoski CG (ed) Handbook of electrochemistry, Elsevier, pp 73–110
189. Zhutaeva GV, Shumilova NA (1985) In: Bard AJ, Parsons R, Jordan J (eds) Standard potentials in aqueous solution. Dekker, New York, Chapter 11.II
190. Pourbaix M (ed) (1966) Atlas of electrochemical equilibria in aqueous solutions. Pergamon Press, Oxford

191. Gabel J, Vonau W, Shuk P, Guth U (2004) Solid State Ionics 169:75
192. Lukowski R, Guth U, Schäf O (1999) DE—Pat 19.823.056:A1
193. Maier J, Warhus U (1986) J Chem Thermodyn 18:309
194. Maier J, Holzinger M, Sitte W (1994) Solid State Ionics 74:5
195. Salem F, Birke P, Weppner W (1999) Electrochem Solid State Lett 2:201
196. Zhang YC, Tagawa H, Asakura S, Mizusaki J, Narita H (1997) J Electrochem Soc 144:4345
197. Ramirez J, Fabry P (2001) Sens Actuators B 77:339

Chapter 6
Reference Electrodes for Use in Nonaqueous Solutions

Kosuke Izutsu

This chapter deals with the problem of the reference electrodes for use in conventional nonaqueous solvents, mainly from practical aspects.[1] The reference electrodes used in nonaqueous solvents can be classified into two groups. One group uses, in constructing reference electrodes, the same solvent as that of the solution under study. The other group uses a solvent different from that of the solution under study; in most cases, aqueous reference electrodes are used but, in some cases, nonaqueous solvents other than that of the solution under study are used. Aqueous reference electrodes are usually an aqueous silver/silver chloride (Ag/AgCl) electrode or a calomel electrode (mostly saturated calomel electrode, SCE). Here, the reference electrodes of these two groups are discussed in detail in Sects. 6.1 and 6.2. There are some review articles concerning the reference electrodes for use in nonaqueous solutions [1–4].

The nonaqueous solvents that are considered in this review and their abbreviations (in parentheses) are as follows:

Acids: acetic acid (HOAc); acetic anhydride ($(Ac)_2O$); formic acid; hydrogen fluoride.

Alcohols: cellosolve or monoethyl ether of ethylene glycol; ethanol (EtOH); ethylene glycol (EG); methanol (MeOH); 1-propanol (1-PrOH); 2-propanol (2-PrOH).

Amides: *N*,*N*-dimethylacetamide (DMA); *N*,*N*-dimethylformamide (DMF); formamide (FA); hexamethylphosphoric triamide (HMPA); *N*-methylacetamide (NMA);

[1] In this book, there are other chapters related to nonaqueous systems. Chapter 1 by Inzelt is on the electrode potentials and includes a section on the problem to relate the electrode potentials between different media. Chapter 2 by Gritzner is on the reference redox systems in nonaqueous systems and their relation to water. Chapter 3 by Tsirlina is on the liquid junction potential and somewhat deals with the problem between different solvents. Chapter 7 by Bhatt and Snook is on the reference electrodes for room temperature ionic liquids. See these chapters as well.

K. Izutsu (✉)
Faculty of Science, Shinshu University, Matsumoto 390-8621, Japan

4-31-6-208 Kichijoji-honcho, Musashino, Tokyo 180-0004, Japan
e-mail: izutsu@almond.ocn.ne.jp

G. Inzelt et al. (eds.), *Handbook of Reference Electrodes*,
DOI 10.1007/978-3-642-36188-3_6,

N-methylformamide (NMF); *N*-methylpropionamide; *N*-methyl-2-pyrrolidinone (NMP); 1,1,3,3-tetramethylurea (TMU).

Amines: ammonia; ethylenediamine (en); methylamine; pyridine (Py).

Ethers: anisole or methoxybenzene; diglyme or diethylene glycol diethylether; 1,4-dioxane; 2-methyl-tetrahydrofuran (2Me-THF); monoglyme or 1,2-dimethoxyethane (DME); tetrahydrofuran (THF).

Ketones: acetone (Ac); acetylacetone (Acac); diethyl ketone or 3-pentanone; 4-methyl-2-pentanone or methyl isobutyl ketone (MIBK).

Nitriles: acetonitrile (AN); benzonitrile (BzN); butyronitrile (BuN); isobutyronitrile; propionitrile (PrN).

Sulfur compounds: dimethyl sulfoxide (DMSO); dimethylthioformamide (DMTF); hexamethylthiophosphoric triamide; *N*-methyl-2-thiopyrrolidinone (NMTP); sulfolane or tetramethylene sulfone (TMS); sulfur dioxide; 2,2′-thiodiethanol.

Others: benzene; γ-butyrolactone (γ-BL); chlorobenzene; 1,2-dichloroethane (DCE); dichloromethane (DCM); dimethyl carbonate; ethyl acetate; ethylene carbonate (EC); heptane; methyl acetate (MA); 3-methyl-2-oxazolidone; nitrobenzene (NB); nitromethane (NM); propylene carbonate (PC); toluene; xylene.

Besides these usual reference electrodes, mercury pool electrodes and pseudo- or quasi-reference electrodes of platinum or silver have often been used in nonaqueous solutions. Though these electrodes can have potentials approximately constant under appropriate conditions, the potentials are usually not defined.[2] Thus, in this chapter, the use of these electrodes in nonaqueous solutions is not dealt with in a separate section. But see Chap. 14 for the problem of pseudo-reference electrodes.

6.1 Reference Electrodes That Use the Same Solvent as the Solution Under Study

The reference electrodes that use the same solvent as the solution under study should have properties as follows[3]: (1) the potential should be reproducible and stable with time; (2) it should be reversible and obey the Nernst equation with respect to the potential-determining species in the solution; (3) it should return to the initial value when a small current is passed through the electrode and then stopped; and (4) it should show no hysteresis with temperature cycling. The reference electrodes of this group are listed in Table 6.1, in the alphabetical order of solvents. In popular solvents such as AN, DMF, DMSO, and PC, many types of reference electrodes have been used. Some explanations are given below for each type of reference electrodes.

[2] (1) See footnote 11 for examples of the quasi-reference electrode of metal wire coated with a redox couple. (2) Supercritical fluids are not dealt with in this chapter, but, in the electrochemistry in them, pseudo- or quasi-reference electrodes are usually used.

[3] These properties are not specific to the reference electrodes of this group. All reference electrodes, including ones for aqueous solutions, must have these properties in general.

Table 6.1 Reference electrodes that use the same solvent as the solution under study

Type of electrode	Examples of the electrode construction[a]	References
Acetic acid (HOAc)		
Ag/AgCl	Ag|AgCl(s)|AgCl(satd.) + KCl(satd.)	[5]
Hg/Hg_2Cl_2	$Hg\|Hg_2Cl_2(s)\|Hg_2Cl_2$(satd.) + LiCl(satd.); {LiCl(satd.)}	[6]
	$Hg\|Hg_2Cl_2(s)\|Hg_2Cl_2$(satd.) + NaCl(satd.) + $NaClO_4$(satd.); {0.05 M NaOAc}	[7]
$Hg/Hg_2(OAc)_2$	$Hg\|Hg_2(OAc)_2(s)\|Hg_2(OAc)_2$(satd.) + 0.5 M or satd. $NaClO_4$; {0.5 or 0.1 M $NaClO_4$}	[8–10]
$Pt/I^- - I_2$	Pt|0.10 M I_2−0.05 M KI (Actually Pt|0.05 M I_2−0.05 M I_3^-)	[11]
Acetic anhydride ($(Ac)_2O$)[#1]		
#1 Ag|AgCl(s)|AgCl(satd.) + 0.3 M LiCl (HOAc) and $Hg\|Hg_2(OAc)_2(s)\|Hg_2(OAc)_2$ (satd.) (HOAc) have been used as reference electrodes [12, 13].		
Acetone (Ac)[#2]		
Ag/Ag^+ [#3]	Ag|0.01 M Ag^+ + 0.05 M Et_4NClO_4 or 0.1 M Bu_4NClO_4	[14, 15]
$Ag/AgCryp^+$	Ag|0.002 M Ag^+ + 0.02 M Cryp(222) + 0.05 M Et_4NClO_4	[15]
Ag/AgCl	Ag|AgCl(s)|AgCl(satd.) + HCl(*c*)	[16]
	Ag|AgCl(s)|AgCl(satd.) + LiCl(satd.) or 0.1 M LiCl; {0.1 M Et_4NClO_4}	[17, 18]
Hg/Hg_2Cl_2	$Hg\|Hg_2Cl_2(s)\|Hg_2Cl_2$(satd.) + LiCl(satd.)	[19]
#2 Ag|AgCl(s)|AgCl(satd.) + 0.1 M Bu_4NCl (AN) has been used by inserting it into the salt bridge of 0.1 M Bu_4NPF_6 (Ac) [20]. #3 The electrode, $Ag\|AgClO_4$ + $KClO_4$; {$KClO_4$}, was also used [21].		
Acetonitrile (AN)		
Ag/Ag^+	Ag|0.01 M $AgNO_3$; {0.1 M Et_4NClO_4, satd. Et_4NPic, etc.}	[22–26]
	Ag|0.01 M $AgClO_4$; {0.1 M $LiClO_4$ or $NaClO_4$}	[27]
	Ag|0.1 M $AgClO_4$ + 0.5 M $NaClO_4$ or 0.1 M Bu_4NClO_4	[14, 28]
$Ag/AgCryp^+$	Ag|0.005 M $AgClO_4$ + 0.01 M Cryp(22) + 0.05 M Et_4NClO_4; {0.05 M Et_4NClO_4}	[29]
	Ag|0.002 M Ag^+ + 0.02 M Cryp(222) + 0.05 M Et_4NClO_4	[15]
Ag/AgCl	Ag|AgCl(s)|AgCl(satd.) + Me_3EtCl(satd.)	[30]
	Ag|AgCl(s)|AgCl(satd.) + 0.1 M Bu_4NCl; {0.1 M Bu_4NPF_6}	[20]
	Ag|AgCl(s)|AgCl(satd.) + LiCl(satd.); {2 % $LiClO_4$(agar)}	[31]
Hg/Hg^{2+}	Hg|0.01 M Hg^{2+} + 0.1 M Bu_4NClO_4	[14]
Tl(Hg)/TlBr	Tl(Hg)|TlBr(s)|TlBr(satd.) + 0.005 to 0.05 M LiBr; (cell without liquid junction, 5−35 °C, deaerated)	[32]
$Pt/Fc-Fc^+$	Pt|0.187 mM Fc + 0.173 mM FcPic, with or without 0.1 M Et_4NClO_4 (deaerated)	[33]
$Pt/DMFc-DMFc^+$	Pt|4 mM DMFc + 4 mM $DMFcPF_6$ + 0.1 M Bu_4NBF_4 (DMFc: decamethylferrocene)	[34, 35]
$Pt/I^- - I_3^-$	Pt|0.05 M I_2 + 0.1 M NaI; {0.1 M $NaClO_4$}	[36]
Pd(satd. H_2 or D_2)/ H^+ or D^+	Pd(H_2 or D_2)|2 M $NaClO_4$ (use in coulometric–potentiometric titration of bases)	[37]
Acetylacetone (Acac)		
Ag/Ag^+	Ag|0.1 M $AgClO_4$; {0.1 M Bu_4NClO_4}	[38]
Ammonia		
Ag/AgCl	Ag|AgCl(satd.) + KCl(satd.) (NH_3 at 25 °C/10 atm or at −40 °C/1 atm)	[39]

(continued)

Table 6.1 (continued)

Type of electrode	Examples of the electrode construction[a]	References
Pb/Pb^{2+}	Pb wire|$Pb(NO_3)_2$(satd.) + $LiNO_3$(satd.) (oxygen-free, 0 °C)	[40]
$Zn(Hg)/ZnCl_2$	Zn(Hg, 2 phase amalgam)|$ZnCl_2 \cdot 6NH_3$(satd.) (deaerated, −36 °C)	[41]
$e^-(Pt)/e^-_{solv}$	e^-(Pt)|0.001 M Na(e^-_{solv}) (electron electrode, deaerated, −77 °C)	[42]

Anisole (methoxybenzene)[#4]

#4 An Ag|0.1 M Ag^+ reference electrode in AN and the aqueous SCE have been used [43].

Benzene[#5]

#5 An Ag/Ag^+ reference electrode in AN (Ag|0.1 M $AgNO_3$ + 0.2 or 0.5 M Hex_4NClO_4 (AN)) [44, 45] and a Pt-wire pseudo-reference electrode [46] have been used.

Benzonitrile (BzN)[#6]

Ag/Ag^+	Ag|0.01 M $AgNO_3$ + 0.1 M Bu_4NClO_4 (Potentials were reported versus Fc/Fc^+ couple.)	[47]
	Ag|0.01 M Ag^+ + 0.05 M Et_4NClO or 0.1 M Bu_4NClO_4	[14, 15]
$Ag/AgCryp^+$	Ag|0.002 M Ag^+ + 0.02 M Cryp(222) + 0.05 M Et_4NClO_4	[15]
Ag/AgCl	Ag|AgCl(s)|satd. Cl^- (?)	[48, 49]
Hg/Hg^{2+}	Hg|0.01 M Hg^{2+} + 0.1 M Bu_4NClO_4	[14]
Pd(satd. H_2 or D_2)/ H^+ or D^+	Pd(H_2 or D_2)|2 M $NaClO_4$ (use in coulometric–potentiometric titration of bases)	[37]

#6 Aqueous reference electrodes and the Ag/Ag^+ reference electrode in AN (Ag|0.01 M $AgClO_4$ + 0.09 M Bu_4NClO_4 (AN)) [50] have been used.

γ-Butyrolactone (γ-BL)

Ag/Ag^+	Ag|0.1 M $AgClO_4$	[51]
	Ag|0.01 M Ag^+ + 0.1 M Bu_4NClO_4	[14]
	Ag|5 mM $AgClO_4$ + 5 mM Et_4NClO_4; {0.01 M Et_4NClO_4}	[52]
Ag/AgCl	Ag|AgCl(s)|AgCl(satd.) + 0.1 M LiCl	[51]
Li/Li^+	Li(strip)|0.5 M $LiAsF_6$ or $LiClO_4$ (argon atmosphere)	[53]
$Pt/I^- - I_3^-$	Pt|0.05 M I_2 + 0.10 M KI; {0.01 M Et_4NClO_4}	[54]

Butyronitrile (BuN)[#7]

Ag/Ag^+	Ag|0.01 M Ag^+ + 0.1 M Bu_4NClO_4	[14]
$Ag/AgCryp^+$	Ag|0.002 M Ag^+ + 0.02 M Cryp(222) + 0.05 M Et_4NClO_4	[15]
Hg/Hg^{2+}	Hg|0.01 M Hg^{2+} + 0.1 M Bu_4NClO_4	[14]

#7 An Ag/AgCl electrode in DCM (Ag|AgCl(s)|AgCl(satd.) + LiCl(satd.) + 0.1 M Bu_4NClO_4 (DCM); {0.1 M Bu_4NClO_4 (BuN)}) has been used [55].

Cellosolve (Monoethyl ether of ethylene glycol)

Ag/Ag^+	Ag|0.1 M $AgClO_4$	[56]

Chlorobenzene[#8]

#8 An Ag/Ag^+ reference electrode in AN (Ag|0.1 M $AgNO_3$ + 0.2 or 0.5 M Hex_4NClO_4 (AN)) has been used [44, 45].

1,2-Dichloroethane (DCE)

Ag/Ag^+	Ag|0.01 M Ag^+ + 0.1 M Bu_4NClO_4	[14]
Ag/AgCl	Ag|AgCl(s)|AgCl(satd.) + Me_4NCl(satd.) (20 °C)	[57]

(continued)

Table 6.1 (continued)

Type of electrode	Examples of the electrode construction[a]	References
Dichloromethane (DCM)[#9]		
Ag/Ag^+	Ag|0.1 M $AgBF_4$[#10]	[58]
	Ag|0.01 M Ag^+ + 0.1 M Bu_4NClO_4	[14]
Ag/AgCl	Ag|AgCl(s)|AgCl(satd.) + LiCl(satd.); {0.07 M Et_4NClO_4 or 0.1 M Bu_4NPF_6}	[17, 18, 59]
	Ag|AgCl(s)|AgCl(satd.) + Bu_4NCl(satd.) + 0.2 M Bu_3HNClO_4 or 0.5 M Bu_4NClO_4	[60, 61]
Ag/AgI	Ag|AgI(s)|AgI(satd.) + 0.05 M Bu_4NI + 0.42 M Bu_4NPF_6	[62]
#9 Ag|AgCl(s)|AgCl(satd.) + 0.1 M Bu_4NCl (AN) has been used by inserting it into 0.1 M Bu_4NPF_6 (DCM) [20]. #10 Ag|0.1 M $AgBF_4$ (AN) and aqueous SCE have also been used [58].		
Diethyl ketone (3-Pentanone)[#11]		
#11 Ag|AgCl(s)|AgCl(satd.) + 0.1 M Bu_4NCl (AN) has been used by inserting it into 0.1 M Bu_4NPF_6 (diethyl ketone) [20].		
Diglyme (Diethylene glycol diethylether)[#12]		
#12 Aqueous reference electrodes have usually been used.		
1,2-Dimethoxyethane (Monoglyme, DME)		
Ag/Ag^+	Ag|$AgNO_3$(satd.) (separated from the test solution by two sintered-glass disks, under nitrogen atmosphere, at −30 and 23 °C)	[63]
	Ag|$AgNO_3$(satd.) + 0.10 M Bu_4NClO_4	[64]
Li/Li^+	Li(foil)|0.1 M $LiClO_4$ + 0.1 M Bu_4NClO_4; {0.1 M Bu_4NClO_4} (argon atmosphere)	[65]
N,N-Dimethylacetamide (DMA)[#13]		
Ag/Ag^+	Ag|0.01 M $AgNO_3$; {satd. Et_4NPic}	[25]
	Ag|0.01 M Ag^+ + 0.05 M Et_4NClO_4 or 0.1 M Bu_4NClO_4	[14, 15]
$Ag/AgCryp^+$	Ag|0.002 M Ag^+ + 0.02 M Cryp(222) + 0.05 M Et_4NClO_4	[15]
Ag/AgCl	Ag|AgCl(s)|AgCl(satd.) + KCl(satd.); {0.1 M or satd. Et_4NClO_4, gelled with methyl cellulose}	[66–68]
Tl(Hg)/TlBr	Tl(Hg)|TlBr(s)|TlBr(satd.) + 0.02–0.1 M LiBr; (cell without liquid junction, 15−35 °C, deaerated)	[32]
#13 Ag|0.01 M $AgNO_3$ + 0.01 M Et_4NClO_4 (AN) has been used [69]. Ag|AgCl(s)|AgCl (satd.) + 0.1 M Bu_4NCl (AN) has also been used by inserting it into 0.1 M Bu_4NPF_6 (DMA) [20].		
Dimethyl carbonate (DMC)		
Cd/Cd^{2+}	Cd (wire)|$Cd(ClO_4)_2$ in poly(methyl methacrylate)-PC gel (solid-state reference electrode)	[70]
N,N-Dimethylformamide (DMF)[#14]		
Ag/Ag^+	Ag|0.01 M $AgNO_3$; {satd. Et_4NPic}	[25]
	Ag|0.01 M Ag^+ + 0.1 M Bu_4NClO_4	[14]
	Ag|0.1 M $AgClO_4$ + 0.1 M Pr_4NClO_4	[71]
	Ag|0.1 M $AgNO_3$ + 0.1 M Et_4NClO_4; {Et_4NClO_4(satd.)}	[72]
$Ag/AgCryp^+$	Ag|0.005 M $AgClO_4$ + 0.01 M Cryp(22) + 0.05 M Et_4NClO_4; {0.05 M Et_4NClO_4}	[29]
	Ag|0.002 M Ag^+ + 0.02 M Cryp(222) + 0.05 M Et_4NClO_4	[15]
Ag/AgCl	Ag|AgCl(s)|AgCl(satd.) + 0.1 M Et_4NCl; {0.1 M Et_4NClO_4}	[73]

(continued)

Table 6.1 (continued)

Type of electrode	Examples of the electrode construction[a]	References
	Ag|AgCl(s)|AgCl(satd.) + Et_4NCl(satd.) + methyl cellulose (satd.); {25 %(w/v) Et_4NClO_4 + 5 %(w/v) methyl cellulose}	[74]
Hg/Hg^{2+}	Hg|0.01 M Hg^{2+} + 0.1 M Bu_4NClO_4	[14]
$M(Hg)/M^+$	Na(Hg, satd.)|$NaClO_4$(satd.); {0.1 M $NaNO_3$ or Et_4NClO_4} (deaerated)	[75]
	Mg(Hg, mole fraction 4.88×10^{-3})|0.105 M $Mg(ClO_4)_2$; {0.1 M Et_4NClO_4} (deaerated)	[76]
M(Hg)/MX	Cd(Hg)|$CdCl_2$(s)|$CdCl_2 \cdot H_2O$(satd) + NaCl(satd.); {$NaClO_4$(satd.)} (deaerated)	[77]
	Cd(Hg)|$CdCl_2$(s)|$CdCl_2$(satd.) + LiCl(satd.) (deaerated)	[78]
	Tl(Hg)|TlCl(s)|TlCl(satd.) + LiCl(satd.) (deaerated)	[78]
$Pt/I^- - I_3^-$	Pt|0.1 M KI + 0.01 M I_2 + 0.5 M $NaNO_3$	[79, 80]

#14 Besides the aqueous SCE and the aqueous Ag/AgCl electrode, the SCE in MeOH (Hg|Hg_2Cl_2(s)|Hg_2Cl_2(satd.) + KCl(satd.) (MeOH)) has also been used [81]. Ag|AgCl(s)|AgCl (satd.) + 0.1 M Bu_4NCl (AN) has also been used by inserting it into 0.1 M Bu_4NPF_6 (DMF) [20].

Dimethyl sulfoxide (DMSO)[#15]

Ag/Ag^+	Ag|0.05 M $AgClO_4$; {0.1 M Et_4NClO_4}	[82]
	Ag|0.01 M $AgNO_3$; {satd. Et_4NPic}	[25]
	Ag|0.01 M $AgNO_3$ (flowing junction)	[83]
	Ag|0.01 M Ag^+ + 0.1 M Bu_4NClO_4	[14]
$Ag/AgCryp^+$	Ag|0.005 M $AgClO_4$ + 0.01 M Cryp(22) + 0.05 M Et_4NClO_4; {0.05 M Et_4NClO_4}	[29]
	Ag|0.002 M Ag^+ + 0.02 M Cryp(222) + 0.05 M Et_4NClO_4	[15]
Ag/AgX	Ag|AgCl(s)|AgCl(satd.) + KCl(satd.)	[84]
	Ag|AgCl(s)|AgCl(satd.) + NaCl(satd.)	[85]
	Ag|AgCl(s)|AgCl(satd.) + Et_4NCl(satd.); {0.01 M Et_4NClO_4}	[86]
	Ag|AgCl(s)|AgCl(satd.) + 0.04 M NaCl + 0.5 M $NaClO_4$	[87]
	Ag|AgI(s)|AgI(satd.) + 0.04 M NaI + 0.5 M $NaClO_4$	[87]
$Ag/AgCl_2^-$	Ag|0.001 M $AgCl_2^-$ + 0.1 M LiCl	[88, 89]
Hg/Hg^{2+}	Hg|0.01 M Hg^{2+} + 0.1 M Bu_4NClO_4	[14]
Hg/Hg_2Cl_2	Hg|Hg_2Cl_2(s)|Hg_2Cl_2(satd.) + LiCl(satd.); {0.1 M NH_4NO_3}	[90]
$Li(Hg)/Li^+$	Li(Hg)|0.5 M LiCl (deaerated)	[91]
$Cd(Hg)/Cd^{2+}$	Cd(Hg)|0.02 M $Cd(ClO_4)_2$ + 1 or 0.15 M NH_4ClO_4; {1 or 0.15 M NH_4ClO_4} (deaerated)	[92]
$Zn(Hg)/Zn^{2+}$	Zn(Hg,satd.)|$Zn(ClO_4)_2 \cdot 4DMSO$(satd.); {0.1 M $NaNO_3$ or Et_4NClO_4} (deaerated)	[75]
Tl(Hg)/TlX	Tl(Hg)|TlCl(s)|TlCl(satd.) + 0.01 M LiCl (deaerated)	[93]
	Tl(Hg|TlCl(s)|TlCl(satd.) + 0.5 M LiCl, etc. (deaerated)	[91]
	Tl(Hg)|TlBr(s)|TlBr(satd.) + 0.01–0.09 M LiBr; (cell without liquid junction, 20−35 °C, deaerated)	[32]
$Pt/I^- - I_3^-$	Pt|0.015 M I_2 + 0.031 M NaI + 0.5 M $NaClO_4$	[87]

#15 Ag|AgCl(s)|AgCl(satd.) + 0.1 M Bu_4NCl (AN) has been used by inserting it into 0.1 M Bu_4NPF_6 (DMSO) [20].

Dimethylthioformamide (DMTF)

Ag/Ag^+	Ag|0.01 M Ag^+ + 0.05 M Et_4NClO_4 or 0.1 M Bu_4NClO_4	[14, 15]
Hg/Hg^{2+}	Hg|0.01 M Hg^{2+} + 0.1 M Bu_4NClO_4	[14]

(continued)

Table 6.1 (continued)

Type of electrode	Examples of the electrode construction[a]	References
1,4-Dioxane[#16]		
#16 This solvent is usually used as mixtures with water and aqueous reference electrodes are employed.		
Ethanol (EtOH)		
Ag/Ag^+	$Ag\|0.01\ M\ AgNO_3 + 0.1\ M\ NaClO_4$	[94]
	$Ag\|0.01\ M\ Ag^+ + 0.1\ M\ Bu_4NClO_4$	[14]
Ag/AgCl	$Ag\|AgCl(s)\|AgCl(satd.) + 0.01\ M\ LiCl$	[95]
Hg/Hg^{2+}	$Hg\|0.01\ M\ Hg^{2+} + 0.1\ M\ Bu_4NClO_4$	[14]
Hg/HgI_2	$Hg\|0.005\ M\ HgI_2 + 0.05\ M\ KI$	[96]
$Pt/I^- - I_3^-$	$Pt\|0.05\ M\ I_2 + 0.1\ M\ NaI;\ \{0.1\ M\ NaClO_4\}$	[36]
Ethyl acetate[#17]		
#17 Only aqueous reference electrodes (SCE and Ag/AgCl) have been used.		
Ethylene carbonate (EC)		
Li/Li^+	$Li\|1\ M\ LiAsF_6$ (argon atmosphere)	[97]
Cd/Cd^{2+}	Cd (wire)$\|Cd(ClO_4)_2$ in poly(methyl methacrylate)-PC gel (solid state reference electrode)	[70]
Pd(satd. H_2 or D_2)/ H^+ or D^+	Pd(H_2 or D_2)$\|2\ M\ NaClO_4$ (40 °C, use in coulometric–potentiometric titration of bases)	[37]
Ethylenediamine (en)		
Ag/Ag^+	$Ag\|0.01\ M\ AgClO_4 + MX(c)$, $MX(c) = 0.23$ M LiCl, LiI (satd.), 0.5 M NaI, KI, and CsI and 0.2 M $NaClO_4$	[98–100]
$Hg/HgCl_2$	$Hg/HgCl_2$(satd.) + LiCl(satd.)	[101]
$Zn(Hg)/ZnCl_2$	Zn(Hg,satd.)$\|ZnCl_2(s)\|ZnCl_2$(satd.) + LiCl(satd. or 0.25 M) (deaerated)	[102]
Ethylene glycol (EG)		
Ag/Ag^+	$Ag\|0.01\ M\ Ag^+ + 0.05\ M\ Bu_4NClO_4$	[14]
Formamide (FA)		
Ag/Ag^+	$Ag\|0.01\ M\ Ag^+ + 0.1\ M\ Bu_4NClO_4$	[14]
	$Ag\|0.01\ M\ AgNO_3;\ \{satd.\ Et_4NPic\}$	[25]
Ag/AgCl	$Ag\|AgCl(s)\|AgCl(satd.)$ + HCl or NaCl (molalities: 0.0024–0.0516); (cell without liquid junction)	[103]
Formic acid		
Ag/AgCl	$Ag\|AgCl(s)\|AgCl(satd.) + HCl(variable)$; (cell without liquid junction)	[104]
Quinhydrone electrode	Pt|0.05 M quinhydrone + 0.25 M Na-formate	[105, 106]
Heptane[#18]		
#18 An Ag-wire pseudo-reference electrode has been used [107].		
Hexamethylphosphoric triamide (HMPA)		
Ag/Ag^+	$Ag\|0.01\ M\ AgNO_3;\ \{satd.\ Et_4NPic\}$	[25]
	$Ag\|0.01\ M\ AgNO_3 + 0.5\ M\ NaClO_4$	[108]
	$Ag\|0.01\ M\ Ag^+ + 0.1\ M\ Bu_4NClO_4$	[14]
	$Ag\|0.01\ M\ AgNO_3 + 0.5\ M\ NaClO_4;\ \{0.5\ M\ NaClO_4\}$	[109]
	$Ag\|0.1\ M\ AgClO_4;\ \{0.05\ M\ Et_4NClO_4\}$	[110]
Ag/AgCl	$Ag\|AgCl(s)\|AgCl(satd.)$ + NaCl(satd. ≈0.01 M) + 0.5 M $NaClO_4$	[108]

(continued)

Table 6.1 (continued)

Type of electrode	Examples of the electrode construction[a]	References
Hg/Hg^{2+}	$Hg\|0.01\ M\ Hg^{2+} + 0.1\ M\ Bu_4NClO_4$	[14]
$e^-(Pt)/e^-_{solv}$	Solvated-electron electrode under vacuum conditions: Pt|sodium metal(e^-) + 0.2 M $NaClO_4$	[111]
Hexamethylthiophosphoric triamide (HMTPA)		
Ag/Ag^+	$Ag\|0.01\ M\ Ag^+ + 0.1\ M\ Bu_4NClO_4$	[14]
Hg/Hg^{2+}	$Hg\|0.01\ M\ Hg^{2+} + 0.1\ M\ Bu_4NClO_4$	[14]
Hydrogen fluoride (HF)[#19]		
Cu/CuF_2	$Cu\|CuF_2(s)\|CuF_2$(satd.) + 1 M KF (0 °C)	[112–114]
	$Cu\|CuF_2(s)\|CuF_2$(satd.) + 0.1 M NaF (18 ± 2 °C)	[115]
	$Cu\|CuF_2(s)\|CuF_2$(satd.) + LiF(satd.) (15 °C)	[116]
Hg/Hg_2F_2	$Hg\|Hg_2F_2(s)\|Hg_2F_2$(satd.) + NaF (0, 10 and −20 °C)	[117, 118]
$Pt(H_2)/H^+$	Platinized $Pt(H_2)\|1\ M\ H_2O$	[119]
$Pd(H_2)/H^+$	$Pd(H_2)\|0.01$ M NaF + 1.0 M $NaBF_4$ (0 °C)	[120]
#19 A Cu-wire pseudo-reference electrode has been used [121].		
Isobutyronitrile[#20]		
Ag/Ag^+	$Ag\|0.01\ M\ Ag^+ + 0.1\ M\ Bu_4NClO_4$	[14]
#20 An aqueous SCE has been used [122].		
Methanol (MeOH)		
Ag/Ag^+	$Ag\|AgNO_3 + KNO_3$	[123]
	$Ag\|0.01\ M\ Ag^+ + 0.1\ M\ Bu_4NClO_4$	[14]
$Ag/AgCryp^+$	$Ag\|0.005\ M\ AgClO_4 + 0.01$ M Cryp(22) + 0.05 M Et_4NClO_4; {0.05 M Et_4NClO_4}	[29]
Ag/AgCl	$Ag\|AgCl(s)\|AgCl$(satd.) + 0.1 M LiCl + 0.66 M H_2O	[124]
Hg/HgI_2	$Hg\|0.005\ M\ HgI_2 + 0.05$ M KI	[96]
N-Methylacetamide (NMA)		
Ag/AgCl	$Ag\|AgCl(s)\|AgCl$(satd.) + KCl(satd.)	[125]
	$Ag\|AgCl(s)\|AgCl$(satd.) + NaCl(satd.); {0.1 M Et_4NClO_4}	[126]
Methyl acetate (MA)[#21]		
Ag/AgBr	$Ag\|AgBr(s)\|AgBr$(satd) + 0.005 M Me_4NBr	[127]
Li/Li^+	$Li\|1\ M\ LiClO_4$	[128]
	$Li(strip)\|2.4\ M\ LiAsF_6$	[129]
#21 In [130], an $Ag\|0.1\ M\ AgNO_3$ (AN) reference electrode has been used, though all potentials were reported as values versus Li/Li^+ electrode.		
Methylamine		
Ag/Ag^+	$Ag\|0.02\ M\ AgNO_3$ (−50 °C)	[131]
Pb/Pb^{2+}	$Pb\|Pb(NO_3)_2$(satd.) (−50 °C)	[131]
N-Methylformamide (NMF)[#22]		
Ag/Ag^+	$Ag\|0.01\ M\ AgNO_3 + 0.1\ M\ Et_4NClO_4$	[14, 132]
Ag/AgCl	$Ag\|AgCl(s)\|AgCl$(satd.) + 0.1 M MCl (M: Li, Na, K, Cs)	[133]
#22 $Ag\|AgCl(s)\|AgCl$(satd.) + 0.1 M Bu_4NCl (AN) has been used by inserting it into 0.1 M Bu_4NPF_6 (NMF) [20].		
3-Methyl-2-oxazolidone		
Ag/Ag^+	$Ag\|0.1\ M\ AgClO_4$	[134]

(continued)

Table 6.1 (continued)

Type of electrode	Examples of the electrode construction[a]	References
4-Methyl-2-pentanone (Methyl isobutyl ketone, MIBK)		
Ag/Ag^+	$Ag\|AgNO_3$(satd.); {0.1 M Bu_4NClO_4}	[135]
	$Ag\|5$ mM $AgClO_4$ + 25 mM Et_4NClO_4; {25 mM Et_4NClO_4}	[136]
N-Methylpropionamide[#23]		
#23 An aqueous normal calomel electrode has been used [137].		
N-Methyl-2-pyrrolidinone (NMP)		
Ag/Ag^+	$Ag\|0.01$ M Ag^+ + 0.1 M Bu_4NClO_4	[14]
	$Ag\|0.01$ M $AgClO_4$ + 0.05 M Et_4NClO_4	[15]
	$Ag\|0.01$ M $AgSO_3CF_3$ + 0.1 M Bu_4NClO_4; {c Bu_4NClO_4}	[138]
$Ag/AgCryp^+$	$Ag\|0.002$ M Ag^+ + 0.02 M Cryp(222) + 0.05 M Et_4NClO_4	[15]
Ag/AgCl	$Ag\|AgCl(s)\|AgCl$(satd.) + NaCl(satd.) + Et_4NClO_4(satd.); {Et_4ClO_4(satd.) + 5% methyl cellulose}	[139]
Hg/Hg^{2+}	$Hg\|0.01$ M Hg^{2+} + 0.1 M Bu_4NClO_4	[14]
Hg/Hg_2^{2+} + Hg^{2+}	$Hg\|0.01$ M (Hg_2^{2+} + Hg^{2+}) + 0.1 M $HClO_4$; {$KClO_4$ + methyl cellulose}	[140, 141]
2-Methyl-tetrahydrofuran (2Me-THF)		
Li/Li^+	Li(wire)$\|0.6$ M $LiAsF_6$ (dry box, argon atmosphere)[#24]	[142]
#24 The solvent and the electrolyte are not stable.		
N-Methyl-2-thiopyrrolidinone (NMTP)		
Ag/Ag^+	$Ag\|0.01$ M Ag^+ + 0.1 M Bu_4NClO_4	[14]
	$Ag\|0.01$ M $AgSO_3CF_3$ + 0.1 M Bu_4NClO_4; {c Bu_4NClO_4}	[138]
Hg/Hg^{2+}	$Hg\|0.01$ M Hg^{2+} + 0.1 M Bu_4NClO_4	[14]
Monoglyme[#25]		
#25 See 1,2-Dimethoxyethane		
Nitrobenzene (NB)[#26]		
Ag/Ag^+	$Ag\|0.01$ M Ag^+ + 0.05 M Et_4NClO_4 or 0.1 M Bu_4NClO_4	[14, 15]
$Ag/AgCryp^+$	$Ag\|0.002$ M Ag^+ + 0.02 M Cryp(222) + 0.05 M Et_4NClO_4	[15]
Hg/Hg^{2+}	$Hg\|0.01$ M Hg^{2+} + 0.1 M Bu_4NClO_4	[14]
#26 In most cases, aqueous SCE or Ag/AgCl electrode is used.		
Nitromethane (NM)		
Ag/Ag^+	$Ag\|0.01$ M $AgClO_4$ + 0.1 M $LiClO_4$	[143]
	$Ag\|0.01$ M Ag^+ + 0.1 M Bu_4NClO_4	[14]
Ag/AgCl	$Ag\|AgCl(s)\|AgCl$(satd.) + Me_4NCl(satd.); {0.09 M Me_4NClO_4}	[143]
Hg/Hg^{2+}	$Hg\|0.01$ M Hg^{2+} + 0.1 M Bu_4NClO_4	[14]
Pd(satd. H_2 or D_2)/ H^+ or D^+	Pd(H_2 or D_2)$\|NaClO_4$(satd.) (use in coulometric–potentiometric titration of bases)	[37]
1-Propanol, 2-Propanol (PrOH)[#27]		
Ag/Ag^+	$Ag\|AgNO_3$ + KNO_3	[123]
#27 A modified SCE, prepared by replacing the inner solution with KCl(MeOH), has been used [144].		

(continued)

Table 6.1 (continued)

Type of electrode	Examples of the electrode construction[a]	References
Propionitrile (PrN)		
Ag/Ag^+	Ag|0.01 M $AgClO_4$	[145]
	Ag|0.01 M Ag^+ + 0.05 M Et_4NClO_4 or 0.1 M Bu_4NClO_4	[14, 15]
$Ag/AgCryp^+$	Ag|0.002 M Ag^+ + 0.02 M Cryp(222) + 0.05 M Et_4NClO_4	[15]
Hg/Hg^{2+}	Hg|0.01 M Hg^{2+} + 0.1 M Bu_4NClO_4	[14]
Propylene carbonate (PC)		
Ag/Ag^+	Ag|0.004 M $AgClO_4$	[146, 147]
	Ag|0.01 M Ag^+ + 0.1 M Bu_4NClO_4	[14]
	Ag|0.01 M $AgClO_4$ + 0.1 M Et_4NClO_4; {0.1 M Et_4NClO_4}	[148]
	Ag|0.02 M $AgClO_4$ + 0.2–1.0 M $LiClO_4$; {0.2–1.0 M $LiClO_4$}	[149]
$Ag/AgCryp^+$	Ag|0.005 M $AgClO_4$ + 0.01 M Cryp(22) + 0.05 M Et_4NClO_4; {0.05 M Et_4NClO_4}	[29]
	Ag|0.002 M Ag^+ + 0.02 M Cryp(222) + 0.05 M Et_4NClO_4	[15]
Ag/AgCl	Ag|AgCl(s)|AgCl(satd.) + 0.004 M Et_4NCl	[146, 147]
Li/Li^+	Li(ribbon)|1 M $LiClO_4$ (argon atmosphere)	[150]
	Li(foil)|0.1 M $LiClO_4$ or 0.2 M $LiAsF_6$ or $LiSO_3CF_3$ (argon atmosphere)	[151]
	Li(foil)|0.1 M $LiClO_4$ + 0.1 M Bu_4NClO_4; {0.1 M Bu_4NClO_4} (argon atmosphere)	[65]
Cd/Cd^{2+}	Cd(wire)|$Cd(ClO_4)_2$ in poly(methyl methacrylate)-PC gel (solid state reference electrode)	[70]
Hg/Hg^{2+}	Hg|0.01 M Hg^{2+} + 0.1 M Bu_4NClO_4	[14]
Hg/Hg_2Cl_2	Hg|Hg_2Cl_2(s)|Hg_2Cl_2(satd.) + KCl(satd.) + 0.10 M Et_4NClO_4	[152]
Tl/TlCl	Tl(wire)|TlCl(s)|TlCl(satd.) + 1 mM LiCl (deaerated)	[153]
Tl(Hg)/TlCl	Tl(Hg)|TlCl(s)|TlCl(satd.) + 1 mM LiCl (deaerated)	[78, 153]
$Pt/I^- - I_3^-$	Pt|3.8 mM I^- + 2.93 mM I_3^- + 0.83 M $LiClO_4$	[154]
	Pt|0.05 M I_2 + 0.1 M NaI; {0.1 M $NaClO_4$}	[36]
$Pt/Fc - Fc^+$	Pt|0.01 M Fc + 0.01 M $FcClO_4$ + 0.1 M $LiClO_4$ or Et_4NClO_4; {0.1 M $LiClO_4$ or Et_4NClO_4} (deaerated)	[155]
	Pt|0.005 M Fc + 0.005 M FcPic (deaerated)	[156]
Pyridine (Py)		
Ag/Ag^+	Ag|1 M $AgNO_3$; {1 M $LiNO_3$}	[157–159]
	Ag|1−5 mM AgPic	[160]
	Ag|0.01 M Ag^+ + 0.1 M Bu_4NClO_4	[14]
Hg/Hg^{2+}	Hg|0.01 M Hg^{2+} + 0.1 M Bu_4NClO_4	[14]
$Hg/HgCl_2$	Hg|$HgCl_2$(s)|$HgCl_2$(satd.)	[160]
$Zn(Hg)/ZnCl_2$	Zn(Hg)|$ZnCl_2$(s)|$ZnCl_2 \cdot 2C_5H_5N$(satd.) (deaerated)	[162, 163]
$Cu^+ - Cu^{2+}$	Pt|2.5 mM Cu(I)Cl + 25 mM $Cu(II)Cl_2$ + 0.1 M Et_4NCl; {0.1 M Et_4NClO_4 + 6 % methyl cellulose gel}	[164]
Sulfolane (Tetramethylene sulfone, TMS)		
Ag/Ag^+	Ag|0.01 M $AgClO_4$ + 0.1 M $LiClO_4$; {0.1 M $LiClO_4$}	[165, 166]
	Ag|0.1 M $AgClO_4$; {0.1 M Bu_4NClO_4}	[167, 168]
	Ag|0.01 M Ag^+ + 0.05 M Et_4NClO_4 or 0.1 M Bu_4NClO_4	[12, 13, 21]
$Ag/AgCryp^+$	Ag|0.002 M Ag^+ + 0.02 M Cryp(222) + 0.05 M Et_4NClO_4	[15]

(continued)

Table 6.1 (continued)

Type of electrode	Examples of the electrode construction[a]	References
Ag/AgCl	Ag|AgCl(s)|AgCl(satd.) + Et_4NCl(satd.); {0.1 M Et_4NClO_4}	[169]
$I^- - I_3^-$	Pt|0.01 M I_3^- + 0.1 M I^-	[165, 166]
Pd(satd. H_2)/H^+	Pd(H_2)|2 M $NaClO_4$ (30 °C) (use in coulometric–potentiometric titration of bases)	[37]
Sulfur dioxide[#28]		
#28 Only aqueous reference electrodes (SCE and Ag/AgCl) have been used.		
Tetrahydrofuran (THF)		
Ag/Ag^+	Ag|$AgNO_4$(satd., ca.10^{-3} M) + 0.3 M $LiClO_4$	[170, 171]
	Ag|0.01 M Ag^+ + 0.1 M Bu_4NClO_4	[14]
	Ag|$AgNO_3$(satd.) + Bu_4NPF_6; {Bu_4NPF_6}	[172]
Hg/Hg^{2+}	Hg|0.01 M Hg^{2+} + 0.1 M Bu_4NClO_4	[14]
Li/Li^+	Li(foil)|0.1 M $LiClO_4$ + 0.1 M Bu_4NClO_4; {0.1 M Bu_4NClO_4} (argon atmosphere)	[65]
Polysulfide reference electrode	Porous, Teflon-bonded carbon electrode|4 mM Li_2S_6 + 0.8 M $LiClO_4$	[173, 174]
Fc/Fc^+	Pt|4 mM Fc + 4 mM $FcPF_6$ + 0.1 M Bu_4NPF_6; {0.1 M Bu_4NPF_6} (deaerated)	[175]
1,1,3,3-Tetramethylurea (TMU)[#29]		
Ag/Ag^+	Ag|0.01 M Ag^+ + 0.1 M Bu_4NClO_4	[14]
#29 An SCE has been used by replacing the saturated KCl(H_2O) with saturated KCl(MeOH) [176].		
2,2′-Thiodiethanol		
Ag/Ag^+	Ag|0.01 M Ag^+ + 0.1 M Bu_4NClO_4	[14]
Hg/Hg^{2+}	Hg|0.01 M Hg^{2+} + 0.1 M Bu_4NClO_4	[14]
Toluene[#30]		
#30 Ag- and Pt-wire pseudo-reference electrodes have been used [46, 107].		
Xylene[#31]		
#31 A Pt-wire pseudo-reference electrode has been used [46]		

[a]Salt bridges are shown in braces

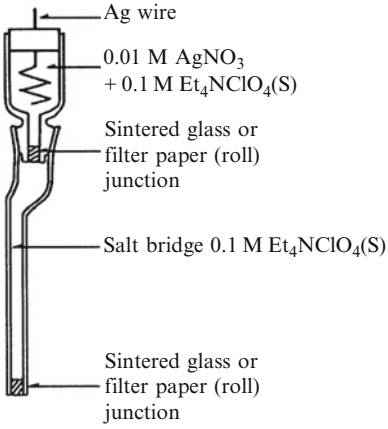

Fig. 6.1 An example of the Ag/Ag^+ reference electrode with a salt bridge

6.1.1 Silver Reference Electrodes

6.1.1.1 Silver–Silver Ion Reference Electrodes

This type is the most popular reference electrode used in nonaqueous solutions. Since Pleskov employed $Ag/AgNO_3$ in AN in 1948 [22], this type of electrode has been employed in most nonaqueous solvents for electrochemical use. $AgNO_3$ and $AgClO_4$[4] have mainly been used as silver salts, though some others ($AgBF_4$, $AgAsF_6$, $AgSO_3CF_3$, etc.) have also been employed. The electrode can be a simple structure as, for example, in Fig. 6.1 and, by dissolving the silver salt in the solvent under study and by using an Ag wire, it can easily be constructed. Ag^+ ions may also be generated by the anodic dissolution of the Ag metal in the solution of the supporting electrolyte, the Ag^+ concentration being controlled by the quantity of electricity passed. The electrode is, moreover, easy to use, the deaeration of the solution of the reference electrode being unnecessary.

Its potential can be expressed, in principle, by $E_{(S)} = E^{\ominus}_{(S)} + (RT/F) \ln a_{(Ag^+,S)} = E^{\ominus'}_{(S)} + (RT/F) \ln c_{(Ag^+,S)}$, where $E^{\ominus}_{(S)}$ and $E^{\ominus'}_{(S)}$ are the standard and the formal potentials of the Ag^+/Ag electrode in the solution under study (solvent S) and $a_{(Ag^+,S)}$ and $c_{(Ag^+,S)}$ are the activity and the concentration of Ag^+ in S. If the potential is expressed in solvent-independent scale[5] using solvent R as a reference, it can be

[4] Silver perchlorate ($AgClO_4$, hygroscopic) may explode by friction or by heating and it must be handled with care. The use of other silver salts ($AgNO_3$, $AgBF_4$, $AgSO_3CF_3$, etc.) is recommended.

[5] Solvent-independent potential scale is obtained by using, as the potential reference, a redox couple that is considered to have the same potentials in all solvents. Such redox couple, $\mathbf{I}^+/\mathbf{I}^0$ or $\mathbf{I}^0/\mathbf{I}^-$, should have the relation $\Delta G^{\ominus}_{t(I^+,R\to S)} = \Delta G^{\ominus}_{t(I^0,R\to S)}$ or $\Delta G^{\ominus}_{t(I^0,R\to S)} = \Delta G^{\ominus}_{t(I^-,R\to S)}$, where $\Delta G^{\ominus}_{t(i,R\to S)}$ shows the variation in the solvation energy of species i between R (reference solvent) and S (the solvent under study). This relation is nearly satisfied by redox couples like BCr^+/BCr and Fc^+/Fc, especially when R and S are both aprotic (see page 41 of [177]).

expressed by $E_{(S)} = E^{\ominus'}_{(R)} + (RT/F) \ln \gamma_{t(Ag^+,R\to S)} + (RT/F) \ln c_{(Ag^+,S)}$, where $E^{\ominus'}_{(R)}$ is the formal potential of the Ag^+/Ag electrode in R and $\gamma_{t(Ag^+,R\to S)}$ is the transfer activity coefficient of Ag^+ from R to S. $\gamma_{t(Ag^+,R\to S)}$ is related to the standard Gibbs energy of transfer of Ag^+ from R to S, $\Delta G^{\ominus}_{t(Ag^+,R\to S)}$, by $\log \gamma_{t(Ag^+,R\to S)} = \Delta G^{\ominus}_{t(Ag^+,R\to S)}/(2.302RT)$. Since the value of $\gamma_{t(Ag^+,R\to S)}$ varies considerably from one solvent to another,[6] the potential of the Ag^+/Ag electrode should vary considerably by the solvent used. The potentials of the 0.01 M Ag^+ + 0.1 M Bu_4NClO_4|Ag electrode in various solvents have been obtained as shown in Table 6.2 against the potential of the *bis*(biphenyl)chromium(I)/*bis*(biphenyl)chromium(0) (BCr^+/BCr) couple which is considered to be nearly solvent independent [14]. In the table, the potentials of the 0.01 M Hg^{2+} (0.1 M Bu_4NClO_4)/Hg electrode and the *bis*(cyclopentadienyl)iron(III)/*bis*(cyclopentadienyl)iron(II) (ferrocenium ion/ferrocene or Fc^+/Fc) couple are also included. The potentials of the Ag^+/Ag electrode expressed versus BCr^+/BCr couple are more positive in the solvents that less easily solvate to the Ag^+ ion (e.g., NM 1.571 V, DCM 1.562 V, NB 1.546 V, and PC 1.514 V) than in the solvents that easily solvate to the Ag^+ ion (e.g., Py 0.611 V, HMPA 0.891 V, DMSO 0.958 V, DMA 1.025 V, AN 1.030 V, NMP 1.032 V, and TMU 1.036 V). In NMTP and DMTF, which are soft solvents in the soft and hard acids and bases (HSAB) concept, the potentials of the Ag^+/Ag electrode vs. BCr/BCr^+ are even more negative and 0.181 V and 0.261 V, respectively, because the solvation of Ag^+ is extremely strong in these solvents.

The potential of this electrode is usually reproducible within several millivolts, if it is prepared freshly using pure solvent and pure electrolyte. But the stability of the potential is not always good enough. In AN, the potential of the Ag^+/Ag electrode is very stable, because Ag^+ ion is strongly solvated, and it is not much influenced by the addition of small amounts of water or other impurities. It is not so difficult to keep the potential drift within a few millivolts in a month [26]. In PC, the potential of the Ag^+/Ag electrode is kept fairly stable if the contamination of impurity and water can perfectly be avoided. But, because the solvation of Ag^+ is weak, the influence of impurity and water is much more serious than in AN: for the electrode of 0.01 M $AgClO_4$ + 0.05 M Et_4NClO_4(S)|Ag, the addition of 0.1 % water shifted the potential by −9.2 mV (i.e., to the negative side) in the case S = PC, though, in the cases S = AN, MeOH, DMSO, and DMF, the shifts were +0.07, −0.26, +0.41, and −0.14 mV, respectively (Table 6.3) [29]. Thus, under usual conditions, the stability of the Ag^+/Ag electrode in PC is not enough; it is much improved if a small amount of AN (e.g., 2 %) is added to the PC solution, though, of course, the potential much varies by the addition of AN [178].[7] In NM, the Ag^+/Ag electrode behaves reversibly

[6] The values of $\log \gamma_{t(Ag^+,H_2O\to S)}$ are 3.2 for (S=) PC, 1.6 for Ac, 1.2 for MeOH, −0.7 for TMS, −3.0 for DMF, −4.1 for AN, −4.6 for NMP, −5.1 for DMA, −6.1 for DMSO, −7.7 for HMPA, and −17.9 for DMTF (see Table 2.7 of [177]).

[7] This reference electrode was used in the potentiometric study of acid–base equilibria in PC using a pH glass electrode, in which the potential of the reference electrode should be very stable [178].

Table 6.2 Potentials of the Ag^+/Ag and Hg^{2+}/Hg electrodes and Fc^+/Fc reference redox system in various organic solvents (V vs. BCr^+/BCr reference redox system; in 0.1 M Bu_4NClO_4 unless otherwise stated in footnote; at 25 °C)

Solvents	$E(Ag^+/Ag)$[a]	$E(Hg^{2+}/Hg)$[b]	Fc^+/Fc[c]
Alcohols			
MeOH	1.337		1.134[d]
EtOH	1.275	1.349	1.134[d]
EG	1.217		1.132[e]
Ketones			
Ac	1.315		1.131[d,f]
Ethers			
THF	1.297	1.367	1.209[f]
Esters, Lactones			
γ-BL	1.364		1.112[d]
PC	1.514	1.606	1.114[d]
Amides			
FA	1.200		1.135
NMF	1.120[d]		1.135
DMF	1.112	1.144	1.127[d]
DMA	1.025		1.135
NMP	1.032	1.118	1.126[d]
TMU	1.036		1.129[g]
Nitriles			
AN	1.030	1.336	1.119
PrN	1.026	1.423	1.132
BuN	1.059	1.427	1.145[g]
Isobutyronitrile	1.071		1.131[f]
BzN	1.112	1.448	1.149
Nitro compounds			
NM	1.571	1.686	1.112[d]
NB	1.546	1.601	1.140[f]
Amine			
Py	0.611	0.783	1.149
Halogen compounds			
DCM	1.562		1.148[f]
DCE	1.503		1.131
Sulfur compounds			
DMSO	0.958	1.022	1.123[d]
TMS[h]	1.349		1.114[d]
2,2′-Thiodiethanol	0.691	0.979	1.121
DMTF	0.261	0.501	
NMTP	0.181	0.452	
Hexamethylthiophosphoric triamide	0.445	0.699	1.153
Phosphorus compounds			
HMPA	0.891	0.929	1.140

From Gritzner G (1990) Pure Appl Chem 62:1839

[a]0.01 M Ag^+ (0.1 M Bu_4NClO_4)/Ag electrode

[b]0.01 M Hg^{2+} (0.1 M Bu_4NClO_4)/Hg electrode

[c]Cyclic voltammetric $(E_{pc} + E_{pa})/2$ of ferrocene (E_{pc} and E_{pa}: cathodic and anodic peak potentials)

[d]0.1 M Et_4NClO_4

[e]0.05 M Bu_4NClO_4

[f]Polarographic half-wave potential

[g]Pulse-polarographic peak potential

[h]30 °C

Table 6.3 Effect of water on the potentials of some electrodes used as reference electrodes [29][a]

	Shift of potential (mV/0.1 vol.% H_2O) in				
Electrodes	AN	PC	MeOH	DMSO	DMF
Ag^+/Ag	+0.07	−9.2	−0.26	+0.41	−0.14[b]
$AgCryp(22)^+/Ag$	+0.82	+1.4	+0.10	+0.27	+0.27
$AgCryp(222)^+/Ag$	+0.22	+0.63	[c]	−0.18	−0.17
$I_3^- - I^-/Pt$	+2.0	+2.4	+0.30	+0.46	+0.75
$Fc^+ - Fc/Pt$	−0.43	−0.48	−0.51	[d]	[d]

Cells of the type "electrode in $S_{||}^{||}$0.05 M Et_4NClO_4 $(S)_{||}^{||}$electrode in (S + trace amount of H_2O)" were prepared for five electrodes, i.e., 0.01 M $AgClO_4$ + 0.05 M Et_4NClO_4|Ag, 0.005 M $AgClO_4$ + 0.010 M Cryp(22) + 0.05 M Et_4NClO_4|Ag, 0.005 M $AgClO_4$ + 0.010 M Cryp(222) + 0.05 M Et_4NClO_4|Ag, 0.005 M I_2 + 0.01 M Et_4NI + 0.05 M Et_4NClO_4|Pt, and 0.01 M Fc + 0.01 M FcPic + 0.05 M Et_4NClO_4|Pt. When trace amount of H_2O was added stepwise, the potential difference of the cell varied near-linearly against its vol.%

[a]Each value is an average of two measurements. The effect on the LJP is included but to an extent of less than 0.1 mV/0.1 % H_2O

[b]Ag^+ was slowly reduced to Ag

[c]The solubility of Cryp(222) was insufficient in MeOH

[d]Fc^+ was rapidly reduced to Fc

but, because the solvation of Ag^+ is very weak, the influence of impurity and water is so serious that the reproducibility and the stability of potential are not good enough for use as a reference electrode (potential shift: 3–4 mV day^{-1}) [143]. In DMF, NMF, and FA, on the other hand, Ag^+ is slowly reduced to Ag metal (for example, $2Ag^+ + HCONMe_2 + H_2O \rightarrow 2Ag^0 + Me_2NCOOH + 2H^+$ in the presence of trace water) and it causes a gradual potential shift to the negative direction [179]. Though the potential is reproducible when the electrode is freshly prepared, its shift reaches a few tens millivolts after several days. Thus, it is necessary to renew the solution every day before measurement. Benedetti et al. [180] studied the behavior of the Ag/Ag^+ reference electrode in DMF and considered it to be promising for its simple preparation, fast response, and fairly high exchange current density (4.0×10^{-6} A cm^{-2} at 1 mM $AgClO_4$ + 0.2 M $NaClO_4$ (DMF)|Ag, 1.3×10^{-6} A cm^{-2} at 1 mM $AgClO_4$ + 0.2 M $LiClO_4$ (DMF)|Ag). Ag^+ of 0.5–59 mM and $NaClO_4$ or $LiClO_4$ of 0.1–0.5 M were appropriate but Et_4NClO_4 gave a sluggish result. The potential of the electrode was stable for about 10 days in case if a millimolar quantity of $HClO_4$ was added.[8]

The Ag/Ag^+ reference electrodes are often used with a salt bridge of an indifferent or supporting electrolyte. Coetzee and Gardner [36] proposed a double-junction assembly combined with a salt bridge terminated in a Teflon (roll) junction (Fig. 6.2a) to prepare an Ag/Ag^+ reference electrode and compared its performance with a $Pt/I^- - I_3^-$ reference electrode in the same double-junction assembly. The flow rate of the Teflon junction with 0.1 M $NaClO_4$ (AN) was 2.6 μL h^{-1}. The solution

[8] In DMSO, if the electrode is 1 mM in Ag^+ (Ag|1 mM Ag^+ + 0.1 M $LiClO_4$ (DMSO)), black precipitate of Ag^0 is formed and the potential shifts by 150 mV to the negative direction in 10 days [89]. With 10 mM Ag^+, the stability of the potential is much improved.

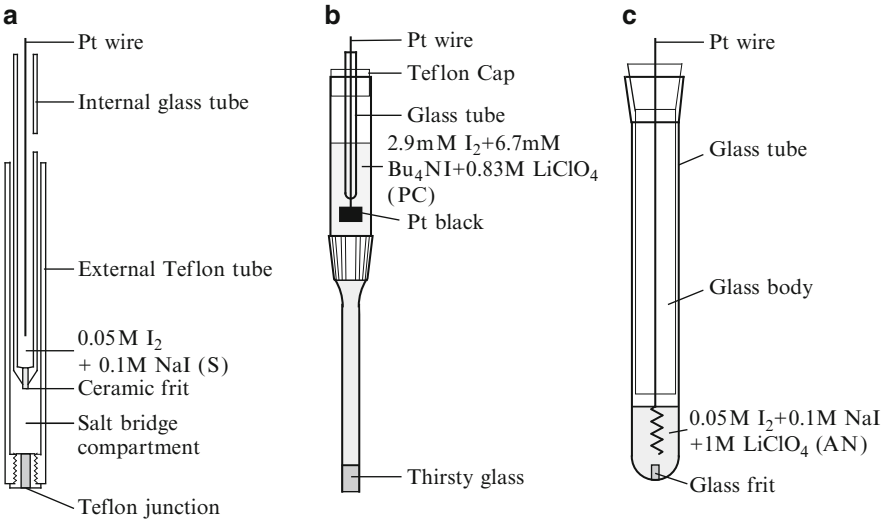

Fig. 6.2 Various $Pt/I^- - I_3^-$ reference electrodes. (**a**) Double-junction assembly for various solvents [36], (**b**) for PC [154], and (**c**) for AN [181]. (**a**) is also usable for Ag/Ag^+ reference electrode, though the electrode and the solution should be replaced. Original figures have been modified

used in the salt bridge was 0.1 M Et_4NClO_4 in AN, PC, and DMSO, 0.1 M $NaClO_4$ in EtOH, and 1 M KCl in H_2O. The potential fluctuation was <0.1 mV over the time of 4 h in H_2O and EtOH, <0.1 mV over the time of 5 h in AN, and <0.2 mV over the time of 8 h in PC. In DMSO, the fluctuation was <0.2 mV (time not shown), but the performance of the junction was less satisfactory than in other solvents. The exchange current density, measured in AN and PC, was of the order of 10^{-7} A cm^{-2} and much smaller than that for the I_3^-–I^-/Pt electrode. The small exchange current density was associated with the slow process of the crystallization of Ag metal. In these solvents, if a current density of 15 μA cm^{-2} was passed for several hundred seconds and then stopped, the Ag^+/Ag electrode needed several hours for the potential to return to the original value.

The use of the Ag/Ag^+ reference electrodes can be recommended as a first choice, because the electrodes are easy to construct and to use. The duration at which the potential is kept stable varies considerably by solvents and experimental conditions employed. The solutions of most Ag/Ag^+ reference electrodes must be refreshed every day before use, but it is not so troublesome.

6.1.1.2 Silver–Silver Cryptate Reference Electrodes

This type of electrodes has been developed in order to improve the stability of the Ag/Ag^+ reference electrodes, though its actual applications are fairly rare.

Ag/AgCryp(22)$^+$ Reference Electrode

The present author used cryptand(22) (1,4,10,13-tetraoxa-7,16-diazacyclooctadecane) for a silver reference electrode with a structure of Ag|5 mM AgCryp(22)$^+$·ClO_4^- + 5 mM Cryp(22) + 50 mM Et_4NClO_4 (S), where Cryp(22) and AgCryp(22)$^+$ show cryptand(22) and its complex with Ag^+, respectively [29]. It can be prepared in various solvents by adding $AgClO_4$, Cryp(22), and Et_4NClO_4 to the solvent to make them 5 mM, 10 mM, and 50 mM, respectively. The concentration of free Ag^+ can be expressed by $c_{(Ag^+)} = (1/K)\left(c_{(AgCryp(22)^+)}/c_{(Cryp(22))}\right)$, where K is the formation constant of AgCryp(22)$^+$ (reaction: Ag^+ + Cryp(22) $\rightleftarrows$ AgCryp(22)$^+$) and is equal to $10^{7.94}$ in AN, $10^{15.57}$ in PC, $10^{9.99}$ in MeOH, $10^{7.39}$ in DMSO, and $10^{9.91}$ in DMF [182]. The concentration of free Ag^+ is thus very small and is buffered if the ratio $c_{(AgCryp(22)^+)}/c_{(Cryp(22))}$ is kept constant. The potential of this electrode is given by $E = E^{\circ\prime}_{(Ag^+/Ag)} - 0.059 \log K + 0.059 \log\left(c_{(AgCryp(22)^+)}/c_{(Cryp(22))}\right)$. It is independent of the total concentration of Ag^+ ions, $c_{(Ag^+)total}$; for example, in 0.05 M Et_4NClO_4–AN, the potential variation due to the variation of $c_{(Ag^+)total}$ between 2×10^{-4} M and 1.6×10^{-2} M was within ±0.2 mV, as expected from the constant free Ag^+ concentration if the ratio $c_{(AgCryp(22)^+)}/c_{(Cryp(22))}$ is kept constant at 1.0. When the ratio $c_{(AgCryp(22)^+)}/c_{(Cryp(22))}$ is varied, however, $c_{(Ag^+)}$ varies and the potential should vary obeying the Nernst equation. In order to maintain the potential variation within ±0.5 mV, the ratio $c_{(AgCryp(22)^+)}/c_{(Cryp(22))}$ should be kept constant within ±2 %.

If referred to the half-wave potentials ($E_{1/2}$) of the Fc^+/Fc couple, the potentials for the AgCryp(22)$^+$/Ag electrode in AN, PC, DMF, and DMSO were −422, −400, −466, and −463 mV, respectively, while those for the Ag^+/Ag electrode (0.01 M Ag^+ + 0.05 M Et_4NClO_4 (S)|Ag) were −104, +381, −23, and −166 mV, respectively. Here, $E_{1/2}$ of the Fc^+/Fc couple is considered to be nearly solvent independent in dipolar aprotic solvents. If the potential is expressed in solvent-independent scale, the shift of the formal potentials of the AgCryp(22)$^+$/Ag electrode between solvents S and R is given by $E^{\circ\prime}_{(S)} - E^{\circ\prime}_{(R)} = 0.059 \log \gamma_{t(AgCryp(22)^+,R\rightarrow S)} - 0.059 \log \gamma_{t(Cryp(22),R\rightarrow S)}$. If S and R are both aprotic, Ag^+ ion in AgCryp(22)$^+$ is almost trapped inside the cavity of Cryp(22) and, thus, a relation $\log \gamma_{t\,(AgCryp(22)^+,R\rightarrow S)} \approx \log \gamma_{t\,(Cryp(22),R\rightarrow S)}$ is expected. Therefore, $E^{\circ\prime}_{(S)} - E^{\circ\prime}_{(R)} \approx 0$ or $E^{\circ\prime}_{(S)} \approx E^{\circ\prime}_{(R)}$ and the potentials of AgCryp(22)$^+$/Ag electrode in dipolar aprotic solvents should be approximately solvent independent.

The exchange current densities of the AgCryp(22)$^+$/Ag electrode were 5.0×10^{-6} A cm^{-2} in AN, 3.2×10^{-6} A cm^{-2} in PC, 3.7×10^{-6} A cm^{-2} in MeOH, 4.1×10^{-6} A cm^{-2} in DMSO, and 4.6×10^{-6} A cm^{-2} in DMF, and were a little larger than those in the case of the Ag^+/Ag electrode. The reproducibility and the stability of the electrode potential were fairly good as shown in Table 6.4. The potentials of the Ag/AgCryp(22)$^+$ reference electrode in various solvents varied

Table 6.4 Reproducibility and stability of the potential of the AgCryp(22)$^+$/Ag electrode [29]

	Reproducibility[a]		Stability[b]
Solvent	1 h	24 h	24 h
AN	±0.35 mV	±0.29 mV	+1.4 mV
PC	±0.28	±0.39	+1.6
MeOH	±0.28	±0.27	−0.1
DMSO	±0.20	±0.27	+0.1
DMF	±0.27	±0.31	+0.9

[a]Standard deviation of the potentials of 6–10 electrodes prepared at the same time. Values after 1 and 24 h

[b]Difference between average potentials of the original electrodes and of the new electrodes prepared after 24 h. Average of two measurements

Table 6.5 Formation constants of AgCryp(222)$^+$ and potentials of Ag^+/Ag and AgCryp(222)$^+$/Ag electrodes [15]

Solvent	log *K* of AgCryp(222)$^+$	*E* of Ag^+/Ag[a]	*E* of AgCryp(222)$^+$/Ag[b]
Ac	13.64	305 mV	−440 mV
AN	8.88	0	−464
PrN	9.07	54	−421
BuN	9.04		−423
BzN	9.98	104	−424
DMA	8.78	−22	−455
DMF	9.92	59	−466
NMP	8.82	−2	−462
DMSO	7.34	−122	−485
PC	16.27	415	−484
TMS	14.88	312	−487
NB	17.13	503	−438

[a]Potential difference of Ag|0.01 M Ag^+, 0.05 M Et_4NClO_4 (AN)|0.01 M Ag^+, 0.05 M Et_4NClO_4 (S)|Ag

[b]Potential difference of Ag|0.01 M Ag^+, 0.05 M Et_4NClO_4 (AN)|0.002 M Ag^+, 0.02 M Cryp(222), 0.05 M Et_4NClO_4 (S)|Ag

near-linearly with the amounts of a little water added; the effects of 0.1 vol.%-water are shown in Table 6.3. The effects are moderate; especially the effect in PC is much smaller than that for the Ag^+/Ag electrode. The influence by solvent impurities is also expected to be moderately small.

Ag/AgCryp(222)$^+$ Reference Electrode

Lewandowski et al. [15] used cryptand(222) (4,7,13,16,21,24-hexaoxa-1,10-diazabicyclo[8.8.8]hexacosane) to develop a similar reference electrode as above. They constructed a cell as shown by Ag|0.01 M Ag^+ + 0.05 M Et_4NClO_4 (AN)|0.002 M Ag^+ + 0.02 M Cryp(222) + 0.05 M Et_4NClO_4 (S)|Ag and got the results as in Table 6.5. The potential differences for S of 12 dipolar aprotic solvents were nearly constant (454 ± 33 mV), as compared to the maximum variation of ca.

620 mV for the potential differences of Ag|0.01 M Ag^+ + 0.05 M Et_4NClO_4 (AN) |0.01 M Ag^+ + 0.05 M Et_4NClO_4 (S)|Ag. In both cells, there is a liquid junction between AN and S, but the liquid-junction potential (LJP) there seems to be relatively small (probably within ±20 mV (Sect. 6.2.3)) and it does not give serious influence on the result that the potential of the AgCryp(222)$^+$/Ag electrode is nearly solvent independent. Because, in dipolar aprotic solvents, AgCryp(222)$^+$ and AgCryp(22)$^+$ resemble in formation constants and in behaviors, this is understandable. The potential of the AgCryp(222)$^+$/Ag electrode is also not much influenced by impurities. For example, the potential of the Ag^+/Ag electrode in Ac varies to the negative direction by the addition of Cl^- (in two steps, i.e., at $c_{(Cl^-)total}/c_{(Ag^+)total}$ of 1 and 2) and the total variation reaches ca. −900 mV for $c_{(Cl^-)total}/c_{(Ag^+)total}$ of 3. However, the potential of the AgCryp(222)$^+$/Ag electrode does not change by more than 10 mV by the addition of the same amount of Cl^-.

6.1.1.3 Silver–Silver Chloride Reference Electrodes

In protic solvents like MeOH, this type of electrode can be constructed similarly as in aqueous solutions. However, in aprotic (mostly dipolar) solvents, it is difficult to prepare an AgCl/Ag electrode of high Cl^- concentrations. The Ag^+ ion in aprotic solvents strongly interacts with chloride ion to form $AgCl_2^-$ or higher complex [183, 184].

$$\begin{array}{lcllll} Ag^+ & + & Cl^- & \rightleftarrows & AgCl & K_{sp} = c_{(Ag^+)}c_{(Cl^-)} \\ Ag^+ & + & 2Cl^- & \rightleftarrows & AgCl_2^- & \beta_2 = c_{(AgCl_2^-)}/(c_{(Ag^+)}c_{(Cl^-)}^2) \\ Ag^+ & + & 3Cl^- & \rightleftarrows & AgCl_3^{2-} & \beta_3 = c_{(AgCl_3^{2-})}/(c_{(Ag^+)}c_{(Cl^-)}^3) \end{array}$$

Table 6.6 shows the values of $pK_{sp}\left(=-\log K_{sp}\right)$, $\log\beta_2$, and $K_{sp}\beta_2$ $\left(=c_{(AgCl_2^-)}/c_{(Cl^-)}\right)$. From this table, the ratio $c_{(AgCl_2^-)}/c_{(Cl^-)}$ is 2.0×10^{-5} in H_2O and 7.9×10^{-6} in MeOH but near to 5 in AN, near to 8 in PC, and near to 20 in DMSO. Thus, in aprotic solvents, the precipitate of AgCl is easily dissolved in solutions of high Cl^- concentrations, forming $AgCl_2^-$.[9] When we construct an AgCl/Ag electrode in an aprotic solvent, we must keep the free Cl^- concentration low, using a solution of a chloride salt that is either sparingly soluble or dilute in concentration, and saturate AgCl in it.

The Ag/AgCl reference electrode has been prepared in aprotic solvents such as Ac, AN, BzN, γ-BL, DCE, DCM, DMA, DMF, DMSO, HMPA, NM, NMP, PC, and TMS and protic solvents such as HOAc, NH_3, EtOH, FA, formic acid, MeOH, NMA, and NMF.

[9] This applies to aprotic solvents that are hard base in HSAB concept. In soft base aprotic solvents like DMTF, AgCl is considerably dissolved by being dissociated into Ag^+ and Cl^-, because Ag^+ is solvated extremely strongly.

Table 6.6 Solvent effects on the formation of precipitates and complexes of the silver ion with chloride ions[a,b]

Solvent	Indifferent electrolyte		
H_2O	5 M $NaClO_4$	pK_{sp}	10.10
		$\log \beta_2$	5.40
		$K_{sp}\beta_2$	$10^{-4.70}$
MeOH	1 M $LiClO_4$	pK_{sp}	13.0
		$\log \beta_2$	7.9
		$K_{sp}\beta_2$	$10^{-5.1}$
AN	0.1 M Et_4NClO_4	pK_{sp}	12.4
		$\log \beta_2$	13.1
		$K_{sp}\beta_2$	$10^{0.7}$
PC	0.1 M Et_4NClO_4	pK_{sp}	20.0
		$\log \beta_2$	20.9
		$K_{sp}\beta_2$	$10^{0.9}$
DMSO	0.1 M Et_4NClO_4	pK_{sp}	10.4
		$\log \beta_2$	11.7
		$K_{sp}\beta_2$	$10^{1.3}$

[a]Taken from Table X in [185]. Somewhat different values are found in Table 4 of [184]
[b]$K_{sp}\beta_2 = {}^{C}(AgCl_2^-)/{}^{C}(Cl^-)$

Popov and Geske [30] prepared an Ag/AgCl reference electrode in AN for polarographic use. It consisted of an Ag/AgCl electrode placed in AN saturated with AgCl and Me_3EtNCl. Here, the solubility of AgCl in AN was limited by the amount of free Cl^- present, which in turn was governed by the solubility of Me_3EtNCl. The saturated condition for the 250 ml reference electrolyte solution was achieved in ca. 80 h at 25 °C and was 0.015 M in AgCl and 0.118 M in Me_3EtNCl. The performance of the Ag/AgCl reference electrode (surface area: 23.4 cm^2)[10] was tested by placing identical half-cells in the arms of an H-cell with a fine sintered-glass frit separating the arms. A linear current–voltage relationship was obtained from 0 to 2 V and 0 to 100 μA. Polarization was less than 1 mV on such a run, and less than 2 mV when a current of 100 μA was passed through the cell for 20 min. There was no variation in potential on shaking the cell. The measurements of the potential difference of the cell Ag|AgCl(s)| AgCl (satd.) + Me_3EtNCl(satd.) (AN)¦0.01 M $AgNO_3$ (AN)|Ag, carried out six times with different electrolyte preparations over a period of 6 months, gave a value of 638 ± 1 mV at 25.0 °C. The temperature coefficient was 0.6 mV K^{-1}. Hanselman and Streuli [31] used an Ag/AgCl reference electrode in AN for coulometry. It was prepared by coating an Ag wire with AgCl and by immersing the wire in AN saturated with AgCl and LiCl.

[10] A reference electrode of large area was used because the polarograph was a two-electrode instrument. With this instrument, the reference electrode also played the role of the counter electrode and considerable current passed through it. With a three-electrode instrument, which is now in common use, the reference electrode can be much smaller in size.

Headridge et al. [74] used for polarography an Ag/AgCl reference electrode in DMF. It consisted of a sheet of Ag (2 × 5 cm) coated with AgCl and was immersed in DMF saturated with AgCl, Et_4NCl, and methyl cellulose. The horizontal cross arm of an H-cell, as a salt bridge, contained a gel of 25(w/v)% Et_4NClO_4−5(w/v)% methyl cellulose in DMF. Headridge et al. [169] also used an Ag/AgCl reference electrode in TMS for polarography. They used an H-cell: the reference electrode was a sheet of Ag (2 × 5 cm) coated with AgCl and immersed in TMS saturated with AgCl and Et_4NCl, and the central horizontal cross arm, separated from the compartment of the reference electrode by sintered-glass disk, contained 0.1 M Et_4NClO_4 in TMS.

The Ag/AgCl reference electrode in DMSO used by Kolthoff and Reddy [85] had a construction Ag|AgCl(s)|AgCl(satd.) + NaCl(satd.), while that used by Simonova et al. [86] was Ag|AgCl(s)|AgCl(satd.) + Et_4NCl(satd.) immersed in a salt bridge of 0.01 M Et_4NClO_4. In DMSO, a reference electrode of the type Ag|10^{-3} M $AgCl_2^-$ + 0.1 M LiCl has also been used [88, 89]. It was prepared in the presence of excess Cl^- ion. The potential responded fast and it was reproducible within 5 mV and stable for more than 1 month.

Bréant reported an Ag/AgCl reference electrode for use in NMP [139]. It had a structure of Ag|AgCl(s)|AgCl(satd.) + NaCl(satd.) + Et_4NClO_4(satd.) in NMP and was connected to the salt bridge of NMP containing saturated Et_4NClO_4 and gelled with 5 % methyl cellulose. The reference electrolyte was prepared by agitating AgCl, NaCl, and Et_4NClO_4 in NMP for 3 days. The potential of the electrode was −500 ± 5 mV vs. Fc^+/Fc couple, being reproducible to nearly 5 mV, and stable to nearly 5 mV at least for 2 months.

Cauquis and Serve [143] used an Ag/AgCl reference electrode in NM: the structure was Ag|AgCl(s)|AgCl(satd.) + Me_4NCl(satd.)|0.09 M Me_4NClO_4. The electrode was prepared by immersing an Ag wire (8 cm in length and 1 mm in diameter) in NM saturated with Me_4NCl (concentration: ca. 0.08 M) and, by the anodic dissolution of the Ag wire, the solution was saturated with AgCl and the wire was covered with AgCl. To saturate the solution of 5 ml with AgCl, the current of 0.1 mA was passed for 6 h. To avoid the diffusion of Cl^- ion to the test solution, the compartment of the reference electrode was connected to a salt bridge of 0.09 M Me_4NClO_4 separated by a fritted glass. $LiClO_4$ was not used instead of Me_4NClO_4 in order to avoid the precipitation of LiCl in the fritted glass. The potential of the reference electrode was −0.35 V vs. aq. SCE. An example of the Ag/AgCl reference electrodes in PC was Ag|AgCl(s)|AgCl(satd.) + 0.004 M Et_4NCl [146, 147]. On the other hand, an example of the Ag/AgCl reference electrode in HMPA had the construction Ag|AgCl(s)|AgCl(satd.) + NaCl (satd.≈0.01 M) + 0.5 M $NaClO_4$ [108].

Usually it takes considerable time to prepare the AgCl-saturated solutions in aprotic solvents. But the Ag/AgCl reference electrodes in such solvents have the advantages that good potential reproducibility and long-term potential stability can be obtained.

6.1.2 Metal and Metal Amalgam Reference Electrodes Other Than Silver

6.1.2.1 M/M$^+$- and M/MX-Type Reference Electrodes

Among the M/M$^+$-type reference electrodes, a Li/Li$^+$ reference electrode is often used in solvents such as PC, γ-BL, and MA, especially in the studies of battery technologies [53, 130, 150]. It can be prepared by immersing lithium (wire, ribbon or foil) into the solution of $LiClO_4$ or $LiAsF_6$. Though its potential is reproducible and stable, it must be used in a glove box under argon atmosphere. Besides the Li/Li$^+$ electrode, a Cd/Cd^{2+} reference electrode has been used in PC, EC, DMC, and their mixtures [70]: it is all solid state and was designed by using poly(methyl methacrylate) (PMMA)−propylene carbonate polymer electrolyte with immobilized Cd $(ClO_4)_2$ solution and a Cd wire. The electrode was good in reproducibility, stability, and durability and the potential of the PMMA–Cd–Cd^{2+} electrode in PC was −0.439 ± 0.013 V vs. aq. SCE. An Hg/Hg_2^{2+} + Hg^{2+} reference electrode, used in NMP [140, 141], had a structure Hg|0.01 M (Hg_2^{2+} + Hg^{2+}) + 0.1 M $HClO_4$ with a salt bridge of $KClO_4$ + methyl cellulose. Its potential was reproducible to 1 mV but was not stable enough and shifted to negative direction because both Hg_2^{2+} and Hg^{2+} were reduced to metallic Hg, though it could be used for 5 days if 10 mV of the potential variation was allowed. A Pb/Pb^{2+} reference electrode, used in ammonia [40], had a structure Pb|Pb $(NO_3)_2$(satd.) + $LiNO_3$(satd.) and was prepared from a cracked glass tube filled with NH_3 solution saturated with $LiNO_3$ and $Pb(NO_3)_2$ and containing a strip of Pb wire. The electrode was immersed in a solution of NH_4NO_3−NH_3 (mole fraction of NH_4NO_3: 0.37) at 0 °C. Because the ohmic resistance across the cracked glass was about 5×10^5 Ω, an instrument of high internal resistance should be used for measurements.

As to the reference electrodes of the M/MX type, there are reports on the Hg/Hg_2Cl_2 and $Hg/Hg_2(OAc)_2$ electrodes in HOAc [6–10], the Hg/Hg_2Cl_2 electrode in Ac [19] and DMSO [90], the $Hg/HgCl_2$ electrode in en [101] and Py [161], the Hg/HgI_2 electrode in EtOH and MeOH [96], the Cu/CuF_2 and Hg/Hg_2F_2 electrodes in hydrogen fluoride (HF) [112–118], and the Hg/Hg_2Cl_2 and Tl/TlCl electrodes in PC [152, 153]. Details for the preparation of the Hg/Hg_2Cl_2 electrode in Ac have been described in [19]. When Ac saturated with LiCl is brought into contact with calomel, Hg_2^{2+} is partly reduced to Hg and partly oxidized to Hg^{2+} complex that is soluble in Ac. To prepare the Hg/Hg_2Cl_2 electrode, a paste of calomel and Hg should be placed on an Hg pool and covered with Ac that has been saturated with LiCl at 30 °C. The system quickly reaches equilibrium by this process and the electrode is reasonably reversible, non-polarizable, stable, and reproducible. In order to avoid the influence of the evaporation of Ac, a paste should be prepared using solid LiCl, calomel, and Hg and the electrolyte solution should be made separately by allowing excesses of LiCl and calomel to come to equilibrium in Ac. The $Hg/HgCl_2$ electrodes in en and Py have a structure Hg|$HgCl_2$(satd.) + LiCl(satd.) [122, 161]. $HgCl_2$ was used

because Hg_2Cl_2 of the calomel electrode instantaneously reacted with the solvent to give a black precipitate, while LiCl was added to reduce the electric resistance of the electrode. The Hg/HgI_2 electrode in EtOH and MeOH with a construction of Hg|0.005 M HgI_2 + 0.05 M KI (EtOH or MeOH) had a flowing junction and its potential was reproducible and stable in both solvents [96]. The $Hg/Hg_2(OAc)_2$ electrode in HOAc [8–10] had a structure $Hg|Hg_2(OAc)_2(s)|Hg_2(OAc)_2$ (satd.) + 0.5 M $NaClO_4$ and was immersed in the salt bridge of 0.5 M $NaClO_4$. The Tl/TlCl electrode in PC had the structure Tl|TlCl(s)| TlCl (satd.) + 1 mM LiCl and oxygen had strictly to be excluded from the system, since solid Tl, as well as Tl(Hg), undergoes oxidation very rapidly [153]. The TlCl layer well adhering to the Tl-electrode surface was formed by anodizing inside the sealed cell and the dissolution of this layer was prevented by pre-saturating the electrolyte solution with TlCl. Compared with the Tl(Hg)/TlCl reference electrode, the solid Tl/TlCl electrode was somewhat less reproducible and required a longer time after its preparation to reach equilibrium. But the solid Tl electrode has some advantage over the Tl(Hg) electrode in the easiness of the practical use.

In using these types of reference electrodes, the toxicities of Cd, Hg, Pb, and Tl metals and their salts should be considered seriously. This also applies to the reference electrodes in the next section.

6.1.2.2 M(Hg)/M^+- and M(Hg)/MX-Type Reference Electrodes

As M(Hg)/M^+-type reference electrodes, there exist Na(Hg)/Na^+ [75] and Mg(Hg)/Mg^{2+} [76] electrodes in DMF and Li(Hg)/Li^+ [91], Cd(Hg)/Cd^{2+} [92], and Zn(Hg)/Zn^{2+} [75] electrodes in DMSO. The Na(Hg)/Na^+ electrode in DMF had a structure Na (Hg, satd.)|$NaClO_4$(satd.) with a salt bridge of 0.1 M $NaNO_3$ or Et_4NClO_4. The saturated Na amalgam was prepared by dissolving Na metal in pure Hg. As to the Mg(Hg)/Mg^{2+} electrode, dilute Mg amalgam (mole fraction: 4.88×10^{-3}) was prepared by discharging a Mg disk into a pool of Hg at a current density of 0.42 mA cm^{-2} from a solution of 1 mM $MgCl_2$ in DMF and it was immersed in 0.105 M $Mg(ClO_4)_2$ (DMF). With the two amalgam electrodes, the measurements must be performed in an argon-filled glove box. The Li(Hg)/Li^+ electrode in DMSO [91] had a structure Li(Hg)|0.5 M LiCl and was used in a glove box under argon. The Li(Hg) amalgam was a saturated one and ca. 2.0 mol% in Li. The Li(Hg)/Li^+ electrode of 1.22 mol% Li amalgam and 0.1 M LiCl had also been used in DMF and DMSO [78]. The Cd(Hg)/Cd^{2+} electrode in DMSO [92] had a structure Cd(Hg)| 0.02 M $Cd(ClO_4)_2$ + 1 or 0.15 M NH_4ClO_4 with a salt bridge of 1 or 0.15 M NH_4ClO_4. The solution of Cd^{2+} was prepared using $Cd(ClO_4)_2 \cdot 6DMSO$ and the Cd (Hg) was prepared by the procedure in [185]. The Zn(Hg)/Zn^{2+} electrode in DMSO [75] had the structure Zn(Hg, satd.)|$Zn(ClO_4)_2 \cdot 4DMSO$(satd.) with a salt bridge of 0.1 M $NaNO_3$ or Et_4NClO_4. The saturated Zn amalgam was prepared by the electrolytic deposition of Zn into a layer of pure Hg from an aqueous solution of $ZnSO_4$.

As M(Hg)/MX-type reference electrodes, there exist Tl(Hg)/TlCl in DMF [78], DMSO [78, 93], and PC [78, 153], Tl(Hg)/TlBr in AN, DMA, and DMSO [32], Cd

(Hg)/$CdCl_2$ in DMF [77, 78], and Zn(Hg)/$ZnCl_2$ in en [102], Py [162, 163], and NH_3 [41]. All of these electrodes must be used under argon or nitrogen atmosphere. The amalgams of Tl, Cd, and Zn were prepared by dissolving the respective metals in pure Hg. The solubilities of TlCl in DMF, DMSO, and PC were 5.48×10^{-5} M, 1.76×10^{-3} M, and 6.07×10^{-7} M, respectively, while those of $CdCl_2$ in DMF and PC were 6.09×10^{-2} M and 2.35×10^{-2} M, respectively [78]. According to another study in DMSO, the solubility product of TlCl was 5.5×10^{-7} and the formation constants of thallous chloride complexes were $\beta_1 = 5 \times 10^2$ for TlCl and $\beta_2 = 9 \times 10^3$ for $TlCl_2^-$ in a LiCl−$LiClO_4$ medium of constant ionic strength, 0.5 [91]. The exchange current of the Tl(40 mol% in Hg)/TlCl(s)/Cl^- electrode in 0.5 M LiCl–DMSO was 7×10^{-4} A cm^{-2} and behaved reversibly [91]. The potential of the Tl(Hg)/TlCl electrode was extremely stable in DMSO, though it varied considerably in DMF [78]. Contrarily, the potential of the Cd(Hg)/$CdCl_2$ electrode was extremely stable in DMF but varied significantly in DMSO because of the high solubility of $CdCl_2$ in DMSO. The Zn(Hg)/$ZnCl_2$ electrode in Py was set up by adding a saturated solution of $ZnCl_2$·2Py in Py to the Zn amalgam (prepared by direct dissolution or by electrolysis) already placed in the electrode vessel [161, 162]. A quantity of solid $ZnCl_2$·2Py was added to the $ZnCl_2$ solution to ensure saturation. The electrode thus obtained was allowed to equilibrate for at least 24 h before use. All measurements were performed in a glove box avoiding exposure to air.

6.1.3 Redox Reference Electrodes

6.1.3.1 Ferrocene−Ferrocenium Ion Reference Electrode

Kolthoff and Thomas [33] used in oxygen-free AN a redox electrode composed of a spiral Pt wire and 0.187 mM Fc + 0.173 mM Fc^+ + 0.1 M Et_4NClO_4. The standard potential vs. Ag/0.01 M $AgNO_3$ (AN) was 0.074 V. In AN containing dissolved oxygen, the decomposition of Fc^+ ion was observed [187]. The mechanism for the process of this decomposition has intensively been studied [188]. During Fc oxidation in an incompletely degassed solution, soluble and insoluble substances were formed; the insoluble substance was a mixture of hydrous Fe(III) oxide and organic polymer material (poly(cyclopentane-1,3-dione-4,5-diyl)) and caused electrode fouling, while the soluble products were mainly constituted from Fe(III) perchlorate, 4-cyclopentene-1,3-dione, tricyclo[5.1.2.0(2,6)]deca-4,8-dien-3,10-dione, and related oligomers. Courtot-Coupez and L'Her [148, 155] used the reference electrode of Pt/0.01 M Fc + 0.01 M $FcClO_4$ + 0.1 M $LiClO_4$ or Et_4NClO_4 in PC in oxygen-free conditions. The normal potential of the electrode vs. Ag/0.01 M Ag^+ (PC) was −0.385 V. In DMF and DMSO, Fc^+ ions are reduced to Fc and the use of the Pt/Fc−Fc^+ system as a reference electrode is impossible even in oxygen-free conditions. Zara et al. [189] reported the mechanism for the decomposition of Fc^+ in strongly donor solvents (S) like DMF and DMSO to be $2FeCp_2^+ + 6S \rightarrow FeCp_2 + FeS_6^{2+} + 2Cp$, where $FeCp_2^+$ and $FeCp_2$ are Fc^+ and Fc, respectively, and Cp is cyclopentadienyl. Recently, Paddon and Compton

[175] studied the Pt|Fc−Fc^+ reference electrode for electrochemical and cryoelectrochemical uses in THF. The electrode had a structure Pt|4 mM Fc + 4 mM $FcPF_6$ + 0.1 M Bu_4NPF_6 with a salt bridge of 0.1 M Bu_4NPF_6 and was used under an inert atmosphere. It was found that the chemical reactivity of Fc^+, which was observed in the supporting electrolyte of Bu_4NClO_4, was suppressed in the supporting electrolyte of Bu_4NPF_6 by ion-pairing between Fc^+ and PF_6^-. But, because the suppression was not complete, the reference electrode had to be freshly prepared on a daily basis.

The Fc^+/Fc couple has been recommended by Gritzner and Kuta as a reference redox system for potentials in nonaqueous solutions (see Chap. 2 or [190]). Because the reference electrode of the couple can be used only under limited conditions, the potential of the couple should be measured, in general, as a half-wave potential in cyclic voltammetry.

Efforts have been made to prepare oxygen-stable ferrocene-type reference electrodes; the most promising is a decamethylferrocene (DMFc) reference electrode.[11] It had a structure Pt|0.004 M DMFc + 0.004 M $DMFcPF_6$ + 0.1 M Bu_4NBF_4 (AN) and could be used in the presence of oxygen [34]. It was prepared for AN solutions, but similar reference electrodes should be possible for a variety of solvents. Moreover, the $DMFc^+$/DMFc couple can be used as a potential reference redox system and its potential is considered to be more solvent independent than that of the Fc^+/Fc couple [194]. However, the reduction of oxygen by DMFc may occur in acidic DCE [35].

6.1.3.2 Pt/I^-−I_3^- Reference Electrodes

The reaction mechanism of the iodine−iodide (I_2−I^-) couple at a Pt electrode has been studied in various solvents, including aprotic solvents such as Ac [195], AN [195–197], DMF [79, 80, 198], DMSO [199], NM [195, 200, 201], THF [202] and TMS [203]. The oxidation of I^- to I_2 in aprotic solvents usually occurs in two steps, i.e., $3I^- \rightarrow I_3^- + 2e^-$ and $2I_3^- \rightarrow 3I_2 + 2e^-$. From the difference in the standard potentials of the two steps, the formation constant of I_3^- can be determined: the values of formation constant, $\log K = \log\left\{c_{(I_3^-)}/\left(c_{(I_2)}c_{(I^-)}\right)\right\}$, are shown in Table 6.7 [204, 205]. Triiodide ion (I_3^-) in aprotic solvents is very stable and, in the presence of excess I^-, most I_2 forms I_3^-. In aqueous solutions, $\log K = 2.85$, and I_3^- is not stable enough to determine the formation constants by this method.

[11] Peerce and Bard [191] coated a Pt electrode with poly(vinylferrocene) (PVFc) and the electrode was kept at the half-wave potential of the PVFc–$PVFc^+$ couple to make their ratio 1:1. The electrode potential was constant and reproducible in deaerated AN over 21 h, but it was unstable in other nonaqueous solvents, probably because of the gradual dissolution of $PVFc^+$. Efforts to prevent the dissolution of $PVFc^+$ did not much improve the stability of the potential [192]. Bard's group also prepared metal/polypyrrole quasi-reference electrode (QRE) for voltammetry in nonaqueous solutions [193]. It was easily fabricated by cyclic voltammetry of the metal electrode in 10 mM pyrrole + 0.1 M Bu_4NPF_6 (AN or DMC). Its potential was more stable than the Ag- and Pt-wire QREs and even a very small size for use in nanocells was possible.

Table 6.7 Standard potentials of $I_2-I_3^-$ and $I_3^--I^-$ couples and formation constants of I_3^- [204, 205]

	Solvents						
	NM	PC	TMS	DMF	AN	DMSO	MeOH
$E^\circ(I_2-I_3^-)$	+0.365	+0.39	+0.35	+0.245	+0.16	+0.16	+0.24
$E^\circ(I_3^--I^-)$	−0.275	−0.28	−0.31	−0.39	−0.315	−0.32	−0.13
log K	7.4	7.6	7.5	7.2	7.3	5.4	4.2

The potentials are V vs. $Pt/Fc-Fc^+$

Table 6.8 Exchange current densities at the $I_3^--I^-$/Pt electrode in various solvents [36]

Electrode (temperature)	Exchange current (A cm^{-2})
0.05 M I_2 + 0.1 M NaI (PC)|Pt (21.3 °C)	9.0×10^{-5}
0.05 M I_2 + 0.1 M KI (PC)|Pt (22.0 °C)	6.6×10^{-5}
0.05 M I_2 + 0.1 M NaI (AN)|Pt (23 °C)	3.5×10^{-4}
0.015 M I_2 + 0.025 M NaI + 0.4 M $NaClO_4$ (AN)|Pt (24.9 °C)	8.3×10^{-4}
0.018 M I_2 + 0.044 M NaI + 0.4 M $NaClO_4$ (DMSO)|Pt (29.7 °C)	1.59×10^{-3}
0.05 M I_2 + 0.1 M NaI (EtOH)|Pt (21.7 °C)	5.6×10^{-5}
0.05 M I_2 (satd.) + 0.1 M NaI (H_2O)|Pt (22.3 °C)	3.2×10^{-4}

The $I_3^--I^-$ system can be used as a reference electrode. Sutzkover et al. [154] developed a $Pt/I^--I_3^-$ reference electrode for use in PC, the structure being a Pt-black electrode immersed in a solution of 2.93 mM I_3^-, 3.8 mM I^- (use of Bu_4NI), and 0.83 M $LiClO_4$ (PC) (Fig. 6.2b). Coetzee and Gardner [36] proposed a double-junction-type reference electrode based on the $I_3^--I^-$ couple for use in various organic solvents. Its schematic diagram is shown in Fig. 6.2a: a $Pt/I^--I_3^-$ electrode is combined with a salt bridge terminated in a Teflon-roll junction, the solvent in the two compartments being the same as that of the analyte solution. It is easy to construct in many solvents and the potential is stable and reproducible. The exchange current densities for the $I_3^--I^-$ couple have been determined in various solvents and the values are shown in Table 6.8. The values at a Pt electrode were much larger than those at a stainless steel electrode and a glassy carbon electrode. The large exchange current densities at a Pt electrode were considered to be associated with the strong adsorption of monatomic iodine (I_{ads}) on the Pt electrode surface. Due to this large exchange current density, after passing a current density of 15 μA cm^{-2} for several hundred seconds and then stopping the current, the electrode potential returned to within 0.04 mV of its equilibrium value after 60 s, though an Ag^+/Ag electrode required several hours for it. The electrode potential was stable even in the presence of trace amounts of impurities or of halide ions. The intense color of I_3^- ion is a useful indicator of leakage through junctions. In order to improve the usability of this reference system, a new type of electrode, with a structure of Pt|0.05 M I_3^- + 0.05 M I^- + 1 M $LiClO_4$ (AN) (Fig. 6.2c), has been proposed [181]. This reference electrode does not have a salt bridge, but the contaminations of I^- and I_3^- are prevented keeping the solution level of the cell above that of the reference electrode.

6.1.3.3 $Pt/Cu^{+}-Cu^{2+}$ Reference Electrode

The $Cu^{2+}-Cu^{+}$ couple in Py has been used as a reference electrode [164]. A Pt sheet (2 cm^2) was immersed in the solution of 2.5 mM Cu^{+} + 25 mM Cu^{2+} + 0.1 M Et_4NCl and was connected to a salt bridge of 0.1 M Et_4NClO_4 + 6 % methyl cellulose gel. The potential of the $Cu^{2+}-Cu^{+}|Pt$ electrode was −0.047 V vs. Ag| 1.0 M $AgNO_3$ in Py. After polarization for 30 s at 20 μA cm^{-2}, the equilibrium potential was regained in 60 s. The potential of the electrode was reproducible and stable, though a very slow drift to more negative potential occurred after 5 days and, for accurate work, the solution in the reference compartment should be replenished once a week.

6.1.3.4 Solvated-Electron Reference Electrodes

Laitinen and Nyman showed in 1948, in the polarographic study in liquid ammonia (NH_3), that solvated electrons are generated from the surfaces of a dropping mercury electrode and a platinum electrode, if the cation of the supporting electrolyte is not reducible [98]. Besides in NH_3 (bp −33.3 °C), electrolytic generation of solvated electrons occurs in solvents such as HMPA (bp 232 °C), methylamine (bp −6 °C), and ethylenediamine (bp 116 °C). The electrochemistry of solvated electrons has been reviewed [99]. The electrode of solvated electrons has been used as reference electrodes in NH_3 [42] and HMPA [111]. In the case of NH_3, a sheet of Pt was immersed in a solution of sodium metal in liquid NH_3 (−77 °C). Sodium metal (Na) was dissolved in NH_3 forming e^{-}_{solv} and Na^{+}. The concentration of Na in the reference electrolyte was 0.001 M, but it could be varied widely without a change in the potential. In the case of HMPA, the weighed sodium metal was distilled directly into the evacuated cell. The 0.2 M $NaClO_4$−HMPA solution was introduced into the cell through a break-seal to prepare the solution of solvated electrons. All processes were carried out under high vacuum (~10^{-5} mmHg) and below 15 °C. The determination of the concentration of solvated electrons could be done polarographically. For the blue color of solvated electrons to disappear, it took about 4 h at 25 °C but 24 h at 5 °C.

6.2 Reference Electrodes That Use a Solvent Different from That Under Study

With the reference electrodes of this group, there is a liquid junction between different solvents, i.e., between the solvent of the solution under study and that of the solution of the reference electrode. Of course, the reference electrodes themselves should fulfill the requirements that the electrode potentials are stable and reproducible. However, in this case, the LJP between different solvents should also be stable and reproducible. The reference electrodes of this group can be divided into two subgroups: the case using aqueous solutions and the case using nonaqueous solutions.

Hereafter, the two cases are discussed (Sects. 6.2.1 and 6.2.2) and then the problems of the LJP between different solvents are discussed in some detail (Sect. 6.2.3).

6.2.1 *The Case of the Reference Electrodes Using Aqueous Solutions*

Aqueous reference electrodes, such as calomel electrodes (mainly SCE) and Ag/AgCl electrodes, have often been used in almost all nonaqueous solvents. Thus, these electrodes are very important. They are usually used by their tips being dipped into nonaqueous solutions of the salt bridge. In this case, a concentrated aqueous KCl is in contact with a nonaqueous solution. By direct contact of concentrated aqueous KCl and a nonaqueous solution, KCl will gradually be solidified on nonaqueous side and, if ClO_4^- exists in nonaqueous side, $KClO_4$ will gradually be solidified in aqueous side, both causing clogging at the diaphragm (sintered-glass disk or ceramic plug) separating the two solutions. In some case, the tip of the reference electrode is first dipped into an aqueous salt bridge of less concentrated salt other than KCl (e.g., $NaClO_4$ and KNO_3). Anyway, the tip of the aqueous reference electrode or the aqueous salt bridge should not be dipped directly into the nonaqueous *test* solution, because the test solution will be contaminated with water and the electrolyte.

When we use aqueous reference electrodes, we must take the LJP between aqueous and nonaqueous solutions into account. Because the problem of the LJP is discussed in detail in Sect. 6.2.3, only the junctions between aqueous KCl (saturated or concentrated) and nonaqueous solutions of moderate electrolyte concentrations (0.1 M or less) are considered here. Moreover, the tip of the aqueous reference electrode, which is inserted into nonaqueous solutions, is assumed, as generally the case, to be restrained by a diaphragm. If the compositions of the solutions at the junction are carefully reproduced, the LJP can usually be reproducible within ± 10 mV for a few tens minutes after formation of the junction. This may be the reason why aqueous reference electrodes are often used for nonaqueous systems. However, after that time, the composition of the electrolytes and solvents in the diaphragm varies in complicated ways. Thus, the LJP can shift by a few tens millivolts or more. If the tip of aqueous KCl is first inserted into the aqueous $NaClO_4$ or KNO_3 salt bridge and, then, the tip of the salt bridge is inserted into nonaqueous solutions, the value of the LJP will vary quite drastically (by more than 50 mV) from the case of direct contact of aqueous KCl and nonaqueous solutions. For these reasons, the use of aqueous reference electrodes should be avoided, if possible. If aqueous reference electrodes should be used, the composition of the junction, especially the solutions on the two sides of the diaphragm, should be described in detail in reporting the potentials. Moreover, it is highly recommended to measure, at the same time, the half-wave potential of the reference potential system (Fc^+/Fc or BCr^+/BCr Chap. 2 or [190]) in the nonaqueous test solution against the aqueous reference electrode.

The LJPs at the junction of satd. KCl(H_2O)¦0.1 M Et_4NPic(S) have been estimated by Diggle and Parker [206] under the assumption of reference electrolyte of tetraphenylarsonium tetraphenylborate (Ph_4AsBPh_4) (see Sect. 6.2.3): the values of the LJP were 172 mV for H_2O/DMSO, 174 mV for H_2O/DMF, 93 mV for H_2O/AN, 135 mV

for H_2O/PC, 152 mV for H_2O/HMPA, 59 mV for H_2O/NM, 30 mV for H_2O/EtOH, and 25 mV for H_2O/MeOH (with H_2O side more negative).

Pavlishchuk and Addison [207] studied the mutual potentials between various Ag^+/Ag electrodes in AN and the Fc^+/Fc couple in AN and also between these electrodes and various types of aqueous reference electrodes (standard hydrogen electrode, SCE, etc.). In the report, they showed that the literature data on the half-wave potential of Fc^+/Fc couple in AN versus aqueous reference electrodes were scattered from one report to another. For example, the data versus aqueous SCE were scattered between 315 and 480 mV. Because most of the literature did not give detailed compositions of the junction, the reasons for the scattering are not known. But the variation in the composition of the liquid junction between H_2O and AN solutions and thus the variation in the LJP there seem to be one reason for that.

6.2.2 *The Case of the Reference Electrodes Using Nonaqueous Solutions*

The Ag/Ag^+ electrode in AN has often been used as a reference electrode for other aprotic solvents. As described in Table 6.1, Ag/Ag^+ electrode in AN was used for anisole [43], benzene and chlorobenzene [44, 45], BzN [50], DCM [58], DMA [69], and MA [130]. Though not included in Table 6.1, Lewandowski et al. [15] used Ag| 0.01 M Ag^+ + 0.05 M Et_4NClO_4 (AN) for solvents such as Ac, PrN, BuN, BzN, DMA, DMF, DMSO, PC, TMS, NB, and DMTF. The Ag/AgCl electrode in AN (Ag|AgCl(s)| AgCl(satd.) + 0.1 M Bu_4NCl (AN)) has been used by Tsierkezos [20] for Ac, DMA, DMF, DMSO, NMF, DCM, and 3-pentanone by inserting it into a salt bridge of 0.1 M Bu_4NPF_6 in respective solvents. The use of the electrodes in AN as the reference electrodes for other aprotic solvents has the advantage that the LJPs between AN and other aprotic solvents are relatively small, as discussed in Sect. 6.2.3.

As other examples, Ag/AgCl and $Hg/Hg_2(OAc)_2$ electrodes in HOAc have been used for $(Ac)_2O$ [12, 13]. Moreover, the calomel electrode (mainly SCE) has been used for some nonaqueous solvents by replacing the aqueous KCl solution to the methanolic KCl solution (e.g., [81]).

6.2.3 *Information on the LJP Between Solutions in Different Solvents*[12]

When a reference electrode that uses a solvent other than that under study is employed, an LJP exists at the junction between the solution under study (solvent S) and the solution of the reference electrode (solvent R). The problem of the LJP between

[12] The LJP between two solutions in the same (aqueous or nonaqueous) solvent has been discussed in Chap. 3 by Tsirlina. However, the LJP between two solutions in *different solvents* is quite different from that.

different solvents is important because it gives a direct influence to the measured potentials. But this problem was often considered to be very complicated and difficult to solve. One method of approach to this problem was to indirectly estimate the LJP by using an extra-thermodynamic assumption. For example, the LJPs between the aqueous saturated KCl solution and nonaqueous solutions have been obtained under various extra-thermodynamic assumptions [206, 208–212]. In the study by Diggle and Parker [205], Ph_4AsBPh_4 was used as a reference electrolyte and it was assumed that $\Delta G^{\ominus}_{t\,(Ph_4As^+,R\to S)} = \Delta G^{\ominus}_{t\left(BPh_4^-,R\to S\right)} = (1/2)\Delta G^{\ominus}_{t\,(Ph_4AsBPh_4,R\to S)}$, where $\Delta G^{\ominus}_{t\,(i,R\to S)}$ is the standard Gibbs energy of transfer of i from solvent R to solvent S. Starting from this assumption, $\Delta G^{\ominus}_{t\,(i,R\to S)}$ values for Ag^+ ion were obtained thermodynamically by measuring the solubilities of $AgBPh_4$ in R and S, and the theoretical difference, ΔE (estimated), in the potentials of the Ag^+/Ag electrode in R and S was calculated. Along with this, the practical difference, ΔE(practical), in the potentials of the Ag^+/Ag electrode in S and R was obtained experimentally. There exists the relation ΔE (practical) = ΔE(estimated) + E_j, where E_j shows the LJP between R and S and, thus, the value of the LJP (E_j) can be obtained from the values of ΔE(estimated) and ΔE(practical). The LJPs at the junction between saturated KCl in water and 0.1 M Et_4NPic in various organic solvents, estimated by Diggle and Parker [206], have been described in Sect. 6.2.1. Here, the reliability of the estimated LJPs depends on the reliability of the extra-thermodynamic assumption.[13] However, this approach cannot clarify the details of the LJP between different solvents. The other approach to this problem was to clarify the details of the LJP, i.e., to clarify the roles of the electrolytes and the solvents in determining the LJP. Several groups [213–217] tried this approach; however, they were not successful enough. We also carried out a series of studies to know the roles of the electrolytes and the solvents [218–234]. The problem of the LJP between different solvents has recently been reviewed, mainly based on our results [235]. The LJPs between different solvents are much larger in magnitudes than those between the same solvent. In order to employ a reference electrode that uses a solvent different from that under study, it seems necessary to have some information about the LJP between different solvents or about how the LJPs are influenced by the solvents and the electrolytes. In the following, this problem is outlined.

The LJP between different solvents contains three components: i.e., (a) a component related to electrolyte concentrations and ionic mobilities, (b) a component related to ion solvation (and ionic mobilities), and (c) a component related to solvent–solvent interactions. Component (a) is somewhat similar to the LJP between solutions in the same solvent, but components (b) and (c) are specific to the LJP between different solvents. Here, a free-diffusion junction with the same electrolyte on the two sides (c_1 MX(S_1)/c_2 MX(S_2)) is considered (see [221] for the case with different electrolytes on the two sides). We found that, under appropriate conditions, we can experimentally measure the variation in each of the three

[13] The reliability of the reference electrolyte (Ph_4AsBPh_4) assumption has been considered to be the best among various extra-thermodynamic assumptions (see page 41 in [177]).

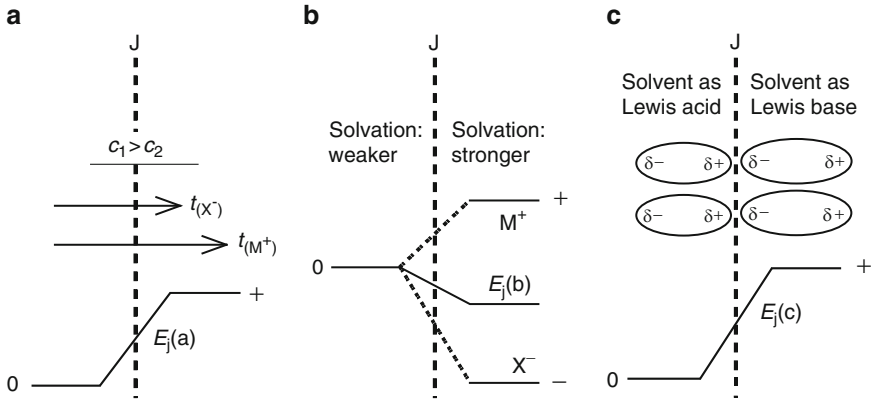

Fig. 6.3 Three components for the LJP between electrolyte solutions in different solvents. Junction: c_1 MX(S_1)|c_2 MX(S_2)

components separately.[14] Thus, we can study the characteristics of each component. The characteristics of the three components are schematically shown in Fig. 6.3.

6.2.3.1 Components (a) and (b)

Components (a) and (b) are diffusion potentials. Component (a) is due to the ionic diffusion by the gradients in ionic concentrations, while component (b) is due to the ionic diffusion by the gradients in ionic standard chemical potentials or solvation energies. The equations for components (a) (Eq. (6.1)) and (b) (Eq. (6.2)) have been obtained for MX of 1:1 electrolyte (see [222] for z_1:z_2 electrolyte)[15]:

[14] (1) The variations in the actual (experimental) values of components (a) and (b) were obtained by measuring the potential differences of Cell (I): Ag|5 mM $AgClO_4$, 20 mM Et_4NClO_4 (S_1)$^{\|}_{\|}$20 mM Et_4NClO_4 (S_1)|c_1 MX (S_1)|c_2 MX (S_2)|20 mM Et_4NClO_4 (S_2)$^{\|}_{\|}$5 mM $AgClO_4$, 20 mM Et_4NClO_4 (S_2)|Ag. In the case of component (a), the values of c_1 and c_2 were varied and necessary corrections were made. In the case of component (b), the electrolyte MX was varied, keeping the values of c_1 and c_2 constant and making appropriate corrections. $E_{corrected}$ in Figs. 6.4, 6.6, and 6.7 shows the corrected potential differences. (2) For the actual (experimental) variations in component (c), Cell (II): Ag|5 mM $AgClO_4$, 25 mM Et_4NClO_4 (S_1=AN)$^{\|}_{\|}c$ Et_4NClO_4 (S_1=AN)|c_3 MX (S_3)|c Et_4NClO_4 (S_2)$^{\|}_{\|}$5 mM $AgClO_4$, 25 mM Et_4NClO_4 (S_2)|Ag, was used and its potential differences were measured by varying solvent S_3 for fixed MX, S_1, and S_2 and making necessary corrections. The values detected in this case (E) were the sum of the variations in component (c) at junctions S_1/S_3 and S_3/S_2.

[15] Equations (6.1) and (6.2) were obtained by integrating the first and second terms on the right hand of Eq. (A), assuming linear variations in $a_{(i)}$, $t_{(i)}$, and $\mu^{\ominus}_{(i)}$ from the values in S_1 to the values in S_2 (Fig. 6.5a).

$$E_j = -(RT/F)\int_{S_1}^{S_2}\sum (t_{(i)}/z_{(i)})\mathrm{d}\ln a_{(i)} - (1/F)\int_{S_1}^{S_2}\sum (t_{(i)}/z_{(i)})\mathrm{d}\mu^{\ominus}_{(i)} + E_{j,solv}. \quad (A)$$

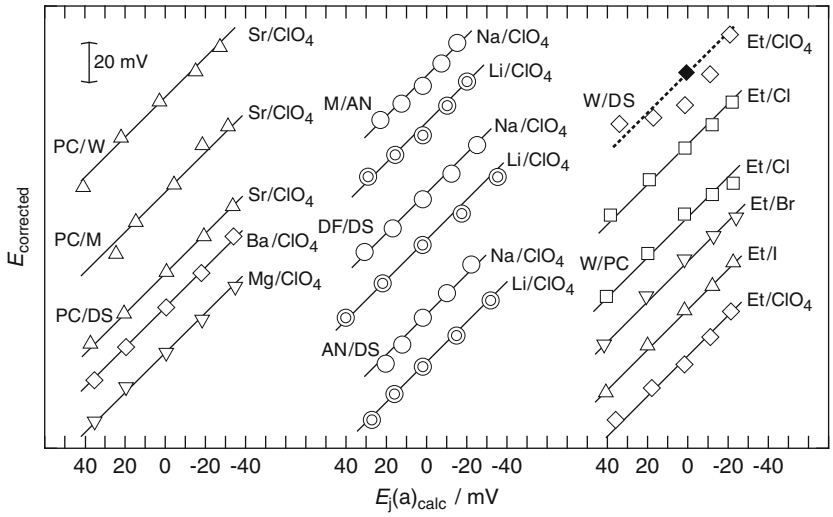

Fig. 6.4 Actual variation in component (a) versus component (a) calculated by Eq. (6.1). Junctions c_1 MX(S_1)|c_2 MX(S_2). S_1/S_2, and M/X are shown on the *lines* and W, M, DS, and Et show H_2O, MeOH, DMSO and Et_4N, respectively; (c_1, c_2)/mM are, from *left* to *right*, (100, 1), (10, 1), (1, 1), (1,10), (1, 100); *filled diamond* (25, 25). *Lines* have unit slopes. The relation for "W/DS, Et/ClO_4" deviates from linearity, but this is due to the influence of the electrolyte concentration on component (c)

$$E_j(a) = \left(-\frac{RT}{F}\right)\left[\left(t_{(M^+)_1} - t_{(X^-)_1}\right)\ln\frac{a_{(MX)_2}}{a_{(MX)_1}} + \left(t_{(M^+)_2} - t_{(M^+)_1} - t_{(X^-)_2} + t_{(X^-)_1}\right) \times\left(1 - \frac{a_{(MX)_1}}{a_{(MX)_2} - a_{(MX)_1}}\ln\frac{a_{(MX)_2}}{a_{(MX)_1}}\right)\right], \tag{6.1}$$

$$E_j(b) = \left(-\frac{1}{2F}\right)\left[(t_{(M^+)_1} + t_{(M^+)_2})\Delta G^{\ominus}_{t(M^+,S_1\to S_2)} - (t_{(X^-)_1} + t_{(X^-)_2})\Delta G^{\ominus}_{t(X^-,S_1\to S_2)}\right]. \tag{6.2}$$

In Eq. (6.1), t is the ionic transport number, a is the electrolyte activity, and the subscripts 1 and 2 refer to the left and right sides of the junction. $E_j(a) = 0$ for $a_{(MX)_1} = a_{(MX)_2}$. In Eq. (6.2), $\Delta G^{\ominus}_{t(i,S_1\to S_2)}$ is the standard Gibbs energy of transfer of i from solvent S_1 to S_2, and is equal to the difference in the standard chemical potential of i, $\mu^{\ominus}_{(i)}$, in S_1 and S_2.

Linear relations of unit slopes are generally observed between the actual (experimental) variations in component (a) and the values obtained by Eq. (6.1) (Fig. 6.4). Thus, Eq. (6.1) is applicable to estimate the values of component (a). The magnitudes

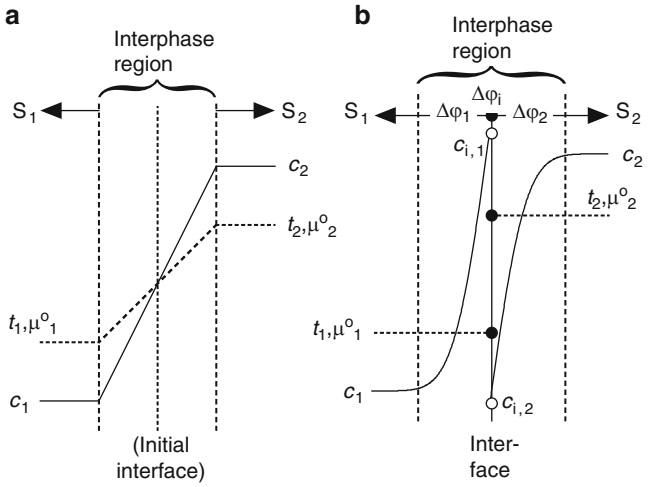

Fig. 6.5 (**a**) Linear variations of c, t, and μ^e (μ° is used instead) at the interphase region of the miscible junction, assumed in deriving Eqs. (6.1) and (6.2), and (**b**) those at the immiscible junction. $\Delta\varphi_i$ is the distribution potential, while $\Delta\varphi_1$ and $\Delta\varphi_2$ are the LJPs in S_1 and S_2, respectively

are of the order of $\pm$40 mV for the variation in electrolyte concentrations (c_1/c_2, mM) from 100/1 to 1/100.

We can predict the characteristics of component (b) by Eq. (6.2): (1) cation M^+ makes the side on which the solvation is stronger more positive (in potential), while anion X^- makes the side on which the solvation is stronger more negative (see Fig. 6.3, component (b)); (2) this component is not influenced by electrolyte concentrations. The independence of component (b) from electrolyte concentrations can easily be confirmed. However, the relations of the experimental (actual) variations in component (b) against the values calculated by Eq. (6.2) are somewhat complicated. For the junctions between water and organic solvents (H_2O/S), near-linear relations are observed, but the slopes are much smaller than unity, i.e., the average is 0.46 $\pm$ 0.029 for five S (i.e., AN, DMF, DMSO, and MeOH) (Fig. 6.6).[16] At the junctions between two aprotic solvents, on the other hand, the slopes are much smaller and, although some contributions of anions and tetraalkylammonium ions are observed, the contributions of alkali metal and silver ions are practically equal to zero

[16] At immiscible junctions H_2O/NB and H_2O/DCE, the slopes of the near-linear relations between experimental (actual) variations in component (b) and the values calculated by Eq. (6.2) are 1.0. Generally, the slopes approach 1.0 with the decrease in miscibility of the solvents on two sides [223]. Actually, at immiscible junctions, ions are distributed at the abrupt interface (thickness ~1 nm), as in Fig. 6.5b, and the distribution potential, $\Delta\varphi_i$, is generated. Moreover, on both sides of the interface, the LJPs between the same solvent, $\Delta\varphi_1$ and $\Delta\varphi_2$, are generated [223]. The potential difference at the immiscible junction is, therefore, the sum of $\Delta\varphi_i$, $\Delta\varphi_1$, and $\Delta\varphi_2$. Here, for immiscible c MX(H_2O)|c MX(NB), this potential difference was confirmed to agree fairly well with the results calculated by Eq. (6.2). It is interesting that Eq. (6.2) is nearly applicable even to immiscible junctions.

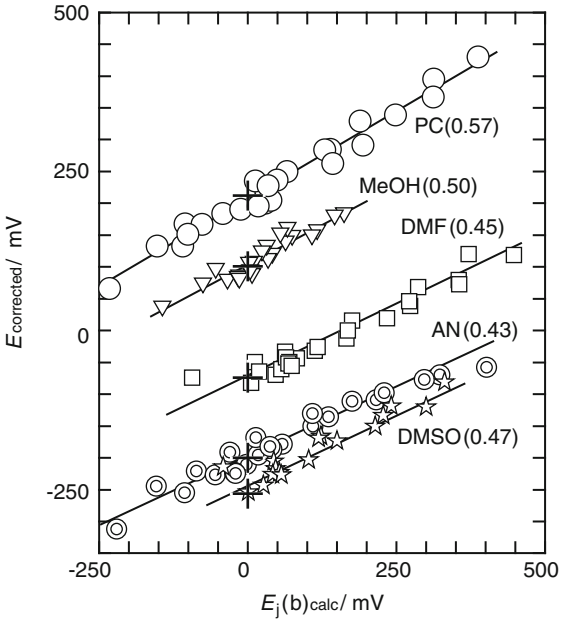

Fig. 6.6 Component (b) of the LJP between different solvents: experimental results versus the values calculated by Eq. (6.2). The case of the junction between water and organic solvents, 10 mM MX $(H_2O)|$10 mM MX(S). Solvent S and the slopes are shown on each *line*. The electrolyte MX are shown by the number as follows: 1 Bu_4NCl, 2 Bu_4NBr, 3 Bu_4NI, 4 Bu_4NClO_4, 7 Pr_4NClO_4, 8 Me_4NClO_4, 9 Et_4NCl, 10 Et_4NBr, 11 Et_4NI, 12 Et_4NClO_4, 13 Et_4NPic, 14 LiCl, 15 LiBr, 16 LiI, 17 $LiClO_4$, 18 LiPic, 19 NaBr, 20 NaI, 21 $NaClO_4$, 22 NaPic, 23 $NaBPh_4$, 24 $KClO_4$, 25 $RbClO_4$, 26 $CsClO_4$. MX (from *right* to *left*): S = PC (1, 2, 9, 14, 3, 19, 11, 15, 4, 7, 13, 20, 12, 26, 16, 8, 25, 24, 21, 17, 22, 18, 23); MeOH (1, 2, 3, 4, 9, 14, 10, 15, 11, 12, 16, 17, 20, 21, 24, 26, 25, 13, 18, 22, 23); DMF (1, 14, 9, 2, 15, 10, 19, 3, 16, 20, 11, 4, 7, 26, 24, 25, 21, 17, 12, 8, 22, 18, 13, 23); AN (1, 2, 9, 10, 3, 14, 11, 4, 15, 7, 12, 20, 13, 16, 8, 26, 25, 24, 21, 17, 22, 18, 23); DMSO (14, 9, 15, 19, 10, 16, 20, 11, 26, 24, 21, 17, 25, 12, 8). *Plus marks* show the estimated $E_{corrected}$ in the absence of component (b)

(Fig. 6.7). The average slopes for the junctions of EG/S, FA/S, and MeOH/S are between these two extremes and 0.33, 0.32, and 0.26, respectively. The exact reason for the slopes of much less than unity or near to zero has not been elucidated yet; some discussions are described in the footnote.[17]

[17] At miscible junctions, solvents on both sides mutually diffuse and the thickness of the diffusion layer expands with time (0.05–5 mm). Ions also diffuse between the two solvents; here, the ionic diffusion due to the gradients in ionic $\mu^{e}_{(i)}$ value will cause a kind of ionic distribution at or near the layers of solvent diffusion. However, the fact that the experimental variations in component (b) are much less than the values calculated by Eq. (6.2) seems to show that the actual ionic distribution is much less in extent than the ionic distribution expected from the theoretically variation in $\mu^{e}_{(i)}$ value. The cause for it must be elucidated, but ionic random walks which result in ionic diffusion seem to play some role [223]. Because the time and the distance of an average step of the random walk are very short, the solvation/desolvation processes cannot catch up with the theoretical $\mu^{e}_{(i)}$ value, making component (b) smaller.

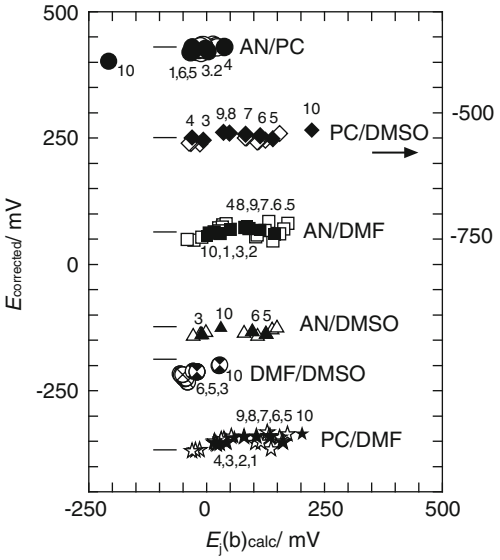

Fig. 6.7 Component (b) of the LJP between different solvents: experimental results versus the values calculated by Eq. (6.2). The case of the junction between two aprotic solvents. *Solid marks* are for MX of perchlorates. "M" is Bu_4N for *1*, Pr_4N for *2*, Et_4N for *3*, Me_4N for *4*, Li for *5*, Na for *6*, K for *7*, Rb for *8*, Cs for *9*, and Ag for *10*. *Minus marks* show the values of $E_{corrected}$ estimated in the absence of component (b)

Although the slopes are less than unity, component (b) is nearly proportional to the calculated E_j(b); thus, we can estimate the actual values of component (b) by multiplying the calculated E_j(b) and the slope. For the junctions H_2O/S, the actual values of component (b) vary considerably with the electrolyte species: for example, the largest variations for H_2O/PC and H_2O/AN are ca. 350 mV and ca. 250 mV, respectively, between MX of $NaPh_4B$ and Bu_4NCl. These values are much larger than the magnitudes of components (a) and (c).

6.2.3.2 Component (c)

Component (c), which is due to the solvent–solvent interactions at the junction, is nearly independent of electrolyte species and concentrations (Fig. 6.8, for example). Its characteristics can be understood if we consider that the two solvents at the junction interact with each other as a Lewis acid and a Lewis base and some of the solvent molecules are oriented perpendicularly to the interphase (see component (c) in Fig. 6.3); the solvent side as a Lewis acid is more negative than that as a Lewis base and the value increases with the increase in the strength of the solvent interaction. The authors of [213–217] considered that component (c) is a diffusion potential, which is due to the transfer of solvent molecules across the junction that occurs being associated with ion transfer. But our result shows that it is not a diffusion potential but a dipole potential; it is due to the orientation of solvent molecules due to the solvent–solvent interactions. The reason for the conflict of opinions is described in [235]. We have no theoretical way to estimate the value of this component, but from the experimental results and under some assumptions, a

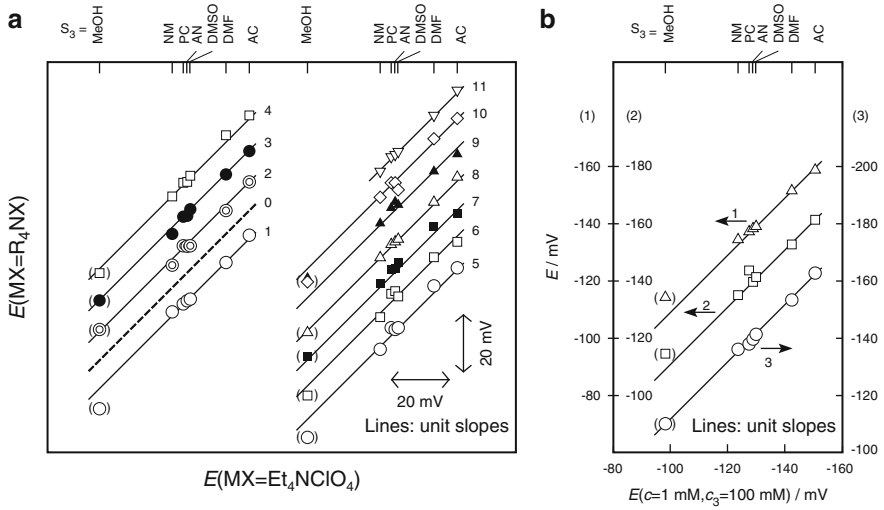

Fig. 6.8 Potential differences of Cell (II) in the footnote 14 in which S_1 = AN and S_2 = DMSO (the data for S_3 = MeOH are only for reference). (**a**) Influence of electrolyte species. The abscissa is for MX = Et_4NClO_4. MX for ordinate: *0*, Et_4NClO_4; *1*, Me_4NClO_4; *2*, Pr_4NClO_4; *3*, Bu_4NClO_4; *4*, Hex_4NClO_4; *5*, Et_4NCl; *6*, Et_4NBr; *7*, Et_4NI; *8*, Et_4NNO_3; *9*, Et_4NPic; *10*, Et_4NBF_4; *11*, Bu_4NBPh_4. In all cases, c = 1 mM and c_3 = 100 mM. (**b**) Influence of electrolyte concentrations. MX = Et_4NClO_4. The abscissa is for c = 1 mM and c_3 = 100 mM and the ordinate (*1*) c = 100 mM, c_3 = 1 mM; (*2*) $c = c_3$ = 50 mM; (*3*) $c = c_3$ = 10 mM

rough estimation is possible. Component (c) between strongly interacting solvents, like H_2O/DMF or H_2O/DMSO, is expected to be a little over 100 mV with the H_2O side more negative.[18] However, at a junction between two aprotic solvents, it is usually within ±20 mV, because these solvents interact only weakly. The dipole-potential mechanism can also explain the important characteristics of component (c) that, at a junction with a mixed solvent on one side or mixed solvents on the two sides, component (c) often changes linearly with the volume fraction of the mixed solvent(s).

The above is the summary of the characteristics of the three components. The value of the total LJP can be obtained by summing up the values of the three components [233]. Table 6.9 shows some examples of the LJP estimated by the three-component method and they are compared with the values estimated by the

[18] The values of component (c) at H_2O/S can be estimated by assuming that the values of component (c) at H_2O/NB and at AN/other aprotic solvent(s) are negligible. At the electrolyte concentration of 1 mM, the values estimated by this method are 122 mV for H_2O/DMF and H_2O/DMSO, 44 mV for H_2O/AN, and 30 mV for H_2O/PC, though the values somewhat decrease with the increase in electrolyte concentrations [235].

Table 6.9 LJPs between different solvents estimated by the three-component method and by the conventional method (mV)[a]

		Three-component method				Traditional method	Difference
S=	MX=	(a)	(b)	(c)	$E_j(1)$	$E_j(2)$	$E_j(1)$–$E_j(2)$
AN	Et_4NPic	0	8	37	45	39	+6
	Et_4NClO_4	−2	18	37	53	55	−2
	Et_4NI	−2	60	38	96	105	−9
	Et_4NCl	−2	131	39	168	169	−1
DMF	Et_4NPic	0	2	107	109	111	−2
	Et_4NClO_4	−2	30	107	135	131	+4
	Et_4NI	−2	73	110	181	177	+4
	Et_4NCl	−2	157	116	271	252	+19
MeOH	Et_4NPic	1	−18	30	13	6	7
	Et_4NClO_4	−2	18	30	46	40	6
	Et_4NI	−2	22	30	50	49	1
	Et_4NCl	−1	40	30	69	81	−12

$E_j(1)$ = (a) + (b) + (c) and is the result by the three-component method
$E_j(2)$ is the result obtained by the traditional indirect method based on the reference electrolyte (Ph_4AsBPh_4) assumption
From [233], but corrections were made for the values of component (c)
[a]Liquid junction of the type 25 mM $MX(H_2O)$¦25 mM MX(S)

traditional indirect method based on the reference electrolyte (Ph_4AsBPh_4) assumption. The results obtained by the two methods agree fairly well. Good agreements between these two methods were observed also for other liquid junctions. Thus, probably, we may consider that the two methods of estimation are fairly reliable.

At a free-diffusion junction, the LJP reaches a steady value within a few seconds after its formation, is reproducible within ±1 mV, and is very stable, although the thickness of the junction expands with time by the mutual diffusions of both the solvents and the electrolytes, as far as the electrolytes on the two sides are the same; the drift is within ±1 mV h^{-1} even when the LJP is near to 200 mV [218]. Even when the electrolytes on the two sides are of different kinds, if the concentration on one side is more than 20 times that on the other and if the junction is a free-diffusion type, the LJP is almost decided by the more concentrated electrolyte and it is stable with time [218, 219]. This justifies, to some extent, the use of aqueous reference electrodes for the measurements in nonaqueous solutions. In reality, however, the junctions between different solvents are usually not free-diffusion type but restrained with a diaphragm. The situation is thus complicated: the composition of solvents and electrolytes in the diaphragm is indefinite and sometimes a clog of electrolyte is formed, making the LJP less reproducible and less stable. This applies to the case when an aqueous reference electrode is inserted into a nonaqueous solution.

Parker et al. [236] employed, in studying ion solvation, the assumption of negligible LJP, considering that the LJP across the following cell is within ±20 mV:

$$\mathrm{Ag|10\ mM\ AgNO_3\ (AN)||100\ mM\ Et_4NPic\ (AN)||10\ mM\ AgNO_3\ (S)|Ag}$$

The assumption is based on that (1) the mobilities of Et_4N^+ and Pic^- are close to each other, (2) $\Delta G^{e}_{t(i,\ AN\rightarrow S)}$ (i: ionic species) values of these ions are small, and (3) AN interacts only weakly with other aprotic solvents. Our results also support this assumption if S is aprotic. As described in Sect. 6.2.2, the Ag/Ag^+ reference electrode in AN is sometimes used for other aprotic solvents (S). In case if the electrolyte on the two sides is Et_4NPic, all three components of the LJP between AN and S are usually small and the total LJP will be also small. When the electrolyte is Et_4NClO_4, the same is expected to be true, if the concentrations of Et_4NClO_4 in AN and S are kept equal in order to keep component (a) small.

6.3 Conclusion

Various reference electrodes hitherto reported for nonaqueous solutions have been reviewed. Some are often used, but some others are rarely used. Some are easy to construct and easy to use. Some are not easy to construct but easy to use and give excellent reproducibility and stability of potentials. Some must be used in a glove box and it is troublesome. Some use metals and their salts that are now considered to be harmful. An appropriate reference electrode should be selected considering these points. Unless special requirements exist, the use of silver reference electrodes (Ag/Ag^+, Ag/AgCryp$^+$, and Ag/AgCl electrodes) and a $Pt|I^- - I_3^-$ reference electrode may be preferable, though especially in the case of Ag/Ag^+ electrode, the Ag^+ solution is desirable to be renewed every time before use. To use the Li/Li^+ reference electrode may be appropriate in the study of lithium battery technology, because argon atmosphere in a glove box is absolutely necessary for this study. When aqueous reference electrodes are used, fairly large LJP between aqueous and nonaqueous solutions is a problem and it must be kept reproducible and stable or their use should be avoided. The use of Ag/Ag^+ reference electrode in AN for studying in other aprotic solvents may be a good idea because the LJPs between AN and other aprotic solvents are fairly smaller. Anyway, it is recommended to measure the half-wave potential of the reference redox system (Fc^+/Fc or BCr^+/BCr) against the potential of the selected reference electrode as often as possible, so that the potential measured against the selected reference electrode can be converted to the potential against these reference systems (see Chap. 2 of this book).

References

1. Lund H (2001) Practical problems in electrolysis. In: Lund H, Hammerich O (eds) Organic electrochemistry, 4th edn. Marcel Dekker, New York, p 246
2. Mann CK (1969) Nonaqueous solvents for electroanalytical use. In: Bard AJ (ed) Electroanalytical chemistry, vol 3. Marcel Dekker, New York, p 57
3. Butler JN (1970) Reference electrodes in aprotic organic solvents. In: Delahay P, Tobias CW (eds) Advances in electrochemistry and electrochemical engineering, vol 7. Interscience, New York, p 77
4. Hills GJ (1961) Reference electrodes in nonaqueous solutions. In: Ives DJG, Janz GJ (eds) Reference electrodes, theory and practice. Academic, New York, p 433
5. Glenn RA (1953) Anal Chem 25:1916
6. Číhalík J, Šimek J (1958) Collect Czech Chem Commun 23:615
7. Bruckenstein S, Kolthoff IM (1956) J Am Chem Soc 78:2974
8. Larson WD, MacDougall FH (1937) J Phys Chem 41:493
9. Al-Qaraghuli N, Stone KG (1959) Anal Chem 31:1448
10. Mather WB, Anson FC (1959) Anal Chim Acta 21:468
11. Maccà C, Soldà L (2002) Ann Chim 92:249
12. Mather WB, Anson FC (1961) Anal Chem 33:1634
13. Piccardi G, Guidelli R (1971) Anal Chem 43:1646
14. Gritzner G (1990) Pure Appl Chem 62:1839
15. Lewandowski A, Szukalska A, Galinski M (1995) New J Chem 19:1259
16. Everett DH, Rasmussen SE (1954) J Chem Soc 1954:2812
17. Bond AM, Hendrickson AR, Martin RL (1973) J Am Chem Soc 95:1449
18. Bond AM, Grabaric BS, Jackowski JJ (1978) Inorg Chem 17:2153
19. Arthur P, Lyons H (1952) Anal Chem 24:1422
20. Tsierkezos NG (2007) J Solut Chem 36:289 (This electrode has been used in such solvents as Ac, AN, DCM, DMA, DMF, DMSO, NMF, and 3-pentanone)
21. Mackor EL (1951) Rec Trav Chim 70:457
22. Pleskov VA (1948) Zh Fiz Khim 22:351
23. Larson RC, Iwamoto RT, Adams RN (1961) Anal Chim Acta 25:371
24. Coetzee JF, Padmanabhan GR (1962) J Phys Chem 66:1708
25. Alexander R, Ko ECF, Mac YC, Parker AJ (1967) J Am Chem Soc 89:3703
26. Kratochvil B, Lorah E, Garber C (1969) Anal Chem 41:1793
27. Billon JP (1959/60) J Electroanal Chem 1:486
28. Lund H (1957) Acta Chem Scand 11:491
29. Izutsu K, Ito M, Sarai E (1985) Anal Sci 1:341
30. Popov AI, Geske DH (1957) J Am Chem Soc 79:2074
31. Hanselman RB, Streuli CA (1956) Anal Chem 28:916
32. Barthel J, Neueder R, Schröder A (1997) Can J Chem 75:1500
33. Kolthoff IM, Thomas FG (1965) J Phys Chem 69:3049
34. Bashkin JK, Kinlen PJ (1990) Inorg Chem 29:4507
35. Su B, Hatay I, Ge PY, Mendez M, Corminboeuf C, Samec Z, Ersoz M, Girault HH (2010) Chem Commun 46:2918
36. Coetzee JF, Gardner CW Jr (1982) Anal Chem 54: 2530, 2625
37. Mihajlović R, Simić Z, Mihajlović L, Jokić A, Vukašinović M, Rakićević N (1996) Anal Chim Acta 318:287
38. Lee HL, Fujinaga T (1979) Bull Inst Chem Res Kyoto Univ 57:285
39. Navaneethakrishnan R, Warf JC (1974) J Inorg Nucl Chem 36:1311
40. Tiedemann WH, Bennion DN (1970) J Electrochem Soc 117:203
41. Sedlet J, De Vries T (1951) J Am Chem Soc 73:5808
42. Hammer RN, Lagowski JJ (1962) Anal Chem 34:597
43. Jaworski JS, Cembor M, Orlik M (2005) J Electroanal Chem 582:165

44. Lines R, Parker VD (1977) Acta Chem Scand B 31:369
45. Howell JO, Wightman RM (1984) J Phys Chem 88:3915
46. Bond AM, Mann TF (1987) Electrochim Acta 32:863
47. Kim K, Kim I, Maiti N, Kwon SJ, Bucella D, Egorova OA, Lee YS, Kwak J, Churchill DG (2009) Polyhedron 28:2418
48. Abou-Elenien GM, Ismail NA, Hassanin MM, Fahmy AA (1992) Can J Chem 70:2704
49. Abou-Elenien GM, Ismail NA, Magd Eldin AA (1992) Monatsh Chem 123:1117
50. Fawcett WR, Opallo M, Fedurco M, Lee JW (1993) J Am Chem Soc 115:196
51. Dey AN (1968) J Electrochem Soc 115:160
52. Izutsu K, Ohmaki M (1996) Talanta 43:643
53. Aurbach D (1989) J Electrochem Soc 136:906
54. Coetzee JF, Chang TH, Deshmukh BK, Fonong T (1993) Electroanalysis 5:765
55. Bond AM, Mann TF, Tondreau GA, Sweigart DA (1990) Inorg Chim Acta 169:181
56. Beal JL, Mann CA (1937) J Phys Chem 42:283
57. Bos M, Dahmen EAMF (1973) Anal Chim Acta 63:185
58. Yaman ŞÖ, Esentürk E, Kayran C, Önal AM (2002) Z Naturforsch 57b:92
59. Bond AM, Oldham KB, Snook GA (2000) Anal Chem 72:3492
60. Pournaghi-Azar MH, Dastangoo H (2000) Microchem J 64:187
61. Pournaghi-Azar MH, Dastangoo H (2000) Anal Chim Acta 405:135
62. Röhrscheid F, Balch AL, Holm RH (1966) Inorg Chem 5:1542
63. Ito N, Aoyagui S, Saji T (1981) J Electroanal Chem 130:357
64. Hoffman AK, Hodgson WG, Maricle DL, Jura WH (1964) J Am Chem Soc 86:631
65. Aurbach D, Daroux M, Faguy P, Yeager E (1991) J Electroanal Chem 297:225
66. Scrosati B, Pecci G, Pistoia G (1968) J Electrochem Soc 115:506
67. Bréant M, Georges J, Imbert J-L, Schmitt D (1971) Ann Chim 6:245
68. Paris J, Plichon V (1981) Electrochim Acta 26:1823
69. Nakamura T, Ren J, Hinoue T, Umemoto K (2003) Anal Sci 19:991
70. Reiter J, Vondrák J, Mička Z (2007) Solid State Ionics 177:3501
71. Rieger PH, Bernal I, Reinmuth WH, Fraenkel GK (1963) J Am Chem Soc 85:683
72. Aylward GH, Garnett JL, Sharp JH (1967) Anal Chem 39:457
73. Butler JN (1968) J Phys Chem 72:3288
74. Headridge JB, Ashraf M, Dodds HLH (1968) J Electroanal Chem 16:114
75. McMasters DL, Dunlap RB, Kuempel JR, Kreider LW, Shearer TR (1967) Anal Chem 39:103
76. Dueber RE, Dickens PG (1991) J Electrochem Soc 138:L79
77. Marple LW (1967) Anal Chem 39:844
78. Synnott JC, Butler JN (1969) Anal Chem 41:1890
79. Barbasheva IE, Povarov YM, Lukovtsev PD (1967) Sov Electrochem 3:1027 (Elektrokhimiya 3:1149)
80. Povarov YM, Barbasheva IE, Lukovtsev PD (1967) Sov Electrochem 3:1071 (Elektrokhimiya 3:1202)
81. Juillard J (1966) J Chim Phys 63:1190
82. Ritchie CD, Uschold RE (1967) J Am Chem Soc 89:1721
83. Kolthoff IM, Chantooni MK Jr, Bhowmik S (1968) J Am Chem Soc 90:23
84. Johnson EL, Pool KH, Hamm RE (1966) Anal Chem 38:183
85. Kolthoff IM, Reddy TB (1962) Inorg Chem 1:189
86. Simonova OR, Sheinin VB, Berezin BD (2007) J Anal Chem 62:680
87. Giordano MC, Bazán JC, Arvia AJ (1966) Electrochim Acta 11:741
88. Courtot-Coupez J, LeDemezet M (1966) CR Acad Sci Paris 263:997
89. Courtot-Coupez J, LeDémézet M (1967) Bull Soc Chim Fr 1967:4744
90. Rumbaut NA, Peeters HL (1967) Bull Soc Chim Belg 76:33
91. Cogley DR, Butler JN (1966) J Electrochem Soc 113:1074
92. Ahrland S, Persson I (1980) Acta Chem Scand A 34:645

93. Smyrl WH, Tobias CW (1966) J Electrochem Soc 113:754
94. Zara AJ, Bulhões LOS (1982) Anal Lett 15:775
95. MacFarlane A, Hartley H (1932) Philos Mag 13:425
96. Goodhue LD, Hixon RM (1935) J Am Chem Soc 57:1688
97. Aurbach D, Gofer Y, Ben-Zion M, Aped P (1992) J Electroanal Chem 339:451
98. Laitinen HA, Nyman CJ (1948) J Am Chem Soc 70:3002
99. Alpatova NM, Krishtalik LI, Pleskov YV (1987) Top Curr Chem 138:149
100. Harima Y (1988) J Electroanal Chem 252:53
101. Bruckenstein S, Mukherjee LM (1960) J Phys Chem 64:1601
102. Schaap WB, Bayer RE, Siefker JR, Kim JY, Brewster PW, Schmidt FC (1961) Rec Chem Prog 22:197
103. Mandel M, Decroly P (1958) Nature 182:794
104. Mukherjee LM (1957) J Am Chem Soc 79:4040
105. Pinfold TA, Sebba F (1956) J Am Chem Soc 78:2095
106. Arnac M, Verboom G (1973) Anal Chem 45:1954
107. Geng L, Ewing AG, Jernigan JC, Murray RW (1986) Anal Chem 58:852
108. Dubois JÉ, Lacaze PC, Ficquelmont AM (1966) CR Acad Sci Paris 262:181
109. Gal JY, Yvernault T (1971) Bull Soc Chim Fr 1971:2770
110. Izutsu K, Sakura S, Fujinaga T (1972) Bull Chem Soc Jpn 45:445
111. Kanzaki Y, Aoyagui S (1972) J Electroanal Chem 36:297
112. Burrows B, Jasinski R (1968) J Electrochem Soc 115:348 (detailed study on Cu/CuF_2 electrode)
113. Clifford AF, Zamora E (1961) Trans Faraday Soc 57:1963
114. Clifford AF, Pardieck WD, Wadley MW (1966) J Phys Chem 70:3241
115. Macleod ID, Bond AM, O'Donnell TA (1973) J Electroanal Chem 45:89
116. Vinnikov YY, Shavkunov SP, Bil'dinov KN (1976) Sov Electrochem 12:1022 (Elektrokhimiya 12:1113)
117. Koerber GG, DeVries T (1952) J Am Chem Soc 74:5008
118. Hackerman N, Snavely ES Jr, Fiel LD (1967) Electrochim Acta 12:535
119. Kaurova GI, Grubina LM, Adzhemyan TA (1966) Sov Electrochem 3:1092 (Elektrokhimia 3:1222)
120. Doughty AG, Fleischmann M, Pletcher D (1974) J Electroanal Chem 51:329
121. Wang CM, Mir Q-C, Maleknia S, Mallouk TE (1988) J Am Chem Soc 110:3710
122. Coetzee JF, Hedrick JL (1963) J Phys Chem 67:221
123. Pemberton JE, Shen A (1999) Phys Chem Chem Phys 1:5671
124. Brossia CS, Kelly RG (1996) Electrochim Acta 41:2579
125. Johari GP, Tewari PH (1966) J Phys Chem 70:197
126. Knecht LA, Kolthoff IM (1962) Inorg Chem 1:195
127. Irish DE, Deng Z, Odziemkowski M (1995) J Power Sources 54:28
128. Rauh RD, Brummer SB (1977) Electrochim Acta 22:85
129. Plichta E, Salomon M, Slane S, Uchiyama M, Chua D, Ebner WB, Lin HW (1987) J Power Sources 21:25
130. Fung YS, Lai HC (1989) J Appl Electrochem 19:239
131. Harima Y, Kurihara H, Aoyagui S (1981) J Electroanal Chem 124:103
132. Gritzner G (1983) J Electroanal Chem 144:259
133. Luksha E, Criss CM (1966) J Phys Chem 70:1496
134. Salomon M (1974) J Phys Chem 78:1817
135. Juillard J, Kolthoff IM (1971) J Phys Chem 75:2496
136. Izutsu K, Yamamoto H (1996) Anal Sci 12:905
137. Payne R (1969) J Phys Chem 73:3598
138. Mayrhofer W, Lasia A, Gritzner G (1991) J Electroanal Chem 317:219
139. Bréant M (1976) Bull Soc Chim Fr 1976:28
140. Bréant M, Bazouin M, Buisson C, Dupin M, Rebattu JM (1968) Bull Soc Chim Fr 1968:5065

141. Bréant M, Buisson C (1970) J Electroanal Chem 24:145
142. Odziemkowski M, Krell M, Irish DE (1992) J Electrochem Soc 139:3052
143. Cauquis G, Serve D (1966) Bull Soc Chim Fr 1966:302
144. Mihajlović L, Nikolić-Mandić S, Vukanović B, Mihajlović R (2009) Cent Eur J Chem 7:900
145. Salomon M, Stevenson BK (1973) J Phys Chem 77:3002
146. Butler JN (1967) Anal Chem 39:1799
147. Butler JN, Cogley DR, Zurosky W (1968) J Electrochem Soc 115:445
148. Courtot-Coupez J, L'Her M (1969) Bull Soc Chim Fr 1969:675
149. Kirowa-Eisner E, Gileadi E (1970) J Electroanal Chem 25:481
150. Burrows B, Jasinski R (1968) J Electrochem Soc 115:365
151. Aurbach D, Daroux ML, Foguy PW, Yeager E (1987) J Electrochem Soc 134:1611
152. Piljac I, Iwamoto RT (1969) J Electroanal Chem 23:484
153. Baucke FGK, Tobias CW (1969) J Electrochem Soc 116:34
154. Sutzkover E, Nemirovsky Y, Ariel M (1972) J Electroanal Chem 38:107
155. Courtot-Coupez J, L'Her M (1970) Bull Soc Chim Fr 1970:1631
156. Boden DP, Mukherjee LM (1973) Electrochim Acta 18:781
157. Cisak A, Elving PJ (1963) J Electrochem Soc 110:160
158. Bertocci U (1957) Z Elektrochem 61:431
159. Bertocci U (1957) Z Elektrochem 61:434
160. Mukherjee LM (1972) J Phys Chem 76:243
161. Mukherjee LM, Kelly JJ, Richards M, Lukacs JM Jr (1969) J Phys Chem 73:580; [101]
162. Mukherjee LM, Kelly JJ (1967) J Phys Chem 71:2348
163. Mukherjee LM, Kelly JJ, Baranetzky W, Sica J (1968) J Phys Chem 72:3410
164. Broadhead J, Elving PJ (1969) Anal Chim Acta 48:433
165. Desbarres J, Pichet P, Benoit RL (1968) Electrochim Acta 13:1899
166. Benoit RL, Pichet P (1973) J Electroanal Chem 43:59
167. Coetzee JF, Simon JM, Bertozzi RJ (1969) Anal Chem 41:766
168. Armstrong NR, Quinn RK, Vanderborgh NE (1974) Anal Chem 46:1759
169. Headridge JB, Pletcher D, Callingham M (1967) J Chem Soc A 1967:684
170. Badoz-Lambling J, Sato M (1962) Acta Chim Hung 32:191
171. Perichon J, Buvet R (1964) Electrochim Acta 9:587
172. Markle RJ, Lagowski JJ (1986) Organometallics 5:595
173. Yamin H, Penciner J, Gorenshtain A, Elam M, Peled E (1985) J Power Sources 14:129
174. Yamin H, Gorenshtein A, Penciner J, Sternberg Y, Peled E (1988) J Electrochem Soc 135:1045
175. Paddon CA, Compton RG (2005) Electroanalysis 17:1919
176. Culp SL, Caruso JA (1969) Anal Chem 41:1329
177. Izutsu K (2009) Electrochemistry in Nonaqueous Solutions, 2nd edn. Wiley-VCH, Weinheim
178. Izutsu K, Kolthoff IM, Fujinaga T, Hattori M, Chantooni MK Jr (1977) Anal Chem 49:503
179. Pastoriza-Santos I, Liz-Marzán LM (2000) Pure Appl Chem 72:83
180. Benedetti AV, Fugivara CS, Cilense M, Rabockai T (1983) Anal Lett 16:1357
181. Zeyer C, Grüniger HR, Dossenbach O (1992) J Appl Electrochem 22:304
182. Cox BG, Firman P, Horst H, Schneider H (1983) Polyhedron 2:343
183. Luehrs DC, Iwamoto RT, Kleinberg J (1966) Inorg Chem 5:201
184. For reviews, see Ahrland S (1990) Pure Appl Chem 62:2077 and [184]
185. Arland S (1978) In: Lagowski JJ (ed) Chemistry of nonaqueous solvents, vol VA. Academic, New York, Chapter 1
186. Persson H (1970) Acta Chem Scand 24:3739
187. Sato M, Yamada T, Nishimura A (1980) Chem Lett 1980:925
188. Zotti G, Schiavon G, Zecchin S, Favretto D (1998) J Electroanal Chem 456:217
189. Zara AJ, Machado SS, Bulhoes LOS, Benedetti AV, Rabockai T (1987) J Electroanal Chem 221:165
190. Gritzner G, Kuta J (1984) Pure Appl Chem 56:461

191. Peerce PJ, Bard AJ (1980) J Electroanal Chem 108:121
192. Kannuck RM, Bellama JM, Blubaugh EA, Durst RA (1987) Anal Chem 59:1473
193. Ghilane J, Hapiot P, Bard AJ (2006) Anal Chem 78:6868
194. Noviandri I, Brown KN, Fleming DS, Gulyas PT, Lay PA, Masters AF, Phillips L (1999) J Phys Chem B 103:6713
195. Nelson IV, Iwamoto RT (1964) J Electroanal Chem 7:218
196. Desbarres J (1961) Bull Soc Chim Fr 1961:502
197. Popov AI, Geske DH (1958) J Am Chem Soc 80:1340
198. Sinicki C (1966) Bull Soc Chim Fr 1966:194
199. Giordano MC, Bazán JC, Arvía AJ (1966) Electrochim Acta 11:1553
200. Voorhies JD, Schurdak EJ (1962) Anal Chem 34:939
201. Lopez B, Iwasita T, Giordano MC (1973) J Electroanal Chem 47:469
202. Behl WK, Chin DT (1988) I Electrochem Soc 135:16
203. Benoit RL, Guay M, Oesbarres J (1968) Can J Chem 46:1261
204. Benoit RL (1968) Inorg Nucl Chem Lett 4:723
205. Badoz-Lambling J, Cauquis G (1974) Analytical aspects of voltammetry in non-aqueous solvents and melts. In: Nürnberg HW (ed) Electroanalytical chemistry. Wiley, New York, p 386
206. Diggle JW, Parker AJ (1974) Aust J Chem 27:1617
207. Pavlishchuk VV, Addison AW (2000) Inorg Chim Acta 298:97
208. Kolthoff IM (1965) J Polarogr Soc 10:22 and [24]
209. Coetzee JF, Campion JJ (1967) J Am Chem Soc 89:2513, 2517
210. Kotočová A (1980) Chem Zvesti 34:56
211. Krishtalik LI, Alpatova NM, Ovsyannikova EV (1991) Electrochim Acta 36:435
212. Bunakova LV, Khanova LA, Topolev VV, Krishtalik LI (2004) J New Mater Electrochem Syst 7:241
213. Alfenaar M, De Ligny CL, Remijnse AG (1967) Recl Trav Chim Pay-Bas 86:986
214. Cox BG, Parker AJ, Waghorne WE (1973) J Am Chem Soc 95:1010
215. Murray RC Jr, Aikens DA (1976) Electrochim Acta 21:1045
216. Senanayake G, Muir DM (1987) J Electroanal Chem 237:149
217. Kahanda C, Popovych O (1994) Aust J Chem 47:921 and references therein
218. Izutsu K, Nakamura T, Yamashita T (1987) J Electroanal Chem 225:255
219. Izutsu K, Nakamura T, Muramatsu M, Aoki Y (1991) J Electroanal Chem 297:49
220. Izutsu K, Nakamura T, Aoki Y (1992) J Electroanal Chem 334:213
221. Izutsu K, Muramatsu M, Aoki Y (1992) J Electroanal Chem 338:125
222. Izutsu K, Arai T, Hayashijima T (1997) J Electroanal Chem 426:91
223. Izutsu K, Kobayashi N (2005) J Electroanal Chem 574:197
224. Izutsu K (2005) Rev Polarogr 51:73 (in Japanese)
225. Izutsu K, Nakamura T, Takeuchi I, Karasawa N (1983) J Electroanal Chem 144:391
226. Izutsu K, Nakamura T, Muramatsu M (1990) J Electroanal Chem 283:435
227. Izutsu K, Gozawa N (1984) J Electroanal Chem 171:373
228. Izutsu K, Nakamura T, Gozawa N (1984) J Electroanal Chem 178:165
229. Izutsu K, Nakamura T, Gozawa N (1984) J Electroanal Chem 178:171
230. Izutsu K (2008) Bull Chem Soc Jpn 81:703
231. Izutsu K (2010) Bull Chem Soc Jpn 83:39
232. Izutsu K (2010) Bull Chem Soc Jpn 83:777
233. Izutsu K, Nakamura T, Muramatsu M, Aoki Y (1991) Anal Sci 7(suppl):1411
234. Izutsu K, Nakamura T, Arai T, Ohmaki M (1995) Electroanalysis 7:884
235. Izutsu K (2011) Anal Sci 27:685
236. Alexander R, Parker AJ, Sharp JH, Waghorne WE (1972) J Am Chem Soc 94:1148

Chapter 7
Reference Electrodes for Ionic Liquids and Molten Salts

Anand I. Bhatt and Graeme A. Snook

Acronyms

AAILs	Amino acid ionic liquid
An	Anion
BCr	*Bis*(phenyl)chromium(I) tetraphenylborate
BdMIm	1-Butyl-2,3-dimethylimidazolium
BMIm	1-Butyl-3-methylimidazolium
BOB	*Bis*(oxalatoborate)
BuPy	*N*-butylpyridinium
BzSEt	2-Ethylthiobenzolium
C_4mpyr	*N*-butyl-*N*-methylpyrrolidinium
C_8MIm	1-Octyl-3-methylimidazolium
C_{10}MIm	1-Decyl-3-methyl-imidazolium
Cat	Cation
Cc	Cobaltocene
ChCl	Choline chloride
DEA	Diethanolamine
DIECARB	*N*,*N*-diethylammonium *N*′,*N*′-dialkylcarbamate
dIL	Distillable ionic liquid
DIMCARB	*N*,*N*-dimethylammonium *N*′,*N*′-dialkylcarbamate
DmFc	Decamethylferrocene
DPA	Di-*N*-propylamine

A.I. Bhatt (✉) • G.A. Snook
Division of Energy Technology and Process Science and Engineering, Commonwealth Scientific and Industrial Research Organisation (CSIRO), Box 312, Clayton South, VIC 3169, Australia
e-mail: Anand.Bhatt@csiro.au; Graeme.Snook@csiro.au

G. Inzelt et al. (eds.), *Handbook of Reference Electrodes*,
DOI 10.1007/978-3-642-36188-3_7,

EAN	Ethyl ammonium nitrate
EMIm	1-Ethyl-3-methylimidazolium
FAP	Tris(pentafluoroethyl)trifluorophosphate
Fc	Ferrocene
FcC_1C_1Im	1-Ferrocenylmethylimidazolium
FcC_1MIm	1-Ferrocenylmethyl-3-methylimidazolium
FcC_1NMe_3	*N*,*N*,*N*,*N*-trimethylferrocenyl-methylammonium
FcMeOH	Ferrocenemethanol
HMIm	1-Hexyl-3-methylimidazolium
IL	Ionic liquid
ImCl	Imidazolium chloride
Me_4P	Tetramethylphosphonium
$MeBu_3N$	*N*-methyl,*N*-tributylammonium
MeCN	Acetonitrile
MEETCARB	*N*-methyl,*N*-ethylammonium *N*′,*N*′-dialkylcarbamate
MEPRCARB	*N*-methyl,*N*-propylammonium *N*′,*N*′-dialkylcarbamate
MIMSBu	1-Methyl-2-butylthiolonium
MIMSEt	1-Methyl-2-ethylthiolonium
mtzSEt	1-Methyl-2-ethylthiotetrazolium
$N_{6,2,2,2}$	Triethyl-hexylammonium
NPr_4	Tetrapropylammonium
OTf	Trifluoromethanesulfonate
$P_{6,6,6,14}$	Trihexyl(tetradecyl)phosphonium
PIL	Protic ionic liquid
PMIm	1-Propyl-3-methylimidazolium
PVdFHFP	Poly(vinylidene fluoride-co-hexafluoropropylene)
QAm	Quaternary ammonium
RTIL	Room temperature ionic liquid
SCE	Saturated calomel electrode
SEI	Solid electrolyte interphase
SHE	Standard hydrogen electrode
TDMATPFPB	Tridodecylmethylammonium tetrakis(pentafluorophenyl)borate
TEA	Triethanolamine
TFSI	*Bis*(trifluoromethylsulfonyl)imide
TMPD	*N*,*N*,*N*′,*N*′-tetramethyl-*p*-phenylenediamine

7.1 Introduction to Ionic Liquids and Molten Salts

High temperature molten salts and low temperature ionic liquids (RTILs or ILs) share commonalities in that they are both composed of ions in the molten state without any additional solvent. These liquids can act as media for chemical and electrochemical reactions. Indeed since there is a high ionic concentration, these liquids can have beneficial properties for electrochemical studies. Generally wide electrochemical windows and differences in coordination properties mean that

these solvents are useful in particular for deposition of metals that cannot be deposited in molecular solvents, or accessing redox couples not readily investigated in molecular or aqueous solvents. However, there are significant differences between the two which are mainly due to the nature of the ions and the melting temperature and liquidus ranges. For high temperature molten salts these are typically composed of simple salts based on alkali metal-halide or small polyatomic anions whereas low temperature ionic liquids are generally composed of organic cations and inorganic or organic anions where a large degree of covalent bonding exists as well as a charged centre (which may be delocalised over several atoms). Molten salts have been extensively studied as solvents for electrochemical reactions for a large number of years (many decades). Ionic liquids on the other hand are relatively new to the electrochemistry field and have only been studied for the past two decades with any significant efforts.

Since the operating temperature of conventional ionic liquids is close to that of room temperature or for a large proportion of reported liquids below 100 °C, cells and equipment used for electrochemical measurements are similar to those employed with traditional aqueous or non-aqueous solvents. The electrochemical responses of a variety of redox processes have been investigated in ionic liquids and show the importance of these solvent systems in future electrochemical devices and applications.

Molten salt electrochemistry on the other hand has been widely investigated and can be considered a mature field of research. Due to the very high temperatures of operation and general corrosive nature of the molten salts, cells and equipment for electrochemical measurements have by necessity been more complex when compared with those used with traditional aqueous or non-aqueous systems.

To perform electrochemical measurements in both molten salts and ionic liquids, a reliable reference electrode is required when accurate determination of electrode potentials is necessary. For the purposes of this chapter, we will only deal with measurements that are based on a three electrode set-up and not on a two electrode systems. We will first begin by defining both ionic liquids and molten salts before describing the properties of an ideal reference electrode for these systems. After this we shall describe a selected number of literature reports on use of reference electrodes and then finish with a discussion on how to construct reference electrodes for IL and molten salt measurements. Since much of the theoretical treatments are similar to those describing aqueous or non-aqueous reference electrodes we will not go into details, rather refer the reader to the previous sections in this book.

7.1.1 Description of Binary, Ternary or Higher Ionic Liquids/Molten Salts

Ionic liquids are defined as an ionic salt which is liquid in the pure state and is composed solely of cations and anions. Accepted practice within the field is to define ionic liquids as those liquids which have a melting point below 100 °C; however, this is not a ubiquitous definition [1]. Defining ionic liquids in this manner means that many

subclasses of ionic liquids such as protic and distillable are not recognized as ionic liquids. Indeed there is still debate in the field as to a universal definition which can encompass all the subclasses of ILs. At present only the room temperature ionic liquid is strictly defined within the field as an ionic liquid which is liquid at room temperature or below. However, simple changing of cationic or anionic functionalities can significantly affect physical properties such as melting points and electrochemical windows. Furthermore, the number of potential cations and anions which can combine to create an ionic liquid is vast [2]. Thus, it is not difficult to see that the definition of an ionic liquid can encompass a large variety of salts and liquidus temperature regimes. In addition, the boundary in definition between a classical high temperature molten salt such as liquid $NaAlCl_4$ (157 °C) and high temperature ionic liquids is not clearly stipulated within the field. Furthermore, the definition of ILs becomes further complicated when properties such as acidity (Brönsted or Lewis acidity) [3, 4], biological activity (e.g. Amino Acid ILs, AAILs [5]) or stability (e.g. energetic ILs [6]) are taken into account. As such it is important to define an ionic liquid prior to discussing the use of reference electrodes in IL media. Since there is not an accepted field definition of an ionic liquid, we here propose a definition of ILs based on liquidus temperature and physical properties in an attempt to define both ILs and their subclasses of ILs as well as conventional molten salts.

We will first begin by defining the simplest form of an ionic liquid where the IL consists of a binary salt, $[Cat^+][An^-]$, which by and large is the most common class of ionic liquid researched at present. At present the only strictly defined binary IL is the room temperature IL where the salt has to be a liquid at 25 °C. Using this definition we will now define ILs and molten salts based on their liquidus temperatures. Ionic liquids that are liquid at or below 25 °C are defined as RTILs. $NaAlCl_4$ has been extensively studied in the past [7] and is here defined as a molten salt with a melting point of 157 °C [8]. Again by using this point as a fixed reference, we now define a high temperature ionic liquid which has a melting point between 25 and 157 °C. Using this definition we can now encompass the majority of binary ILs that have a higher than room temperature melting point as well as encompassing a proposed higher limit of 100 °C. Above the melting point of $NaAlCl_4$, the conventional/classical molten salts are defined. The definitions are shown diagrammatically in Fig. 7.1. This temperature-based definition also has implications in the complexity of the cations and anions. As the liquidus temperature range is increased the cation and anion molecular complexity is reduced. As the temperature range is increased typically, the level of covalent bonding within the ions decreases and ionic character is increased.

Ternary or higher ionic liquids, where the IL exists as a mixture of cations and/or anions are defined as:

$$[Cat_1^+]_a[An_1^-]_b[Cat_2^+]_c[An_2^-]_d \cdots \tag{7.1}$$

where a, b, c, d,... = 0, 1, 2, 3, 4, ... and the subscripts 1, 2, ... = different ion chemical identity.

Clearly, the binary IL is a subset of this class of IL systems. Hence the melting temperature-based classification system is also applicable for this type of IL. Again

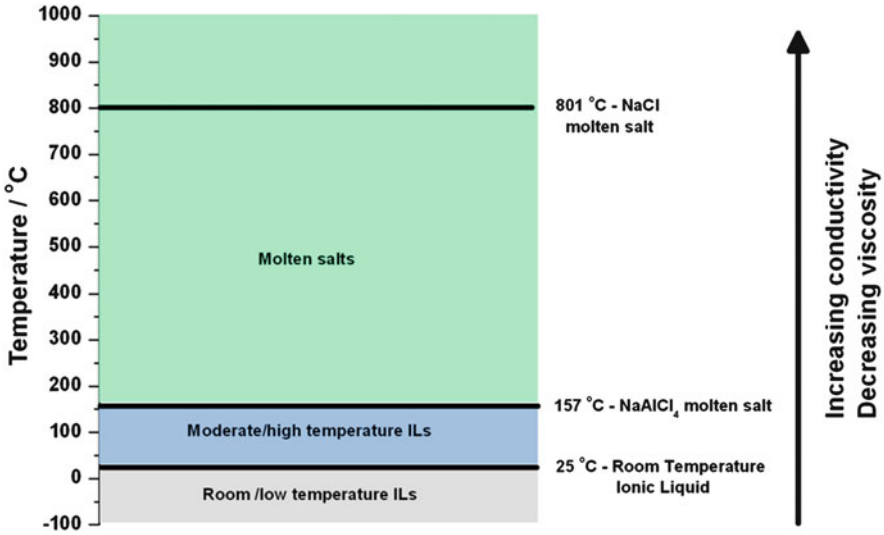

Fig. 7.1 Classification of ionic liquids/molten salts as a function of melting temperature

the two fixed reference points of 25 and 157 °C are used. At this point it is worthwhile noting that for many electrochemical studies on ionic complexes, dissolution of the solute into a binary IL will create a ternary or higher IL system to some extent. The level of higher IL formation will be dependent on the concentration of the solute within the IL media.

Next we define molten salts simply as those salts whose melting temperature is above the 157 °C melting point of $NaAlCl_4$. Thus we do not differentiate whether the molten salt has a relatively simple ionic structure such as NaCl or $NaAlCl_4$ or if the ions have a more complex structure typically associated with room temperature ionic liquids. Thus a clear distinction between moderate or high temperature ionic liquids and molten salts can be made. Similar to the distinction between binary and ternary or higher ionic liquids a similar reasoning can be applied to molten salts where mixing of multiple anions and cations can form a ternary or higher molten salt. This then allows the eutectic mixtures of various salts to be classified as molten salts if the melting temperature is above the 157 °C.

7.1.2 Description of Other Subsets of Ionic Liquids

Having defined the distinction between the relatively simple ionic liquid and molten salts we now need to define the subsets of the IL classes. There are literature reports on studies of IL systems where the atypical physical properties such as low/negligible volatility or inertness have been modified. These ILs thus form a subset of the typically studied IL systems. We begin first with the properties of inertness. There

is a class of IL systems which possess either Brönsted or Lewis acidity due to the IL ions interactions. Protic ILs (PILs) are formed by proton transfer between a Brönsted acid and a Brönsted base [1]. PILs are not required to have negligible vapour pressures associated with conventional ionic liquids. The first reported PIL was the ethanolammonium nitrate which had a melting point of 52–55 °C [9]. Since then a large variety of PILs have been reported [3] and a similar spread in melting point and liquidus range exists as compared to conventional ILs.

Lewis acidic ILs have predominantly been restricted within the field to the investigations of ILs where the anion is based on $[AlCl_4]^-$ and its associated complexes. However, a handful of reports have focussed on other anionic structures that can act as a Lewis base or acid [10, 11]. It is evident that if the associated cation with the $[AlCl_4]^-$ anion is Na^+, then the resulting liquid will be the molten salt. Most researchers have focussed on changing the Na^+ to a more functionalised cation, e.g. $[EMIm]^+$, in order to reduce the melting temperature [12]. Thus for both PILs and Lewis acidic ILs, we can also define these systems using the same temperature reference points as shown in Fig. 7.1.

The next major subset of ILs we will discuss is the distillable ionic liquids or dILs. These IL systems have a significant vapour pressure associated with them and at relatively low temperatures can be dissociated into a gaseous or liquid state and can be reformed at lower temperatures [13, 14], hence the distillable nature of them. Clearly this subset of ILs has unique properties that are a cross between conventional molecular solvent systems and also posses the ionic character associated with ILs. Previous work has shown that again, as for the IL and PIL systems, dILs can have a range of melting points. Thus, as before the temperature distinction shown in Fig. 7.1 can be applied to this special case.

It should be noted the PIL and dIL systems have similarities within their physical properties. Namely, both these classes have ionic characters similar to the more conventional IL/molten salts. However, they also posses properties that are more closely related to those of traditional non-aqueous molecular solvents. Based on this we now need to expand the definitions presented in Fig. 7.1 to encompass these properties, and this is presented in Fig. 7.2.

We will limit our definitions of ionic liquids and molten salts to the above major categories. Although other categories or subsets of ionic liquids exist for the purposes of this chapter, it is not necessary to define them in detail as the arguments and recommendations will equally apply to these subsets with minimal modifications.

7.2 Properties of an Ideal Reference Electrode for Use in IL Media

The properties and theoretical aspects of a reference electrode for use in electrochemical measurements have been described elsewhere in detail (Chap. 1). Here we will limit discussion to those specific properties relevant to application in ionic liquid/molten salt systems.

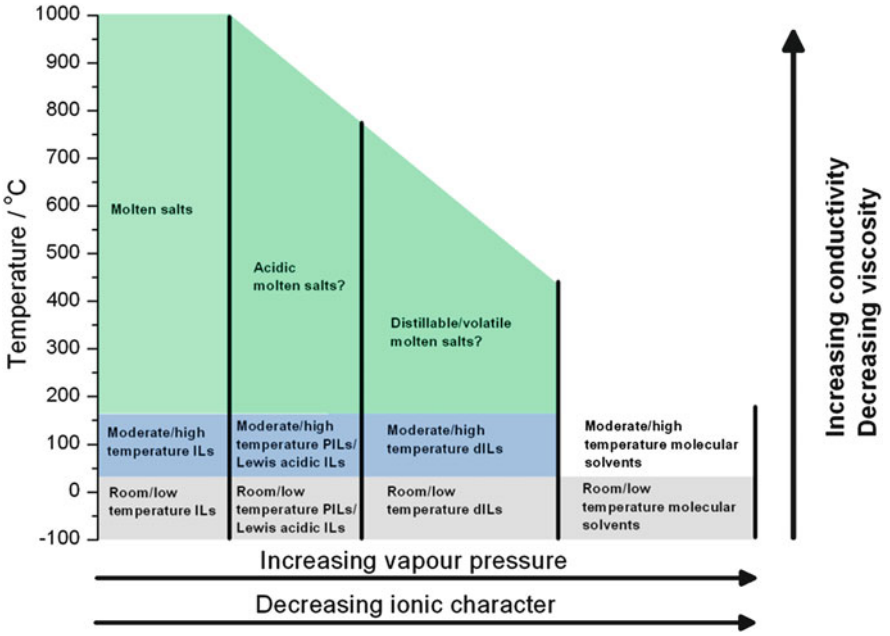

Fig. 7.2 Classification of ionic liquids/molten salts and their subsets as a function of melting temperature

As detailed in Sect. 7.1 there are many classes of ILs each with unique chemical/physical properties and temperature regimes under which electrochemical measurements can be performed. As such, the "holy grail" of a universal reference electrode system for ionic liquids and molten salts cannot exist. For each IL system and operating temperature, careful choice of reference electrode must be made which can operate reliably under the appropriate measurement conditions. Some of the properties to consider are explained in more detail below.

The properties of an ideal reference electrode for IL and molten salt media have been succinctly stated by Barrosse-Antle et al. [15]. First, the reference potential should be stable with time [15], i.e. the reference potential does not drift or shows minimal drift (ideally less than 10 mV per day). A second requirement, as also for non-aqueous and aqueous reference electrodes, is that the reference electrode should have a very small temperature coefficient over the desired operating range [15, 16]. However, for ILs and molten salts this can be a difficult requirement to meet since the liquidus operating range is much larger than for aqueous or non-aqueous systems. Hence, a more accurate statement would be that the reference electrode is stable over the temperature range of data collection. Finally, the reference electrode should be reproducible in its preparation as well as voltage response over the duration of use/measurement as well as being convenient to use [15].

7.2.1 Electrodes of the First Kind

As explained in previous chapters (see Chaps. 1 and 2), an electrode of the first kind is one based on atoms or molecules and their corresponding cation or anion in solution. This type of electrode is most commonly used within the ionic liquids' fields. Requirements for this class of reference electrode are that the atom or molecule used does not react with the ionic liquids. Additionally the corresponding cation or anion should be stable in the solvated form within the IL and should not have any corresponding undesirable chemical reactions with the IL components. If the reference electrode is based on a metal M|metal ion M^{n+} electrode system, and assuming the activity of the metal is 1 (which may not be true for specific cases), then the corresponding potential of the half-cell is given by:

$$E = E_c^{\ominus\prime} + \frac{RT}{nF} \ln a(M^{n+}), \tag{7.2}$$

where E is the measured potential, $E_c^{\ominus\prime}$ the formal potential, R the gas constant, T the temperature, n the number of electrons transferred and a is the activity of the species.

If the reference electrode is based on a gas, G_x, and its corresponding cation or anion in solution $\frac{1}{x}G^n$, then the corresponding potential of the half-cell is given by

$$E = E_c^{\ominus\prime} + \frac{RT}{nF} \ln \frac{a(G^n)}{f_{G_x}^{1/x}}, \tag{7.3}$$

where f is the fugacity of the gas ($f = \gamma p$ where p is the pressure and γ is the fugacity coefficient) and all other symbols are defined in Eq. (7.2).

Clearly similar requirements exist for gas-based reference electrodes. The corresponding gas ions must not react with the IL components to form alternative products.

For both metal-based or gas-based reference electrodes, these definitions in practical terms mean that the concentration of the dissolved ions within the reference electrode remains essentially constant. The electrochemical changes of the reference system should be part of an equilibrium reaction and overall no net reaction should occur during the measurement. However, if a reaction or alternative equilibrium occurs which can change the activities of the reference species in a detectable manner, then the redox couple chosen can be problematic and stability of the reference electrode can be compromised. Therefore, care must be taken to ensure this type of reaction does not take place with the chosen ions.

7.2.2 Electrodes of the Second Kind

Reference electrodes of the second kind are based on three phases in mutual contact where the electrode potential is a function of the common anion (An^-) activity in solution. One such example is the Ag|AgCl|Cl^- (silver–silver chloride) reference electrode and as stated in previous chapters this type of electrode is well known in aqueous electrochemistry. The electrode potential of the half-cell is given by:

$$E = E_c^{\ominus\prime} - \frac{RT}{nF} \ln a(An^-). \tag{7.4}$$

Use of this type of reference electrode requires good solubility and high concentrations of the anion, An^-, in the IL. This is not always straightforward for ILs, where limited or low solubility of anions such as halides (e.g. Cl^-) may be encountered. As a result this type of reference electrode is not commonly used within IL electrochemistry. Another requirement is that the metal halide solid, typically on the surface of the metal wire, should be stable to the IL and should have very low solubility within the IL, otherwise unstable reference electrode potentials will arise. This can be mitigated by having a suitably high concentration of the An^- in the IL phase.

There are a number of reports where the Ag|AgCl reference electrode (where the AgCl phase is deposited onto a Ag wire) is used without addition of Cl^- to the IL phase. This type of electrode is not an electrode of the second kind and is actually a quasi-reference electrode (see Chap. 14). As such this type of reference electrode may show significant drift since lack of Cl^- in the IL phase means that over time the Cl^- and Ag^+ on the electrode will diffuse into the IL phase causing a shift in reference potential.

7.2.3 Inert Electrode Immersed in a Solution Containing a Soluble Redox Couple

This class of reference electrode consists of an inert conducting or semi-conducting material immersed in an IL solution containing a redox couple:

$$Ox + ne^- \rightleftarrows Red. \tag{7.5}$$

Provided that the redox equilibrium (7.5) is electrochemically reversible under potentiometric conditions at the inert electrode, the electrode will assume a potential given by the following equation (Nernst equation):

$$E = E_c^{\ominus\prime} + \frac{RT}{nF} \ln\left(\frac{a(Ox)}{a(Red)}\right). \tag{7.6}$$

Use of this type of electrode with ILs requires that both sides of the redox couple chosen are soluble in the IL system. Furthermore as with the previous classes of electrodes, the IL must not react chemically or electrochemically with the redox couple to produce unwarranted products. Lastly, the redox reaction chosen must exhibit electrochemical reversibility within the IL. Due to the nature of many IL interactions with analytes, this should be confirmed prior to using this type of electrode. Since the reference electrode may be required to operate over a wide temperature regime, the redox couple should also exhibit electrochemical reversibility over the temperature range required.

7.2.4 *Experimental Considerations for an Ideal Reference Electrode in IL Electrochemistry*

For the majority of IL systems reported, the physical properties of the IL mean that issues such as solution resistance become significant. This is much more apparent for IL measurements than compared to non-aqueous solvents or aqueous solvent systems. Barosse-Antle et al. have summarised the physical properties relevant to electrochemistry of a range of ILs [15], and this is summarised in Table 7.1. As is evident from Table 7.1, IL conductivities (which are related to solution resistance as explained below) are lower than those of organic solvents resulting in high resistances.

The effect of solution resistance, IR_u, on the IUPAC recommended cobaltocene|cobaltocenium ($Cc|Cc^+$) [17] and decamethylferrocene|decamethylferrocenium ($DmFc|DmFc^+$) couples in two different IL media is shown in Table 7.2. For both redox couples the peak–peak separation should be 57 mV at the reported temperatures. As can be seen from the data, this is not always the case even when appropriate levels of IR_u compensation have been applied by the potentiostatic software.

In order to minimise effects of IR_u, care should be taken to locate the reference electrode as close as possible to the working electrode. In Fig. 7.3a, this is shown schematically. Ideally the distance between the working and reference electrodes, x, should be minimised without contacting the two electrodes. There are two types of commonly used reference electrode assemblies used in the IL field. The first is where a porous glass or Vycor® frit is used within a glass chamber and separated from the electroactive species by a fritted tube or compartment (Fig. 7.3b), while the second is where the compartment/tube is replaced with a Luggin capillary (Fig. 7.3c).

In IL electrochemistry use of the two commonly reported types of reference electrodes shows significant difference in electrochemical responses. Using the methodology developed by Oldham [19], the level of R_u can be calculated as a function of distance of the reference electrode tip from a disk working electrode by:

$$R_u = \frac{\arctan[x_{R-W}/r_w]}{2\pi r_w \kappa}, \tag{7.7}$$

Table 7.1 Physical properties relevant to electrochemistry of a range of ionic liquids (data from [15] and references therein)

Ionic liquid	η (cP)	ρ (g cm^{-3})	κ (mS cm^{-1})	Electrochemical window (V)
Binary ionic liquids				
[EMIm][TFSI]	34	1.53	8.8	4.3
[BMIm][TFSI]	52	1.44	3.9	4.8
[BdMIm][TFSI]	105	1.42	2.0	5.2
[HMIm][FAP]	74	1.56	1.3	5.3
[C_4mpyr][TFSI]	89	1.4	2.2	5.2
[BMIm][OTf]	90	1.3	3.7	4.9
[BMIm][BF_4]	112	1.21	1.7	4.7
[$N_{6,2,2,2}$][TFSI]	167	1.27	0.67	5.4
[BMIm][PF_6]	371	1.37	1.5	4.7
Brönsted acidic ionic liquids				
[DEA]Acetate	336	1.22	0.14	2.4
[DPA][OTf]	19	0.97	1.19	2.7
[TEA]Acetate	11	0.96	1.27	3.4
[DEA]Cl	305	1.24	0.86	4.0
Distillable ionic liquids				
DIMCARB	77	1.05	1.7	2.0
DIECARB	14	0.91	0.053	2.1
MEETCARB	85	0.98	0.37	1.9
MEPRCARB	70	0.95	0.18	1.8
Organic solvents				
Acetonitrile	0.34	0.79	7.6[a]	5.0[a]
N,*N*-Dimethylformamide	0.92	0.94	4.07[a]	4.3[a]
Dimethylsulphoxide	1.99	1.10	2.7[a]	4.4[a]

Where η = viscosity, ρ = density and κ = conductivity
[a]Data for 0.1 M [NBu_4]ClO_4/solvent solutions at 295 K

Table 7.2 Comparison of peak separations for IUPAC recommended reference compounds (and their derivatives) at macro working electrodes in IL media from cyclic voltammetry measurements

Scan rate (mV s^{-1})	ΔE_{peak} (V) for 1.8 mM DmFc|DmFc$^+$ in DIMCARB [13]	ΔE_{peak} (V) for 5 mM Cc|Cc$^+$ in [C_4mpyr][TFSI] [18]
2	65	–
5	–	63
10	58	64
20	57	65
40	60	–
50	–	74
100	64	80

where x_{R-W} is the reference electrode–working electrode distance, r_w the electrode radius and κ is the solution conductivity.

Figure 7.4a shows the calculated R_u level using Eq. (7.7) for various sizes of disk working electrodes in an IL with conductivity of 2.2 mS cm^{-1} (for example butylmethylpyrrolidinium[TFSI] [20]). It is clear from Fig. 7.4a that the level of R_u is

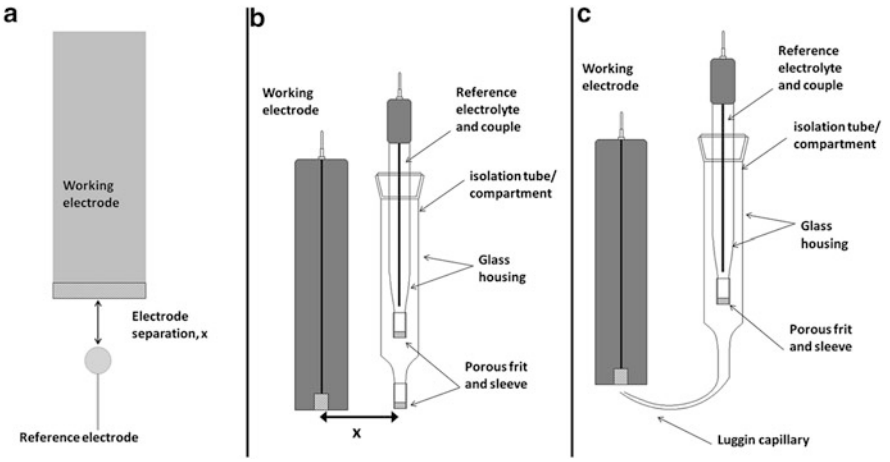

Fig. 7.3 Location of reference electrodes within an electrochemical cell and types of electrode assemblies commonly reported in the literature. (**a**) Schematic showing separation of reference and working electrode; (**b**) porous glass or Vycor® fritted reference electrode separated from the electroactive species by a fritted tube or compartment and (**c**) porous glass or Vycor® fritted reference electrode separated from the electroactive species by a tube/compartment fitted with a Luggin capillary

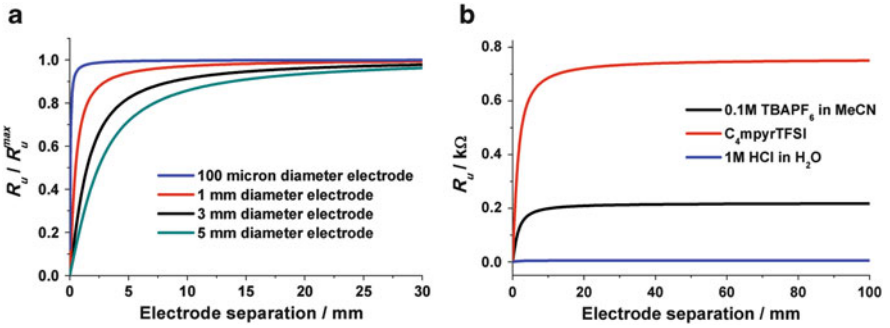

Fig. 7.4 (**a**) Effect of electrode separation on R_u in butyl-methylpyrrolidinium[TFSI] (data normalised to allow comparisons); (**b**) Effect of solution conductivity on R_u for 1 M HCl in water ($\kappa = 33$ S m^{-1} [21]), 0.1 M [NBu$_4$]ClO$_4$ in acetonitrile ($\kappa = 7.6 \times 10^{-3}$ S m^{-1} [15, 21]) and butyl-methylpyrrolidinium TFSI ($\kappa = 2.2 \times 10^{-3}$ S m^{-1} [15, 20])

dependent on both the working electrode size and distance between the reference electrode and working electrode. However, above 20 mm separations a steady state in the R_u values is achieved for an IL with conductivity of 2 mS cm^{-1}. Experimentally this means that the reference electrode placement in IL electrochemical measurements more than 20 mm from the working electrode results in the level of R_u being essentially constant. In other words, the working and reference electrodes are essentially at infinite distance from each other. The second thing to

notice from Fig. 7.4a is for macrosized (1–5 mm diameters) disk working electrodes the region where R_u can be minimised is in the 5–10 mm separation region or below. Again practically this means that a choice of correct reference electrode assembly must be made prior to measurements. For many frit type of reference electrodes (e.g. glass tubes with a Vycor® frit), the frit size itself results in a minimum separation of several millimetres. This in combination with placement of the reference electrode within the cell can result in several millimetre separations. As a result the R_u value can be close to the infinite linear region. Experimentally in order to get electrode separations <5 mm, it is wise to use a Luggin type of reference electrode assembly (see Fig. 7.3). Regardless, whichever electrode assembly type the readers wish to use, care should be made when reporting or analysing electrochemical data in IL media to ensure that any IR_u effects are accounted for or minimised.

It can be seen from Fig. 7.4b that there is a significant effect on R_u when using an ionic liquid electrolyte as compared to aqueous or non-aqueous electrolytes. This is due to the difference in conductivities of ionic liquids when compared to aqueous or non-aqueous electrolytes. Consequently, electrochemical data measured in ionic liquid media will have an inherently higher level of IR_u issues. Thus, reference electrode construction and placement in order to minimise IR_u effects is critical when using IL electrolytes.

7.3 Reference Electrode Systems Used with IL and Molten Salt Media

Although reference electrodes are important for measurements of accurate potentials in electrochemical measurements, little attention has been spent on development of ionic liquid reference electrodes. The following sections will discuss the types of reference electrodes reported within the ionic liquid field or discuss redox systems, which can be modified for use in reference electrodes.

7.3.1 Room Temperature Ionic Liquid Reference Electrodes

7.3.1.1 $Ag|Ag^+$ Reference Electrode

By far the most commonly reported reference electrode system for room temperature or low temperature binary, ternary or higher reference electrodes has been based on the $Ag|Ag^+$ couple. Some selected examples of reference electrodes using the $Ag|Ag^+$ couple in selected ILs are presented in Table 7.3. All of these reported reference electrodes are based on use of a silver wire immersed into an IL containing a dissolved silver salt.

Table 7.3 Selected $Ag|Ag^+$ reference electrodes used in binary, ternary or higher IL media

Ionic liquid	Silver salt	Electrode assembly	Calibrated potential (mV)	Reference
[EMIm][TFSI]	0.1 M AgOTf	Frit	+440 (vs. $Fc\|Fc^+$)	[22]
[BMIm][BF_4]	$AgNO_3$/MeCN/RTIL	Frit	−232 (vs. $Fc\|Fc^+$)	[23]
[BMIm][TFSI]	$AgNO_3$/MeCN/RTIL	Frit	−182 (vs. $Fc\|Fc^+$)	[23]
[BMIm][PF_6]	$AgNO_3$/MeCN/RTIL	Frit	−222 (vs. $Fc\|Fc^+$)	[23]
[C_4mpyr][TFSI]	10 mmol L^{-1} AgOTf/ [C_4mpyr][TFSI]	Frit	+390 (vs. $Fc\|Fc^+$)	[24]
[EMIm][OTf]	10 mmol L^{-1} AgOTf/ [C_4mpyr][TFSI]	Frit	+416 (vs. $Fc\|Fc^+$)	[24]
[EMIm][$EtSO_4$]	10 mmol L^{-1} AgOTf/ [C_4mpyr][TFSI]	Frit	+432 (vs. $Fc\|Fc^+$)	[24]
[BMIm][BF_4]	10 mmol L^{-1} AgOTf/ [C_4mpyr][TFSI]	Frit	+418 (vs. $Fc\|Fc^+$)	[24]
[BdMIm][BF_4]	10 mmol L^{-1} AgOTf/ [C_4mpyr][TFSI]	Frit	+415 (vs. $Fc\|Fc^+$)	[24]
[C_4mpyr][BOB]	10 mmol L^{-1} AgOTf/ [C_4mpyr][TFSI]	Frit	+401 (vs. $Fc\|Fc^+$)	[24]
[C_4mpyr][TFSI]	10 or 100 mMol L^{-1} AgOTF	Frit	+475 (vs. $Ag\|AgNO_3$)	[25]
[C_4mpyr][TFSI]	10 or 100 mMol L^{-1} AgTFSI	Frit	+470 (vs. $Ag\|AgNO_3$)	[25]
[C_4mpyr][TFSI]	10 or 100 mMol L^{-1} $AgNO_3$	Frit	+460 (vs. $Ag\|AgNO_3$)	[25]
[BMIm][TFSI]	10 mMol L^{-1} AgOTf	Frit	+387 (vs. $Fc\|Fc^+$)	[26]
[$MeBu_3N$][TFSI]	10 mMol L^{-1} AgOTf	Frit	+340 (vs. $Fc\|Fc^+$)	[26]
EAN	$Ag/AgNO_3$	Frit	+114 (vs. $Fc\|Fc^+$)	[27]
[C_4mpyr][TFSI]	Ag/AgCl/KCl (aqueous)	Frit	−320 (vs. $Fc\|Fc^+$)	[28]
[BMIm][TFSI]	Ag/AgCl/KCl (aqueous)	Frit	−320 (vs. $Fc\|Fc^+$)	[28]
[TDMA][TPFPB]	Ag/AgCl	Luggin	Not reported	[29]
ChCl	Ag/AgCl/urea/ChCl	None	Not reported	[30]
ChCl	$Ag/AgNO_3$/urea/ ChCl	None	Not reported	[30]

It is clear from Table 7.3 that the reference potential of the $Ag|Ag^+$ couple is dependent on the choice of ionic liquid and also choice of silver salt used for construction of the reference electrode. This is observed in the potential values of the IUPAC recommended $Fc|Fc^+$ couple [17], which are in the range of −440 to 320 mV against the $Ag|Ag^+$ couple. As such it is recommended that once a reference electrode has been constructed, the reference potential is calibrated against an IUPAC recommended internal reference couple. In order to minimise the variations in the reference electrode potential, it is important to dissolve the Ag^+ solution into the same IL as used for the electrochemical measurements, otherwise, a junction potential (ΔE_j) will exist which needs to be determined. For example Snook et al. have constructed an Ag|AgOTf|[C_4mpyr][TFSI] reference electrode

Table 7.4 Plots of ΔE_j for the Ag|AgOTf|[C_4mpyr][TFSI] reference electrode in a variety of ILs [26], where $E_c^{o\prime}$ is the formal potential and ΔE_j is the liquid junction potential

Ionic liquid	$E_c^{o\prime}$ (mV) for Fc|Fc$^+$ vs. Ag|AgOTf|[C_4mpyr][TFSI] electrode	ΔE_j (mV)
[C_4mpyr][TFSI]	−390	0
[EMIm][OTf]	−146	−26
[BMIm][BF_4]	−418	−28
[EMIm][$EtSO_4$]	−432	−42
[BdMIm][BF_4]	−415	−25
[C_4mpyr][BOB]	−401	−11

and have measured its ΔE_j in a variety of ILs by determination of the Fc|Fc$^+$ potential [27]. As can be observed from Table 7.4, significant shifts in the ΔE_j exist. In order to minimise this situation when using an Ag|Ag$^+$ reference system, the silver salt should be dissolved into the same IL as used for the electroactive species, and similarly the same IL should be used within the salt bridge tube or compartment.

As stated in Sect. 7.2.1 of this chapter, for electrodes of the first kind, the metal ions should not react with the ILs. Basile et al. have noted that the presence of water results in the formation of silver nanoparticles for solutions of Ag$^+$ ions dissolved into [C_4mpyr][TFSI] [31]. These authors postulate that this occurs via chelation of Ag$^+$ by the [TFSI] anion and a subsequent disproportionation reaction in the presence of water to form a Ag^{2+}-[TFSI] complex and Ag^0 [31]. Thus, the choice of a reference electrode based on Ag|AgOTf|[C_4mpyr][TFSI] may be problematic. The authors did note that over a short period of time, when chemical reaction rates were low, the Fc|Fc$^+$ reversible potential was close to that reported by Snook et al. [27, 31]. According to Snook et al. [27] the Ag|AgOTf|[C_4mpyr][TFSI] reference electrode is only stable for 3 weeks before the solution needs to be replaced and the electrode remade. Therefore, if the Ag|Ag$^+$ couple is to be used in other ILs, then any potential chemical reactions of Ag$^+$ ions within this IL should be explored prior to use, as well as the stability of the reference electrode over time.

Experimentally, the Ag|Ag$^+$ reference electrode is constructed by dissolution of the silver salt into an IL. This IL solution is then placed into either a fritted tube or into a Luggin capillary tube. The electrical contact is then made via a silver wire immersed into the Ag$^+$/IL solution. In the case of the fritted tube, this should ideally be separated from the electrochemical cell by use of a second fritted tube or compartment depending on cell design, containing only neat IL which is the same for the electroactive species. This is done in order to minimise effects of any potential leakage of silver ions from the reference electrode.

Although adoption has not been widespread, Kakiuchi et al. have constructed a Ag|AgCl|[C_8MIm][TFSI] gel reference electrode [32]. This system is created by anodising an Ag wire in KCl to form a surface layer of AgCl. Onto this layer a solution of [C_8MIm][TFSI] containing PVdF HFP (400,000 Da) as a gelling agent in acetone is coated. The IL is then gelled on the surface by evaporation of the acetone solvent. This gelled RTIL-coated electrode is then used as a reference

Table 7.5 Formal potential of the $H^+|HAn$ couple and peak potential (E_p) for the $HAn \rightarrow ½\ H_2 + An^-$ reduction in ionic liquid media

Ionic liquid	E_p (V) for the $HAn \rightarrow ½\ H_2 + An^-$ reduction	$E^{e'}_{c,2H^+/H_2}$ for the $H^+\|HAn$ couple
[EMIm][TFSI]	1.18 (HTFSI)	1.36
[BMIm][TFSI]	1.19 (HTFSI)	1.36
[BMIm][OTf]	0.68 (HOTf)	0.98
$[N_{6,2,2,2}]$[TFSI]	1.08 (HTFSI)	1.30
[BMIm][PF_6]	1.24 (HPF_6)	1.53
$[P_{6,6,6,14}]$[TFSI]	0.73 (HTFSI)	1.38

All potentials referenced to $Cc^+|Cc^0$ [32]

electrode by placing into a salt bridge tube/compartment containing the same IL as that used for the electroactive species. The $E^{e'}_c$ of this reference electrode is estimated by Kakiuchi et al. to be 0.22 V vs. SHE [32].

7.3.1.2 $H_2|H^+$ Reference Electrode

Although strictly speaking this type of reference electrode has not been used in IL electrochemistry, sufficient data does exist for this type of reference electrode to be constructed. Compton et al. have shown that H_2 can be oxidised in a number of ILs at a platinum electrode (Table 7.5) [33–35]. Additionally for selected ILs the reduction of H^+ can also occur [35]. The formal potential determined for the $H^+|H_2$ redox couple in selected ILs is presented in Table 7.5.

As can be seen from Table 7.5, similar to the case of the $Ag|Ag^+$ couple, when the $H_2|H^+$ is referenced to an internal redox couple a shift in the $E^{e'}_c$occurs and is dependent on the IL studied. Additionally, Compton et al. have reported that the electrochemical reversibility of the $H_2|H^+$ couple is dependent on the identity of the IL [33]. This is most likely due to the difference in proton activity in the different ILs. As such it is important if the reader wishes to use the $H_2|H^+$ couple in a reference electrode; then the reversibility of this reaction is checked prior to use.

Experimentally constructing an $H_2|H^+$ reference electrode in IL media would be similar to construction of the $Ag|Ag^+$. In this particular case a platinum wire should be used and the Ag^+ solution replaced with an H^+ solution. The separation of the reference electrode via a salt bridge tube of compartment (depending on cell designs) is advisable in order to minimise issues with leakage of reference solution into the electroactive solution. Experimentally the set-up would be similar to that used in PILs electrochemistry (see below for further details)

7.3.1.3 $Li|Li^+$ Reference Electrodes

A number of researchers have reported on the use of lithium wires or lithium foils as reference electrodes (see [36] and references therein). Experimentally researchers

usually directly immerse the lithium foil into the IL solution of interest. Whilst this reference electrode can provide a stable reference point for electrochemical measurements, it is not possible to consider this type of electrode as anything other than a quasi-reference electrode. A well-known phenomenon on the lithium electroplating reaction is the formation of a passivating film known as the solid electrolyte interphase (SEI) layer. Thus, the lithium redox couple should be defined as:

$$Li^+ + e^- \xrightarrow{IL} Li^0 \big| SEI \xrightarrow{-e^-} Li^+ + \underset{\substack{\downarrow \\ \text{decomposition products}}}{SEI} \tag{7.8}$$

Since the SEI formation can occur both chemically and frequently electrochemically in ionic liquid media, there will be a shift in the potential of the Li|Li^+ couple. However, the chemical composition of the SEI layer is frequently unknown and thus the shift in potentials cannot be readily ascertained without calibration. Further complications exist when using lithium electrodes as reference electrodes. Compton et al. have studied the Li|Li^+ couple at both Ni and Pt electrodes. For the Li|0.1 M $LiAsF_6$|[C_4mpyr][TFSI] reduction of Li^+ occurs at −3.2 V vs. Fc|Fc^+ at a Ni electrode [37]. Using a combination of simulation and experimental methods, Compton et al. have determined the formal potential of this reaction to be −3.25 V vs. Fc|Fc^+ and is stable between 25 and 45 °C [37]. In [Me_4P][TFSI] the lithium redox couple has been observed at −3.20 V vs. Fc|Fc^+ at a glassy carbon electrode [38], and this potential correlates well with that reported by Compton et al. but does show a difference of 50 mV most likely due to the existence of a different composition of SEI layer. Another potential drawback of using a Li|Li^+ reference electrode is highlighted in the work of Yang et al. where use of lithium foils as both working and counter electrodes results in chemical reaction between the lithium metal and the IL [39]. Consequently, Yang et al. report that voltametric features were detected due to the generation of electroactive impurities from the chemical reaction [39].

7.3.1.4 Quasi-reference Electrodes

Quasi-reference electrodes (Chap. 14) are by and large the most common type of reference electrodes reported in ionic liquid electrochemistry. However, since the potential of this reference electrode is unknown, and the stability of this reference electrode can vary from electrode to electrode and solution to solution, accurate potentials cannot be measured with this type of reference electrode. Quasi-reference electrodes can also show considerable drift, especially when using silver wire directly immersed into the IL solution [15]. If using a quasi-reference electrode in IL electrochemical measurements for accurate determination of potentials, the electrode should be calibrated against an IUPAC recommended redox couple [15]. However, in many IL electrochemical reports, this is not performed and as such any potential data reported cannot be confirmed by other laboratories.

A large variety of quasi-reference electrodes have been used based on metal wires such as silver [40], platinum [41], aluminium [42], tungsten [43], magnesium [44], etc. Typically electrodes are placed directly into the IL solution or separated from the main solution inside a fritted glass tube/compartment. In order to minimise liquid junction potentials in the latter case, the same ionic liquids as per the measurements is used as electrolyte. It is the authors' experience that separation of the quasi-reference electrode allows for a reduction in potential drift when compared to direct insertion into the electrochemical cell.

7.3.2 Redox Reference Electrodes

Many researchers have reported on the use of either $Ag|Ag^+$ reference electrodes or quasi-reference electrodes in IL media. In order to standardise reference potentials, some researchers have used the IUPAC recommended ferrocene or cobaltocene couples or derivatives of these. Indeed, there is some debate in the literature which advocates that IL electrochemical measurements be reported against these redox couples. Tables 7.6, 7.7 and 7.8 show the potentials of ferrocene, its derivatives and cobaltocene in IL media.

For all of the measurements reported in Table 7.6, experimentally they were accomplished by dissolution of ferrocene in the concentration range of 1–50 mM into the IL of choice and after dissolution measurements performed. For the majority of the data presented in Table 7.6 this was collected via analysis of cyclic voltammetric experiments. Consequently, the voltammetric peak potentials were used in order to determine the $E_c^{\ominus\prime}$ values or the $E_{1/2}$ values. Experimentally $E_{1/2}$ values can be converted to $E_c^{\ominus\prime}$ values as shown below (under conditions where $\alpha = 0.5$ and $D_{ox} = D_{red}$):

$$E_{1/2} = E_c^{\ominus\prime} - \frac{RT}{F} \ln \left(\frac{D_{ox}}{D_{red}} \right)^{1/2}. \tag{7.9}$$

This methodology can be used to calibrate potentials if the assumption is adopted that the $Fc|Fc^+$ couple is unaffected by solution. However, there are a number of issues that can prevent the calibration process. First, in some IL systems ferrocene has been reported to not have ideal electrochemistry or indeed chemically react with IL components [13, 46]. In a scenario such as this, use of the $Fc|Fc^+$ couple is not recommended for calibration purposes. Second, the effect of solvation on Fc may not be negligible and may cause a shift in potentials [45]. Therefore, the assumption that the $Fc|Fc^+$ couple is unaffected by solution may not be accurate. Consequently, prior to use of Fc its electrochemistry should be explored in detail to determine if it can be used within the IL system under investigation. A much more serious issue has been explored by Compton and co-workers. This group

Table 7.6 Potentials of ferrocene in selected IL media

Ionic liquid	Compound and concentration	$E_c^{e\prime}$ (mV)	Reference
[BMIm][TFSI]	Fc (various concentrations)	77 vs. Ag|Ag^+ (320 vs. SCE)	[45]
[BMIm][PF_6]	Fc (solid adhered to electrode surface)	+1,332 vs. Cc|Cc^+	[46]
[EMIm][TFSI], [MIMSBu][TFSI], [MIMSEt][TFSI], [MIMSBu][$PO_2(OBu)_2$], [BzSEt][$PO_2(OET)_2$], [mtzSEt][$PO_2(OEt)]_2$, [MIMSEt][OTf], [MIMSBu][OTF], [MIMSEt][PF_6]	3 mM Fc	770 vs. Ag wire QRE	[47]
0.95:1 $AlCl_3$:[ImCl]	20 mM Fc	+654 vs. Ag wire QRE	[48]
0.8:1 $AlCl_3$:[ImCl]	15 mM Fc	+806 vs. Ag wire QRE	[48]
0.6:1 $AlCl_3$:[ImCl]	40 mM Fc	+863 vs. Ag wire QRE	[48]
0.45:1 $AlCl_3$:[ImCl]	50 mM Fc	+863 vs. Ag wire QRE	[48]
[EMIm][BF_4]	4.39 mM Fc	+477–481 vs. Ag|Ag^+| cryptand RE (dependent on electrode material)	[49]
[BMIm][BF_4]	5 mM Fc	+324 vs. SCE	[50]
[BMIm][PF_6]	5 mM Fc	+176 vs. SCE	[50]
[BMIm][BF_4]	1 mM Fc	+375 vs. Ag|AgCl	[51]
[EMIm][TFSI]	1 mM Fc	+230 vs. SCE (reported as $E_{1/2}$)	[52]
[PMIm][TFSI]	1 mM Fc	+258 vs. SCE (reported as $E_{1/2}$)	[52]
[BMIm][TFSI]	1 mM Fc	+270 vs. SCE (reported as $E_{1/2}$)	[52]
[HMIm][TFSI]	1 mM Fc	+250 vs. SCE (reported as $E_{1/2}$)	[52]
[BdMIm][TFSI]	1 mM Fc	+309 vs. SCE (reported as $E_{1/2}$)	[52]
[BuPy][TFSI]	1 mM Fc	+280 vs. SCE (reported as $E_{1/2}$)	[52]
[BuPy][BF_4]	1 mM Fc	+370 vs. SCE (reported as $E_{1/2}$)	[52]
[BMIm][BF_4]	1 mM Fc	+370 vs. SCE (reported as $E_{1/2}$)	[52]
[BMIm][PF_6]	1 mM Fc	+270 vs. SCE (reported as $E_{1/2}$)	[52]
[C_4mpyr][TFSI]	5 mM Fc	−390 vs. Ag|AgOTf| C_4mpyrTFSI	[24]
[EMIm][OTf]	5 mM Fc	−416 vs. Ag|AgOTf| C_4mpyrTFSI	[24]
[BMIm][BF_4]	5 mM Fc	−418 vs. Ag|AgOTf| C_4mpyrTFSI	[24]
[EMIm][$EtSO_4$]	5 mM Fc	−432 vs. Ag|AgOTf| C_4mpyrTFSI	[24]
[C_4mpyr][BOB]	5 mM Fc	−401 vs. Ag|AgOTf| C_4mpyrTFSI	[24]

Table 7.7 Potentials of ferrocene derivatives in selected IL media

Ionic liquid	Compound and concentration	E_c^e (mV)	Reference
[EMIm][TFSI]	3 mM [FcC_1MIm][TFSI]	−263 V vs. $Ag\|Ag^+$	[55]
[BMIm][PF_6]	$Fe(CpCH_3)_2$ (solid adhered to electrode)	+1,233 vs. $Cc\|Cc^+$	[46]
[BMIm][PF_6]	$Fe(CpCOCH_3)_2$ (solid adhered to electrode)	+1,813 vs. $Cc\|Cc^+$	[46]
[BMIm][PF_6]	CpFeCpCOH (solid adhered to electrode)	+1,627 vs. $Cc\|Cc^+$	[46]
[BMIm][PF_6]	$Fe(Cp(CH_3)_5)_2$ (solid adhered to electrode)	+856 vs. $Cc\|Cc^+$	[46]
[BMIm][PF_6]	10 mM $CpFeCpCH_2CH_3$	+1,285 vs. $Cc\|Cc^+$	[46]
[EMIm][TFSI], [MIMSBu][TFSI], [MIMSEt][TFSI], [MIMSBu][$PO_2(OBu)_2$], [BzSEt][$PO_2(OET)_2$], [mtzSEt][$PO_2(OEt)_2$], [MIMSEt][OTf], [MIMSBu][OTf], [MIMSBu]Cl	5 mM $Fe(Cp(CH_3)_5)_2$	−510 vs. $Fc\|Fc^+$	[47]
[C_nC_1Im][TFSI] ($n = 2$, 4 or 8)	FcMeOH	250 vs. Ag QRE	[56]
[EMIm][TFSI]	[FcC_1Im][TFSI]	105 vs. $Fc\|Fc^+$	[57]
[EMIm][TFSI]	[FcC_1NMe_3][TFSI]	234 vs. $Fc\|Fc^+$	[57]
[EMIm][TFSI]	[FcC_1C_1Im][TFSI]	168 vs. $Fc\|Fc^+$	[57]
[EMIm][TFSI]	1 mM DmFc	−310 vs. SCE (reported as $E_{1/2}$)	[52]
[PMIm][TFSI]	1 mM DmFc	−260 vs. SCE (reported as $E_{1/2}$)	[52]
[BMIm][TFSI]	1 mM DmFc	−250 vs. SCE (reported as $E_{1/2}$)	[52]
[HMIm][TFSI]	1 mM DmFc	−250 vs. SCE (reported as $E_{1/2}$)	[52]
[BdMIm][TFSI]	1 mM DmFc	−214 vs. SCE (reported as $E_{1/2}$)	[52]
[BuPy][TFSI]	1 mM DmFc	−250 vs. SCE (reported as $E_{1/2}$)	[52]
[BuPy][BF_4]	1 mM DmFc	−30 vs. SCE (reported as $E_{1/2}$)	[52]
[BMIm][BF_4]	1 mM DmFc	−80 vs. SCE (reported as $E_{1/2}$)	[52]
[BMIm][PF_6]	1 mM DmFc	−210 vs. SCE (reported as $E_{1/2}$)	[52]

measurements on ferrocene under a flow of inert gas or increasing temperature show that ferrocene can volatilise from some ILs [53, 54]. Previously Vorotynsev and co-workers have suggested using UV/vis spectroscopy to determine the exact concentration of ferrocene in the IL solution prior to making measurements [45].

Indeed if Eq. (7.9) is to be used to determine the $E_c^{\ominus\prime}$, then it is important to know the exact concentration of ferrocene in order to determine the diffusion coefficients of the oxidised and reduced forms.

These reports would suggest that for some IL systems, ferrocene can be used for calibration of potentials. However, prior to proceeding with this technique it is advisable that the electrochemical response of ferrocene is checked in the IL system under investigation in order to determine if ferrocene can be used. If the ferrocene is not behaving as an ideal reference couple, then use of derivatised ferrocenes or cobaltocene, or alternative redox couples is suggested. There can also be problems with dissolving enough ferrocene in the IL of interest to carry out the cyclic voltammetry. Ferrocene is largely insoluble or only partially soluble in many ILs.

In cases where use of ferrocene is compromised due to poor electrochemical reversibility of chemical reactions with IL functionalities, then some researchers have proposed use of derivatised ferrocenes. A list of either the standard potentials or midpoint potentials for a series of derivatised ferrocenes is given in Table 7.7. In many cases the derivatised ferrocenes show more stable electrochemical response and less reaction with IL components. Consequently, they have been used to calibrate potentials in ILs either as a standard of choice or as a replacement for ferrocene. The methodology in use of these complexes is the same as for ferrocenes. After dissolution of the complexes in the IL, the potential is measured (usually but not limited to voltametric techniques) and from this the $E_c^{\ominus\prime}$ determined and hence calibrate potentials. If the ferrocene or derivatised ferrocene redox processes are in the same potential range as those of the electroactive species, alternative redox couples should be used.

In those instances where use of ferrocenes or derivatised ferrocenes is problematic due to non-ideal electrochemistry of the metallocenes or overlap of potentials with those of electroactive species making potential calibration problematic, the cobaltocene|cobaltocinium couple has been suggested as a reference redox couple [15]. The $Cc|Cc^+$ couple is also an IUPAC recommended redox couple for electrochemical potential calibration [17]. Table 7.8 lists selected data for the $Cc|Cc^+$ couple in IL media. The cobaltocene electrochemical response is similar to that of the ferrocenes and the methodology of calibration is again similar. Many researchers typically use the same voltametric techniques as discussed for the ferrocene and derivatised ferrocene couples to determine the $E_c^{\ominus\prime}$ value for the $Cc|Cc^+$ couple.

An alternate redox reference compound to metallocenes has been proposed by Compton and co-workers [25]. The redox chemistry of *N*,*N*,*N*′,*N*′-tetramethyl-*p*-phenylenediamine (TMPD) is two electron transfer processes as shown below:

$$\mathrm{TMPD} \rightleftarrows \mathrm{TMPD}^{+\bullet} + \mathrm{e}^- \tag{7.10}$$

$$\mathrm{TMPD}^{+\bullet} \rightleftarrows \mathrm{TMPD}^{2+} + \mathrm{e}^- \tag{7.11}$$

Table 7.8 Potentials of cobaltocene in selected IL media

Ionic liquid	Compound and concentration	$E_c^{e\prime}$ (mV)	Reference
[BMIm][PF_6]	10 mM $CcPF_6$	−1,146 vs. Ag|Ag + QRE	[46]
[EMIm][TFSI], [MIMSBu][TFSI], [MIMSEt][TFSI], [MIMSBu][$PO_2(OBu)_2$], [MIMSEt][OTf], [MIMSBu][OTf], [MIMSEt][PF_6], [MIMSBu]Cl	Cc	−1,340 vs. Fc|Fc+	[47]
[EMIm][BF_4]	5.13 mM $CcPF_6$	−608 to 858 vs. Ag|Ag^+|cryptand (reported as $E_{1/2}$ dependent on electrode material)	[49]
[C_4mpyr][TFSI]	5–100 mM $CcPF_6$	−1,737 to −1,706 (reported as $E_{1/2}$ dependent on electrode material)	[18]

Table 7.9 Potential of TMPD vs. Ag|10 mmol Ag^+ or calibrated to the $Cc|Cc^+$ couple

Ionic liquid	$E_{1/2}$ vs. $Ag|Ag^+$ (mV)	$E_{1/2}$ vs. $Cc|Cc^+$ (mV)
[EMIm][TFSI]	167	1,076
[BMIm][TFSI]	498	1,069
[C_4mpyr][TFSI]	186	1,088
[$N_{6,2,2,2}$][TFSI]	242	1,079
[BMIm][BF_4]	166	1,093
[BMIm][PF_6]	183	1,092

All potentials determined from cyclic voltametric measurements

The first redox process has been determined to be reversible in [C_4mpyr][TFSI], [$P_{6,6,6,14}$][TFSI], [C_{10}MIm][TFSI] and [EMIm][TFSI] and has a faster rate of electron transfer then the $Ag|Ag^+$ couple in [C_4mpyr][TFSI] [25]. In a variety of ILs investigated by Compton et al., the potential of this process [Eq. (7.10)] against $Cc|Cc^+$ and the $Ag|Ag^+$ reference is shown in Table 7.9.

As can be seen from Table 7.9, the potential difference between the $Cc|Cc^+$ couple and the TMPD first redox process is constant for the ILs tested. The approximate 20 mV shifts observed are most likely due to experimental uncertainties. Thus, the TMPD complex offers an alternative to the ferrocene or cobaltocene couples for reference potential calibration. If the potential of the TMPD couple is close to that of the electroactive species, then use of the *bis* (phenyl)chromium(I) tetraphenylborate (BCr) redox couple with ILs has also been proposed by Lewandowski et al. [49]. Studies of this redox reference compound in [EMIm][BF_4] show that it has a stable potential at +0.236 to +0.248 V vs. $Cc|Cc^+$ (range dependent on electrode material) [49].

Experimentally, both the TMPD and BCr complexes potentials are determined from solutions of <10 mM in the IL using voltametric techniques. The electroactive species is then referenced to the determined potentials of the reference couple.

An alternative reference couple based on the $I^-|I_3^-$ couple has been used by Bonhôte and co-workers [58] and also Matsumoto and co-workers [59, 60] to evaluate the electrochemical windows of a range of ionic liquids. This reference electrode was calibrated to the ferrocene couple in [EMIm] trifluoroacetate and found to have a potential of −0.195 V vs. $Fc|Fc^+$ [58]. Experimentally this reference electrode is constructed by dissolution of 15 mM I_2 and 60 mM NPr_4I in an ionic liquid and electrical connection via an inert Pt wire. The reference solution and Pt wire are separated from the electroactive species via use of a fritted glass tube.

7.3.3 *Moderate or High Temperature Ionic Liquid Reference Electrodes*

Thus far we have discussed reference electrodes that have been used primarily at room temperature or close to room temperature. However, there are many IL systems that exhibit liquidus ranges starting above room temperature. This increase in operating temperature poses significant problems for choice of reference electrode. Thus, far the majority of literature reports have used quasi-reference electrodes based on metallic wires. Indeed calibration of these reference potentials is complicated by the increase in temperature. If the temperature is suitably high enough, then use of metallocenes such as ferrocene is not possible due to evaporation of ferrocene from the IL medium. Compton and co-workers have shown that if the temperature is increased, then ferrocene evaporation can take place at a rate dependent on operating temperature (this also occurs under a flow of inert gas, though at a lesser rate) [53, 54]. Indeed this work has shown the rate constants for ferrocene evaporation increase almost fivefold upon increase of temperature from 25 to 37 °C [53, 54].

Similar effects were noted by Bhatt et al. on electrochemical studies of ILs at elevated temperatures [38]. However, the operating temperature of 190 °C meant that only a single voltametric scan of ferrocene could be achieved prior to evaporation, whereas studies at the temperatures investigated by Compton et al., should allow for several more scans albeit with a constantly decreasing ferrocene concentration. Bhatt et al. used the $Li^+|Li^0$ (via dissolution of LiTFSI into the IL) couple in combination with a quasi-reference electrode for calibration purposes. Since at 190 °C, lithium is liquid (hence effects of SEI formation are negligible) and calibration could be achieved. However, as will be shown in the following section, increasing temperature further results in formation of intermetallic complexes, and the electrochemical response of lithium differs at significantly elevated temperatures.

7.3.4 Molten Salt Reference Electrodes

Experimental techniques for handling high temperature molten salts have been developed for many more years than those for room temperature ionic liquids. Considerable experimental challenges need to be overcome to find a stable reference electrode that will survive high temperatures (often up to 1,000 °C) and highly corrosive molten salt environments.

7.3.4.1 Quasi-reference Electrodes for Molten Salts

In the harsh environment of a high temperature molten salt, it is often necessary to resort to quasi-reference electrodes. Examples of this approach include the use of a stable metal or graphite dipped into the molten salt being investigated [61–67]. The use of quasi-reference electrodes rely on a close to constant environment of ions maintaining a similar potential for long periods, i.e. a stable environment of ions in which the potential will not drift significantly with electrolysis time. Of course, long-term stability is rarely achieved and only an approximate indication of potential is usually possible using this strategy. Some of these studies used an internal standard redox couple to determine the initial position of the reference electrode [65–67]. In electrochemical studies, however, there is often a need to use a reference electrode to avoid uncertainty in which electrochemical processes are occurring [68].

7.3.4.2 $Ag|Ag^+$ Reference Electrode for LiCl–KCl Eutectics

For electrochemical studies involving LiCl or LiCl–KCl (eutectic mix) molten salts, generally the reference electrode of choice is a $Ag|Ag^+$ based reference electrode [69, 70]. Typically, this reference electrode is constructed with a silver wire immersed in 1 mol% AgCl in the LiCl–KCl eutectic melt which is contained within the reference electrode casing. However, Shirai et al. [70] suggest that 1–10 mol% is much more stable. Work by this group [70] suggests that the positive shift in potential with prolonged use (typically seen in experiments) is a result of a decrease of the AgCl concentration. The experimental observation of the reference electrode shows a black stain at the closed end of the Pyrex tube as well as dendritic Ag metal growth. The origin of the concentration loss is attributed to the escape of Ag^+ and minute Ag particles into the closed-end tube by ion exchange and absorption or attributed to the reaction between Ag^+ and the O^{2-} in the melt to form silver oxide (Ag_2O) precipitate.

The electrochemical reaction for the $Ag|Ag^+$ reference electrode for molten salt experiments is as follows [70]:

$$Ag^+{}_{(\text{molten salt})} + e^-{}_{(\text{Ag wire})} \rightleftarrows Ag_{(\text{Ag wire})} \tag{7.12}$$

Studies by Shirai et al. [70], look at the temperature dependence of the reversible potential of the reference electrode versus a $Cl^-|Cl_2$ reference electrode (see later section for description of this electrode). They find that the potential is slightly lowered compared to what is theoretically expected by complexation of the Ag^+ ions with the chloride (Cl^-) ions in the melt, which lowers the activity of Ag^+ ions.

This reference electrode is used in other eutectic chloride melts. Another example is $MgCl_2$–NaCl–KCl [71]. Here the reference electrode utilised contained 0.01 mol% AgCl in a LiCl–KCl eutectic. In other words, two different melts were used—where the one in the reference compartment is different to the one in the working compartment. This will create junction potentials, and if the reference electrode is not properly characterised, this will be a problem.

7.3.4.3 Sealed Ag|AgCl Reference Electrode for Calcium Chloride Melts

The typical set-up of a reliable Ag|AgCl reference electrode for molten chloride melts is shown in Fig. 7.5 as a schematic representation. This involves a thinned and sealed lower end of the quartz tube which acts as an ion conducting membrane. This thin wall is achieved using glass blowing while the bottom is in the flame. The wall thickness is controlled by the blowing operation. Above this thin-walled membrane is the much thicker quartz tube. While this tube is still open, a silver wire attached to a longer piece of tungsten wire is inserted within the glass and subsequent to this the electrolyte (typically a mixture of AgCl, NaCl, KCl at a molar ratio of 10:45:45) is added so that it rests in the bottom of the arrangement. This long quartz tube is then sealed (under vacuum) around the tungsten wire in the middle of the tube using a hydrogen–oxygen flame. This means the reference compartment is sealed, which overcomes the problem of the molten chloride volatility. More details of the construction are given in reference [68]. Although the reference electrode is referred to as a Ag|AgCl electrode, technically it is a $Ag|Ag^+$ electrode as there is no AgCl coating on the electrode. However, it is arguable whether the traditional classifications of reference electrodes are applicable to molten salts. This particular reference electrode is affected by the coordination of chloride anions around the silver cations. If the molten salt was a fluoride-based molten salt, the reference potential would be different. This would not be the case, for example, in non-aqueous reference electrodes as, in general, the solvent molecules solvate the silver cation and negate the effect of anions on the potential of the reference electrode.

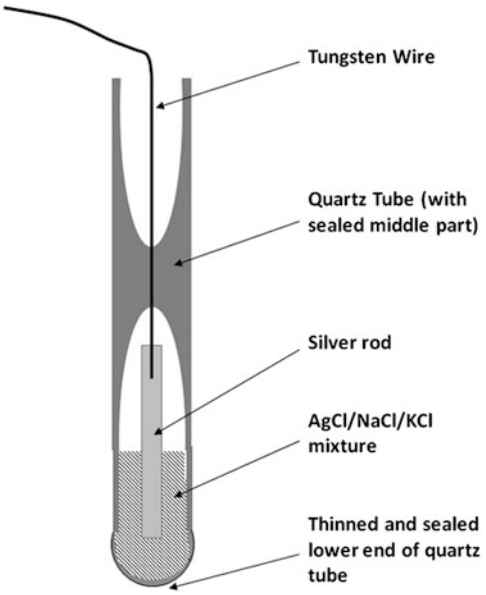

Fig. 7.5 Ag|AgCl reference electrode schematic for chloride baths

This reference electrode system is suitable for use between 700 and 950 °C, below which the reference system has too high impedance (typically above 10^4 Ω) and above which the silver melts ($T_m = 962$ °C). Internal standards are used to measure the stability of the electrode. Here, reduction of silicon dioxide and calcium metal deposition (from Ca^{2+}) can be used as indicator potentials and show that the electrode can give stable potentials for times between hours and days. In practice, while carrying out long electrolysis reactions in chloride melts, the group at CSIRO (Australia) have found that the electrodes typically last about 8 h. This is, however, sufficient to carry out many types of experiments.

The other stability test carried out by Gao et al. [68] was to add AgCl and KCl to a level of 10 wt% to the molten salt melt. These had insignificant effect on the potential of the reference electrode. However, addition of small amounts of NaCl affected the potential of the reference electrode by 0.1522 V per decade. This is related to the changing concentration of Na^+, as well as Ca^{2+}, which indicates conduction of these ions through the membrane and a build up of a junction potential. Multiple reference electrodes constructed by the group [68] (by different workers) resulted in reference electrodes with potentials varying no more than 15 mV but typically with a variance smaller than 8 mV.

7.3.4.4 Li|Li$^+$ Reference Electrodes

Work by Okabe et al. [72, 73] utilises a Li|Li$^+$ reference electrode for the study of additions of Li_3N into molten LiCl at 900 K. This reference electrode was constructed by passing a current of 2 A for 100 s between a nickel sheath cathode

and a graphite anode immersed in LiCl. This results in lithium metal plated in-situ onto the nickel electrode as an intermetallic compound. Further deposition (longer deposition times) would result in growth of Li metal as liquid due to the low melting point of lithium (180.5 °C). In all, these experiments, with addition of Li_3N to the bath the lithium deposition process onto either a nickel or molybdenum working electrode [as described in Eq. (7.13) below], resulted in a reversible potential at 0 V vs. the Li|Li^+ reference electrode [72]. Therefore, the reference electrode was believed to be stable during the measurements.

$$Li^+ + e^- \rightarrow Li(\text{on Ni, Mo}) \tag{7.13}$$

7.3.4.5 Al^{3+}|Al Reference Electrode for Eutectic Chlorides

Another less commonly used reference electrode for eutectic mix chloride melts is the Al^{3+}|Al reference [70], where an aluminium wire is utilised in an $AlCl_3$ (e.g. 0.419 mol%) mixture in the LiCl–KCl salt.

7.3.4.6 $Cl^-|Cl_2$ Reference Electrode for Chloride Melts

A standard reference electrode for chloride melts is shown in schematic form in Fig. 7.6. This is the standard chlorine or $Cl^-|Cl_2$ reference electrode [70, 74, 75]. This electrode is analogous to the standard hydrogen electrode (SHE) for aqueous solutions. Here the gas (Cl_2) is passed over the reference compartment chloride melt at 1 atm (standard pressure), and the potential of the reference system is determined by the ratio of the chloride concentration to the chlorine gas pressure as described in the Nernst equation. As with the SHE this is a difficult reference electrode to maintain and utilise and is consequently less commonly used in modern experiments. In the work by Shirai et al. [70], the reference electrode is used as a standard reference point for measuring other reference electrode potentials. Sometimes the measurements are done using, for example, a Ag|Ag^+ reference electrode and then converted to the standard chlorine scale [76, 77]. This is much like aqueous results being shifted to the SHE scale even though the measurements were not done using this reference electrode.

7.3.4.7 Nickel-Based Reference Electrodes

The Ni–Ni(II) couple is used as a reference electrode because it exhibits Nernstian behaviour [78–80]. However, diffusion of the strongly oxidising Ni^{2+} into the test solution is a problem. This couple can be used in fluoride melts.

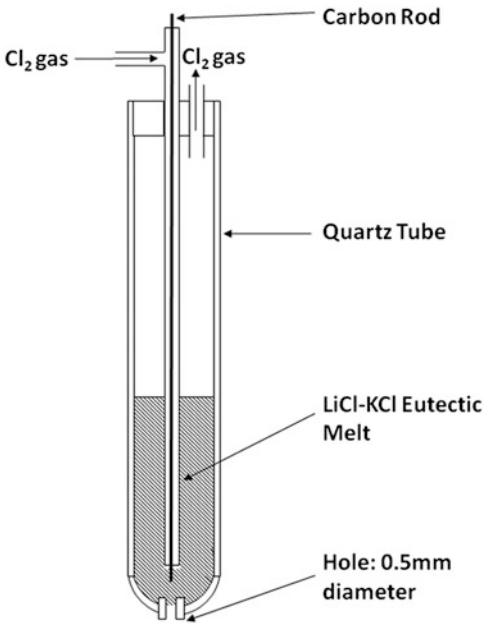

Fig. 7.6 $Cl^-|Cl_2$ reference electrode for chloride eutectics

7.3.4.8 Al_2O_3|Al Reference for Cryolite

Perhaps the most difficult molten salt environment for reference electrode survival and maintenance of key qualities of robustness and stability is sodium cryolite (Na_3AlF_6), often termed the "Universal Solvent". This molten salt is the only solvent that can appreciably not only dissolve alumina (to allow electrowinning of aluminium metal) but also dissolves most other materials used for reference electrode casings. Thus, the reference electrode of choice for this particular molten salt almost invariably is a quasi-reference electrode such as carbon (often the graphite crucible housing the molten salt itself) or a metal (for example molybdenum or tungsten).

However, there have been suggestions in the literature for reference electrodes based on the alumina|aluminium couple. An electrode comprising a molten salt and aluminium was first described by Drossbach [81]. Common types of reference electrodes involve a molten aluminium pool covered by molten cryolite contained within a thin walled tube of sintered alumina or boron nitride. This housing must be electrically insulating but able to transfer ions (i.e. porous and ionically conductive). Also it must be resistive to corrosion. Electrolytes must be in contact and a tortuous path is required such that the different melts do not mix but establish a stable liquid junction.

This requires a medium from which aluminium can be reversibly deposited and stripped and consequently requires some form of cryolite in the reference compartment along with aluminium metal. There are two main types of reference electrodes suggested for aluminium research in cryolite. The distinction between the two types

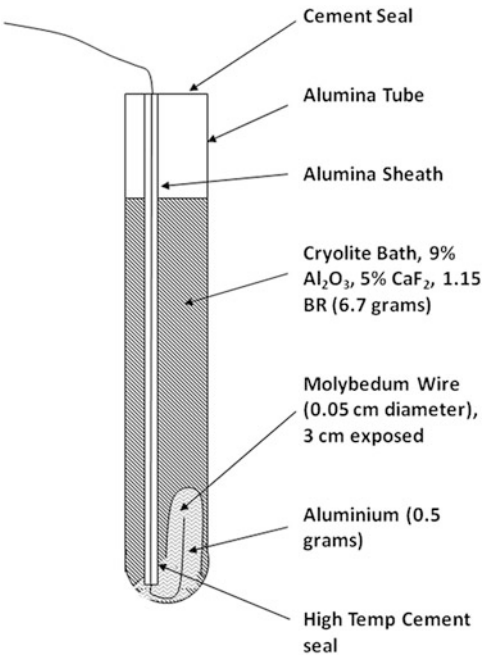

Fig. 7.7 Wetted molybdenum hook (WMH) design reference electrode for cryolite [82]

of reference electrode is based on whether the aluminium rests at the bottom of the cryolite bath (this utilises a standard cryolite bath) and is referred to as the wetted molybdenum hook (WMH) design reference electrode by Burgman et al. [82] (Fig. 7.7) or the aluminium floats above the cryolite bath (this utilises a modified bath of high density) known as the densified bath inverted (DBI) design reference electrode [82] (Fig. 7.8).

The standard bath in the reference electrode by Burgman et al. [82] contains 9 wt % alumina, 5 wt% CaF_2 and a bath ratio (NaF:AlF_3 molar ratio) of 1.15 as shown in Fig. 7.7. The reference potential is established (according to the Nernst equation) by the ratio of the concentration of the saturated Al_2O_3 (~8–9 wt%) and the activity of the aluminium liquid (assumed to be constant and at unity). The mechanism of conversion of Al_2O_3 to Al metal is much debated [83] and involves complex fluoride intermediates, but for simplicity sake the potential can still be considered to be derived from the concentration ratio of alumina to aluminium. This experimental set-up, according to the literature [82], is stable for measurements as long as 8 hours and is reliable to within 5 mV. In this particular work [82] the alumina tube was partially protected from dissolution (alumina is soluble in cryolite) by a surrounding boron nitride block. This alumina tube is found to be porous enough and this combined with the Na^+ content in the alumina means that it can establish a liquid junction and operate as a reference electrode. This so-called wetted molybdenum hook (WMH) design was considered the successful of the two types and is recommended by Burgman et al. [82].

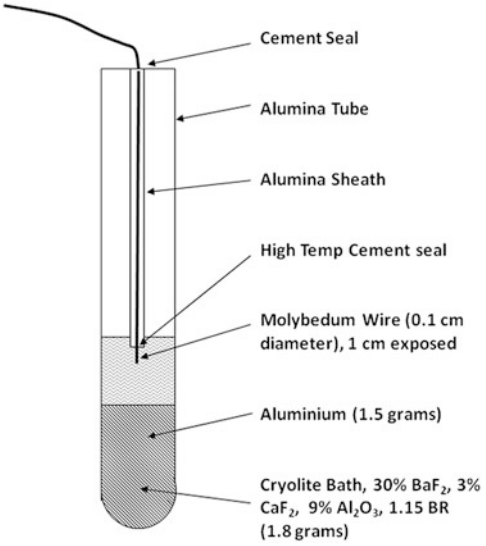

Fig. 7.8 Densified bath inverted (DBI) design reference electrode for cryolite, where aluminium floats above the cryolite bath (modified bath of low density) [82]

The problem with contact between the electrolyte and lead wire is the partial dissolution (e.g. tungsten wire) and the resulting mixed potential that is established. CaF_2 and BaF_2 can be mixed with the bath to increase the density of the bath or Li, Na, K, Ru, Ce, etc. can be mixed with aluminium to lower the density of the metal so that the aluminium liquid floats above the bath material and contact is made between the tungsten wire and the molten Al. The densified bath for the densified bath inverted (DBI) design described in [82] utilises a high BaF_2 content to increase the density above that of the aluminium liquid metal. Again the potential is established by the ratio of alumina to aluminium liquid according to the Nernst equation. This design was found to be stable for measurements as long as 8 hours and was reliable to within 10 mV. This DBI design was not deemed as reliable by the authors [82] as the WMH design. However, the patent by Sadoway et al. [84] which came out at a similar period of time to the work by Burgman et al. [82] claims the best design for an aluminium reference electrode uses a densified bath due to the lack of contact of the cryolite bath with the tungsten wire.

7.3.5 Brönsted Acidic, Lewis Acidic and Distillable IL Reference Electrode Systems

7.3.5.1 Brönsted Acidic Ionic Liquids

Electrochemical measurements using protic or Brönsted acidic ILs as electrolytes have not received as high a research effort as observed for binary or ternary IL systems. Nevertheless, the proton mobility within these systems results in simplification of reference electrodes available for use.

Some researchers have reported on use of a silver wire quasi-reference electrode ($Ag|Ag^+$ couple) [85–87]. Experimentally this is accomplished by direct immersion of the silver wire into the PIL of interest. Bond and co-workers have reported the electrochemical response of cobaltocene and ferrocene in PILs using this reference electrode [85]. They have shown that the $Cc|Cc^+$ couple is -1.34 V vs. $Fc|Fc^+$. However, they do note that the ferrocene can react chemically with the PIL moieties whereas the cobaltocinium cation does not appear to exhibit this reaction on the electrochemical timescale [85].

An alternate reference electrode based on H_2 has also been developed by a number of groups [88–90]. This area is split into two broad sections. The first area is the reversible hydrogen electrode where a platinum wire is inserted into the PIL in a glass tube with a Luggin capillary [88, 89]. Into this reference compartment, H_2 gas is bubbled. Since there are available protons within the PIL, the reference couple becomes the $H^+|H_2$ reference system. The experimental set-up is shown schematically in Fig. 7.9.

An alternative variation of this reference system is the Pd–H reference electrode [90]. For this system a Pd wire is sealed into a soda glass tube and cycled at 100 mA cm^{-2} in H_2SO_4 (aq) solution to adsorb H_2 onto the surface [91]. After this preparative step, the reference electrode is cleaned in distilled water and placed into the PIL system of interest. This electrode demonstrates stable reference potentials for ca. 24 h and has a reference potential value of +35 mV vs. SHE [90, 91].

An alternate reference system to that of the H_2 electrode is the Ag|AgCl reference electrode. Due to the difference in solvation ability of PILs compared to ILs, the dissolution of halide salts such as KCl is far more readily accomplished. As such some researchers have constructed Ag|AgCl|KCl (saturated in PILs) reference electrode systems [92, 93]. This reference electrode exhibits a very stable potential of 0.216 V vs. SHE [92, 93]. Experimentally the reference electrode is constructed by placing a silver wire with a AgCl surface layer into a reference compartment containing a saturated solution of KCl in the PIL of choice.

7.3.5.2 Lewis Acidic or Basic Ionic Liquids

Ionic liquids based on chloroaluminates (the most common form of Lewis acidic or basic ionic liquids) are formed by reacting a quaternary ammonium chloride salt $[QAm]^+$ with aluminium chloride ($AlCl_3$) in various ratios [94]. Common examples are 1-ethyl-3-methyl imidazolium chloride ([EMIm]Cl) and 1-(1-butyl)pyridinium chloride ([BuPy]Cl) [95]. A Lewis base, neutral species or acid is formed by varying the ratio of the two components of the ionic liquid. Using the letter N to represent the mole fraction of $AlCl_3$ in the melt [96], the following classification is given for these ionic liquids:

$N < 0.5$: Lewis base, excess chloride from QAmCl present
$N = 0.5$: Neutral, with $[QAm]^+$ and $[AlCl_4]^-$ present

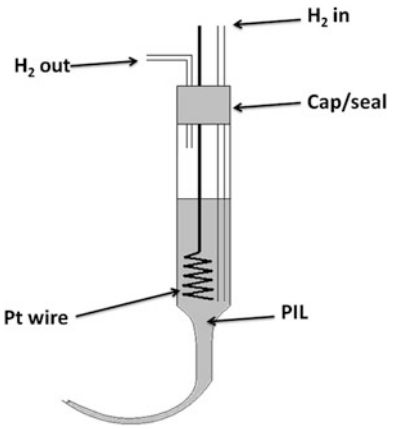

Fig. 7.9 Diagram of a reversible hydrogen electrode for PIL electrochemistry [88]

$N > 0.5$: Lewis acid, with $[AlCl_4]^-$ present along with polymeric forms such as $[Al_2Cl_7]^-$ and $[Al_3Cl_{10}]^-$

The most commonly used reference electrodes in these IL types have used a fritted compartment with an aluminium wire dipped into a melt with a fixed N value. Literature examples [96–103] commonly use an aluminium wire in an $N = 0.60$ (acidic melt) ionic liquid, which is also referred to as a 1.5:1.0 QAm^+: $AlCl_3$ ratio. A slight variation in the reference half-cell with 66.7 mol% of $AlCl_3$ was used to match the melt of interest in work by Xu et al. [95]. In all cases, a major aluminium species in the melt is $[Al_2Cl_7]^-$ from which aluminium can be deposited and stripped off from the wire. This means the electrode is a reference electrode of the first kind ($M|M^{x+}$) or ($Al|Al^{3+}$).

7.3.5.3 Distillable Ionic Liquids

Distillable ILs are formed from combination of CO_2 (or in principle other gases) and dialkyamines to form dialkycarbamates. In a correct stoichiometric ratio of CO_2 to amine, simple dialkycarbamate salts are formed [13]. However, if the CO_2 is limited then a liquid is formed which has the properties of ionic liquids but is readily volatile at low temperatures and can be distilled [13]. Typically electrochemical measurements in this class of IL is performed using silver wire quasi-reference electrodes separated from the electroactive species via a salt bridge [13, 14, 104–106]. Potential calibration is then performed using either cobaltocene or decamethylferrocene. The formal potentials of Cc and Fc in a variety of dILs are shown in Table 7.10. Ferrocene is not used in calibration of the quasi-reference electrode in DIMCARB as it has been shown to react with the dIL components.

Table 7.10 Formal potentials of $Cc^+|Cc^0$ and $Fc^+|Fc^0$ in distillable ionic liquids against an $Ag|Ag^+$ quasi-reference electrode

Distillable ionic liquid	$E_c^{\ominus\prime}$ of $Cc\|Cc^+$	$E_c^{\ominus\prime}$ of $DmFc\|DmFc^+$	References
DIMCARB	−613	238	[14]
DIMCARB	−602	238	[13, 104]
DIECARB	−682	280	[14]
MEETCARB	−668	270	[14]
MEPRCARB	−666	284	[14]

7.4 Considerations for Constructing Reference Electrodes for Ionic Liquid/Molten Salt Electrochemical Measurements

As with the reference electrode configurations for molecular solvents, it is generally recommended that a separated/fritted reference half-cell be used in all reference electrode configurations for ionic liquids (see also Chap. 4). This separation ensures that, even in the case of a quasi-reference electrode, the solution surrounding the metal wire will remain relatively constant, allowing a stable reference potential to be established. As minimal current will flow through this separate fritted half-cell, there will be minimal change in concentration in this half-cell solution. Ionic liquids tend to be much more viscous than molecular solvents such as acetonitrile or water. Consequently, wetting of the frit of the reference electrode half-cell with IL can be slow in the case of the commonly used Vycor® tip and may take over 24 h when starting from a dry state. In contrast, ultrafine porous glass frits can wet in $<$10 min. This feature may lead to the recommendation of the use of such frits when using ionic liquids [24]. However, the risk of contamination and leaking of solution to the working compartment of the cell is much greater than with Vycor® tips. On balance, the Vycor® tip is superior, as once it is wetted, refreshing of the reference half-cell solution and re-wetting out of the Vycor® tip are relatively rapid.

As previously discussed in this chapter, the physical positioning of the working electrode and reference electrode to minimise the electrode separation and thus to minimise IR_u can be restrictive due to the physical size of the electrode, especially when using macrosized electrodes. For many working electrodes the inert electrode housing itself can be up to several millimetres thick which can impact upon the separation distance (see Fig. 7.3). If consideration is not given to the experimental set-up, it may be difficult to reduce the electrode separation sufficiently to avoid working in the infinite linear R_u region (see Fig. 7.4). Luggin capillaries can be used to alleviate this problem and ensure closer working electrode to reference electrode separation. Using a Luggin capillary, much closer positioning (within 1–5 mm) is possible. However, care needs to be taken to use a capillary that is small enough in diameter that it does not screen the electrode and block part of the current density flowing between the auxiliary and working electrodes.

Experimentally it is best to utilise the same ionic liquid within the reference electrode compartment as also used in the test solution or working electrode compartment. This ensures that junction potentials are kept to a minimum. As

geometry and configuration of the cell changes from experiment to experiment, it is possible for junction potentials to vary in unpredictable ways. Thus, it is best to minimise ΔE_j effects as far as practicable. Using the same ionic liquid can be restrictive when, for example, a range of ionic liquids are being investigated. However, in all instances, it is advisable to fully characterise the reference electrode of choice, using a reference compound (such as ferrocene or cobaltocinium). Often, this will need to be done before or after the experiment to ensure the reference electrode is functioning properly and to ensure that any electrode drift effects are taken into consideration when evaluating experimental data.

When operating at higher temperatures with ILs, the choice of reference electrode systems is limited as stated above. Hence, a suitable reference couple must be chosen which is stable over the temperature range of experimentation. Similar to the lower temperature versions, the reference electrode should be separated from the electroactive species by use of a salt bridge. The choice of frit material is crucial as conventional frits such as Vycor® can experience problems at elevated temperatures. However, glass frits should be stable for most applications. Prior to running measurements, it is important to allow sufficient time for the reference electrode and salt bridge to calibrate to the operating temperature. Ideally, the reference electrode should be calibrated to a suitable reference couple in order to allow accurate determination of potentials. The choice of reference couple will be dependent on the operating temperature. However, if metallocenes are used, the volatility of these should be checked prior to calibration.

In the case of PILs, choice of reference electrode is simplified. As shown in Sect. 7.3.5.1 the Ag|AgCl|$KCl_{(PIL)}$ reference electrode appears to be suitable for use and shows stable reference potentials. Alternatively, the $H_2|H^+$ reference electrode can be used; however, care should be taken when using H_2 gas. Since well defined reference systems are available the use of quasi-reference electrodes is not recommended. For Lewis acidic ILs the $Al|Al^{3+}$ reference electrode has been shown to be suitable for use in a large variety of systems; hence, it is recommended that this reference electrode be used as a standard.

In molten salt electrochemistry all reference electrodes face similar issues due to the elevated temperatures of operation. Mostly, this is due to the type of electrode casing materials used for construction of the reference electrode. Thus, for molten salts operated between 450 and 600 °C, sodium glass (or pyrex) can be sufficient as the electrode housing (encasing) [9]. This is easily fabricated into thin walled (ion conducting) junctions, using conventional glass blowing techniques. However, due to the melting temperature of 820 °C, the use is precluded above around 600 °C due to softening and deformation of the glass. Ionic conduction through the glass membrane is typically achieved with the sodium ion content in the glass.

For higher temperature applications (up to 1,200 °C), quartz is commonly used, which begins to soften at around 1,400 °C. However, as was seen with the Ag|AgCl reference for chloride melts employed by Gao et al. [68], the lower temperature use (below 700 °C) was limited due to the high impedance (~4×10^5 Ω) of the reference electrode. The thickness of the end-wall is such that insufficient ionic conduction at temperatures below 750 °C is common. The majority of potentiostats

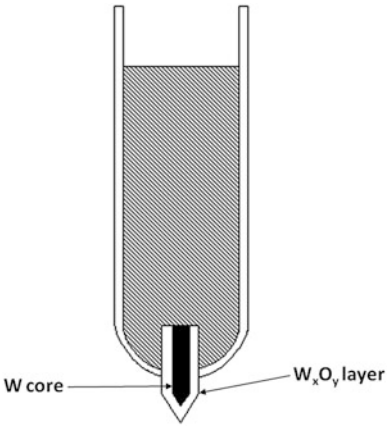

Fig. 7.10 Tungsten tip junction for molten salt reference electrodes

do not provide a stable response when high reference electrode impedance is encountered resulting in extremely noisy voltammograms.

In work by Park et al. [69], it is suggested that a tungsten tip junction, which contains a porous metal oxide layer for ionic conduction, can overcome this problem at temperatures between 450 and 600 °C. A schematic of this reference electrode junction is shown in Fig. 7.10. Here the tungsten wire which is embedded in the quartz tube is oxidised to tungsten oxide. The tungsten oxide is much more porous (with a density of 7.16 g cm^{-3}) compared to the tungsten metal (with a density of 19.35 g cm^{-3}). Consequently, the tungsten oxide layer (formed in the melt) allows an ionic conduction pathway for ions across the reference electrode liquid junction. In electrochemical measurements in which the stability over time of this type of reference electrode casing was measured, it was found that these electrodes were stable at 700 °C for over 12 h [69].

For work in fluoride melts, such as cryolite [82] and LiF–NaF–KF (FLINAK) [80], boron nitride has been suggested as a reference electrode containment material. In work by Kontoyannis et al. [80], pyrolytic boron nitride is slowly impregnated by the melt to provide ionic contact. Boron nitride has a resistivity of about 2.3×10^{10} Ω cm at 500 °C [78]. However, it becomes ionically conductive as it is impregnated with the molten salt, thus providing good ionic contact between the two half-cells while limiting diffusion between them. This encasing was used successfully between 500 and 550 °C [80]. At higher temperatures the BN tends to degrade and mixes into the melt. Also, boric oxide binders used in the tube will dissolve and change the electrode potential via contamination of the melt. In this same work [80], it is suggested that a boron nitride-coated graphite container is used as the reference compartment. The bottom is left free with the rest of the container electrically insulated by the boron nitride.

Finally, in the past [107, 108], a sodium ion conducting porcelain reference electrode casing has been suggested. These can be used to much higher temperatures than glass (1,000 °C) and was typically composed of 2.5 % Na_2O,

73.1 % SiO_2 and 24.4 % Al_2O_3 by weight. A major problem with these types of casings is the durability; they are quite fragile.

7.5 Conclusions

As has been shown in the preceding sections, there is no universal reference electrode system which works for all kinds of molten salts or ionic liquid electrochemistry. Indeed the reference electrodes that can be used are dependent upon the solvent system. Consequently, careful consideration should be made for choice of reference electrode and thought given to its use within the solvent system under investigation.

Prior to use of any reference electrode system for molten salts or ionic liquids, the electrode must be characterised fully in the solvent and calibrated. The reference electrode selection criteria are the same as found for non-aqueous electrodes (see Chaps. 3 and 6), and the final choice of reference system must also follow those guidelines of stability with time (no drift in potential) and temperature (stable over the operating range to be used), and it should be reproducible and convenient to use. In the case of ionic liquids, much work still needs to be performed in order to fully characterise reference electrode systems that can be used.

References

1. MacFarlane DR, Seddon KR (2007) Aus J Chem 60:3
2. Wasserschied P, Welton T (eds) (2003) Ionic liquids in synthesis. Wiley-VCH, Germany
3. Greaves TL, Drummond CJ (2008) Chem Rev 108:206
4. Boon JA, Levisky JA, Pflug JL, Wilkes JS (1986) J Org Chem 51:480
5. Ohno H, Fukumoto K (2007) Acc Chem Res 40:1122
6. Katritzky AR, Yang H, Zhang D, Kirichenko K, Smiglak M, Holbrey JD, Reichert WM, Rogers RD (2006) New J Chem 30:349
7. Pelton AD, Skeaff JM, Bale CW, Lin PL (1982) Can J Chem 60:1664
8. Robelin C, Chartrand P, Pelton AD (2004) J Chem Thermodyn 36:683
9. Gabriel S (1888) Ber 88:89
10. Duan Z, Gu Y, Deng Y (2006) Catal Commun 7:651
11. Li C, Liu W, Zhao Z (2007) Catal Commun 8:1834
12. Wilkes JS, Levisky JA, Wilson RA, Hussey CL (1982) Inorg Chem 21:1263
13. Bhatt AI, Bond AM, MacFarlane DR, Zhang J, Scott JL, Strauss CR, Iotov PI, Kalcheva SV (2006) Green Chem 8:161
14. Wang H, Zhao C, Bhatt AI, MacFarlane DR, Lu AM, Bond J-X (2009) ChemPhysChem 10:455
15. Barrosse-Antle LE, Bond AM, Compton RG, O'Mahony AM, Rogers EI, Silvester DS (2010) Chem Asian J 5:202
16. Ives DJG, Janz GJ (1961) Reference electrodes theory and practice. Academic, London
17. Gritzner G, Kuta J (1982) Pure Appl Chem 54:1527

18. Sukardi SK, Zhang J, Burgar I, Horne MD, Hollenkamp AF, MacFarlane DR, Bond AM (2008) Electrochem Commun 10:250
19. Bond AM, Oldham KB, Snook GA (2000) Anal Chem 72:3492
20. From the MSDS and data listed on the Aldrich website. http://www.aldrich.com. Accessed 28 July 2011
21. Zoski CG (ed) (2007) Handbook of electrochemistry. Elsevier, Netherlands
22. Katayama Y, Fukui R, Miura T (2007) J Electrochem Soc 154:D534
23. Saheb A, Janata J, Josowicz M (2006) Electroanalysis 18:405 [Erratum: Saheb A, Janata J, Josowicz M (2007) 19:1222
24. Snook GA, Best AS, Pandolfo AG, Hollenkamp AF (2006) Electrochem Commun 8:1405
25. Rogers EI, Silvester DS, Ward Jones SE, Aldous L, Hardacre C, Russell AJ, Davies SG, Compton RG (2007) J Phys Chem C 111:13957
26. Nikitenko SI, Cannes C, Le Naour C, Moisy P, Trubert D (2005) Inorg Chem 44:9497
27. Snook GA, Greaves TL, Best AS (2011) J Mater Chem 21:7622
28. O'Toole S, Pentlavalli S, Doherty AP (2007) J Phys Chem B 111:9281
29. Langmaier J, Samec Z (2007) Electrochem Commun 9:2633
30. Anicai L, Cojocaru A, Florea A, Visan T, Studia Universitatis Babes-Bolyai (2008) Chemia 53:119
31. Basile A, Bhatt AI, O'Mullane AP, Bhargava SK (2011) Electrochim Acta 56:2895
32. Kakiuchi T, Yoshimatsu T, Nishi N (2007) Anal Chem 79:7187
33. Silvester DS, Ward KR, Aldous L, Hardacre C, Compton RG (2008) J Electroanal Chem 618:53
34. Silvester DS, Aldous L, Hardacre C, Compton RG (2007) J Phys Chem B 111:5000
35. Aldous L, Silvester DS, Pitner WR, Compton RG, Lagunas MC, Hardacre C (2007) J Phys Chem C 111:8496
36. Bhatt AI, Snook GA, Lane GH, Rees RJ, Best AS (2010) Application of room temperature ionic liquids in lithium battery technology. In: Torriero AAJ, Shiddiky MJA (eds) Electrochemical properties and applications of ionic liquids. Nova, New York
37. Wibowo R, Ward Jones SE, Compton RG (2009) J Phys Chem B 113:12293
38. Bhatt AI, May I, Volkovich VA, Hetherington ME, Lewin B, Thied RC, Ertok N (2002) J Chem Soc Dalton Trans 24:4532
39. Fang S, Yang L, Wei C, Peng C, Tachibana K, Kamijima K (2007) Electrochem Commun 9:2696
40. Zell CA, Endres F, Freyland W (1999) Phys Chem Chem Phys 1:697
41. Zein El Abedin S, Farag HK, Moustafa EM, Welz-Biermann U, Endres F (2005) Phys Chem Chem Phys 7:2333
42. Campbell JLE, Johnson KE (1995) J Am Chem Soc 117:7791
43. Smolenskii VV, Bove AL, Khokhryakov AA, Osipenko AG (2003) Radiochemistry 45:449
44. NuLi Y, Yang J, Wang J, Xu J, Wang P (2005) Electrochem Solid State Lett 8:C166
45. Vorotynsev MA, Zinovyeya VA, Konev DV, Picquet M (2009) J Phys Chem B 113:1085
46. Hultgren VM, Mariotti AWA, Bond AM, Wedd AG (2002) Anal Chem 74:3151
47. Torriero AAJ, Siriwardana AI, Bond AM, Burgar IM, Dunlop NF, Deacon GB, MacFarlane DR (2009) J Phys Chem B 113:11222
48. Zarpinski ZJ, Song S, Osteryoung RA (1994) Inorganica Chim Acta 225:9
49. Waligora L, Lewandowski A, Gritzner G (2009) Electrochim Acta 54:1414
50. Cruz H, Gallardo I, Guirado G (2008) Electrochim Acta 53:5968
51. Eisele S, Schwarz M, Speiser B, Tittel C (2006) Electrochim Acta 51:5304
52. Bizzarri C, Conte V, Floris B, Galloni P (2011) J Phys Org Chem 24:327
53. Fu C, Aldous L, Dickinson EJF, Manan NSA, Compton RG (2011) Chem Commun 47:7083
54. Fu C, Aldous L, Dickinson EJF, Manan NSA, Compton RG (2011) ChemPhysChem 12:1708
55. Taylor AW, Qui F, Hu J, Licence P, Walsh DA (2008) J Phys Chem B 112:13292
56. Lovelock KRJ, Ejigu A, Loh SF, Men S, Licence P, Walsh DA (2011) Phys Chem Chem Phys 13:10155

57. Taylor AW, Licence P, Abbott AP (2011) Phys Chem Chem Phys 13:10147
58. Bonhôte P, Dias A-P, Papageorgiou N, Kalyanasundaram K, Grätzel M (1996) Inorg Chem 35:1168
59. Matsumoto H, Matsuda T, Miyazaki Y (2000) Chem Lett 12:1430
60. Matsumoto H, Matsuda T, Tsuda T, Hagiwara R, Ito Y, Miyazaki Y (2001) Chem Lett 12:922
61. Mehmood M, Kawaguchi N, Maekawa H, Sato Y, Yamamura T, Kawai M, Kikuchi K (2003) Mater Trans 44:259
62. Schwandt C, Alexander DTL, Fray DJ (2009) Electrochim Acta 54:3819
63. Schwandt C, Fray DJ (2007) Z Naturforsch Sect A-J Phys Sci 62:655
64. Gaur HC, Jindal HL (1968) Curr Sci 37:49
65. Jin XB, Gao P, Wang DH, Hu XH, Chen GZ (2004) Angew Chem Int Ed 43:733
66. Nohira T, Yasuda K, Ito Y (2003) Nat Mater 2:397
67. Chen GZ, Fray DJ, Farthing TW (2000) Nature 407:361
68. Gao P, Jin XB, Wang DH, Hu XH, Chen GZ (2005) J Electroanal Chem 579:321
69. Park YJ, Jung YJ, Min SK, Cho YH, Im HJ, Yeon JW, Song K (2009) Bull Korean Chem Soc 30:133
70. Shirai O, Nagai T, Uehara A, Yamana H (2008) J Alloy Compd 456:498
71. Ghosh S, Vandarkuzhali S, Venkatesh P, Seenivasan G, Subramanian T, Reddy BP, Nagarajan K (2006) Electrochim Acta 52:1206
72. Okabe TH, Horiuchi A, Jacob KT, Waseda Y (2000) Mater Trans JIM 41:822
73. Okabe TH, Horiuchi A, Jacob KT, Waseda Y (2001) J Electrochem Soc 148:E219
74. Novoselova A, Khokhlov V, Shishkin V (2001) In: Nianyi C, Zhiyu Q (eds) 6th international symposium on molten salt chemistry and technology. Shanghai University, Shanghai, Peoples Republic of China, pp 253–256
75. Novoselova A, Shishkin V, Khokhlov V (2010) In Meeting of the NATO-Advanced-Study-Institute, Verlag Z Naturforsch, Kas, Turkey, pp 754–756
76. Caravaca C, Laplace A, Vermeulen J, Lacquement J (2008) J Nucl Mater 377:340
77. Bourges G, Lambertin D, Rochefort S, Delpech S, Picard G (2006) In: 4th topical conference on plutonium and actinides/plutonium futures—the science 2006, Elsevier Science Sa, Pacific Grove, CA, pp 404–409
78. Jenkins HW, Mamantov G, Manning DL (1968) J Electroanal Chem 19:385
79. Jenkins HW, Mamantov G, Manning DL (1970) J Electrochem Soc 117:183
80. Kontoyannis CG (1995) Electrochim Acta 40:2547
81. Drossbach P (1936) Z Elektrochem Angew Phys Chem 42:65
82. Burgman JW, Leistra JA, Sides PJ (1986) J Electrochem Soc 133:496
83. Thonstad J, Fellner P, Haarberg GG, Hives J, Kvande H, Sterten A (2001) In: Aluminium electrolysis: fundamentals of the Hall-Heroult process, 3rd edn. Alumunium, Dusseldorf, pp 186–215
84. Sadoway DR (1988) Massachusetts Inst Technology (Masi), US patent 4764257
85. Zhao C, Burrell G, Torriero AAJ, Separovic F, Dunlop NF, MacFarlane DR, Bond AM (2008) J Phys Chem B 112:6923
86. MacFarlane DR, Meakin P, Sun J, Amini N, Forsyth M (1999) J Phys Chem B 103:4164
87. Rochefort D, Pont A-L (2006) Electrochem Commun 8:1539
88. Noda A, Susan MABH, Kudo K, Mitsushima S, Hayamizu K, Watanabe M (2003) J Phys Chem B 107:4024
89. Nakamoto H, Noda A, Hayamizu K, Hayashi S, Hamaguchi H, Watanabe M (2007) J Phys Chem C 111:1541
90. Bautista-Martinez JA, Tang L, Belieres JP, Zeller R, Angell CA, Friesen C (2009) J Phys Chem C 113:12586
91. Fleischmann M, Hiddleston JN (1968) J Phys E Sci Instrum 1:667
92. Anouti M, Caillon-Caravanier M, Dridi Y, Galiano H, Lemordant D (2008) J Phys Chem B 112:13335

93. Mysyk R, Raymundo-Piñero E, Anouti M, Lemordant D, Béguin F (2010) Electrochem Commun 12:414
94. Snook GA, Bond AM (2010) Reference electrodes for electrochemical studies in room temperature ionic liquids. In: Torriero AAJ, Shiddiky MJA (eds) Electrochemical properties and applications of ionic liquids. Nova, New York
95. Xu XH, Hussey CL (1993) J Electrochem Soc 140:1226
96. Ryan DM, Riechel TL, Welton T (2002) J Electrochem Soc 149:A371
97. Fuller J, Osteryoung RA, Carlin RT (1995) J Electrochem Soc 142:3632
98. Hanz KR, Riechel TL (1997) Inorg Chem 36:4024
99. Piersma BJ, Ryan DM, Schumacher ER, Riechel TL (1996) J Electrochem Soc 143:908
100. Riechel TL, Wilkes JS (1992) J Electrochem Soc 139:977
101. Riechel TL, Wilkes JS (1993) J Electrochem Soc 140:3104
102. Scordiliskelley C, Carlin RT (1993) J Electrochem Soc 140:1606
103. Scordiliskelley C, Fuller J, Carlin RT, Wilkes JS (1992) J Electrochem Soc 139:694
104. Bhatt AI, Bond AM, Zhang J (2007) J Solid State Electrochem 11:1593
105. Bhatt AI, Bond AM (2008) J Electroanal Chem 619–620:1
106. Zhang J, Bhatt AI, Bond AM, Wedd AG, Scott JL, Strauss CR (2005) Electrochem Commun 7:1283
107. Labrie RJ, Lamb VA (1958) J Electrochem Soc 105:C160
108. Labrie RJ, Lamb VA (1959) J Electrochem Soc 106:895

Chapter 8
Reference Electrodes in Oxidic Glass Melts

Friedrich G.K. Baucke

8.1 General

Reference electrodes to be used in oxidic glass melts are either based on the redox system oxygen/oxide or—in more rare cases—on systems metal/metal oxide [1]. Either of them must be constructed so that it yields a constant potential difference between the oxidic melt of interest and the metal parts of the electrode, i.e., it must represent a constant potential, the "reference potential (difference)" between the glass melt of interest and the metal contact of the electrode. In this chapter the first electrode type treated is the oxygen/oxide reference electrode, which is more often applied than the second type, the metal/metal oxide electrode, whose application is more complicated and thus usually less often applied than the oxygen/oxide reference electrode.

8.1.1 Oxygen/Oxide-Based Electrodes

The reference electrode of these oxygen sensors consists of a platinum electrode in a reference gas with defined oxygen partial pressure, which is separated from the melt by a wall of doped zirconia solid electrolyte with unit oxide transport number. Yttria (Y_2O_3) is used as the second oxide (dopant), which renders the doped oxide solid electrolyte more stable than calcium oxide (CaO) and magnesium oxide (MgO), which have also been tried as the second component of the doped ceramic but were found rather unsatisfactory. Practical units applied in laboratory and industrial glass melts consist of a combination of the essential (platinum) electrode and the zirconia electrolyte, which are constructed for easy handling. These units are called

F.G.K. Baucke (†)
Formerly affiliated with SCHOTT AG, Mainz, Germany

G. Inzelt et al. (eds.), *Handbook of Reference Electrodes*,
DOI 10.1007/978-3-642-36188-3_8,

"reference electrodes," "zirconia reference electrodes," or briefly "zirconia electrodes," although the solid electrolyte is only part of the unit. The latter term, however, can quite generally be used as long as the underlying mechanism is clear to the user. This terminology will thus also be applied in this chapter.

It is emphasized, however, that the expression given to the electrodes is not merely a matter of semantics but concerns also the potential differences within the electrodes due to the different materials (e.g., zirconia, platinum, gas with certain oxygen contents) and their arrangements. Thus, the "potential" of a "zirconia electrode" $\varphi_{\text{zirconia electrode}}$, i.e., the Galvani potential difference between the oxygen-bathed platinum electrode and the glass melt, is actually the sum of two Galvani potential differences, i.e., the Galvani potential difference between inner electric potentials (ϕ) of the platinum and the zirconia (wall) and that between the zirconia (wall) and the oxidic melt, as demonstrated by Eq. (8.1),

$$\varphi_{\text{zirconia electrode}} = \left(\phi_{\text{Pt}} - \phi_{\text{ZrO}_2}\right) + \left(\phi_{\text{ZrO}_2} - \phi_{\text{m}}\right) = \left(\varphi_{\text{Pt}} - \varphi_{\text{m}}\right) \tag{8.1}$$

which, under isothermal conditions, reduces to the potential difference between platinum and melt because of the uniform potential of the solid electrolyte (ZrO_2) (Y_2O_3). This, however, is not the case if the zirconia within the electrode is subject to temperature gradients (see below). Also, Eq. (8.1) demonstrates that a zirconia electrode can be understood to be a platinum electrode within a glass melt whose oxygen partial pressure can be arbitrarily changed by outside means.

8.1.2 Construction of Zirconia Electrodes

The basic composition of zirconia electrodes allows (and necessitates) the construction of several different types of electrodes.

The simplest form is the *zirconia tube reference electrode*, whose prototype was already tested by *Besson* [2] and applied in laboratory glass melts by *Plumat* [3]. The cross section of this type presented in Fig. 8.1 shows that the zirconia is arranged as a closed-end tube, which contains a four-bore alumina tube in which three platinum wires are contained: one wire connecting the outside contact in the electrode head to the platinum electrode at the lower end of the tube, and two wires connecting the outside to a thermocouple, which is buried in the zirconia grit at the lower end of the tube so that the temperature of the zirconia grit, which contacts the zirconia tube, is measured at the lower end of the electrode. The reference gas is supplied through the fourth bore (or, alternatively, through one of the other three bores of the alumina tube) to the zirconia grit. The reference gas leaves the grit at the interior of the zirconia tube through the space between the Al_2O_3 and the ZrO_2 tubes and the insulated metal head of the arrangement, which also serves to stabilize the electrode mechanically. The electrochemically active part of zirconia tube electrodes is thus the bottom part of the arrangement and is strictly isothermal. Zirconia tube electrodes thus yield the most accurate results of all constructions developed.

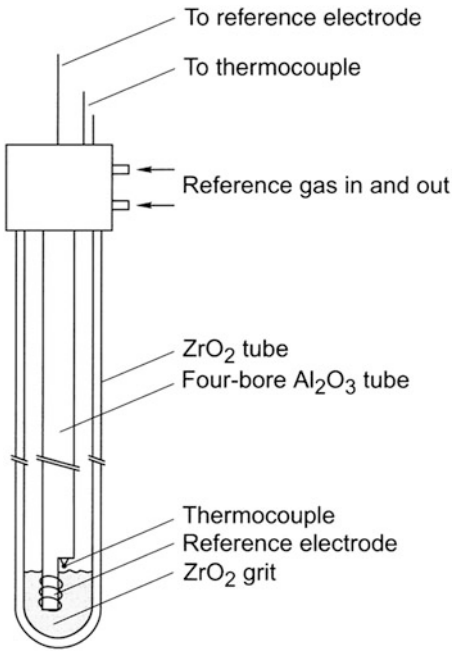

Fig. 8.1 Cross section of zirconia reference tube electrode. Only the bottom part of the zirconia tube contains the platinum contact and the thermocouple both buried in zirconia grit and in intimate contact with the zirconia tube. The reference potential is thus strictly isothermal. Because it is easily broken, the use of the zirconia tube is restricted to laboratory measurements

A basically similar construction is given by the *zirconia disk electrode*. Its inner parts are the same as those of the zirconia tube electrode. The zirconia tube is merely replaced by a platinum tube, which is closed at its lower end by a zirconia disk sintered onto the lower open end of and thus closing the platinum tube. Different from zirconia tube electrodes, this arrangement is rather insensitive to thermal shock. However, it exhibits the phenomenon of "bubble boring" or "bubble drilling" through the horizontal zirconia disk [4] that "captures" gas bubbles at its lower horizontal surface, which, due to their strong movements at the contacting plane of zirconia and melt, dissolve part of the ceramic disk and thus "drill" holes through the zirconia. Bubble drilling through perpendicular ceramic walls is thus less often observed than that through horizontal walls. Perpendicular ceramic walls, however, are not or less often given by zirconia disk electrodes.

8.1.2.1 Zirconia Electrodes with Longer Lifetime

One of the disadvantages of more or less all zirconia electrodes is the rather strong corrosion (or "solubility") of the zirconia ceramics in oxidic melts. This fact prompted us to construct electrode units especially for application in industrial glass melting tanks, which are distinguished by rather long lifetimes despite the relatively high corrosion of the zirconia.

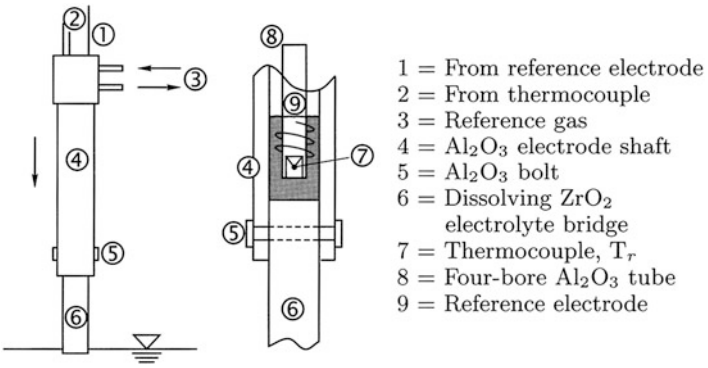

Fig. 8.2 Essential upper part (*left*) and cross section (*right*) of the upper part of a dissolving zirconia reference electrode. The upper part is contained in an alumina tube, which is similar to that shown on the *left side* and closed by the upper end (*right*) of a zirconia rod. The zirconia electrolyte bridge is kept in place by an alumina bolt. The zirconia rod serves as an electrolyte bridge between the upper zirconia and the melt. Its slow dissolution in the melt determines the lifetime of the unit

8.1.2.2 Dissolving Zirconia Electrodes

A dissolving zirconia reference electrode is schematically depicted in Fig. 8.2. It is specifically designed for application in technical (industrial) melting tanks [5–8]. Its considerably longer lifetime compared to, e.g., zirconia tube electrodes is achieved by an ~10–12 cm long electrolyte bridge consisting of a doped zirconia rod, which provides the ionic contact between the upper reference electrode and the surface of the melt and slowly dissolves away at its lower end. The upper end of the rod-shaped electrolyte bridge is inserted into an inert alumina tube where it is kept in place by a horizontal alumina bolt because alumina and zirconia (and doped zirconia) cannot be joined by sintering due to their slightly different coefficients of thermal expansion. However, the mechanical construction necessitates a slight overpressure of the reference gas within the alumina shaft in order to avoid diffusion of gases above the melt through the slits between zirconia rod and alumina electrode shaft and thus a contamination of reference gas and platinum electrode. The perpendicular electrode is continuously or stepwise lowered according to the dissolution rate of the zirconia rod in order to maintain the contact of zirconia rod and melt. Dissolving zirconia electrodes are thus also particularly suited for streaming glass melts which remove traces of dissolved zirconia from the melt near the lower end of the corroding rod and thus eliminate even slight changes of the melt composition near the surface.

8.1.2.3 Temperature Influence

Because, however, the temperatures of glass melt and upper reference electrode at the alumina electrode shaft differ considerably, measuring cells employing

dissolving zirconia electrodes are nonisothermal electrochemical cells as indicated by the electrode scheme, cell (I),

$$\mathrm{Pt, O_2(r)}(T_\mathrm{r})|\mathrm{ZrO_2}|(T_\mathrm{m})\mathrm{melt, O^{2-}, O_2}(T_\mathrm{m})|\mathrm{Pt} \tag{8.I}$$

where T_r and T_m are reference and melt temperature, respectively, and ZrO_2 is the nonisothermal dissolving ZrO_2 electrolyte bridge. As demonstrated by Eq. (8.2), the standard thermoelectric emf, $E_{\mathrm{Th},\mathrm{ZrO_2}}(T_\mathrm{r}, T_\mathrm{m})$, of the zirconia electrolyte must be known for correcting the thermoelectric emf, $E_{\Delta T}(T_\mathrm{r}, T_\mathrm{m})$, along the zirconia bridge in order to obtain the oxygen partial pressure of the melt [5, 6],

$$p_{\mathrm{O_2,m}}(T_\mathrm{m}) = \exp\left\{\frac{4F}{RT_\mathrm{m}}\left[E_{\Delta T}(T_\mathrm{r}, T_\mathrm{m}) - E_{\mathrm{Th},\mathrm{ZrO_2}}(T_\mathrm{r}, T_\mathrm{m})\right] + \frac{T_\mathrm{r}}{T_\mathrm{m}} \ln p_{\mathrm{O_2,r}}\right\}, \tag{8.2}$$

which is assumed isothermal in this equation. This quantity had been measured before when thermoelectric data of molten glasses were thoroughly studied [9, 10].

8.1.2.4 Measurement of the Thermoelectric Power (emf) of Yttria-Doped Zirconias

The thermoelectric emf, $E_{\Delta T}(T_\mathrm{r}, T_\mathrm{m})$, of yttria-doped zirconia, which is applied in Eq. (8.2), must be known with extremely high accuracy if sufficiently correct oxygen partial pressures are to be determined. The accuracy of most literature data, however, turned out to be less accurate to guarantee the degree of accuracy needed for the calculations. In addition, the exact magnitude of the thermoelectric power depends on the exact yttria concentration of the ceramics and on the properties of the individual zirconia charges, such as possible trace impurities and special sintering conditions [9]. It was thus unavoidable to measure and compare the thermoelectric data of all individual zirconia specimens, $ZrO_2(Y_2O_3)$, applied to the construction of the reference electrodes. For this reason we devised a reproducible method of checking each individual zirconia material before its application as electrode material [11].

The principle of these measurements is sketched in Fig. 8.3. The arrangement consists of two zirconia electrodes with 1 bar oxygen partial pressure at different temperatures, which are snugly pressed against the ends of the 10–12 cm long nonisothermal zirconia rod under investigation [9, 10]. Variable temperature profiles of the rod are provided by a specially designed temperature furnace [11], the heating alumina tube of which contains the actual measuring arrangement according to

$$\mathrm{Pt, O_2}(T_1)|\mathrm{ZrO_2\ specimen}|(T_2)\mathrm{Pt, O_2} \tag{8.II}$$

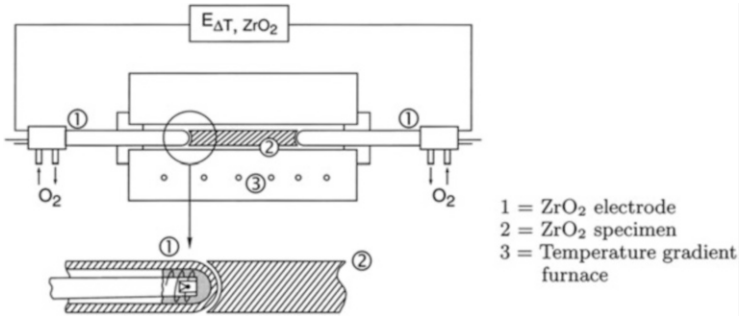

Fig. 8.3 Arrangement for measuring thermoelectric emfs of doped zirconia rods used as zirconia electrolyte bridges. The specimen is clamped between two zirconia electrodes with equal oxygen partial pressure. The zirconia rod is kept in a temperature field due to the specially designed temperature gradient furnace

and thus yields the emf of the ZrO_2 specimen as a function of the temperature difference. Additionally, the temperature gradients can be subdivided and reversed, which increases the accuracy of the measured data by eliminating any asymmetries of the arrangement.

8.1.2.5 Properties of Doped Zirconia Materials

In agreement with the literature, standard Seebeck coefficients of yttria-doped zirconias are independent of temperature and proportional to the molar yttria concentration of the ceramics [10, 12]. For the material most frequently applied during this investigation they can be represented by the linear relationship [11]:

$$\frac{\mathrm{d}E_{\mathrm{Th,ZrO_2}}(T)}{\mathrm{d}T} = ac_{\mathrm{Y_2O_3}} + b, \tag{8.3}$$

where the constants are $a = 4.643 \times 10^{-3}\,\mathrm{mV/(K\,mol\%)}$ and $b = -0.4949\,\mathrm{mV\,K^{-1}}$. For example, the standard Seebeck coefficient of the most frequently applied zirconia composition in this study, i.e., $(ZrO_2)_{0.9547}\ (Y_2O_3)_{0.0453}$, is (-0.4793 ± 0.0015) $\mathrm{mV\,K^{-1}}$ within the temperature range 700–1,550 °C.

8.1.2.6 Zirconia Reference Electrodes with Special Protection Devices

In addition to the electrode specimens described so far, we have constructed four more electrode types.

1. *The corrosion-protected zirconia electrode* is protected from corrosion by a platinum tube around the alumina shaft, which protects the ceramics from condensing vapors of melt components with high vapor pressure. An additional

gutter at the lower end of the Pt tube ensures that condensed liquid compounds of the melt trickle down from the Pt tube to the zirconia and corrode the zirconia electrolyte bridge [13].

2. *The isothermal zirconia electrode* involves a heating device, which keeps the temperature of the reference electrode automatically equal to that of the measuring electrode by means of an additional electronic control unit and thus eliminates thermoelectric voltages in the first place [14].
3. *The contamination-protected zirconia electrode* incorporates a second closed-end zirconia tube within the alumina shaft which is ionically contacted by the electrolyte bridge through zirconia grit and contains the platinum reference electrode, which is thus protected from melt vapors when the overpressure of the reference gas accidentally drops to the pressure of the tank atmosphere [15].
4. *Various designs of a hook-shaped zirconia electrode* with horizontal electrode shaft and perpendicular zirconia electrolyte bridge allow the sensors to be applied through windows in the side walls of glass melting tanks. "Top application" through the melt surface is thus unnecessary by these considerably more practicable constructions [16].

All zirconia reference electrodes described above can be checked for correct functioning by defined changes of the oxygen reference partial pressure, which must be "answered" by the theoretical emf change if the electrode functions correctly. This check can even be accomplished during the application of the electrodes due to the short response times of the Pt, O_2 electrode on changing the oxygen partial pressure.

8.1.3 Metal/Metal Oxide Electrodes: An Alternative Solution

Although dissolving zirconia reference electrodes as described above provide the maximum lifetime possible and a relatively high mechanical stability because of their construction, a small remaining possibility of breakage and corrosion of the ceramic parts, especially in melts with, e.g., a high lead content, made an alternative reference electrode without these disadvantages highly desirable.

8.1.3.1 Discovery and Development of Metal/Metal Oxide Electrodes

Surprisingly, we observed during experiments with metal rods, which were applied as heating electrodes in industrial melters, that, e.g., molybdenum rods, if not applied for heating, i.e., being nonpolarized, exhibited extremely constant potentials. This observation was the beginning of the development of alternative electrodes, i.e., of metal/metal oxide electrodes, which function similarly as do metal/sparingly soluble metal anion electrodes, for instance, silver/silver halide electrodes, in aqueous solutions, and are known as well-behaving reference

electrodes in aqueous solutions. After this discovery, our goal was thus to develop a similar kind of electrode on the basis of our experience, which would be a metal/metal oxide electrode with the favorable properties of molybdenum rods in oxidic melts. This work resulted in an understanding of the stability of the potential of metal/metal oxide systems, as we had observed them in oxidic melts.

8.1.3.2 The Basic Reaction of Metal/Metal Oxide Electrodes in Oxidic Melts

The studied molybdenum rods were actually covered by a thin tight layer of one of their (yellow) oxides, which were in equilibrium with each other during their application for reference purposes. They function thus on the basis of their oxide formation, Eq. (8.III),

$$x\mathrm{M} + y\mathrm{O} \rightleftarrows \mathrm{M}_x\mathrm{O}_y \tag{8.III}$$

and are represented by the electrode scheme $\mathrm{M} \rightleftarrows \mathrm{M}_x\mathrm{O}_y$. If the oxide forms a tight layer at the metal surface, which, after some time, assumes a steady state with relatively small formation and dissolution rates, it represents approximately an equilibrium as indicated by Eq. (8.III), and its equilibrium constant can be written as

$$K(T) = \frac{a_{\mathrm{M}_x\mathrm{O}_y}}{(a_{\mathrm{M}})^x (a_{\mathrm{O}})^y}, \tag{8.4}$$

where a is the activity of the species indicated, and a_{O} is the oxygen activity at the metal/metal oxide phase boundary.

Because both metal and metal oxide are pure condensed phases, and their activities are constant and defined to be unity, the oxygen activity at the phase boundary is fixed by the temperature according to the phase law or, expressed in a different way, its temperature dependence is given by that of the equilibrium constant,

$$a_{\mathrm{O}}(T) = f(K(T)), \tag{8.5}$$

which can be calculated according to (8.6),

$$\frac{\mathrm{d} \ln p_{\mathrm{O}_2(\mathrm{M}/\mathrm{M}_x\mathrm{O}_y)}}{\mathrm{d}(1/T)} = \frac{2\Delta H^{\ominus}}{yR}, \tag{8.6}$$

where $\Delta H^{\ominus}$ is the standard chemical energy of formation of the pure oxide. Melts contacting the oxide can lead to several interferences, for example, chemical reactions with the oxide, formation of additional solid phases, and alloying the metal with reduced metal from the melt. It is thus unavoidable for practical quantitative applications of the electrodes to conduct measurements which either

confirm the absence of interfering reactions or serve as standardizing measurements and yield the "practical $\Delta H^{\Theta\prime}$" for each particular glass melt studied.

Several requirements must thus be met for a satisfactory functioning of metal/metal oxide electrodes. (1) The metal must have a sufficiently high melting point and (2) must not be too inert to allow the oxide to be formed at a sufficient rate; it must, however, (3) be inert enough not to form the oxide at too high a rate so that (4) the lifetime of the electrodes is long enough in the particular melt. (5) The oxide also must have a high melting point, and (6) it must be extremely sparingly soluble in the melt so that, instead of being dissolved after its formation, it forms a steady-state surface layer with a thickness in the range of several atomic dimensions to about 10 nm. For this reason (6) it must be sufficiently tight to ensure that reaction (III) takes place entirely at the phase boundary between metal and oxide after the oxygen has diffused through the layer. Also, (7) it should be a pure oxide ion—or a pure cation conductor for the ideal functioning of the electrode, although the effect of mixed conduction could be taken into account by measurements during the steady state of the electrode.

8.1.3.3 The Main Advantages of Metal/Metal Oxide Electrodes

The main advantage is the absence of ceramic parts so that high corrosion rates and the probability of breakage are excluded. The thermal and mechanical stability enables their introduction and application through the wall and the bottom of technical melters even during the melting process.

A disadvantage, however, is the time-consuming necessity *to standardize the electrodes in each envisaged melt* before their application. This is conducted by means of three different electrodes: a platinum electrode, a zirconia electrode, and the metal/metal oxide electrode to be standardized, which form interconnected electrochemical cells in the oxidic melt of interest.

First, the "standardizing cell" containing the zirconia as the reference electrode has the cell scheme

$$\mathrm{Pt, O_2(r)|ZrO_2|melt, O_2|Pt} \tag{8.IV}$$

exhibits the emf

$$E_1(T) = \varphi_{\mathrm{Pt}}(T) - \varphi_{\text{zirconia electrode}}(T), \tag{8.7}$$

and yields the temperature-dependent oxygen partial pressure of the melt according to

$$E(T) = \frac{RT}{4F} \ln \frac{p_{\mathrm{O_2}}(\mathrm{m})}{p_{\mathrm{O_2}}(\mathrm{r})} \tag{8.8}$$

(m: melt; r: reference).

Second, The "reference cell" according to the cell scheme

$$\mathrm{Pt, O_2(r)|ZrO_2|melt, O_2\big|M_xO_y\big|Pt} \tag{8.V}$$

refers the potential of the metal/metal oxide electrode to that of the zirconia electrode,

$$E_2(T) = \varphi_{\mathrm{M/M_xO_y}}(T) - \varphi_{\text{zirconia electrode}}(T), \tag{8.9}$$

which thus serves as the ultimate reference electrode.

Third, the "measuring cell" containing the metal/metal oxide as the reference electrode and has the cell scheme

$$\mathrm{M\big|M_xO_y\big|melt, O_2|Pt} \tag{8.VI}$$

It is the cell actually to be applied during the practical measurements envisaged and thus yields the emf of interest,

$$E_3(T) = \varphi_{\mathrm{Pt}}(T) - \varphi_{\mathrm{M/M_xO_y}}(T). \tag{8.10}$$

Combination of Eqs. (8.7)–(8.10) finally yields

$$E_3(T) = E_1(T) - E_2(T), \tag{8.11}$$

which shows that either the directly measured emf $E_3(T)$ of the "measuring cell" and the oxygen partial pressure $p\mathrm{O_2}(T)$ obtained from $E_1(T)$ or the measured emf $E_2(T)$ of the "reference cell," the measured emf $E_1(T)$ of the "standardizing cell," and the oxygen partial pressure $p\mathrm{O_2}(T)$ (from $E_1(T)$) yield the isothermal standardization curve $p\mathrm{O_2}(T_\mathrm{m}) = f(E_3(T_\mathrm{m}))$ at any measuring temperature T_m, which is required for the evaluation of the measurements. For application in nonisothermal melts the temperature of measuring and reference electrode and the possibly temperature-dependent Seebeck coefficient(s) of the glass melts must be known and taken into account.

8.1.3.4 Test Application of Metal/Metal Oxide Electrodes

Various metal/metal oxide electrodes were tested in several glass melts with the result that particularly the systems $\mathrm{Mo/MoO_2}$, $\mathrm{W/WO_2}$, and $\mathrm{Ta/Ta_2O_3}$, the metals and oxides of which exhibit the required sufficiently high melting points (see Table 8.1), show good agreement of practical and theoretical thermodynamic data, i.e., standard chemical energies and standard entropies of oxide formation. These results were obtained in sodium calcium silicate glass melts containing antimony as the fining agent as well as in technical glass melts, for instance, in

Table 8.1 Melting points of some metals and their oxides and temperature-dependent free energies of formation of the oxides, which are of interest for application as alternative reference electrodes in glass-forming melts

		$-\Delta G^{\ominus}$ (kJ mol^{-1})			
Melting point (°C)		1,000 K	1,200 K	1,400 K	1,600 K
Ta	2,996				
Ta_2O_5	1,877	1,607	1,523	1,443	1,364
Mo	2,010				
MoO_2	1,927	389			318
W	3,410				
WO_2	1,570	401	367	333	

borosilicate glass melts fined with sodium chloride. Molybdenum showed the least corrosion, which appeared as thin yellow surface layers. The electrodes did not cause any technical problems during several weeks of application. The logarithm of the equilibrium oxygen at the partial pressure at the metal/metal oxide interfaces is a linear function of the reciprocal absolute temperature. It ranges from approximately $\log p_{O_2} = -15$ at 1,000 °C to $\log p_{O_2} = -8$ at 1,600 °C in the cases of molybdenum/molybdenum oxide and tungsten/tungsten oxide and from $\log p_{O_2} = -22$ at 1,000 °C to $\log p_{O_2} = -12$ at 1,600 °C with tantalum/tantalum oxide. These results promise a general application of metal/metal oxide electrodes in technical glass melters in the future in parallel to the well-established use of zirconia electrodes for research purposes in laboratories and for the standardization of the alternative electrodes.

8.1.3.5 The Essential Steps of the Development of Reference Electrodes for Use with Oxygen-Indicating Electrodes

The first electrodes were based on calcia- and magnesia-stabilized zirconia tubes, respectively, and were applied for short-time activity measurements in molten steel and slags in the steelmaking industry. As with the alternative electrodes for glass melts just described, the reference oxygen partial pressure of these electrodes was fixed by a metal/metal oxide system, for instance, iron/iron oxide, nickel/nickel oxide, cobalt/cobalt oxide, chromium/chromium oxide, and others, which were contained in the zirconia tubes. These first electrodes actually represented combinations of zirconia tube electrodes and the alternative metal/metal oxide electrodes contained in the zirconia tubes. Their oxygen partial pressure was fixed by a solid state reaction (metal/metal oxide) but the lack of suitable properties of these oxides, i.e., chemical inertness with respect to glass melts, and tightness and a sufficient ionic conductivity of thin layers of the oxides necessitated an additional protecting and oxide ion-conducting solid electrolyte, for instance, zirconia, between the reference system and the glass melt. Incidentally, at the early stages of our development, zirconia electrodes with nickel/nickel oxide and with cobalt/cobalt oxide reference systems were also tested for applicability in glass melts. However, they were found unsuited for long-term application because of the

rather limited lifetime of the metal/metal oxide reference systems, which is caused by the relatively high oxygen partial pressures at high temperatures, and result in a fast decomposition of the fine-grain oxides and the following fast exhaustion and loss of their oxygen content.

8.1.3.6 The Three Preferable Reference Electrodes for Use in Oxidic Melts

As a consequence of these studies, three alternative reference electrodes with particular properties and fields of applicability can be recommended.

First: *zirconia tube electrodes* employ a reference gas (and an outside determined source of oxygen). An advantage is thus a temperature-independent reference oxygen partial pressure and a strictly isothermal functioning. A disadvantage, on the other hand, is their temperature shock sensitivity due to the fragility of the ceramic tube. Zirconia tube electrodes are thus *the choice* in research and development and even *the only choice* if standard Seebeck coefficients of glass melts are to be determined [17].

Second: *dissolving zirconia reference electrodes* also employ a reference gas with temperature-independent oxygen partial pressure. Also, they employ a rather sturdy electrolyte bridge (doped zirconia rod) between upper Pt electrode and melt surface. The electrolyte bridge, however, introduces the additional problem of temperature-dependent measurements of standard Seebeck coefficients and a material check of each zirconia specimen (rod) before its use. Due to the electrolyte bridge, the lifetime of dissolving reference electrodes is much longer than that of zirconia tube electrodes and thus also well suited for industrial melters.

Third: *metal/metal oxide electrodes, particularly molybdenum, tungsten, etc. oxides* offer the advantage of extremely high mechanical stability. They can be inserted into the hot glass melt without any danger of breakage. The number of useful metals, however, is rather limited. Another disadvantage is the cumbersome and time-consuming standardization of the electrodes with respect to other (zirconia) electrodes before application in each envisaged oxidic melt.

References

1. Baucke FGK (2001) Reference electrodes. In: Bach H, Baucke FGK, Krause D (eds) Electrochemistry of glasses and glass melts, including glass electrodes. Springer, Berlin, p 308
2. Besson J, Deportes C, Darcy M (1960) Compt Rend Acad Sci 251:1630–1632
3. Plumat E, Toussaint F, Boffe M (1966) J Am Ceram Soc 49:551–558
4. Schaeffer HA, Frey T, Löh I, Baucke FGK (1982) J Non-Cryst Solids 49:179–189
5. Baucke FGK (1992) High-temperature sensors for oxygen glass-forming melts. In: Göpel W, Jones TA, Kleitz M, Lundström I, Seiyama T (eds) Sensors. A comprehensive survey. Chemical and biochemical sensors, part II, vol 3. Wiley-VCH, Weinheim, pp 1155–1180
6. Baucke FGK (1983) Glastechn Ber 56K:307–312
7. Baucke FGK, Röth G (1987) Sonde zur Messung von Sauerstoffpartialdrücken in hochaggressiven Medien. DE 3109454

8. Baucke FGK, Röth G (1985) Sauerstoffsonde unter Verwendung eines nichtleitenden Keramikrohres. DE G8513976
9. Fridman SL, Pal'guev SF, Chebotin VN (1969) Elektrokhimiya 5:357–358
10. Fischer W (1967) Z Naturforsch 22a:1575–1581
11. Veith JA (1983) Ermittlung von Standard-Seebeck-Koeffizienten von Yttrium-dotierten Zirkonoxid-Keramiken zwischen 700 °C und 1500 °C. Diploma-thesis, FH-Rheinland-Pfalz, Bingen
12. Pizzini S, Riccardi C, Wagner V, Sinistri C (1970) Z Naturforsch 25a:559–565
13. Baucke FGK, Röth G, Werner R-D (1989) Messvorrichtung zum Messen des Sauerstoffpartialdruckes in aggressiven Flüssigkeiten hoher Temperatur. DE 3811865
14. Baucke FGK, Röth G, Werner R-D (1990) Messvorrichtung zum Messen des Sauerstoffpartialdruckes in aggressiven Flüssigkeiten hoher Temperatur. DE 3811864
15. Baucke FGK, Röth G, Werner R-D (1990) Messvorrichtung zum Messen des Sauerstoffpartialdruckes in aggressiven Flüssigkeiten hoher Temperatur. DE 3811915
16. Baucke FGK, Röth G (1993) Referenzelektrodenanordnung einer Messkette zur Messung des Sauerstoffpartialdruckes in aggressiven Medien von hoher Temperatur. DE 4138409
17. Baucke FGK (2001) Non-isothermal glass forming melts. In: Bach H, Baucke FGK, Krause D (eds) Electrochemistry of glasses and glass melts, including glass electrodes. Springer, Berlin, pp 367–384

Chapter 9
Reference Electrodes for Solid-Electrolyte Devices

Vladislav V. Kharton and Ekaterina V. Tsipis

9.1 Introduction

Solid electrolytes are a class of solids where electrical conduction occurs predominantly via migration of ions and the overall level of ionic transport is high enough for practical applications, whilst electronic contribution to the total electrical conductivity is negligible. This term is commonly used for the materials with ion transport numbers (t_{ion}) equal to or higher than 0.99 under given external conditions. The range of conditions (temperature, pressure, and thermodynamic activities of components) where $t_{ion} \geq 0.99$ is often called the electrolytic domain. A large number of solid electrolytes (SEs) with mono-, bi-, and trivalent ion charge carriers are known. The groups important from the practical point of view include [1–5]:

(i) Solids with fast diffusion of monovalent cations (Li^+, Na^+, K^+, Ag^+, Cu^+, etc.), which find their applications in many types of batteries, sensors, fuel cells, accumulators, alkali-metal thermal to electric converters (AMTECs), and electrochromic and ionic memory devices. Examples are the families of β-alumina and NASICON ($Na_{1+x}Zr_2Si_xP_{3-x}O_{12}$), their analogues and derivatives where almost all alkaline-metal cations and protons may have high mobility, numerous alkaline-metal salts, and also oxide, halide, sulfide, and nitride compounds such as Li_4SiO_4, Li_2SO_4, Li_3N, KMO_2 (M = Al, Ga, Fe), $KAlSi_2O_6$, AgI, CuI, $RbAg_4I_5$, and $Rb_4Cu_{16}I_7Cl_{13}$.

V.V. Kharton (✉)
Department of Materials and Ceramic Engineering, CICECO, University of Aveiro, 3810-193 Aveiro, Portugal
e-mail: kharton@ua.pt

E.V. Tsipis
UCQR, IST/ITN, Instituto Superior Técnico, Universidade Técnica de Lisboa, CFMC-UL, Estrada Nacional 10, 2686-953 Sacavém, Portugal
e-mail: katya@itn.pt

G. Inzelt et al. (eds.), *Handbook of Reference Electrodes*,
DOI 10.1007/978-3-642-36188-3_9,

(ii) Oxygen-anion conductors, which are used for solid oxide fuel cells (SOFCs), high-temperature electrolyzers of carbon dioxide and water vapor, electrochemical oxygen pumps and compressors, gas dosage, various electrochemical reactors where oxygen is involved in catalytic and/or electrocatalytic processes over an anion-conducting membranes or electrodes, gas sensors, and a variety of other appliances for thermodynamic and analytical measurements. Key families of the oxygen ion-conducting solid electrolytes include stabilized high-temperature polymorphs of ZrO_2, Bi_2O_3, $Bi_4V_2O_{11}$, $La_2Mo_2O_9$ and $Ba_2In_2O_5$, apatite-type $La_{10-x}(MO_4)_6O_{2\pm\delta}$ (M = Si, Ge), acceptor-doped CeO_2 with fluorite structure, perovskite-type $LaMO_3$ (M = Ga, Al), and pyrochlore-type titanates and zirconates such as $(Gd, Ca)_2Ti_2O_{7-\delta}$.

(iii) Protonic conductors have numerous potential and current applications in hydrogen-separation membranes, hydrogen pumps and dosing devices, catalytic processes, steam electrolysis, SOFCs with proton-conducting oxide electrolyte membranes, and sensors of H-containing components in gaseous and liquid phases, including hydrogen in molten metals. These solid electrolytes are often classified into several subgroups, namely low-temperature (particularly acids and salts, such as CsH_2PO_4, $CsHSO_4$, and $H_3PW_{12}O_{40}{\cdot}nH_2O$), intermediate-temperature [for example, hydrated or ammoniated β-alumina- and NASICON-based frameworks, $H_2M_2O_6{\cdot}H_2O$, and NH_4MWO_6 with M = Nb or Ta, $(NH_4)_4Ta_{10}WO_{30}$, $Zr(HPO_4)_2$], and high-temperature oxide materials (primarily acceptor-doped perovskites, fergusonites, fluorites, and pyrochlores such as AMO_3 (A = Ba, Sr; M = Zr, Ce), $LaNbO_4$, $La_{6-x}WO_{12-\delta}$, and $La_2Zr_2O_7$).

Although a number of solid electrolytes with substantially high diffusivity of small di- and trivalent cations (Mg^{2+}, Ca^{2+}, Al^{3+}, Sc^{3+}) are documented in the literature, these materials are still of rather academic interest. The same is true for the solids where larger trivalent cations and anions like CO_3^{2-} were reported to be mobile; thorough experimental studies of the relevant microscopic migration mechanisms and macroscopic mass transfer and redox processes are often necessary in these cases. The materials and electrochemical systems, which are still far from practical applications, are excluded from consideration in this chapter. Nonetheless, the general principles and key methods discussed below and in Preface and Chaps. 1 and 8 remain applicable unless additional limitations due to specific features of a given material or system may appear. Such limitations are usually associated with electrochemical cell materials interaction, surface reactions and phase separation affecting electrode kinetics and potentials, dependence of redox states and electronic transport in a solid electrolyte on the applied electrical field or other external conditions, the presence of several ionic charge carriers and/or parallel processes influencing the charge-carrier concentration and mobility, kinetic demixing, and similar factors. To a significant extent, these factors cannot be even neglected a priori when selecting reference electrodes, electrochemical cell configuration, and operation conditions for the relatively stable systems considered below.

This chapter is mainly focused on the reference electrodes used for the developments of SOFCs and other electrochemical cells with solid oxide electrolytes,

as well as for the solid-state potentiometric sensors and thermodynamic measurements involving solid-electrolyte membranes. These applications require reference electrodes (REs) for two major goals: (1) correct determination of kinetic parameters (overpotentials, polarization resistance, exchange currents, ohmic drop) of the working electrode(s), and (2) accurate extraction of the thermodynamic activity or concentration of the potential-determining species at the working electrode (WE) from the cell electromotive force (emf) measured between WE and RE (see Chaps. 1 and 8). For the latter goal, the RE should provide, at least, a well-defined and fixed activity of the potential-determining component and a sufficiently high reversibility; other relevant aspects are addressed below. Note that in the case of galvanic and electrolytic cells, the requirements to the RE potential stability and electrode reversibility remain critical as well, whilst the measuring cell configurations are often selected to provide similar equilibrium potentials of the RE and WE in order to minimize errors due to WE concentration polarization and diffusion between the electrodes. Taking into account the practical application domains of solid electrolytes, the use of REs in the fuel cells and electrolyzers is primarily analyzed for the systems with oxygen-anion and proton conductors.

9.2 Reference Electrodes in the Solid and Liquid Electrolyte-Based Electrochemical Cells: Selected Similarities and Differences

Most experimental techniques to study electrode kinetics in solid-electrolyte cells, including the three-electrode method with reference electrodes, were developed on the basis of their analogues existing in the electrochemistry of liquid electrolytes [3, 5–7]. The same is essentially true for the solid-state electrochemical sensors and other appliances. On the other hand, there exist substantial differences between these areas of the electrochemical science, associated primarily with different basic properties of ion-conducting solids and liquids. First of all, most solid electrolytes used in practice exhibit dominant transport of one type of ionic charge carriers (important exceptions are related to the proton-conducting electrolytes where both protons and oxygen anions may provide significant contributions to the conductivity, depending on external conditions, and systems with mixed alkaline-metal cation charge carriers). Furthermore, possibilities to vary the ionic charge-carrier concentration in solid electrolytes are limited. As a rule, the phases with fast ionic transport (so-called fast ionic conductors) exist in relatively narrow compositional domains; large variations in their composition lead often to phase segregation, conductivity drop, and/or changing other physicochemical properties hampering potential applications. It should also be mentioned that processing of ion-conducting materials is associated with relatively high costs and stringent requirements to the mechanical properties, density, and necessity to form stable electrodes with well-defined

microstructure and good adhesion to the solid-electrolyte surface. These factors make it impossible to use supporting electrolytes and to vary the electrolyte transport properties as for the liquid systems; the range of possible cell geometries becomes also very narrow. For instance, the electrochemical cells discussed below all have relatively simple geometries, primarily planar, tubular, or cylindrical. The electrical resistivity of SEs is, in general, higher compared to liquid electrolytes. Other important features relate to local inhomogeneities in solid-electrolyte materials (e.g., grain boundaries, extended defects, local deviations from stoichiometric composition, ordered microdomains), which are determined by the electrolyte prehistory and may change at elevated temperatures, and to significant electronic transport that may be induced by electrical and/or chemical potential gradients and interdiffusion at the electrode/electrolyte interfaces. The former factor may limit, in particular, minimization of the electrode size; the latter factor causes additional requirements to the electrode compositions and makes it necessary to account for the electrolytic-domain boundaries when selecting the cell operation conditions and measurement regimes. Notice that, in the case of excessive electrochemical potential gradients, a number of other detrimental phenomena may also occur in the solid-electrolyte cells, including phase decomposition and microstructural degradation of the electrolyte, fast kinetic demixing, and even mechanical decomposition of the cell. If the electrolytic-domain restrictions are however observed, the crystal electroneutrality condition and substantially high concentration of ionic charge carriers, governed by doping and structural features, lead usually to negligible concentration gradients in the solid-electrolyte phase, except for the cells with protonic conductors. In other words, contrary to the liquid electrolytes, the concentration polarization phenomena in the solid-electrolyte cells are typically associated with transport processes over electrolyte surface, i.e., at the electrode and/or in the gaseous or liquid phase.

In addition to the limitations originating from the SE properties, practical constraints to the selection and placement of reference electrodes in the solid-electrolyte cells are much greater compared to the cells with liquid electrolytes [7–9]. Whilst the REs in the latter case can be immersed in the liquid electrolyte, the reference electrodes in SE cells should always be located on an electrolyte surface exposed to given media and should usually provide electrochemical reaction involving third (gaseous, solid, or liquid) phase. The only exceptions include electrochemical cells with cation-conducting electrolytes when the electrode can be made using a metal forming mobile cations in the electrolyte phase (e.g., Na/Na^+ or Ag/Ag^+). Second, in most devices the SE membranes are used to separate two compartments. This increases the importance of hermetization, often at elevated temperatures and in aggressive environments, and electrolytic permeation under chemical potential gradients, resulting from minor electronic conduction in the solid electrolyte. Any leakage may shift the activity of the potential-determining species at the RE. Moreover, in the case of electrolytic permeability, the presence of small ionic currents charge-compensated by electronic transport in the SE membrane may apparently shift the RE potential due to polarization [9]. Consequently, the reference electrodes in model fuel cells, batteries, and electrolyzers

should be preferably located under conditions identical to those for WEs [7]. Another necessary comment is that the role of permeation processes increases with decreasing electrolyte membrane thickness. For the practical applications of fuel cells and other electrochemical devices, the solid-electrolyte thickness should usually be minimized to decrease ohmic resistance, simultaneously preserving gas tightness; the typical range is 10–1,000 μm, whereas the electrode dimensions vary from micro- to centimeter scale. Although such cells provide high power density and efficiency, their configurations are often unsuitable for fundamental studies of electrode kinetics owing to the permeation and current-distribution problems analyzed below.

When studying electrode kinetics in solid-electrolyte cells by the three-electrode technique involving impedance spectroscopy or current interruption approaches, the current distributions in the SE membrane and in the electrodes should always be taken into account, unless the simplest cell configuration is employed and the electrode behavior is close to ideal. The importance of current-distribution problems in the impedance measurements appears primarily due to the frequency dependence of the distribution, a result of the influence of interfacial polarization combined with the geometrical aspects of the cell arrangement [6]. At high frequencies the primary current distribution is observed for the AC part of the current as the electrode capacitance short-circuits the interface; increasing the interface impedance with decreasing frequency results in a changeover to the secondary distribution different from the primary distribution if the latter is not uniform [6]. Such effects lead to distortions of the impedance spectra and various artifacts, as for the liquid electrolyte electrochemistry. In these conditions, incorrect use of a reference electrode can readily lead to inaccurate and misleading results [10]. The aspects related to the RE placement and current-distribution problems are addressed below, by the example of electrochemical cells with solid oxide electrolytes.

9.3 Reference Electrodes for Electrode Potential Measurements in Fuel Cells, Gas Electrolyzers, Gas Pumps, and Electrochemical Converters with Solid-Electrolyte Membranes

9.3.1 Definitions and General Aspects

Since the operation principles of fuel cells and other electrochemical devices are widely described in the literature [2–5, 11–16], this section presents only short definitions and introductory information necessary for understanding of the main approaches to the reference electrode design. Briefly, solid oxide fuel cells are the devices directly converting chemical energy of fuel into the electrical energy and heat, using solid oxide as an electrolyte (oxygen-anion or high-temperature protonic conductor). The SE membrane serves also as a barrier that prevents

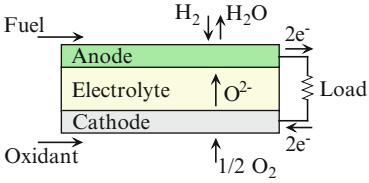

Fig. 9.1 Schematic representation of H_2-fueled SOFC with an oxygen ion-conducting solid electrolyte

mixing of the fuel and oxidant steams. With respect to the other types of fuel cells, such as alkaline fuel cell (AFC), polymer electrolyte membrane fuel cell (PEMFC), phosphoric acid fuel cell (PAFC), and molten carbonate fuel cell (MCFC), SOFCs attract a great interest due to their high-energy conversion efficiency, fuel flexibility including the prospects to directly operate on natural gas, possibility to recover exhaust heat as SOFCs operate at elevated temperatures, and other advantages [3, 11, 14]. A single cell comprises a dense solid electrolyte in contact with porous anode and cathode, onto which a fuel and an oxidant, respectively, are continuously supplied (Fig. 9.1). A variety of fuels including hydrogen, carbon monoxide, light hydrocarbons and alcohols, and even solid carbon can be used in SOFCs. Electrical current is generated due to the electrochemical reactions at the electrodes; for the oxygen ion-conducting electrolytes, these reactions include oxygen reduction at the cathode:

$$\frac{1}{2}O_2(g) + 2e^- \rightarrow O^{2-}(s) \tag{9.1}$$

and fuel oxidation at the anode, for example:

$$H_2(g) + O^{2-}(s) \rightarrow H_2O(g) + 2e^- \tag{9.2a}$$

$$CO(g) + O^{2-}(s) \rightarrow CO_2(g) + 2e^- \tag{9.2b}$$

$$CH_4(g) + 4O^{2-}(s) \rightarrow 2H_2O(g) + CO_2(g) + 8e^- \tag{9.2c}$$

Notice that due to high operating temperatures, a variety of other processes such as reforming of hydrocarbons, carbon oxidation, and water gas shift reaction may also occur at the anode. The inverse electrode reactions occur in the solid oxide electrolysis cells (SOECs) used to convert steam and carbon dioxide into hydrogen and carbon monoxide, respectively. The operation of the electrochemical reactors with SE membranes, which can also be used to cogenerate electricity and valuable chemical products, is typically based on incomplete oxidation or reduction of the reactants; as an example, synthesis gas can be produced in SOFCs via the partial oxidation of methane (POM):

$$CH_4(g) + O^{2-}(s) \rightarrow 2H_2(g) + CO(g) + 2e^- \tag{9.2d}$$

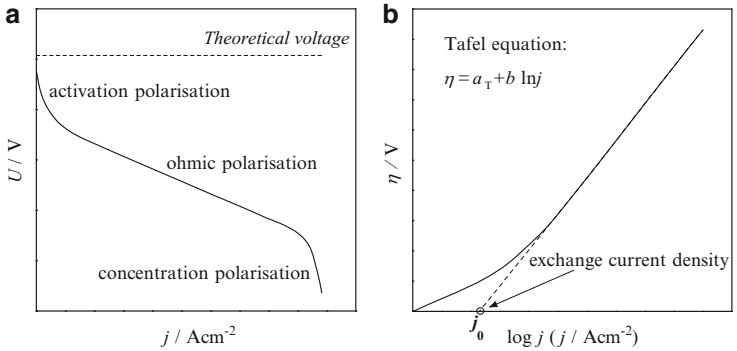

Fig. 9.2 Current-density dependencies of fuel cell voltage (**a**) and working electrode overpotential (**b**)

The electrode processes in solid-electrolyte systems consist always of a number of serial and/or parallel steps. The characteristic steps of the gas electrode reactions include transport in the gas phase to (or from) the gas/electrode or gas/electrolyte interface, adsorption (or desorption) at these surfaces, diffusion to (or from) the reaction zone, and transfer reactions [14–24]. As a rule, the electrochemical reaction is believed to occur in the vicinity (within a few microns) of triple-phase boundary (TPB), the junction of the gas, electronic or mixed ionic-electronic conductor (electrode), and ionic conductor (electrolyte); the TPB length is mostly determined by the electrode microstructure formed during the cell fabrication. Actual location of the electrochemically active sites depends generally on the bulk and surface transport properties of the electrode and solid-electrolyte materials. When the current I is passed or drawn through the cell, the working electrode potential E_{WE} deviates from the equilibrium value E_e. This deviation is characterized by the quantity of overpotential $\eta = E_{WE} - E_e$ (see Chap. 1). The electrode polarization resistance defined as

$$R_p = \frac{d\eta}{dI} \tag{9.3}$$

in the case of small polarization and linear $I - \eta$ dependencies, is directly interrelated with the exchange or limiting current under given external conditions. Typical current-density dependencies of the fuel cell voltage and electrode overpotential are schematically shown in Fig. 9.2.

For the developments of solid-state electrochemical devices and optimization of their operation regimes, it is necessary to accurately evaluate the overall performance of individual electrodes, reflected primarily by the area-specific polarization resistance and overpotentials, and to collect reliable information on the electrochemical reaction mechanisms. In the three-electrode arrangement, the working electrode is polarized with respect to the reference electrode (RE), i.e., a voltage is applied between the WE and counter electrode (CE) and electrical current

flows through the cell. The WE overpotential can be experimentally determined from the measured electrode potential vs. RE, corrected for ohmic losses:

$$\eta = (E_{\mathrm{WE}} - E_{\mathrm{RE}}) - IR_{\Omega}, \tag{9.4}$$

where R_{Ω} is the corresponding ohmic resistance obtained usually by the electrochemical impedance spectroscopy (EIS) with AC signal superimposed on DC polarization, or by the current interruption method. These measurements require an adequacy of the reference electrode, including its reversibility and appropriate placement. The cell configuration can be examined experimentally (e.g., by testing different RE positions and/or comparing the measurement results in different cells with similar electrodes) and by modeling of the current and potential distributions. It should also be mentioned that R_{p} under zero DC conditions can be measured employing symmetrical cells with two nearly identical electrodes when no RE is necessary; however, these two-electrode measurements cannot be used to study overpotentials and, thus, performance of the electrodes under the real operation conditions of the electrochemical devices.

The simulation approaches involve often the assumptions that the solid electrolyte has constant composition and conductivity, and operates below its dielectric response frequency, when the electrical state obeys Laplace's equation (e.g., [8, 23–25]):

$$0 = \nabla^2 \dot{\phi}, \tag{9.5}$$

where ϕ is the quasielectrostatic potential based on the majority charge carriers and the symbol "˙" indicates complex quantity due to the applied AC voltage. Note that this starting hypothesis may become invalid when local inhomogeneities in the ceramic electrolytes (e.g., grain boundaries, pores, interfaces, composition gradients) should be taken into account. The current density (j) consists of two parts proportional to the real and imaginary parts of potential gradient [27]:

$$j = -\dot{\kappa}(\mathrm{Re}[\nabla\dot{\phi}] + \mathrm{iIm}[\nabla\dot{\phi}]), \tag{9.6}$$

where κ is the electrolyte conductivity ($\dot{\kappa} = \kappa + \mathrm{i}\ \omega\varepsilon$), i is the imaginary unity, ω is the angular frequency of the applied AC voltage, and ε is the dielectric permittivity. With appropriate boundary conditions, Eq. (9.5) can be solved for a specific geometry using numerical or analytical methods. Typical boundary conditions for the two-dimensional structures, assuming a linear electrode polarization, are [25, 26]:

$$j_{\perp} = \kappa n_{\perp} \nabla\phi = 0 \quad \text{at any insulating surface(exposed electrolyte)}, \tag{9.7a}$$

$$j_{\perp} = \kappa n_{\perp} \nabla\phi = -\chi(\phi - \Psi) \quad \text{at any electrode surface}, \tag{9.7b}$$

where $n_{\perp}$ is the normal vector of the interface, χ is the electrode conductivity, and Ψ is the potential of working electrode relative to reference electrode of the

same type located in the electrolyte outside the double layer. The finite-element method is usually used to solve this system of equations numerically and to determine current/potential distributions for various cell geometries in a desired frequency range. For a potential difference between the two electrodes, the total complex impedance for a given complex conductivity is [27]:

$$\dot{Z} = \frac{\dot{\Psi}}{\int_X -\dot{\kappa}\nabla\dot{\phi}\mathrm{d}x}, \tag{9.8}$$

where the integration is along an equipotential line X with the differential normal vector element dx.

As mentioned above, for the correct and accurate determination of potential difference in the three-electrode cells, the RE potential must remain constant when the electrical current is passed, making it necessary to appropriately select the RE location, size, shape, composition, and microstructure. Obviously, these parameters cannot be considered without relevance to the entire cell design, materials, and fabrication and measurement conditions. In general, the current-induced deviations in the RE potential are associated with changing the current-density and chemical potential distributions in the cell, including the RE itself. When even the cell geometry is selected adequate, such deviations may still be caused by the poor electrode activity, excessive local current densities, or cell materials interaction, and may lead to erroneous results. Needless to stress that the potential gradient along any electrode in the measuring cell should be minimized, whilst the reference electrode should exhibit a high electronic conduction and reversibility.

Finally, the above discussion is also applicable to more complex configurations of the electrochemical cells, such as four-electrode one. The four-electrode cells with two reference electrodes placed at the cathode and anode sides can be used to assess kinetics of both current-bearing electrodes, sampling the potential differences relative to each RE and cell emf [28, 29]. Their advantages include, in particular, a possibility for continuous validation of the measurement results by comparing the cathodic and anodic overpotentials, relevant ohmic contributions, total cell voltage and ohmic resistance, and electromotive force measured between the REs. Two or more reference electrodes may also be used for averaging the potential difference between RE and WE [30] or for monitoring chemical potential drop along tubular SOFCs and SOECs, thus serving as an integrated electrochemical oxygen sensor [17].

9.3.2 *Effects of the Electrode Asymmetry and Solid-Electrolyte Thickness*

As for the electrochemistry of liquid electrolytes, nonuniform current-density distributions at the working electrode of solid-electrolyte cells require always a

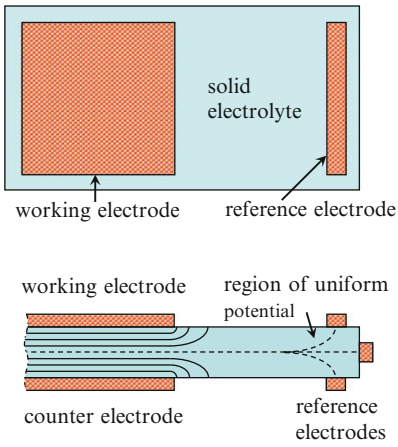

Fig. 9.3 Illustration of the electrical potential distribution calculated for the flat-plate cell with ideally symmetrical working and counter electrodes, according to [25]. *Solid lines* correspond to the equipotential surfaces. Possible positions of reference electrodes are indicated

special attention when deriving the electrode polarization resistance and ohmic contributions [6, 8]. In the planar cells with geometrically symmetric WE and CE, for the correct determination of the electrode overpotential against RE, the reference electrode should usually be placed far away enough from the current-bearing electrodes, in the area with uniform potential (Fig. 9.3); several alternative configurations are considered below. For a square-planar cell geometry, both experimental measurements and numerical calculations of the potential distribution within a thin solid electrolyte show that the electrolyte is approximately equipotential beyond a distance (ℓ) of about three electrolyte thicknesses (d) from the edge of the WE and CE [25, 26, 31]. Here, a reference electrode may be placed anywhere in this region, avoiding potential gradients and making the experimental data insensitive to exact RE location. The aspect ratio of $(\ell/d) > 8$ was suggested based on experimental results for the cells with thin solid electrolyte [28]. Another important limitation originates from the fact that the precision of processing methods commonly applied for the electrode fabrication is always limited. For instance, screen-printing provides an accuracy of the order of ~125–500 μm (e.g., [26, 28]). Misalignments between the WE and CE may significantly bias the RE potential towards the overhanging electrode, if even the RE is far from the active region (Fig. 9.4a). Moreover, in this situation the potential distributions become different in the high- and low-frequency limits (or under applied DC current and when it is interrupted), i.e., where primary and secondary distributions are observed; this difference leads to large errors in the determination of the electrode and electrolyte resistances [8, 25, 26, 31–34]. As an example, when the WE and CE have the same geometric area, displacing the CE towards RE leads to overestimated ohmic and WE polarization resistances, whereas the CE displacement away from the RE results in an opposite effect accompanied also with a pronounced decrease in the peak frequency of the WE impedance [8, 31]. One illustration of this behavior is presented in Fig. 9.4b. Analogously, extension of the counter electrode over WE leads to higher apparent R_p and R_Ω values.

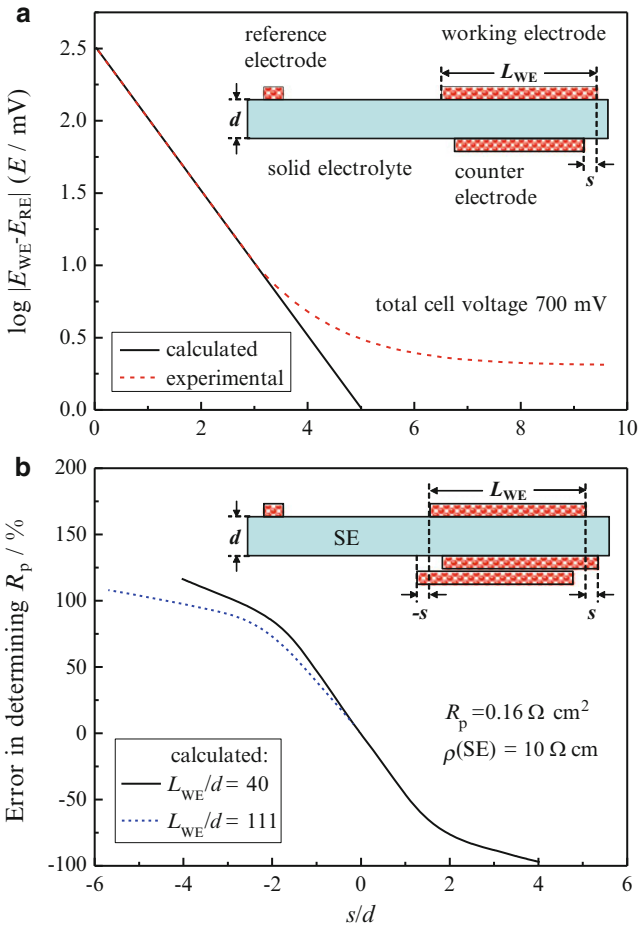

Fig. 9.4 Potential difference between the working and reference electrodes (**a**) and relative error in the determination of WE polarization resistance (**b**) as functions of misalignment between the WE and CE normalized by the solid-electrolyte thickness (s/d), as calculated by the finite-element analysis assuming linear electrode kinetics [8, 25]. At high s/d ratios, the experimentally measured value stabilizes at a small Nernst potential due to gas-phase polarization of the working electrode, whereas the predicted value reaches zero (**a**). The error in (**b**) is defined as $\frac{R_p^{apparent}-R_p^{true}}{R_p^{true}} \times 100\ \%$. RE is placed at a distance equal to at least $3d$ away from the WE

If the WE and CE possess different polarization resistances and time constants defined as $\tau = R_P \times C$ (where C is the area-specific capacitance of the electrode/electrolyte interface), this extension may also introduce artifacts in the impedance data [25, 31, 35]. In other words, when shifting the CE to RE, the equipotential surface probed by the RE approaches the CE/electrolyte interface at $\omega \rightarrow 0$ and the RE may no longer isolate the potential drop of the WE. In addition to the apparent increase in the electrolyte resistance, this causes a partial introduction of the CE impedance into the measured WE impedance [26, 31].

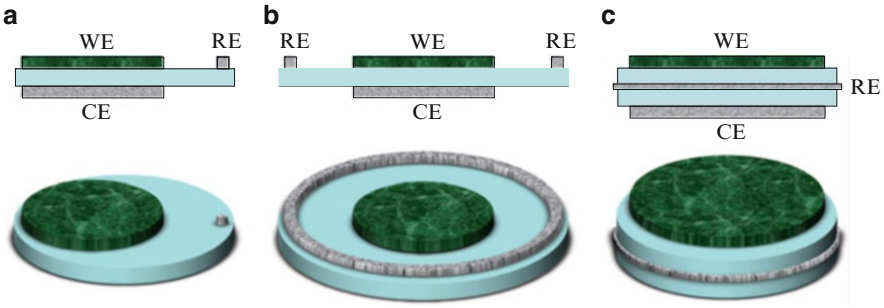

Fig. 9.5 Examples of possible flat-plate geometries of three-electrode cells for the determination of the WE overpotential and polarization resistance. The solid electrolyte should preferably be thick enough and the alignment of the working and counter electrodes should be as precise as possible in all cases. The reference electrode may be placed at a distance corresponding to at least 3–8 electrolyte thicknesses away from the WE and CE (**a** and **b**), or in the middle of electrolyte edge (**c**)

As the uncertainty associated with these frequency-dependent effects increases when the electrolyte thickness and conductivity decrease, accurate measurements of electrode overpotentials in thin solid-electrolyte cells become challenging [8, 25, 26, 28, 31, 33, 35, 36]. The thickness threshold values vary usually in the range 0.2–1 mm, depending on other parameters. In a hypothetic case when the WE and CE polarization resistances are equal, possible maximum electrode displacement corresponds to ~10 % electrolyte thickness [8]. When the electrode kinetics of the WE and CE are different, large errors may appear if even the electrode alignment is essentially precise, for the measurements on thin-electrolyte cells wherever the RE is located [8, 25, 26, 28, 35]. At the same time, if the reference electrode enables correct determination of the steady-state potential difference between the WE and RE, and if there are no other sources of experimental uncertainties, the WE overpotential may still be measured employing EIS by extracting the associated ohmic losses from high-frequency part of the impedance spectra under a given applied DC voltage. In order to ensure an uniform current distribution, alternative designs were proposed [26, 30] on the basis of standard cell arrangements shown in Figs. 9.5a and 9.6a. For the RE placement, these designs require to form a relatively thin extension of the SE membrane or a groove isolating RE [26, 30]; in many cases, this complex geometry may be quite problematic due to the SE processing constraints and insufficient mechanical strength at elevated temperatures. Other simple approaches are based on the use of two or more REs to correct and/or to average the data affected by the WE and CE misalignments [30]. Such averaging may be, in fact, naturally achieved using the cell configurations illustrated in Fig. 9.5b, c.

For thick SE membranes where possible electrode misalignments are relatively small compared to the electrolyte thickness, the location of the equipotential surface probed by the reference electrode remains essentially frequency independent [25]. However, large SE thicknesses are not always appropriate due to extra

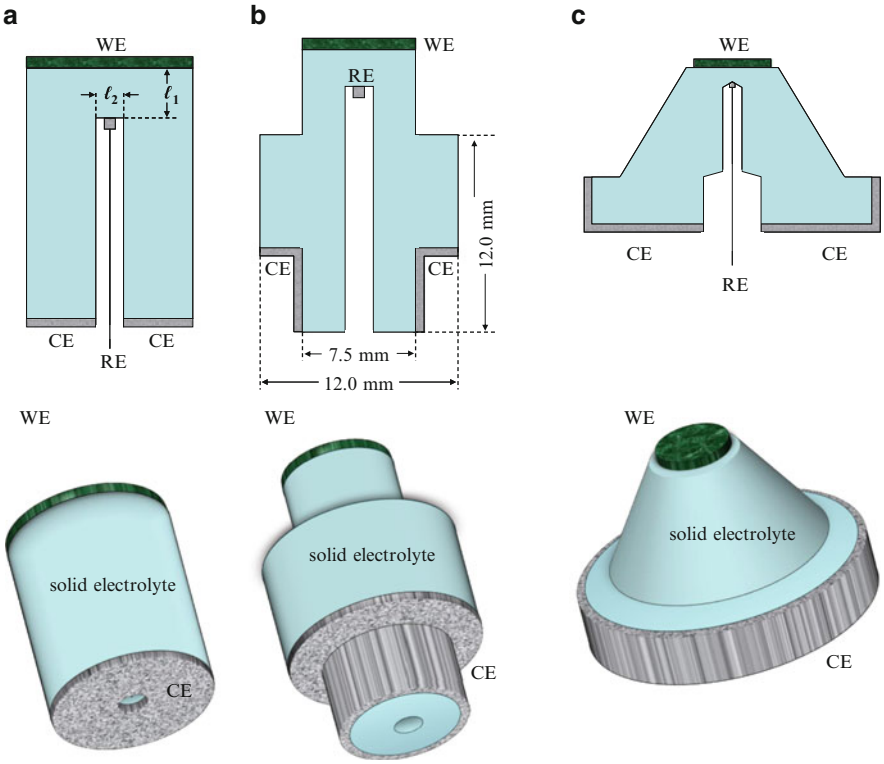

Fig. 9.6 Examples of possible three-electrode cell geometries with embedded RE located at the counter side of solid electrolyte close to the WE [8, 26, 35], essentially similar to the use of a Luggin capillary probe in liquid-electrolyte systems. For (**b**), the cell dimensions according to [8] are given. The advantages and disadvantages of specific configurations shown in (**a**), (**b**) and (**c**) are discussed in the text

limitations on the range of applied current densities, associated with possible electrolyte decomposition, induced electronic transport, and Joule heating. For many electrolyte materials, processing of very thick dense ceramics without defects is also constrained. These factors are often important for the cell configurations presented in Fig. 9.6, where the reference electrode is placed right next to the WE. Such an approach can only be used in combination with large solid-electrolyte thicknesses, typically 1–2 cm. For the cells shown in Fig. 9.6, the inaccuracy due to nonuniform current distribution increases with increasing hole diameter (ℓ_2) and with decreasing distance between the WE and RE (ℓ_1) when the central channel is too thick; the condition $\ell_1 > \ell_2$ should be maintained [8]. In the case of so-called Risø design (Fig. 9.6b), the estimated relative errors in R_p determination can be minimized down to 3–5 % [8].

Figure 9.7 illustrates the microelectrode configurations with narrow coplanar or point WE and RE, where the CE has an effective infinite width and the potential

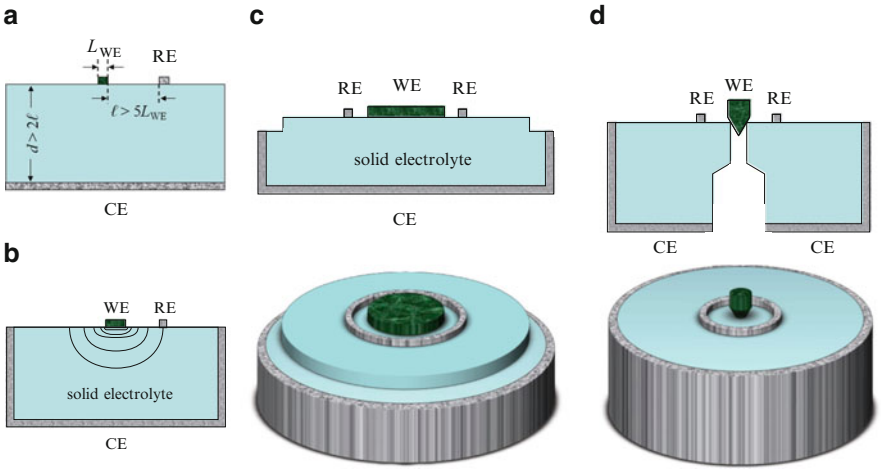

Fig. 9.7 Examples of thick pellet-based cell geometries with a small working electrode and essentially radial distribution of equipotential surfaces, as shown by *solid lines* in (**b**) [26, 35]. L_{WE} is the width of the working electrode, ℓ is the distance between WE and RE, and d is the solid-electrolyte thickness. (**a**), (**c**) and (**d**) illustrate the configurations with small WE and RE having similar sizes, an axially symmetric configuration, and point WE, respectively. The advantages and disadvantages of these configurations are discussed in the text

distribution around WE is nearly cylindrical or spherical, respectively [26, 34, 35]. In these cases the distortions of impedance spectra are minor and can be easily taken into account. The latter geometry is often preferable as the potential variations along the WE can be avoided. For the former case, one design was suggested with inter-digitated WE and RE patterns formed by photolithography with very small gaps, thus minimizing the ohmic drop [30, 36]. The main limitations are associated, again, with the cell processing and stability at elevated temperatures.

9.3.3 Other Relevant Factors

9.3.3.1 Electrochemical Potential Distribution at the Reference Electrodes

Another important source of errors is linked with the electrical potential gradient along the reference electrode, which may cause in-plane currents, an appearance of local overpotentials at the RE, and other parasitic effects [8, 25, 31]. Therefore, the RE width in the direction parallel to the potential gradient should be decreased down to a possible minimum. Figure 9.8 displays the range of suitable combinations of the geometric parameters, when the potential difference along RE becomes negligible, for a standard planar cell illustrated in the inset. This criterion appears relatively easy to satisfy. For example, if the RE is placed at the distance of $\ell = 3d$ from WE, its width may well be larger than the solid-electrolyte thickness. Usually, the fabrication of RE with the width or diameter of around 1 mm presents no practical problems.

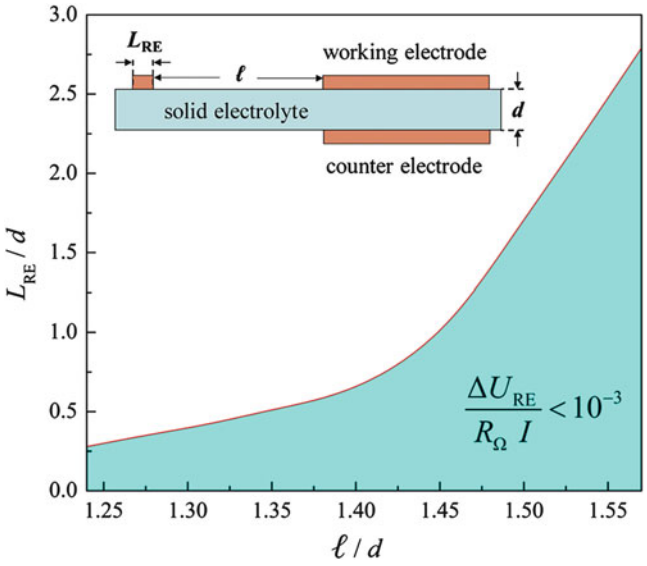

Fig. 9.8 Schematic diagram showing the domain of possible combinations of the reference electrode width (L_{RE}), distance between working and reference electrodes (ℓ), and solid-electrolyte thickness (d) in the planar cells with symmetric WE and CE, illustrated in the inset [8]. *Solid line* corresponds to the condition $\Delta U_{RE}/(R_\Omega\, I) = 10^{-3}$ where ΔU_{RE} is the potential difference along the RE, R_Ω is the total ohmic resistance of the cell, and I is the total electrical current. Blue area corresponds to the region where normalized ΔU_{RE} does not introduce any significant error in the measurements

The situation changes, however, when the solid electrolyte exhibits a significant electronic transport, either in the bulk or along the surface, and when surface diffusivity of any ionic species is high. The former case may appear due to the thermodynamic properties of solid electrolyte itself (e.g., for ceria-based membranes and a number of high-temperature protonic conductors exposed to reducing environments [37–39]), processes in the electrochemical device (e.g., deposition of carbon from fuel mixtures or chromium oxide from the SOFC current collectors), or diffusion of variable-valence cations from other cell components. Notice that, sometimes, electronic conduction in the electrolyte surface is intentionally induced by doping in order to promote surface exchange (e.g., [40–42]). As for the bulk electronic transport, in-plane electronic currents along the SE surface result in partial short-circuiting of the reference and working electrodes, and may shift the RE potential if parasitic electrochemical reactions occur. These phenomena lead to underestimating the overpotentials and should be taken into account [29, 43]. Similar processes may occur in the electrochemical cells with cation conductors where the surface diffusion may involve both foreign species and ions immobile in the bulk lattice. For the EIS data, a "cross talk" between the working and reference electrodes mediated by surface diffusion of charged adsorbed species results in an additional inductive loop contribution in the impedance spectra [44]. When the electron

transference numbers in the electrolyte bulk are significant and the cell is placed under chemical potential gradient of the neutral species involved in the electrode reactions, the electrode polarization may even occur under the open-circuit conditions due to non-negligible ionic currents compensated by the electronic transport [9, 30, 45]. The apparent equilibrium potentials of WE and RE become then generally different due to differences in the electrode kinetics. The true η and R_p values cannot be experimentally measured in this case unless the RE is isolated from the bulk electrolyte by a purely ionically conducting interlayer [43]. Finally, effects of the chemical potential gradient across the reference electrode under nonequilibrium conditions, shifting the RE potential, cannot be a priori neglected as well [32]. These problems may arise, for example, in nonequilibrium gas mixtures, in the case of high solubility of the potential-determining species in the reference electrode material, or due to continuous reaction between the RE and SE compositions.

9.3.3.2 Electrochemical Properties of the Reference, Working, and Counter Electrodes

High-impedance reference electrodes may cause serious distortions and artifacts in the EIS data for both high- and low-frequency ranges and affect the potentiostatic measurements, a consequence of complex voltage divider effect [46–48]. The methods for its minimization and correction were discussed in [47–49]. When the RE impedance is significant with respect to the instrument input impedance, errors appear as the frequency response analyzer (FRA) fails to account for the voltage drop across the RE [46, 47]. The threshold of tolerable RE impedance can be estimated as ~1 % of the FRA input resistance at all frequencies. Figure 9.9 illustrates the influence of RE impedance on the accuracy of WE polarization resistance measured by the three-electrode technique, for the low-frequency range.

Ion-blocking reference electrodes placed inside the solid electrolyte without controlling chemical potential of the electrochemically active species (e.g., exposure to gaseous phase or introducing mixed conductor) cannot be used, in general, to measure WE characteristics; such electrodes may however serve as selective potential probes in order to estimate the electrochemical potential of electrons in the bulk of solid-electrolyte or mixed-conducting membranes [50, 51]. Nevertheless, a number of attempts to incorporate REs inside the electrolyte are known in the literature (e.g., [52, 53]).

The constraints to the relative dimensions and placement of the cell components become more stringent when the electrochemical activity of working electrodes is high; as a rule, the precision in R_p determination increases with increasing R_p/R_Ω ratio [8, 30, 31, 33, 35]. When any significant misalignment of the WE and CE takes place, artifacts may even appear in the impedance spectra of relatively passive working electrodes [31]. As a criterion for the WE impedance determination accuracy, the impedance should be independent of the solid-electrolyte thickness and frequency range. The three-electrode measurements may also be influenced by the electrochemical activity of the counter electrode.

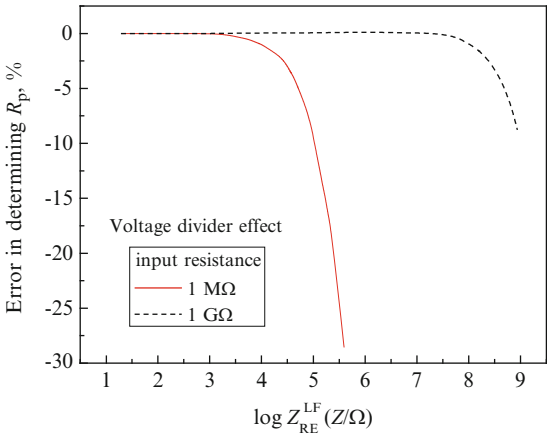

Fig. 9.9 Effect of the low-frequency (LF) impedance of reference electrode, reflecting the sum of contact and charge-transfer resistances, on the error in polarization resistance of the working electrode measured using three-point LO-pin configuration [46]. The error, calculated as $\frac{R_p^{apparent}}{R_p^{true}} = \frac{R_{input}}{R_{input} + Z_{RE}^{LF}}$ where R_{input} is the analyzer unit input resistance, coincides with experimental values collected at 20 mHz

In particular, the electrode response cross-contamination effect mentioned above appears due to nonuniform current-density distribution, leading to distortions in the impedance spectra [26, 31, 33, 35]; these distortions may result in erroneous R_p and η values and may become misleading for interpretation of the EIS data. Generally, the CE polarization resistance should be negligibly low compared to that of WE. For the cell configuration similar to that in Fig. 9.4b, it was shown that the error in R_p determination is kept within few percent when the ratio of WE and CE interfacial resistances is $\geq$10 [33]. In the cells with microelectrodes, the influence of counter electrodes having large geometric area can be usually neglected.

9.3.3.3 Effects of Operating and Testing Conditions: Brief Comments

During testing of the three-electrode cells, external DC bias is often applied between the WE and CE in order to simulate the fuel cell operation conditions. In this case, however, the chemical potential of the electrochemically active species (e.g., oxygen) and electrochemical potential of electrons at the WE can be independently varied, whereas in fuel cells these potentials are interrelated. As a particular consequence, the oxygen chemical potential in the electrolyte surface layers may eventually become lower with respect to the electrolytic-domain or phase decomposition boundary. At high applied voltages in the model SOFC-type cells, the electrochemical activity of the cathode may be overestimated owing to increasing oxygen deficiency or reductive decomposition processes in the solid-electrolyte surface layers, both manifesting as an excess current [9]. This situation is illustrated by Fig. 9.10. The same or even more harmful effects may appear in SOECs where the cathode is already exposed to reducing atmospheres, and in the electrochemical oxygen and hydrogen pumps

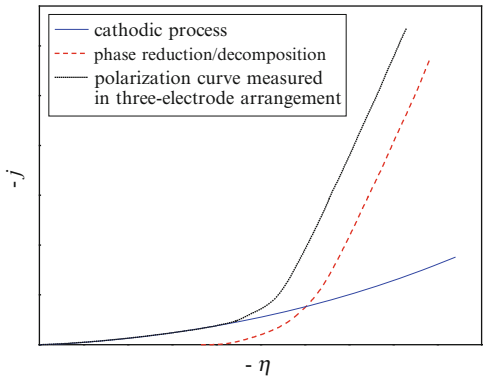

Fig. 9.10 Schematic representation of the WE polarization curve collected by three-electrode method, illustrating the effect of solid electrolyte reduction [9]. When the applied DC voltage becomes excessively high, the current originating from the progressive increase of local electrolyte nonstoichiometry and/or phase decomposition at the SE membrane surface starts to dominate over the cathodic current

when the gas is extracted from highly diluted mixtures. In addition, the appearance of substantially high electronic conduction in the reduced electrolyte layers near interface or formation of phases blocking ionic and/or electronic transport may also affect the electrode kinetics. In order to estimate the voltage limits, information on the SE transport properties and interfacial kinetics as function of the chemical potential of the electrochemically active species is necessary, often in combination with thermodynamic data (see [7, 54] and references cited). If the working electrode concentration polarization dominates, the solid-electrolyte reduction may occur at even lower applied voltages [9].

The RE potential in the three-electrode cells may only remain constant when the external conditions (composition of the surrounding atmosphere and temperature) are fixed. For SOFCs, the steady-state oxygen chemical potential at the RE is often affected by the applied current-density and gas flow rates [24, 28]. These effects become usually more pronounced on increasing the working electrode geometric area and on decreasing distance between the WE and RE. In such cases, the RE should be placed in a separate chamber essentially isolated from the WE and CE environments, and/or the reactant flow rates should be selected high enough to eliminate the influence of changing chemical potentials of the potential-determining species under high current densities. In all cases, temperature gradients in the electrochemical cells should be minimized or taken into account.

9.3.4 Comparison of the Measuring Cell Designs

Summarizing the discussion on possible configurations of the three-electrode cells with solid electrolytes, one should stress again two key issues, namely: (1) the cell must provide an essentially uniform current-density/potential distribution, and (2) the reference electrode must be located in an equipotential region, ensuring that

its potential is not affected by the WE polarization and potential gradients. In practice, there exist usually a number of specific variables enabling alternative technical solutions. The most common geometry for three-electrode electrochemical testing is the flat-plate one, or so-called button cell. When relatively high current densities are necessary and/or SE ceramics with more complex geometries is unavailable, the cells shown in Fig. 9.5 can be used in most cases, subject to the constraints discussed above; one should provide, in particular, that the solid-electrolyte membrane is thick enough and the WE and CE can be applied with minimum misalignments. In the case of moderate current densities, or when the WE and CE cannot be aligned, even thicker cells with the RE placed near WE (Figs. 9.6 and 9.7c) present an optimum choice. When using the cell configurations shown in Figs. 9.5a, 9.6, and 9.7a, the voltage divider problems may arise when the RE impedance increases (e.g., on decreasing temperature) if the RE is too small; for excessively large reference electrodes the potential shift due to in-plane currents may be observed. Several arrangements (for example, Fig. 9.7d) present also potential technical difficulties for separation of the WE and CE gas compartments. Nonetheless, these designs can be modified for specific experimental goals.

Microelectrodes and microelectrode arrays are inevitably studied in the asymmetric cells with relatively thick electrolyte and RE placed near WE (Fig. 9.7). The thin-film microelectrodes are a very useful tool for the analysis of polarization phenomena, providing well-defined geometry and morphology, flexibility enabling fast verification and reproducibility inspection, statistical averaging, precise investigations of irreversible processes, and minimization of ohmic drops in the electrolyte [26, 34, 35]. However, the electrode behavior in these configurations may substantially differ from that of large porous layers having the same composition. Patterned electrodes with relatively large overall area can be studied using any cell geometry, provided that the general requirements discussed above are satisfied; for instance the cell shown in Fig. 9.5a has been adapted for this purpose [55].

The general conclusions drawn for the planar geometries are also valid for tubular cells. In this case, most available configurations (Fig. 9.11) are quite similar to the planar cells (Fig. 9.4a, b). The same care should be taken to the WE and CE alignment, RE placement, and dimensions of all three electrodes with respect to the electrolyte thickness. Moreover, gas diffusion problems may arise in addition to the concentration gradients along the tubular SE membranes [24], especially if the cathode and anode surface areas are large; use of excessively high gas flow rates causes temperature gradients. These aspects may lead to additional complications, including the need to place at least one reference electrode at each side of the tubular membrane and to combine the polarization measurements with monitoring chemical potential gradient of the electrochemically active species across the cell. At the same time, the use of such integrated sensors operating on the basis of Nernst voltage enables to estimate additional parameters such as fuel utilization efficiency [17]. Tubular reactors combined with an online mass spectrometer for continuous monitoring of the outlet gas composition can be used to study catalytic activity of the electrodes, the chemistry of reactions at their surface, and, simultaneously, the electrochemical performance of working electrodes and entire cells, avoiding the problems associated with sealing and leakage [56].

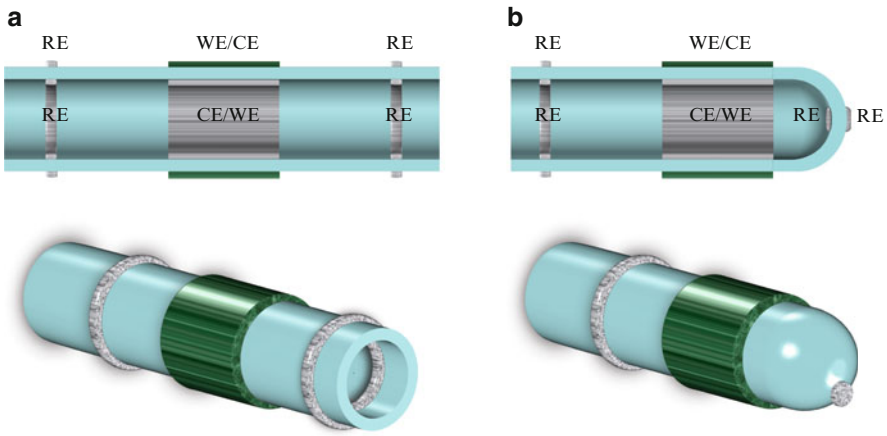

Fig. 9.11 Examples of tubular configurations of the three- or multiple-electrode cells for determination of the electrode overpotentials and polarization resistance

For both planar and tubular configurations, numerous experimental problems are to be solved when testing electrochemical cells with very thin SE layers. Under open-circuit conditions, the polarization resistance in such cells can be correctly determined using symmetrical two-electrode arrangements where both electrodes have the same composition and microstructure and are exposed to the same atmosphere. In the case of electrode-supported electrolyte layers, the cell arrangements are often selected in order to minimize ohmic losses; these losses, or the impedance of supporting CE, can then be neglected if the WE size is sufficiently small. Usually such approaches may give, however, only limited information on the electrode kinetics. On the other hand, it was demonstrated that the overpotentials of both current-bearing electrodes can be correctly measured by the current interruption method in square-planar cells (Fig. 9.3) where the solid-electrolyte thickness was ~200 μm, the effective geometric areas of symmetric cathode and anode were ~10.9 cm^2, and the reference electrodes (width 3 mm) were placed 5 mm away from the cathode and anode sides [28]. The use of thinner SE membranes shifts partitioning of the relative anodic and cathodic contributions to the ohmic resistance and leads to the corresponding errors in the measured overpotentials.

In all cases, suitability of a selected cell arrangement for the given external conditions, materials, and fabrication approaches should be validated experimentally. Possible approaches include examination of the impedances measured using different electrode pairs (WE/RE, RE/CE, WE/CE) in the three- or four-electrode configurations [28, 47, 49], comparing the R_p values derived from the impedance spectra and calculated from the polarization curves, analyzing the effects of RE replacement and other variations in the cell geometry, monitoring the ohmic contributions associated with solid-electrolyte resistivity under open-circuit and applied bias conditions [31], and measuring the steady-state potential difference between the reference electrodes located at opposite sides of the SE membrane as a function of the current density [28].

Table 9.1 Properties of selected metal electrode materials [7, 17]

Metal	Electrical conductivity ($S\ cm^{-1}$)	TEC $\times 10^6$ (K^{-1}) at 280–1,200 K	Vapor pressure at 1,173 K ($N\ m^{-2}$)	Melting point (K)	Potential of the metal/oxide redox couple at 1,273 K (V)
Pt	2.4×10^6 (1,200 K)	8.9–11.4	3×10^{-11}	2,045	Decomposition at 780 K (Pt_3O_4)
Ag	1.6×10^7 (1,000 K)	18.7–28.1	1.1×10^{-1}	1,234	Decomposition at 460 K (Ag_2O)
Pd	2.8×10^6 (1,200 K)	11.8–16.7	–	1,827	Decomposition at 1,150 K (PdO)
Ni	1.9×10^6 (1,270 K)	16.5	1.1×10^{-5}	1,728	−0.700
Co	2.3×10^6 (1,270 K)	12.5	8.5×10^{-7}	1,768	−0.719
Cu	1.0×10^7 (1,270 K)	16.6	7.5×10^{-4}	1,357	−0.449 (Cu_2O)

9.3.5 *Typical Reference Electrode Materials and Relevant Constraints*

The key criteria for the selection of RE materials include: (1) high electronic conductivity; (2) high electrochemical activity, including fast interfacial exchange and, in many cases, fast diffusion of the potential-determining species to the TPB or electrode|electrolyte interface; (3) thermodynamic and morphological stability under the cell fabrication and operation conditions, including an absence of phase transitions and volatilization; (4) negligible interaction with other cell components, primarily solid electrolyte; (5) feasibility to form appropriate microstructures, enabling to preserve constant electrochemical potentials of the species involved in the electrode reaction; (6) good adhesion to the solid electrolyte, compatibility of the thermal expansion coefficients (TECs), and an absence of contact phenomena which may rise the RE impedance; (7) easy processing, availability of the components, and moderate costs. For the high-temperature electrochemical cells operating often in aggressive media, these severe requirements limit the range of RE materials, primarily to the noble metals (e.g., Pt, Au, Ag) and ceramic–metal composites (cermets) on their basis. For instance, numerous studies focused on the reference electrodes for SOFCs, high-temperature electrolyzers, oxygen sensors, and pumps deal usually with the RE and CE made using porous metallic Pt, often in combination with zirconia-based ceramics selected as a model solid electrolyte (e.g., [5, 7, 16–19, 31, 32, 35, 47] and references therein). Platinum is well known to possess a high chemical stability, thermal expansion compatible with those of most solid oxide electrolytes, lower sinterability, and volatility under operation conditions with respect to other candidate metals (Table 9.1), high catalytic activity, and a relatively good performance as an oxygen or hydrogen electrode. As a rule, porous reference electrodes of platinum or cermets containing Pt and yttria-stabilized zirconia (YSZ) electrolyte are deposited onto SE membranes via sputtering, painting, screen-printing, or other methods, and then sintered at 1,270–1,400 K, depending on the starting materials and cell operation temperatures; use of Pt wires or meshes pressed mechanically onto the electrolyte membrane is rarely possible due to resultant high-impedance values. Under specific

experimental conditions when porous Pt electrodes may undergo oxidation (e.g., during testing at high oxygen partial pressures) or when their catalytic activity may play a negative role (e.g., due to parasitic chemical reactions), less active gold is used for the reference electrodes [17, 57].

In the intermediate-temperature range, 670–970 K, the impedance of small Pt-based reference electrodes in contact with solid oxide electrolytes becomes often excessively high; their potential may also be affected by surface oxidation processes at high oxygen pressures. These problems make it often necessary to use other RE materials with higher electrochemical activity and/or FRAs with larger input impedance, or to compensate the EIS spectra distortions [46, 47, 49]. For this temperature range, a better reversibility in oxygen-containing atmospheres is characteristic of metallic Ag and silver-based alloy and cermet electrodes [47, 58–60] (Fig. 9.12). These provide also an easy deposition, relatively high oxygen diffusivity in the bulk enabling to mitigate microstructural requirements, and lower costs compared to platinum. The disadvantages of silver REs include the relatively low melting point, high volatilization and thermal expansion (Table 9.1), and serious microstructural changes on oxygen dissolution and heating. Notice also that Ag electrodes possess rather poor activity for fuel oxidation and NO reduction, and tend often to exfoliation from the SE surface due to sintering and thermal expansion mismatch [7, 17, 58, 60, 61]. The oxide mixed-conducting compositions, such as perovskite-related cobaltites and nickelates, may be advantageous in oxygen-containing atmospheres due to fast surface exchange and diffusion [62]. However, owing to the problems associated with their interaction with solid electrolytes and relatively slow oxygen nonstoichiometry variations which may affect RE potential in the intermediate-temperature range, their use as reference electrodes is still essentially limited to the microelectrode arrays where the electrode layer is thin and excessively high temperatures are avoided. Nevertheless, applying similar electrode compositions for the oxide WE and RE (e.g., [29]) is an effective approach enabling to minimize errors. The same approach is relevant for the fuel electrodes when several parallel reactions may occur and potential difference between the WE and RE may arise due to different electrocatalytic activities of the electrodes [35]; the presence of non-negligible electronic transport in the SE membrane also leads to the necessity to use essentially identical electrode compositions as discussed above. In particular, metallic Ni can be utilized for REs in reducing environments [55], despite its lower redox stability with respect to Pt. The polarization resistance of nickel electrodes is comparable to that of platinum or even lower (Fig. 9.12).

The microscopic mechanisms responsible for the electrochemical behavior of metallic and oxide electrodes were exhaustively analyzed in the literature [17–22, 24, 60, 62–69] and are outside of the main scope of this chapter. One should only mention that the solid-electrolyte additions into the electrode composition make it possible to increase reversibility and to enlarge the domain of temperatures and chemical potentials where the electrode can be safely used, a result of the TPB expansion and microstructural stabilization. Although the mixed-conducting and catalytically active additives such as doped ceria might also be useful from the cell impedance point of view, their use for the reference electrodes is limited if oxygen nonstoichiometry changes may occur under the cell operation conditions.

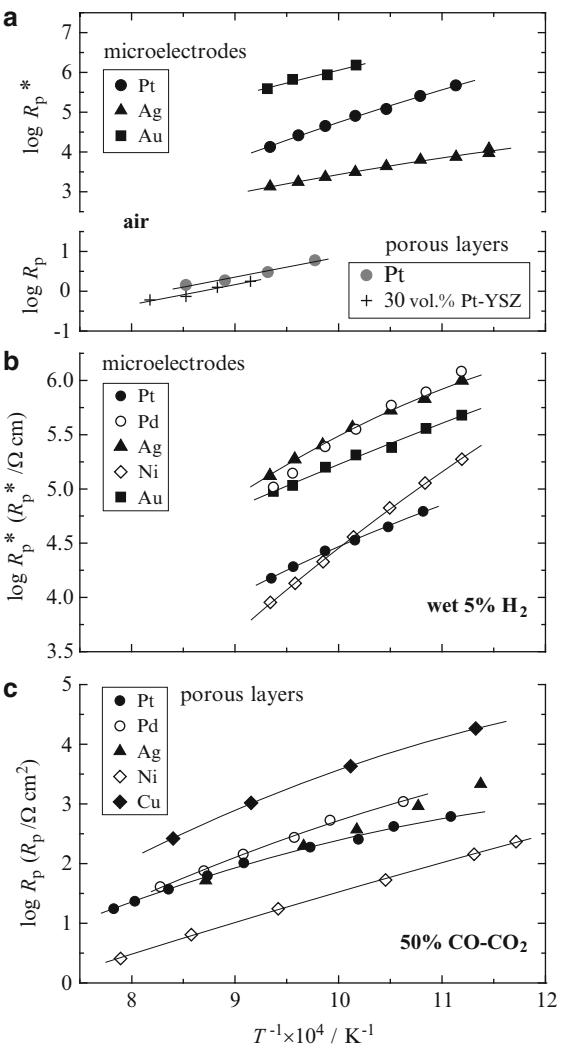

Fig. 9.12 Polarization resistances of various metallic microelectrodes and porous layers in air (**a**), in 5 vol.% H_2–5 vol.% H_2O–90 vol. % N_2 (**b**), and in 50 vol.% CO–50 vol.% CO_2 gas mixture (**c**), in contact with stabilized zirconia solid electrolytes [17, 60, 63]. For the microelectrodes, the R_p* (Ω × cm) values were corrected for the length of triple-phase boundary between the electrode, electrolyte, and gaseous phase, and cannot be directly compared to the polarization resistances (Ω × cm^2) of the porous electrodes normalized to their geometric area

9.3.6 Solid Oxide Electrolyte-Related Limitations: Selected Examples

The major electrolyte-related constraints affecting selection of the reference electrodes for SOFCs, SOECs, and electrochemical gas pumps are associated with the following factors: (1) electronic transport and electrolytic permeability of the SE membranes; (2) possible interdiffusion and reactions between the SE and RE materials, which may result in the formation of blocking layers, an increase of the electronic conductivity in the SE surface, RE potential shift during the cell

operation, charge-carrier concentration gradients in the SE membrane, and other parasitic phenomena; (3) electrolyte degradation, including phase decomposition and kinetic demixing under the cell operation conditions; and (4) thermal expansion mismatch that may cause RE failure on thermal cycling. The limitations originating from surface diffusion in solid oxide electrolytes play, in general, a less important role compared to the cation conductors.

The n-type electronic conduction may originate from the partial electrolyte reduction under operating conditions, for instance, at the SOFC anode side. One classical example refers to the ceria-based electrolytes [29, 37, 43, 70]. Due to the mixed oxygen-ionic and n-type electronic conductivity, the oxygen chemical potential in the fuel-exposed surface layers of these materials becomes very close to that in the gas phase [50, 51, 71]; the voltage drop in the oxygen concentration cells occurs mainly across the oxygen electrode/electrolyte interface, implying that almost entire SE membrane is partially reduced. Whilst an appearance of n-type electronic transport on reduction is characteristic for most solid oxide electrolytes, their electrolytic-domain boundaries vary in a very large range and are often far below the oxygen chemical potentials necessary for SOFC/SOEC operation [2, 3, 7, 68, 70]. As an example, the effects of electronic conduction on the RE reliability can be neglected in the case of zirconia- and thoria-based ceramics unless the electrolyte is modified with variable-valence dopant cations or is reduced by high applied voltage. However, opposite situations may take place for many other solid electrolytes, including stabilized $Bi_4V_2O_{11-\delta}$ (so-called BIMEVOX) and $La_2Mo_2O_9$ (LAMOX), acceptor-substituted ceria such as $Ce(Gd)O_{2-\delta}$, pyrochlore-type $(Gd, Ca)_2Ti_2O_{7-\delta}$, and a number of protonic conductors based on doped cerates, niobates, tantalates, and titanates, such as $BaCe(Y)O_{3-\delta}$, $Ba_2(Ca, Nb, Ta)_2O_{6-\delta}$, or $LaNbO_4$ [38, 39, 68, 70, 72–79]. The electron–hole transport under oxidizing conditions leads often to similar problems. Depending on the oxygen chemical potential and temperature, the p-type electronic contribution to the total conductivity may achieve non-negligible levels for the transition metal-doped (La, Sr)(Ga, Mg)$O_{3-\delta}$ (LSGM) and acceptor-doped $Gd_2Ti_2O_7$ and ThO_2; substantially high electron–hole conduction is characteristic of the proton-conducting oxide materials where, however, the transference numbers are also dependent on the water vapor partial pressure. Another major methodological difference in the electrode polarization analysis for the cells with oxygen-anion and proton-conducting solid electrolytes refers to non-negligible effects of diffuse charge [80] and charge-carrier concentration gradients in the latter case; for oxygen ionic conductors these effects can usually be ignored. The aspects related to reactivity of the solid-electrolyte and electrode materials become less pronounced when noble metals are used for the REs. Nonetheless, Ag and Pt may interact with Bi_2O_3-based electrolytes [81]; platinum promotes interfacial decomposition of LSGM in reducing atmospheres and may even form Pt–Zr intermetallic compounds in contact with zirconia on reduction [82, 83]. Whilst the latter process is not observed under the SOFC operating conditions, topotactic reactions between YSZ and oxide electrode materials leading to the formation of ion-blocking zirconate layers have a critical importance for selection of the fuel cell fabrication and operation regimes

[14, 17, 68]. The transition from cubic to tetragonal zirconia phase caused by interaction with Ni was reported in [67]. On the other hand, the thermodynamic stability of zirconia electrolytes is higher with respect to many other electrolytes, such as perovskite-type LSGM or apatite-type $(La, Sr)_{10-x}Si_6O_{26\pm\delta}$, and the combination of Pt and YSZ is commonly selected for the model cells with reference electrodes. Information on the behavior of electrochemical cells with silicate-based electrolytes is still scarce. Silica diffusion from these electrolytes, leading to partial blocking of the interface and electrode surface poisoning [84], is however expected to substantially affect the RE stability and reversibility. LSGM may readily react with metallic Ni and numerous oxide electrode materials due to the high solubility of transition metal cations and formation of relatively stable secondary phases (e.g., [85] and references cited). This interaction makes it necessary to incorporate protective sublayers between the electrolyte membrane and electrodes, and to use noble metals for the REs.

9.4 Reference Electrodes in Solid-State Potentiometric Sensors and Appliances for Thermodynamic Measurements

9.4.1 Sensors

The operation of potentiometric sensors is based on the measurements of concentration cell emf (see Chaps. 1 and 8), which makes it possible to extract the activity, concentration, or partial pressure of potential-determining species at the working electrode vs. RE. The WE potential may be established by a thermodynamic equilibrium or by a nonequilibrium steady state, whereas key requirements to the reference electrodes are related to their reversibility, stability, and, often, fast equilibration on changing external conditions. The solid-state potentiometric sensors are used for a wide variety of technological applications and probed species [2, 3, 5, 15, 18, 86–91]; their application for oxidic glass melts is addressed in Chap. 8.

The common solid electrolytes used in the potentiometric sensors include stabilized ZrO_2, CaF_2 and other fluorides which are often preferable due to higher stability under heavily reducing conditions compared to zirconia, and cation conductors such as β-alumina and NASICON [3–5]. Note that the use of metal salts, formed by the target gas species, as electrolytes enables to directly probe activity of these species; as an example, mixtures of carbonates and sulfates were employed for CO_2 and SO_2 sensors, respectively [92, 93]. However, the sensors with the common electrolytes provide generally better stability and reliability. Apart from the stability issues, the solid electrolyte should possess minimum electronic transport, zero physical leakages, and thermomechanical and chemical compatibility with other sensor components, primarily WE and RE. These criteria are essentially similar to those for the fuel cells and electrolyzers, discussed above. It should be separately stressed that, as a general criterion for the SE selection, the ion transference numbers under operation conditions should not be lower than 0.99 in order to avoid significant

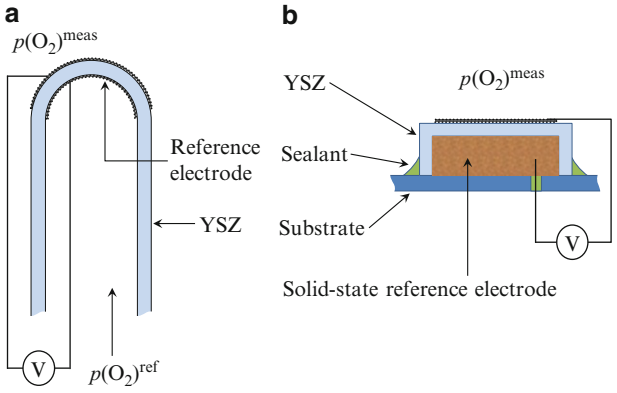

Fig. 9.13 Typical configurations of potentiometric oxygen sensors with yttria-stabilized zirconia solid electrolyte, where the oxygen chemical potential over porous metallic reference electrode is fixed by supplying a gas mixture of known composition (**a**) and where a solid-state RE is used (**b**)

deviations of the measured sensor emf (E_{obs}) from the theoretical Nernst voltage (E_N). In the case when the electrode polarization resistance can be neglected, this deviation is described by the Wagner equation [1–3]:

$$E_{obs} = t_{ion} E_N, \tag{9.9}$$

where the transference number is averaged for a given chemical potential range. For any solid electrolyte, such constraints limit also the range of possible chemical potential variations at the reference electrode. Namely, although a large difference in the activities of electrochemically active species at the electrodes is often desirable to increase the sensor response, the RE should always be selected to provide the reference chemical potential within the electrolytic domain when $t_{ion} \geq 0.99$.

Figure 9.13 illustrates two typical configurations where the reference electrode potential is fixed supplying a gas mixture of known composition onto RE (a) and a solid-state reference electrode is used (b), by the example of gaseous oxygen sensors with YSZ electrolyte. Essentially similar concepts are used for the analysis of oxidic glass melts (Chap. 8). Table 9.2 presents the approximate low-temperature limits of metal | YSZ electrode reversibility vs. composition of O_2-, H_2-, and CO-containing gas mixtures passed over porous electrodes, as reported in [94]. Although the infiltration of catalytically active nonstoichiometric oxides, such as $CeO_{2-\delta}$ or PrO_x, expands the electrode reversibility domain, their use for reference electrodes may be limited if the oxygen nonstoichiometry variations affect the sensor response and equilibration kinetics.

For the solid-state RE, the reference chemical potential is established by a mixture of two compounds whose equilibrium involves electrochemically active species, similar to the buffer solutions enabling fixing pH in the electrochemistry of aqueous electrolytes. In the case of oxygen sensors, these mixtures comprise

Table 9.2 Approximate low-temperature reversibility limits of porous metal and cermet electrodes in contact with YSZ according to [94]

Metal	Infiltrated additive	Atmosphere		
		100 % O_2	21 % O_2 in inert gas	0.01 % O_2 in inert gas
Pt	–	740 K	770 K	840 K
Au	–	800 K	780 K	–
Ag	–	780 K	800 K	1,000 K
Pd	–	860 K	870 K	870 K
Pt	PrO_x	650 K	700 K	790 K
Au	PrO_x	660 K	690 K	870 K
Ag	PrO_x	620 K	700 K	860 K
Pd	PrO_x	630 K	730 K	760 K
		95 % CO in CO–CO_2	50 % CO in CO–CO_2	5 % CO in CO–CO_2
Pt	$CeO_{2-\delta}$	900 K	880 K	870 K
Au	$CeO_{2-\delta}$	790 K	760 K	750 K
Ag	$CeO_{2-\delta}$	790 K	820 K	930 K
Pd	$CeO_{2-\delta}$	940 K	900 K	800 K
		95 % H_2 in H_2–H_2O	50 % H_2 in H_2–H_2O	5 % H_2 in H_2–H_2O
Pt	–	640 K	620 K	620 K
Au	–	740 K	590 K	620 K
Ag	–	650 K	610 K	620 K
Pd	–	760 K	740 K	780 K
Pt	$CeO_{2-\delta}$	630 K	610 K	560 K
Au	$CeO_{2-\delta}$	750 K	670 K	600 K
Ag	$CeO_{2-\delta}$	670 K	640 K	570 K
Pd	$CeO_{2-\delta}$	610 K	650 K	600 K

usually a metal and its binary oxide (such as Ni and NiO) or two oxides (such as Cu_2O and CuO); the oxygen chemical potential at the reference electrode is determined by the reactions like

$$\mathrm{Ni} + \frac{1}{2}\mathrm{O_2} \rightleftarrows \mathrm{NiO} \tag{9.10a}$$

or

$$\mathrm{Cu_2O} + \frac{1}{2}\mathrm{O_2} \rightleftarrows 2\mathrm{CuO} \tag{9.10b}$$

The reference electrodes with liquid components can be equally used, provided that the relevant equilibrium is achieved and there are no concentration polarization and secondary chemical reactions at the RE. The latter requirement common for all electrochemical systems is often crucial for the molten electrodes with high corrosion activity. On the contrary, all-solid-state sensors offer important technical advantages including compactness, easy fabrication and miniaturization, and the possibility to use relatively simple designs and thin-film approaches. Table 9.3 lists several reactions in the metal-oxide and binary oxide mixtures used for reference

Table 9.3 Equilibrium oxygen partial pressures over metal-oxide and binary oxide mixtures used as reference electrodes for thermodynamic measurements and sensors, and the standard free energy changes of the corresponding redox reactions [95, 96]

T (K)	Reaction	log $p(O_2)$ at 1,273 K (atm)	$\Delta_r G^o$ (kJ mol^{-1})
900–1,150	$Pd + \frac{1}{2}O_2 \rightleftarrows PdO$	1.09[a]	$-114 + 0.100\ T$
880–1,125	$2Mn_3O_4 + \frac{1}{2}O_2 \rightleftarrows 3Mn_2O_3$	0.31[a]	$-113 + 0.092\ T$
890–1,300	$Cu_2O + \frac{1}{2}O_2 \rightleftarrows 2CuO$	−0.87	$-131 + 0.095\ T$
1,395–1,720	$\frac{3}{2}UO_2 + \frac{1}{2}O_2 \rightleftarrows \frac{1}{2}U_3O_8$	−4.94	$-167 + 0.084\ T$
970–1,370	$2Fe_3O_4 + \frac{1}{2}O_2 \rightleftarrows 3Fe_2O_3$	−5.47	$-247 + 0.142\ T$
925–1,330	$2Cu + \frac{1}{2}O_2 \rightleftarrows Cu_2O$	−6.24	$-163 + 0.071\ T$
990–1,390	$3MnO + \frac{1}{2}O_2 \rightleftarrows Mn_3O_4$	−6.63	$-223 + 0.111\ T$
1,160–1,370	$Pb(liq) + \frac{1}{2}O_2 \rightleftarrows PbO(liq)$	−7.82	$-191 + 0.075\ T$
770–1,160	$Pb(liq) + \frac{1}{2}O_2 \rightleftarrows PbO$	–	$-215 + 0.096\ T$
910–1,370	$Ni + \frac{1}{2}O_2 \rightleftarrows NiO$	−10.30	$-234 + 0.085\ T$
1,170–1,370	$Co + \frac{1}{2}O_2 \rightleftarrows CoO$	−11.89	$-236 + 0.072\ T$
950–1,270	$3\text{``}FeO\text{''} + \frac{1}{2}O_2 \rightleftarrows Fe_3O_4$	−12.75	$-312 + 0.123\ T$
770–980	$Sn(liq) + \frac{1}{2}O_2 \rightleftarrows SnO$	–	$-293 + 0.108\ T$
970–1,270	$\frac{1}{2}W + \frac{1}{2}O_2 \rightleftarrows \frac{1}{2}WO_2$	−14.7	$-288 + 0.085\ T$
900–1,540	$Fe + \frac{1}{2}O_2 \rightleftarrows \text{``}FeO\text{''}$	−14.84	$-264 + 0.065\ T$
1,025–1,325	$\frac{1}{2}Mo + \frac{1}{2}O_2 \rightleftarrows \frac{1}{2}MoO_2$	−14.86	$-288 + 0.084\ T$
1,050–1,300	$2NbO_2 + \frac{1}{2}O_2 \rightleftarrows Nb_2O_5$	−17.58	$-314 + 0.078\ T$
690–1,180	$Zn(liq) + \frac{1}{2}O_2 \rightleftarrows ZnO$	−17.98	$-356 + 0.108\ T$
1,300–1,600	$\frac{2}{3}Cr + \frac{1}{2}O_2 \rightleftarrows \frac{1}{3}Cr_2O_3$	−21.8	$-372 + 0.084\ T$
1,050–1,300	$NbO + \frac{1}{2}O_2 \rightleftarrows NbO_2$	−22.0	$-360 + 0.072\ T$
920–1,270	$Mn + \frac{1}{2}O_2 \rightleftarrows MnO$	−23.9	$-389 + 0.076\ T$
1,070–1,270	$\frac{2}{5}Ta + \frac{1}{2}O_2 \rightleftarrows \frac{1}{5}Ta_2O_5$	−24.4	$-403 + 0.082\ T$
1,050–1,300	$Nb + \frac{1}{2}O_2 \rightleftarrows NbO$	−25.1	$-420 + 0.090\ T$
300–1,400	$\frac{1}{2}U + \frac{1}{2}O_2 \rightleftarrows \frac{1}{2}UO_2$	−35.5	$-540 + 0.084\ T$
920–1,380	$Mg(liq) + \frac{1}{2}O_2 \rightleftarrows MgO$	−39.3	$-609 + 0.105\ T - 10^{-3}\ T \log T$
1,125–1,760	$Ca(liq) + \frac{1}{2}O_2 \rightleftarrows CaO$	−41.5	$-643 + 0.107\ T$

[a]Extrapolated

electrodes in the potentiometric oxygen sensors and appliances for thermodynamic measurements, addressed below; the standard free energy changes are given for the reactions $Red + \frac{1}{2}\ O_2 \rightleftarrows Ox$ involving one oxygen atom. In cases when the electronic conductivity of solid-state REs is insufficient, sublayers or meshes made of chemically inert metals are often incorporated at the RE interface in order to reduce the cell impedance. The same solid-state REs can also be employed for CaF_2 and other fluoride-based electrolytes owing to the exchange by F^- and O^{2-} anions and substantial oxygen solubility in the fluorite-type lattices.

Whatever the type of reference electrodes, the oxygen partial pressure over working electrodes of the sensors shown in Fig. 9.13, $p(O_2)^{meas}$, can be calculated from the measured emf and reference oxygen pressure, $p(O_2)^{ref}$:

$$E = \frac{RT}{4F} \ln \frac{p(O_2)^{meas}}{p(O_2)^{ref}}. \tag{9.11}$$

Similar approaches can be used to determine activity of alkaline and alkaline earth cations, halogens, hydrogen, sulfur, and other species in gas mixtures, liquid media, and solids [2, 3, 5, 7, 15, 86–91]. As an example, for a galvanic cell with a Na^+ cation-conducting electrolyte and sodium metal present at the electrode, the sodium activity can be calculated from the Nernst voltage:

$$E = \frac{RT}{F} \ln \frac{a_{Na}{}^{meas}}{a_{Na}{}^{ref}}. \tag{9.12}$$

Furthermore, when the sodium cation conductor is an oxide, Na_2O in the electrolyte surface layers may equilibrate with gaseous oxygen

$$2Na^+(s) + \frac{1}{2}O_2(g) + 2e^- \rightleftarrows Na_2O(s) \tag{9.13}$$

In this case, the Na^+ concentration and the cell emf are related to the oxygen partial pressure; sodium oxide should not be necessarily present as a separate phase, but Na_2O activity should remain constant in order to provide stable emf. If the target species are not present in the ion-conducting phase, the measurements can be performed using so-called auxiliary electrodes, e.g., Na_2SO_4 for SO_2 detection:

$$2Na^+(s) + SO_2(g) + O_2(g) + 2e^- \rightleftarrows Na_2SO_4(s) \tag{9.14}$$

Notice that, although metallic sodium might theoretically provide a stable reference potential for Na^+ cation-conducting solid electrolytes, its use in reference electrodes is associated with serious technical difficulties due to high reactivity, as for other alkaline metals. As a rule, more stable compounds and mixtures, such as $NaCl–Na_2CO_3$ [97] or $Na_{1-x}CoO_2$ [98], are used for REs in such sensors. Another attractive approach is to use two solid electrolytes, exchanging cations or anions at the interface and forming so-called electrolyte chains. Irrespective of the system complexity and additional contributions to the cell impedance, this approach expands the choice of potential reference electrodes and the sensor application domain. Furthermore, the electrolyte chain concept makes it possible to combine commercially available and/or low-cost electrolytes as the primary structure and an applied layer of optimized electrolyte composition.

Other important aspects affecting the RE selection in the developments of reliable electrochemical sensors include the reference potential established under target

operation conditions, potential drifts caused by sintering and other morphology-related factors, equilibration kinetics, and cell impedance. The RE placement becomes critical when miniaturizing the sensors [99], as for the components interaction. In order to improve the output stability, the reference potential should be selected, in general, relatively close to the sensing electrode potential range. In particular, the redox couples formed by the transition metals and their oxides, such as Mo–MoO_2 (Table 9.2), are quite suitable for REs in the electrochemical sensors detecting oxygen activity in molten steel, which operate at very high temperatures and low oxygen chemical potentials [100–102]. The reference electrodes comprising Pd–PdO or Cu_2O–CuO couples provide a good performance for moderate oxygen partial pressures typical, as an example, for the detection of oxygen traces in inert gases [15, 103]. As the stagnated reaction kinetics on reducing temperature leads to prolonged transient times, metals with a low melting point (e.g., In, Bi, Sn) are often used in these conditions [104–106]. Finally, one may note Ti–TiH_2 reference electrodes used in hydrogen sensors based on proton-conducting electrolyte, for molten aluminum analysis [107]. The development of such systems always faces, however, significant challenges associated with stability limitations.

9.4.2 *Thermodynamic Analysis*

As for thermodynamic measurements using liquid electrolytes, galvanic cells with solid ion conductors are widely applied to study thermodynamic properties of solids and melts. These measurements are based on the determination of galvanic cell emf (Chap. 1) when the reference electrode potential is known. In a simplest case, when A^{z+} cation-conducting electrolyte is employed and the RE comprises metal A, the cells

$$(-)\mathrm{A}|\mathrm{A}^{z+}|\mathrm{A}_{1-x}\mathrm{B}_x(+) \tag{9.15}$$

make it possible to calculate changes of the A chemical potential on its transfer from the standard state in $A_{1-x}B_x$, which may correspond to an alloy, solid or liquid solution, compound, or phase mixture in equilibrium:

$$\Delta\mu_\mathrm{A} = -zFE. \tag{9.16}$$

The partial molar enthalpy ($\Delta\overline{H}_\mathrm{A}$) and entropy ($\Delta\overline{S}_\mathrm{A}$) can then be extracted from the temperature dependencies of the cell emf:

$$\Delta\overline{S}_\mathrm{A} = zF\left(\frac{\partial E}{\partial T}\right)_\mathrm{P}, \tag{9.17}$$

$$\Delta\overline{H}_{\mathrm{A}} = zF\left[T\left(\frac{\partial E}{\partial T}\right)_{\mathrm{P}} - E\right]. \tag{9.18}$$

In combination with coulometric titration, this approach gives information on the activity variations of potential-determining species vs. composition, phase boundaries, and free energy changes of target reactions, provided an appropriate arrangement of the working and reference electrodes is made. Following the pioneering works by Kiukkola and Wagner [108], the solid-electrolyte appliances became a common tool for the thermodynamic measurements [1–3, 5, 7, 54, 70, 95, 96, 109–112]. The most widespread are solid oxide electrolytes, such as YSZ and yttria-doped thoria, and fluorides, such as CaF_2; the use of cation conductors and other ion-conducting materials was also well documented in the literature, but is less common as the relevant equilibria can often be examined in the galvanic cells with liquid electrolytes. The general requirements to the reference electrodes are essentially similar to those in electrochemical sensors, with a few exceptions related to the cell fabrication, size, and measuring regimes. In particular, RE selection for the thermodynamic experiments is primarily governed by the factors associated with the measurement accuracy, verification, and durability; the criteria related to compactness, easy processing, and fast equilibration important for the sensors can frequently be neglected. On the contrary, any parasitic phenomena which may lead to experimental uncertainties (e.g., electronic transport in solid electrolyte, interaction between the cell materials, contact potentials, temperature gradients, impurities in the RE) should be properly taken into account and, when possible, minimized. For example, critical errors appear due to reactions between solid-state electrode components and ZrO_2-based electrolytes forming interfacial zirconate layers at elevated temperatures [109]. Iron diffusion from the Fe–$Fe_\gamma O$ reference electrodes into yttria-doped thoria solid electrolyte results in $YFeO_3$ formation and in the reference potential deviations up to 40 mV [113]; the interaction between metallic platinum and wüstite makes it often necessary to separate iron-containing components and Pt | zirconia interface at the RE [114]. As a rule, thermodynamic data collected in the solid-state cells are to be validated using the measurements with two or more reference electrodes and, often, different solid electrolytes.

Figures 9.14 and 9.15 illustrate typical arrangements of the galvanic cells with anion-conducting solid electrolytes. For the cells with solid-state reference electrodes (Fig. 9.14), metal-oxide and binary oxide mixtures provide a wide range of accessible potentials (Table 9.3). As for potentiometric sensors, the reference potential should always be selected close enough to that of the working electrode where a compound, alloy, or phase mixture under study is placed, in order to suppress effects of electrolytic and physical leakages. For the same reason, the measuring cell with two electrode compartments separated by the SE membrane is often introduced in a controlled-atmosphere chamber. The use of external reference cells to measure oxygen chemical potential over WE is usually possible, but may be associated with additional errors due to stagnated mass transfer. The diffusion limitations in the gaseous phase may play a positive role when gas compartments over the electrodes

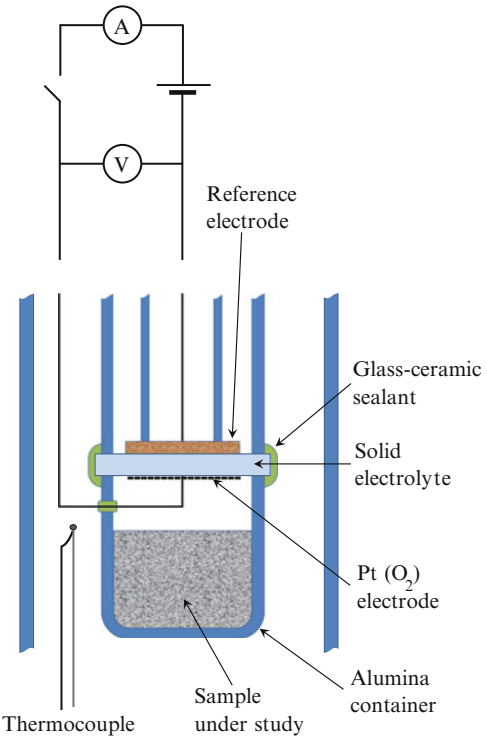

Fig. 9.14 Example of the solid-electrolyte galvanic cell for thermodynamic measurements, where the solid-state RE is pressed onto electrolyte membrane separating two gas compartments

are not separated; however, the results collected using such measuring cells require always a careful verification [96].

For the galvanic cells with fluoride solid electrolytes, electrodes with either gaseous oxygen, oxide mixtures, or fluoride components can be employed. As an example, emf of the cell [116]

$$O_2, Pt|CaO|CaF_2|CaSiO_3, SiO_2|Pt, O_2 \tag{9.19}$$

is governed by the reactions

$$CaO(s) + 2F^- \rightleftarrows CaF_2(s) + \frac{1}{2}O_2(g) + 2e^- \tag{9.20}$$

$$CaF_2(s) + SiO_2(s) + \frac{1}{2}O_2(g) + 2e^- \rightleftarrows CaSiO_3(s) + 2F^- \tag{9.21}$$

and can be used to calculate free energy change for the formation of $CaSiO_3$ from silica and calcium oxide. The cells

$$Mo|Th, ThF_4|CaF_2|ThF_4, ThC_2, C|Mo \tag{9.22}$$

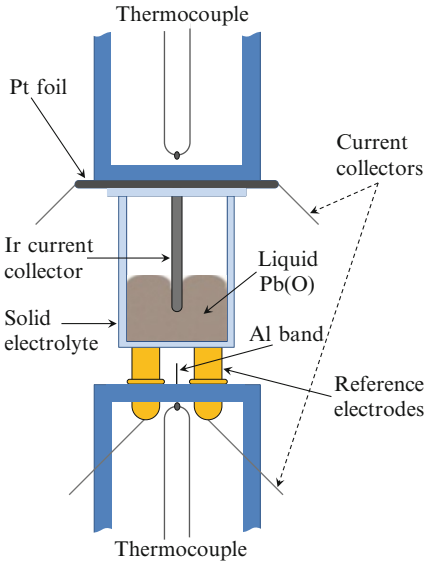

Fig. 9.15 Schematic drawing of the galvanic cells proposed to study oxygen activity in liquid Pb [115], using zirconia- and thoria-based solid electrolytes and reference electrodes made of Ni–NiO and Cu–Cu_2O mixtures

$$\mathrm{Mo|Th, ThF_4|CaF_2|ThF_4, ThC_{1-\delta}|Mo} \tag{9.23}$$

have been proposed to study thermodynamic functions of the thorium carbides [117, 118]. Taking into account the electrolytic-domain limitations of common solid oxide electrolyte materials at very low oxygen chemical potentials, later similar approaches were widely applied for the analysis of numerous carbides and intermetallic compounds (e.g., [119–122]).

References

1. Kröger FA (1964) The chemistry of imperfect crystals. North-Holland, Amsterdam
2. Rickert H (1982) Electrochemistry of solids. An introduction. Springer, Berlin
3. Gellings PJ, Bouwmeester HJM (eds) (1997) Handbook of solid state electrochemistry. CRC Press, Boca Raton, FL
4. Bard AJ, Inzelt G, Scholz F (eds) (2012) Electrochemical dictionary, 2nd edn. Springer, Heidelberg
5. Kharton VV (ed) (2009) Solid state electrochemistry I: fundamentals, materials and their applications. Wiley-VCH, Weinheim
6. Barsoukov E, Macdonald JR (eds) (2005) Impedance spectroscopy: theory, experiment and applications, 2nd edn. Wiley-Interscience, Hoboken, NJ
7. Chebotin VN, Perfiliev MV (1978) Electrochemistry of solid electrolytes. Technical Information Center, US Department of Energy, Oak Ridge
8. Winkler J, Hendriksen PV, Bonanos N, Mogensen M (1998) J Electrochem Soc 145:1184
9. Virkar AV (2005) J Power Sources 147:8

10. Brett DJL, Kucernak AR, Aguiar P, Atkins SC, Brandon NP, Clague R, Cohen LF, Hinds G, Kalyvas C, Offer GJ, Ladewig B, Maher R, Marquis A, Shearing P, Vasileiadis N, Vesovic V (2010) Chem Phys Chem 11:2714
11. Takahashi T, Kozawa A (eds) (1980) Applications of solid electrolytes. JEC Press, Cleveland, OH
12. Goto KS (1988) Solid state electrochemistry and its applications to sensors and electronic devices. Elsevier, Amsterdam
13. Munshi MZA (ed) (1995) Handbook of solid state batteries and capacitors. World Scientific, Singapore
14. Sammes N (ed) (2006) Fuel cell technology: reaching towards commercialization. Springer, London
15. Zhuiykov S (2007) Electrochemistry of zirconia gas sensors. CRC Press, Boca Raton, FL
16. Kharton VV (ed) (2011) Solid state electrochemistry II: electrodes, interfaces and ceramic membranes. Wiley-VCH, Weinheim
17. Perfilyev MV, Demin AK, Kuzin BL, Lipilin AS (1988) High-temperature electrolysis of gases. Nauka, Moscow
18. Murygin IV (1991) Electrode processes in solid electrolytes. Nauka, Moscow
19. Fabry P, Kleitz M (1974) J Electroanal Chem 57:165
20. Wang DY, Nowick AS (1981) J Electrochem Soc 128:55
21. Mitterdorfer A, Gauckler LJ (1999) Solid State Ionics 117:187
22. Mitterdorfer A, Gauckler LJ (1999) Solid State Ionics 117:203
23. Steele BCH (1997) Solid State Ionics 94:239
24. Mizusaki J, Tagawa H, Isobe K, Tajika M, Koshiro I, Maruyama H, Hirano K (1994) J Electrochem Soc 141:1674
25. Adler SB, Henderson BT, Wilson MA, Taylor DM, Richards RE (2000) Solid State Ionics 134:35
26. Adler SB (2002) J Electrochem Soc 149:E166
27. Fleig J, Maier J (1996) Electrochim Acta 41:1003
28. Jiang SP (2004) J Appl Electrochem 34:1045
29. Riess I, Gödickemeier M, Gauckler LJ (1996) Solid State Ionics 90:91
30. Rutman J, Riess I (2007) Electrochim Acta 52:6073
31. Cimenti M, Co AC, Birss VI, Hill JM (2007) Fuel Cells 5:364
32. Nagata M, Itoh Y, Iwahara H (1994) Solid State Ionics 67:215
33. Kato T, Momma A, Kaga Y, Nagata S, Kasuga Y, Kitase M (2000) Solid State Ionics 132:287
34. Fleig J, Baumann FS, Brichzin V, Kim H-R, Jamnik J, Cristiani G, Habermeier H-U, Maier J (2006) Fuel Cells 6:284
35. Cimenti M, Birss VI, Hill JM (2007) Fuel Cells 5:377
36. Hashibon A, Raz S, Riess I (2002) Solid State Ionics 149:167
37. Steele BCH (2000) Solid State Ionics 129:95
38. Norby T (1999) Solid State Ionics 125:1
39. Bonanos N (2001) Solid State Ionics 145:265
40. Thampi KR, McEvoy AJ, Van herle J (1995) J Electrochem Soc 142:506
41. Scholten D, Burggraaf AJ (1985) Solid State Ionics 16:147
42. Kharton VV, Viskup AP, Figueiredo FM, Naumovich EN, Shaulo AL, Marques FMB (2002) Mater Lett 53:160
43. Chebotin VN, Glumov MV, Palguev SF, Neuimin AD (1971) Elektrochimiya 7:491
44. Boukamp BA (2001) Solid State Ionics 143:47
45. Frade JR, Kharton VV, Shaula AL, Marques FMB (2008) Sens Lett 6:370
46. Hsieh G, Ford SJ, Mason TO, Pederson LR (1996) Solid State Ionics 91:191
47. Hsieh G, Mason TO, Pederson LR (1996) Solid State Ionics 91:203
48. Hsieh G, Mason TO, Garboczi EJ, Pederson LR (1997) Solid State Ionics 100:297
49. Lagos GE, Bonanos N, Steele BCH (1983) Electrochim Acta 28:1581
50. Lim H-T, Virkar AV (2008) J Power Sources 180:92

51. Lim H-T, Virkar AV (2008) J Power Sources 192:267
52. Burmistrov I, Bredikhin S (2009) Ionics 15:465
53. Reed DM, Anderson HU, Huebner W (1996) J Electrochem Soc 143:1558
54. Chebotin VN (1989) Chemical diffusion in solids. Nauka, Moscow
55. Bohac P, Orliukas A, Gauckler L (1994) Lowering of the cathode overpotential of SOFC by electrolyte doping. In: Waser R, Hoffmann S, Bonnenberg D, Hoffmann Ch (eds) Electroceramics IV, vol II. IWE, University of Technology, Augustinus Buchhandlung, Aachen, pp 771–774
56. Finnerty CM, Cunningham RH, Kendall K, Ormerod RM (1998) Chem Commun 915
57. Thomsen EC, Coffey GW, Pederson LR, Marina OA (2009) J Power Sources 191:217
58. Kharton VV, Naumovich EN, Vecher AA (1999) J Solid State Electrochem 3:61
59. Kharton VV, Naumovich EN, Yaremchenko AA, Marques FMB (2001) J Solid State Electrochem 5:160
60. Baker R, Guindet J, Kleitz M (1997) J Electrochem Soc 144:2427
61. Reinhardt G, Baitinger V, Göpel W (1995) Ionics 1:504
62. Tsipis EV, Kharton VV (2008) J Solid State Electrochem 12:1367
63. Barbucci A, Bozzo R, Cerisola G, Costamagna P (2002) Electrochim Acta 47:2183
64. Mizusaki J, Tagawa H, Miyaki Y, Yamauchi S, Fueki K, Koshiro I, Hirano K (1992) Solid State Ionics 53–56:126
65. Mizusaki J, Tagawa H, Saito T, Kamitani K, Yamamura T, Hirano K, Ehara S, Takagi T, Hikita T, Ippommatsu M, Nakagawa S, Hashimoto K (1994) J Electrochem Soc 141:2129
66. Schwandt C, Weppner W (1997) J Electrochem Soc 144:3728
67. Aaberg RJ, Tunold R, Mogensen M, Berg RW, Ødegård R (1998) J Electrochem Soc 145:2244
68. Tsipis EV, Kharton VV (2008) J Solid State Electrochem 12:1039
69. Tsipis EV, Kharton VV (2011) J Solid State Electrochem 15:1007
70. Etsell TH, Flengas SN (1970) Chem Rev 70:339
71. Mineshige A, Taji T, Muroi Y, Kobune M, Fujii S, Nishi N, Inaba M, Ogumi Z (2000) Solid State Ionics 135:481
72. Kramer S, Spears M, Tuller HL (1994) Solid State Ionics 72:59
73. Yaremchenko AA, Avdeev M, Kharton VV, Kovalevsky AV, Naumovich EN, Marques FMB (2002) Mater Chem Phys 77:552
74. Marozau IP, Marrero-Lopez D, Shaula AL, Kharton VV, Tsipis EV, Nunez P, Frade JR (2004) Electrochim Acta 49:3517
75. Jacquens J, Farusseng D, Georges S, Viricelle JP, Gaudillere C, Corbel G, Lacorre P (2010) Fuel Cells 10:433
76. Song SJ, Wachsman ED, Dorris SE, Balachandran U (2003) J Electrochem Soc 150:A790
77. Kharton VV, Marozau IP, Mather GC, Naumovich EN, Frade JR (2006) Electrochim Acta 51:6389
78. Haugsrud R, Risberg T (2009) J Electrochem Soc 156:B425
79. Solis C, Serra JM (2011) Solid State Ionics 190:38
80. Biesheuvel PM, Franco AA, Bazant MZ (2009) J Electrochem Soc 156:B225
81. Yaremchenko AA, Kharton VV, Naumovich EN, Marques FMB (2000) J Electroceram 4:235
82. Yamaji K, Horita T, Ishikawa M, Sakai N, Yokokawa H (1999) Solid State Ionics 121:217
83. Yokokawa H, Horita T, Sakai N, Kawada T, Dokiya M (1995) Solid State Ionics 78:203
84. Tsipis EV, Kharton VV, Frade JR (2007) Electrochim Acta 52:4428
85. Huang P, Horky A, Petric A (1999) J Am Ceram Soc 82:2402
86. Weppner W (1987) Sens Actuators 12:107
87. Weppner W (1992) Mater Sci Eng B15:48
88. Yamazoe N, Miura N (1998) J Electroceram 2:243
89. Park CO, Akbar SA (2003) J Mater Sci 38:4611
90. Park CO, Fergus JW, Miura N, Park J, Choi A (2009) Ionics 15:261
91. Fergus JW (2011) J Solid State Electrochem 15:971

92. Currie JF, Essalik A, Marusic JC (1999) Sens Actuators B 59:235
93. Eastman CD, Etsell TH (2000) Solid State Ionics 136–137:639
94. Fadeev GI, Perfilyev MV (1988) Studying equilibrium potentials of gas electrodes in the cells with ZrO_2–O_3 electrolyte at reduced temperatures by the thermo-emf method. In: Perfilyev MV (ed) Electrode processes in solid-electrolyte systems. Ural Branch of the Academy of Sciences of USSR, Sverdlovsk, pp 85–95
95. Rapp RA, Shores DA (1970) Techniques in metal research. In: Rapp RA (ed) Physicochemical measurements in metals research, vol 4, Part 2. Interscience, Chichester, NY, pp 123–192
96. Tretiakov YD (1974) Chemistry of nonstoichiometric oxides. Moscow University Publications, Moscow
97. Zhang L, Fray DJ, Dekeyser JC, Schutter FD (1996) Metall Mater Trans B 27:794
98. Yao PC, Fray DJ (1985) J Appl Electrochem 15:379
99. Rutman J, Riess I (2008) Solid State Ionics 179:108
100. Li F, Zhu Z, Li L (1994) Solid State Ionics 70/71:555
101. Weyl A, Tu SW, Janke D (1994) Steel Res 65:167
102. Lou TJ, Kong XH, Huang KQ, Liu QG (2006) J Iron Steel Res Int 13:18
103. Kaneko H, Okamura T, Taimatsu H, Matsuki Y, Nishida H (2005) Sens Actuators B 108:331
104. Konys J, Muscher H, Voß Z, Wedemeyer O (2004) J Nucl Mater 335:249
105. Colominas S, Abella J, Victori L (2004) J Nucl Mater 335:260
106. Kaneko H, Okamura T, Taimatsu H (2003) Sens Actuators B 93:205
107. Schwandt C, Fray DJ (2006) J Appl Electrochem 36:557
108. Kiukkola K, Wagner C (1957) J Electrochem Soc 104:308
109. Schmalzried H (1966) The EMF method in studying thermodynamic and kinetic properties of compounds at elevated temperatures. In: Thermodynamics: proceedings of symposium 1965, vol 1. International Atomic Energy Agency, Vienna, pp 97–110
110. Alcock CB (ed) (1968) Electromotive Force measurements in high-temperature systems. Institution of Mining and Metallurgy, London
111. Ray HS (2006) Introduction to melts: molten salts, slags and glasses. Allied Publishers, New Delhi
112. Kara S (ed) (2011) Electromotive force and measurement in several systems. InTech, Rijeka
113. Markin TL, Rand MH (1966) Thermodynamic data for plutonium oxides. In: Thermodynamics: Proceedings of Symposium 1965, vol 1. International Atomic Energy Agency, Vienna, pp 144–156
114. Kaul AR, Oleinikov NN, Tretiakov YD (1971) Elektrokhimiya 7:1395
115. Alcock CB, Belford TN (1964) Trans Faraday Soc 60:822
116. Sundaresen M, Gerasimov YI, Geiderikh VA, Vasilyeva IA (1963) Sov J Phys Chem 37:2462
117. Egan JJ (1954) J Phys Chem 68:978
118. Aronson S, Sadofsky J (1965) J Inorg Nucl Chem 27:1769
119. Sichen D (1990) Metall Trans B 21:313
120. Coltters RG, Nava Z (1991) Metall Trans B 22:661
121. Jacob KT, Seetharaman S (1994) Metall Trans B 25:149
122. Alqasmi R, Egan JJ (1995) Metall Trans A 26:1025

Chapter 10
Direct Solid Contact in Reference Electrodes

Andrzej Lewenstam

10.1 The Concept of Solid Contact

As a part of the electrodes used in galvanic cells, the role of direct (internal) contact is to facilitate communication between the meter and the electrochemical cell. This is usually solid contact (SC) and is referred to by names such as solid contact ion-selective electrodes (SC ISEs) or solid contact reference electrodes (SC REs). The main reason for introducing solid contact into indicator/working or reference electrodes is to eliminate their watery compartments, often called internal solution. This solution can be an obstacle in many applications where there are restrictive maintenance and/or service demands (e.g., in clinical chemistry), there is contamination of the sample by a leakage of the internal solution (e.g., in cellular biology), there is a need for other than a vertical position (e.g., in industrial process analysis), or specific reference electrode shapes (e.g., in disposable clinical analyzers) are required.

The internal solution in conventional ion-selective membrane (ISE) and reference electrodes has two roles. One is to support ion-to-electron transduction, or ion-to-electron current, between the internal solution and the electronically conducting substrate, e.g., metal, which is (or is a part of) the lead to the meter. For instance, in a silver–silver chloride reference electrode, it is the chloride ion in the potassium chloride solution that makes the transduction process possible, according to the reaction (see Sect. 5.2 and Chapter 6):

$$\mathrm{Ag} + \mathrm{Cl}^- \rightleftharpoons \mathrm{AgCl} + \mathrm{e}^- \tag{10.1}$$

A. Lewenstam (✉)
Center for Process Analytical Chemistry and Sensor Technology 'ProSens', Process Chemistry Center, Åbo Akademi University, Åbo, Finland

Faculty of Materials Science and Ceramics, AGH University of Science and Technology, Krakow, Poland
e-mail: Andrzej.Lewenstam@abo.fi

G. Inzelt et al. (eds.), *Handbook of Reference Electrodes*,
DOI 10.1007/978-3-642-36188-3_10,

Another role of the internal solution is to support the proper functioning of the electroactive electrode element, whether it is a membrane in the case of an ISE or electrolytic bridge (junction) in the case of a reference electrode (see Chap. 4). In the former instance, a well-defined, reversible, and fast single ion transfer is preferred. In the latter case, the most advantageous is concurrent transfer by ion and co-ion, ideally, both of equal transference numbers.

The solid contact in the electrodes should correspondingly, in SC ISE and SC RE, support these two roles.

Additionally, the solid contact should be stable over time, insensitive to bathing solution matrix effects and changes, easy to cast, well adhering to the substrate phase and electroactive element, thermally resistant, mechanically processable. It would be advantageous if the same or similar SCs are used for fabrication of both the indicator and reference electrodes. If this is the case, then the solid-contact electrode provides an opportunity to fabricate a robust sensor, with the chance to be miniaturized or sterilized [1].

As indicated above, the internal solid contact mediates between the electronically conducting contact (lead to the meter) and ionically conducting electroactive element, which is either a membrane (e.g., ion-selective membrane) or electrolytic bridge (e.g., equitransferent gel).

To ensure mediating role, the SC should exhibit mixed conductivity. For this reason, two types of solid contact were introduced. In the first type the layer of conducting polymer is employed (Scheme 10.1) while in the second the redox polymers confined in a close space are used (Scheme 10.2). Both schemes are shown graphically in Fig. 10.1.

The charge transfer for at least one carrier at the interface I (i.e., electronically conducting substrate/solid contact) and at the interface II (solid contact/electroactive element) should be unblocked (=non-polarized interface), thus allowing for faradaic current. This current is characterized by small charge transfer resistance, making it in particular favorable for potentiometric (zero-current) measurements, because capacitive effects at these interfaces are negligible [2, 3]. The phase of solid contact should support a stable chemical potential (activity) of the charge carriers in SC (electrons and ions), which are fully dissociated and in equilibrium. This ensures reversible ion-to-electron coupling in the solid contact phase, with a "smooth" transition from ionic conduction between the membrane or reference junction to the electronic one of the substrate and supports stable electric potential drops inside the SC and at the SC boundaries, which are controlled by electrons on the electronically conducting substrate side and ions on the SC | membrane/bridge interface [4].

In the case of a thick layer SC, it will allow for "dissipative" unblocking over distance. The stability in this case is provided by the SC bulk, which can be treated as highly loaded redox buffer and ion exchanger. With reduction of the SC thickness, the ion-to-election transduction zone can be downscaled to a "functionalized" (mono)layer covering the substrate, where ion-to-electron coupling and unblocking concurrently take place. The stability can in such a case be achieved by increasing the

electronically conducting substrate (C, Pt, Au) | mixed conducting solid contact (conducting polymer) | ISE or RE membrane/bridge

interface I

interface II

Scheme 10.1 Conducting polymer-based solid contact

electronically conducting substrate (C, Pt, Au) | mixed conducting solid contact (redox polymer) | ISE or RE membrane/bridge

interface I

interface II

Scheme 10.2 Redox polymer-based solid contact

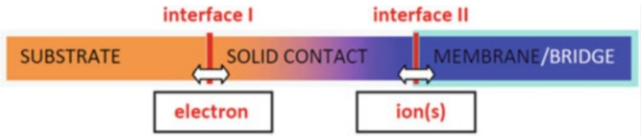

Fig. 10.1 Solid contact as ion-to-electron transducer. Ion-to-electron coupling scheme

effective wiring surface using nanostructures. However, in essence, the mechanisms underlying functionality of SC, as just described, remain the same (see Sect. 10.2).

The fundamental problem of a reference potential when solid contact is applied has been discussed in seminal papers. Initially, thermodynamic criteria of stability for solid-state sparingly soluble sulfide membranes were presented [5, 6], while other authors showed the application of mixed conductor AgF as a solid contact for an ionically conducting LaF_3 solid-state ISE membrane [7, 8]. Different contacts for ion-selective electrodes with glass membrane were reviewed by Nikolskii and Materova [9].

The solid contact for plastic ISE membranes, made by applying conducting polymer (CP) and supported by a comprehensive theoretical model, was introduced by Lewenstam group [4, 10]. The CP used was poly(pyrrole) doped deliberately with tetrafluoride anions [see Eq. (10.10) and adjacent comment]. Since then different conducting polymers were used by numerous authors, mainly conjugated p-doped poly(tiophene), poly(aniline) and poly(pyrrole), and their derivates were applied [11, 12].

CPs as mixed conductors support the conditions for SC, formulated above [4]. In fact, in p-doped polymer the redox reaction is similar to the one given above for silver chloride:

$$CP^0 + X^- \rightleftharpoons CP^+X^- + e^- \tag{10.2}$$

where CP^0 and CP^+ represent reduced and oxidized form of conducting polymer, respectively.

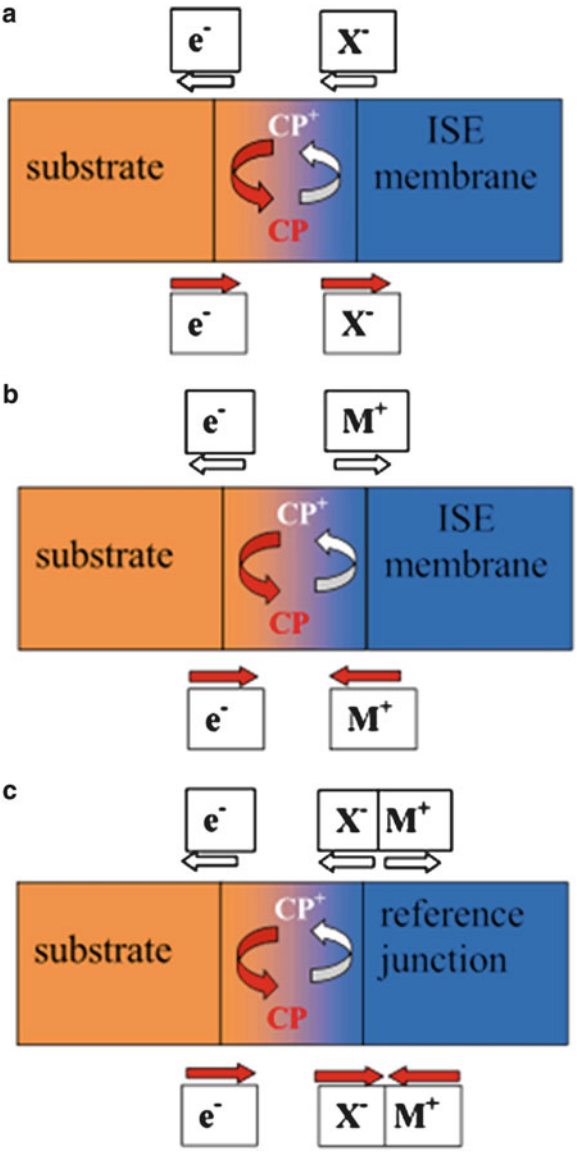

Fig. 10.2 Conducting polymer-based solid contact. Schematic representation of the charge transfer for anion-sensitive (**a**), cation-sensitive (**b**) and reference junction (**c**)

Reaction (10.2) supports anion-to-electron coupling and is used for anion (X^-)-sensitive membranes [13] (see Fig. 10.2a).

Correspondingly, redox reaction in the CP involving cation has the form:

$$CP^0(M^+X^-) \rightleftharpoons CP^+X^- + M^+ + e^- \tag{10.3}$$

Reaction (10.3) supports cation (M^+)-sensitive membranes [13]. This sensitivity is especially pronounced if doping anion X^- is immobile in the CP phase [14] (see Fig. 10.2b).

In a process of repeated oxidation and reduction of the same polymer film with the same charge, it is possible to dope the CP with a salt MX, in particular for immobile M^+ and X^- [13]. This occasion is of importance for reference elements in which MX, in particular equitransferent MX, plays a role of junction electrolyte.

$$CP^0(M^+X^-) \rightleftharpoons CP^0 + M^+ + X^- \tag{10.4}$$

A generalized thermodynamic scheme has been introduced to describe redox and ionic sensitivity of CP [4]. In this theory the polymer is treated as the "sparingly soluble mixed salts," $CP^+e^- \bullet CP^+X^- \bullet N^+X^-$ with reduced and oxidized forms of the CP denoted as red′ and ox′, respectively. A half-cell reaction for the CP | electroactive element (membrane or bridge) is then written as:

$$\overline{\text{red}'} + \frac{\delta}{2}X^- \rightleftharpoons \overline{\text{ox}'} + \frac{\gamma}{2}N^+ + \frac{\delta+\gamma}{2}e^-, \tag{10.5}$$

where barred terms refer to CP phase, and N^+ and X^- are the ions present in the phase in contact with CP (membrane or bridge); γ and δ are stoichiometric coefficients.

It was shown that conducting polymer as the phase characterized with mixed conductivity exhibits metallic behavior in the open-circuit (identical to noble metals or carbon) in contact with the element (membrane, junction, solution) containing the redox pair, according to the Nernst equation:

$$E = E_c^{\ominus\prime} + \frac{RT}{F}\ln\frac{[\text{ox}]}{[\text{red}]}. \tag{10.6}$$

The same CP may exhibit an ionic response (cationic or anionic), which is also Nernstian:

$$E = E_c^{\ominus\prime} + \frac{RT}{F}\ln\left(\frac{[\overline{\text{ox}'}]}{[\overline{\text{red}'}]}\right)^{2/(\delta+\gamma)} + \frac{RT}{F}\ln\frac{[N^+]^{(\gamma)/(\gamma+\delta)}}{[X^-]^{(\delta)/(\gamma+\delta)}}. \tag{10.7}$$

For $\delta = 0$ Eq. (10.7) reduces to the Nernstian form describing cationic sensitivity:

$$E = E_c^{\ominus\prime} + \frac{RT}{F}\ln\left(\frac{[\overline{\text{ox}'}]}{[\overline{\text{red}'}]}\right)^{2/(\gamma)} + \frac{RT}{F}\ln[N^+] \tag{10.8}$$

while for $\gamma = 0$ and the limiting sensitivity is anionic:

$$E = E_c^{\ominus\prime} + \frac{RT}{F} \ln \left(\frac{[\overline{\text{ox}'}]}{[\overline{\text{red}'}]} \right)^{2/(\delta)} - \frac{RT}{F} \ln[\text{X}^-]. \tag{10.9}$$

For the case depicted by reaction (10.4), when $\delta = \gamma$, cationic and anionic sensitivity of CP compensate, with resulting favorable set point for reference electrodes, i.e., potentiometric "zero-slope."

Redox and ion sensitivity of CP that is used as a solid contact is schematically illustrated in Fig. 10.2.

By virtue of the arguments, just given by Eqs. (10.6), (10.8), and (10.9) and Fig. 10.2, justification for applying the mixed conductor, e.g., conducting polymer, as a solid contact, was found and supported. Moreover, it was shown [4, 11, 13] that a desired sensitivity can be exposed by optimizing the composition of the polymer phase (described by parameters γ and δ), which is crucial for favorable application of SC sensors in any electrochemical configuration and variety of samples in which sensor is applied.

From the point of view of a cogent theory, the conducting polymer as a solid contact can reliably work because because it supports electron exchange, and a stable potential difference (pd) on the electronically conducting substrate | CP interface as well as the ion exchange, and a stable pd on the CP | electroactive element interface, as indicated in the schemes Fig. 10.1 and 10.2. Additionally, the theory shows that to get optimal stability of CP-based SC, its redox buffer capacity $[\overline{\text{ox}'}]/[\overline{\text{red}'}]$ and coupled ion loadings ($\overline{\text{N}^+}$ and/or $\overline{\text{X}^-}$) have to be ideally at their maximum, while the activity of electron in the phase in contact with SC (i.e., ISE membrane or reference junction) possibly minimal [4]. It ensures that exchange current density, due to the redox reaction at the substrate and/or a direct electron transfer between the substrate and CP (see [15]), has to be sufficiently high in order to dominate any other competing redox systems such as an oxygen half-cell. Concurrently, high ion loading in the membrane or reference junction in contact with SC allows interfacial potential at this interface to be controlled by ions and not by parasitic redox influences [4, 13, 14, 16–18]. The interfacial potential at this SC interface can be built up by different unblocking mechanisms. Single ion-charge transfer and multiple ion charge transfer (charge partition) are the mechanisms described above. However, the interface can be also unblocked by a local ion-exchange process. That mechanism can be used for the interface with no common ions, as it actually happened with classical system where sodium SC ISE with a plastic membrane was described for the first time [10]. In this system poly(pyrrole) doped with tetrafluoroborate (BF_4^-) as the SC and PVC-based ISE membrane containing tetra(phenyl)borate ($\text{B}\Phi_4^-$) were used.

Assuming ion-exchange equilibrium between BF_4^- and $B\Phi_4^-$ at the conducting polymer (CP)—ISE membrane (M) interface, an expression for a stable Galvani potential difference can be derived [Lewenstam A (1992) unpublished notes]:

$$\varphi_{\mathrm{M}}^{\mathrm{CP}} = \mathrm{const} + \frac{RT}{F} \ln \frac{[\mathrm{BF}_4^-]_{\mathrm{M}} + K_{\mathrm{BF}_4^-,\mathrm{B}\Phi_4^-}[\mathrm{B}\Phi_4^-]_{\mathrm{M}}}{[\mathrm{BF}_4^-]_{\mathrm{CP}} + [\mathrm{B}\Phi_4^-]_{\mathrm{CP}}} = \mathrm{const}', \tag{10.10}$$

where $\varphi_{\mathrm{M}}^{\mathrm{CP}}$ is the electrical potential drop at CP|M interface, surface ion concentrations of ions in the CP and M are denoted using respective symbols, and $K_{\mathrm{BF}_4^-,\mathrm{B}\Phi_4^-}$ is the selectivity coefficient.

A constant bulk concentration of BF_4^- in CP and $B\Phi_4^-$ in PVC provides a sufficient driving force to control a local equilibrium at this interface and to maintain there a constant gradient of electrical potential. (It should be noticed that for ion exchange of the same common ion, the selectivity coefficient can be formally given as $K_{\mathrm{X}^\pm,\mathrm{X}^\pm} = 1$ and Eq. (10.10) is reduced to $\varphi_{\mathrm{M}}^{\mathrm{CP}} = \mathrm{const}'$.) This mechanism is often used in the area of SC-based sensors, see the text below.

In the thermodynamic sense, the interfacial potentials, redox on the left, and ion exchange on the right (Fig. 10.1 and/or Fig. 10.2) contribute to the overall potential of the SC sensor. The bulk of the solid contact supports the process of ion-to-electron coupling, since all of these phase components, including the electrons and (doping or inserted) ions are in equilibrium, and their respective chemical potentials are constant, see [12]. In other words, the high buffer redox capacity and high ionic loading support stability of electric potentials that relate to SC. Recently this theory was generalized by a kinetic approach using the Nernst–Planck–Poisson coupled equation system, and in this way criteria of stability became accessible in an explicit time and space domains [19, 20].

The application of solid contact according to Scheme II with the activity of electron stabilized by redox polymer has been first reported by Hauser group [21]. The authors reported on a poly(vinylferrocene) as a solid contact between the membrane and the metallic substrate.

The solid contact made of a composite of poly(methyl methacrylate) (PMMA) and modified graphite with a surface-confined hydroquinone/quinone redox system was described by Scholz and coworkers [18]. The hydroquinone/quinone redox system was entrapped on the surface of carbon by covalent bonding via an electrochemical preoxidation treatment, which was followed by immobilization of the hydroquinone precursor, 2-(2,5-dimethoxyphenyl)alkaneamine (DMPAA), by carbodiimide chemistry and a final demethylation reaction [18]. Redox-active self-assembled monolayers of a lipophilic redox-active compound [22] and ferrocene-terminated alkanethiols containing amide moieties [23] were used as the intermediate layers between the ISE membrane and gold in the solid-state ISEs. The fabrication of SC ISE with self-assembled redox layer was found tedious, and the long-term stability of SAMs is not guaranteed; the application of poly(*n*-octyl) thiophene (POT) deposited on Au was found advantageous [24]. The poly (vinyl chloride) (PVC) covalently modified with ferrocene groups (FcPVC) was

described as promising ion-to-electron transducer in electrochemical ion sensors, especially in view of designing all solid-state voltammetric ion sensors [25].

Recently the idea of solid contact made of monolayer-protected nanocluster (MPC) characterized by an equimolar mixed-valent $MPC^{0/+1}$ functionalized to interact with tetra(phenyl) borate ($B\Phi_4^-$), namely tetrakis(4-chlorophenyl) borate, was shown to be a good SC for potassium SC ISE [26]. This result shows that the concept of SC and ion-to-electron scheme showed above is valid for solid contacts made with advanced functionalized materials.

Historically important is the porous carbon contact described by Ruzicka and Lamm [27]. It seems that these approaches have paved the way for the present research in sensor technology, in which new nanomaterials are applied. In this research, multiphase (heterogenous) SCs are of interest. They are realized by the introduction of carbon nanostructures (single-walled carbon nanotubes (SWCNTs) [28], carbon cloth [29], carbon black [30], graphene [31]) or nanoparticles (bare or functionalized gold nanoparticles [32], conducting polymers decorated by metal nanoparticles [33]). Although typically the mechanism is not specified, one can assume that it is similar to the ion-to-electron coupling mechanism as described above. An increase in electrode potential stability often reported by the authors, in absence of dedicated coupling, can be in general attributed to the increase of apparent surface area of the metallic contact vs. the geometric area of this contact.

10.2 Solid-Contact Reference Electrodes

Solid-contact reference electrodes, based on contacts made of polypyrrole (PPy) or poly(3,4-ethylenedioxythiophene) (PEDOT), have been presented [34].

Planar and disposable reference electrodes have been described. The method is essentially the same as used for obtaining all-plastic ion-selective electrodes. Aqueous dispersion of poly(3,4-ethylenedioxythiophene) doped by poly(4-styrenesulfonate) ions (PEDOT-PSS, Baytron P).

In both systems the CP layer was covered by a nonselective poly(vinyl chloride)-based membrane containing solid AgCl and KCl, added to obtain a stable potential [35].

Polypyrrole doped by chloride ions PPy(Cl) was used as the SC mediating between the poly(*n*-butyl acrylate) membranes and the glassy carbon electrode [36].

Glassy carbon (GC) disks covered with the conductive polymer [poly(3,4-ethylenedioxythiophene)] doped with chloride (PEDOT-Cl) and covered with the tetrabutylammonium tetrabutylborate (TBA-TBB, single salt) dispersed in PVC have been reported [37]. This system is the example of literal realization of a scheme described by the reaction given by (10.4).

Poly(3-octylthiophene-2,5 diyl) (POT) was used as an intermediate polymer layer, carbon ink substrates and the membranes were prepared using only polymer (PVC) and an ionic liquid (IL) as the plasticizer [38].

Glassy carbon covered with poly(octylthiophene) was used to obtain PVC membrane-based all-solid-state reference electrodes. The reference membrane

was plasticized poly(vinyl chloride) with heterogeneous additives: solid KCl and AgCl encapsulated in polypyrrole microvessels were found to enhance the properties of reference system [39].

The solid contact reference electrodes are so far mainly dedicated to applications in clinical analyzers in potentiometric measurements. Without any doubt, this vividly expanding area of research will soon provide examples of successful application in other measurements.

References

1. Blaz T, Migdalski J, Lewenstam A (2005) Analyst 130:637
2. Janata J (2009) Principles of chemical sensors, 2nd edn. Springer, Dordrecht
3. Buck RP (1978) In: Freiser H (ed) Ion-selective electrodes, vol 2. Plenum, New York, p 1
4. Lewenstam A, Bobacka A, Ivaska A (1994) J Electroanal Chem 368:23
5. Buck RP, Shepard VR (1974) Anal Chem 46:2097
6. Koebel M (1974) Anal Chem 46:1559
7. Lyalin OO, Turayewa MS (1976) J Anal Chem (Russ) 31:1879
8. Fjeldly TA, Nagy K (1980) J Electrochem Soc 127:1299
9. Nikolskii BP, Materova EA (1985) Ion-Selective Electrode Rev 7:1
10. Cadogan A, Gao Z, Lewenstam A, Ivaska A, Diamond D (1992) Anal Chem 64:2496
11. Bobacka J, Ivaska A, Lewenstam A (2008) Chem Rev 108:329
12. Inzelt G (2012) In: Scholz F (ed) Conducting polymers. A new era in electrochemistry, 2nd edn, Monographs in Electrochemistry. Springer, Heidelberg
13. Bobacka A, Ivaska A, Lewenstam A (1994) J Electroanal Chem 368:3333
14. Migdalski J, Blaz T, Lewenstam A (1996) Anal Chim Acta 322:151
15. Maksymiuk K, Nyback A-S, Bobacka J, Ivaska A, Lewenstam A (1997) J Electroanal Chem 430:243
16. Buck RP (1989) J Electroanal Chem 271:l
17. Vorotyntsev MA (1993) Synth Met 55–57:4556
18. Scholz F, Kahlert H, Hasse U, Albrecht A, Kuate AC, Jurkschat K (2010) Electrochem Commun 12:955
19. Sokalski T, Lewenstam A (2001) Electrochem Commun 3:107
20. Lewenstam A (2011) J Solid State Electrochem 15:15
21. Hauser PC, Chiang DWL, Wright GA (1995) Anal Chim Acta 302:241
22. Fibbioli M, Bandyopsdhyay K, Liu S-G, Echegoyen L, Enger O, Diederich F, Bühlmann P, Pretsch E (2002) Chem Mater 14:1721
23. Grygołowicz-Pawlak E, Wygladacz K, Sek S, Bilewicz R, Brzozka Z, Malinowska E (2005) Sens Actuators B 111–112:310
24. Sutter J, Radu A, Peper S, Bakker E, Pretsch E (2004) Anal Chim Acta 523:53
25. Pawlak M, Grygolowicz-Pawlak E, Bakker E (2010) Anal Chem 82:6887
26. Zhou M, Gan S, Cai B, Li F, Ma W, Han D, Niu L (2012) Anal Chem 84:3480
27. Ruzicka J, Lamm CG (1971) Anal Chim Acta 54:l
28. Crespo GA, Macho S, Rius FX (2008) Anal Chem 80:1316
29. Mattinen U, Rabiej S, Lewenstam A, Bobacka J (2011) Electrochim Acta 56:10683
30. Paczosa B Talanta (2012) 93:424
31. Li F, Ye J, Zhou M, Gan ZG, Zhang Q, Han D, Niu L (2012) Analyst 137:618.
32. Jaworska E, Wojcik M, Kisiel A, Mieczkowski J, Michalska A (2011) Talanta 85:1986
33. Li X-G, Feng H, Huang M-R, Gu G-L, Moloney MG (2012) Anal Chem 84:134
34. Kisiel A, Marcisz H, Michalska A, Maksymiuk K (2005) Analyst 130:1655
35. Kisiel A, Michalska A, Maksymiuk K (2007) Bioelectrochemistry 71:75

36. Kisiel A, Michalska A, Maksymiuk K, Hall EAH (2008) Electroanalysis 20:318
37. Mattinen U, Bobacka J, Lewenstam A (2009) Electroanalysis 21:1955
38. Cicmil D, Anastasova S, Kavanagh A, Diamond D, Mattinen U, Bobacka J, Lewenstam A, Radu A (2011) Electroanalysis 23:1881
39. Kisiel A, Kijewska K, Mazur M, Maksymiuk K, Michalska A (2012) Electroanalysis 24:165

Chapter 11
Micro-reference Electrodes

Heike Kahlert

11.1 Introduction

Rapid and accurate determination of ions in solutions is an increasing demand in medicine, research, routine work in laboratories as well as in process control. The development of portable chemical analysers is dependent on the ability to miniaturise the sensors. With voltammetric or amperometric techniques, the tolerated uncertainty in the potential is still relatively large since the analyte concentration is related primarily to the measured current, which is quite constant in a certain potential window. So, pseudo-reference electrodes or quasi-reference electrodes have been successfully implemented in voltammetric and amperometric microsystems. With potentiometric sensors, however, the zero-current potential is directly related to the activity of the analyte ion. The potential change at the reference electrode as a function of the sample composition must therefore be kept reliably small. Considerable effort has been made to improve the performance of ion selective electrodes. As a result, miniaturised ISEs having analytical performance comparable to macro-ISEs are now available for many ions. However, true miniaturisation of ion sensor is often hampered by the lack of suitable micro-reference electrodes. The understanding of the dimensions of a microsystem differs in the literature. The dimension of a true microelectrode should be ca. 1 μm; however, this dimension refers to the active area. The size of the electrode housing may be orders of magnitude larger. Very often, the term micro-reference electrode refers to electrodes with outer dimensions in the lower millimetre range. (cf. Janata [1]). As always, there are three basic requirements that a reference electrode has to satisfy: (1) it should have a stable potential (i.e. the potential should not depend on the composition of the sample solution), (2) the potential should establish reversibly (i.e. the potential will return rapidly to its equilibrium value after a small transient

H. Kahlert (✉)
Institute of Biochemistry, University of Greifswald, 17487 Greifswald, Germany
e-mail: hkahlert@uni-greifswald.de

G. Inzelt et al. (eds.), *Handbook of Reference Electrodes*,
DOI 10.1007/978-3-642-36188-3_11,

perturbation), (3) the potential should be reproducible (i.e. the same electrode potential should be obtained when the reference electrode is constructed from the same electrode/solution combination; esp. also in series production). When miniaturising a reference half-cell, the main question is to which extent these basic requirements have to be fulfilled by the reference electrode. On one hand side, when developing low-cost disposable electrodes, a simple design with cheap component parts is required; a special long-term stability must not be fulfilled. On the other hand side, sophisticated technologies are required to develop sensor systems with increased lifetime without curtailment of the performance of a macroscopic electrode. The development of new technological approaches such as the thick film and thin film techniques supported arrangements with planar reference electrodes. Although thick and thin film technologies have been optimised to a great extent, special problems with miniaturised reference electrodes have to be considered. Because the adhesion of silver to substrates like glass or SiO_2 is poor, an adhesive layer of chromium or titanium is used to provide adequate adhesion. Exposed edges of these adhesive layers could be responsible for the appearance of mixed potentials, or in extreme cases chromium and titanium can be oxidised resulting in a positive potential shift. The contamination of the silver layer by interdiffusion of atoms from the underlying layer can also fatally affect the electrode performance, especially during the conversion of silver to silver chloride [2]. In contrast to macro-reference electrodes, the lifetime of miniaturised reference electrodes is limited because of the non-negligible solubility of AgCl in solutions of high Cl^- concentrations (formation of chloro complexes of Ag(I)). This problem is severe in case of electrodes with AgCl layers of only a few hundred nanometres thickness. The incorporation of a liquid reservoir in miniaturised devices is technically not easy to achieve. In addition, because of the miniaturisation, the electrolyte volume is substantially reduced and rapid contamination as well as exhaustion and drying out of the reference electrolyte, even at low leakage rates, become limiting factors, i.e. attempts to miniaturise macro-reference electrodes of the second kind resulted in a serious reduction of the lifetime. Moreover, a leakage of the inner filling electrolyte of the reference compartment can disturb the response of the working electrode tremendously in small sample volumes. To avoid a dry out of the electrolyte containing gel, one can think about the miniaturisation of the liquid junction. But, the miniaturisation of the contact area between the reference electrolyte and the sample is also limited. By using a dense diaphragm, instable diffusion potentials can occur. Small pores can easily be blocked, and the contact between the reference electrolyte and the sample is interrupted. Additionally, interfering ions (e.g. redox systems from the sample, complexing agents for silver ions, or ions forming sparingly soluble compounds with silver ions) reach the reference electrode surface much faster and in higher concentrations than in the macroscopic arrangement.

Numerous scientific papers and patents have been published describing special constructions of integrated micro-reference electrodes for a certain sensor or sensor array arrangement. It is very difficult to find a general role for the conception of an integrated micro-reference because of the variety of problems to be solved. In the

following, the basic principles, strategies and materials to prepare miniaturised reference electrodes will be discussed. In practice, the user has to decide individually the conception of the reference electrode according to the demands.

11.2 Construction of Miniaturised Reference Electrodes

For the miniaturisation of cylindrical reference electrodes, in general thin silver wires with diameters of about 0.3–0.5 mm were used. By immersing the wires into nitric acid (60 %) for around 30 s, the wires are cleaned. In case of miniaturised planar reference electrodes, different substrates like silicon-based materials, ceramics, glass, heat sealing films or flexible polyimide films (Kapton) can be used. Commercially available silicon wafers with a 100 orientation are cleaned with standard procedures (e.g. by washing with a fluoride containing solution and rinsing with deionised water). After cleaning and drying the surface is oxidised. Kapton materials are cleaned by a series of solvent rinses followed by a dry etch in an oxygen–argon plasma [3]. Because the flexibility of the Kapton material often gives rise to a number of difficulties in further structuring processes, a hard silicon wafer was recommended as support during electrode fabrication [4].

For further structuring, either photolithographic processes (lift-off processes) or screen printing methods (cf. Chap. 13) can be used. In case of photolithographic methods, one can distinguish between positive and negative processes. In both cases, in the first step a light-sensitive photoresist is evenly applied to the substrate, e.g. by spin coating. A mask (e.g. a quartz glass plate with structures of a chromium layer) is placed onto the photoresist, and the wafer is irradiated with UV light only where no chromium is on the glass plate. In case of positive processes, the photoresist at the irradiated areas is dissolved in the next step. In case of negative processes, the irradiated areas stay on the wafer, whereas the other areas are dissolved in the following step. The metal layers can be evaporated sequentially by an electron gun. To avoid the corrosion of titanium and chromium, edges are protected by a hydrophobic polymer [5]. A thin layer of Pt or Pd can be used as a diffusion barrier between Ti and Ag [6]. The last step is the lift-off of the photoresist together with the overlaying metals. Screen printing has the main advantage that the paste can be deposited directly onto the substrate with the help of a mask, i.e. it is not so time consuming as the photolithographic process.

In many cases, where the reference electrode is not required to exhibit a specified and thermodynamically determined potential, the conventional reference electrode is replaced by a pseudo-reference electrode (see Chap. 14). These can be (1) in its most simple form, metal wires (or layers) of Au, Ag or Pt (cf. Fig. 11.1), or (2) in a more sophisticated form, Ag-salt covered Ag electrodes; however, lacking the usual salt reservoir (e.g. KCl) and salt bridge afforded for a complete and thermodynamically controlled reversible reference electrode (see Preface and Chaps. 1–10). The metal layers can be deposited either by photolithographic processes or by screen printing methods (cf. above) [7]. Such micro-pseudo-reference electrodes are parts of voltammetric and amperometric analysing systems and commercially available.

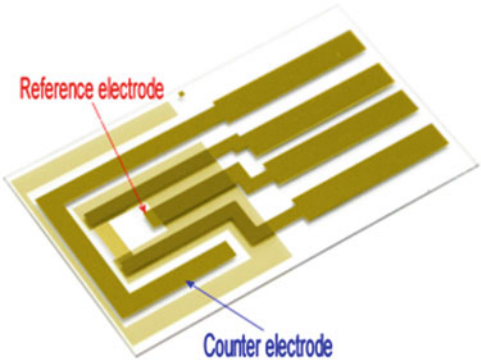

Fig. 11.1 Typical miniaturised pseudo-reference electrode

Pseudo-reference electrodes are preferably used for miniaturised lab-on-chip systems (μTAS = micro total analysis systems) operating under well-defined conditions (e.g. [8]). The Ag/AgCl reference system is the most easily producible planar micoreference electrode with micromachining techniques. The basic structure of the thin film Ag/AgCl element consists of a silver layer deposited and patterned on a dielectric substrate with an adhesive intermediate metallic layer followed by a chemical or electrochemical chlorination. The chemical chlorination can be performed, e.g. in a 0.05 M $FeCl_3$ solution [9]. The electrochemical chlorination can be performed in a solution containing 0.1 mol L^{-1} hydrochloric acid by applying either a constant voltage of 1.0 V or a constant current. Best results are achieved by using constant currents in the microampere range [10]. By screen printing of an Ag/AgCl-containing paste onto an appropriate substrate like structured silicon wafers or polyester foil, rather thick films between 50 μm and some hundred micrometres are obtained [11, 12]. Polymer-based pastes with silver or a mixture of silver/silver chloride are commercially available.

Bratten et al. [13] have investigated the application of semiconductor processing techniques in making devices for electrochemical measurements in sub-nanolitre volumes: integrated micro Ag/AgCl reference electrodes led to increasingly distorted voltammograms, whereas similar Ag/AgI reference electrodes should be undistorted and stable over several hours. An Ag/AgBr pseudo-reference electrode has been described as an integral part of a miniaturised oxygen sensor [14].

Zhang et al. [15] have described carbon fibre microelectrodes with an integrated silver/silver chloride reference electrode for voltammetric measurement. The carbon fibre microelectrodes are sealed into a glass capillary. This capillary is coated with a thin silver film by sputtering procedure. The top layer is then converted into AgCl electrochemically (cf. Fig. 11.2).

To cope with the dissolution of AgCl, different strategies have been followed:

(i) Making the silver and silver chloride layers very thick by electrodeposition (electroplating of thick silver layers onto appropriate substrates) or screen printing. The lifetime of Ag/AgCl quasi-reference electrodes depends also on the degree of conversion of the silver layer to AgCl. The AgCl layer adheres best only when 10–30 % are converted [8, 16].

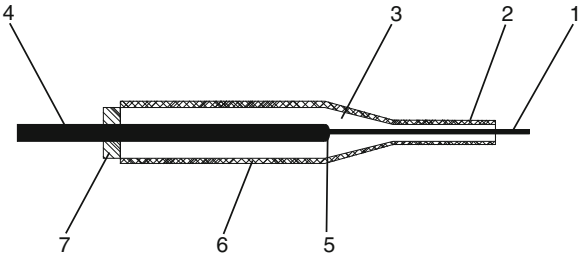

Fig. 11.2 Scheme of a carbon fibre nanoelectrode with an integrated micro Ag/AgCl reference electrode: *1* carbon fibre tip, *2* Ag/AgCl tin film, *3* glass capillary tube, *4* copper wire, *5* carbon fibre-copper wire joint, *6* Ag tin film, *7* epoxy resin (according to [15])

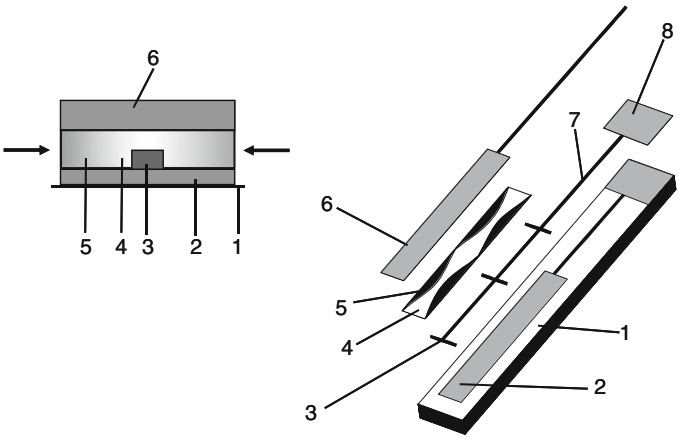

Fig. 11.3 (**a**) Cross section and (**b**) decomposed structure of an Ag/AgCl planar electrode with a protective layer according to Suzuki [2]. *1* Silicon substrate, *2* adhesive layer, *3* gold layer, *4* silver layer, *5* AgCl layer, *6* upper polyimide layer, *7* lead, *8* pad

(ii) Application of diluted Cl^- containing electrolyte solutions.

(iii) Covering the Ag layer by a protecting layer so that the conversion of Ag to AgCl starts at the margins and the Ag/AgCl is vertically sandwiched between the base and the protecting layer [2, 17]. To avoid solution contact with the base metal, a special architecture has been suggested as shown in Fig. 11.3.

(iv) Covering the surface of the entire surface with a porous polymer like Nafion, polyurethane [18, 19], or a combination of conducting polymers covered with PVC or poly(*n*-butyl acrylate) [20, 21]. Schnakenberg [22, 23] used a combination of Ag/AgCl/Ag applying evaporation technique and a photosensitive polyHEMA (hydroxyethyl methacrylate) layer as protection against variation of chloride concentration in the analyte. p-HEMA covered Ag/AgCl layers were successfully used by Cosofret et al. as a reference electrode in a microfabricated sensor array onto a flexible polyimide substrate (Kapton) for

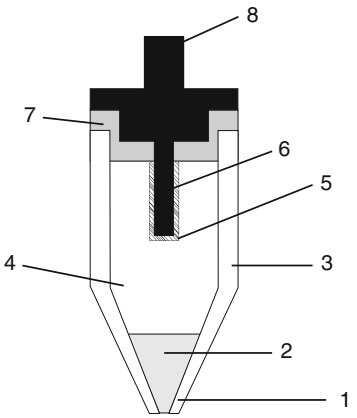

Fig. 11.4 Micro-reference glass electrode tip according to Hassel [27]. *1* Tip diameter 5–100 µm, *2* saltbridge (KNO_3 + 2 % agar in water), *3* glass capillary, *4* electrolyte (sat. KCl 2–4 % agar in water), *5* AgCl, *6* silver wire (Ø = 150 µm), *7* polymer block, *8* gold plated connector

measurements in beating heart [24]. Bakker suggested [25] that the liquid junction free reference electrode based on hydrophobic polymer may function, because the membrane material would be microporous and acts as a liquid junction itself. However, coatings will either produce additional interfacial potentials varying depending on the ionic environment or make the electrode potential more fluctuating by blocking the exchange current.

In case of potentiometric measurements with microelectrode arrays, "complete micro-reference electrodes" have been suggested. The term "complete micro-reference electrode" is used here for such reference electrodes that consist of the same parts as conventional macroelectrodes. Their operating principle is essentially identical to that of the latter. Major difference is the size. Needle-type reference electrodes are frequently used for miniaturisation. The Ag/AgCl system (or a similar one) is hosted in a capillary with dimensions in the millimetre range. The capillary is thinned at one end, and the orifice houses the liquid junction. Commercially available complete reference microelectrodes have capillaries with an outer diameter of 1–2 mm at the end. The liquid junction is realised by a ceramic frit or a fibre. A real micro-reference electrode has been described by Kitade and coworkers [26]. They used a commercially available Femtotip® capillary tube as the electrode body. Such tips have a capillary with an outer diameter of 1 µm and are usually used for microinjection into adherent and suspension cells. The tip is filled with a KCl agar gel to realise the liquid junction. The bare part of the silver wire has to be covered with a polystyrene membrane to avoid any additional potential between the inner electrolyte solution and the bare silver wire.

The same configuration in a glass capillary was used by Hassel et al. [27] (see Fig. 11.4).

The problem with such ultra-micro-reference electrode was that the potential can be strongly influenced by electromagnetic interferences. Therefore, a shielded wire between the electrode and the potentiometer is demanded. The main lack is that the electrodes remain functional for only 7 days after fabrication and are applicable only for disposable use. The leakage of the inner electrolyte solution, the dry out of

the electrolyte reservoir via the agarose gel as well as the dissolution of the silver chloride layer can be responsible for the short lifetime of the electrodes. However, the reproducibility is very high and the difference to macroscopic reference electrodes is nearly zero. Of course, such ultra-thin glass capillaries are very fragile.

More promising for applications are planar micro-reference electrodes. The basic structure of planar miniaturised reference electrodes is the same as for quasi-reference electrodes. Additionally, a reservoir containing an electrolyte, mostly potassium chloride, or an electrolyte containing membrane will be used. The limitation of the scaling down of conventional reference electrodes of the second kind lies in the fact that the miniaturisation of the volume of the reference electrolyte leads to shorter lifetimes because the outflow of the reference electrolyte as well as the penetration of the measuring electrolyte change the concentration of the reference electrolyte very quickly. To solve that problem, several authors have used potassium chloride containing gels like KCl-agarose [6, 10]. These electrodes showed good reproducibility, insensitivity towards pH changes and towards differences in chloride ion concentrations, but nothing is said about the storage of the electrodes. The problem is that the agarose gel can dry out during storage; hence, such electrodes are only useful for laboratory use immediately after preparation. Other authors used polyacrylamide hydrogel doped with KCl as an internal electrolyte [28].The deposition of solid KCl in the reference electrolyte volume can prolong the lifetime of the reference compartment, but because of the solubility of the salt the reservoir is quickly consumed.

Yee [29] has suggested a miniature liquid junction reference electrode with a micromachined silicon cavity. The electrode essentially consists of four parts: (1) a silicon-based cavity in combination with two side channels, (2) a layer of Corning 7930 porous glass as the ion-exchange membrane, (3) a layer of Corning 7740 glass as the back cover and (4) a Ag/AgCl wire. The cavity is formed by anisotropic etching from both sides of a silicon wafer using SiO_2 as a mask material and standard silicon etching procedure. The volume of the cavity can be controlled by the thickness of the silicon wafer and the back opening of the SiO_2 mask. After the cavity is formed, the back cover Corning 7740 glass is electrostatically bonded to the silicon. The front end of the electrode is then covered with the Corning 7930 porous glass by using epoxy. The cavity is filled with saturated KCl solution by connecting the porous glass side with a vacuum pump and injecting the electrolyte solution into one of the two side channels. A fine silver wire is electrochemically chloridised and then inserted from the other side channel. Finally, epoxy is used to close up both channels. The miniaturised electrodes showed an offset between electrodes with different areas of front opening; i.e. the reproducibility seems to be a problem with this kind of miniaturised reference electrodes. The electrodes showed a potential drift of 0.25 mV h^{-1} in 1 M KCl indicating a diffusion of Cl^- ions out of the electrode cavity. A similar approach was suggested by Suzuki [30] (cf. Fig. 11.5). The lifespan of this kind of electrodes could be expanded to 100 h with a fluctuation of the potential of ± 1 mV.

Mroz [31] described a disposable reference electrode based on the Ag/AgCl system without a diaphragm (see Fig. 11.6). The internal electrolyte solution is

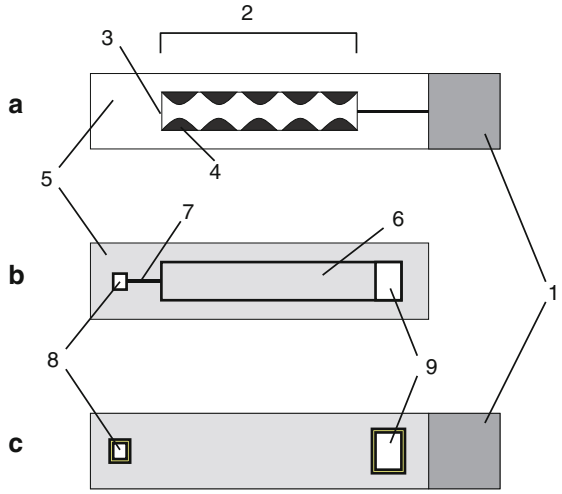

Fig. 11.5 Structure of the miniature liquid-junction Ag/AgCl reference electrode suggested by Suzuki [30]: (**a**) glass substrate on which the Ag/AgCl reference element is formed, (**b**) silicon substrate on which the recess for the electrolyte solution and the liquid junction are formed, (**c**) completed electrode. *1* Pad, *2* Ag/AgCl element, *3* gold backbone, *4* AgCl, *5* surfaces to be bonded, *6* recess in which the electrolyte is filled, *7* liquid junction, *8* end of liquid junction (thru-hole), *9* thru-hole to introduce the electrolyte solution

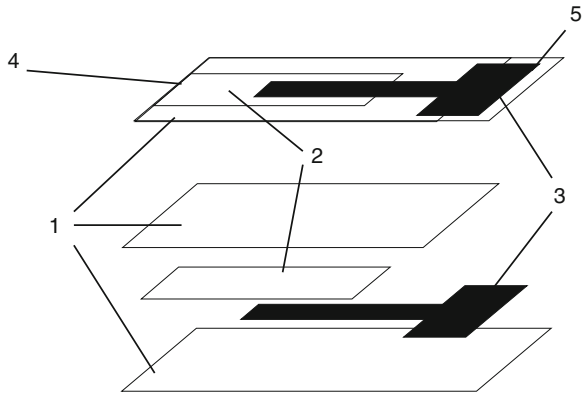

Fig. 11.6 Scheme of the disposable reference electrode suggested by Mroz [31]. *1* Sealing film, *2* glass fibre with the internal electrolyte, *3* strip conductor, *4* electrolyte contact opening, *5* contact to the potentiometer

enclosed in a glass-fibre filter medium, which provides limited leakage. The electrodes were produced by depositing an Ag/AgCl screen printing ink on a sheet of heat sealing film. Glass-fibre filter medium was positioned over the conducting line and a second sheet was placed on top and the three layers were laminated together. The filter paper was filled by immersing the electrode in 3 M

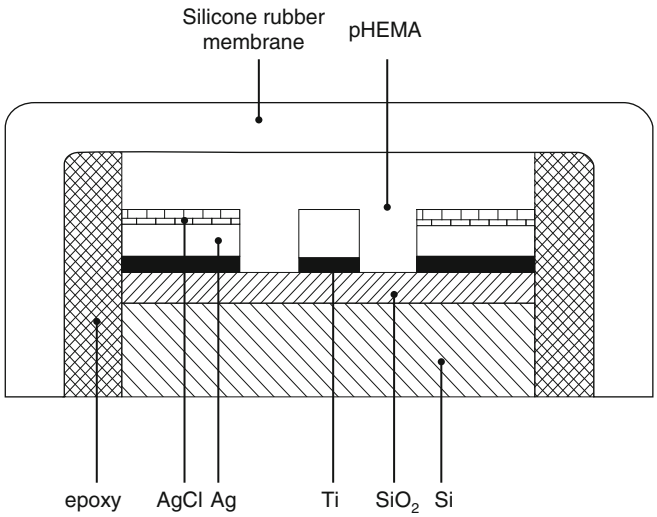

Fig. 11.7 Cross section of the planar two-electrode oxygen sensor according to Koudelka [16]

KCl. The filling is spontaneous, caused by capillary forces. In order to make a contact with the measured solution, the lower part of the electrode will be cut just before the measurement. The influence of moderate concentrations of KCl and NaCl and of the pH of the test solution in the range from 3 to 11 on the potential of the disposable reference electrodes is very small. The potential of the electrodes is sufficiently stable for at least 1 day with a drift of about 0.5 mV h^{-1}.

An alternative to overcome problems with the miniaturisation of the diaphragm is the use of salt containing polymers like polyvinyl acetate, quaternary polychloromethylstyrene, PVC, or pHEMA. The reference electrode design by Kinlen [32] involves coating a silver–silver chloride surface with a chloride-ion containing polymer (e.g. triethylamine quarternised polychloromethylstyrene). Here, the chloride ion is trapped within the polymer layer by encapsulating it with Nafion. After annealing, the Nafion cation-selective membrane effectively blocks chloride-ion diffusion to the test solution and maintains a constant chloride ion activity on the Ag/AgCl surface.

Koudelka [16] has introduced a planar two-electrode oxygen sensor with a planar Ag/AgCl/Cl^- reference electrode with a hydrogel internal electrolyte (Fig. 11.7). The electrode was covered with poly(2-hydroxyethyl methacrylate), pHEMA, by polymerisation at room temperature. After polymerisation, the pHEMA was soaked in an electrolyte solution containing potassium chloride. Finally, the entire sensor was covered with silicon rubber (50 μm) to stabilise the fragile pHEMA layer after water uptake.

Authors stated that the reference potential is stable and reproducible within 10 mV for several days of continuous testing. To avoid a drying out of the KCl containing gel, a covering of the gel with a polymer like silicone, PVC, Nafion,

cellulose nitrate or a combination of thin protection membranes has been recommended [33, 34]. Tymecki has presented a method for the fabrication of a planar Ag/AgCl/KCl reference electrode on a flexible polyester foil [35] by screen printing. The best results have been obtained with the following structure: (1) protective paste (highly hydrophobic paste, usually applied for screen printing of protective layers) doped with KCl, (2) Ag/AgCl paste, (3) protective paste doped with KCl and (4) non-modified protective paste with a small hole to enable the contact between the KCl and the solution (see also Chap. 13). Here, the process of water penetration and electrolyte leakage is relatively slow. Such electrodes showed acceptable stability over a time period of 10 days. Also, the reproducibility was quite good (sd = 4.1 mV for eight electrodes). The electrodes could be stored at ambient conditions for at least 9 months.

Mamińska and co-workers [36, 37] presented a miniaturised reference electrode consisting of planar Ag/AgCl layers covered with PVC membranes containing an ionic liquid (1-dodecyl-3-methylimidazolium chloride, IL). The membrane with the additive provides an internal solid electrolyte with a constant chloride concentration and thus a constant potential. The reproducibility of such electrodes is acceptable (within 10 mV). The lifetime depends on the amount of the IL and can reach nearly 2 months. Kakiuchi has described the direct covering of an Ag/AgCl wire with a gelled AgCl containing ionic liquid 1-methyl-3-octylimidazolium bis (trifluoromethylsulfonyl)imide [38]. The ionic liquid serves as a salt bridge. The problem is that a partial leaching of the IL from the membrane to the test solution can occur.

11.3 R(E)FETs

The ISFET, developed from the fabrication techniques of semiconductor devices, is an important sensor device used in potentiometry. The main advantages are the extremely small size, solid-state structure and the ability to fabricate multi-ion sensors. More than 30 years ago, methods have been proposed to work with a differential arrangement, i.e. the integration of an ion-sensitive and an ion-insensitive structure, the later one working as the reference element (R(E)FET). The main problem is that semiconductor-modified surfaces required for R(E)FET are also not always in thermodynamical equilibrium with the test solution and can be sensitive to aggressive or interfering dissolved species or not well characterised aging phenomena.

Comte and Janata [39] were the first using a modified pH-ISFET as a reference field effect transistor (R(E)FET). A small compartment filled with buffered agarose gel is built on the membrane of the reference gate and is connected with the sample solution via a glass capillary (see Fig. 11.8).

A similar approach with a fluoride-sensitive ISFET, a reservoir containing CaF_2 and a polymer membrane (cellulose-2,4-acetate) was suggested by Lisdat and Moritz [40] as a reference compartment in a differential arrangement with a fluoride-sensitive

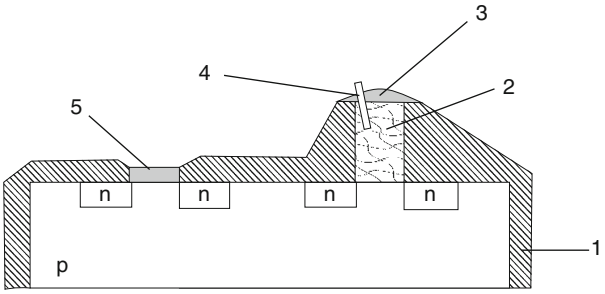

Fig. 11.8 Schematic description of a transistor chip with an ISFET and a reference gate (cf. [39]). *1* Epoxy resin, *2* compartment filled with buffered agarose, *3* reference gate, *4* glass capillary, *5* ion-sensitive gate

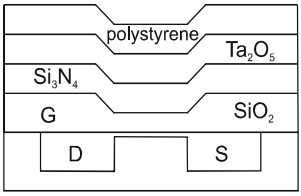

Fig. 11.9 Schematic configuration of the REFET described by Tahara et al. [46]. *D* drain, *S* source, *G* gate

ISFET to determine fluoride concentrations. At first sight, this concept seems rather promising. However, because of the limited lifetime, limitation in miniaturisation and rather complicate preparation, it did not obtain acceptance.

More promising seemed the fabrication of R(E)FESTs by coating ISFET gate surfaces with hydrophobic, insulating and ion-blocked films by vacuum deposition, ion beam sputtering and plasma polymerisation, chemically grafting an aliphatic chain, covalently anchoring an ion-blocking polymeric membrane formed by photopolymerisation, coating a bilayer, etc. [41–44]. Oyama [45] suggested a R(E)FET, the gate of which is coated with two kinds of polymeric films in a bilayer state. The inner layer is the electroactive electropolymerised poly(*p*,*p*′-biphenol) film, and the outer one is the polyimide film prepared by radical polymerisation of the photosensitive polyimide precursor by UV radiation. The bilayer film-coated R(E)FETs were nearly insensitive to Cl^- ion under a constant concentration of $NaClO_4$. The concentration of the electroactive sites in the inner film is very high (in the order of 1 M), thus it was expected that the redox couples in the film determine the potential level of the electrode surface, i.e. the inner film is considered to function as an "internal" standard solution. The drift of the reference electrodes was within 0.2 mV during continuous measurement of 11 h. Tahara [46] reported on a R(E)FET, that is, the gate insulator of the pH-ISFET is directly coated with a plasma polymerised styrene thin film soaked with potassium chloride (c.f. Fig. 11.9).

This film prevents the variations of the interface potential, which is located between the gate insulator and electrolyte from being affected by the species and activities of ions dissolved in sample solutions. The special structure of the film shows that potassium chloride solution is tightly held on the surface of the film and works as a salt bridge. Matsuo [47] proposed a parylene-gate ISFET as a reference electrode. Parylene film is an almost hydrophobic and ion-blocked membrane, and parylene-gate ISFETs showed very low pH sensitivity and negligible sensitivities towards other ions like sodium ions or chloride ions. The authors have analysed the electrolyte–insulator–semiconductor system theoretically by applying the site-binding model to the electrolyte–insulator interface and considering the interactions between the charge in the electrolyte and the charge in the semiconductor surface through the gate capacity (field effect). From the results they have derived the required conditions of the parameters for a reference ISFET, i.e. the relationship between the low dissociated site density of the insulator and the semiconductor charge density which will make the surface potential of the insulator constant.

In summary, it can be stated that a lot of attempts have been made to create REFETS, but so far no long-term stable and reliable device was successful. Additionally, theoretical explanations are contrary.

11.4 Other Alternatives

Yoon et al. [48] proposed a liquid junction free polymer membrane-based reference electrode system for blood analysis under flowing conditions. They used silicon wafers as well as ceramic substrate to fabricate ion selective sensors with an integrated reference electrode. The silver chloride layer was coated with a membrane based on aromatic polyurethane (PU 40 membrane) with equimolar amounts of both cathodic and anodic lipophilic additives (TDMACl and KTpClPB) to reduce the electrical resistance (see Chaps. 12 and 13). The ceramic-based sensors were fabricated by screen-printing methods. Both reference electrodes showed a rather stable potential in various electrolyte solutions with different pH values and different concentrations of clinically relevant ions, providing that the ionic strength of the solution is over 0.01 M. The integrated ISE cartridge based on the ceramic chip could be used continuously for a week.

Anastasova et al. [49] have described solid contact reference electrode based on conducting polymer and traditional plasticised PVC membrane doped with lipophilic electrolyte. Here, Au/PEDOT, TBA-TBB, o-NPOE and PVC are parts of a pen-like multisensor probe (diameter 13 mm with seven integrated electrodes each of which has a diameter of 1 mm). The response time is of ca. 2 min due to kinetic hindrance of the surface ion-exchange process; the electrodes showed good long-term stability and no significant deviation in response after 3 months.

In an approach suggested by Nagy et al. [50], the reference signal will be produced by two separate electrodes consisting of Ag/AgCl layers covered with an anion and cation conducting membrane, respectively. The electrodes are connected in parallel via a resistor and intrinsically respond to monovalent cations

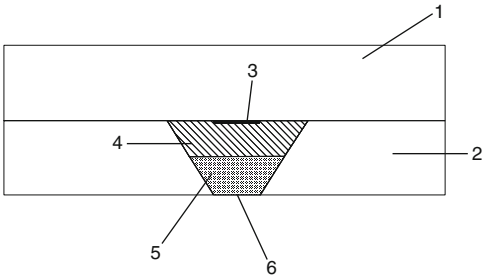

Fig. 11.10 Schematic description of a reference electrode with a perchlorate-sensitive membrane suggested by Dumschat [52]. *1* Glass substrate, *2* Silicium, *3* Ag contact, *4* perchlorate-sensitive membrane, *5* perchlorate containing gel, *6* contact area to the electrolyte solution

and anions in solution according to the Nernst equation. The resulting EMF is then nearly independent on sample concentration changes. This approach has a number of shortcomings (e.g. measured potential will change as the nature of the sample electrolyte varies).

Lee proposed reference electrodes [51] with polymer membranes directly deposited onto the surface of a metal. The polymer membrane incorporate both anion- and cation-exchange sites (i.e. potassium tetrakis(*p*-chlorophenyl)borate and tridodecylmethylammonium chloride). Best results were obtained with polyurethane combined with poly (tetramethylene ether glycol) (PTMEG).

Dumschat [52] has suggested a reference electrode containing a perchlorate-sensitive membrane (see Fig. 11.10).

A silver contact was deposited onto a glass substrate and covered with the perchlorate-sensitive membrane. The electrolyte cavity is filled with a potassium perchlorate-containing gel and has a small contact area with the sample solution. The lifetime of such electrodes is longer than that for comparable potassium chloride containing electrodes as the solubility of potassium chloride is higher than of potassium perchlorate. The same concept can be used for REFETs consisting of a perchlorate-sensitive membrane in contact with a mixture of solid potassium perchlorate and $CaSO_4 \cdot 2H_2O$ and covered with a polyethylene/polyester film. A small hole in the film serves as a liquid junction [53].

An interesting alternative is disposable electrodes developed by Diekmann and co-workers [54]. Here, a microfibre matrix, e.g. a filter paper is filled with a redox electrolyte solution. Graphite serves as a strip conductor. The filter paper is laminated with a heat sealing film. To fill the filter paper, a small strip is cut and the electrode can be immersed into a solution containing KCl and an equimolar mixture of $K_4[Fe(CN)_6]$ and $K_3[Fe(CN)_6]$ in a nitrogen atmosphere. To store the electrodes, the opening has to be closed. Of course, the lifetime of such electrodes is very short (2 days) and storage shows complications because of the oxidation of $K_4[Fe(CN)_6]$ with O_2 and drying out of the inner solution. Additionally, the temperature dependence and the influence of other redox systems have to be taken into consideration. However, because of the simple and low cost preparation, it is an interesting approach for laboratory use.

11.5 Conclusions

Considerable efforts have been made to develop reliable micro-reference systems. As a result, different strategies have been proposed to construct micro-reference compartments mostly for short-time measurements in research laboratories or for disposable devices. However, the main problems with long-term stability of micro-reference electrodes could not be solved satisfactorily up to now. The development of all-solid state reference electrodes is still in an early stage, and basic research is required to add the knowledge in the field of the electrochemical processes at solid-state electrodes. The main question is if it is really possible from a theoretical point of view to create a reliable reference system in the micrometre scale.

References

1. Janata J (1990) Chem Rev 90:691
2. Suzuki H, Hiratsuka A, Sasaki S, Karube I (1998) Sens Actuators B 46:104
3. Lindner E, Cosofret VV, Ufer S, Buck RP, Kusy RP, Ash RB, Nagle HT (1993) J Chem Soc Faraday Trans 89:361
4. Lindner E, Cosofret VV, Ufer S, Johnson TA, Ash RB, Nagle HT, Neuman MR, Buck RP (1993) Fresenius J Anal Chem 346:584
5. Bousse LJ, Bergveld P, Geeraedts HJM (1986) Sens Actuators 9:179
6. Huang IY, Huang RS (2002) Thin Solid Films 406:255
7. Jenkins DM, Song C, Fares S, Cheng H, Barrettino D (2009) Sens Actuators B 137:222
8. Gernet S, Koudelka M, de Rooij NF (1989) Sens Actuators 18:59
9. Polk BJ, Stelzenmueller A, Mijares G, MacCrehan W, Gaitan M (2006) Sens Actuators B 114:239
10. Huang IY, Huang RS, Lo LH (2003) Sens Actuators B 94:53
11. Desmond D, Lane B, Alderman J, Glennon JD, Diamond D, Arrigan DWM (1997) Sens Actuators B 44:389
12. Cranny AWJ, Atkinson JK (1998) Meas Sci Technol 9:1557
13. Bratten CDT, Cobbold PH, Cooper JM (1997) Anal Chem 69:253
14. Wittkampf M, Chemnitius GC, Cammann K, Rospert M, Mokwa W (1997) Sens Actuators B 43:40
15. Zhang X, Ogorevc B, Tavčar G, Grabec Švegl I (1996) Analyst 121:1817
16. Koudelka M (1986) Sens Actuators 9:249
17. Suzuki H, Hirakawa T, Sasaki S, Karube I (1999) Anal Chim Acta 387:103
18. Nolan MA, Tan SH, Kounaves SP (1997) Anal Chem 69:1244
19. Moussy F, Harrison DJ (1994) Anal Chem 66:674
20. Kisiel A, Macisz H, Michalska A, Maksymiuk K (2005) Analyst 130:1655
21. Kisiel A, Michalska A, Maksymiuk K, Hall EAH (2008) Electroanalysis 20:318
22. Schnakenberg U, Lisec T, Hintsche R, Kuna I, Uhlig A, Wagner B (1996) Sens Actuators B 34:476
23. Uhlig A, Dietrich F, Lindner E, Schnakenberg U, Hintsche R (1996) Sens Actuators B 34:252
24. Cososfret VV, Erdösy M, Johnson TA, Buck RP, Ash RB, Neuman MR (1995) Anal Chem 67:1647
25. Bakker E (1999) Electroanalysis 11:788
26. Kitade T, Kitamura K, Takegami S, Miyata Y, Nagamoto M, Sakaguchi T, Furukawa M (2005) Anal Sci 21:907

27. Hassel AW, Fushimi K, Seo M (1999) Electrochem Commun 1:180
28. Arquint P, van den Berg A, van der Schoot BH, de Rooji NF, Bühler H, Morf WE, Dürselen LFJ (1993) Sens Actuators B 13–13:340
29. Yee S, Jin H, Lam LKC (1988) Sens Actuators 15:337
30. Suzuki H, Hirakawa T, Sasaki S, Karube I (1998) Sens Actuators B 46:146
31. Mroz A, Borchardt M, Diekmann C, Cammann K, Knoll M, Dumschat C (1998) Analyst 123:1373
32. Kinlen PJ, Heider JE, Hubbard DE (1994) Sens Actuators B 22:13
33. Simonis A, Lüth H, Wang J, Schöning MJ (2003) Sensors 3:330
34. Ha J, Martin SM, Jeon Y, Yoon IJ, Brown RB, Nam H, Cha GS (2005) Anal Chim Acta 549:59
35. Tymecki L, Zwierkowska E, Koncki R (2004) Anal Chim Acta 526:3
36. Mamińska R, Dybko A, Wróblewksi W (2006) Sens Actuators B 115:552
37. Mamińska R, Dybko A, Wróblewksi W (2006) Electroanalysis 18:1347
38. Kakiuchi T, Yoshimatsu T, Nishi N (2007) Anal Chem 79:7187
39. Comte PA, Janata J (1978) Anal Chim Acta 101:247
40. Lisdat F, Moritz W (1993) Sens Actuators B 15–16:228
41. Perrot H, Jaffrezic-Renault N, De Rooji NF, Van den Vlekkert HH (1989) Sens Actuators 20:293
42. Skowronska-Ptasinska M, Van der Wal PD, Van den Berg A, Bergveld P, Sudhölter EJR, Reinhoudt DN (1990) Anal Chim Acta 230:67
43. Chovelon JM, Fombon JJ, Clechet P, Jaffrezic-Renault N, Martelet C, Nyamsi A (1992) Sens Actuators B 8:221
44. Jaffreczic-Renault N, Chovelon JM, Perrot H, Le Perchec P, Chevalier Y (1991) Sens Actuators B 5:67
45. Oyama N, Ohsaka T, Ikeda S, Okuaki K (1989) Anal Sci 5:729
46. Tahara S, Yoshii M, Oka S (1982) Chem Lett 3:307–310
47. Matsuo T, Nakajima H (1984) Sens Actuators 5:293
48. Yoon HJ, Shin JH, Lee SD, Nam H, Cha GS, Strong TD, Brown RB (2000) Sens Actuators B 64:8
49. Anastasova-Ivanova S, Mattinen U, Radu A, Bobacka J, Lewenstam A, Migdalski J, Danielewski M, Diamond D (2010) Sens Actuators B 146:199
50. Nagy K, Eine K, Syverud K, Aune O (1997) J Electrochem Soc 144:L1
51. Lee HJ, Hong US, Lee DK, Shin JH, Nam H, Cha GS (1988) Anal Chem 70:3377
52. Dumschat C (1993) DE 4302322 A1
53. Pötter W, Dumschat C, Cammann K (1995) Anal Chem 67:4586
54. Diekmann C, Dumschat C, Cammann K, Knoll M (1995) Sens Actuators B 24–25:276

Chapter 12
Conducting Polymer-Based Reference Electrodes

Jan Migdalski and Andrzej Lewenstam

12.1 Introduction

Conducting polymers [1] in reference electrodes are used for two reasons/in two roles:

- Conducting polymer (CP) is an active part of the reference electrode (i.e., CP-based reference membrane)
- Conducting polymer is a solid contact between plastic reference membrane and electronic conductor (for theoretical background see Chap. 10)

In comparison with the conventional reference electrodes (see Chap. 5), application of conducting polymer increases the reference electrodes' integrity by elimination of water-containing compartments. This allows the electrode miniaturization and eliminates problems resulting from uncompensated transport and undesired leakages from the bridge. The elimination of water compartments from the reference electrodes by use of conducting polymers enables their application at higher temperatures and over a wide pressure range as well as in the measurements in nonaqueous solvents.

Numerous attempts were undertaken to apply conducting polymers for the reference electrodes design. They cover the following aspects: (1) adjusting of the electrode response by dispersing molecules enhancing its stability, (2) adjusting ion

J. Migdalski (✉)
AGH University of Science and Technology, Faculty of Materials Science and Ceramics, Mickiewicza 30 Ave., 30-059 Krakow, Poland
e-mail: migdal@agh.edu.pl

A. Lewenstam
Center for Process Analytical Chemistry and Sensor Technology 'ProSens', Process Chemistry Center, Åbo Akademi University, Åbo, Finland

Faculty of Materials Science and Ceramics, AGH University of Science and Technology, Krakow, Poland
e-mail: Andrzej.Lewenstam@abo.fi

G. Inzelt et al. (eds.), *Handbook of Reference Electrodes*,
DOI 10.1007/978-3-642-36188-3_12,

transport to get compensated, i.e., equitransferent (out) flux, (3) direct application of partially oxidized and (or) over-oxidized conducting polymers, or (4) introducing special designs in which conducting polymer is used as a part of the system.

This chapter provides a description of the main concepts as well as their concise summary in a tabulated form.

12.2 Dispersing Stability Enhancing Molecules in a Conducting Polymer

12.2.1 Incorporation of Hg/Hg_2Cl_2 or Ag/AgCl Particles Inside Polypyrrole Layer Doped with Chloride Ions

Pickup et al. [2] have investigated the feasibility of constructing a polypyrrole/mercury/mercury chloride reference electrode. Initially, polypyrrole/mercury/mercury chloride films were obtained by electrodeposition of the polypyrrole on a mercury pool with an area 27 cm^2 from the solution containing 0.5 M sodium para-toluene sulfonate, 0.3 M pyrrole, and 1 M sodium chloride all dissolved in sodium acetate buffer with pH = 4.5. Deposition was conducted galvanostatically using 20 mA for 3.5 h. It was shown that in this procedure, insufficient amount of mercury was incorporated in the polypyrrole film for further reaction with chloride ions to yield a mercury/mercury chloride half cell.

Better polypyrrole/mercury/mercury chloride films were obtained by multistep procedure. At first polypyrrole films were deposited on a glassy carbon (GC) disk substrate from the solution containing 0.1 M pyrrole and 0.1 M sodium para-toluene sulfonate in 0.5 M acetate buffer with pH = 4.90. Constant current 5 mA was applied, and total charge was equal to 750 mC. Subsequently, Hg was potentiostatically deposited onto PPy layer from 0.5 M $Hg(NO_3)_2$ in 1 % HNO_3 solution under −0.5 V during 20 min. Obtained PPy/Hg film was soaked subsequently in 0.5 M NaOH for 15 min and in 10 M HCl for 3 min to exchange the para-toluene sulfonate counter anions by chlorides. After immersion in 10 M HCl, the CV cycles in the range −2 to +1 V with scan rate 100 mV/s were applied to form Hg_2Cl_2 inside film. The obtained PPy/Hg/Hg_2Cl_2 films were tested as possible reference electrodes. Negligible potential difference in 3 M KCl solution versus commercial calomel electrode filled with 3 M KCl was observed. Bigger potential differences ranging from −25 to −60 mV were observed if KCl concentration was changed in the range 10^{-6}–1 M. According to the authors, the deviation from the expected zero potential difference is due to the leakage of mercury and/or mercury chloride from the polypyrrole-coated electrode in chloride solutions less concentrated than the saturated KCl. Additionally, chloride counter ions and other ions influence potentiometric measurements by doping/dedoping mechanism.

Similar approach was used by Mangold et al. [3]. In order to reduce ionic sensitivity of the conducting polymer film, Ag/AgCl particles were introduced

into the chloride-doped polypyrrole matrix as a reference system. According to the authors' assumption, Ag/AgCl potential is determined by chloride anions dispersed inside polypyrrole layer. PPy films were deposited potentiodynamically (scan rate 200 mV/s, range of potential cycling −0.7 to +0.9 V) from 0.1 M pyrrole and 0.1 M NaCl solution on the Ag surface. The formation of silver and silver chloride particles embedded in PPy film was evidenced by scanning electron microscopy and X-ray diffraction. The films obtained exhibited strong potential dependence of NaCl concentration.

12.2.2 Reference Membrane Obtained by Dispersing pH Buffer Ligands Inside Conducting Polymer Films

Reference membranes of this kind were obtained by Blaz et al. [4] incorporating pH buffer ligands containing a sulfonate group, in particular ligand bases constituting biological buffers, as doping anions in the process of p-doping during electrodeposition. The ligands used were those which form weak complexes with ions, in particular with alkaline and/or alkaline-earth metal cations, as it is in biological buffers. Then the CP films were soaked in a buffer solution at pH that corresponds to the maximum buffer capacity of the pH buffer dispersed in the film. The films were ready for use after soaking.

By incorporating the pH buffer system into the CP film, the fundamental operational property of the pH buffer, which is defined as "a solution that does not change pH after the addition of a small amount of strong acid or base or if diluted," was kept valid. In this way CP films insensitive to pH in certain pH ranges and giving electric potential of the CPs independent of pH were obtained. By using conducting polymers insensitive to pH as the reference electrodes, several advantages like mixed conductivity, insolubility in certain solvents, and processability of conducting polymers were achieved, keeping valid the possibility of application of such reference electrodes in numerous amphiprotic solvents.

Apparently, small amounts of strong base or acid additions did not change the potential of the CP reference electrode, which complies with a definition of pH buffer, and the practical use of the described reference electrodes.

The CP film exhibits insensitivity to pH because:

1. The immobile doping ion inhibits anionic response and promotes a cationic one [5–7].
2. The selectivity to the hydrogen ion is enhanced by using doping ions unable to form complexes with cations other than hydrogen [8, 9].
3. The sensitivity to the hydrogen ion is hampered by the pH buffering capacity of the CP film induced via high pH pair loading and soaking.
4. The insensitivity to redox potential for mild redox changes is due to the inability of the redox system to gain control of the overall potential determining electrode process [7, 10–14] pronounced in the case of overoxidized CP [15, 16].

The films were deposited on the working electrode by potential cycling at a scan rate of 20 mV/s or potentiostatically under constant potential. The electrodeposition of the poly(3,4-ethylenedioxythiophene) films doped with 1-hydroxy-4-sulfobenzoic acid (PEDOT–SSA film) was performed from solutions containing 0.001, 0.1, or 3 M SSA and 0.01 M EDOT. The ranges of potential cycling were chosen so that the maximal current density was in the range 1.1–1.7 mA/cm^2 for 0.1 M and 3 M SSA or 0.55–0.65 mA/cm^2 for 0.001 M SSA. The usual ranges of potential cycling and scan numbers performed were as follows: 500–1050 mV and 40 scans for 0.001 M SSA, 500–870 mV and 20 scans for 0.1 M SSA, and 500–850 mV and 20 scans for 3 M SSA.

The PEDOT films doped with benzenesulfonic acid (PEDOT–BSA) were deposited from 0.1 M BSA and 0.01 M EDOT solution by cycling the potential in the range 500–950 mV with the number of cycles equal to 20.

The poly(1-methylpyrrole) films and PEDOT films doped with 2-(*N*-morpholino) ethanesulfonic acid (PMPy–MES and PEDOT–MES films) were deposited potentiostatically from 0.4 or 1.33 M MES and 0.1 M MPy or 0.01 M EDOT solutions. The applied potential was equal to 750 mV for PMPy film deposition and 1050 mV for PEDOT film deposition, and the deposition time was (usually) equal to 600 s.

The poly(1-methylpyrrole) films and PEDOT films doped with 3-(*N*-morpholino) propanesulfonic acid (PMPy–MOPS as well as PEDOT–MOPS films) were deposited potentiostatically from 1.4 M MOPS and 0.1 M MPy or 0.01 M EDOT solutions. The applied potential was usually equal to 800 mV for PMPy film deposition and 1050–1100 mV for PEDOT film deposition, and the deposition time was (usually) equal to 1200 s.

The poly(1-methylpyrrole) and PEDOT films doped with Piperazine-1-4-bis(2-ethanesulfonic acid (PMPy–PIPES as well as PEDOT–PIPES films) were deposited potentiostatically from saturated PIPES solution (about 0.005 M) and 0.1 M MPy or 0.01 M EDOT. The applied potential was equal to 900 mV for PMPy film deposition and 1050 mV for PEDOT film deposition, and the deposition time was (usually) equal to 600 s.

The pH sensitivity of such films was tested in universal buffer solutions prepared according to the Perrin and Dempsey prescription [17]. The main solution consisted of 0.1 M citric acid, 0.1 M KH_2PO_4, 0.1 M $Na_2B_4O_7$, 0.1 M TRIS, and 0.1 M KCl. pH of the buffer solution was adjusted either with HCl or NaOH to cover the pH range from 2 to 10.

Alternatively, three pH/electrolyte standards, to mimic those used in blood electrolyte analyzers with the following pH and concentrations of main electrolytes (in mmol/dm^3), were also used:

STD1: pH = 7.00 and Na^+ = 120.0, K^+ = 6.0, Ca^{2+} = 0.58, Cl^- = 93.4,
STD2: pH = 7.40 and Na^+ = 140.0, K^+ = 4.5, Ca^{2+} = 1.25, Cl^- = 113.1,
STD3: pH = 7.80 and Na^+ = 150.0, K^+ = 3.0, Ca^{2+} = 2.23, Cl^- = 118.2,

It was shown that the pH buffer system in the film behaves as a pH buffer in a solution.

For PEDOT films doped with SSA, it was observed that the sensitivity towards pH changes can be hampered in both alkaline and acidic pH ranges. If PEDOT–SSA films were conditioned in the mixture of SSA with NaOH, pH = 11.6, apparent pH insensitivity was observed in the pH range from 10 to 7, and typical potential change of the film did not exceed few mV. If the mixture of SSA with NaOH, pH = 2.6, was used for film conditioning then hampered pH sensitivity was observed in the pH range from 3 to 6 and typical potential changes of the film did not exceed few mV as well.

The best resistance to pH change (highest buffer capacity) was observed for the films deposited from most concentrated SSA solution, which indicates that the vicinity of CP film-solution behaves as a pH buffer in a certain pH range. For example, smaller than 1 mV potential changes were observed in the pH range 10–8 for the PEDOT–SSA films deposited from 3 M SSA. Under the same conditions three times bigger potential changes were observed for the films deposited from 0.01 M SSA.

A similar pH insensitivity pattern was observed for several other films used like PEDOT or PMPy doped with MES, MOPS, and PIPES.

Very pronounced pH insensitivity in commercial buffers used as calibrating solutions for multiparameter clinical analyzer, with stability of readout within 1 mV in the pH range 7.0–7.8, was observed for the PEDOT–MES films. On the other hand, the PEDOT film doped with benzenesulfonic acid (BSA, which cannot form a buffer pair) indicated much stronger pH sensitivity [18, 19].

The standard deviation of the potential of the PEDOT–SSA films, in comparison to a conventional Ag | AgCl electrode, measured in the universal buffer solution of pH = 9 during 60 min, did not exceed 0.7 mV. In general, the reproducibility of readouts between three electrodes was better than 10 mV.

It was shown that pH insensitivity effect depends on the acid–base properties of dopant and resulting pH buffering properties of the films. Magnitude of this effect was determined during titration of diluted HCl with NaOH to obtain pH change from 5.65 to 9.00. For the PEDOT–SSA films used outside of their optimal pH range, only limited pH sensitivity (in comparison to a glass electrode) was observed during titration. On the contrary, for the films matching the relevant pH buffer range (PEDOT–MES), the change of the potential was insignificant.

Obtained results indicate that there is pH range optimal for each film to be used and that outside this range other processes may contribute to apparent pH insensitivity as secondary processes.

All tested films were also insensitive to the redox potential changes induced by subsequent pumping argon and air. For PEDOT–SSA films conditioned in the mixture of SSA and NaOH, pH = 11.6, potential changes recorded during subsequent pumping argon and air through universal buffer solutions of pH = 10 or pH = 9 were smaller than 1 mV. For comparison, potential changes recorded in parallel with Pt electrode exceeded 100 mV.

The possibility of application of the PEDOT–SSA film as reference membrane was confirmed during F-ISE calibration in TISAB buffer. Since TISAB is the solution with constant pH and ionic strength (from sodium chloride), the CP-based reference electrode was expected to be a perfect substitute for a conventional electrode. In fact, almost the same slopes equal to 57.5 or 58.5 mV/pF were obtained using the PEDOT–SSA film and a conventional Ag | AgCl electrode as reference electrode.

Additionally, PEDOT–SSA films stabilized by conditioning in alkaline or acidic solutions were successfully used in classical Me–EDTA titration. Titration of Ca was performed in borate buffer of pH = 9.2, and Cu titration was performed in acetate buffer of pH = 5.

It was also shown, for the first time, that potentiometric titrations in water–methanol solution can be performed using pair of "plastic" electrodes, CP-based Pb^{2+}-sensitive indicator electrode and CP-based reference electrode [3] or CP-based Cu^{+2}-sensitive indicator electrode and CP-based reference electrode [20].

Furthermore, it was shown that it is possible to integrate and miniaturize indicator and reference electrodes while maintaining the characteristics of macro-conventional potentiometric sensors [21]. In consequence, it was shown that such electrodes can be placed together on a flat surface. In this way the miniature galvanic cells for flow-through modules, for direct measurements in small sample volumes can be obtained.

Usability of such miniature galvanic cells equipped with CP-based reference membrane was confirmed experimentally [21]. One of such microcells, with a solid-contact type Ca-sensitive electrode and the PEDOT–SSA reference membrane, was used for end-point detection in the course of calcium titration with EDTA in a borate buffer (pH 9.2). The potential changes were measured against an external Ag/AgCl electrode and potential change for the PEDOT–SSA membrane was negligible during the whole titration.

Other galvanic microcells with the solid contact type Ca-, K-, Na-, and Cl-sensitive electrodes as well as PMPy film doped with MOPS as reference membrane were used for numerous applications. The changes of the reference membrane potential as low as 0.27 mV were recorded during repeated microcell calibration with clinical standard solutions. Within 30 days of use, standard potential of such PMPy–MOPS reference membrane increased for about 30 mV, but potential changes recorded in clinical standards solutions were practically unchanged.

This way it was shown that by incorporation of a pH buffering system in conducting polymer matrix, it is possible to merge the advantageous properties of pH buffer (known form amphiprotic solutions) and those of conducting polymer films (as mixed conductivity and processability), and to obtain a reference electrode that offers a wide range of potentiometric applications. This electrode can be applied in amphiprotic solvents, including mixed solvents. By using such reference membranes, some analytical disadvantages associated with the use of conventional reference electrodes can be avoided, e.g., contamination of the sample with water and ions flowing from the bridge. Such electrodes are easy to manufacture, service-free, durable, easy to miniaturize, and cheap.

12.3 Compensating Ion Fluxes

12.3.1 Compensation of the Anionic and Cationic Sensitivity of the Conducting Polymer Films

Several attempts were undertaken in order to minimize diffusion potential effect resulting form uneven cationic and anionic fluxes. For this purpose monolayers or bilayers of the conducting polymer films with mixed anionic/cationic sensitivity were investigated.

Bilayers of conducting polymers with different redox potentials, e.g., polypyrrole and poly(3-methylthiophene), and/or with different ion exchanger properties (i.e., cation or anion exchangers) were investigated by Mangold et al. [3]. Polypyrrole (PPy) films were deposited potentiodynamically (scan rate 200 mV/s, range of potential cycling −0.7 to +0.9 V) from 0.1 M pyrrole, 0.1 M NaCl, or 0.1 M sodium polystyrene sulfonate solution (PSS), whereas poly(3-methylthiophene) films (PMT) were deposited galvanostatically (1 mA/cm^2) from propylene carbonate solution containing 0.2 M 3-methylthiophene and 0.03 M tetrabutylammonium hexafluorophosphate. The most stable potential was observed for bilayer composed of PPy doped with chloride anions (anion exchanger) as an inner layer and PPy doped with PSS (cation exchanger) as an outer layer. Distinct anionic sensitivity was observed if conducting polymer with anion exchanger properties was used as an outer layer. For PPy(Cl)/PPy(PSS) bilayer, the slope of −4 mV/p[NaCl] in the concentration range 0.001–0.1 M was observed. Incorporation of Ag/AgCl system into PPy(Cl) film did not improve bilayer potential stability.

It was shown that bilayer composed of both polymers with anion exchanger properties, e.g., PMT(PF_6^-)/PPy(PF_6^-) exhibited strong dependence of the open circuit potential on NaCl concentration with the slope 52 mV/p[NaCl]. Distinct redox sensitivity of such bilayers, with the slope −48 mV/p[Ox/Red], was observed as well.

In the further works of this group, Mangold et al. [22] have shown that bilayers composed of conducting polymers with different redox properties and with different ion exchanger properties exhibit stable open circuit potential in organic solvents. In this case polypyrrole films were deposited in galvanostatic or potentiodynamic mode from the solution containing 0.1 M pyrrole and 0.1 M NaCl or 0.1 M sodium polystyrene sulfonate. Poly(3-methylthiophene) films were deposited from acetonitrile solutions containing 0.1 M 3-methylthiophene and 0.1 M tetrabutylammonium hexafluorophosphate. For bilayers composed of poly(3-methylthiophene) doped with hexafluorophosphate as an inner layer and polypyrrole doped with polystyrene sulfonate as an outer layer, potential changes did not exceed few mV if measurements were performed in propylene carbonate solution, and concentration change of tetrabutylammonium hexafluorophosphate was in the range 0.0001–0.1 M. A stable open circuit potential was observed if a sequence of layers has been reversed and poly(3-methylthiophene) doped with hexafluorophosphate used as an outer layer.

The observed potential changes did not exceed few mV if measurements have been performed in acetonitrile solution and concentration of tetrabutylammonium hexafluorophosphate changed in the range 0.001–1 M. Such anhydrous bilayers could be promising candidates for the reference electrodes to be applied in organic solvents.

Similar observations were reported by Wojda and Maksymiuk [23]. According to these authors, a stable open circuit potential of bilayer is a result of compensation of anion and cation exchange processes, and permeability of the outer layer for ions is of major importance. It was observed that a sequence of polymer layers with the cation-exchanging component on the top (e.g., polypyrrole layer doped with polystyrene sulfonate or dodecylbenzenesulfonate anions) allows access of electrolyte ions to both layers, owing to the hydrophilic environment within outer layer, assured by immobilized anions. However, for the reversed sequence of layers (anion-exchanging polymer as the outer component) some charge trapping effects are present, due to the limited permeability of the anion-exchanging polymer for cations, as shown by Maksymiuk [24]. In this case an anionic slope of the potentiometric response was always obtained.

An attempt for applying conducting polymer bilayers as reference membranes was described also by Kisiel et al. [25]. It was shown that potentiometric response of bilayers composed of polypyrrole doped with perchlorate (inner layer) and polypyrrole doped with polystyrene sulfonate (PSS) or dodecylbenzenesulfonate (DBS) (outer layer) strongly depends on the thickness of both layers, established by deposition charge. Polypyrrole films were deposited in potentiostatic mode from the solutions containing 0.05 M pyrrole and 0.1 M sodium salt of perchlorate, polystyrene sulfonate, or dodecylbenzenesulfonate, and applied potential was equal to +0.800 V. The best results for PPy(ClO_4)/PPy(PSS) films were obtained if charge ratio was equal to 7:3 (i.e., inner layer was thicker). After overnight conditioning in 0.1 M KCl solution, the slope for such bilayer was equal to 1.6 mV/p[KCl] in the KCl concentration range from 10^{-5} up to 10^{-2} M.

For PPy(ClO_4)/PPy(DBS) bilayer the best charge ratio was equal to 6:1. After overnight conditioning in 0.1 M KCl solution, the slope was equal to −0.7 mV/p[KCl] in the KCl concentration range from 10^{-5} up to 10^{-2} M.

As shown by Kisiel et al. [25] an ionic response of the conducting polymer monolayer can be diminished by a parallel doping with both mobile and/or immobile dopants. Conducting polymer films were deposited under potentiostatic mode (E = +0.800 V) from the solutions containing 0.05 M pyrrole monomer and two types of doping anions: perchlorate (mobile anion, responsible for anionic sensitivity) and polystyrene sulfonate or dodecylbenzenesulfonate (anions immobilized inside polypyrrole film, responsible for cationic sensitivity). Total concentrations of both anions were kept constant and equal to 0.1 M, whereas their molar ratio was changed. Deposited films were conditioned overnight in 0.1 M KCl and calibrated with KCl solutions. Depending on molar ratio of the mobile and immobile anions, the potentiometric response of the films has changed from cationic to anionic, and smallest slope values were obtained for the films deposited from 0.04 M ClO_4^-, 0.06 M PSS^- solution (slope equal to 0.6 mV/p[KCl] within KCl concentration

range 10^{-3}–1 M) or 0.06 M ClO_4^-, 0.04 M DBS^- solution. In the last case slopes as small as −0.3 mV/p[KCl] were the typical for KCl concentration range 10^{-5}–10^{-1} M.

12.3.2 Inhibition of the Ion Exchange Processes at Conducting Polymer/Solution Interface

It was shown [25] that the monolayer of polypyrrole doped with dodecylbenzenesulfonate (DBS) can be used as a reference membrane. According to the authors, DBS anions not only assure cation exchange properties of the conducting polymer, but being anionic surfactants can be accumulated at the polymer/solution interface. In consequence, ion exchange processes are inhibited and suppressed dependence of potential on electrolyte concentration is observed. Further reduction of the potential vs. concentration dependence was obtained by proper protocol of precipitate formation in the polymer layer with DBS anions and potassium or barium cations. After overnight conditioning in 1 M KCl solution or in saturated $BaCl_2$ solution, the slopes of −1.7 mV/p[KCl] and −1.1 mV/p[KCl] for 10^{-5}–10^{-1} M KCl concentration range were observed. The films exhibited redox sensitivity, and in the presence of $K_3[Fe(CN)]_6/K_4[Fe(CN)]_6$ redox pair (both 0.5 mM), the open circuit potential is ca 150 mV higher than in the absence of the redox pair.

12.4 Direct Application of Conducting Polymers

12.4.1 Polypyrrole Films as a Quasi-reference Electrode in both Aqueous and Organic Solvents

It is obvious that aqueous reference electrodes are not well suited for use in nonaqueous solvents, since unknown and irreproducible liquid junction potentials exist between the aqueous and nonaqueous phases. Furthermore, contamination of the sample by water and other ions associated with the reference electrode may occur.

For nonaqueous electrochemistry, IUPAC recommended the use of a redox couple such as ferrocene/ferrocenium ion (Fc/Fc^+) as an internal standard [26]. An alternative to the liquid junction electrode is one based on an entirely solid-state design. Peerce and Bard [27] fabricated such an electrode by coating poly (vinylferrocene) (PVFc) on platinum. The polymer-coated electrode was brought to a 1:1 ratio of ferrocene to ferrocenium by poising the electrode at the $PVFc/Fc^+$ half-wave potential (0.39 V vs. SCE). Although this electrode maintained a constant, reproducible potential in deaerated acetonitrile over 21 h, it was unstable in other

nonaqueous solvents, including benzonitrile, DMF, and methanol. The electrode's rapid potential drift in these solvents was attributed to gradual dissolution of $PVFc^+$, and it was predicted that higher molecular weight PVFc should be more useful in a wide range of solvents.

To overcome solubility problems, cross-linking strategies for PVFc were employed by Kannuck et al. [28], but this design still suffered from poor stability (lifetimes of 24 h in MeCN and 7 h in H_2O). Also the reference electrodes prepared by electrochemically copolymerizing vinylferrocene and vinylpyrrole onto platinum were found to be stable for several hours in deaerated acetonitrile but unstable in the presence of air [29]. It has shown clearly that polymer solubility was not the only important contributor to the stability of ferrocene-based electrodes.

Fc^+ is a stabilized 17-electron radical that is stable in aqueous acid but decomposes in neutral or basic solution to give ferrocene and iron hydroxides [30, 31]. It was shown also that DMSO solutions of Fc^+ rapidly decompose in the presence of O_2 [32], as well as the irreversible behavior of Fc^+ in hydroxylic solvents has been described Thus, a poised $PVFc/Fc^+$ electrode exposed to air in pH $\geq$ 7 would be expected to drift as Fc^+ is consumed and would therefore fail in any practical application.

To overcome this problem Bashkin and Kinlen [33, 34] have shown that sufficient methyl substitution of the cyclopentadienyl rings can render ferrocenium stable to O_2, and ring-methylated Fc^+ analogues may be used to fabricate stable reference electrodes.

A bis(pentamethylcyclopentadienyl)iron reference electrode was described; its potential was pH independent in aqueous buffer solutions. Unlike any other ferrocene electrodes previously reported, these electrodes were stable in aqueous solvents in air as well.

Ghilane et al. [35] have described solid-state quasi-reference electrodes (QRE) based on metal (Pt or stainless steel) coated with partially oxidized polypyrrole PPy. It was shown that such QRE can be used in both aqueous and aprotic media. As in the cases discussed above, characteristic of this approach is the absence of any liquid component in the electrode design.

The PPy film was electrodeposited on Pt or stainless steel substrate from a solution containing 0.1 M tetrabutylammonium hexafluorophosphate (Bu_4NPF_6) and 0.01 M pyrrole dissolved in acetonitrile (CH_3CN) (MeCN) or dichloromethane (CH_2Cl_2). The electrodeposition of PPy was carried out in potentiodynamic mode by potential sweeping in the range of −0.6 to +1.2 V versus the Ag/AgCl (sweep rate 100 mV/s, 50 cycles). During the final scan, the working electrode was disconnected at a potential of +0.4 V versus Ag/AgCl. In this way partially oxidized film composed of $PPy^0/PPy^+PF_6^-$ was obtained. The polymerization charge was 360 mC/cm^2 corresponding to the film thickness of about 40 μm.

To check the stability of the Pt/PPy QRE, CV voltammograms were recorded in organic and aqueous solutions containing supporting electrolyte and ferrocenemethanol (FcMeOH) as a redox species.

Long-term open circuit potential stability of such Pt/PPy QRE was observed in both aqueous as well as organic solutions. For example, in the aqueous solution

containing 0.1 M KCl as supporting electrolyte and 1 mM ferrocenemethanol (FcMeOH), $E_{1/2}$ was shifted only by 2 mV after the Pt/PPy QRE had remained in the cell for 12 h. If Pt/PPy QRE was kept 1 week in air without any protection, the shift of the peak potential of FcMeOH was equal to 10 mV.

The experiments performed with various organic solvents like dimethylformamide (DMF) or MeCN containing 1 mM FcMeOH with 0.1 M tetrabutylammonium hexafluorophosphate (Bu_4NPF_6) as supporting electrolyte have shown superior Pt/PPy ORE stability. $E_{1/2}$ drift observed was lower than 3 or 10 mV after 1 or 3 days of use, respectively. Good potential stability of the Pt/PPy QRE was observed also in 1:2 mixtures of MeCN with benzene or tetrahydrofurane.

Moreover, by using several redox mediators with $E_{1/2}$ in range −1.5 to 0.3 V versus Pt/PPy QRE in both oxidation and reduction CV (with the open circuit potential of the solution and CV scans starting near 0 V), good agreement with the results obtained with FcMeOH was observed.

Stainless steel/PPy QRE has shown also very good open circuit potential stability.

To prove it, CV voltammograms were recorded in a DMF solution containing 0.1 M Bu_4NBF_4 and 1 mM FcMeOH with stainless steel/PPy QRE and, for comparison, with Ag wire QRE. For stainless steel/PPy QRE, drift of the peak potential between the first and the 1000th cycle was smaller than 3 mV, whereas for Ag QRE potential shift above 56 mV was observed already after 50 cycles.

It was shown also that PPy layers are very compact, and corrosion effect of stainless steel was not observed after immersion of QRE in 1 M H_2SO_4 for several hours, suggesting low permeability of the PPy layer on the metal surface.

The potential of the QREs was dependent on the kind of the electrolyte used (Table 12.1); however, the potential stability was good in all tested electrolytes.

Interestingly, the potential of Pt/PPy QRE was stable even in silver plating solution containing 1 M KCN, 0.3 M K_2CO_3, and 0.2 M AgCN showing stability similar to that found in KCl.

The solution redox potential affected both the potential and potential stability of the Pt/PPy QRE.

The reported Pt/PPy electrode was found to be a useful RE in both aqueous and organic solvents. These QREs exhibited good stability over several days in different media and has several advantages compared to conventional RE, like the SCE and Ag/AgCl electrode. The electrode is easy to fabricate, and the PPy film can be formed on different metals such as stainless steel [35].

12.4.2 Reference Electrodes Based on Overoxidized Polypyrrole Films

Chou group described the conducting polymer reference electrodes (CPRE) based on overoxidized polypyrrole films [36–38]. Polypyrrole films were deposited

Table 12.1 Open circuit potential (OCP) of Pt/PPy vs. SCE as a function of the supporting electrolyte anion in aqueous solution

Supporting electrolyte (0.1 M)	K_2SO_4	KBF_4	KPF_6	KCl	$KClO_4$	KBr	KF	K_2CO_3	KCN
OCP of Pt/PPy (V vs. SCE)	0.270	0.226	0.226	0.186	0.175	0.173	0.151	0.074	0.039

electrochemically onto indium tin oxide or screen-printed Ag substrate. According to the authors polymerization is performed in the solution containing 1 M acetonitrile, 0.1 M KCl, and 0.3 M pyrrole, all dissolved in 0.1 M phosphate buffer solution of pH = 7.

Two-electrode electrochemical cells with ITO glass [36, 38] or screen printed Ag layer [37] as an anode and platinum wire as cathode were used. Polypyrrole was deposited under +5 V on the ITO glass or under +2.5 V on the screen printed Ag layer, and deposition time was equal to 30 min.

After electrodeposition, the ITO covered with polypyrrole was immersed in deionized water for 30 min, next allowed to dry for 12 h and finally was placed into 6 M NaOH solution for 30 s. According to the authors, the last operation reduced the conductivity of polypyrrole by several orders of magnitude and increased its stability. Occasionally polypyrrole film was additionally covered with Nafion layer to block the ingress of anions.

The potentiometric characteristics of the solid-state CPRE were investigated using an extended gate type Field Effect Transistor (FET) and current–voltage (I–V) measurement system. Drain current equal to 300 μA was kept constant by changing V_{GS} voltage (although V_{DS} voltage used was not specified).

According to the authors the developed solid-state CPRE exhibits sufficient stability and reproducibility in acid–base, sodium chloride, and potassium chloride solutions. According to the presented results, performance of such CPREs were exceptionally good, even better than performance of the conventional Ag/AgCl electrode. pH sensitivity of CPRE was very small and was almost unchanged within 600 days of dry storage. Unfortunately, despite encouraging information presented, the reports do not provide sufficient data to be reproduced experimentally.

12.5 Special Designs

12.5.1 Conducting Polymers as an Anode or Cathode in Two-Electrode Electrochemical Cell

In a few particular cases, the biosensor can be simplified into a weakly polarized two-electrode device. This avoids the use of a third reference electrode and requires

only a stabilized voltage source. This has been, for example, possible by coupling the first biochemical reaction of substrate recognition:

$$\text{Substrate} + \text{NAD}^+ \rightleftarrows \text{Product} + \text{NADH} + \text{H}^+ \tag{12.1}$$

with a second reaction that regenerates the oxidized form of the coenzyme NAD by ferricyanide ($[Fe(CN)_6]^{3-}$) catalyzed by a diaphorase:

$$\text{NADH} + 2\left[\text{Fe(CN)}_6\right]^{3-} \rightleftarrows \text{NAD}^+ + 2\left[\text{Fe(CN)}_6\right]^{4-} + \text{H}^+ \tag{12.2}$$

Detection of ferrocyanide ($[Fe(CN)_6]^{4-}$) instead of NADH makes it possible to decrease the potential of the working electrode from 0.8 V versus a saturated calomel electrode (SCE) to 0.25 V. A convenient biosensor based on these reactions has then been proposed by adding $[Fe(CN)_6]^{3-}$ in high concentration comparing to that of $[Fe(CN)_6]^{4-}$ produced by the reaction with NADH [39].

Given the high rate of the heterogeneous electron transfer reaction between $[Fe(CN)_6]^{3-}/[Fe(CN)_6]^{4-}$ system and a platinum electrode, overpotential of the cathodic reaction is very low even at relatively high current. A weakly polarized two-electrode device is then sufficient to make anode potential corresponding to ferrocyanide oxidation plateau without involving the reference electrode. Nevertheless, these analytical tools are not reagent-less since ferricyanide ions have to be introduced into the solution before measurements. To overcome this problem Gros et al. [40] has entrapped $[Fe(CN)_6]^{3-}$ ions at the auxiliary electrode surface by means of an electrosynthesized polypyrrole film. Modified in such a way, the electrode was used as a pseudo-reference electrode in a weakly polarized two-electrode device to design amperometric biosensors.

Polypyrrole was deposited at +0.8 V versus SCE from the aqueous solution containing 0.1 M pyrrole and 0.1 M $K_4[Fe(CN)_6]$ and subsequently oxidized electrochemically in 0.1 M phosphate buffer, pH = 7 at +0.4 V. It was shown that the electron transfer rate between the $[Fe(CN)_6]^{3-}/[Fe(CN)_6]^{4-}$ redox system entrapped in the film and the polypyrrole backbone was rapid and reversible, and reduction of the entrapped $[Fe(CN)_6]^{3-}$ ions took place prior to PPy backbone reduction. As long as the ratio of $[Fe(CN)_6]^{3-}/[Fe(CN)_6]^{4-}$ redox couple inside film was not significantly changed, potential changes of the film were small and allowed to maintain working electrode potential in the region of limiting current. This way Pt electrode modified with PPy doped with $[Fe(CN)_6]^{3-}$ can be used as a auxiliary/reference electrode in a weakly polarized two-electrode device and had an operating lifetime longer than 2 months if stored in dry state.

Linear dependence of the oxidation current on $[Fe(CN)_6]^{4-}$ concentration recorded for a cell containing 0.5 mm diameter platinum disk working electrode

and 5 mm diameter polypyrrole-coated platinum disk pseudoreference electrode has proved it (both electrodes were immersed in the phosphate buffer, and 100 mV potential difference between the electrodes was applied).

The modified pseudoreference electrode has been successfully used in construction of NAD-dependent amperometric biosensors for D-lactic acid with the linear response ranging from 0.01 to 2 mM of D-lactic acid and detection limit as low as 0.0025 mM.

In conclusion it was said that PPy doped with $[Fe(CN)_6]^{3-}$ can be used as efficient auxiliary/reference electrode in weakly polarized two-electrode devices if low current is measured for a short time, e.g., in disposable amperometric microsensors devoted for a single use.

Yoshida et al. [41] have shown that indium tin oxide electrode (ITO) coated with poly(3,4-ethylenedioxythiophene), PEDOT, can be used as a reference/counter electrode in an organic phase and can be applied to a thin-layer cell of a two-electrode system for voltammetry at the liquid | liquid interface. By using oxidized by 50 % PEDOT film, to achieve maximum redox buffer capacity, doped with supporting electrolyte anions present in an organic phase, suitable depolarization was realized at the PEDOT | organic phase interface. It was shown that partially oxidized PEDOT–ITO electrode showed Nernstian response to the supporting electrolyte anion concentration in the organic phase. For selected concentrations, the electrode potential was stable within ± 3 mV for 12 h, and showed a consistent value among the PEDOT–ITO prepared according to the same procedure (error range was about 7 mV, $n = 8$).

If a supporting electrolyte ion in an organic phase is doped into/dedoped from the polymer, the conducting polymer-coated electrode can work as a good counter electrode in organic phase, because the reaction product of the electrode does not contaminate organic phase. Moreover, the electrode potential in organic phase is determined by the concentration of the dopant ion, which can be exchanged between the polymer and organic phase. If concentration changes are not too high, the conducting polymer-coated electrode can be used also as a reference electrode in organic phase. Yoshida et al. have shown that an indium tin oxide glass electrode coated with partially oxidized PEDOT film can be used as a reference/counter electrode and applied to a two-electrode thin layer cell designed for voltammetry at the liquid | liquid interface. Depolarization at the interface between PEDOT and the organic phase was achieved by doping/dedoping of the PEDOT film with hydrophobic anion of the supporting electrolyte, i.e., tetrakis[3,5-bis(trifluoromethyl)-phenyl] borate, $TFPB^-$ anion.

According to the authors, PEDOT–ITO electrodes were prepared as follow.

Three-electrode electrochemical cell with an ITO glass working electrode, tetrapentylammonium ion selective electrode TPenA–ISE as a reference, and Pt

mesh as an auxiliary electrode was used. Electrodeposition of PEDOT was carried out potentiostatically on the ITO glass electrode from deoxygenated 0.1 M solution of the bis(triphenylphosphoranylidene)ammonium perchlorate (BTPPA-ClO_4) and 0.1 M EDOT, both dissolved in 1.2 dichloroethane (DCE); constant potential of 2.0 V was applied for 20 s.

The used DCE was purified three times by washing with distilled water and by drying with molecular sieves. After electrodeposition, the film was reduced at −0.1 V for 60 s in order to remove ClO_4^- ions from the PEDOT film. Doping with $TFPB^-$ ions was achieved by repeating oxidation and reduction of the PEDOT in DCE containing 0.1 M BTPPA-TFPB, and 15 potential scans in the range of −0.8 and 1.5 V at potential scan rate of 0.1 V/s were executed. According to the authors, the short-chain fraction of PEDOT, more soluble in organic media, was removed from the film during CV as well. PEDOT films oxidized by 50 %, were obtained by means of partial reduction of the fully oxidized film, and soaked for 12 h in DCE containing 10^{-3} M BTPPA-TFPB. The PEDOT films prepared in this way were used as counter or reference electrodes.

The potential of such electrodes measured in BTPPA-TFPB solution in DCE with respect to TPenA–ISE showed a Nernstian response, with the slope of 54.5 mV/decade. For selected BTPPA-TFPB concentrations, however, the potential stability was better than ±3 mV within 12 h and the standard potential repeatability was quite good (95 % confidence interval 0.169–0.155 V in 10^{-3} M TFPB).

According to the authors, the following points contributed to reproducibility of the electrode potential: (1) using a conducting polymer of low oxidation potential, such as PEDOT, (2) controlling the ratio of the oxidized form to the reduced one of the PEDOT. (Purification of DCE solvent was found advantageous to get a stable reduced PEDOT, which was completely oxidized if not purified DCE solvent was used).

It was shown that almost ideal depolarization was achieved at the PEDOT | DCE interface at a potential scan rate slower than 50 mV/s. Additionally, if total charge used was below 20 μC/cm^2, potential shift was smaller than 15 mV. Thus, such electrode can be used as a reference/counter electrode in organic phase.

In fact, the described PEDOT–ITO electrode was used as a reference/counter electrode in organic phase, and ion transfer at the liquid | liquid interface was investigated using two-electrode cell. Additional advantage of PEDOT–ITO is that the ionic product of the electrode reaction does not inhibit voltammetric measurement at the liquid | liquid interface.

The deposition conditions, postdeposition treatment, ionic and redox sensitivity, and selected applications of the conducting polymer-based reference electrodes are summarized in Table 12.2.

Table 12.2 Deposition conditions, postdeposition treatment, ionic and redox sensitivity, and selected applications of the conducting polymer-based reference electrodes

CP deposition method	Postdeposition treatment	The best ionic insensitivity	Redox sensitivity	Applications	Remarks	Reference
0.1 M Py and 0.1 M NaPTS in 0.5 M acetate buffer with pH = 4.90	Deposition of the Hg, soaking with 5 M NaOH, electro-oxidation in 10 M HCl	$\Delta E \approx 50$ mV within 10^{-6}–1 M KCl concentration range	Not checked	Not indicated		[2]
0.1 M Py, 0.1 M NaCl, Ag substrate	–	Distinct anionic sensitivity in NaCl solution		Not indicated		[3]
0.01 M EDOT, 0.001 M, 0.1 or 3 M SSA	Soaking with mixture 0.1 M SSA + NaOH, pH = 2.6 or 11.6	5 mV in the pH range 3–6, 1 mV in the pH range 8–10	Nonsensitive to dissolved oxygen	Direct potentiometry and potentiometric titrations	Calibration of F-ISE and Cu-ISE, titration of H^+, Ca^{+2}, Cu^{+2}, Pb^{+2}, last titration with both CP-based REF and ISE	[4]
0.01 M EDOT, 0.4 M or 1.33 M MES	Soaking with clinical standard pH = 7.8	<1 mV in the pH range 7.0–7.8	Not checked	Potentiometric titrations	Titration of H^+	[4]
0.01 M EDOT, 0.005 M PIPES	Soaking with clinical standard pH = 7.8	2 mV in the pH range 7.0–7.8	Not checked	Not indicated		[4]
0.01 M EDOT, 0.1 M BSA	Soaking with clinical standard pH = 7.8	10 mV in the pH range 7.0–7.8	Not checked	Not indicated		[4]
0.1 M MPy, 0.4 M or 1.33 M MES	Soaking with clinical standard pH = 7.8	2 mV in the pH range 7.0–7.8	Not checked	Not indicated		[4]
0.1 M MPy, 0.005 M PIPES	Soaking with clinical standard pH = 7.8	3 mV in the pH range 7.0–7.8	Not checked	Not indicated		[4]
0.01 M EDOT, 1.33 M MES	Soaking with clinical standard pH = 7.0	Not checked	Not checked	Potentiometric titration of the Cu^{2+}		[20]
0.01 M EDOT, 3 M SSA	Soaking with a mixture 0.1 M SSA + NaOH, pH = 11.6	Not checked	Not checked	Potentiometric titration of the Ca^{2+} with EDTA in borate buffer pH = 9.2	Potential changes <1 mV during titration	[21]

0.1 M MPy, 1.4 M MOPS	Soaking with clinical standard pH = 7.4	<0.5 mV in the pH range 7.0–7.8	Not checked	Determination of the selected ions with flow-through system, determination of ions in the samples of microliters volume	Applied as REF in multielectrode galvanic microcell	[21]
0.1 M pyrrole and 0.1 M NaCl or 0.1 M NaPSS 0.2 M MT and 0.03 M TBA-PF_6 in PC		−4 mV/p[NaCl] for PPy(Cl)/PPy(PSS) Distinct sensitivity for PMT(PF_6)/PPy(PF_6)	Distinct sensitivity for PMT(PF_6)/PPy(PF_6)	Not indicated	CP bilayers	[3]
0.1 M Py and 0.1 M NaCl or 0.1 M NaPSS 0.2 M MT and 0.03 M TBA-PF_6 in MeCN		For PPy(PSS)/PMT(PF_6) and PMT(PF_6)/PPy(PSS) few mV/p[X], X = $TBAPF_6$ dissolved in PC or MeCN	Not checked	Not indicated	CP bilayers	[22]
0.05 M Py, 0.1 M $NaClO_4$ or 0.1 M NaPSS or 0.1 M NaDBS	Soaking with 0.1 M KCl	1.6 mV/p[KCl] for PPy(ClO_4)/PPy(PSS) −0.7 mV/p[KCl] for PPy(ClO_4)/PPy(DBS)	Not checked	Not indicated	CP bilayers inner/outer layer deposition charge ratio 7:3 for PSS and 6:1 for DBS	[25]
0.05 M Py ($NaClO_4$ and NaPPS or NaDBS) total concentration 0.1 M and different concentration ratios	Soaking with 0.1 M KCl	0.6 mV/p[KCl] for PPy(ClO_4, PSS) −0.3 mV/p[KCl] for PPy(ClO_4, DBS)	Not checked	Not indicated	CP monolayer doped parallel with two anions. Best concentration ratio 2:3 for ClO_4, PSS or 3:2 for ClO_4, DBS	[25]
0.05 M Py, 0.1 M NaDBS	Soaking with 1 M KCl or saturated $BaCl_2$	−1.7 mV/p[KCl] after soaking with KCl −1.1 mV/p[KCl] after soaking with $BaCl_2$	Distinct sensitivity	Not indicated		[25]

(continued)

Table 12.2 (continued)

CP deposition method	Postdeposition treatment	The best ionic insensitivity	Redox sensitivity	Applications	Remarks	Reference
0.3 M Py, 1 M MeCN, 0.1 M KCl in 0.1 M phosphate buffer, pH = 7 Two-electrode cell, PPy deposition on ITO glass under +5 V	30 min soaking with H_2O, next 12 h in dry place, next soaking for 30 s with 6 M NaOH	3.21×10^{-4} mV/pH? Excellent long-term stability within 600 days Excellent long-term stability within 600 days?? pH sensitivity between 1 and 1.29 mV/pH	Not checked	Calibration of the RuO_2-based pH sensor with using extended gate FET		[36]
0.3 M Py, 1 M MeCN, 0.1 M KCl in 0.1 M phosphate buffer, pH = 7 Two-electrode cell, PPy deposition on ITO glass under +5 V or on Ag substrate under +2.5 V	30 min soaking with H_2O, next 12 h in dry place, next soaking for 30 s with 6 M NaOH	Parameters better than for Ag/AgCl REF?	Not checked	Ascorbic acid biosensor with RuO_2-based pH-ISE and CP-based REF		[37]
0.3 M Py, 1 M MeCN, 0.1 M KCl in 0.1 M phosphate buffer, pH = 7 Two-electrode cell, PPy deposition on ITO glass under +5 V	30 min soaking with H_2O, next 12 h in dry place, next soaking for 30 s with 6 M NaOH Sometimes covered with Nafion membrane	Average ionic sensitivity: 1.53 mV/pH, 7.45 mV/pNaCl, 2.14 mV/pKCl	Not checked	Calibration of the H-ISE, Na-ISE, and K-ISE using extended gate FET		[38]

0.01 M Py and 0.1 M Bu_4NPF_6 in MeCN or CH_2Cl_2		Good long-term potential stability	Too high or too low solution redox potential affected both the potential and potential stability of the QRE	Different application in voltammetry with aqueous and organic solutions	Used as quasi-reference electrode in voltammetry	[35]
0.1 M Py and 0.1 M $K_4Fe(CN)_6$	10 min of electrooxidation under +0.4 V in phosphate buffer, pH = 7	Nonpolarizable, good enough potential stability	Not checked	Construction of NAD-dependent amperometric biosensor	Used as reference/ counter electrode in two-electrode cell	[40]
0.1 M EDOT, 0.1 M BTPPA-ClO_4 in DCE TPenA–ISE as REF	Reduction under 60 s, next 15 scans in the range −0.8 to +1.5 V, 100 mV/s, next oxidizing and reducing by 50 %, all in 0.1 M BTPPA-TFPB in DCE 12 hours soaking in 10^{-3} M BTPPA-TFPB in DCE	Nonpolarizable, good enough potential stability	Not checked	Used as reference/ counter electrode in two-electrode system of voltammetry at the liquid/liquid interface	Used as reference/ counter electrode in two-electrode cell	[41]

Py pyrrole, *MPy* 1-methylpyrrole, *PPy* polypyrrole, *PMPy* poly(1-methylpyrrole), *EDOT* 3,4-ethylenedioxytiophene, *PEDOT* poly(3,4-ethylenedioxytiophene), *MT* 3-methylthiophene, *PMT* poly(3-methylthiophene), *NaPSS* sodium polystyrene sulfonate, *NaDBS* sodium dodecylbenzenesulfonate, *NaPTS* sodium para-toluene sulfonate, *BSA* benzenesulfonic acid, *SSA* 2-hydroxy-5-sulfobenzoic acid, *MES* 2-(*N*-morpholino) ethanesulfonic acid, *MOPS* 3-(*N*-morpholino) propanesulfonic acid, *PIPES* piperazine-1,4-bis(2-ethanesulfonic) acid, *MeCN* acetonitrile, *DCE* 1,2-dichloroetane, *Bu_4NPF_6* tetrabutylammonium hexafluor-ophosphate, *BTPPA-ClO_4* bis(triphenylphosphoranylidene)ammonium perchlorate, *BTPPA-TFPB* bis(triphenylphosphoranylidene)ammonium tetrakis[3,5-bis (trifluoromethyl)phenyl]borate, *TPenA* tetraphenylammonium

References

1. Inzelt G (2012) In: Scholz F (ed) Conducting polymers. A new era in electrochemistry, 2nd edn, Monographs in electrochemistry. Springer, Heidelberg
2. Pickup NL, Lam M, Milojevic D, Bi RY, Saphiro JS, Wong DKY (1997) Polymer 38:2561
3. Mangold KM, Schafer S, Juttner K (2000) Fresenius J Anal Chem 367:340
4. Blaz T, Migdalski J, Lewenstam A (2005) Analyst 130:637
5. Migdalski J, Blaz T, Lewenstam A (1996) Anal Chim Acta 322:151
6. Michalska A, Ivaska A, Lewenstam A (1997) Anal Chem 69:4060
7. Lewenstam A, Bobacka A, Ivaska A (1994) J Electroanal Chem 368:23
8. Migdalski J (2002) Chem Anal (Warsaw) 47:595
9. Michalska A, Lewenstam A (2000) Anal Chim Acta 406:159
10. Migdalski J, Blaz T, Kowalski Z, Lewenstam A (1999) Electroanalysis 11:735
11. Michalska A, Lewenstam A, Ivaska A, Hulanicki A (1993) Electroanalysis 5:261
12. Maksymiuk K, Nyback AS, Bobacka A, Ivaska A, Lewenstam A (1997) J Electroanal Chem 430:243
13. Vazquez M, Bobacka J, Ivaska A, Lewenstam A (2002) Sens Actuators B 82:7
14. Vazquez M, Danielsson P, Bobacka J, Lewenstam A, Ivaska A (2004) Sens Actuators B 97:182
15. Arrigan DWM, Gray DS (1999) Anal Chim Acta 402:157
16. Ersoz A, Gavalas VG, Bachas LG (2002) Anal Bioanal Chem 372:786
17. Perrin DD, Dempsey B (1974) Buffers for pH and metal ion control. Chapman and Hall, London
18. Lewenstam A, Blaz T, Migdalski J, Duda L (2010) Polish Patent PL 206043
19. Lewenstam A, Blaz T, Migdalski J, Duda L (2008) European Patent 06716825.2
20. Migdalski J, Błaz T, Zrałka B, Lewenstam A (2007) Anal Chim Acta 594:204
21. Migdalski J, Bas B, Blaz T, Golimowski J, Lewenstam A (2009) J Solid State Electrochem 13:149
22. Mangold KM, Schafer S, Juttner K (2001) Synth Met 119:345
23. Wojda A, Maksymiuk K (1998) J Electroanal Chem 441:205
24. Maksymiuk K (1994) J Electroanal Chem 373:97
25. Kisiel A, Marcisz H, Michalska A, Maksymiuk K (2005) Analyst 130:1655
26. Gritzner G, Kuta J (1984) Pure Appl Chem 56:461
27. Peerce PJ, Bard AJ (1980) J Electroanal Chem 108:121
28. Kannuck RM, Bellama JM, Blubaugh EA, Durst RA (1987) Anal Chem 59:1473
29. Haimerl A, Merz A (1986) Angew Chem Int Ed Engl 25:180
30. Prins R, Korswagen AR, Kortbeek AGTG (1972) J Organomet Chem 39:335
31. Wilkinson G (1952) J Am Chem Soc 74:6146
32. Sato M, Yamada T, Nishimura A (1980) Chem Lett 8:925
33. Bashkin JK, Kinlen PJ (1989) US Patent 4,857,167
34. Bashkin JK, Kinlen PJ (1990) Inorg Chem 29:4507
35. Ghilane J, Hapiot P, Bard AJ (2006) Anal Chem 78:6868
36. Liao YH, Chou JC (2008) J Electrochem Soc 155:J257
37. Jung CC, Yen HT, Chen CC (2008) IEEE Sens J 8:1571
38. Chen CC, Chou JC (2009) Jpn J Appl Phys 48:111501
39. Durliant H, Comtat M, Mahenc J, Baudras A (1976) Anal Chim Acta 85:31
40. Gros P, Durliant H, Comtat M (2000) Electrochim Acta 46:643
41. Yoshida Y, Yamaguchi S, Maeda K (2010) Anal Sci 26:137

Chapter 13
Screen-Printed Disposable Reference Electrodes

Agata Michalska, Anna Kisiel, and Krzysztof Maksymiuk

13.1 Introduction

In recent years there has been a pronounced interest in miniaturized, disposable electrochemical systems dedicated for electrochemical analysis. One of the most attractive approaches to yield such sensors (judging on the number of papers published) is screen printing of single electrodes or electrodes sets in various arrangements (i.e., combining all three electrodes required for classical electrochemical cell). Screen printing apart from miniaturization allows efficient large-scale production of sensors of relatively low cost and high reproducibility, which are of special interest for simple, fast electrochemical (both potentiometric and amperometric) determination of a range of analytes. Moreover, screen-printed electrodes can be obtained on a variety of substrates, although in practice the preference is given to synthetic polymeric materials (plastic foil). One of the big advantages of application of screen-printing technology is the possibility of developing own designs of electrodes and electrodes setups—even commercial, specialized suppliers of screen-printed electrodes usually allow custom designs. Moreover, the sequential printing of different layers, using different formulation of pastes, is especially suited for making miniaturized setups containing electrodes of different functions to be printed on one piece of support, e.g., reference, working (optionally modified with sensing layer), and counter electrodes. Screen-printing pastes in current use most often are designed to be cured at relatively low temperatures (compared to those used initially).

Screen-printing technology is well established for electrochemical sensor preparation: commercial sensors are available on the market for many years now; nevertheless many laboratories are still producing sensors in-house for their need/of their own design using commercially available pastes or preparing own ones. Usually an integral part of these arrangements are reference electrodes, prepared similarly as

A. Michalska (✉) • A. Kisiel • K. Maksymiuk
Department of Chemistry, University of Warsaw, Pasteura 1, 02-093, Warszawa, Poland
e-mail: agatam@chem.uw.edu.pl; akisiel@chem.uw.edu.pl; kmaks@chem.uw.edu.pl

G. Inzelt et al. (eds.), *Handbook of Reference Electrodes*,
DOI 10.1007/978-3-642-36188-3_13,

other electrodes using just other formulation of pastes. Although applications, modifications, and benefits of screen-printed working electrodes have been reviewed in a few papers (e.g., [1–3]), to authors' best knowledge the screen-printed reference electrodes have not been summarized in a review paper, yet.

It should be stressed that depending on intended electrochemical sensing methodology different requirements are set on reference electrodes affecting also the methodology of their production, although in all cases disposable use is intended.

In general, application of screen-printing technology is used to scale down the Ag/AgCl reference electrode, taking the advantage of commercial or homemade printing pastes containing silver and/or silver chloride to obtain layers of these materials. For potentiometric applications the key issue is to achieve supply of electrolyte (KCl) to stabilize potential over the electrode life; however, for electrochemical techniques based on recording current usually the presence of Ag or Ag/AgCl layers is sufficient for ensuring significant potential stability.

13.2 Screen-Printed Reference Electrodes for Potentiometric Purposes

Microreference elements (reference electrodes or reference field-effect transistors—REFETs) micromachined in silicon were precursors of screen-printed reference electrodes (e.g., [4–7]). The major motivation to look for optimal layered reference system was usually to build a potentiometric "chip" containing disposable sensing and reference electrode, preferably made in the same or similar layer application technology, e.g., thin-film technology, which can be regarded as direct ancestor of nowadays screen-printed reference elements.

Most of those systems were using (thin film) Ag/AgCl elements, which are not free from problems in manufacturing (e.g. related to poor adhesion of silver to glass/silicone) leading to poor potential stability [8]. Improvements proposed [8] included application of intermediate polyimide layer instead of previously applied metal ones and special formation of AgCl layer on top of silver film. Thus obtained sensors were characterized with increased stability of potentials in KCl (up to 8 h) as well as in interferent (KI or K_2S) solutions [8].

Application of screen-printing technology made preparation of reference electrodes significantly easier; the initial application of those devices was potentiometrically orientated; thus the stability of potential in time was an issue. Significant progress was achieved when Ag/AgCl layer, screen printed, was covered with a layer containing KCl [9–11]; the screen-printed Ag/AgCl electrode has been also reported recently as chloride-selective solid-state sensor [12] (i.e., indicator electrode).

Initially the research interest was on optimization of applied materials. One of the works [9] has used alumina substrate, on which sequentially layers of silver, silver

chloride, and KCl containing layer of glass paste or silicone polymer paste, using glass dielectrics film as insulator, were applied. This work [9] was also looking at the difference between commercially available epoxy polymer Ag/AgCl pastes and homemade pastes. Post printing each layer was dried and then either fried at high-temperature furnace or thermally cured depending on paste composition. Depending on composition of the electrode layers different performance was observed. Due to the presence of KCl outer layer relatively low potential drifts were observed (close to 4.5 mV/day) and long lifetimes (up to 40 days) were obtained; however the optimal sensor required about 10 h time equilibration with solution [9].

A disposable reference electrode, intended for environmental or medical analysis [10], was obtained using filter paper, heat-sealing film with screen-printed conducting lines. In this simple arrangement glass fiber was used as material containing KCl [10]. Initially this concept was used to prepare reference electrode using $K_4[Fe(CN)_6]/K_3[Fe(CN)_6]$ electrolyte to stabilize potential, which however was found to be inappropriate for biomedical analysis [13]. The improved system containing KCl [10] was found to yield stable potentials over range of KCl or NaCl activities. The electrodes were characterized with potential drift close to 0.5 mV/h and could be stored for about 10 weeks in wet atmosphere without loss of stability.

The approach developed by Suzuki et al. [8] was further optimized supplementing the electrode with screen-printed layer of poly(ethylene glycol) resin containing powdered (grinded) KCl and poly(vinyl pyrrolidone) [11]. The polymer and KCl were dispersed in 2-propanol, which was (after printing) allowed to evaporate in room temperature. Thus obtained reference electrodes were able to maintain relatively stable (± 1 mV) potential over 100 h, which was insignificant to change of KCl activity or solution pH.

Other reports confirmed that not only application of KCl containing layer is crucial for screen-printed reference electrode potential stability, but also protection of KCl from (instant) leaching is important [14]. Looking at range of arrangements (from evaporated Ag layer partially converted to AgCl to screen-printed Ag/AgCl layer) it was shown that application of KCl containing gelated layer of agar, covered by poly(vinyl chloride)/cellulose nitrate layer or poly(vinyl chloride)/Nafion layer, was beneficial, allowing to extend the stable potential readings from hours (for systems free from KCl containing layer) to 2 months.

Application of low-temperature or UV curable pastes has brought a significant simplification from manufacturing point of view—it allowed application of polyester flexible foil as substrate for screen printing [15]. The idea of application of screen-printed layer of protective (insulating) paste supplemented with solid KCl beneath as well as on the top of Ag/AgCl layer and protecting its insulation layer with relatively small opening yields highly stable reference electrodes [15] Fig. 13.1. The superior performance of these reference electrodes was confirmed over long-term stability tests (over 240 h), but also by changing electrolytes (including halides, buffers, redox or complexing reagents) or chloride ion activity. Apart from stability of herein proposed reference electrodes, the clear benefit of the

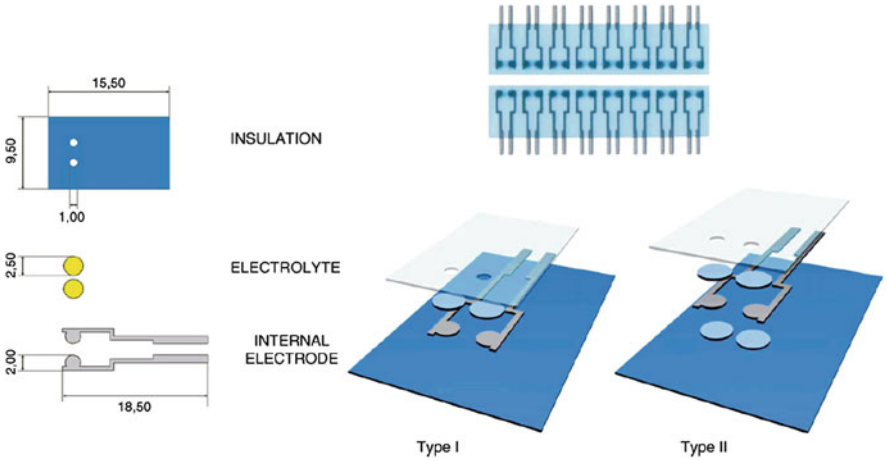

Fig. 13.1 The arrangement of screen-printed reference electrodes from work [15]. Reprinted with permission from Elsevier

proposed approach was screen printing of KCl containing layer and insulating layer of the top, which definitely simplifies preparation procedure and makes it feasible for mass scale production.

Yet another system in which KCl containing layer was also screen printed was applying electrolyte paste containing saturated KCl in sodium alginate, which was gelated after printing with $CaCl_2$ solution, and then after drying covered with hydrophilic polymer-coated polyester film [16]. Authors reported a long-term potential stability; moreover due to ability of alginate to gelate in sample solution, the potential did stabilize after 4 min and remained stable over about 1 h.

There is a significant, application driven interest in integration of screen-printed reference electrodes on one substrate together with indicator electrode. A reference electrode integrated with pH sensor on the same alumina substrate [17] was obtained by screen-printing silver paste, followed by drying and calcination at 850 °C. Then, the silver layer printed was chemically oxidized by $FeCl_3$ to form AgCl layer, which was further covered with agar containing KCl (applying agar solution—simply by pipette—prior gelation). The protecting layer of chloroprene rubber was coated on top. Potentiometric responses recorded in various electrolytes solutions have proven high stability of potential of thus obtained electrode.

The other report dealing with integrated screen-printed device was using extremely simple reference element obtained by screen printing of Ag/AgCl on the top of PET films; cured Ag/AgCl was serving as reference for screen-printed pH sensor [18]. Authors claim stability of reference element close to ± 1 mV over a period of 7 days.

The applicability of screen-printed (on polyester foil) Ag/AgCl layer as internal reference, i.e., in the arrangement in which it was covered by hydrogel layer doped with electrolyte and then by ion-selective membrane to work as internal

solution-free ion-selective electrode, was also tested [19]. Thus obtained sensor was characterized with performance comparable with that of conventional ion-selective electrodes with internal solution.

Also other systems intended to be used as disposable reference electrodes (although tested for weeks or months to prove their superiority performance) for potentiometric measurements were proposed; these were generally using approaches developed originally for indicator electrodes. The Ag/AgCl layer coated on metallized printed board, covered with poly(vinyl chloride) membrane containing ionic liquids, has been proposed [20]. These miniature planar electrodes were characterized with good stability of potentials for relatively long time (3 months). For miniature, disposable ion-selective electrodes using conducting polymer as a conducting path and ion-to-electron transducer (all-plastic electrodes) a reference electrode was also proposed [21]. This system was based on heterogeneous membrane of plasticized poly(vinyl chloride) containing solid AgCl (with traces of Ag), solid KCl, and equimolar mixture of anion and cation exchangers: tridodecylmethylammonium chloride (MTDDACl) and sodium tetrakis[3,5-bis(trifluoromethyl)phenyl]borate, respectively. This system, intended as disposable electrode, was showing stable potentials.

13.3 Reference Electrodes for Amperometric/Voltammetric Sensing

In the case of screen-printed sets of electrodes intended for amperometric applications there is variety of proposed/available commercially arrangements, including different shapes and materials/modified materials of working and/or counter electrodes. Reference elements intended for amperometric/voltammetric sensing are most often silver or silver/silver chloride, used without any additional outer coating layer. The main concern is in reproducibility of obtained sets intended for disposable applications, not in stability of potential of reference element in time (which is hardly ever studied in amperometric applications).

Commercially available sets of screen-printed electrodes (including customized designs) utilizing Ag or Ag/AgCl reference electrodes are available from several companies.

References

1. Hart JP, Wring SA (1997) Trends Anal Chem 16:89
2. Honeychurch KC, Hart JP (2003) Trends Anal Chem 22:456
3. Tymecki L, Glab S, Koncki R (2006) Sensors 6:390
4. Comte PA, Janata J (1978) Anal Chim Acta 101:247
5. Lisdat F, Moritz W (1993) Sens Actuators B 15:228
6. van den Berg A, Grisel A, van den Vlekkert HH, de Rooij NF (1990) Sens Actuators B 1:425
7. Chudy M, Wróblewski W, Brzózka Z (1999) Sens Actuators B 57:47

8. Suzuki H, Hiratsuka A, Sasaki S, Karube I (1998) Sens Actuators B 46:104
9. Cranny AWJ, Atkinson JK (1998) Meas Sci Technol 9:1557
10. Mroz A, Borchardt M, Diekmann C, Cammann K, Knoll M, Dumschat C (1998) Analyst 123:1373
11. Suzuki H, Shiroishi H, Sasaki S, Karube I (1999) Anal Chem 71:5069
12. Cranny A, Harris NR, Nie M, Wharton JA, Wood RJK, Stokes KR (2011) Sens Actuators A 169:288
13. Diekmann C, Dumschat C, Cammann K, Knoll M (1995) Sens Actuators B 24:276
14. Simonis A, Lüth H, Wang J, Schöning MJ (2003) Sensors 3:330
15. Tymecki L, Zwierkowska E, Koncki R (2004) Anal Chim Acta 526:3
16. Koutarou I, Miyuki Ch, Naoki N, Eiichi T, Yuzuru T (2010) Jpn J Appl Phys 49:097003-1-097003-3
17. Liao W-Y, Chou T-C (2006) Anal Chem 78:4219
18. Musa AE, del Campo FJ, Abramova N, Alonso-Lomillo MA, Domínguez-Renedo O, Arcos-Martínez MJ, Brivio M, Snakenborg D, Geschke O, Kutter JP (2011) Electroanalysis 23:115
19. Walsh S, Diamond D, McLaughlin J, McAdams E, Woolfson D, Jones D, Bonner M (1997) Electroanalysis 17:1318
20. Mamińska R, Dybko A, Wróblewski W (2006) Sens Actuators B 115:552
21. Kisiel A, Michalska A, Maksymiuk K (2007) Bioelectrochem 71:75

Chapter 14
Pseudo-reference Electrodes

György Inzelt

Both the terms of pseudo-reference (literally "false" reference) electrode and quasi-reference ("almost" or "essentially") electrode are used in the literature, often synonymously or interchangeably. The essential difference between a true reference electrode (as defined in Chap. 1) and a pseudo-reference electrode is the lack of thermodynamic equilibrium in the latter case [1–4]. In many cases simply platinum or silver or Ag/AgCl wires serve as pseudo- or quasi-reference electrodes. Obviously, thermodynamic equilibrium cannot exist, since there is no common component (anion or cation) in the two adjacent phases. However, usually they are calibrated by a reference redox system by adding the internal reference during the experiments into the electrolyte (preferred) or measuring their potential after the experiments by using a reference redox system or a conventional reference electrode. Sometimes when a reference redox system (e.g., ferrocene or cobaltocane) [5] is also used in situ, this reference electrode is called a quasi-reference electrode. These types of reference electrodes are used almost exclusively in nonaqueous systems (See Chaps. 2 and 6), in molten salts or at elevated temperatures, in ionic liquids (see Chap. 7), and mostly in three-electrode potentiostatic or potentiodynamic experiments. The advantages of the use of pseudo-reference electrodes are their simplicity, and because those are immersed directly into the electrolyte used in the cell, the ohmic resistance (impedance) effect is small, no liquid junction potential appears, and usually there is no contamination of the test solution by solvent molecules or ions that a conventional reference electrode might transfer. There are several disadvantages of the use of these reference electrodes. First is the lack of the thermodynamic equlibrium; therefore, one cannot calculate their potential. Second, because these are not ideally nonpolarizable electrodes, there is a shift of their potential during the measurements, which depends on the current density applied. Third, most pseudo-reference electrodes work over a limited range of conditions such as pH or temperature; outside of this

G. Inzelt (✉)
Department of Physical Chemistry, Eötvös Loránd University, Pázmány Péter sétány 1A, Budapest 1117, Hungary
e-mail: inzeltgy@chem.elte.hu

G. Inzelt et al. (eds.), *Handbook of Reference Electrodes*,
DOI 10.1007/978-3-642-36188-3_14,

range the electrodes' behavior becomes unpredictable. However, it should be mentioned that, although under suitably selected conditions the potential of the pseudo-reference electrode, although unknown, might be surprisingly constant during the experiments.

References

1. Kahlert H (2010) Reference electrodes. In: Scholz F (ed) Electroanalytical methods, 2nd edn. Springer, Berlin, pp 302–303
2. Inzelt G (2012) Reference electrode. In: Bard AJ, Inzelt G, Scholz F (eds) Electrochemical dictionary, 2nd edn. Springer, Berlin, pp 795–798
3. Bard AJ (2012) Quasi-reference electrodes (QRE). In: Bard AJ, Inzelt G, Scholz F (eds) Electrochemical dictionary, 2nd edn. Springer, Berlin, p 776
4. Bard AJ, Faulkner LR (2001) Electrochemical methods, 2nd edn. Wiley, New York, NY, pp 53–54, Chap 2
5. Gritzner G, Kuta J (1984) Pure Appl Chem 56:461

Chapter 15
The Kelvin Probe Technique as Reference Electrode for Application on Thin and Ultrathin Electrolyte Films

Michael Rohwerder

The Kelvin probe technique is a unique reference electrode that allows non-contact measurement of electrode potentials. It can be used for measuring electrode potentials through insulating dielectric media such as air or polymeric films. It is mainly used where standard electrochemical techniques, which require a finite ionic resistance between working and reference electrodes, will fail.

It was invented by W. Thomson [1], the later Lord Kelvin, and was originally only used for measuring work functions of materials. In the classical set-up sample surface and the Kelvin probe plate form a parallel plate capacitor. If the capacitance between probe plate and sample surface is known, the work function difference between probe (reference material) and sample can be calculated, although the measurement of the charge is not easily performed. This problem can be overcome by measuring the discharge current when the distance between probe and sample is varied [1, 2], first introduced by Lord Kelvin. Zisman developed the technique further to the vibrating capacitor technique, in which the probe plate vibrates periodically, thus causing a steady ac current to flow [3]. Nowadays the vibrating capacitor set-up is the established technique for Kelvin probe.

While the Kelvin probe is widely used in surface physics to study adsorption of molecules or reconstruction processes of single crystal surfaces (see e.g. [4]), which both cause a change in the surface or dipole potential, its application in electrochemistry is quite recent. As it is the only reliable reference electrode that can be applied to electrodes covered by ultrathin electrolyte layers, a common situation in atmospheric corrosion, it was first applied for electrochemical studies in corrosion science. Stratmann et al. [5–14] were the first who used a Kelvin probe as reference electrode.

Using the Kelvin probe as reference electrode is directly related to measuring absolute electrode potentials. The concept of absolute electrode potentials dates back to the first works on the relationship between potential at zero charge and work

M. Rohwerder (✉)
Max-Planck-Institut für Eisenforschung, Max-Planck-Str. 1, 40237 Düsseldorf, Germany
e-mail: rohwerder@mpie.de

G. Inzelt et al. (eds.), *Handbook of Reference Electrodes*,
DOI 10.1007/978-3-642-36188-3_15,

function of a metal. Veselovsky [15] pointed out that the difference between the zero charge potentials for silver and mercury electrodes is virtually equal to the difference between the work functions of these metals. According to Grahame [16] Frumkin expressed similar ideas more than 80 years ago [17].

This discussion about an "absolute" electrode potential, referenced like the work function against the vacuum level, experienced a revival in the 1970s by Bockris et al. [18–20] and Gileadi [21]. However, it was essentially S. Trasatti who formed the modern concept of absolute electrode potential [22–28]. The following discussion (see also [29]) is mainly inspired by his ideas published in [27].

Firstly, it is helpful to consider the definition of the work function.

The work function is defined as the minimum work that is required to extract an electron from within the sample to a position just outside the sample (far enough to avoid contributions from image forces). It is comprised of the chemical work and the electrostatic work necessary for transporting the charged electron through the dipole layer at the surface:

$$\Phi = -\mu_e + e\chi = -(\mu_e - e\chi), \tag{15.1}$$

where μ_e is the chemical potential (i.e. the chemical work to transfer the electron from the infinity into the sample and hence the minus sign) and χ is the so-called dipole or surface potential. This is the potential drop between just inside the sample and just outside of it.

The use of the phrase "just outside the sample" for the definition of the work function is unimportant for the case of an uncharged sample, where the energetic position just outside the sample is the same as far away from it, i.e. it is equivalent with the vacuum level. But usually the sample is charged and then an additional work component is required to transfer the electron from just outside the surface to a position infinitely far away: $e{\cdot}\psi$, where ψ is the Volta potential, which is equivalent for the potential drop from the infinity to a position just outside the surface. The Volta potential is due to surface charges; see Fig. 15.1.

The dipole potential χ and the Volta potential ψ sum up to the Galvani potential ϕ, i.e., the potential drop between the vacuum level infinitely far away from the surface and the bulk of the sample:

$$\phi = \chi + \psi. \tag{15.2}$$

Now also for this case the work for transferring an electron from the bulk just outside the electrolyte layer can be defined, which can be considered as a kind of modified work function Φ^*, describing the minimum work to extract an electron from the Fermi level, through the solid/liquid interface (with the potential drop $\Delta\phi_M^{El}$), through the liquid and through the surface layer of the liquid to a position just outside the liquid; see Fig. 15.2a, b. Then the quantity $E_{abs} = \Phi^*/e$ is defined as the absolute electrode potential of a sample covered by an electrolyte layer.

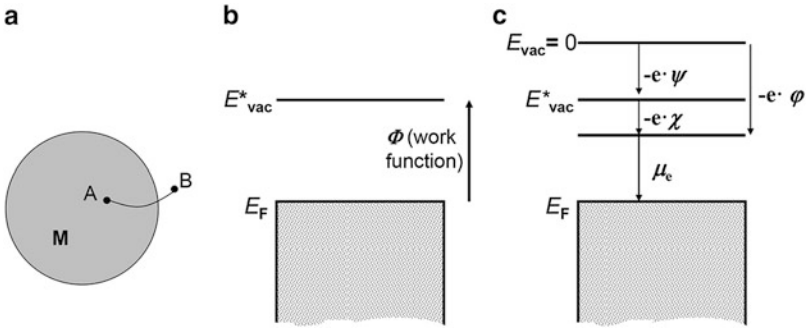

Fig. 15.1 The work function is defined as the minimum work that is required for the removal of an electron from within the sample to a point just outside the sample (**a**). For uncharged samples the energy level at this position is equivalent to the vacuum level $E^*_{vac} = E_{vac}$ (**b**). For charged samples with the external potential $\psi \neq 0$ this is still $-e{\cdot}\psi$ away from the absolute vacuum level E_{vac} (**c**). M denotes the metal, and A and B positions inside the metal and just outside of it

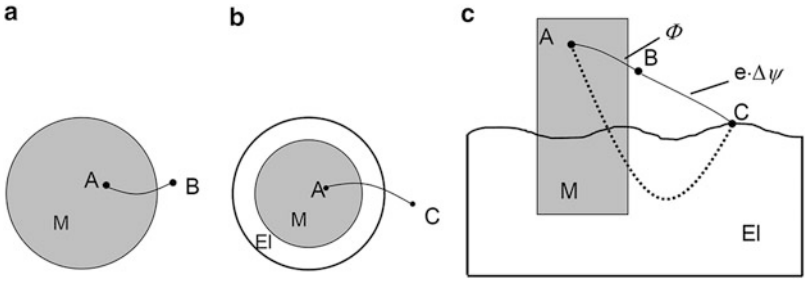

Fig. 15.2 A more general work function Φ^* may be defined, in analogy to the definition of the work function, where the electron is also transferred through the electrolyte layer covering the sample [see (**b**)]. The absolute electrode potential is then defined as $E_{abs} = \Phi^*/e$. (**c**) Both paths AC and ABC for the electron extraction are energetically equivalent. M and El denote the metal and the electrolyte layer, respectively. A a position inside the metal, B a position just outside of it and C a position just outside the electrolyte layer

Hence, $E_{abs} = \Phi^*/e$ is directly obtained from Eq. (15.1) by adding the additional term $\Delta\varphi_M^{El} = \varphi_M - \varphi_{El}$ and exchanging χ_{El} with χ_M:

$$E_{abs} = \frac{1}{e} \cdot \Phi^* = \left(-\frac{\mu_e}{e} + \Delta\varphi_M^{El} + \chi_{El} \right), \tag{15.3}$$

where $\Delta\varphi_M^{El}$ is the potential drop at the metal/liquid interface and χ_{El} the surface potential of the electrolyte layer.

On the other hand, the absolute potential can also be expressed by the work function of the metal and the Volta potential difference between metal and electrolyte (see Fig. 15.2c):

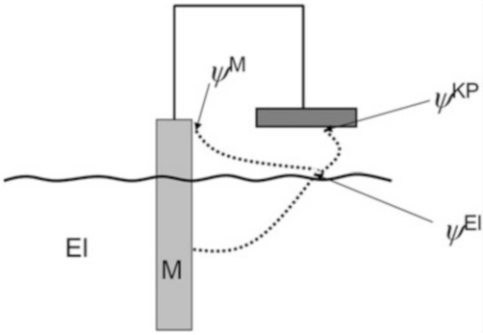

Fig. 15.3 The work for transferring an electron from within the metal M to a point over the surface of the electrolyte is the same for all three indicated transfer paths, and hence, $E_{abs} = \frac{1}{e}\Phi^{*} = \left(-\frac{\mu_e}{e} + \Delta\varphi_{M}^{El} + \chi_{El}\right) = \Phi^{M}/e + (\psi^{M} - \psi^{El}) = \Phi^{KP}/e + (\psi^{KP} - \psi^{El})$. Hence, the Volta potential difference between the Kelvin probe and the electrolyte surface is directly correlated to the electrode potential of the immersed electrode M

$$E_{abs} = \Phi/e + (\psi^{M} - \psi^{El}), \tag{15.4}$$

where ψ^{M} and ψ^{El} denote the Volta potentials outside the metal and outside the solution.

If now a metallic probe KP is positioned near the surface of the electrolyte, thus as sketched in Fig. 15.3, then the following correlation can be made:

$$\begin{aligned} E_{abs} &= \frac{1}{e}\Phi^{*} = \left(-\frac{\mu_e}{e} + \Delta\varphi_{M}^{El} + \chi_{El}\right) = \Phi^{M}/e + (\psi^{M} - \psi^{El}) \\ &= \Phi^{KP}/e + (\psi^{KP} - \psi^{El}) \end{aligned} \tag{15.5}$$

as no work is required for an electron to go from the metal M into the also metallic probe KP.

If the work function of the probe KP is known, the absolute electrode potential can be directly obtained by the measurement of the Volta potential difference $(\psi^{KP} - \psi^{El})$. This potential difference is exactly what the Kelvin probe technique provides. The bottom of the tip of the Kelvin probe and the surface of the electrolyte just beneath it form a plate capacitor which is charged due to the bias $\psi^{KP} - \psi^{El}$ across the gap between tip and electrolyte. When the tip vibrates periodically over the electrolyte layer, such that the distance is modulated periodically, this induces a so-called displacement current. This current can be nulled by applying an external bias compensating $\psi^{KP} - \psi^{El}$. This way this Volta potential differences can be easily obtained; for more details, see e.g. [29, 30]. In this way the Kelvin probe technique may be described as the natural reference electrode, which has the great advantage of being very versatile in application.

The absolute electrode potential can be easily correlated to the conventional reference electrodes as usually applied in electrochemistry. For instance for the

correlation of the absolute electrode potential with the electrode potential referenced vs. the standard hydrogen electrode, we can simply write as follows:

$$E_{\mathrm{SHE}} = E_{\mathrm{abs}} - E^{\ominus}(\mathrm{SHE})_{\mathrm{abs}}, \tag{15.6}$$

where $E^{\ominus}$ $(\mathrm{SHE})_{\mathrm{abs}}$ is the potential of the standard hydrogen electrode in the absolute electrode potential scale.

Obviously, the following correlation between the potential of zero charge and the corresponding modified work function Φ^* measured on the electrolyte-covered metal at the potential of zero charge can be made [27]:

$$\Phi^* = e \cdot E_{\sigma=0,\mathrm{abs}} = e \cdot \left(E_{\sigma=0,\mathrm{SHE}} + E^{\ominus}(\mathrm{SHE})_{\mathrm{abs}}\right), \tag{15.7}$$

i.e., the measurement of the corresponding modified work function Φ^* provides directly $E^{\ominus}(\mathrm{SHE})_{\mathrm{abs}}$, if the potential of zero charge vs. SHE is known. Unfortunately, as it is difficult in ambient environment to make a really precise measurement of the work function of the Kelvin probe, these measurements are not easy. Hence, the values found in the literature scatter in a wide range from about 4.44 to 4.85 V [27].

For this reason it is usually not used for measuring electrode potentials in the absolute potential scale, but it is referenced vs. a standard reference electrode as they are commonly used in electrochemistry. For this a simple calibration has to be carried out.

As the absolute electrode potential E_{abs} is correlated with the corresponding electrode potential vs. a given reference through the relation $E_{\mathrm{ref}} = E_{\mathrm{abs}} - E(\mathrm{ref})_{\mathrm{abs}}$, we can write [see Eq. (15.5)]:

$$\begin{aligned}(\psi^{\mathrm{KP}} - \psi^{\mathrm{El}}) &= \left(-\frac{\mu_{\mathrm{e}}}{e} + \Delta\varphi_{\mathrm{M}}^{\mathrm{El}} + \chi_{\mathrm{El}}\right) - \frac{1}{e}\Phi^{\mathrm{KP}} = E_{\mathrm{abs}} - \frac{1}{e}\Phi^{\mathrm{KP}} \\ &= E_{\mathrm{ref}} + E(\mathrm{ref})_{\mathrm{abs}} - \frac{1}{e}\Phi^{\mathrm{KP}}.\end{aligned} \tag{15.8}$$

Since $E(\mathrm{ref})_{\mathrm{abs}}$ and Φ^{KP} are constant, we can directly write as follows:

$$E_{\mathrm{ref}} = (\psi^{\mathrm{KP}} - \psi^{\mathrm{El}}) + \mathrm{const}(\mathrm{ref}), \tag{15.9}$$

where the constant depends on the chosen standard reference electrode.

The value for const(ref) can be obtained by calibrating the Kelvin probe by means of a suitable reference system, as e.g. copper in a Cu^{2+}-containing electrolyte or zinc in Zn^{2+}-containing electrolyte (i.e. vs. Cu/Cu^{2+} or Zn/Zn^{2+}), or by direct calibration vs. an electrode polarised potentiostatically to different potentials, such as schematically depicted in Fig. 15.4.

From the example shown in Fig. 15.4 it becomes obvious that through the application of the Kelvin probe an active potentiostatic control of surfaces covered by ultrathin electrolyte layers should be possible and hence performing

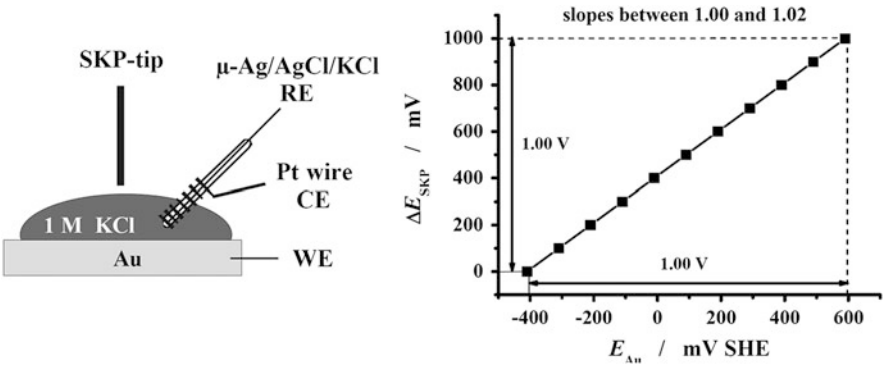

Fig. 15.4 *Left*: A very instructive way for calibrating the Kelvin probe is by positioning it over an electrolyte-covered surface potentiostatically polarised to different potentials. A typical calibration curve is shown on the *right*. As can be seen, there is a linear relation between measured Kelvin probe signal and the applied electrode potential. Once the correct functioning of an SKP set-up has been checked this way, it is sufficient to calibrate the offset value (here it is about 400 mV) with just one measurement vs. a reference. This is usually done by positioning the SKP over a small Cu beaker filled with $CuSO_4$ solution of well-known concentration (usually saturated) and referencing the SKP signal to the corresponding Cu/Cu^{2+} potential [31]

electrochemical experiments on such samples, which is of great significance for fundamental studies of atmospheric corrosion [9] and for catalysis, e.g., in fuel cells and modern high rate electrolytical processes where high transport rates are achieved by ultrathin electrolyte layers (as of importance e.g. for modern chloralkali electrolysis [32]).

For such electrochemical experiments under ultrathin electrolyte layers usually a set-up as shown in Fig. 15.5 is used.

With such a set-up it was found, for instance, that the rate-determining step for oxygen reduction on a sufficiently cathodically polarised platinum electrode underneath an ultrathin electrolyte layer below a certain thickness ceases to be the diffusion through it and starts to be controlled by the oxygen uptake at the electrolyte surface (see Fig. 15.6).

Even "dry" surface under typically ambient conditions can be considered as electrodes where it makes sense to interpret the work functions measured on these surfaces as electrode potentials, as these are directly related to the electrochemical activity on these surfaces [33].

Other than for electrodes immersed in bulk electrolyte, on electrodes covered by ultrathin layers the electrode potential may differ significantly across the electrode surface. Hence, localised measurements are of interest, being performed by scanning the tip across the sample. This was first applied for organic coated metals where the coating was electrochemically delaminating, driven by corrosion [12–14, 29]. Even on the submicron scale the Kelvin probe technique can be applied for such studies, and then based on a modified atomic force microscope, see [34, 35]. Recent developments are the combination of Kelvin probe and SECM [36] and the use of Kelvin probe for hydrogen detection [37].

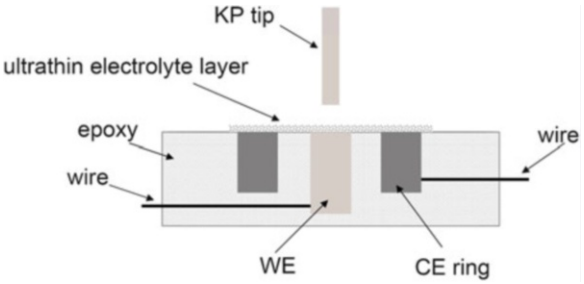

Fig. 15.5 Schematic cross section of a typical set-up for performing electrochemical experiments under ultrathin electrolyte layers. The working electrode is made of a cylinder that is, together with the counter electrode ring positioned around it, embedded in an inert and insulating polymer, e.g. in epoxy. The Kelvin probe tip is positioned over the centre of exposed surface of the working electrode. This way Ohmic drops during polarisation can be minimised

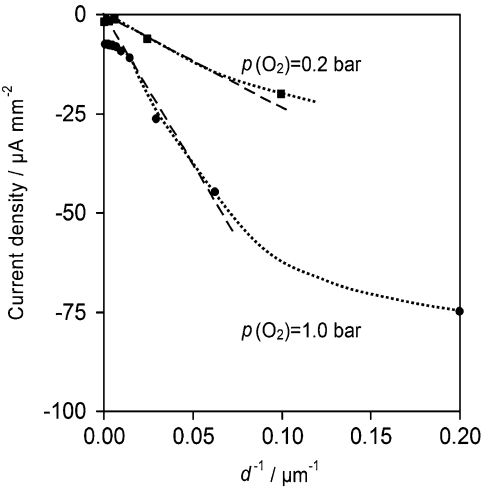

Fig. 15.6 Dependence of the rate of the oxygen reduction on the thickness of the electrolyte layer; Pt, 1 M Na_2SO_4, $E = -0.65$ V_{SHE} (rate plotted vs. $1/d$; *dashed line*: slope that can be used to calculate the diffusion coefficient of oxygen; *dotted line* is indicating the likely further behaviour of the oxygen reduction rate; see [9])

References

1. Thomson W (1898) Philos Mag 46:82
2. Patai IF, Pomerantz MA (1951) J Franklin Inst 252:239
3. Zisman WA (1932) Rev Sci Instrum 3:367
4. Rohwerder M, Benndorf C (1993) Surf Sci 307–309:789
5. Stratmann M, Kim KT, Streckel H (1990) Z Metallkunde 81:715
6. Yee S, Stratmann M, Oriani RA (1991) J Electrochem Soc 138:55
7. Stratmann M, Streckel H (1990) Corr Sci 30:681

8. Stratmann M, Streckel H (1990) Corr Sci 30:697
9. Stratmann M, Streckel H, Kim KT, Crockett S (1990) Corr Sci 30:715
10. Leng A, Stratmann M (1993) Corr Sci 34:1657
11. Stratmann M (1992) Bull Electrochem 8:30
12. Leng A, Streckel H, Stratmann M (1999) Corr Sci 41:547
13. Leng A, Streckel H, Stratmann M (1999) Corr Sci 41:579
14. Leng A, Streckel H, Hofmann K, Stratmann M (1999) Corr Sci 41:599
15. Veselovsky VJ (1939) Acta Physicochim URSS 11:815
16. Grahame DC (1947) Chem Revs 41:441
17. Frumkin AN (1930) Colloid Symposium Annual 7: 89
18. Bockris JOM, Argade SD (1968) J Chem Phys 49:5133
19. Bockris JOM (1970) Energ Conv 10:41
20. Bockris JOM (1972) J Electroanal Chem 36:495
21. Gileadi E, Stoner G (1972) J Electronal Chem 36:492
22. Trasatti S, Damaskin B (1974) J Electroanal Chem 52:313
23. Trasatti S (1975) J Electroanal Chem 66:155
24. De Battisti A, Trasatti S (1977) J Electroanal Chem 79:251
25. Trasatti S (1982) J Electroanal Chem 139:1
26. Trasatti S (1990) Electrochim Acta 3:269
27. Trasatti S (1991) Electrochim Acta 36:1659
28. Trasatti S (1995) Surf Sci 335:1
29. Rohwerder M, Turcu F (2007) Electrochim Acta 53:290
30. Frankel GS, Stratmann M, Rohwerder M, Michalik A, Maier B, Doora J, Wicinski M (2007) Corr Sci 49:2021
31. Ehahoun H, Stratmann M, Rohwerder M (2005) Electrochim Acta 50:2667
32. Jörissen J, Turek T, Weber R (2011) Chem unserer Zeit 5:172
33. Hausbrand R, Stratmann M, Rohwerder M (2008) J Electrochem Soc 155:C369
34. Rohwerder M, Hornung E, Stratmann M (2003) Electrochim Acta 48:1235
35. Senöz S, Rohwerder M (2011) Electrochim Acta 56:9588
36. Senöz S, Maljusch A, Rohwerder M, Schuhmann W (2012) Electroanalysis 24:239
37. Senöz S, Evers S, Stratmann M, Rohwerder M (2011) Electrochem Commun 13:1542

Index

A
Absolute electrode potentials, 333
Accuracy, 22
Acids, 145
Acrylate hydrogels, 55
Ag|AgBr, 61, 98
Ag|AgCl, 80, 86, 163, 213
Ag|AgCryp(22)$^{+}$ reference electrode, 161
Ag|AgI, 100
Ag|$AgNO_3$, 156
Ag|Ag_2O, 132, 135
Ag|Ag^{+} reference electrodes, 28, 159, 201
Ag|Ag_2S, 101
Agar, 55
Agarobiose, 55
Agaropectin, 55
Agarose, 55
Al^{3+}|Al reference electrode, eutectic chlorides, 215
Alcohols, 145
Alkaline fuel cell (AFC), 248
1-Alkyl-3-methylimidazolium bis (trifluoromethanesulfonyl)amide, 64
Al_2O_3|Al reference electrode, cryolite, 216
Amides, 145
Amines, 146
As|As_2O_3, 135

B
Bi|Bi_2O_3, 135
BIMEVOX, 266
Bis(triphenylphosphoranylidene)ammonium perchlorate (BTPPA-ClO_4), 319
Bis(biphenyl)chromium(I) tetraphenylborate (BCr), 27, 30, 36, 210
Brönsted acidic ionic liquids, 218

C
Calcium chloride melts, sealed Ag|AgCl reference electrode, 213
Calcium oxide (CaO), 229, 274
Calomel electrodes, 106
Carbon fibre nanoelectrode, 293
Cd/Cd^{2+} reference electrode, 166
Cell
  diagram, 3
  reaction, 6
  voltage, 3
Cellulose gel, 55
Chloride baths, Ag|AgCl reference electrode, 214
$Cl^{-}|Cl_2$ reference electrode, chloride melts, 215
Cobaltocene/cobaltocenium ($Cc|Cc^{+}$), 13, 27, 209
Compensation method, 16
Compensators, 18
Complete micro-reference electrode, 294
Condensed ionic systems, LJP, 45
Conducting polymer (CP), 305
  films, anionic/cationic sensitivity, 311
Conducting polymer reference electrodes (CPRE), 315
Cryolite, 216

D
Densified bath inverted (DBI) design, 217, 218
Diaphragms, 49
Diffusion potential, elimination, 41
Distillable ionic liquids, 220
du Bois-Reymond–Poggendorff compensation method, 16

G. Inzelt et al. (eds.), *Handbook of Reference Electrodes*,
DOI 10.1007/978-3-642-36188-3, © Springer-Verlag Berlin Heidelberg 2013

E
Electrochemical cells, 3
Electrochemical converters, 247
Electrodes, 2
  asymmetry, 251
  miniaturized, 96
  potential, 5
    thermodynamics, 6
  reaction, kinetics, 13
Electromotive force, 5
Equilibrium electrode potential, 5
Ethers, 146

F
FcPVC, 285
Ferrocene/ferrocenium ($Fc|Fc^+$), 13, 27, 35, 168, 206
Formal potentials, 10
Fuel cells, 247, 259, 338

G
Gas electrolyzers 247
Gas pumps, 247
Gel reference electrodes, 93
Gel-solidified internal electrolyte, 92
Gibbs energy, 6, 26, 58, 157, 174, 176
Ground-joint diaphragm, 50

H
Half-cell, 2
Harned cell, 81
Henderson equation, 39
Heptadecafluorodecyltrioctylphosphonium tetrakis[3,5-bis(trifluoromethyl) phenyl]borate, 65
Hexamethylthiophosphoric triamide (HMTPA), 152
$Hg|Hg_2Cl_2$, 106
Hg|HgO, 127
$H_2|H^+$ reference electrodes, 204
Hydrogen electrodes, 29, 77
  purity, 84
Hydroquinone/quinone redox system, 285
Hydroxyethyl cellulose, 55

I
ILSB|W interface, 62
Immiscible electrolyte solutions (ITIES), 46
Immiscible liquids, 46
Indium tin oxide electrode (ITO), 318
Iodine–iodide electrode, 121
Ion exchange, inhibition, 313
Ionic liquids (IL), 27, 57, 93, 190, 286
  room temperature (RTILs), 34
Ionic liquid salt bridges (ILSB), 57
  dissolution of water, 64
  gelation, 68
  liquid junction potential, 60
Ionic transport, 243
Ion-selective membrane (ISE), 279
Ion-to-electron transducer/coupling, 281
ISFET, 298

K
KCl-based salt bridge (KClSB), 57
Kelvin probe technique, 333
Ketones, 146

L
LAMOX, 266
Lewis acidic/basic ionic liquids, 219
Lewis–Sargent cells, 39
LiCl–KCl eutectics, 212
$Li|Li^+$ reference electrodes, 166, 204, 214
Liquid ammonia, 171
Liquid electrolytes, thermodynamic measurements, 272
Liquid junction (LJ), 67
  potential (LJP), 26, 33
Low-temperature ionic liquids (RTILs), 190
Luggin capillary, 50

M
Magnesium oxide (MgO), 229
Membranes, 46
Mercury electrodes, 105
Mercury/mercury(I) bromide electrode, 112
Mercury/mercury(I) chloride (calomel) electrode, 106
Mercury/mercury(I) sulfate electrode, 112
Mercury/mercury(I) sulfide electrode, 115
Mercury(II) oxide, 127
Mercury–mercury(II) oxide electrode, 127
Metal/metal oxide electrodes, 235
Methacrylate hydrogels, 55
Methyl acetate (MA), 152
1-Methyl-3-octylimidazolium bis (trifluoromethanesulfonyl)amide, 68
Microelectrodes, 289

Miniaturized electrodes, 96
M(Hg)/M(MX)-type reference electrodes, 167
Molten carbonate fuel cell (MCFC), 248
Molten salts, 190
  reference electrodes, 212
Monolayer-protected nanocluster (MPC), 286
Multipotentiostats, 21

N
Nanoparticles, 286
NASICON, 243, 267
Nernst equation, 11
Nickel-based reference electrodes, 215
Ni–Ni(II), 215
Nitriles, 146
Nitrobenzene (NB), 62
Normal hydrogen electrode (NHE), 77

O
Open-circuit conditions, 16
Operational amplifiers (OPAs), 19
Oxidic glass melts, 229
Oxygen-anion conductors, 244
Oxygen-indicating electrodes, 239
Oxygen partial pressure, 271

P
Partial oxidation of methane (POM), 248
PEDOT–SSA film, 308
pH meters, 19, 20
Phosphoric acid fuel cell (PAFC), 248
Platinum black, 78
Platinum hydrogen cell (Harned cell), 81
Platinum hydrogen electrode, 80
Poggendorff compensation circuit, 17
Poly(3,4-ethylenedioxythiophene) (PEDOT), 286, 308
Poly(methyl methacrylate) (PMMA), 285
Poly(octylthiophene) (POT), 285
Poly(3-methylthiophene) films, 311
Poly-2-hydroxyethyl-methacrylate (p-HEMA), 55
Polymer electrolyte membrane fuel cell (PEMFC), 248
Polymer/solution interface, inhibition of ion exchange, 313
Polypyrrole (PPy), 94, 106, 286, 311, 318
  films, overoxidized, 315
  $Hg|Hg_2Cl_2$, 306
Potential measurement, accuracy, 22
Potentiometric sensors, 267
Potentiostats, 19, 20, 64, 114, 222, 308
Protic ionic liquids (PILs), 194
Protonic conductors, 244
Pseudo-reference electrodes, 28, 331
  miniaturised lab-on-chip systems, 292
$Pt/Cu^{+}–Cu^{2+}$ reference electrodes, 171
$Pt/I^{-}–I_3^{-}$ reference electrodes, 160, 169
PVDF-HFP, 68
PVFc, 313

Q
Quasi-reference electrodes, 205
  polypyrrole films, 313

R
$Rb^{+}|Rb$, 26
Redox couple, soluble, 197
Redox reference electrodes, 168, 206
Redox systems, 26
Reference electrodes, aqueous solutions, 77, 172
  bridge, 28
  conducting polymer, 305
  disposable, 296
  electrochemical potential distribution, 256
  ILSB-coated, 69
  ionic liquids, 189
  Kelvin probe technique, 333
  mercury, 105
  miniaturized, 291
  molten salts, 189
  nonaqueous solutions, 145, 173
  oxidic glass melts, 229
  polymer membranes, 301
  screen-printed, disposable, 325
  solid contact, 279, 286
Reference redox systems, 26
REFETs, 298, 326
Reversible hydrogen electrodes (RHE), 78
Room temperature ionic liquid reference electrodes, 201

S
Salt bridges, 42, 49, 57
  diaphragms, 49
  gels, 54
  ionic liquid (ILSB), 57
  KCl-based (KClSB), 57
Saturated calomel electrode (SCE), 23

$Sb|Sb_2O_3$, 135
Screen-printing technology, 325
Sensors, 267
Silver electrodes, 86
Silver–silver bromide electrode, 61, 98
Silver–silver chloride electrode, 80, 86, 163
Silver–silver cryptate reference electrodes, 160
Silver–silver iodide electrode, 100
Silver–silver ion reference electrodes, 156
Silver–silver oxide electrode, 132
Silver–silver sulfide electrode, 101
$SnO_2|Na_2SnO_3$, 136
Sodium cryolite (Na_3AlF_6), 216
Solid contact (SC), 279
  ionselective electrodes (SC ISEs), 279
  reference electrodes (SC REs), 279
Solid electrolytes, 243
  membranes, 247
  thickness, 251
Solid oxide electrolysis cells (SOECs), 248
Solid oxide fuel cells (SOFCs), 244, 248
Solvated-electron reference electrodes, 171
Solvents, nonaqueous, 145
Solvent–solvent interactions, 179
Standard electrode potential, 5
Standard hydrogen electrode (SHE), 29, 77
  pressure dependency, 82
Standard potentials, 9

T
Tetra(phenyl)borates, 284, 286
Tetrabutylammonium hexafluorophosphate, 314
Tetrafluoroborate, 284
Thallium electrode, 119
Thermal expansion coefficients (TECs), 263
Thermal liquid junction potential (TLJP), 44
Thorium carbides, 275
$TiO_2|Na_2TiO_3$, 137
TlCl/Tl(Hg), 120
Triiodide ion, 169
Triple-phase boundary (TPB), 249
Two-electrode electrochemical cells, conducting polymers, 316

U
Ultra-micro-reference electrode, 294

V
Voltage follower (VF), 21
Voltmeters, 19, 20

W
Wetted molybdenum hook (WMH), 217

Y
Yttria (Y_2O_3), 229
Yttria-doped zirconia, 233
Yttria-stabilized zirconia (YSZ), 263

Z
Zirconia electrode/tube reference electrode, 230